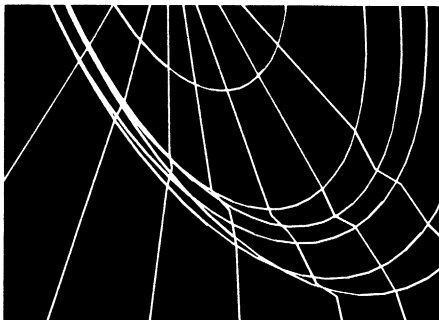


MARC



Volume E

Demonstration Problems

Version K7



Copyright © 1997 MARC Analysis Research Corporation
Printed in U. S. A.

This notice shall be marked on any reproduction of this data, in whole or in part.

MARC Analysis Research Corporation
260 Sheridan Avenue, Suite 309
Palo Alto, CA 94306 USA

Phone: (650) 329-6800
FAX: (650) 323-5892

Document Title: **MARC Volume E: Demonstration Problems, Part IV, Version K7**
Part Number: RF-3018-07.IV
Revision Date: June, 1998

Proprietary Notice

MARC Analysis Research Corporation reserves the right to make changes in specifications and other information contained in this document without prior notice.

ALTHOUGH DUE CARE HAS BEEN TAKEN TO PRESENT ACCURATE INFORMATION, MARC ANALYSIS RESEARCH CORPORATION DISCLAIMS ALL WARRANTIES WITH RESPECT TO THE CONTENTS OF THIS DOCUMENT (INCLUDING, WITHOUT LIMITATION, WARRANTIES OR MERCHANTABILITY AND FITNESS FOR A PARTICULAR PURPOSE) EITHER EXPRESSED OR IMPLIED. MARC ANALYSIS RESEARCH CORPORATION SHALL NOT BE LIABLE FOR DAMAGES RESULTING FROM ANY ERROR CONTAINED HEREIN, INCLUDING, BUT NOT LIMITED TO, FOR ANY SPECIAL, INCIDENTAL OR CONSEQUENTIAL DAMAGES ARISING OUT OF, OR IN CONNECTION WITH, THE USE OF THIS DOCUMENT.

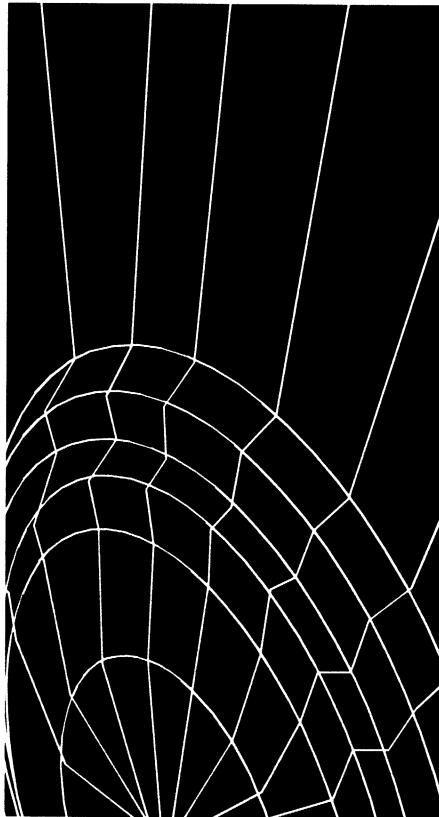
This software product and its documentation set are copyrighted and all rights are reserved by MARC Analysis Research Corporation. Usage of this product is only allowed under the terms set forth in the MARC Analysis Research Corporation License Agreement. Any reproduction or distribution of this document, in whole or in part, without the prior written consent of MARC Analysis Research Corporation is prohibited.

Restricted Rights Notice

This computer software is commercial computer software submitted with "restricted rights." Use, duplication, or disclosure by the government is subject to restrictions as set forth in subparagraph (c)(i)(ii) or the Rights in technical Data and Computer Software clause at DFARS 252.227-7013, NASA FAR Supp. Clause 1852.227-86, or FAR 52.227-19. Unpublished rights reserved under the Copyright Laws of the United States.

Trademarks

All products mentioned are the trademarks, service marks, or registered trademarks of their respective holders.



MARC



Volume E

Demonstration Problems

Version K7

Part IV

- Contact
- Advanced Topics





Part IV

Volume E: Demonstration Problems



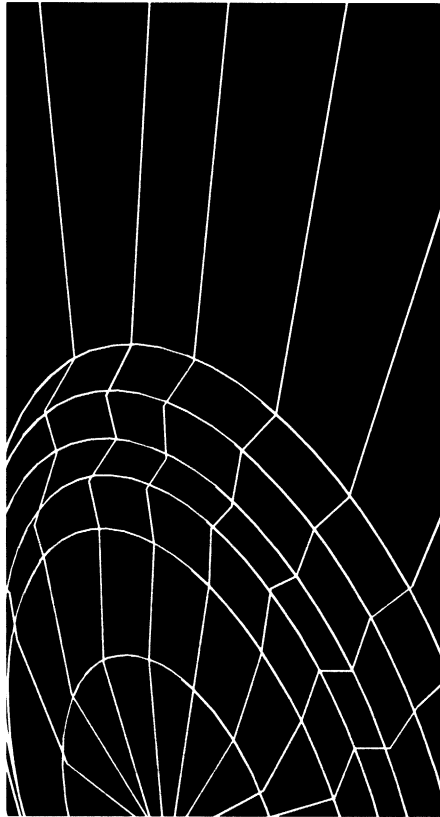
Chapter 7

Contact

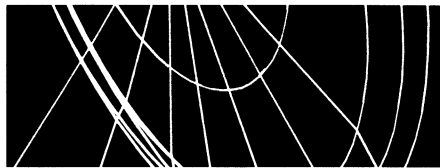
Chapter 8

Advanced Topics





MARC



Volume E

Demonstration Problems

Version K7

Chapter 7
Contact





Contact Contents



Description	Problem
Rigid Perfectly Plastic Extrusion Isothermal and Coupled Analysis	7.1
End-Plate-Aperture Breakaway	7.2
Barrel Vault Shell under Self-weight (Shell Cracking)	7.3
Side Pressing of a Hollow Rubber Cylinder (Mooney Material)	7.4
Analysis of a Thick Rubber Cylinder under Internal Pressure	7.5
Biaxial Stress in a Composite Plate	7.6
Composite Plate Subjected to Thermal Load	7.7
Cylinder under External Pressure (Fourier Analysis)	7.8
Cylinder under Line Load (Fourier Analysis)	7.9
Mesh Qualification.	7.10
Concrete Beam under Point Loads	7.11
Constant Uniaxial Stress Applied to Plate in Plane Strain (Viscoelasticity)	7.12
Analysis of Pipeline Structure	7.13
Viscoelastic Analysis of an Externally Reinforced Thick-Walled Cylinder under Internal Pressure	7.14
Spiral Groove Thrust Bearing with Tilt	7.15
Hydrodynamic Journal Bearing of Finite Width.	7.16
Elastic-Plastic Finite Deformation of a Thick-Walled Cylinder.	7.17
Side Pressing of a Hollow Rubber Cylinder.	7.18
Stretching of a Rubber Sheet with a Hole	7.19
Compression of an O-Ring using Ogden Model	7.20
Stretching of a Rubber Plate with Hole	7.21

Description	Problem
Loading of a Rubber Plate	7.22
Compression of a Foam Tube	7.23
Constitutive Law for a Composite Plate	7.24
Progressive Failure of a Composite Strip	7.25
Pipe Collars in Contact	7.26
Twist and Extension of Circular Bar of Variable Thickness at Large Strains	7.27
Analysis of a Thick Rubber Cylinder under Internal Pressure	7.28
3D Analyses of a Plate with a Hole at Large Strains	7.29
Damage in Elastomeric Materials	7.30
Rezoning in an Elastomeric Seal	7.31
Structural Relaxation of a Glass Cube.	7.32



Contact List of Figures



Figure		Page
7.1-1	50% Reduction Die Problem.	7.1-5
7.1-2	Mesh and Boundary Conditions for 50% Reduction Example.	7.1-6
7.1-3	50% Reduction Extrusion Velocity Field.	7.1-7
7.1-4	Temperature Distribution in the Billet Neglecting Thermal Convection.	7.1-8
7.1-5	Temperature Distribution in the Billet including Convection.	7.1-9
7.1-6	Equivalent Plastic Strains in Billet Neglecting Thermal Convection.	7.1-10
7.2-1	Geometry and Mesh of End Plate-Aperture.	7.2-4
7.2-2	Transient Normal Forces in Bolts.	7.2-5
7.2-3	Transient Shear Force in Bolts.	7.2-6
7.2-4	Radial Displacement at Outside Top (Node 46).	7.2-7
7.3-1	Mesh for the Shell Roof.	7.3-4
7.3-2	Load-Vertical Deflection Curve at Node 3.	7.3-5
7.4-1	Rubber Cylinder and Mesh.	7.4-4
7.4-2	Deformed Mesh Plot.	7.4-5
7.5-1	Cylinder Mesh (8-Node Model).	7.5-4
7.5-2	Radial Stress Through Radius.	7.5-5
7.6-1	Composite Plate.	7.6-5
7.6-2	Finite Element Mesh.	7.6-6
7.6-3	Deformed Mesh Plot.	7.6-7
7.7-1	Plate Geometry and Mesh.	7.7-3
7.7-2	Displaced Mesh.	7.7-4
7.8-1	Cylinder and Mesh.	7.8-5
7.8-2	First Mode Solid Cylinder Plane Strain.	7.8-6
7.8-3	Second Mode Solid Cylinder Plane Strain.	7.8-7



Figure	Page
7.9-1 Cylinder and Mesh	7.9-4
7.9-2 Concentrated Load on a Solid Cylinder	7.9-5
7.10-1 Membrane and Mesh.	7.10-3
7.10-2 Strain Energy Difference	7.10-4
7.11-1 Concrete Beam and Mesh	7.11-4
7.11-2 Deformed Mesh Plot.	7.11-5
7.11-3 Regions of Cracking	7.11-6
7.12-1 Geometry.	7.12-4
7.12-2 Finite Element Model	7.12-4
7.12-3 Normalized Displacement vs. Time	7.12-5
7.12-4 Normalized Out-of-Plane Stress, σ_{zz} vs. Time	7.12-5
7.13-1 Pipe Line Geometry and Model	7.13-5
7.13-2 Load vs. Displacement	7.13-6
7.13-3 Ovalization Behavior Due to Out-of-Plane and In-Plane Moments	7.13-7
7.14-1 Long Thick-Walled Cylinder	7.14-6
7.14-2 Simple Maxwell Model.	7.14-6
7.14-3 Finite Element Model	7.14-7
7.14-4 Radial Stress vs. Time.	7.14-8
7.14-5 Hoop Stress vs. Time	7.14-9
7.15-1 Spiral Groove Thrust Bearing with Tilt	7.15-4
7.15-2 Vector Plot of Mass Flow	7.15-5
7.16-1 Journal Bearing of Finite Width	7.16-5
7.16-2 Path Plot of Pressure Distribution.	7.16-6
7.17-1 Thick-Walled Cylinder	7.17-3
7.17-2 Applied Load History	7.17-4
7.17-3 Deformed Meshes at Increments 6, 10, and 20.	7.17-4
7.17-4 Internal Pressure vs. Inner Radius.	7.17-5

Figure	Page
7.18-1 Rubber Cylinder and Mesh	7.18-3
7.18-2 Deformed Mesh Plot	7.18-4
7.18-3 Displacement History of Node 53	7.18-5
7.18-4 Stress Relaxation	7.18-6
7.19-1 Finite Element Mesh	7.19-4
7.19-2 Incompressible Model Deformed Mesh	7.19-5
7.19-3 Incompressible Model Load Deflection Curve at Node 277	7.19-6
7.19-4 Foam Model Deformed Mesh	7.19-7
7.19-5 Foam Model Load Deflection Curve at Node 277	7.19-8
7.20-1 O-Ring Mesh	7.20-4
7.20-2 Coarse O-Ring Initial Mesh for Data Set e7x20c	7.20-5
7.20-3 Stress-Strain Curve	7.20-6
7.20-4 Deformed Mesh, Increment 10	7.20-7
7.20-5 Deformed Mesh, Increment 30	7.20-8
7.20-6 Deformed Mesh, Increment 50	7.20-9
7.20-7 Mean Stress Distribution	7.20-10
7.20-8 Contact Forces	7.20-11
7.20-9 Adaptive Mesh at Increment 10	7.20-12
7.20-10 Adaptive Mesh at Increment 20	7.20-13
7.20-11 Adaptive Mesh at Increment 40	7.20-14
7.20-12 Adaptive Mesh at Increment 67	7.20-15
7.20-13 Contact Forces for the Updated Lagrange Formulation	7.20-16
7.21-1 Finite Element Mesh	7.21-3
7.21-2 Stress-Strain Curve	7.21-4
7.21-3 Deformed Mesh	7.21-5
7.21-4 Stress Distribution	7.21-6
7.21-5 Strain Distribution	7.21-7
7.22-1 Finite Element Mesh	7.22-5
7.22-2 Stress-Strain Curve	7.22-6
7.22-3 Displacement History of Center Node – Elastic Effects Only	7.22-7
7.22-4 Displacement History of Center Node – Including Damage Effects	7.22-8



Figure	Page
7.22-5 Displacement History of Center Node – Including Damage and Viscoelastic Effects.	7.22-9
7.22-6 Displacement History as a Function of Time – Including Damage and Viscoelastic Effects.	7.22-10
7.23-1 Finite Element Mesh of Tube	7.23-3
7.23-2 Deformed Mesh at Increment 10	7.23-4
7.23-3 Deformed Mesh at Increment 16	7.23-5
7.23-4 Deformed Mesh at Increment 29	7.23-6
7.23-5 Shear Strain in Compressed Tube.	7.23-7
7.24-1 Geometry and Lamination of a Composite Plate	7.24-4
7.25-1 Finite Element Mesh of Strip	7.25-3
7.25-2 History of Deflection of the Tip	7.25-4
7.25-3 History of First Component of Stress in Layer 1	7.25-5
7.25-4 History of First Component of Stress in Layer 5	7.25-6
7.25-5 History of the Reaction Force at Clamped End	7.25-7
7.26-1 Geometric Dimension and Bending Loads.	7.26-3
7.26-2 FEM Model.	7.26-4
7.26-3 Deformed Shape at 0°	7.26-4
7.26-4 von Mises Stress Contour at 0°, Layer 1.	7.26-5
7.26-5 von Mises Stress Contour at 180°, Layer 9.	7.26-6
7.26-6 Plastic Strain Contour at 0°, Layer 1.	7.26-7
7.27-1 Circular Bar and Mesh	7.27-3
7.27-2 Deformed Mesh and Distribution of Equivalent von Mises Stress.	7.27-4
7.28-1 Cylinder Mesh (8-Node Model)	7.28-5
7.29-1 Initial Mesh.	7.29-4
7.29-2 Deformed Model and Distribution of Equivalent von Mises Stress for e7x29a. . .	7.29-5
7.29-3 Deformed Model and Distribution of Equivalent von Mises Stress for e7x29b. . .	7.29-6
7.30-1 Discontinuous Damage.	7.30-4
7.30-2 Continuous Damage	7.30-5



Figure	Page
7.31-1 Deformed Mesh at Increment 0	7.31-4
7.31-2 Deformed Mesh at Increment 7	7.31-5
7.31-3 Deformed Mesh at Increment 14	7.31-6
7.31-4 Deformed Mesh at Increment 15	7.31-7
7.31-5 Deformed Mesh at Increment 29	7.31-8
7.31-6 Contact Force Distribution	7.31-9
7.32-1 Structural Relaxation Phenomenon.	7.32-3
7.32-2 Property (Volume) – Temperature Plot	7.32-3
7.32-3 Volume Change during Cyclic Temperature History	7.32-5



7 *Contact List of Figures*

 **7**

Contact List of Tables



Table		Page
7-1	Special Topics Demonstration Problems	7-2



7 *Contact List of Tables*

 7

Contact



In addition to the various analysis capabilities discussed in previous chapters concerned with problems of linear elasticity, plasticity and creep, large displacement, heat transfer as well as dynamics, this chapter contains demonstration problems for the illustration of additional analysis capabilities in MARC. Detailed discussions of these capabilities can be found in *MARC Volume A: Theory and User Information* and a summary of the various capabilities illustrated is given below.

- Steady, creeping flow of rigid, perfectly plastic material (R-P FLOW).
- The use of gap-friction element (Element Type 12 and Type 97).
- Analysis of concrete (CRACK DATA) structures.
- Analysis of rubber structures (MOONEY, OGDEN, and FOAM).
- Simulation of composite material (COMPOSITE).
- Simulation of viscoelastic material.
- Axisymmetric structure under nonsymmetric loading (Fourier Analysis).
- Study of mesh refinement (QUALIFY).
- Analysis of hydrodynamic bearings.
- Use of the rezoning technique for large deformation analysis.

Compiled in this chapter are a number of solved problems. Table 7-1 shows the MARC elements and options used in these demonstration problems.

Table 7-1 Special Topics Demonstration Problems

Problem Number	Element Type(s)	Parameters	Model Definition	History Definition	User Subroutines	Problem Description
7.1	32	ELSTO R-P FLOW	CONTROL	AUTO LOAD	—	Steady, creeping flow of rigid, perfectly plastic material (R-P Flow).
7.2	10 12	—	OPTIMIZE CONTROL ISOTROPIC GAP DATA	POINT LOADS DIST LOADS AUTO LOAD	—	The use of gap-friction element in the analysis of a manhole cover in a pressure vessel.
7.3	75	SHELL SECT	UFXORD CONTROL CRACK DATA ISOTROPIC	AUTO INCREMENT	UFXORD	Analysis of a concrete barrel vault shell subjected to self-weight.
7.4	12 32	LARGE DISP	RESTART CONTROL MOONEY GAP DATA	PROPORTIONAL AUTO LOAD	—	Side pressing of a hollow rubber cylinder.
7.5	33 82 119	LARGE DISP FOLLOW FOR	NODE FILL CONTROL MOONEY	DIST LOADS	—	Analysis of a thick rubber cylinder.
7.6	75	SHELL SECT	DEFINE COMPOSITE ORIENTATION ORTHOTROPIC PRINT ELEM	—	—	Elastic analysis of a multilayered square plate under uniform pressure (composite material).
7.7	75	SHELL SECT	DEFINE COMPOSITE ORTHOTROPIC PRINT ELEM ORIENTATION INITIAL STATE CHANGE STATE	—	—	Elastic analysis of a multilayered square plate subjected to uniform pressure and thermal loading (composite material).
7.8	62	FOURIER	CONTROL FOURIER RESTART	—	UFOUR	Fourier analysis of a cylinder under external pressure.
7.9	62	FOURIER	CONTROL FOURIER RESTART CASE COMBIN	—	UFOUR	Fourier analysis of a cylinder in plane strain subjected to a line load.

Table 7-1 Special Topics Demonstration Problems (Continued)

Problem Number	Element Type(s)	Parameters	Model Definition	History Definition	User Subroutines	Problem Description
7.10	27	MESH PLOT QUALIFY	POST	—	—	Use of the QUALIFY option for the study of mesh refinement.
7.11	3 9	—	CONTROL CRACK DATA ISOTROPIC RESTART	POINT LOAD	—	Analysis of a simply supported concrete beam subjected to concentrated loads.
7.12	27	—	TYING PRINT CHOICE ISOTROPIC VISCELPROP	AUTO LOAD TIME STEP	—	Analysis of a simply supported concrete beam subjected to concentrated loads.
7.13	14 17	SCALE ELSTO	TYING	AUTO LOAD PROPORTIONAL INC	—	Analysis of pipeline structure using element type 14 and 17, and the pipeline mesh generator MARCPIPE.
7.14	28	—	ISOTROPIC VISCELPROP PRINT CHOICE	AUTO LOAD TIME STEP	—	Internal pressurization of an externally reinforced long, thick walled, viscoelastic cylinder.
7.15	37	BEARING	THICKNESS VELOCITY TYING	—	UFXORD UFCONN UTHICK UVELOC UGROOV	Calculation of the pressure distribution in a spiral groove thrust bearing including grooves.
7.16	39	BEARING	CONN GENER NODE FILL THICKNESS VELOCITY	DAMPING COMPONENTS STIFFNESS COMPONENTS THICKNESS CHANGE	UTHICK UBEAR	Analysis of a journal bearing. Determine the load carrying capacity of the bearing.
7.17	10	UPDATE FINITE LARGE DISP REZONE	FORCDT WORK HARD	AUTO LOAD COORDINATE CHANGE REZONE	FORCDT	Analysis of a thick-walled cylinder under internal pressure. Demonstration of rezoning capability.
7.18	32 12	LARGE DISP	MOONEY GAP DATA VISCELMOONEY	AUTO LOAD TIME STEP	—	Side pressing of a hollow viscoelastic rubber cylinder.

Table 7-1 Special Topics Demonstration Problems (Continued)

Problem Number	Element Type(s)	Parameters	Model Definition	History Definition	User Subroutines	Problem Description
7.19	26	—	MOONEY TYING	AUTO LOAD	—	Plane stress stretching of a rubber sheet with a hole.
7.20	82	FOLLOW FOR PRINT, 5	DEFINE CONTACT CONTROL OGDEN	MOTION CHANGE AUTO LOAD DIST LOADS TIME STEP	—	Compression of an O-ring.
7.21	26	—	OGDEN	DISP CHANGE AUTO LOAD	—	Plane stress stretching of a rubber sheet with a hole.
7.22	75	LARGE DISP SHELL SECT	OGDEN DIST LOADS DAMAGE VISCELOGDEN	AUTO LOAD DIST LOADS TIME STEP	—	Loading of a rubber plate including damage and rate effects.
7.23	11	LARGE DISP	FOAM CONTACT	AUTO LOAD TIME STEP	—	Compression of a foam tube.
7.24	75	—	ORIENTATION ORTHOTROPIC COMPOSITE	—	—	Demonstrate composites.
7.25	22	LARGE DISP	ORIENTATION ORTHOTROPIC FAIL DATA COMPOSITE	POINT LOAD POST INCREMENT AUTO LOAD PROPORTIONAL INC	—	Progressive failure of fiber reinforced composite.
7.26	95 97	—	GAP DATA WORK HARD DIST LOAD	DIST LOADS	—	Pipe collars in contact.
7.27	67	ELASTICITY ALIAS	DIST LOAD TYING	AUTO LOAD POINT LOAD	—	Twist and extension of a circular bar of variable thickness at large strains.
7.28	10 116 28 55	FOLLOW FOR ELASTICITY	DIST LOAD OGDEN NODE FILL	DIST LOAD	—	Analysis of a thick rubber cylinder under internal pressure.
7.29	7 117	User Defaults ELASTICITY PROCESS	OGDEN OPTIMIZE	AUTO LOAD DISP CHANGE	HYPELA2	3D analysis of a plate with a hole at large strains.
7.30	7	ELASTICITY	DEFINE DAMAGE OGDEN'	AUTO INC DISP CHANGE	—	Damage in elastomeric materials.

Table 7-1 Special Topics Demonstration Problems (Continued)

Problem Number	Element Type(s)	Parameters	Model Definition	History Definition	User Subroutines	Problem Description
7.31	11	ELASTICITY REZONE ALIAS	CONTACT CONTACT TABLE OGDEN RESTART CONNECTIVITY CHANGE COORDINATE CHANGE CONTACT CHANGE END REZONE	AUTO LOAD TIME STEP	—	Rezoning in an elastomeric seal.
7.32	7	STATE VARS	SHIFT FUNCTION VISCEL EXP VISCLEPROP CHANGE STATE	AUTO LOAD CHANGE STATE TIME STEP	—	Structural relaxation of a glass cube.



7 *Contact*

7.1 Rigid Perfectly Plastic Extrusion Isothermal and Coupled Analysis

This example illustrates the use of the R-P FLOW option in a classic plastic flow problem – the extrusion of metal in-plane strain through a 50% reduction, frictionless die. The problem is shown in Figure 7.1-1; a uniform velocity is applied at the left-hand side. The required solution is the velocity field and extrusion force. The slip-line solution to this problem is well known [1, 2].

The rigid-plastic flow option uses Herrmann incompressible elements to solve for the velocity field. The material is modeled as a non-Newtonian fluid and MARC iterates for the viscosity,

which is $\frac{2}{3} \frac{\bar{\sigma}}{\dot{\epsilon}}$, where σ is the yield stress and $\dot{\epsilon}$ is the equivalent plastic strain rate.

The second part of this example demonstrates the coupled analysis for steady-state rigid-plastic flow. The comparison between effect of no heat convection contribution and heat convection contribution is made in e7x1b and e7x1c. Uniform velocity and fixed temperature is applied at the left-hand side. The contribution of convection heat is made after the solution of velocity is obtained. The nonsymmetric solver is turned on automatically when heat convection is included. The parameter COUPLE is used to flag the coupling procedures.

This problem is modeled using the three techniques summarized below.

Data Set	Element Type(s)	Number of Elements	Number of Nodes	Differentiating Features
e7x1	32	32	121	Isothermal
e7x1b	32	32	121	Coupled without Convection
e7x1c	32	32	121	Coupled with Convection

Element

In this example, the plane-strain Herrmann element (element 32) is used. This element is a second-order, distorted quadrilateral (plane-strain). There are 32 elements and a total of 121 nodes.

Material Properties

The equivalent von Mises yield stress is entered as 30×10^3 psi in this option. The thermal properties are:

specific heat	4.2117E-2
density	0.3523E-3
thermal conductivity	0.7254E-3

The property is specified for elements 1 through 32.

Geometry

No geometry is specified.

Loading

No loading is specified.

Boundary Conditions

The material entering the die is assigned a velocity of 1 in/sec in the x-direction. The material velocities normal to the die walls are fixed as zero. In the thermal mechanically coupled analysis, the inlet temperature of the material is fixed at 800°F. The wall temperature is fixed at 500°F.

Control

A 10% tolerance on the relative residual force was chosen to determine if convergence was achieved. In a rigid plastic analysis, the computational time would have been reduced if the convergence based upon velocities was requested.

Auto Load

Because the contribution of heat convection is accounted after the solution of velocity distribution is obtained, two fixed time steps are used to simulate the coupling process. In the first increment, the heat transfer analysis is done first and subsequent stress analysis uses this new temperature distribution for material properties to obtain the solution of velocity distribution. In the next increment, the temperature distribution is obtained based on the velocity distribution result of the previous increment.

Results

The solution for the 50% reduction case chosen here is a centered fan – outside the fan the material moves as a rigid body or is stationary. The mesh is confined to the neighborhood of the fan region (Figure 7.1-2).

Note a special consideration for the fully incompressible Herrmann formulation: since the system is semidefinite, it is only possible to solve by Gauss elimination if the first active degree of freedom is a stiffness degree of freedom and not a pressure variable (Lagrange multiplier). Thus, node 1 must have at least one unconstrained velocity component. In this case, one and two are swapped to achieve this by adding additional CONNECTIVITY and COORDINATES set by hand. The value of the input velocity is arbitrary in this case, since the yield is assumed to be rate independent. The accuracy of the solution is determined by the convergency requirements. In this analysis, nine iterations were required.

Extrusion force in 50% reduction, frictionless die. (Normalized by the tensile yield stress and input width).

Calculated at input stream	1.347
Calculated from reaction on die face	1.393
Exact (slip line) solution, $.5(1 + \pi/2)$	1.285

The predicted flow field is illustrated in Figure 7.1-3. Velocity vectors are shown in this figure. The slip-line fan has been superimposed on this picture. The “dead” region in the corner of the die is well predicted by the finite element model, before it reaches the fan. The downstream solution also shows a little rotation of the velocity field just below the corner of the die. This is more accurate than the upstream solution. The strain gradients on entry to the fan are very high. At this point, the slip solution shows a discontinuity in tangential velocity. A finer mesh in this region would improve this part of the solution.

The temperature distributions shown in Figure 7.1-4 and Figure 7.1-6 indicate the effect of heat convection on the plastic extrusion. As the contribution of heat convection is included, the heat transferred into exit from the inlet is faster and the temperature gradient between the wall and the central region is higher. The equivalent plastic strain is shown in Figure 7.1-5. The shear bands are clearly visible.

References

1. Hill, R., *Mathematical Theory of Plasticity*, Chapter 4, (Oxford University Press, 1950.).
2. Prager, W., and Hodge, P. G., *Theory of Perfectly Plastic Solids*, Section 298 (John Wiley, 1951).

Parameters, Options, and Subroutines Summary

Example e7x1.dat:

Parameters	Model Definition Options	History Definition Options
ELEMENT	CONNECTIVITY	AUTO LOAD
ELSTO	CONTROL	CONTINUE
END	COORDINATE	
R-P FLOW	END OPTION	
SIZING	FIXED DISP	
TITLE	ISOTROPIC	

Example e7x1b.dat:

Parameters	Model Definition Options	History Definition Options
COUPLE	CONNECTIVITY	AUTO LOAD
END	CONTROL	CONTINUE
ELEMENTS	COORDINATE	TIME STEP
HEAT	END OPTION	
R-P FLOW	FIXED DISPLACEMENT	
SIZING	FIXED TEMPERATURE	
TITLE	INITIAL TEMPERATURE	
	ISOTROPIC	
	NO PRINT	
	POST	

Example e7x1c.dat:

Parameters	Model Definition Options	History Definition Options
COUPLE	CONNECTIVITY	AUTO LOAD
END	CONTROL	CONTINUE
ELEMENTS	COORDINATE	TIME STEP
HEAT	END OPTION	
R-P FLOW	FIXED DISPLACEMENT	
SIZING	FIXED TEMPERATURE	
TITLE	INITIAL TEMPERATURE	
	ISOTROPIC	
	NO PRINT	
	POST	

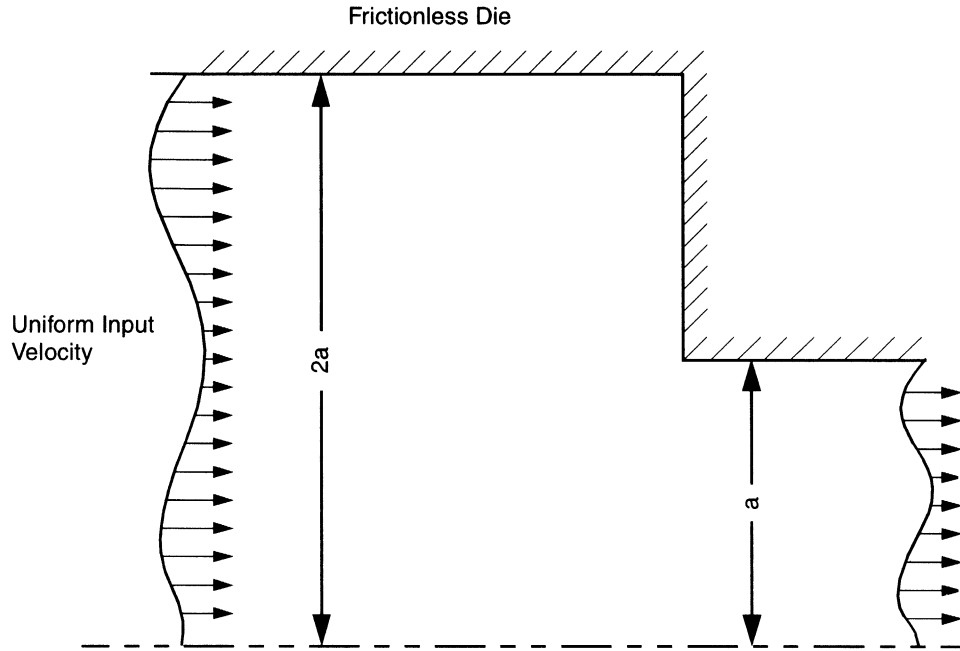


Figure 7.1-1 50% Reduction Die Problem

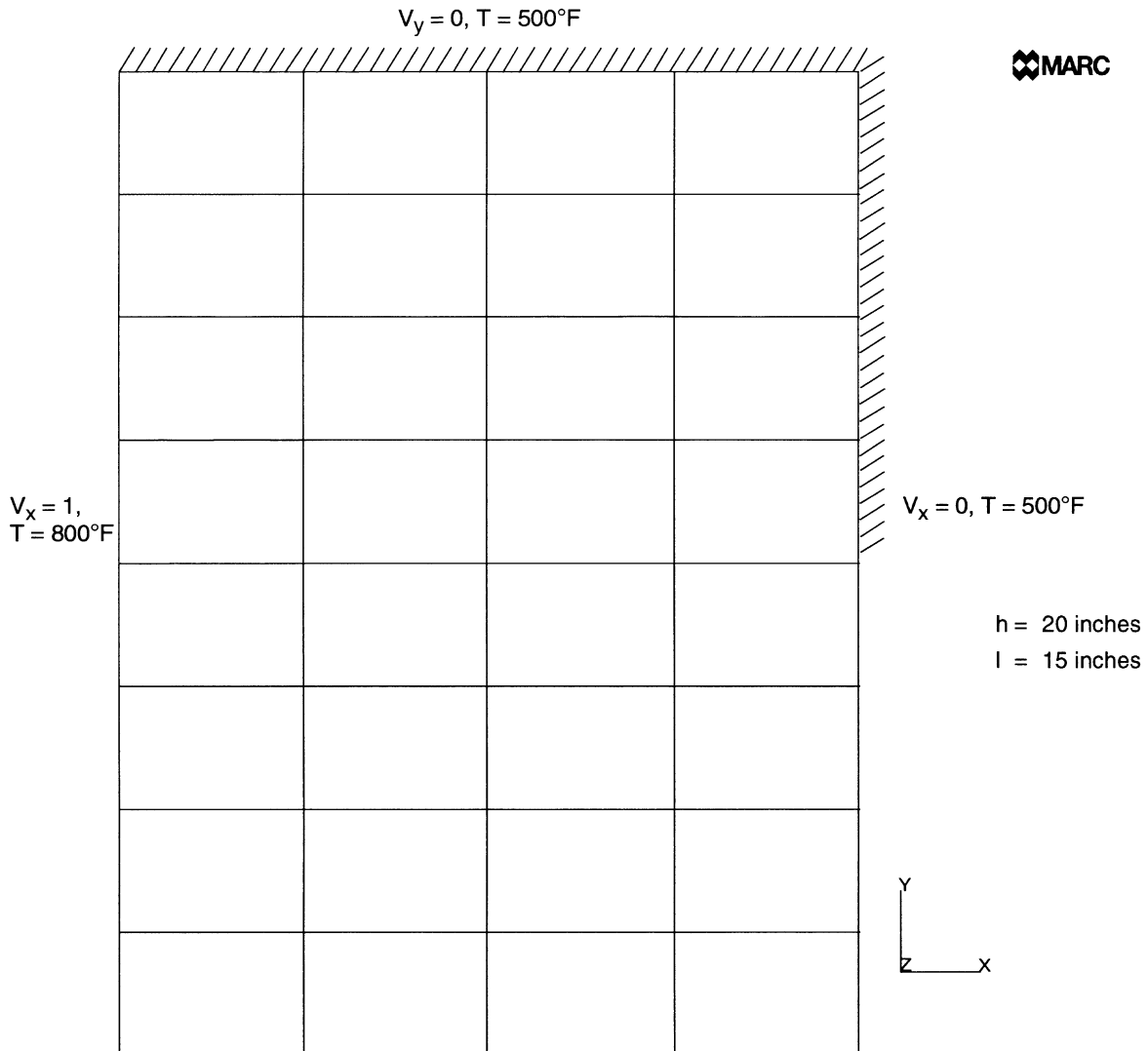


Figure 7.1-2 Mesh and Boundary Conditions for 50% Reduction Example



INC : 1
 SUB : 0
 TIME : 0.000e+00
 FREQ : 0.000e+00

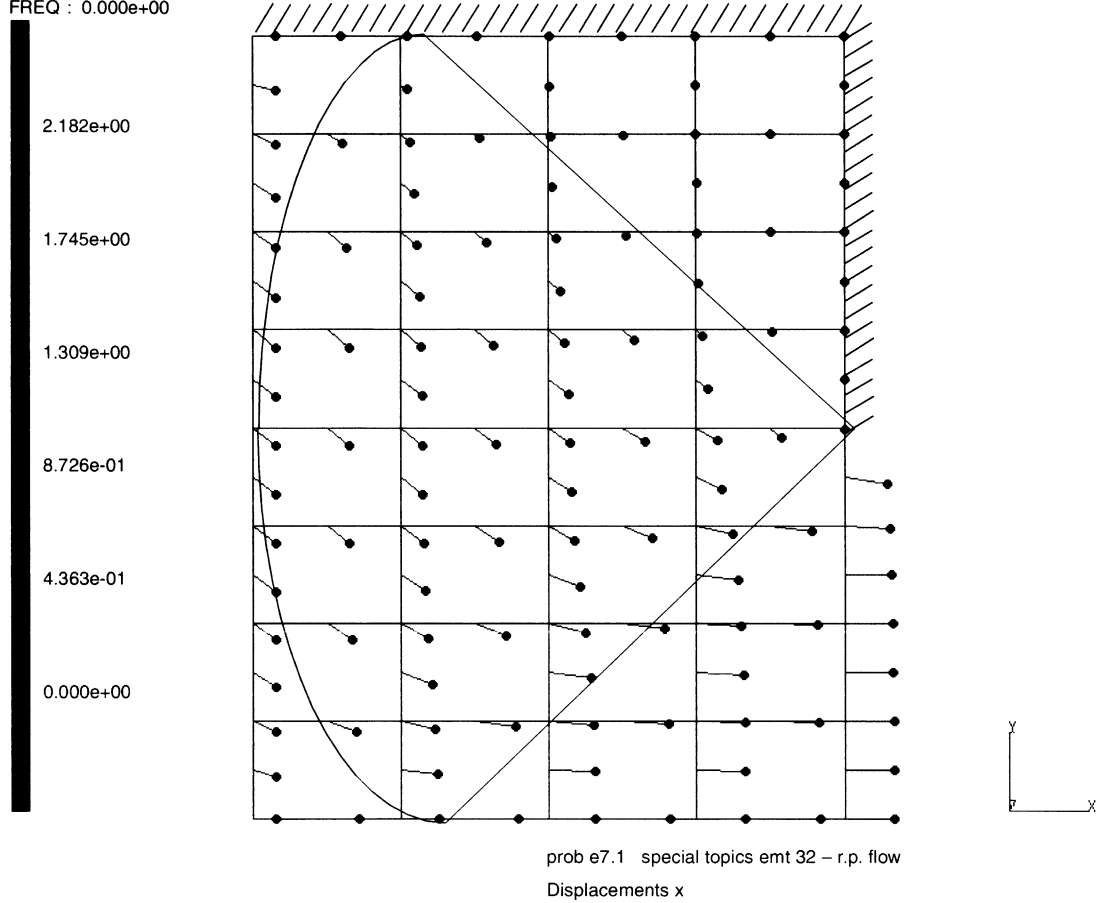
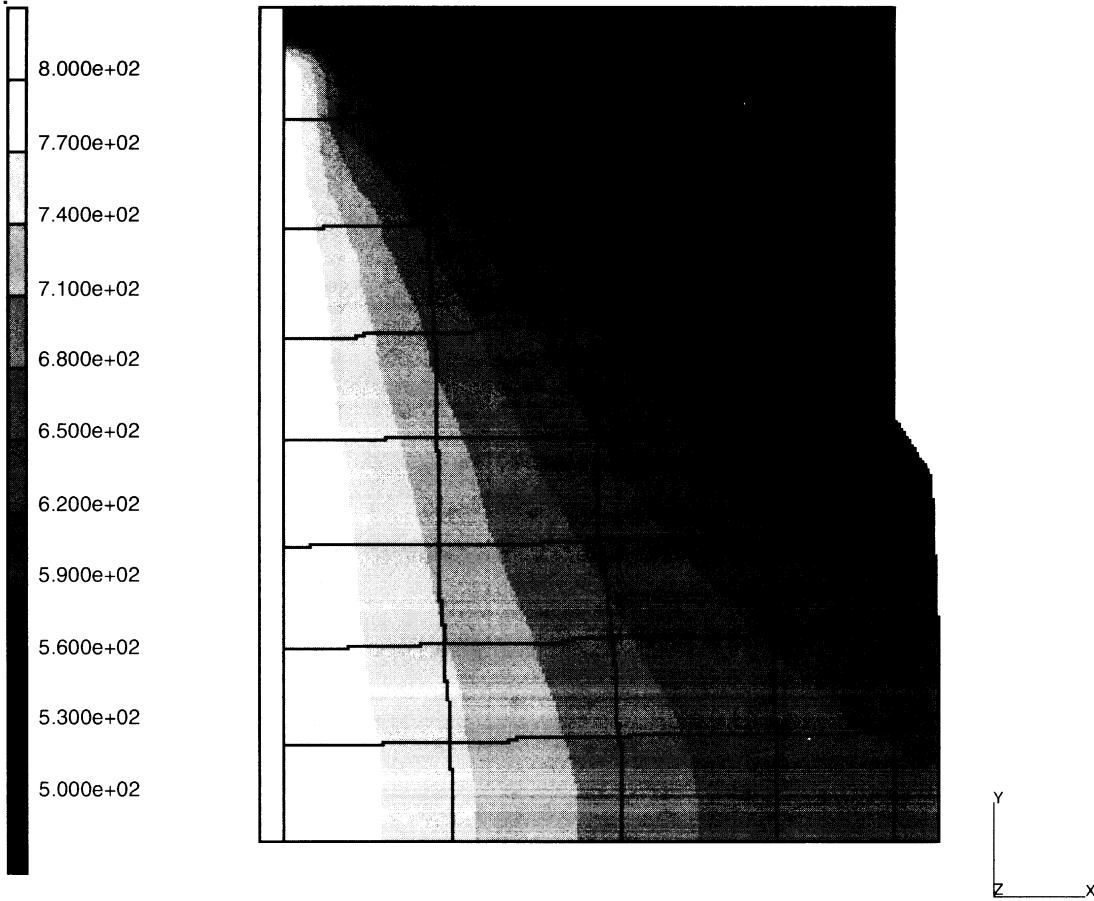


Figure 7.1-3 50% Reduction Extrusion Velocity Field

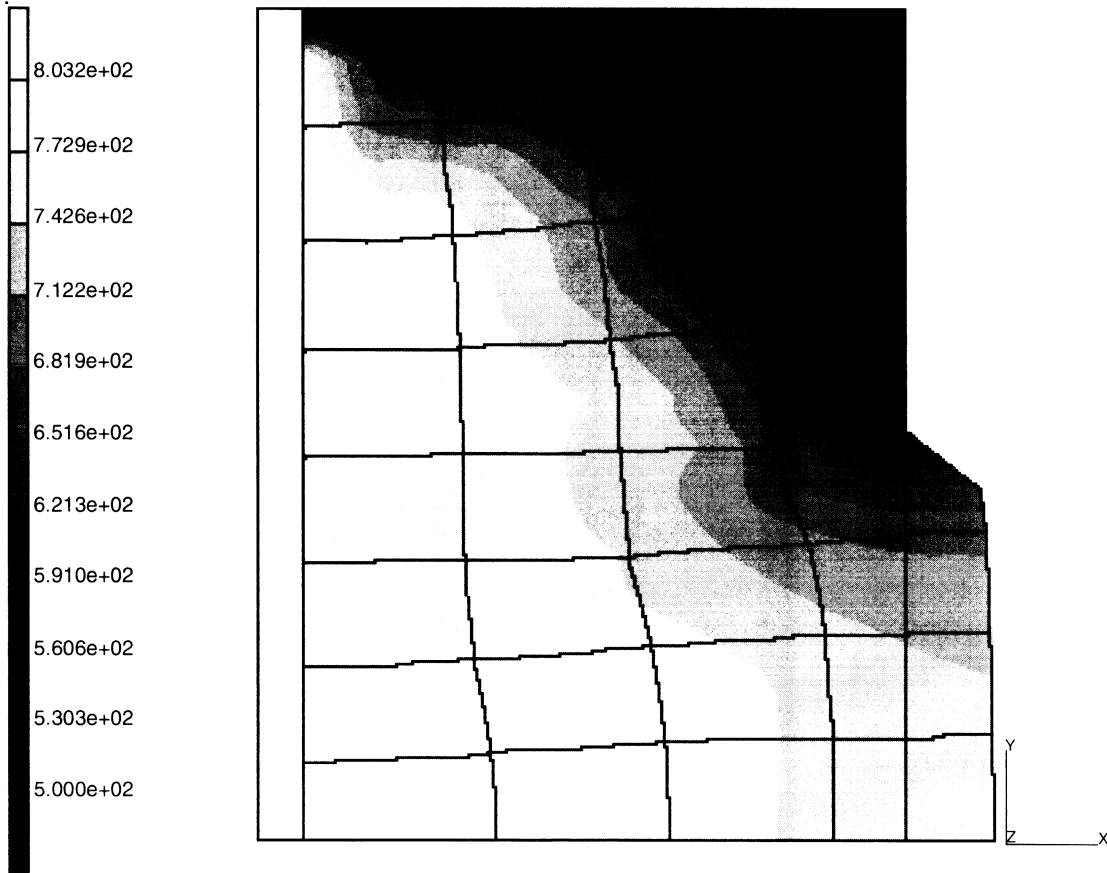
INC : 1
SUB : 0
TIME : 5.000e-01
FREQ : 0.000e+00



prob e7.1b - coupled r.p. flow without heat convection
Temperature t

Figure 7.1-4 Temperature Distribution in the Billet Neglecting Thermal Convection

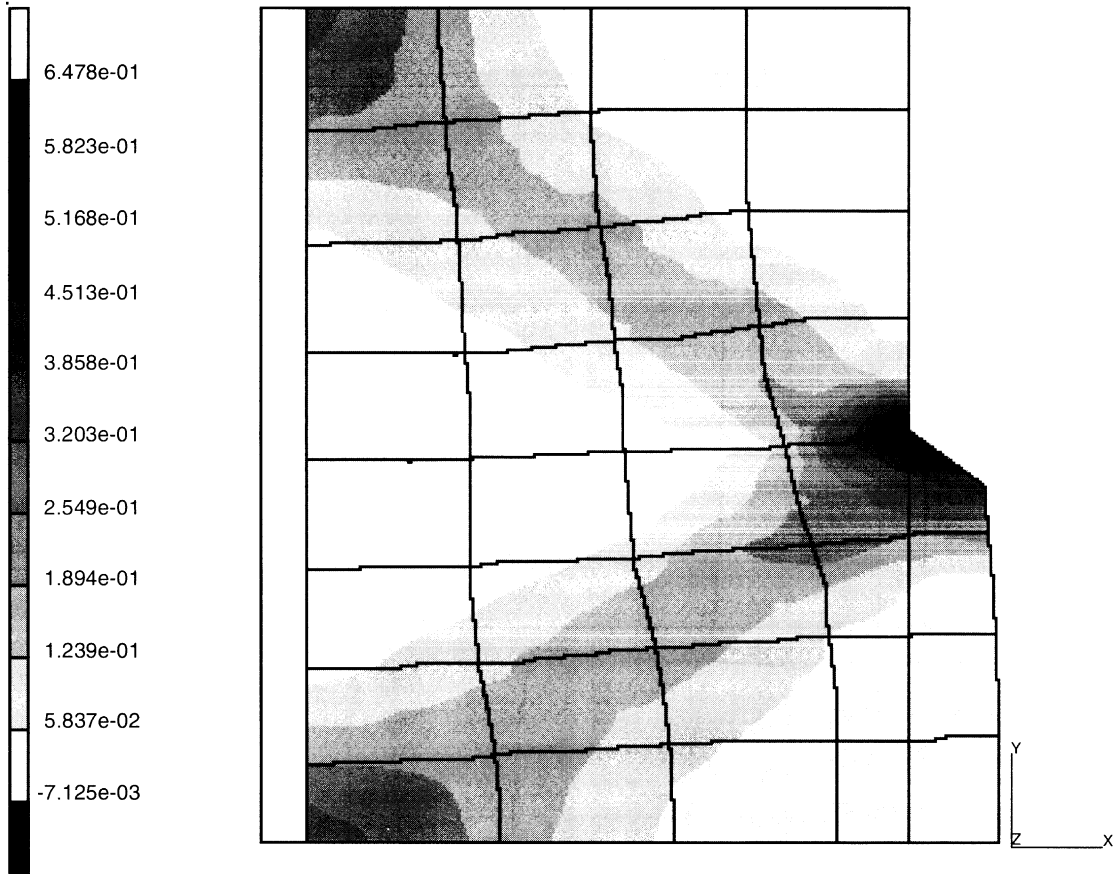
INC : 2
SUB : 0
TIME : 1.000e+01
FREQ : 0.000e+00



prob e7.1c - coupled r.p. flow without heat convection
Temperature t

Figure 7.1-5 Temperature Distribution in the Billet including Convection

INC : 2
SUB : 0
TIME : 1.000e+01
FREQ : 0.000e+00



prob e7.1b - coupled r.p. flow without heat convection
Total Equivalent Plastic Strain

Figure 7.1-6 Equivalent Plastic Strains in Billet Neglecting Thermal Convection

7.2 End-Plate-Aperture Breakaway

This example illustrates the use of the gap and friction link, element type 12. This element allows surface friction effects to be modeled. This example is a simple model of a man-hole cover in a pressure vessel. The axisymmetric mesh is shown in Figure 7.2-1. The object of this analysis is to establish the response of the bolted joint between the manhole cover (elements 1-12) and the vessel (elements 13-27). The bolts are first tightened, and then the main vessel expands radially (as might occur due to thermal or internal pressure effects). You should be aware that this problem is presented only as a demonstration. The mesh is too coarse for accurate results.

Elements

Element 12 is a friction and gap element. It is based on the imposition of a gap closure constraint and/or a frictional constraint via Lagrange multipliers. The element has four nodes: nodes 1 and 4 are the end nodes of the link and each has two degrees of freedom (u , v) in the global coordinate direction; node 2 gives the gap direction cosines (n_x , n_y) and has λ_n , the force in the gap direction, as its one degree of freedom; node 3 gives the friction direction cosines (t_{1_x} , t_{1_y}) and has γ_1 , the frictional shear forces, and p , the net frictional slip, as its two degrees of freedom.

Model

Twenty-seven type 10 elements are used for the two discrete structures, the end cap and the aperture. These are then joined by four type 12 elements. There are 54 nodes and a total of 108 degrees of freedom in the mesh.

Loading

The load history consists of applying bolt loads (that is, tightening down the bolts), then pulling out the outer perimeter of the main vessel model. Bolt loads are modeled here as point loads applied in opposite directions (self-equilibrating) on node pairs 4 and 32, 5 and 33. Since there is a possibility of gaps developing between the facing surfaces of the cover and vessel, the bolt load is initially applied as a small magnitude, then incremented up to the total value of 2000 pounds per bolt ring. This usually requires two runs of the problem: an initial run with a “small” load to see the pattern developing, from which some judgement can be made about the load steps which can be used to apply the total bolt force. In this case, it was determined by this method that no surface separation occurred, so that, in the actual run, the full bolt loads are applied in one increment.

The radial expansion of the main vessel is modeled as a uniform negative pressure on the outer surfaces of the outer elements (15, 21, 27). (Note this is given as load type 8 to apply it to the correct face of the elements.) Again, the purpose of the analysis is to watch the development of slippage between the main vessel and the cover plate, and the analyst cannot easily estimate the appropriate load increments to apply to model this nonlinearity. For this purpose, the RESTART

option can be used effectively. A restart is written at the point where full bolt load is applied, and then a trial increment of pull-out force is applied. Based on the response to this (in the friction links), a reasonable size for the sequence of loading increments can be determined. This procedure is frequently necessary in such problems. For brevity, this example shows only the final load sequence obtained as a result of such trials.

Boundary Conditions

The nodes on the axis of symmetry are constrained radially, and the rigid body mode in the axial direction is removed at node 46.

Isotropic

The ISOTROPIC option is used to enter the mechanical properties of the manhole cover.

Gap Data

In this example, a small negative closure distance of -0.001 is given for the gaps. This indicates that the gaps are initially closed and solve for an interference fit in increment 0. The coefficient of friction μ is 0.8.

Results

The results of the analysis are shown in Figure 7.2-2 through Figure 7.2-4. First of all, it is observed in Figure 7.2-2 that the force at node 53, associated with gap element 31 goes to zero, indicating that the gap has opened. The interested user can investigate here possible model changes and their effect – for example, the effect of inaccurate bolt tightening, so that the two bolt rings have different loadings.

In this case, the initial bolt load is carried quite uniformly (A in Figure 7.2-2), but as the pull-out increases, the inner two links take more of the stress and the outer link (element 31) sheds stress. The shear stress development is followed in Figure 7.2-3 – initially (bold load only), all shear stresses are essentially zero. The two outer links slip first, but then the additional forces required to resist the pull develops in the inner two elements until the shear stress pattern follows the normal stress pattern, when the shear in the pair of links also slip ($\tau = \mu\sigma$). Figure 7.2-4 shows a plot of radial displacement of the outer perimeter against pull-out force. Notice the small loss of stiffness caused by slip developing as the vessel model has to resist the extra force along without any further force transfer to the cover.



Parameters, Options, and Subroutines Summary

Example e7x2.dat:

Parameters

DIST LOADS

ELEMENT

END

SIZING

TITLE

Model Definition Options

CONNECTIVITY

CONTROL

COORDINATE

END OPTION

FIXED DISP

GAP DATA

ISOTROPIC

OPTIMIZE

POINT LOAD

History Definition Options

AUTO LOAD

CONTINUE

DIST LOADS

POINT LOAD

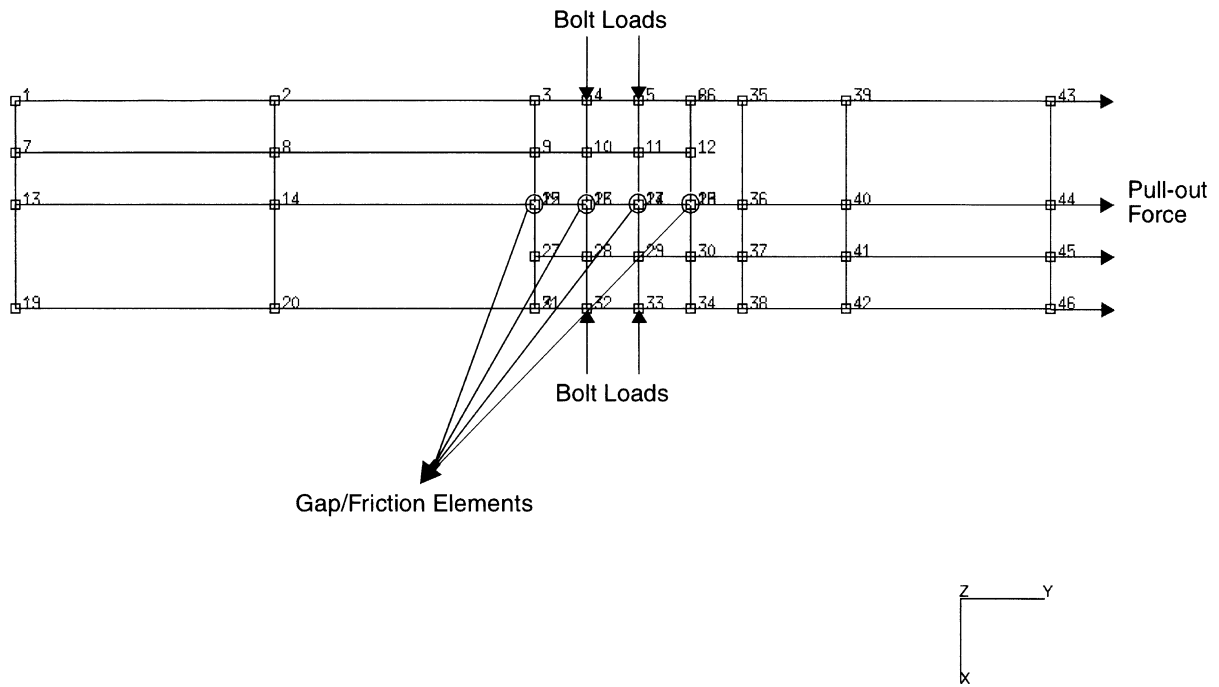


Figure 7.2-1 Geometry and Mesh of End Plate-Aperture

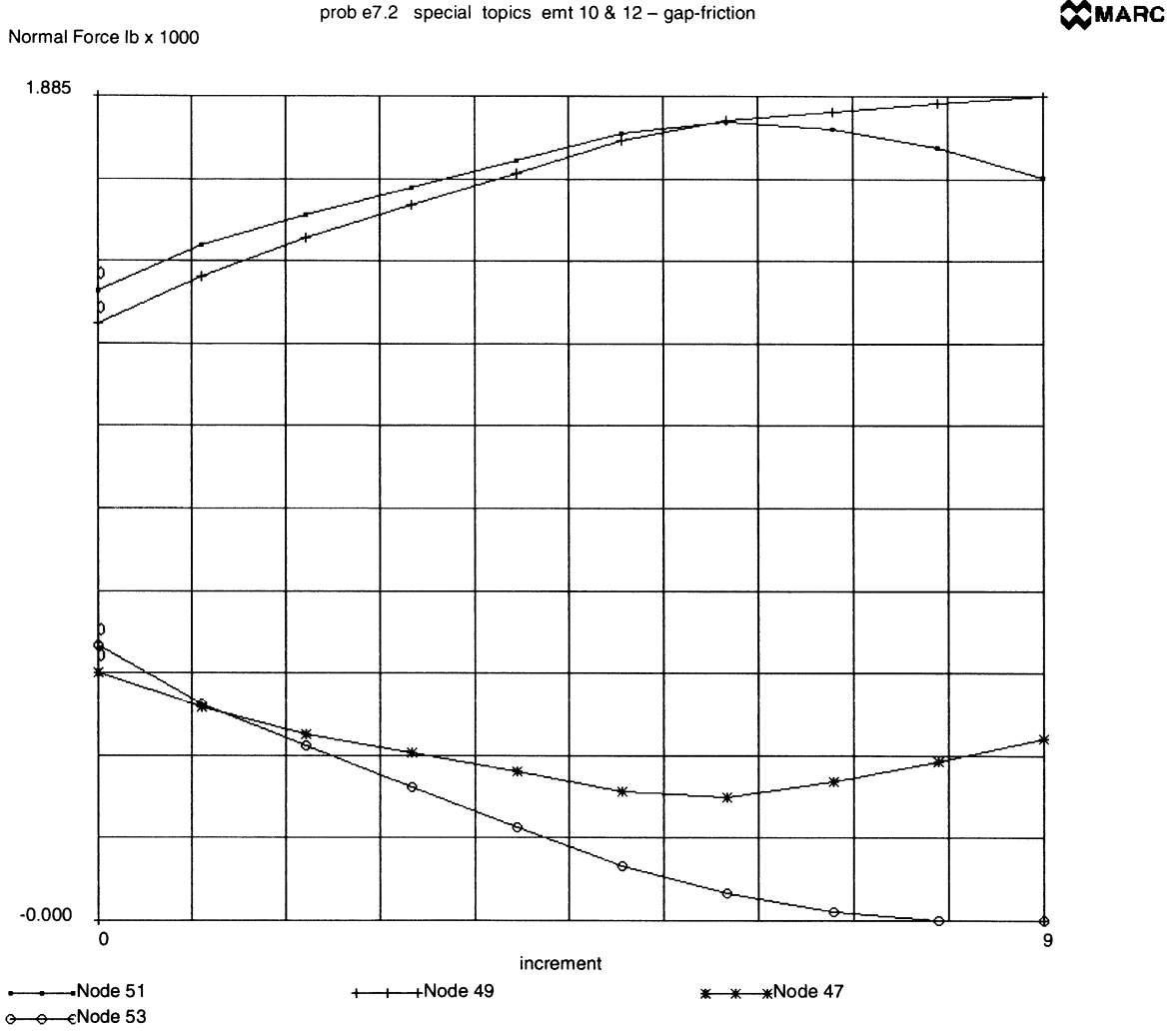


Figure 7.2-2 Transient Normal Forces in Bolts

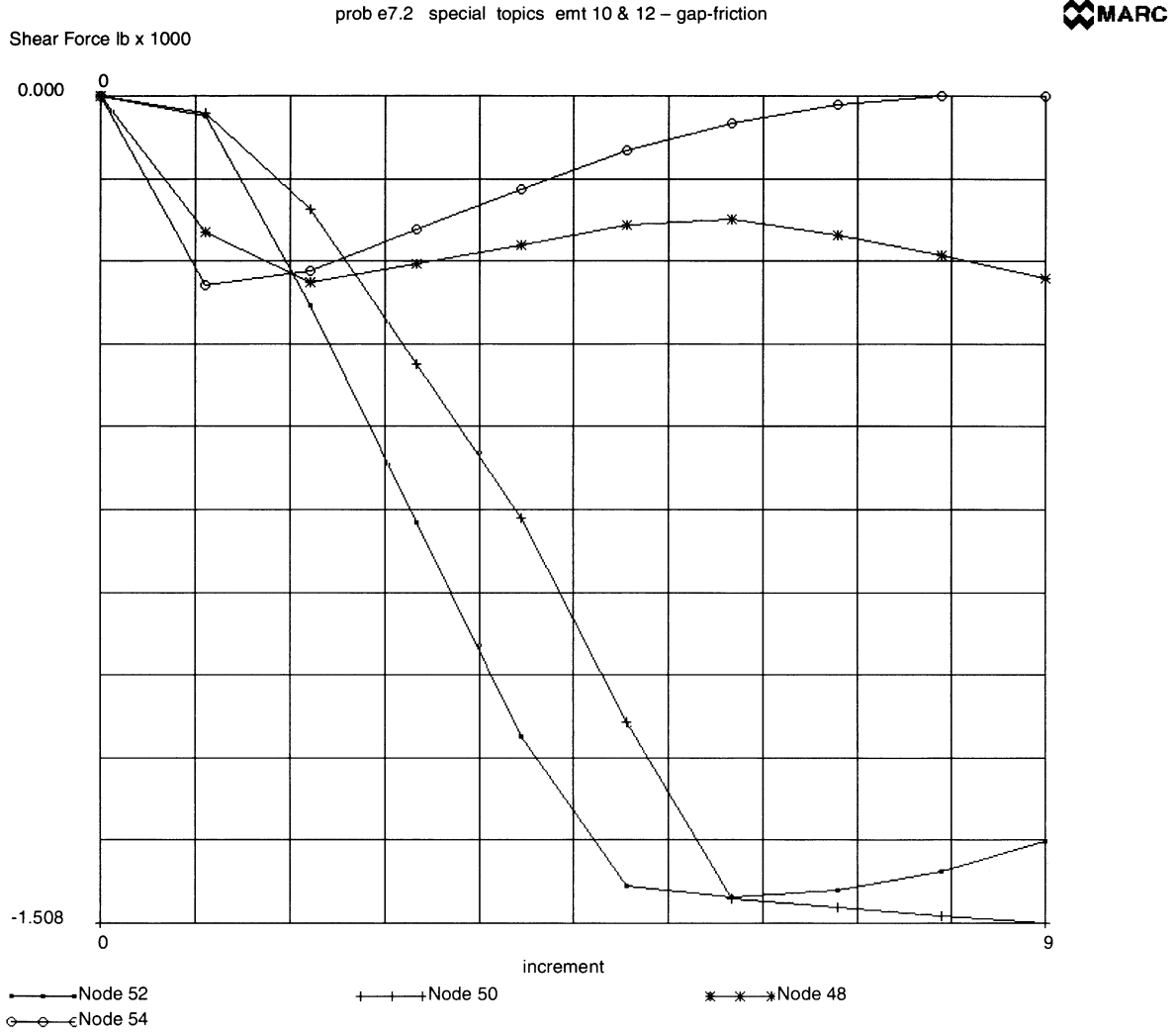


Figure 7.2-3 Transient Shear Force in Bolts

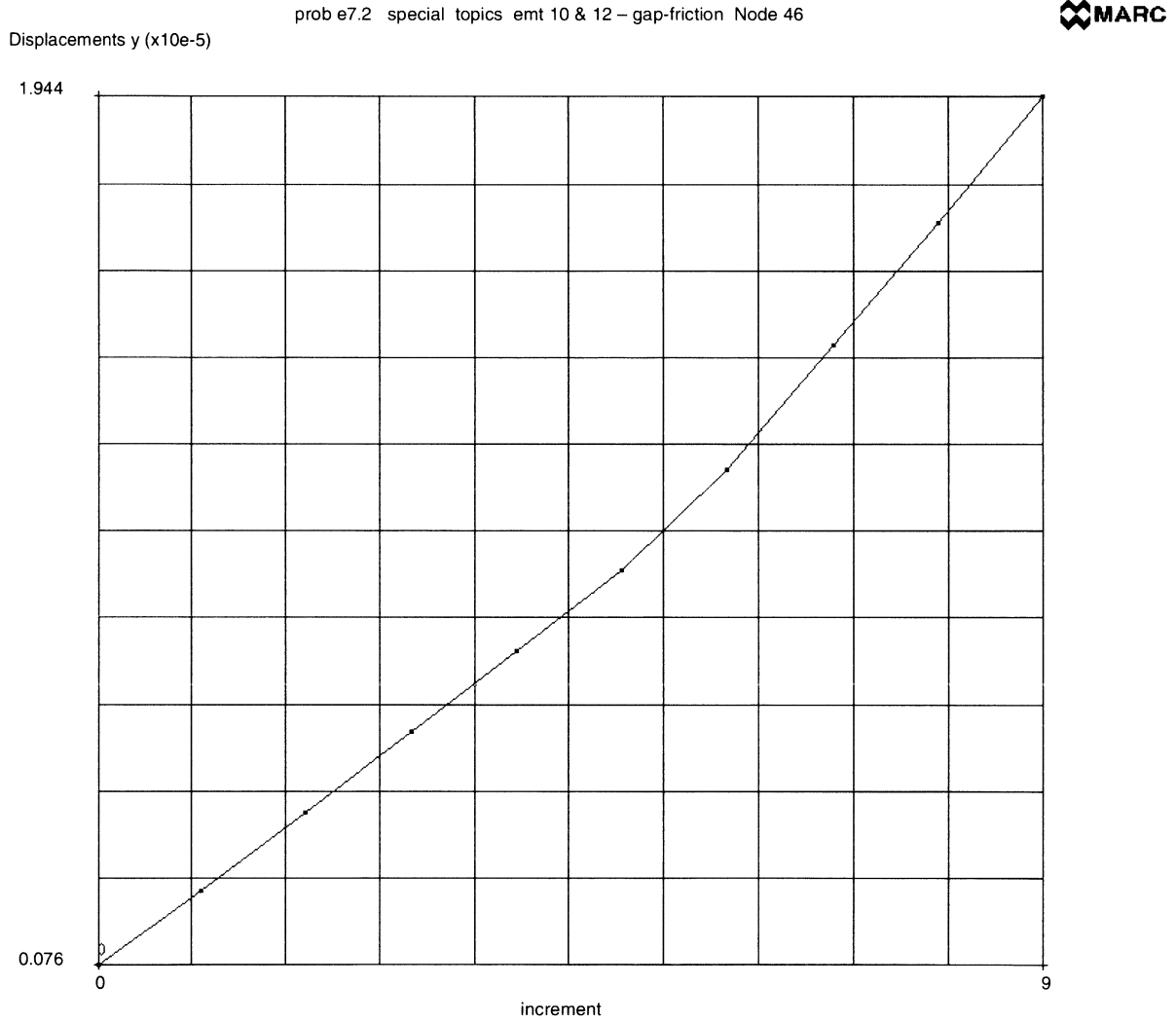


Figure 7.2-4 Radial Displacement at Outside Top (Node 46)

7.3 Barrel Vault Shell under Self-weight (Shell Cracking)

A concrete barrel vault shell is loaded under increasing snow load until cracking is developed. This is the same as problem 3.23 with the addition of nonlinear behavior.

This problem is modeled using the two techniques summarized below.

Data Set	Element Type(s)	Number of Elements	Number of Nodes	Differentiating Features
e7x3	75	36	49	AUTO INCREMENT
e7x3b	75	36	49	AUTO STEP

Element

Element type 75 is a 4 node thick shell element. The cylinder has a half length of 100 inches and a constant thickness of 3 inches. The radius is 300 inches.

Model

Thirty-six elements are used to model one-quarter of the shell taking advantage of symmetry. The model has 49 nodes. The mesh is shown in Figure 7.3-1. Subroutine UFXORD is used to generate the full set of coordinates.

Material Properties

The Young's modulus is 3×10^6 psi, the ultimate compressive strain is 0.002 in/inch. Failure in tension is assumed to occur at 1000 psi. The material is given a strain softening modulus of 3×10^5 psi. A shear retention coefficient of 0.5 is used for the concrete. The ISOTROPIC option is used to indicate that cracking is to be used.

Loading

In e7x3.dat, a total load of 2.0 psi is applied using the AUTO INCREMENT option. The load in the first increment is 10% of the total load.

In the second analysis, the total load of 2.0 psi is applied using the AUTO STEP procedure. The loading criteria is, based upon a maximum change in displacement of 0.5 inch and a maximum change in stress of 200 psi per increment.

Boundary Conditions

The ends of the structure are supported by diaphragms. There are two free edges.

Results

The first cracks occur at the bottom layers of element numbers 24 and 36 during increment 5. Subsequent loading results in formation of new cracks. Increasing loads propagate the cracks through the thickness of the shell.

The load deflection results for the midpoint of the edge of the shell (node 3), as shown in Figure 7.3-2. The effect of cracking is highly pronounced. This results in significant nonlinearity and leads to a reduction in the effective stiffness of the structure. The concrete's failure in tension dominates the response of this structure. In addition, a few points also fail due to crushing.

A rather large tolerance was necessary to obtain convergence in this analysis. This is not unusual for problems involving cracking.

Parameters, Options, and Subroutines Summary

Example e7x3.dat:

Parameters	Model Definition Options	History Definition Options
ELEMENT	CONNECTIVITY	AUTO INCREMENT
END	CONTROL	CONTINUE
SHELL SECT	COORDINATE	DIST LOADS
SIZING	CRACK DATA	
TITLE	DIST LOADS	
	END OPTION	
	FIXED DISP	
	GEOMETRY	
	ISOTROPIC	
	POST	
	PRINT CHOICE	
	RESTART	
	UFXORD	

Example e7x3b.dat:

Parameters

ELEMENT
END
SHELL SECT
SIZING
TITLE

Model Definition Options

CONNECTIVITY
CONTROL
COORDINATE
CRACK DATA
DIST LOADS
END OPTION
FIXED DISP
GEOMETRY
ISOTROPIC
POST
PRINT CHOICE
RESTART
UFXORD

History Definition Options

AUTO STEP
CONTINUE
DIST LOADS

User subroutine in u7x3.f:

UFXORD

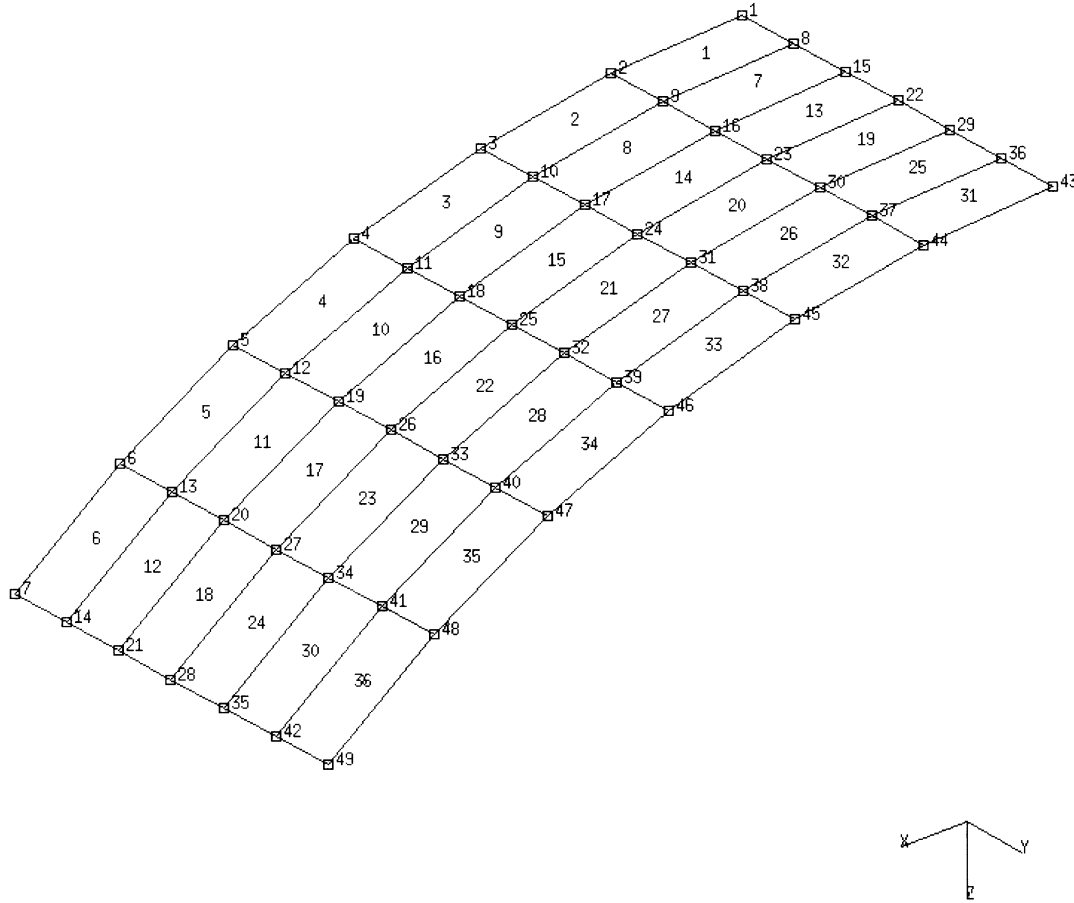


Figure 7.3-1 Mesh for the Shell Roof

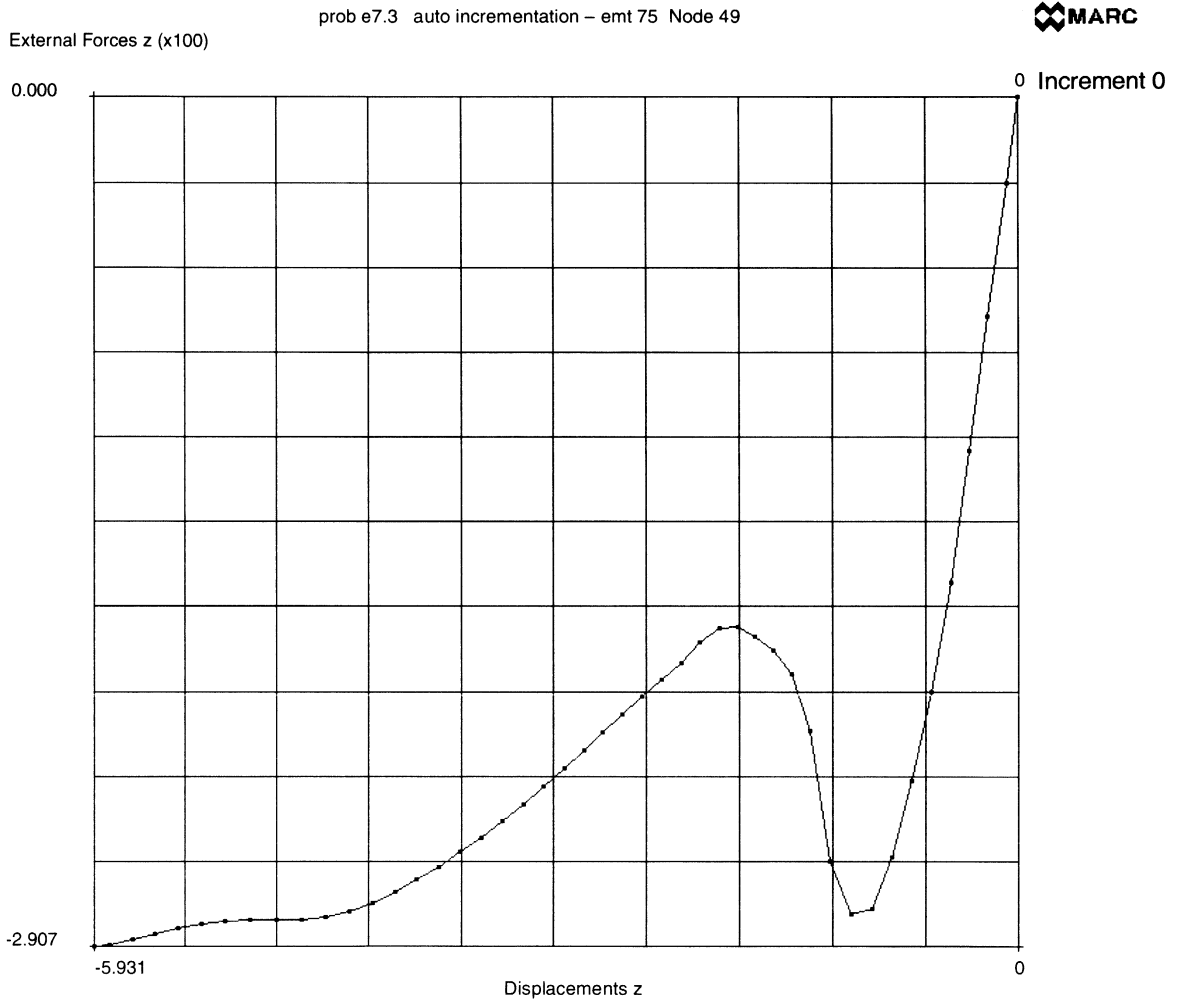


Figure 7.3-2 Load-Vertical Deflection Curve at Node 3

7.4 Side Pressing of a Hollow Rubber Cylinder (Mooney Material)

The behavior of a thick hollow rubber cylinder, compressed between two rigid plates, is analyzed. The cylinder is long; hence, a condition of plane strain in the cross section will be assumed. For reasons of symmetry, only one-quarter of the cylinder needs to be modeled. No friction will be assumed between cylinder and plates. A MOONEY material behavior is used to represent the rubber. The LARGE DISPLACEMENT option is used.

This problem is modeled using the two techniques summarized below.

Data Set	Element Type(s)	Number of Elements	Number of Nodes	Differentiating Features
e7x4	32 & 12	19	53	AUTO LOAD
e7x4b	32 & 12	19	53	AUTO STEP

Element

The quarter cylinder is modeled by using 8-node hybrid plane strain elements (MARC element type 32). This element can be used in conjunction with Mooney material. The corner nodes have an additional degree of freedom to represent the hydrostatic pressure. Seven gap elements are used to model the potential contact.

Model

The outer radius of the cylinder is 3 mm and the inner radius of the cylinder is 2 mm. Twelve elements are used for the cylinder, with two elements specified over the thickness. The geometry of the cylinder and the mesh are shown in Figure 7.4-1.

MOONEY

The MOONEY option is used to specify the rubber properties. The rubber material can be modeled as a Mooney-Rivlin material with $C_{10} = 8 \text{ N/mm}^2$, $C_{01} = 2 \text{ N/mm}^2$.

GAP DATA

The gap closure distance is defined as the initial nodal distance between the cylinder and the plate and is entered via the GAP DATA option.

Loading

In the first analysis, the AUTO LOAD option is used to apply five displacement increments to the plate. The increment is equal to the one applied in increment 0. After load application, one iteration is carried out by using PROPORTIONAL INCREMENT option with zero load increment to insure that the solution is in equilibrium. This is not necessary if the tolerance specified on the CONTROL option is sufficiently small.

In the second analysis, a total displacement of 1 inch is applied using AUTO STEP. The load is controlled by requiring that the incremental strain be less than 10% per increment.

Connectivity

The CONNECTIVITY option is used twice. It is used the first time to read the data of the mesh of the cylinder. The option is then used again to read gap data.

Tying

TYING establishes the connections between the nodal degrees of freedom of the cylinder and that of the gaps. This is necessary because the degrees of freedom of these two elements are not the same.

Results

The cylinder outer diameter is reduced from 6 inches to 4 inches in five increments. The cylinder is in contact with the plate at four nodes (four gaps have been closed). The incremental displacements become very small and equilibrium is satisfied with high accuracy. The incremental full Newton-Raphson method was used to solve the nonlinear system. The total force on the plate may either be calculated by summing up the gap forces, or directly obtained from the reaction force on node 75. For both the data sets, this leads to a total force $F = 1.91$ N. A plot of the deformed cylinder is shown in Figure 7.4-2.



Parameters, Options, and Subroutines Summary

Example e7x4.dat:

Parameters

ELEMENT
END
LARGE DISP
SIZING
TITLE

Model Definition Options

CONNECTIVITY
CONTROL
COORDINATE
END OPTION
FIXED DISP
GAP DATA
MOONEY
RESTART
TYING

History Definition Options

AUTO LOAD
CONTINUE
PROPORTIONAL INCREMENT

Example e7x4b.dat:

Parameters

ELEMENT
END
LARGE DISP
SIZING
TITLE

Model Definition Options

CONNECTIVITY
CONTROL
COORDINATE
END OPTION
FIXED DISP
GAP DATA
MOONEY
RESTART
TYING

History Definition Options

AUTO STEP
CONTINUE
PROPORTIONAL INCREMENT

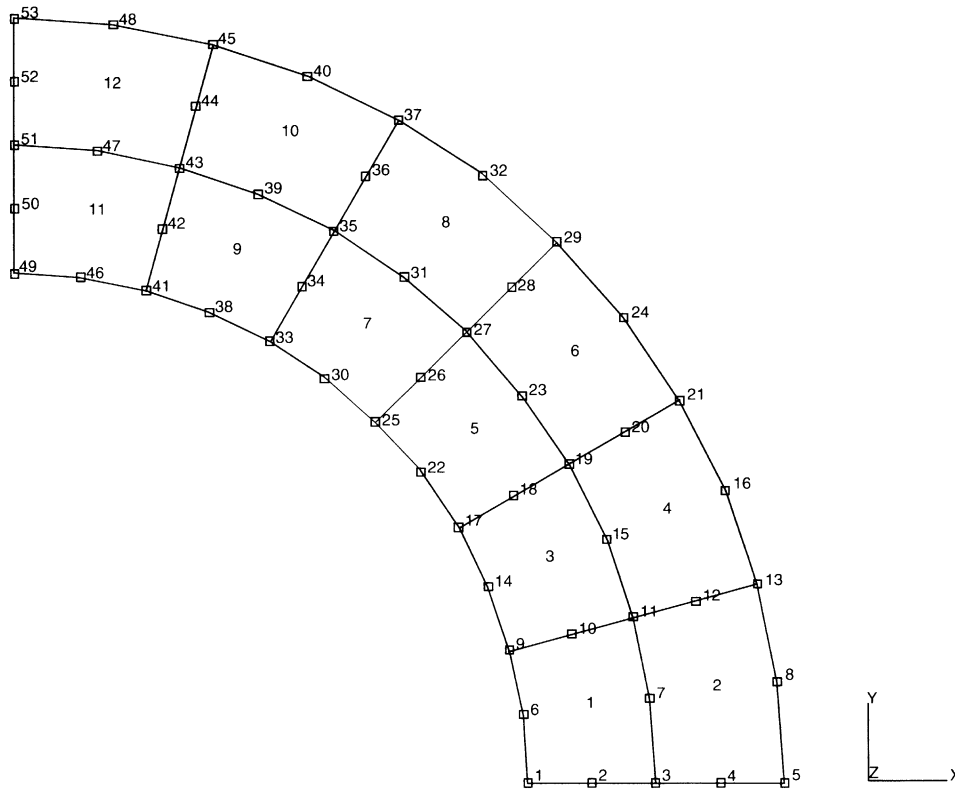
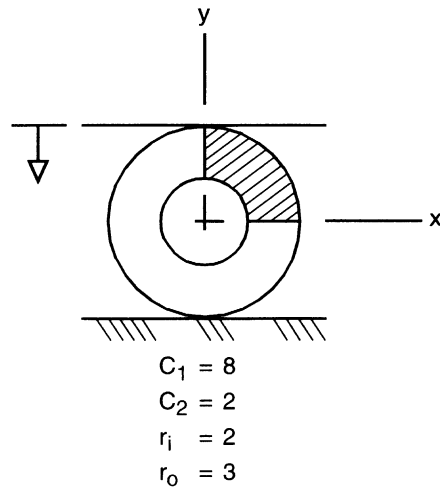
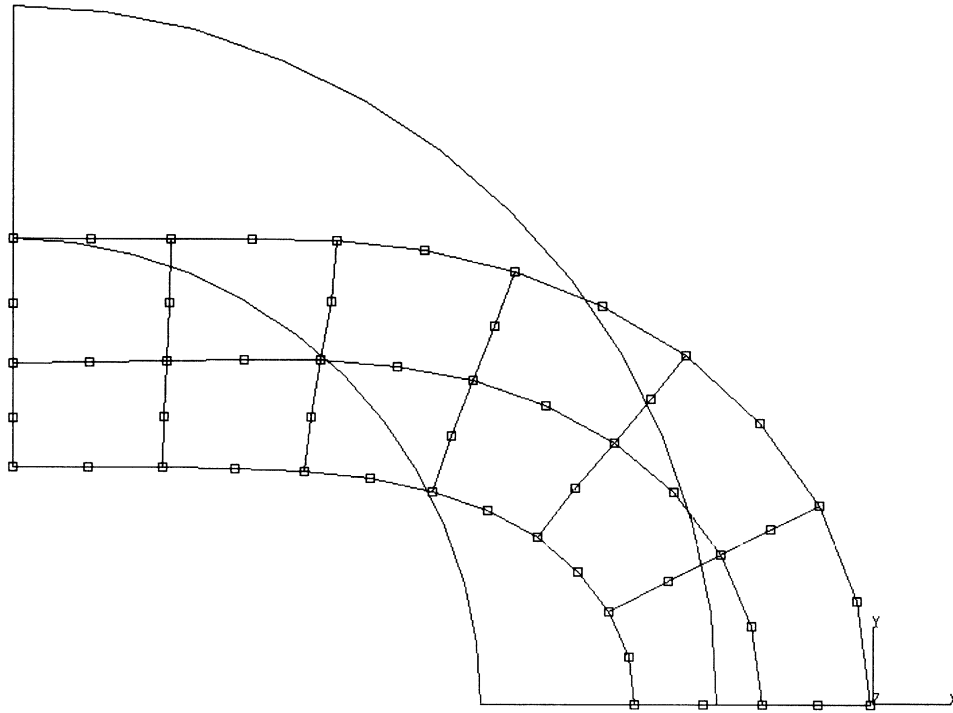


Figure 7.4-1 Rubber Cylinder and Mesh

INC : 6
SUB : 0
TIME : 0.000e+00
FREQ : 0.000e+00



prob e7.4 special topics emt 32 & 12 – mooney
Displacements x

Figure 7.4-2 Deformed Mesh Plot



7 Contact

Side Pressing of a Hollow Rubber Cylinder (Mooney Material)

7.5 Analysis of a Thick Rubber Cylinder under Internal Pressure

This problem illustrates the use of MARC elements types 33, 82, and 120 (8- and 4-node incompressible, axisymmetric elements) and options, LARGE DISP, FOLLOW FOR, and MOONEY for an elastic, large strain analysis of a rubber cylinder subjected to a uniformly distributed internal pressure. The pressure load is applied in a single step, and the Newton-Raphson iteration procedure is used to obtain an equilibrium state.

This problem is modeled using the three techniques summarized below.

Data Set	Element Type(s)	Number of Elements	Number of Nodes
e7x5	33	4	23
e7x5b	82	4	14
e7x5c	119	4	14

Model

The dimensions of the rubber cylinder and finite element meshes are shown in Figure 7.5-1. The 8-node model consists of four elements of type 33 and 23 nodes, and the 4-node model consists of four elements of type 82 or type 120, and 14 nodes.

Material Properties

The material of the rubber cylinder is assumed to be MOONEY material with material constants:

$$C_{10} = 8 \text{ N/mm}^2$$

$$C_{01} = 2 \text{ N/mm}^2$$

Loading

Uniformly distributed internal pressure = 11.5 N/mm^2 is applied on element number 1. This load is applied in increment zero. In MARC, increment 0 is treated as linear so an additional increment, with no additional load, is used to bring the solution to the correct nonlinear state.

Boundary Conditions

$u = 0$ on the planes $z = 0$ and $z = 1.0$ to simulate a plane strain condition.

Note

LARGE DISP is included to obtain the geometric nonlinear effects; the full Newton-Raphson technique is used.

FOLLOW FOR indicates that pressures will be applied on the current geometry of the cylinder. CONTROL block is used to specify the number of increments in the analysis. In this analysis, two increments are specified with a maximum of 15 Newton-Raphson iterations to obtain equilibrium.

Newton-Raphson iterations are obtained with PROPORTIONAL INCREMENT. This indicates that the previous load increment has to be multiplied by a certain user specified factor and has to be added to the current loads. The loads can be pressures, nodal loads, or nonzero kinematic boundary conditions. If the multiplication factor is set to be zero (0), then no load is added. Iterations are performed until the maximum residual force is less than 10% of the maximum reaction force.

Results

A. 8-Node Model (Element Type 33)

After the linear elastic step (increment 0), the radial displacements of the inside nodes (nodes 1, 10 and 15) are:

Node	Radial Displacement (mm) (MARC)
1	0.38351
10	0.38351
15	0.38350

They are in good agreement with analytical solution which predicts a radial displacement of 0.38333.

After ten iterations, the radial displacement at the inside node is 1.0026, and the corresponding pressure can be computed from the following expression:

$$P = (C_1 + C_2) \left[\log \left(\frac{B^2 a^2}{A^2 (B^2 - A^2 + a^2)} \right) + \frac{(a^2 - A^2)(B^2 - A^2)}{a^2 (B^2 - A^2 + a^2)} \right]$$

where A and B are the inner and outer radius of the cylinder in the undeformed state, and “a” is the inner radius in the deformed state, and C₁ and C₂ are material constants.

The computed pressure (11.49) is in very good agreement with the prescribed value of 11.5.

**B. 4-Node Model (Element Type 82, 120)**

After the linear elastic step (increment 0), the radial displacements of the inside nodes (nodes 1 and 6) are:

Node	Radial Displacement (MARC) type 82	Radial Displacement (MARC) type 120
1	0.38174	0.38335
6	0.38174	0.38335

Agreement with analytical solution of 0.38333 is good. After ten iterations, the radial displacement at inside node is 1.0061, and the corresponding pressure is 10.35 for element 82. For element 120, the displacement at the inside node is 1.0063 and the corresponding pressure is 11.5. Agreement with prescribed value or 11.5 is excellent.

Parameters, Options, and Subroutines Summary

Example e7x5.dat:

Parameters	Model Definition Options	History Definition Options
ELEMENT	CONNECTIVITY	CONTINUE
END	CONTROL	CONTROL
FOLLOW FORCE	COORDINATE	DIST LOADS
LARGE DISP	DIST LOADS	
SIZING	END OPTION	
TITLE	FIXED DISP	
	MOONEY	
	NODE FILL	
	POST	

Example e7x5b.dat or e7x5c.dat:

Parameters	Model Definition Options	History Definition Options
ELEMENT	CONNECTIVITY	CONTINUE
END	CONTROL	CONTROL
FOLLOW FORCE	COORDINATE	DIST LOADS
LARGE DISP	DIST LOADS	
SIZING	END OPTION	
TITLE	FIXED DISP	
	MOONEY	
	POST	

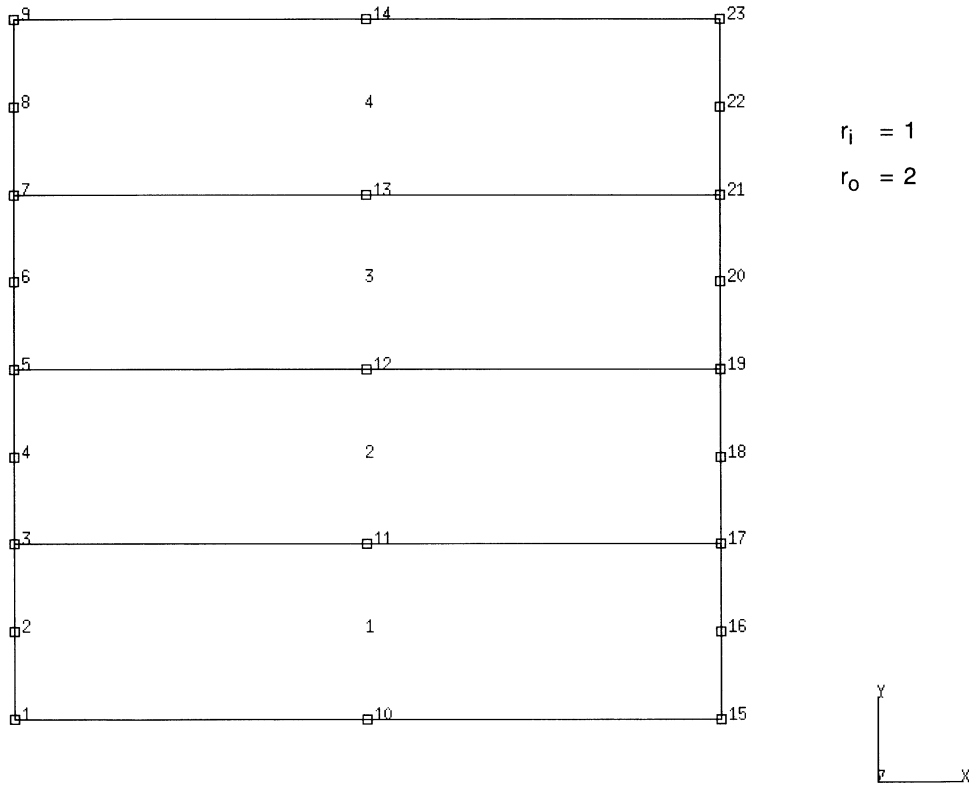


Figure 7.5-1 Cylinder Mesh (8-Node Model)

INC : 0
SUB : 0
TIME : 0.000e+00
FREQ: 0.000e+00

prob e7.5 special topics emt 33 – mooney



2nd comp of cauchy stres (x10)

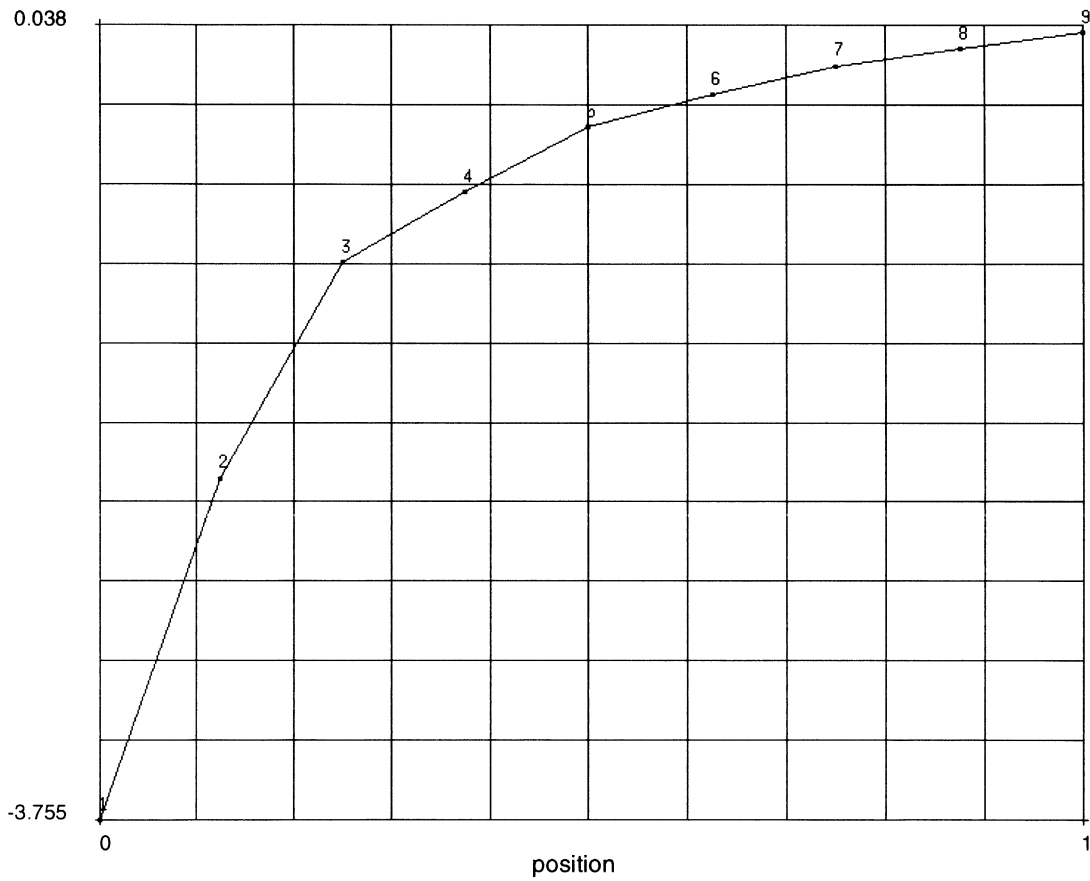


Figure 7.5-2 Radial Stress Through Radius



7 Contact

Analysis of a Thick Rubber Cylinder under Internal Pressure

7.6 Biaxial Stress in a Composite Plate

This problem illustrates the analysis of a plate made of layered composite material as shown in Figure 7.6-1. A biaxial stress field is applied and the results are compared with a textbook solution (Reference 1).

This problem is modeled using the two techniques summarized below.

Data Set	Element Type(s)	Number of Elements	Number of Nodes	Differentiating Features
e7x6	75	20	25	User subroutine ANISOTROPIC
e7x6b	75	20	25	

Element

Shell element 75 is used to model the plate. It is a four-node bilinear thick shell element capable of modeling the behavior of layered composite materials.

Model

A 4 x 4 mesh of shells is used for a total of 16 elements, 25 nodes, and 150 degrees of freedom. (See Figure 7.6-2.)

Material Properties

The plate consists of three layers of an orthotropic material. The top layer is 3 mm thick and is offset 45° from the middle layer. The middle layer is 4 mm thick. The bottom layer is also 3 mm thick and is offset 45° from the middle layer. This data is entered in the COMPOSITE option.

The orthotropic material properties are first entered in the ORTHOTROPIC option. The data entered here are the engineering constants E_{11} , E_{22} , E_{33} , ν_{12} , ν_{23} , ν_{31} , G_{12} , G_{22} , and G_{33} with respect to the three planes of elastic symmetry. In problem e7x6b, the anisotropic stress-strain law is entered directly through the ANISOTROPIC option. When entering the data using the ANISOTROPIC option, you must specify the values (21 values) in the symmetric triangle for a compressed form 6x6 matrix. The ply angle for the various layers is given in the COMPOSITE option.

Element type 75 has only two direct strains. Using the PRINT,11 option, you would observe the following printout:

```
layer stress-strain law in layer coords for elem 5.
```

Column \ Row	1	2	3	4	5
1	.200456E11	.70159E9	0	0	0
2	.70159E9	.200456E11	0	0	0
3	0	0	.7E9	0	0
4	0	0	0	.7E9	0
5	0	0	0	0	.7E9

The input required when using the ANISOTROPIC option is:

Column \ Row	1	2	3	4	5	6
1	.200456E11	.70159E9	0	0	0	0
2	.70159E9	.200456E11	0	0	0	0
3	0	0	.7E9	0	0	0
4	0	0	0	.7E9	0	0
5	0	0	0	0	.7E9	0
6	0	0	0	0	0	0

Loading

The biaxial stresses applied to the plate are $\sigma_x = 1. \times 10^6 \text{ N/m}^2$, $\sigma_y = 2. \times 10^5 \text{ N/m}^2$ and $\tau_{xy} = 0$. These distributed loads are specified in the DIST LOADS option (the units in this problem are m-kg-s). The applied load magnitudes are negative so that the applied loading is directed out of the element.

Boundary Conditions

In order to fully restrain the rigid body modes without introducing any elastic constraints, a special set of boundary conditions is used. Degrees of freedom 1 to 5 are suppressed at node 1 and degree of freedom 1 is suppressed along the entire left-hand edge. Since the layup is symmetric, only in-plane deformations are expected. The specification of additional rotational constraints at the left-hand edge is irrelevant.

Print Control

The use of the suboption PREF under PRINT ELEM allows you to obtain printout of the layer stresses in the preferred (ply) coordinate system. The generalized shell resultant quantities are always expressed in the local shell \tilde{v}^1, \tilde{v}^2 system. Here, these coordinates are parallel to global x and y, respectively.

Results

Results for this problem are given on page 169 in the reference below. They are summarized below:

		Reference	MARC
ϵ_x^o		.00685	.006875
ϵ_y^o		.00332	.003324
ϵ_{xy}^o		-.00784	-.007845
Layers 1,3 $\times 10^6\text{N/m}^2$	σ_1	29.6	29.85
	σ_2	18.8	18.87
	σ_{12}	-2.5	-2.49
Layer 2 $\times 10^6\text{N/m}^2$	σ_1	139.3	139.8
	σ_2	11.4	11.46
	σ_{12}	-5.5	-5.49

Figure 7.6-3 shows the deformed shape of the structure. The displacements are all planar, and there is no coupling between bending and axial extension due to the symmetry of the layup. There is, however, coupling between axial extension and in-plane shear. The results are identical, independent of the way the material is input.

Reference

Agarwal, B.D., Broutman, L., *Analysis and Performance of Fiber Composites*, Wiley, 1980.

Parameters, Options, and Subroutines Summary

Example e7x6.dat:

Parameters	Model Definition Options
ELEMENT	COMPOSITE
END	CONNECTIVITY
SHELL SECT	COORDINATE
SIZING	DEFINE
TITLE	DIST LOADS
	END OPTION
	FIXED DISP
	ORIENTATION
	ORTHOTROPIC
	POST
	PRINT ELEM

Example e7x6b.dat:

Parameters	Model Definition Options
ELEMENT	ANISOTROPIC
END	COMPOSITE
SHELL SECT	COORDINATE
SIZING	DEFINE
TITLE	DIST LOADS
	END OPTION
	FIXED DISP
	ORIENTATION
	POST
	PRINT ELEM

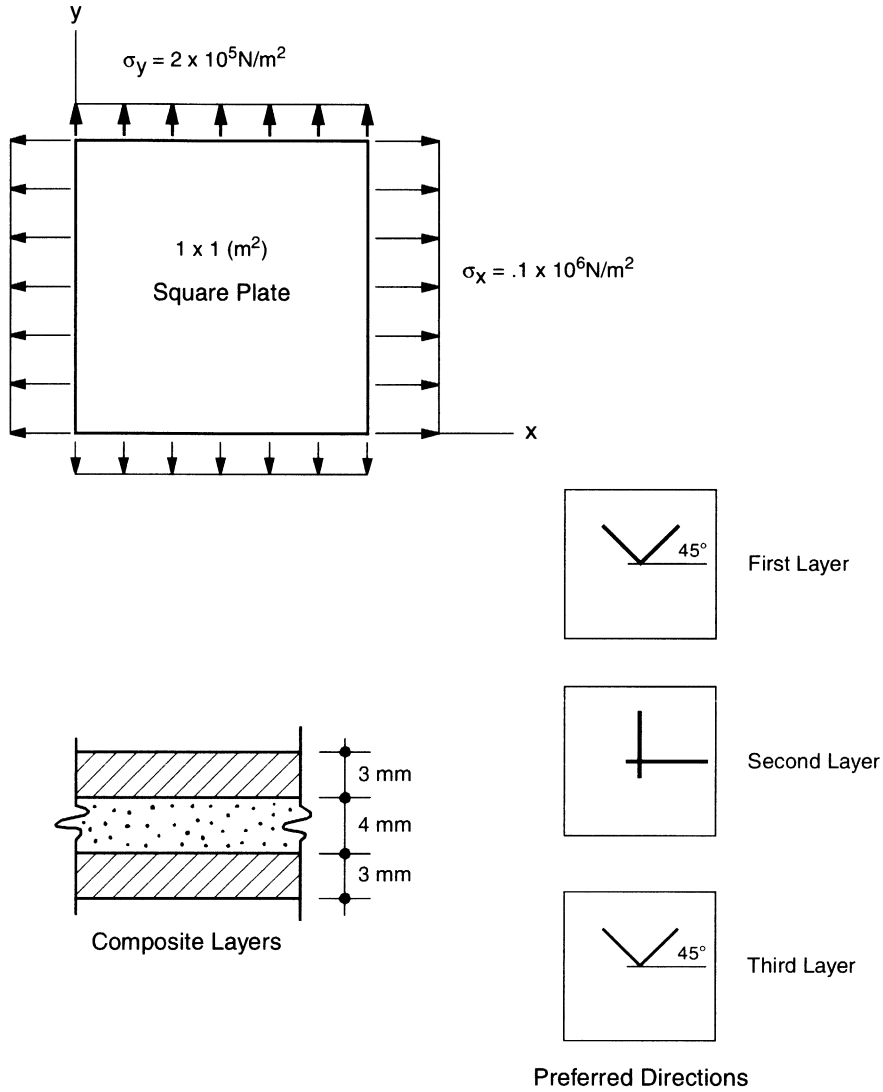


Figure 7.6-1 Composite Plate

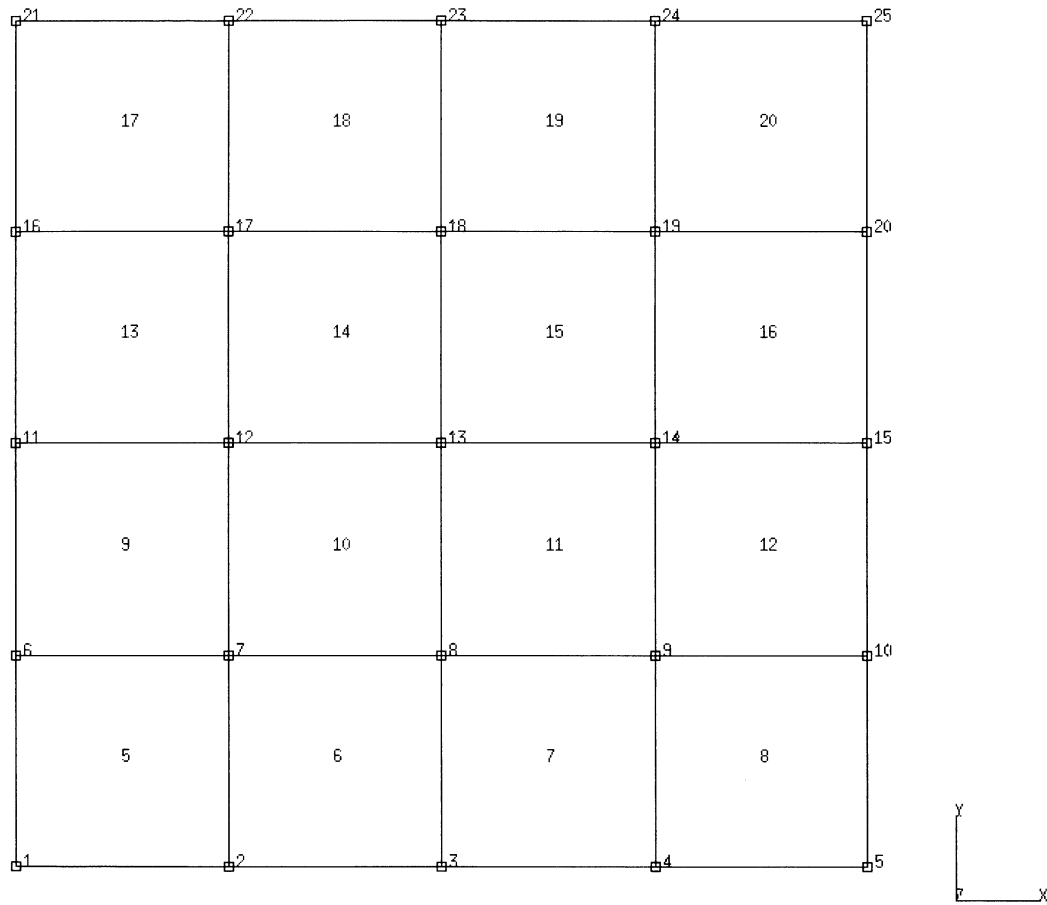
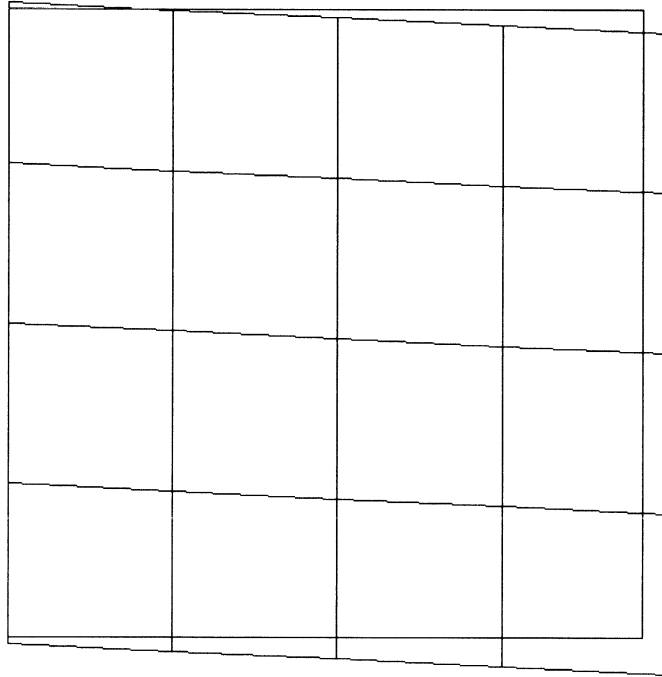


Figure 7.6-2 Finite Element Mesh

INC : 0
SUB : 0
TIME : 0.000e+00
FREQ : 0.000e+00



prob e7.6 special topics – elmt 75
Displacements x

Figure 7.6-3 Deformed Mesh Plot

7.7 Composite Plate Subjected to Thermal Load

A composite plate is subjected to a uniform thermal load.

Element

Element 75, the four-node bilinear thick shell element, is used. In this analysis, three layers will be used through the thickness.

Model

The square plate of 1 inch length has been divided into 16 elements with 25 nodes as shown in Figure 7.7-1. To demonstrate that the element numbers do not need to begin with 1, they are given id's of 5 to 20.

Geometry

No geometry specification is used. The plate thickness on a layer-by-layer basis is specified with the COMPOSITE option. Then the thickness of layers 1 to 3 are 0.003, 0.0025, 0.0025 respectively, giving a total thickness of 0.008 inch.

Loading

The initial temperature for all the layers is 125°F, and the plate is cooled to 25°F in increment 0. All elements, integration points and layers are given the same temperature. The INITIAL STATE and CHANGE STATE options are used to define this data.

Boundary Conditions

The edge $x = 0$, with nodes 1, 6, 11, 16, 21 are prescribed to have no x -displacement. Additionally, node 11 is constrained such that $u_y = u_z = \phi_x = \phi_y = 0$. This eliminates any rigid body motion. Note that if the material was isotropic, there would be free thermal expansion given these boundary conditions, and the stresses would be zero.

Material Properties

The plate is made of a single orthotropic material which is oriented differently between layers 1 and 2 and 3. First the ORTHOTROPIC option is used to define the material properties:

WWW

$$\begin{array}{llll}
 E_{11} = 19.8 \times 10^9 & \nu_{12} = .35 & G_{12} = 70 \times 10^7 & \alpha_{11} = .7 \times 10^{-5} \text{ in/in}^\circ\text{F} \\
 E_{22} = 19.8 \times 10^8 & \nu_{23} = 0.0 & G_{13} = 70 \times 10^7 & \alpha_{22} = .23 \times 10^{-5} \text{ in/in}^\circ\text{F} \\
 E_{33} = 0 & \nu_{31} = 0.0 & G_{31} = 70 \times 10^7 & \alpha_{33} = 0.0
 \end{array}$$

As element 75 has only two direct components of stress ($NDI = 2$), it is not necessary to define E_{33} and α_{33} . Since the element has three components of shear (in-plane and transverse), all values of G were entered. As $\nu_{23} = \nu_{31} = 0$, this is an odd material.

The base material orientation is given in the ORIENTATION block as being at 0° with respect to the 1-2 edge which will place it along the x-axis. The actual orientation is given in the COMPOSITE option as ply angles with respect to this base orientation.

The COMPOSITE option is used to define three layers, each of the same material but with thickness of 0.003, 0.0025 and 0.0025 inch. The stacking sequence is +45./0./0.

There are no temperature dependent effects in this example. If necessary, the ORTHO TEMP option would be used to enter this data.

Controls

The PRINT ELEM option is used to request that the stresses are output in both the conventional elements system and the local preferred system.

Results

The results indicate that the non-isotropic nature of the composite plate results in a generation of out-of-plane displacements as large as 0.05 inch and equivalent stresses as high as 1×10^6 psi.

Parameters, Options, and Subroutines Summary

Example e7x7.dat:

Parameters	Model Definition Options
ELEMENT	CHANGE STATE
END	COMPOSITE
SHELL SECT	CONNECTIVITY
SIZING	COORDINATE
TITLE	DEFINE
	END OPTION
	FIXED DISP
	INITIAL STATE
	ORIENTATION
	ORTHOTROPIC
	POST
	PRINT ELEM

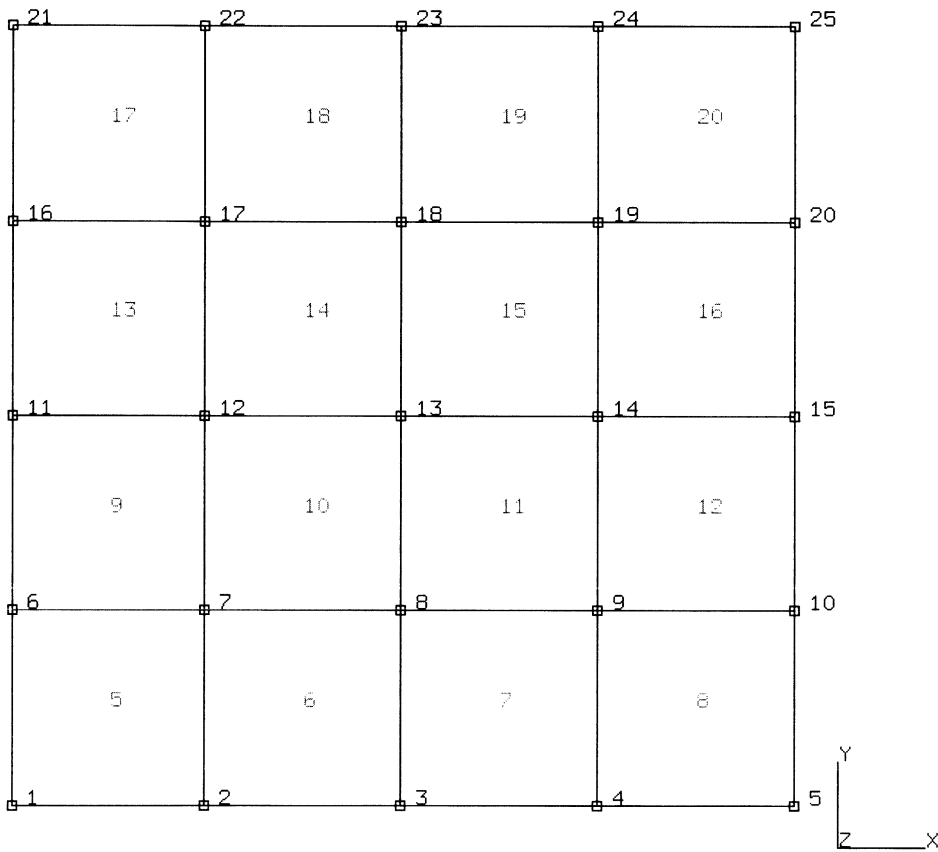
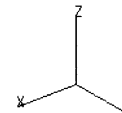
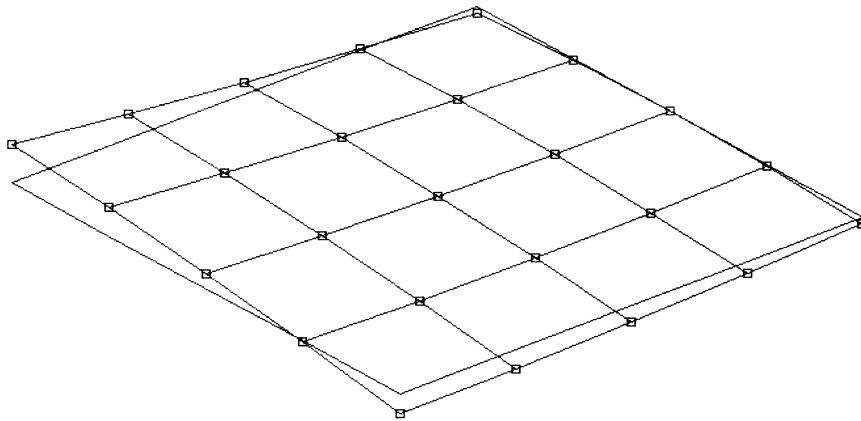


Figure 7.7-1 Plate Geometry and Mesh

INC : 0
SUB : 0
TIME : 0.000e+00
FREQ : 0.000e+00



prob e7.7 special topics – elmt 75
Displacements x

Figure 7.7-2 Displaced Mesh

7.8 Cylinder under External Pressure (Fourier Analysis)

A solid cylinder in plane strain with radius (a) and external pressure (p_o) is elastically analyzed. Love [1] gives the solutions to the first and second modes of this problem as follows:

$$\sigma_{rr} = p_o r \cos\theta$$

$$\sigma_{\theta\theta} = 3p_o r \cos\theta$$

$$\sigma_{r\theta} = p_o r \sin\theta$$

for the first mode, and

$$\sigma_{rr} = p_o \cos 2\theta$$

$$\sigma_{\theta\theta} = p_o \left(\frac{2r^2 - a^2}{a^2} \right) \cos 2\theta$$

$$\sigma_{r\theta} = p_o \left(\frac{r^2 - a^2}{a^2} \right) \sin 2\theta$$

for the second mode. It should be noted that for the first mode, the condition $\sigma_{rr}(a) = p_o \cos\theta$ requires that $\sigma_{r\theta}(a) = p_o \sin\theta$, where “ a ” is 1 inch. Two Fourier series are used for expansion of the 100 psi pressure loading. One series is for the cosine terms and the other for the sine terms. Three different methods, as shown in Problems e7-8a, e7.8b and e7.8c are demonstrated in describing the series. Comparison of the results with Love’s [1] exact solution is presented.

This problem is modeled using the three techniques summarized below.

Data Set	Element Type(s)	Number of Elements	Number of Nodes	Differentiating Features
e7x8a	62	10	53	Fourier coefficients input
e7x8b	62	10	53	Define nonsymmetric
e7x8c	52	10	53	User subroutine UFOUR

Element

Element type 62, the axisymmetric quadrilateral element for arbitrary loading, is used here. Details on this element are found in *MARC Volume B: User Input*.

Model

The geometry and mesh used are shown in Figure 7.8-1. The solid cylinder has a height of 0.1 inch and a radius of 1.0 inch. The mesh has 10 elements and 53 nodes.

Geometry

This option is not required for this problem.

Material Properties

The elastic material data assumed for this example is Young's modulus (E) is $30. \times 10^6$ psi and Poisson's ratio (ν) is 0.25.

Loading

The 100 psi external pressure is specified as a distributed load (IBODY=0) and associated with Fourier series number 1. The -100 psi shear is specified as a uniform load in the circumferential direction (IBODY=14) and associated with Fourier series number 2. Only element 10 is specified with the above loads using the DIST LOAD option.

Boundary Conditions

All nodes on the plane $Z = 0.$ and $Z = 0.1$ are constrained in the axial direction such that only radial motion is permitted. Nodes 1, 2, and 3 on the plane $R = 0$ are also constrained in the radial direction due to symmetry.

Fourier

Three different ways are used to describe the series:

1. Specify the first two nonzero terms for series number 1 by evaluating the following integral:

$$a_n = \frac{1}{\pi} \int_0^{2\pi} \begin{pmatrix} \cos \theta \\ \cos 2\theta \end{pmatrix} \cos n\theta \, d\theta = \begin{cases} 0, & \text{all } n \text{ except} \\ 1, & n = 1, \text{ and } 2 \end{cases}$$

and the first nonzero term for series number 2 by evaluating the following integral:

$$b_n = \frac{1}{\pi} \int_0^{2\pi} \sin \theta \sin n\theta \, d\theta = \begin{cases} 0, & \text{all } n \text{ except} \\ 1, & n = 1 \end{cases}$$

2. Describe the function $F(\theta)$ which is to be expanded into a Fourier series by an arbitrary number (say 5) of $[\theta, F(\theta)]$ pairs of data.
3. Use user subroutine UFOUR to generate an arbitrary number of $[\theta, F(\theta)]$ pairs and let MARC calculate the Fourier series coefficients. Five pairs of $[\theta, F(\theta)]$ are defined in this example.



It should be pointed out that five pairs of $[\theta, F(\theta)]$ have been chosen for demonstration only. It is easy to add more by changing the number 5 in the user subroutine UFOUR. An increased number of $[\theta, F(\theta)]$ pairs would yield better results in comparison with the exact coefficient evaluations.

Results

The results for the radial and circumferential stresses of Problem e7.8a and Love's exact solution are plotted in Figure 7.8-2 and Figure 7.8-3. They indicate that the finite element solutions are in good agreement with the exact solutions.

Reference

Love, A.E.H., *A Treatise on the Mathematical Theory of Elasticity*, Dover, New York.

Parameters, Options, and Subroutines Summary

Example e7x8a.dat:

Parameters	Model Definition Options
ELEMENT	CONNECTIVITY
END	CONTROL
FOURIER	COORDINATE
SIZING	DIST LOADS
TITLE	END OPTION
	FIXED DISP
	FOURIER
	ISOTROPIC
	RESTART



Example e7x8b.dat:

Parameters	Model Definition Options
ELEMENT	CONNECTIVITY
END	CONTROL
FOURIER	COORDINATE
SIZING	DIST LOADS
TITLE	END OPTION
	FIXED DISP
	FOURIER
	ISOTROPIC
	RESTART

Example e7x8c.dat:

Parameters	Model Definition Options
ELEMENT	CONNECTIVITY
END	CONTROL
FOURIER	COORDINATE
SIZING	DIST LOADS
TITLE	END OPTION
	FIXED DISP
	FOURIER
	ISOTROPIC
	RESTART

User subroutine in u7x8c.f:

UFOUR

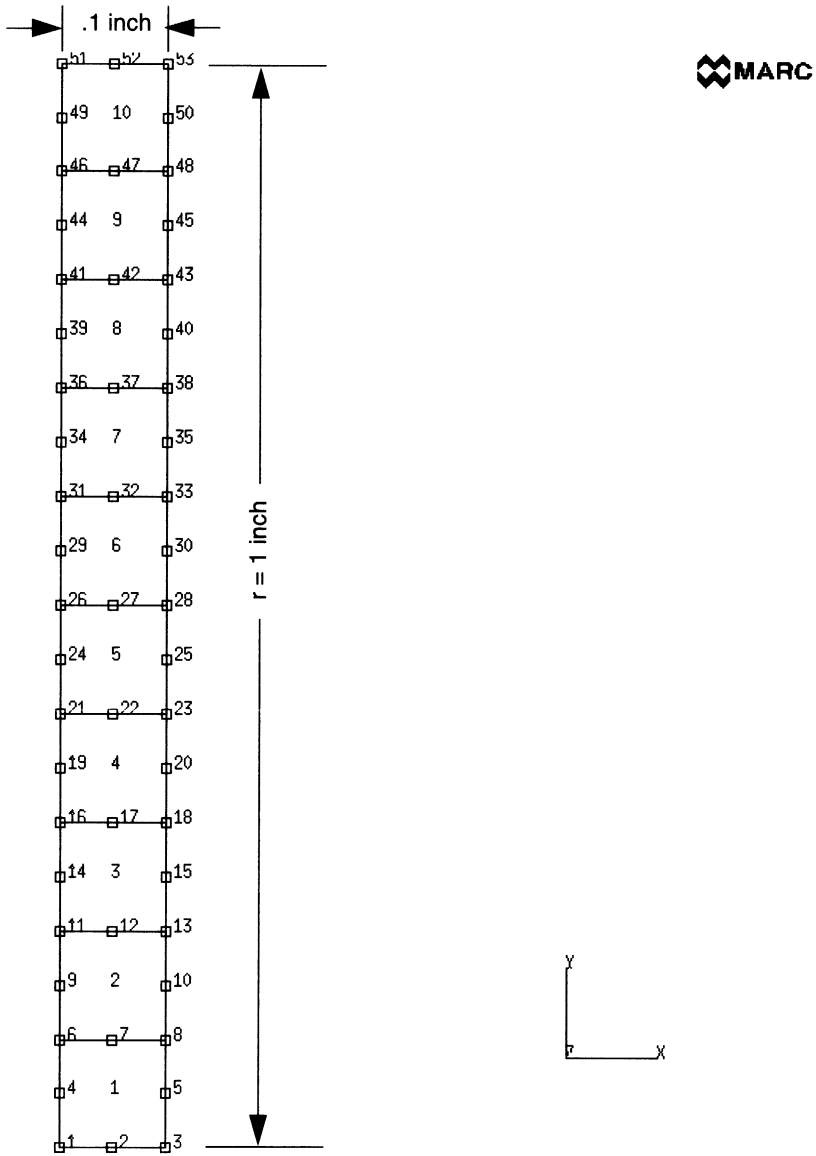


Figure 7.8-1 Cylinder and Mesh

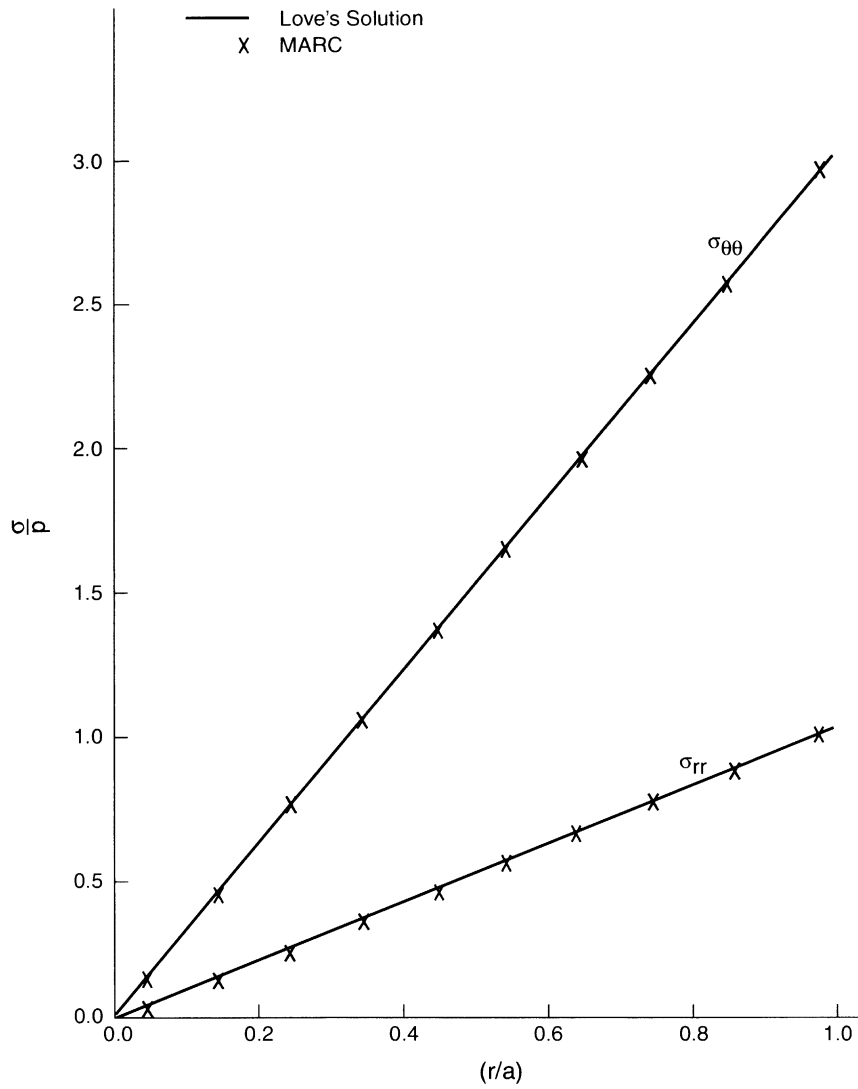


Figure 7.8-2 First Mode Solid Cylinder Plane Strain

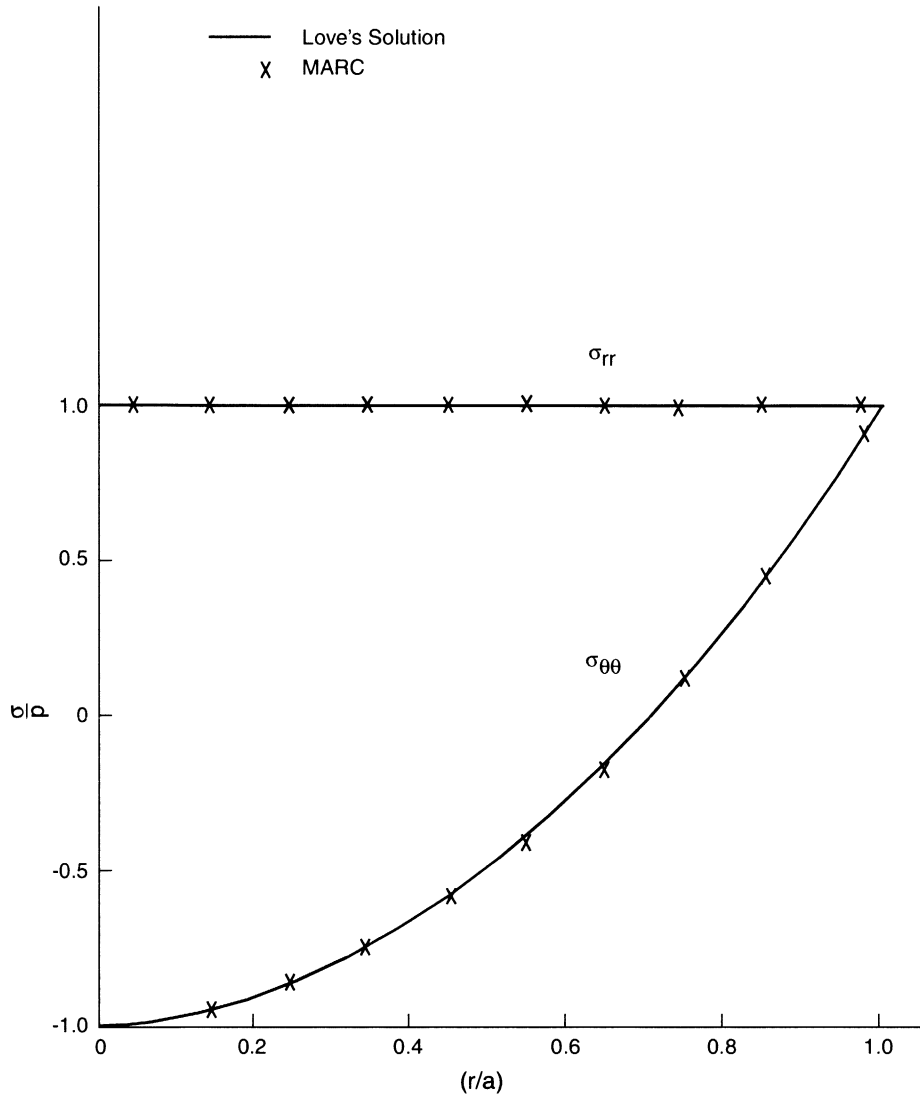


Figure 7.8-3 Second Mode Solid Cylinder Plane Strain

7.9 Cylinder under Line Load (Fourier Analysis)

A solid cylinder in plane strain with a concentrated line load acting across the diameter is elastically analyzed. One FOURIER series with only symmetric terms is used to characterize the circumferential variation of the loading. Two different methods are demonstrated in describing the FOURIER series (problems e7.9a and e7.9b). The CASE COMBIN option is used to obtain the final results by superposition at four equally spaced stations around the circumference in problem e7.9c.

This problem is modeled using the two techniques summarized below.

Data Set	Element Type(s)	Number of Elements	Number of Nodes	Differentiating Features
e7x9a	62	10	53	Specify Fourier Coefficients
e7x9b	62	10	53	User Subroutine UFOUR

Element

Element 62, the axisymmetric quadrilateral for arbitrary loading, is used here. Details on this element are found in *MARC Volume B: User Input*.

Model

The geometry and mesh are shown in Figure 7.9-1. The solid cylinder has a height of 0.1 inch and a radius of 1.0 inch. The mesh consists of 10 elements and 53 nodes.

Geometry

This option is not required for this problem.

Material Properties

The elastic material data assumed for this example is Young's modulus (E) of $30. \times 10^6$ psi and Poisson's ratio (ν) of 0.25.

Loading

The 100 pound line load acting across the diameter is specified as a distributed load (IBODY=0) on element 10 and associated with Fourier series number 1. The force magnitude given in the DIST LOAD block is equal to $100/\pi$.

Boundary Conditions

All nodes on the planes $Z = 0$. and $Z = 0.1$ are constrained in the axial direction such that only radial motion is permitted. Nodes 1, 2 and 3 on the plane $R = 0$ are also constrained in the radial direction due to symmetry.

Fourier

Two different methods are used to describe the series:

1. Specifying the first eight nonzero terms to approximate the infinite series representing the actual loading:

$$a_0 = \frac{1}{2\pi} \int_0^{2\pi} P(\theta) d\theta = \frac{1}{\pi}$$

$$a_n = \frac{1}{\pi} \int_0^{2\pi} P(\theta) \cos n\theta d\theta = \begin{cases} 0, & n\text{-odd} \\ \frac{2}{\pi}, & n\text{-even} \end{cases}$$

2. Using user subroutine UFOUR generates an arbitrary number (say 361) of $[\theta, F(\theta)]$ pairs and the program calculates the series coefficients. The results should compare closely with the above exact calculations. In this example, 6 function pairs are generated by the subroutine.

Results

Figure 7.9-2 gives a comparison of the radial displacements at $\theta = 0^\circ$ predicted by this analysis with the exact solution of Muskhelishvili. For $\theta = 0^\circ$, $a = 1.0$ and $\nu = 0.25$, the solution is:

$$u_r(\theta=0^\circ) = \frac{1}{2\pi} \left[3 \ln \frac{\left(1 + \frac{r}{a}\right)}{\left(1 - \frac{r}{a}\right)} - \frac{r}{a} \right] \frac{P(1 + \nu)}{E}$$

The comparison is very good except at $r = a$. Here, the finite element solution cannot capture the singular behavior of the problem and falls below the unbounded exact solution.

Reference

Muskhelishvili, N. I., *Some Basic Problems of the Mathematical Theory of Elasticity*, translated by J.R.M. Radok, Erven P. Noordhoff, The Netherlands, 1963.



Parameters, Options, and Subroutines Summary

Example e7x9a.dat:

Parameters	Model Definition Options
ELEMENT	CONNECTIVITY
END	CONTROL
FOURIER	COORDINATE
SIZING	DIST LOADS
TITLE	END OPTION
	FIXED DISP
	FOURIER
	ISOTROPIC
	RESTART

Example e7x9b.dat:

Parameters	Model Definition Options
ELEMENT	CONNECTIVITY
END	CONTROL
FOURIER	COORDINATE
SIZING	DIST LOADS
TITLE	END OPTION
	FIXED DISP
	FOURIER
	ISOTROPIC
	RESTART

User subroutine in u7x9b.f:

UFOUR

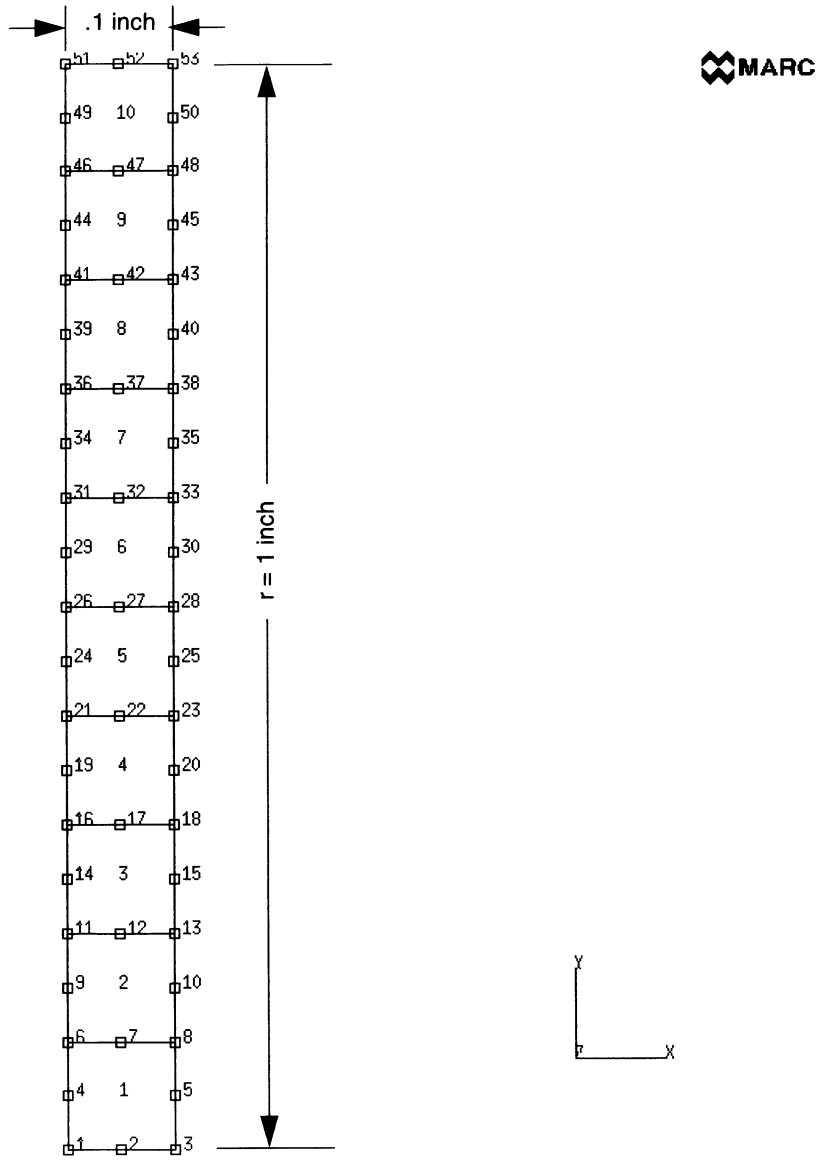


Figure 7.9-1 Cylinder and Mesh

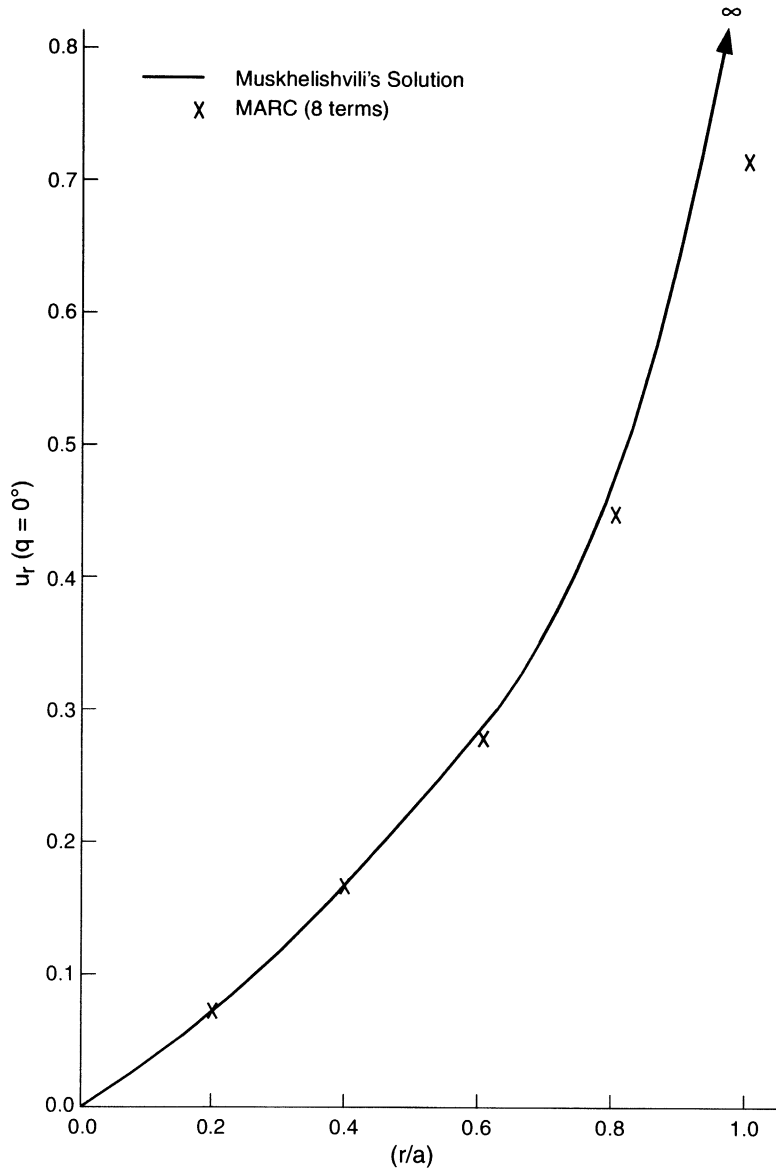


Figure 7.9-2 Concentrated Load on a Solid Cylinder

7.10 Mesh Qualification

This problem uses the QUALIFY option for mesh refinement studies. This option is invoked by adding the QUALIFY parameter. It is only applicable for the higher order isoparametric elements. The model and input data of the problem follow.

Model

A quarter of a square membrane structure is modeled using four 8-node quadrilateral elements type 27 (8-node plane-strain element). Dimensions of the model and a finite element mesh are shown in Figure 7.10-1.

Material Properties

The Young's modulus and Poisson's ratio of the membrane are assumed to be 10E6 psi and 0.3, respectively.

Loading

Two concentrated forces of equal magnitude are applied at the corner of the membrane (node 21). The forces are $F_x = F_y = 7.07$ pounds.

Boundary Conditions

Displacement at lines of symmetry are constrained ($u = 0$ at $x = 0$ and $v = 0$ at $y = 0$).

Geometry

The membrane thickness is 0.1 inch.

Results

Strain Energy Difference (SED) contours are shown in Figure 7.10-2. The large value in the corner implies that for this loading condition the mesh refinement should take place in the corner region of element number 4.



Parameters, Options, and Subroutines Summary

Example e7x10.dat:

Parameters

ELEMENT
END
MESH PLOT
QUALIFY
SIZING
TITLE

Model Definition Options

CONNECTIVITY
COORDINATE
END OPTION
FIXED DISP
GEOMETRY
ISOTROPIC
POINT LOAD

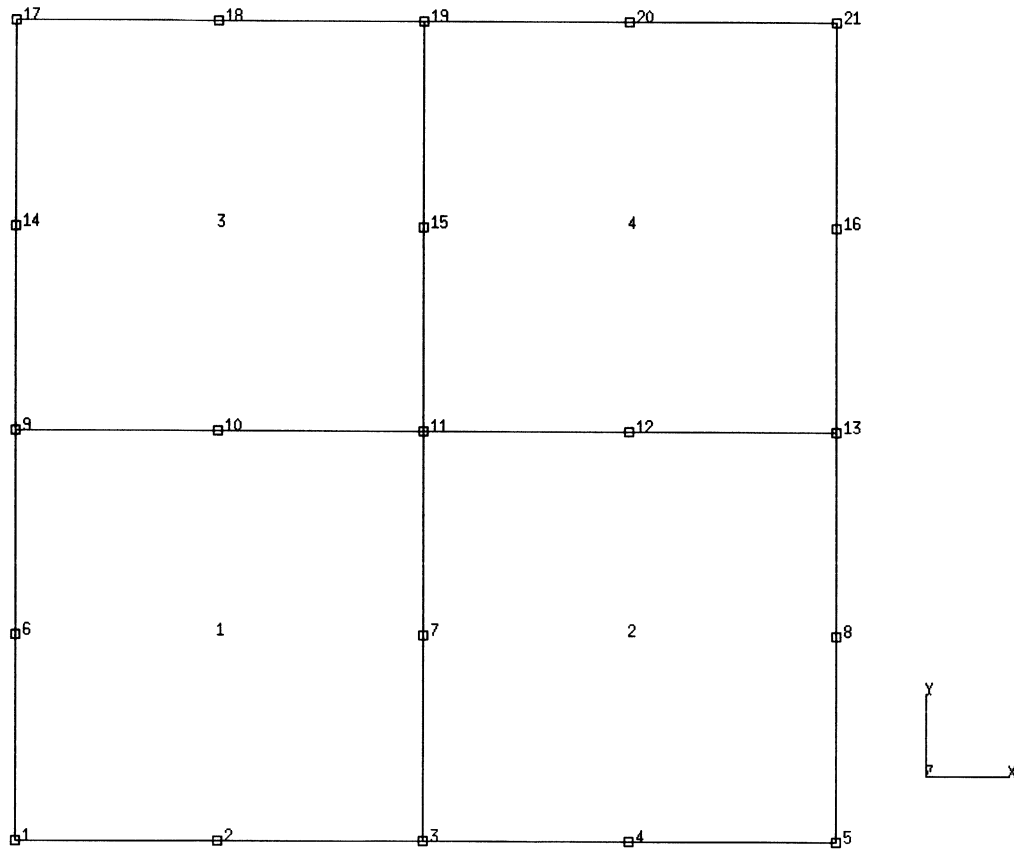
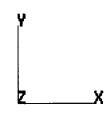
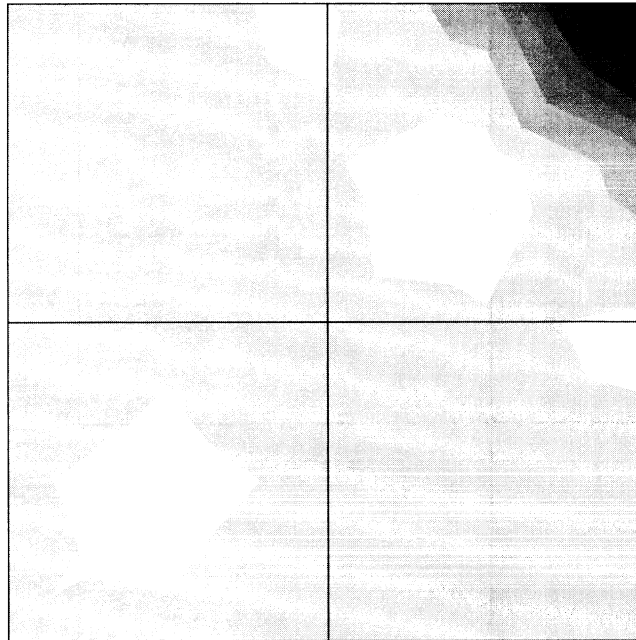
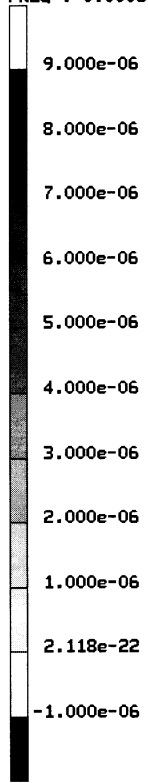


Figure 7.10-1 Membrane and Mesh

INC : 0
SUB : 0
TIME : 0.000e+00
FREQ : 0.000e+00



prob e7.10 special topics emt 27 - mesh qualification
Higher Order Contribution

Figure 7.10-2 Strain Energy Difference

7.11 Concrete Beam under Point Loads

A simply supported concrete beam is subjected to two concentrated loads. The beam is analyzed using the concrete cracking option in MARC. Plane stress element (element type 3) is used for modeling the concrete and truss element (element type 9) is chosen for the simulation of steel reinforcement. The cracking option allows cracks to initiate in the concrete elements.

Model

The dimensions of the beam and the finite element mesh are shown in Figure 7.11-1. The model consists of 80 elements representing the concrete and 10 elements representing the steel.

Material Properties

The elastic-plastic material data is given through the ISOTROPIC option.

For concrete (Elements 1-80), material id of 1

$$E_c = 3.E6 \text{ psi}$$

$$\nu_c = 0.15$$

$$\sigma_{yc} = 1250 \text{ psi}$$

For steel reinforcement (Elements 81-90), material id of 2

$$E_s = 3.E7 \text{ psi}$$

$$\nu_s = 0.3$$

$$\sigma_{ys} = 40,000 \text{ psi}$$

For both the concrete and the rebars, an isotropic plasticity model is used. For the concrete elements the cracking flag is initiated.

Crack Data

The concrete (material id of 1) has an ultimate tensile stress of 700 psi. The shear retention factor is 0.5. The strain softening modulus is 365 psi.

Geometry

Thickness of the concrete beam 1.0 inch; area of the steel reinforcement = 0.1 square inch.

Loading

Two concentrated loads are symmetrically placed near the centerline of the beam. A total of 1175 pounds (2 x 587.5 pounds) is applied to the beam in 10 increments. Variable load increments, through the use of options POINT LOAD, PROPORTIONAL INCREMENT, and AUTO LOAD are:

Inc. No.	Load Increment
0	2 x 250
1	2 x 62.5
2	2 x 62.5
3	2 x 62.5
4	0.
5	2 x 50.
6	0.
7	2 x 50.
8	0.
9	2 x 50.

Boundary Conditions

Out-of-plane degrees of freedom are constrained for all nodal points ($w = 0$ for all nodes). Symmetry conditions are imposed along line $x = 68$ ($u = 0$ for nodes 29, 31, 33, 89, 91, 93, 95, 97, and 99). Simply-supported conditions are placed at node 1 ($v = 0$).

Results

A deformed mesh plot is shown in Figure 7.11-2. Cracking begins in increment 4 and the program begins to iterate. By increment 9, seven elements have developed cracks and the largest crack strain is about 0.034%. Figure 7.11-3 shows the final cracked region consisting of 14 elements near the bottom center portion of the beam.

Parameters, Options, and Subroutines Summary

Example e7x11.dat:

ParametersELEMENT
END
SIZING
TITLE**Model Definition Options**CONNECTIVITY
CONTROL
COORDINATE
CRACK DATA
END OPTION
FIXED DISP
GEOMETRY
ISOTROPIC
POINT LOAD
PRINT CHOICE
RESTART**History Definition Options**AUTO LOAD
CONTINUE
POINT LOAD
PROPORTIONAL INCREMENT

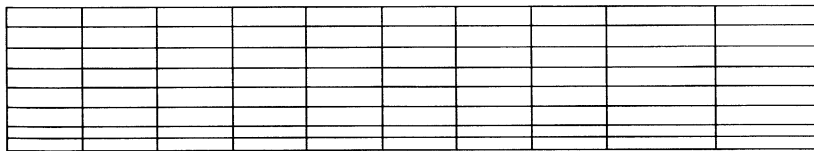
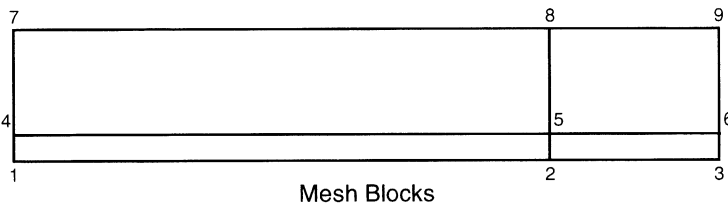
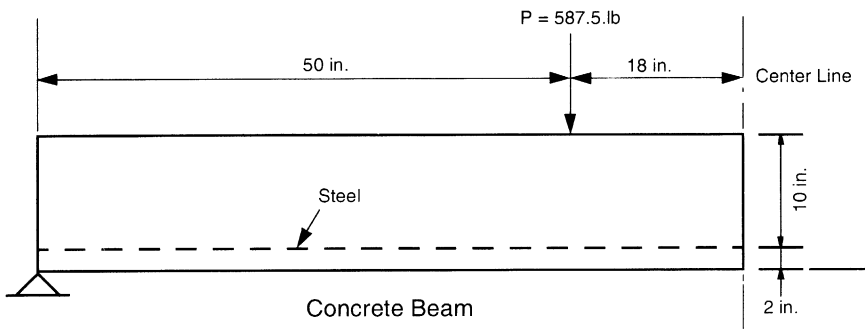
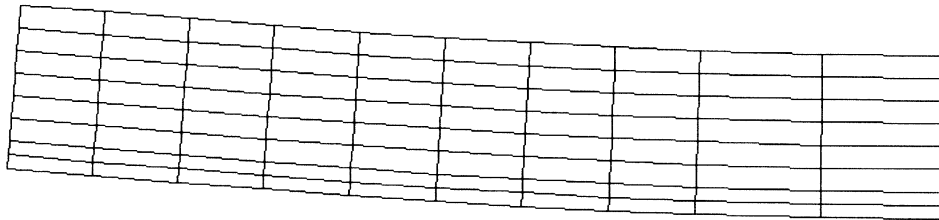


Figure 7.11-1 Concrete Beam and Mesh

INC : 9
SUB : 0
TIME : 0.000e+00
FREQ : 0.000e+00



prob e7.11 special topics emt 3 & 9 – cracking

Figure 7.11-2 Deformed Mesh Plot

61	62	63	64	65	66	67	68	79	80
53	54	55	56	57	58	59	60	77	78
45	46	47	48	49	50	51	52	75	76
37	38	39	40	41	42	43	44	73	74
29	30	31	32	33	34	35	36	71	72
21	22	23	24	25	26	27	28	69	70
9	10	11	12	13	14	15	16	19	20
1	2	3	4	5	6	7	8	17	18

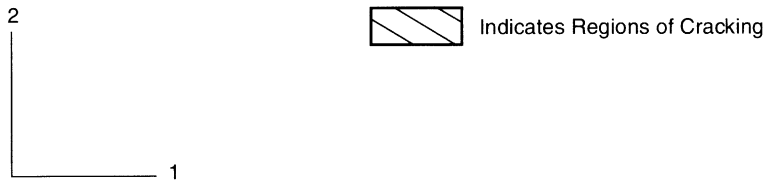


Figure 7.11-3 Regions of Cracking

7.12 Constant Uniaxial Stress Applied to Plate in Plane Strain (Viscoelasticity)

A viscoelastic rectangular plate (Figure 7.12-1) is subjected to a constant and uniform tensile stress of 10 psi in the x-direction. The deformation conforms to the plane strain idealization. The material is isotropic and strictly elastic in dilatational response. The bulk modulus is 20,000 psi. The time-dependent shear relaxation modulus is given as:

$$G(t) = 100 + 9900 e^{-2.3979t} \quad (\text{psi})$$

where the units of time are seconds. The displacements $u_i(x_i, t)$ are required as well as the out-of-plane stress, $\sigma_{zz}(t)$. The numerical results are compared to the closed form solution.

By converting the stress relaxation function defined above to a creep function, you obtain the creep function for isotropic shear behavior. The corresponding stress relaxation is:

$$J(t) = (1 \times 10^{-4}) + 9.9 \times 10^{-3} [1 - \exp(-t/41.703)] \quad \text{sq.in/lb.}$$

The constant elastic dilatational response (bulk modulus, K) is now expressed in reciprocal form compatible with the creep function formulation.

This is:

$$B = \frac{1}{K} = 0.5 \times 10^{-4} \quad \text{sq.in/lb.}$$

Element

Element type 27 is used. This is an isoparametric distorted quadrilateral element for plane strain. There are two degrees of freedom at each node and four nodes per element.

Model

There are four elements and a total of 23 nodes as shown in Figure 7.12-2.

Geometry

The thickness is specified in EGEOM1 as 0.2 inch.

ISOTROPIC/VISCELPROP

The details of any viscoelastic material model are given in the model definition section. For an isotropic material, strictly elastic in dilatational response, the material characteristics can be completely represented by the model definition options ISOTROPIC and VISCELPROP.

Both the Young's modulus (E) and Poisson's Ratio (ν) are entered through the ISOTROPIC option. Recall that the expressions of shear modulus (G) and the bulk modulus (K) are:

$$G = \frac{E}{2(1 + \nu)} \quad ; \quad K = \frac{E}{3(1 - 2\nu)}$$

By eliminating E, we obtain the expression of ν in terms of G and K as:

$$3(1 - 2\nu)K = 2(1 + \nu)G$$

In the current problem, the bulk modulus K is equal to 20,000. The shear modulus G is equal to 10,000 [$G(0) = 100 + 9900$]. So, you obtain the values of $\nu = 0.2857$ and $E = 25714$.

Rewrite the expression of time dependent shear relaxation modulus as:

$$\begin{aligned} G(t) &= 100 + 9900 e^{-(t/0.4170316)} \\ &= G_0 + G_1 * e^{-(t/\tau_1)} \end{aligned}$$

We have $G_1 = 9900$ and $\tau_1 = 0.4170316$ that are entered through the VISCELPROP option.

Loading

The execution of this analysis consisted of three parts. The application of the tensile 10 psi load was accomplished with the DIST LOADS block. The instantaneous elastic response was then determined in increment 0. This load was held constant for the duration of the analysis using a second DIST LOADS block after END OPTION with zero incremental load.

Subsequent to this, two creep stages were applied by means of the TIME STEP and AUTO LOAD history definition options. Knowledge of the closed form solution shows that most of the deformation and stress relaxation occurs in the first five seconds. Consequently, the suggested time step in the first TIME STEP block was specified as 0.1 second for a time span of 5.0 seconds. The number of increments was set at 50 and the time step was to remain fixed for all increments at the suggested value.

In the second TIME STEP load incrementation block, the constant time step size was increased to 4.0 seconds and 50 increments were requested to cover a span of 200 seconds.

It will be noted that the step size in the second creep stage is approximately one-tenth of the retardation time. This is more typical of the appropriate size which should be used in an analysis where no other characteristic times are present. Such other factors that might influence the choice of a time step are:

1. diffusional times for transient thermal analysis;
2. characteristic times associated with the application of external loads; or
3. the existence of a significant shift factor in the analysis of materials classified as being thermo-rheologically simple.



A series of different time step sizes might be used for different stages of an analysis where materials exhibit several characteristic relaxation or retardation times.

It was predetermined, with consideration of the closed form solution, that 100 increments would be sufficient to reach approximately to the steady state condition. A maximum value of 200 was entered in the CONTROL block. Tolerances and control limits for the analysis assume default values.

FIXED DISP

The unloaded face of the plate ($x = 0$) is fixed against displacement in the x-direction. The plane strain assumptions limit all displacements of the plate to the x-y plane.

Results

The exact solution for displacement of the end face, $u_x(2,t)$, is plotted in Figure 7.12-3. The out-of-plane stress, $\sigma_{zz}(t)$, is shown in Figure 7.12-4. The corresponding numerical results, obtained with MARC, are also plotted in these figures. The numerical results were found to be identical to the exact solution even at the point in the numerical analysis where the time step was changed from 0.1 seconds to 4.0 second.

Parameters, Options, and Subroutines Summary

Example e7x12.dat:

Parameters	Model Definition Options	History Definition Options
ELEMENT	CONNECTIVITY	AUTO LOAD
END	CONTROL	CONTINUE
SIZING	COORDINATE	DIST LOADS
TITLE	DIST LOADS	TIME STEP
	END OPTION	
	FIXED DISP	
	GEOMETRY	
	ISOTROPIC	
	PRINT CHOICE	
	TYING	
	VISCELPROP	

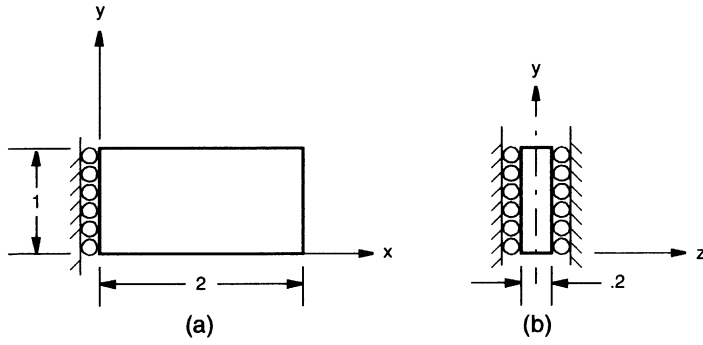


Figure 7.12-1 Geometry

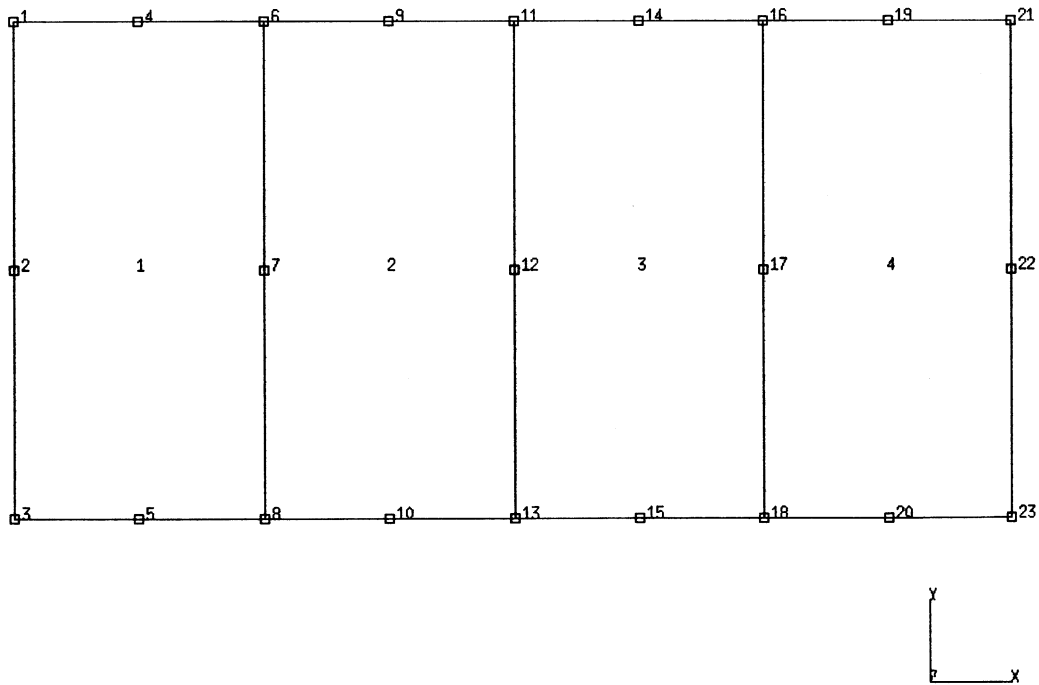


Figure 7.12-2 Finite Element Model

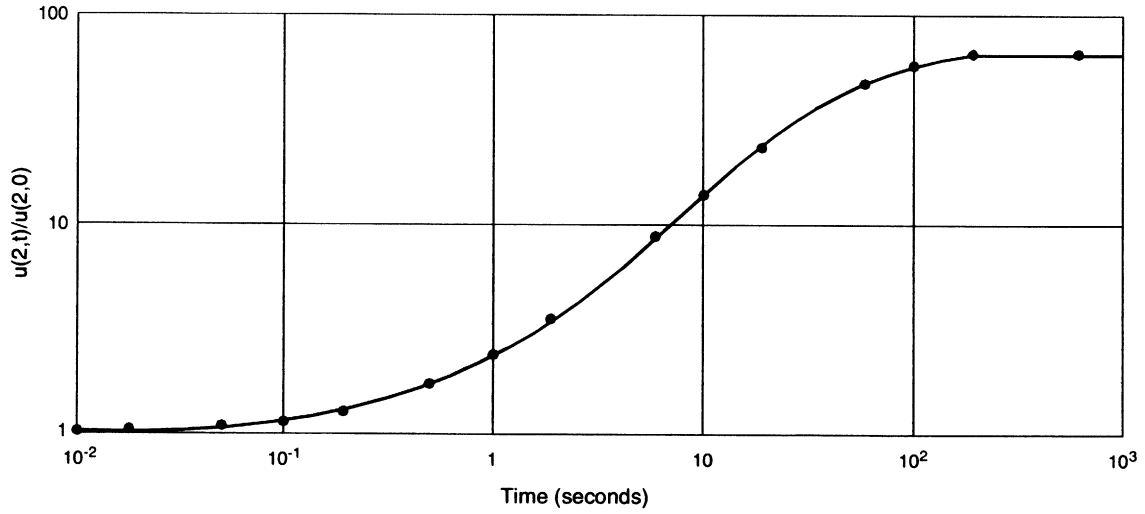


Figure 7.12-3 Normalized Displacement vs. Time

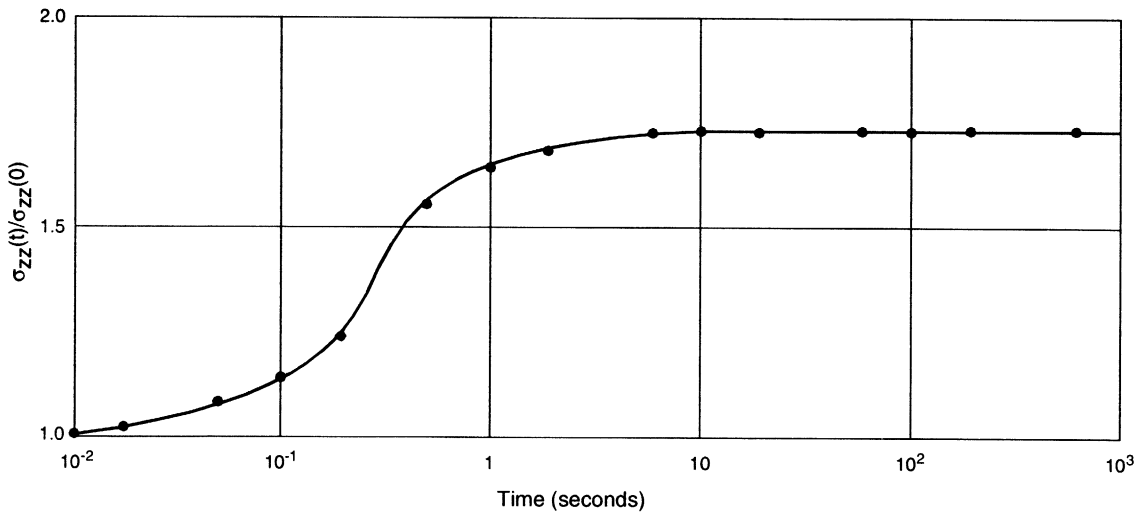


Figure 7.12-4 Normalized Out-of-Plane Stress, σ_{zz} vs. Time



7 Contact

Constant Uniaxial Stress Applied to Plate in Plane Strain (Viscoelasticity)



7.13 Analysis of Pipeline Structure

MARC beam element type 14 and pipe-bend element type 17 are utilized for the elastic analysis of a pipeline structure subjected to either in-plane or out-of-plane bending. The structure is loaded until the limit load is reached. The pipeline mesh generation MARC-PIPE is used for the generation of CONNECTIVITY and COORDINATES data blocks as well as the tying data required for the use of element types 14 and 17.

Model

There are a total of 20 elements in the model, of which 6 are type 14 and 14 are type 17. A total of 26 nodes are used. The dimension of the pipeline structure and a finite element mesh are shown in Figure 7.13-1. MARC-PIPE is used for the mesh generation and the tying information.

Material Properties

The Young's modulus and Poisson's ratio of the pipeline material are 155.53×10^3 (ksi) and 0.3, respectively.

Tractions

An out-of-plane moment of 2.06×10^7 (in-kips) is applied at node 1 in the first analysis. As shown in Figure 7.13-1, the applied load is a moment about the y-axis (the fifth degree of freedom of node 1). The load is increased to a final load of 3.71×10^7 (in-kips) by increment 8. In the second analysis, an in-plane moment of 1.37×10^7 (in-kips) is applied at node 1. The applied load is about the z-axis (the sixth degree of freedom of node 1). The load is increased to a final load of 2.87×10^7 (in-kips) by increment 11.

Boundary Conditions

All degrees of freedom of node 26 are constrained for the fixed-end condition.

Geometry

The wall thickness and mean radius of the beam elements (element type 14) are:

For Elements 1, 2, 19, and 20:

Wall Thickness= 8.8 inches

Mean Radius = 275 inches

For Elements 3 and 18:

Wall Thickness= 10.4 inches

Mean Radius = 274.5 inches

For the pipe-bend elements (element type 17) the geometry data are:

Pipe thickness, $t = 10.4$ inches

The angular extent of the pipe-bend section, $\phi = 90^\circ$

The radius to the center of the pipe in the r-z plane, $R = 838.2$ inches

MARC-PIPE

As shown in Figure 7.13-1 and in the MARC-PIPE input listing, the pipeline structure is subdivided into two straight and one curved segments for mesh generation. As a result, the number of joints and the number of sections on first card series are 4 and 3, respectively. Next, the two straight sections identified by nodal points 1-2 and 3-4, are further divided into three finite elements each, along the pipe direction. The input data for these two straight sections are:

Subdivision				
Section Number	Section Number	Node Numbers		Along the Pipe Direction
1	0	1	2	3
3	0	3	4	3

The curved portion of the pipeline structure, identified by nodes 2-3, is subdivided into 14 elements around the pipe cross section. There is no further subdivision along the pipe direction.

Subdivision					
Section Number	Section Number	Node Numbers		Pipe Direction	Around Pipe Cross Section
2	1	2	3	1	14

Coordinates of Center of Curvature of the Curved Portion

x	y	z	Pipe Radius
1500.0	838.2	0	274.2

Finally, the coordinates of the four joints are given below:

Joint Number	x	y	z
1	0	0	0
2	1500	0	0
3	2338.2	838.2	0
4	2338.2	2338.2	0

Connectivity, Coordinates and Tying Type

Since all three blocks of data are generated from MARC-PIPE, only the key word and the file number on which the data have been stored are required for the input.

Results

In both analyses, the load is scaled such that incipient yield occurs at increment 1. The loading was increased until the limit load was reached. This was due to an inability to obtain a convergent solution. At the limit load, plasticity had occurred through all 11 layers through the thickness of the elbow section. Figure 7.13-2 shows the load-displacement results of this analysis. The special pipe bend element (type 17) allows the analyst to examine the ovalization of the cross section of the pipe. Using the SECTIONING option in the plot description section, we can examine this effect. Figure 7.13-3 shows the ovalization due to the two types of loading conditions.

Parameters, Options, and Subroutines Summary

The data file used for MARC-PLOT is e7x13a.dat:

Example e7x13b.dat:

Parameters	Model Definition Options	History Definition Options
ELEMENT	CONNECTIVITY	AUTO LOAD
ELSTO	CONTROL	CONTINUE
END	COORDINATE	PROPORTIONAL INCREMENT
SCALE	END OPTION	
SIZING	FIXED DISP	
TITLE	GEOMETRY	
	ISOTROPIC	
	POINT LOAD	
	RESTART	
	TYING	

Example e7x13c.dat:

Parameters	Model Definition Options	History Definition Options
ELEMENT	CONNECTIVITY	AUTO LOAD
ELSTO	CONTROL	CONTINUE
END	COORDINATE	PROPORTIONAL INCREMENT
SCALE	END OPTION	
SIZING	FIXED DISP	
TITLE	GEOMETRY	
	ISOTROPIC	
	POINT LOAD	
	RESTART	
	TYING	

Example e7x13d.dat:

Parameters	Model Definition Options	History Definition Options
ELEMENT	BOUNDARY COUNDITIONS	CONTINUE
ELSTO	CONTROL	
END	END OPTION	
MESH PLOT	GEOMETRY	
SCALE	ISOTROPIC	
SIZING	POINT LOAD	
TITLE	RESTART	

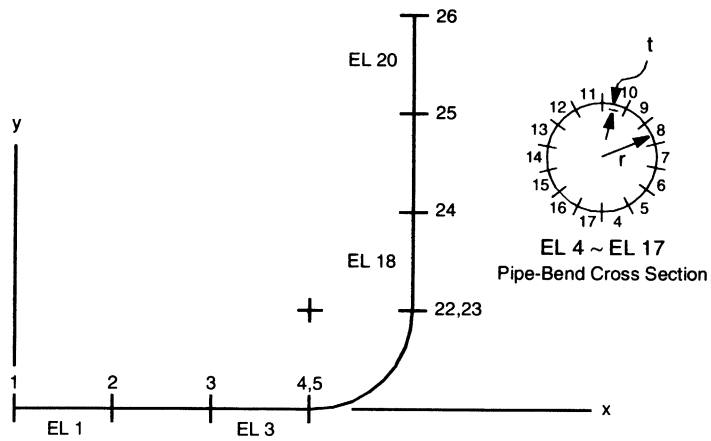
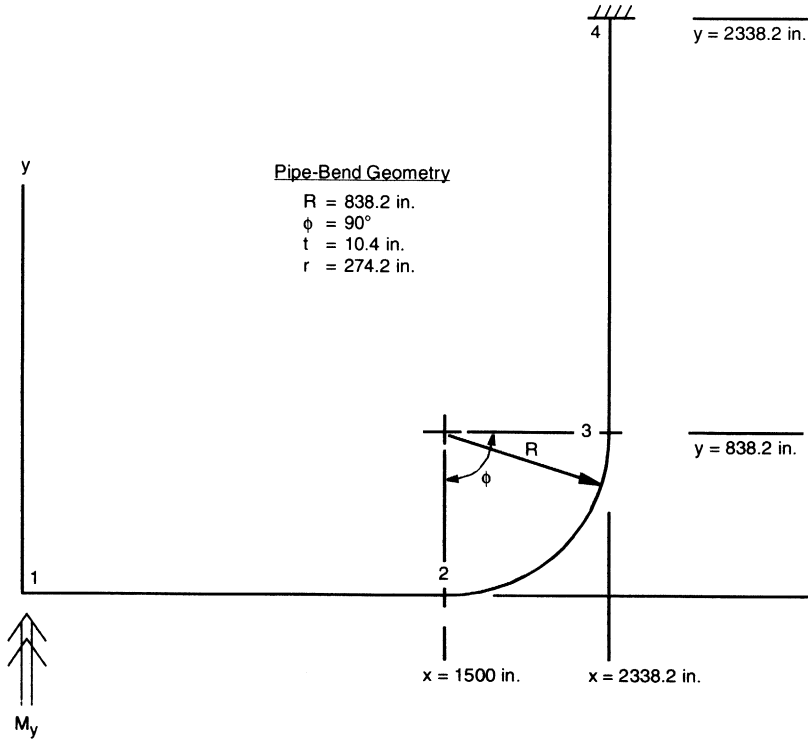


Figure 7.13-1 Pipe Line Geometry and Model

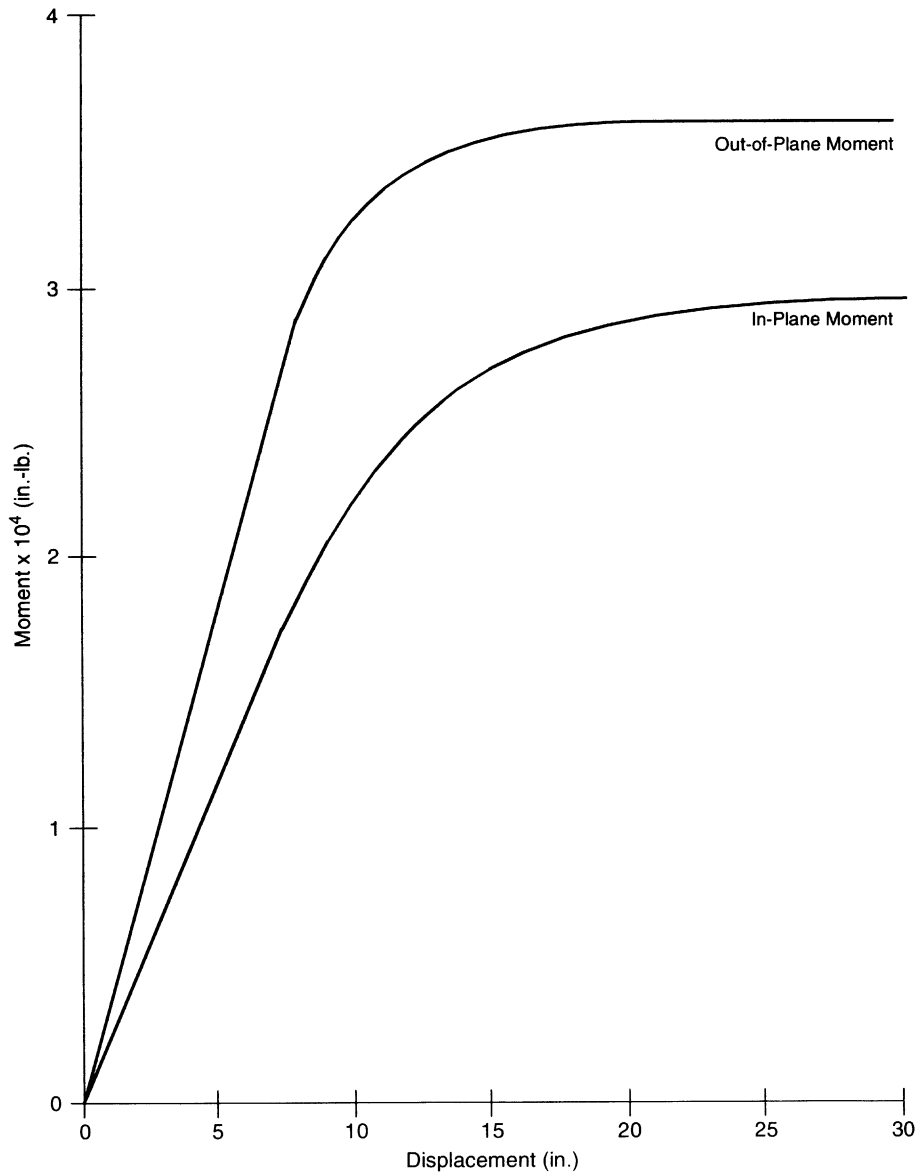
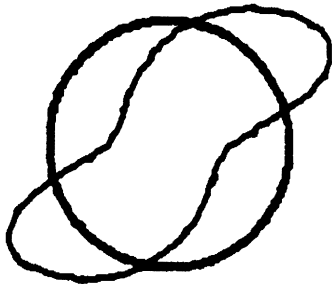
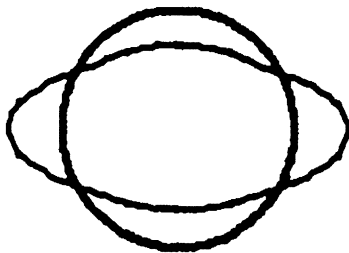


Figure 7.13-2 Load vs. Displacement



(a) Due to Out-of-Plane Moment



(b) Due to In-Plane Moment

Figure 7.13-3 Ovalization Behavior Due to Out-of-Plane and In-Plane Moments

7.14 Viscoelastic Analysis of an Externally Reinforced Thick-Walled Cylinder under Internal Pressure

A very long thick-walled cylinder (Figure 7.14-1) with an internal radius of 2 inches and an external radius of 4 inches is subjected to an internal pressure of 10 psi. The material is assumed to be isotropic and to be strictly elastic in dilatational response, having a constant bulk modulus of 10^5 psi. The time-dependent viscoelastic shear response is assumed to be represented by a simple Maxwell rheological model. A schematic diagram of such a model is shown in Figure 7.14-2. The constitutive representation in differential equation form can be expressed as:

$$A \frac{\partial S_{ij}}{\partial t} + B S_{ij} = \frac{\partial e_{ij}}{\partial t}$$

where S_{ij} is the deviatoric or shear component of stress and e_{ij} is the tensor component of the deviatoric or shear strain (that is, the engineering strain $\gamma_{ij} = 2 e_{ij}$). The values of the coefficients A and B , which appear in the above expression, are those which were used by Lee et al. [1] and Zienkiewicz et al. [2] in their analyses of the same problem (i.e., $A = B = \frac{4}{3} \times 10^{-5}$).

A thin steel cylinder with an inner radius of 4 in. and thickness of 0.1212 in. is rigidly bonded to the outer surface of the viscoelastic cylinder. The Young's modulus for the steel casing is 30.0×10^6 and the Poisson's ratio is 0.3015. It is assumed that both cylinders are sufficiently long so that the deformation is considered to conform to the plane strain idealization with no axial motion.

We are interested in the time varying stresses within the inner viscoelastic cylinder. The numerical results are then compared to the closed form solution, which is readily obtained for this test case and developed in the following.

Constitutive Representation

The differential equation, which describes the shear response, can be re-expressed in the following form:

$$\frac{\partial s_{ij}}{\partial t}(\underline{x}, t) + \frac{1}{\tau_1} S_{ij}(\underline{x}, t) = G_1 \frac{\partial \gamma_{ij}}{\partial t}(\underline{x}, t)$$

where the characteristic relaxation time, in this instance, is given by:

$$\tau_1 = \frac{A}{B} = 1$$

Figure 7.14-5 shows that initial hoop tension occurs adjacent to the bore of the viscoelastic cylinder. The magnitude and sign of this stress depends on the stiffness of the reinforcement and the radius ratio, b/a . This circumferential tension changes to compression as the pressure is maintained, and the limit of uniform hydrostatic compression is reached when the shear strength has relaxed to zero.

It will be noted from the printout for this analysis that assembly of the overall stiffness matrix occurs only for the first three increments. Thereafter, only back-substitution is required to attain each incremental solution for this linear viscoelastic case. The effective incremental stress-strain matrix, $[G_{\text{eff}}]$, which is used to develop the overall stiffness matrix for the third and subsequent increments, was found to be:

$$[G_{\text{eff}}] = \left[[G_{\infty}] + \sum_{i=1}^n \frac{2 \tau_i \beta_i(h_{\epsilon}) [G_i]}{h} \right]$$

This form reflects the assumption of a linearly varying strain rate over each increment.

However, the associated numerical procedure requires that the strain rates at the previous step are known. In the first viscoelastic step, this is not the case. In this increment, the assumption is made that the strain rate is constant. It can then be shown that the incremental stress for this first step is given by:

$$\begin{aligned} \Delta \sigma \Big|_{t = \Delta t} &= \left[[G_{\infty}] + \sum_{i=1}^n \tau_i [1 - \alpha_i(h_{\epsilon})] [G_i] \right] \Delta \epsilon \Big|_{t = \Delta t} \\ &= - \sum_{i=1}^n [1 - \alpha_i(h_{\epsilon})] \sigma_i \Big|_{t = 0^+} \end{aligned}$$

where σ_i is the value of the state variable or stress supported by the i^{th} viscoelastic element in the generalized Maxwell model at the end of the instantaneous initial elastic step. It is given as:

$$(\sigma_i = G_{\infty} + G_i \cdot \epsilon) \Big|_{t = 0^+}$$

The increment in this variable for the first viscoelastic step is given as:

$$\Delta \sigma_i \Big|_{t = \Delta t} = - [1 - \alpha_i(h_{\epsilon})] \sigma_i \Big|_{t = 0^+} + [1 - \alpha_i(h_{\epsilon})] G_i \frac{\Delta \epsilon}{h} \Big|_{t = \Delta t}$$



In situations where there is a sudden and local sharp change in stress (for example, to an abrupt change in temperature in a thermo-rheologically simple solid), a few very small starting steps may be required. This minimizes the effect that any starting approximation error might have on the evaluation of the transient response and on the residual or steady state. For example, without such precautions, this type of error has been found to arise in the analysis of the tempering of thermo-rheologically simple glass sheets [3].

References

1. Lee, E. H., Radok, J. R. M., and Woodward, W. B., "Stress Analysis for Linear Viscoelastic Materials", *Trans. of the Society of Rheology*, Volume III, pp. 41-59 (1959).
2. Zienkiewicz, O. C., Watson, M. and King, I. P., "A Numerical Method of Visco-Elastic Stress Analysis", *Int. J. Mech. Sci.*, Vol. 10, pp. 807-827 (1968).
3. Narayanaswamy, O. S. and Gardon, R., "Calculation of Residual Stresses in Glass", *Journal of the American Ceramic Society*, Volume 52, No. 10, pp. 554-558 (1969).

Parameters, Options, and Subroutines Summary

Example e7x14.dat:

Parameters	Model Definition Options	History Definition Options
ELEMENT	CONNECTIVITY	AUTO LOAD
END	CONTROL	CONTINUE
SIZING	COORDINATE	DIST LOADS
TITLE	DIST LOADS	TIME STEP
	END OPTION	
	FIXED DISP	
	ISOTROPIC	
	PRINT CHOICE	
	VISCELPROP	

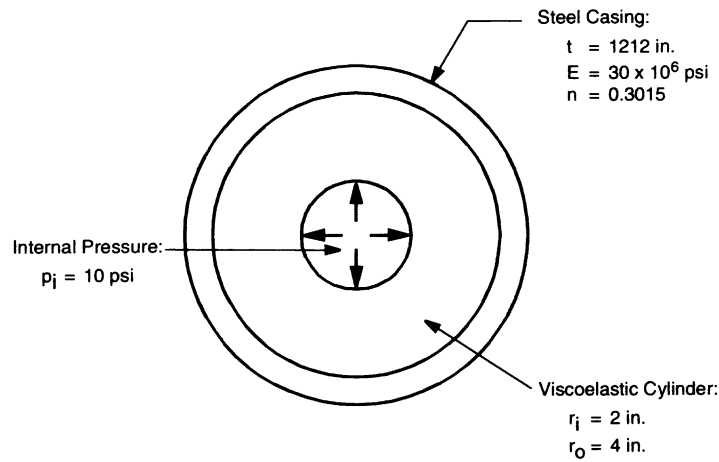


Figure 7.14-1 Long Thick-Walled Cylinder

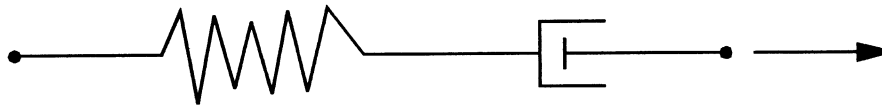


Figure 7.14-2 Simple Maxwell Model

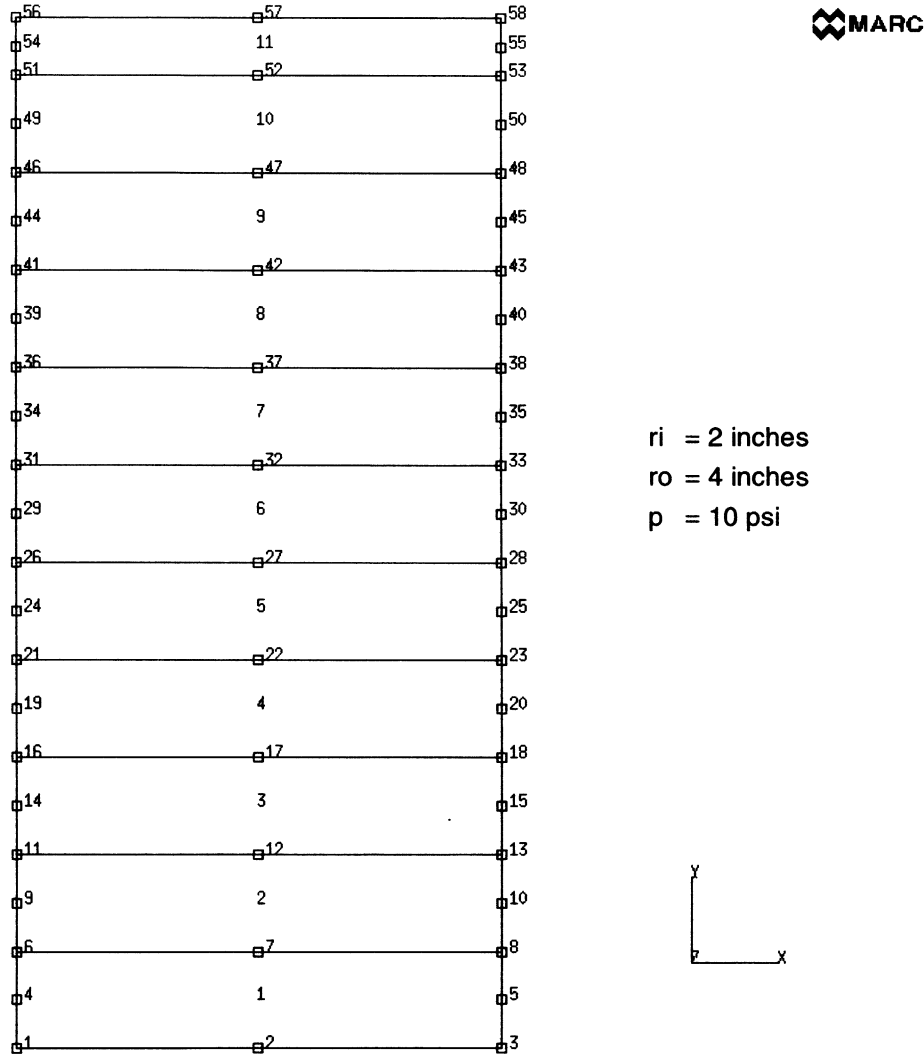


Figure 7.14-3 Finite Element Model

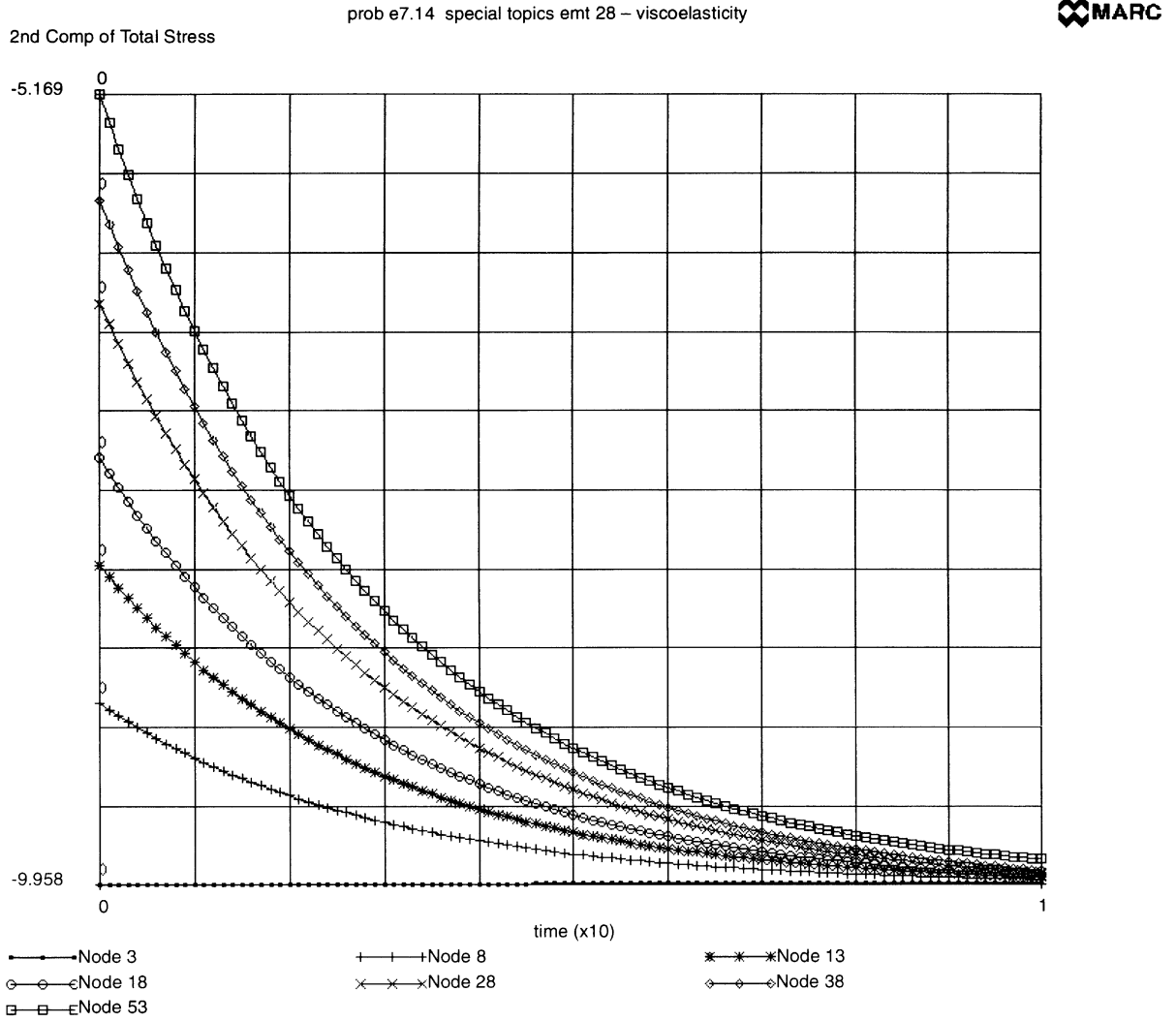


Figure 7.14-4 Radial Stress vs. Time

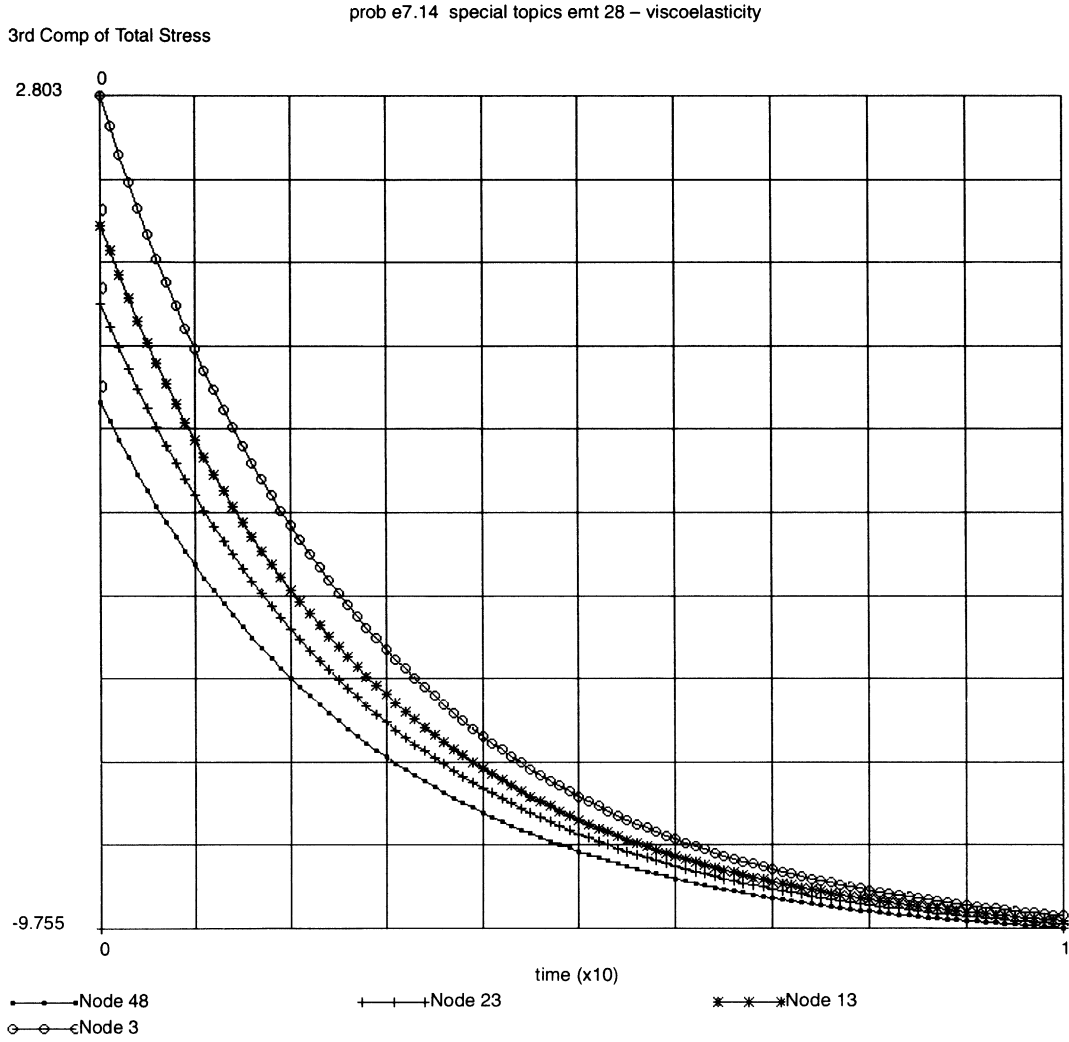


Figure 7.14-5 Hoop Stress vs. Time



7 Contact

Viscoelastic Analysis of an Externally Reinforced Thick-Walled Cylinder under Internal Pressure

7.15 Spiral Groove Thrust Bearing with Tilt

A spiral groove thrust bearing with tilt is analyzed to demonstrate the treatment of discontinuous film profiles as a result of the presence of grooves.

Element

Element type 37 is an arbitrary planar 3-noded triangular element chosen to model the lubricant.

Model

Problem details and the element mesh are shown in Figure 7.15-1. The dotted areas represent the lubricant grooves. The geometric specifications are as follows:

$$h_2 = 30 \times 10^{-6} \text{ m}$$

$$h_3 = 15 \times 10^{-6} \text{ m}$$

$$h_0 = 96.774 \times 10^{-6} \text{ m}$$

$$r_1 = 75 \times 10^{-3} \text{ m}$$

$$r_2 = 150 \times 10^{-3} \text{ m}$$

Due to the tilt of the longitudinal axis, the position with the smallest film thickness occurs on the axis $X = 0$ at the maximum Y -value. A total number of five spiral grooves has to be modeled. The required element mesh is generated by specifying a subset of nodal coordinates and elemental connectivities which subsequently are being used in user subroutines UFXORD and UFCONN to generate the complete mesh.

Thickness Field

The circumferential variation of the lubricant profile is specified per node in user subroutine UTHICK based on the nodal coordinates. In addition, user subroutine UGROOV is used to specify the contribution from the grooves to the total lubricant thickness.

Velocity Field

The relative velocity of the lubricant at the rotor surface, with respect to the grooved stationary part, is specified in user subroutine UVELOC. The angular velocity equals 100 rpm.

Material Properties

Viscosity of $0.020 \text{ N}\cdot\text{sec}/\text{m}^2$ and density of $800 \text{ kg}/\text{m}^3$ are assumed.

Boundary Conditions

Atmospheric pressure is applied at the outer radius. It is assumed that a constant pressure occurs at the internal oil chamber. For this reason, all nodes on the inner radius are tied.

Results

Pressure distribution is calculated in increment 0. In addition, the resulting load-carrying capacity is determined by integrating the pressure distribution over the grooved surface. This results in a bearing force of:

$$F_x = 0 \text{ N}$$

$$F_y = 0 \text{ N}$$

$$F_z = 23.714 \times 10^3 \text{ N}$$

The calculated bearing moment components with respect to the center of the thrust bearing are:

$$M_x = 129.3 \text{ Nm}$$

$$M_y = -70.6 \text{ Nm}$$

$$M_z = 0.0 \text{ Nm}$$

Based on these results, the position of the resulting bearing force can be determined. If the coordinates of this point are denoted by (X_0, Y_0) , it follows that:

$$X_0 = -\frac{M_y}{F_z} = 2.997 \times 10^{-3} \text{ m}$$

$$Y_0 = \frac{M_x}{F_z} = 5.4521 \times 10^{-3} \text{ m}$$

The so-called attitude angle, which is the angle between the point (X_0, Y_0) and the Y-axis equals:

$$\arctan \frac{X_0}{Y_0} = \arctan \frac{M_y}{M_x} = 28.6 \text{ degrees}$$

Since the integration of the pressure distribution was only performed over the grooved surface, the contribution from the oil chamber has to be added. In addition, the contribution from the atmospheric pressure has to be subtracted.

A vector plot of the mass fluxes is shown in Figure 7.15-2. This yields for the actual vertical bearing force component:

$$F_z^* = F_z + \bar{Y}(r_1^2 P_{ch} - r_2^2 P_{at}) = 25.83 \times 10^{-3} \text{ N}$$

where $P_{ch} = \text{N/m}^2$.



Parameters, Options, and Subroutines Summary

Example e7x15.dat:

Parameters

ELEMENT
END
SIZING
TITLE

Model Definition Options

CONNECTIVITY
CONTROL
COORDINATE
DIST LOADS
END OPTION
FIXED DISP
ISOTROPIC
PRINT CHOICE
VISCELPROP

History Definition Options

AUTO LOAD
CONTINUE
DIST LOADS
TIME STEP

User subroutines in u7x15.f:

UFXORD
UFCONN
UTHICK
UVELOC
UGROOV

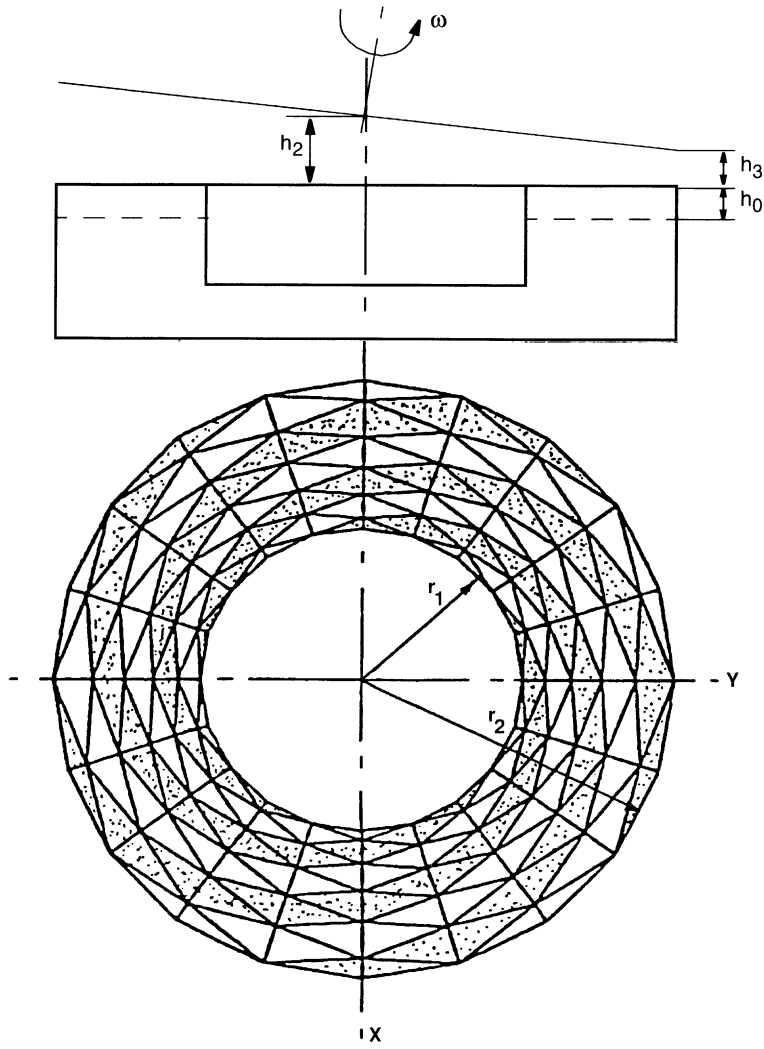
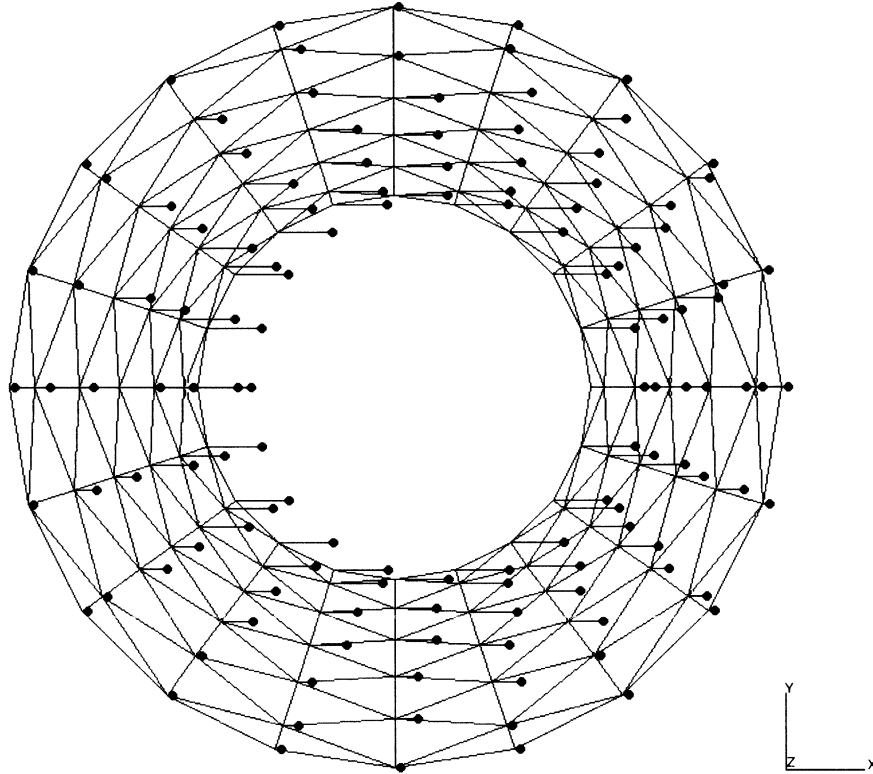


Figure 7.15-1 Spiral Groove Thrust Bearing with Tilt

INC : 0
SUB : 0
TIME : 0.000e+00
FREQ : 0.000e+00



spiral groove thrust bearing with tilt
Displacements

Figure 7.15-2 Vector Plot of Mass Flow

7.16 Hydrodynamic Journal Bearing of Finite Width

In this example, a journal bearing of finite width is analyzed. The load-carrying capacity as well as stiffness and damping properties are determined for a stationary bearing system. In addition, the procedure to be followed when analyzing the dynamic behavior of a nondeformable bearing system due to a change in the applied load vector is demonstrated.

Element

Element type 39, which is an arbitrary 4-node isoparametric quadrilateral element with bilinear pressure interpolation, is used to model the lubricant.

Model

The details of the journal bearing problem are given in Figure 7.16-1. In bearing analyses, the lubricant is modeled by means of planar finite elements. This is possible because it is assumed that the pressure does not vary over the lubricant thickness. Due to symmetry conditions, only half the bearing width needs to be modeled. The incremental mesh generators CONN GENER and NODE FILL are used to generate the element mesh.

Boundary Conditions

It is assumed that atmospheric pressure is acting on the end faces of the bearing system. The BC FILL option is used to generate these boundary conditions.

Tying

Tying was applied to the nodal pressures at both sides of the mesh to simulate the continuous pressure distribution in the circumferential direction.

Thickness Field

The variation of the lubricant thickness over the mesh due to the eccentric position of the rotor is specified in user subroutine UTHICK. This subroutine determines the nodal thickness values using the following expression:

$$h(\theta) = (20 - 10 \cos \theta) 10^{-6} \text{ m}$$

Velocity Field

The relative velocity of the lubricant at the rotor surface, with respect to the stationary surface, is specified in the VELOCITY block. The angular velocity is 1250 rad/second.

Material Properties

All elements have lubricant properties as follows: viscosity of .015 N-sec/m² and density of 800 kg/m³.

Load-Carrying Capacity

The pressure distribution for the given bearing system is calculated in increment 0. Because no external mass flux is prescribed, FLUXES need to be specified. The resulting pressure distribution is integrated to calculate the actual bearing force components. User subroutine UBEAR is included to specify at each node the physical orientation of the lubricant film. The following expressions are used:

$$\begin{aligned} X &= r \sin \theta & n_X &= -\cos \theta \\ Y &= r \cos \theta & n_Y &= -\sin \theta \\ Z &= -y & n_Z &= 0 \end{aligned}$$

In addition, the resulting bearing moment components with respect to the origin of the global coordinate x, y, z system are calculated. Figure 7.16-2 shows a path plot of the calculated pressure distribution along the circumference.

The resulting bearing force yields:

$$\begin{aligned} W_X &= -1046 \text{ N} \\ W_Y &= -1814 \text{ N} \\ W_Z &= 0 \end{aligned}$$

The resulting bearing moment yields:

$$\begin{aligned} M_X &= -6.846 \text{ Nm} \\ M_Y &= 3.938 \text{ Nm} \\ M_Z &= 0 \end{aligned}$$

Because half of the structure was modeled, the components M_X and M_Y are not zero.

Damping and Stiffness Properties

The calculation of bearing characteristics (that is, damping and stiffness properties) is performed in subincrements based on a specified change in lubricant film thickness or thickness rate. This is achieved by activating the DAMPING COMPONENTS and the STIFFNESS COMPONENTS options. The variation of the film thickness is again specified in user subroutine UTHICK. In total, four subincrements are specified. A displacement of the rotor center of 1.0×10^{-7} m in each global direction is given for both damping and stiffness properties.

The calculated properties are as follows:

Specified Thickness Rate	Damping Components
$\dot{h} = -1 \times 10^{-7} * \cos \theta \text{ m/s}$	$B_{XX} = -54.3 \times 10^{-3} \text{ N-sec/m}$ $B_{YX} = -22.4 \times 10^{-3} \text{ N-sec/m}$
$\dot{h} = -1 \times 10^{-7} * \sin \theta \text{ m/s}$	$B_{XY} = -16.8 \times 10^{-3} \text{ N-sec/m}$ $B_{YY} = -28.4 \times 10^{-3} \text{ N-sec/m}$

Stiffness

Specified Thickness Rate	Stiffness Components
$\Delta h = -1 \times 10^{-7} * \cos \theta \text{ m/s}$	$K_{XX} = -62.6 \text{ N/m}$ $K_{YX} = -84.1 \text{ N/m}$
$\Delta h = -1 \times 10^{-7} * \sin \theta \text{ m/s}$	$K_{XY} = 119.8 \text{ N/m}$ $K_{YY} = 31.4 \text{ N/m}$

Load-Carrying Capacity at New Rotor Position

Assume that the actual loading of the bearing system increases to the force $F = (1408, 1390, 0)$. Since the resultant load-carrying capacity is not in equilibrium with this force, the rotor moves to a new position. Based on the calculated damping and stiffness properties, a new rotor position, which implies an incremental thickness change in a particular time period, can be estimated. This is done by investigating the mechanical equilibrium of the total system.

The force equilibrium conditions for a nondeformable bearing requires that:

$$F + W + \Delta W = 0$$

From this equation, the required correction for the load-carrying capacity can be calculated. This yields:

$$\Delta W = (-1362, 424, 0)$$

Any incremental change in position of the rotor center causes a change in the load-carrying capacity according to the following relation:

$$[B] \Delta \dot{u} + [K] \Delta u = \Delta W$$

where u is the incremental movement of the rotor center.

After substituting the previously calculated stiffness and damping properties, the above equation can be solved, which yields:

$$\Delta u = (-.450, -1.832, 0) 10^{-6} \text{ m}$$

where a time increment of 10^{-3} seconds is assumed.

From the difference in magnitude of the damping and stiffness properties, it can be concluded that the initial response is dominated by the damping effects.

The above procedure is applied in increment 1. The incremental thickness change is defined in user subroutine UTHICK, based on the previous calculated bearing properties at the original rotor position. This change in film thickness is automatically added to the previous thickness field if the calculation of damping and/or stiffness properties is not activated.

According to the calculated pressure distribution for increment 2, this results in a bearing force of:

$$W_x = -1296 \text{ N}$$

$$W_y = -1513 \text{ N}$$

$$W_z = 0.0 \text{ N}$$

Parameters, Options, and Subroutines Summary

Example e7x16.dat:

Parameters	Model Definition Options	History Definition Options
BEARING	BC FILL	CONTINUE
ELEMENT	CONN GENER	DAMPING COMPONENTS
END	CONNECTIVITY	STIFFNS COMPONENTS
SIZING	CONTROL	THICKNS CHANGE
TITLE	COORDINATE	
	END OPTION	
	FIXED PRESSURE	
	ISOTROPIC	
	NODE FILL	
	THICKNESS	
	TYING	
	VELOCITY	

User subroutines in u7x16.f:

UTHICK
UBEAR

INC : 0
SUB : 1
TIME : 0.000e+00
FREQ : 0.000e+00

prob e7.16 hydrodynamic analysis of a journal bearing



Bearing Pressure (x100)

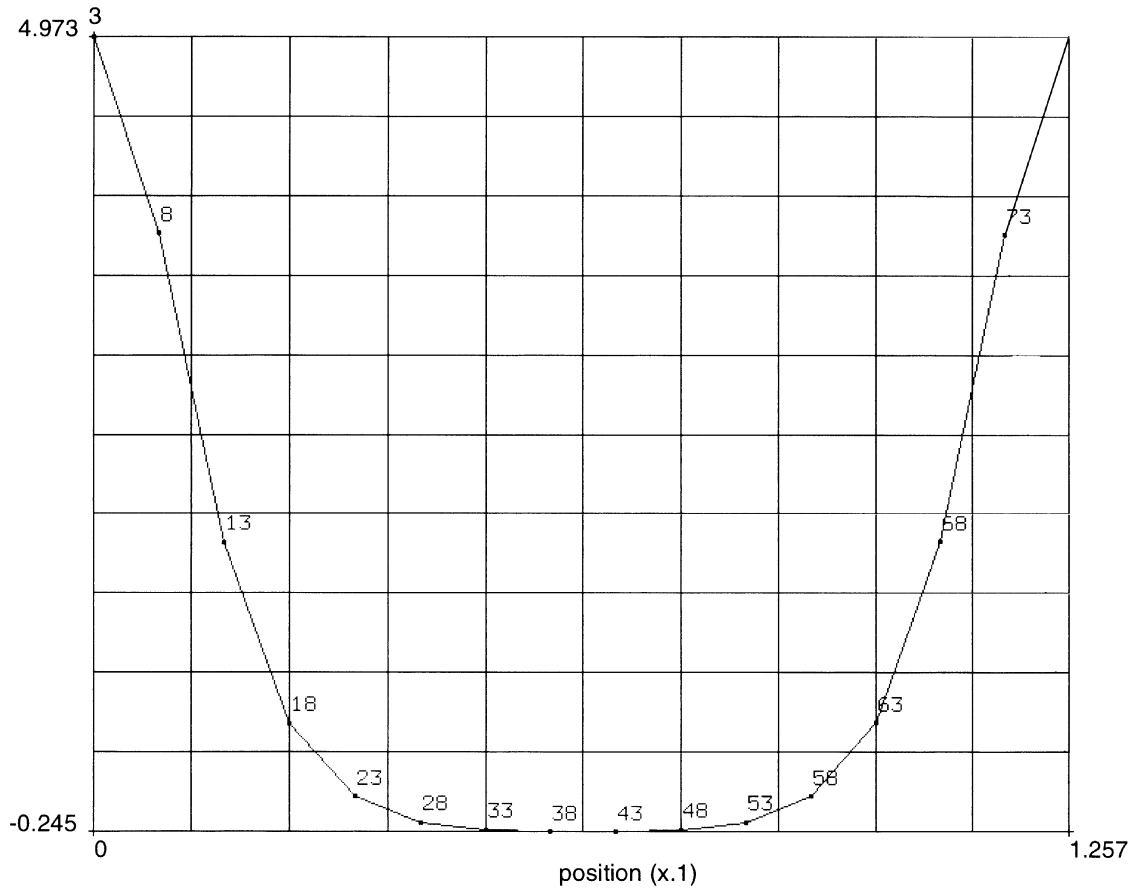


Figure 7.16-2 Path Plot of Pressure Distribution

7.17 Elastic-Plastic Finite Deformation of a Thick-Walled Cylinder

This problem demonstrates the rezoning technique for the elastic-plastic finite deformation of a thick cylinder. The cylinder is subjected to internal pressure which results in large elastic-plastic deformation, after which the load is removed leaving the structure in its permanent plastically deformed shape. Because of the amount of plastic deformation, the FINITE STRAIN option is used in conjunction with the UPDATED LAGRANGE option. Often, in this type of analysis, the mesh becomes seriously distorted, resulting in a low quality solution. This problem demonstrates the REZONING option to resolve this difficulty.

Model

The model consists of five axisymmetric type 10 elements and 12 nodes. The initial inner and outer radii are 1 and 2 m, respectively. The mesh is shown in Figure 7.17-1.

Material Properties

The elastic properties of the material are Young's modulus of 1000 N/m^2 and Poisson's ratio of 0.3. The material has an initial yield stress of 1 N/m^2 and strain hardens at a rate of 3 N/m^2 .

Geometry

No thickness is associated with an axisymmetric element. The constant dilatation method is used for this element by indicating a 1. in the second field of this option.

Boundary Conditions

The thick cylinder is constrained to be under plane-strain conditions ($e_{zz} = 0$).

Loading

An incremental nodal load is prescribed to the nodes on the inner radius (nodes 1 and 2) through the FORCDT option. To determine the current applied pressure, this force needs to be divided by $2\pi R_{\text{current}}$. The prescribed load and resulting pressures are shown in Figure 7.17-2.

Controls

All calculations are saved on the restart file for every increment. The maximum number of increments allowed is 50. The maximum number of recycles was put to 10. This is because very large increments were chosen, and after a rezoning occurs the calculations are not in equilibrium. The PRINT CHOICE option is used to restrict the output to element 1.

Procedure

Using the first input, the analysis is completely carried out in 42 increments. The second input demonstrates the use of the REZONING option. The first analysis is restarted at the end of increment 10. The REAUTO option is used to prematurely discontinue the AUTO LOAD sequence that was defined previously in the first analysis.

The data after the END OPTION, beginning with REZONE and finishing with END REZONE, form one rezoning increment. In this analysis, the coordinates are redefined such that the new inner and outer radii are the same as the deformed radii at increment 10 of the previous analysis. The other points are located such that the new mesh would be regular.

At the conclusion of the rezoning increment, the analysis is continued to the same level of loading.

Results

Figure 7.17-3 shows the deformed mesh during different stages of the analysis. Clearly, the boundary of the deformed cylinder is virtually identical for both analyses. The pressure versus internal radius diagram is shown in Figure 7.17-4, together with the analytical solution for an equivalent rigid workhardening material. Excellent agreement is obtained, both between theory and finite element calculation and between the two analyses.

It should be commented that although rezoning was not necessary in this problem, it is extremely useful in many practical applications in the metal working area.

Parameters, Options, and Subroutines Summary

Example e7x17a.dat:

Parameters	Model Definition Options	History Definition Options
ALL POINTS	CONNECTIVITY	AUTO LOAD
ELEMENT	CONTROL	CONTINUE
END	COORDINATE	
FINITE	END OPTION	
LARGE DISP	FIXED DISP	
REZONE	FORCDT	
SIZING	GEOMETRY	
TITLE	ISOTROPIC	
UPDATE	POST	
	PRINT CHOICE	
	RESTART	
	WORK HARD	

Example e7x17b.dat:

Parameters

ALL POINTS
 ELEMENT
 END
 FINITE
 LARGE DISP
 REZONE
 SIZING
 TITLE
 UPDATE

Model Definition Options

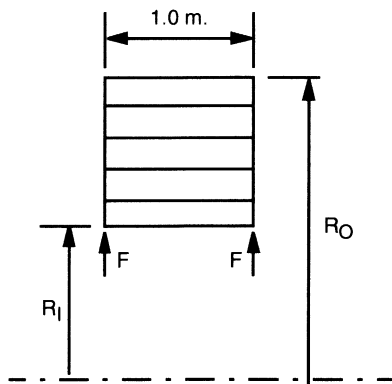
CONNECTIVITY
 CONTROL
 COORDINATE
 END OPTION
 FIXED DISP
 FORCDT
 GEOMETRY
 ISOTROPIC
 POST
 PRINT CHOICE
 REAUTO
 RESTART
 WORK HARD

History Definition Options

AUTO LOAD
 CONTINUE

User subroutine in u7x17.f:

FORCDT



$$R_I = 1.0 \text{ m.}$$

$$R_O = 2.0 \text{ m.}$$

$$E = 1000 \text{ N/m}^2$$

$$\nu = 0.3$$

$$\sigma_y = 1.0 \text{ N/m}^2$$

$$\frac{\partial \bar{\sigma}_y}{\partial \bar{\epsilon}_p} = 3.0$$

Figure 7.17-1 Thick-Walled Cylinder

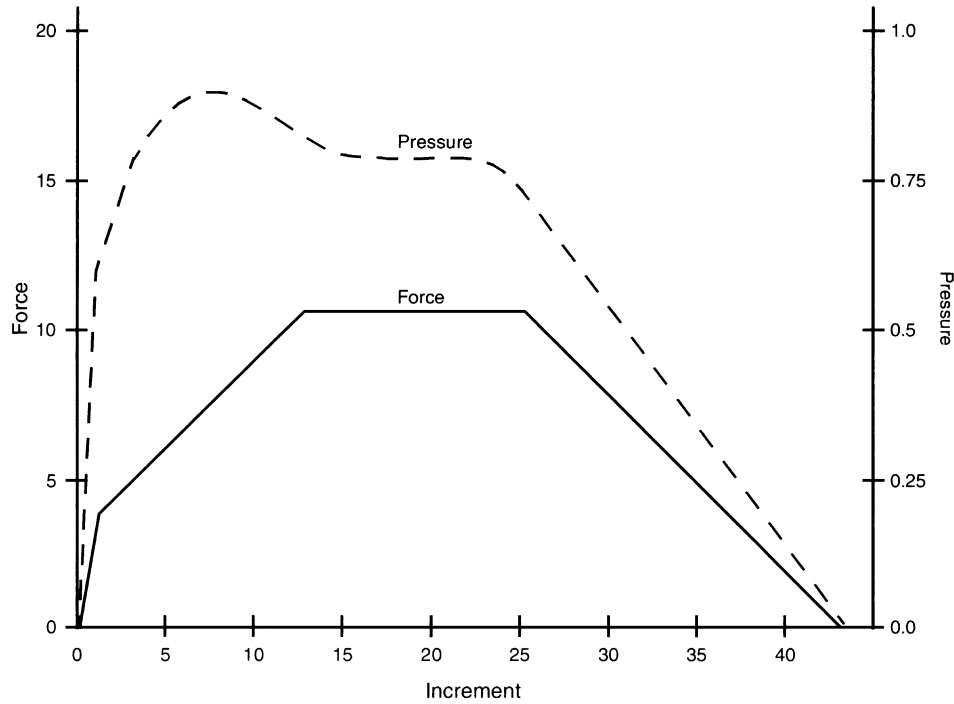


Figure 7.17-2 Applied Load History

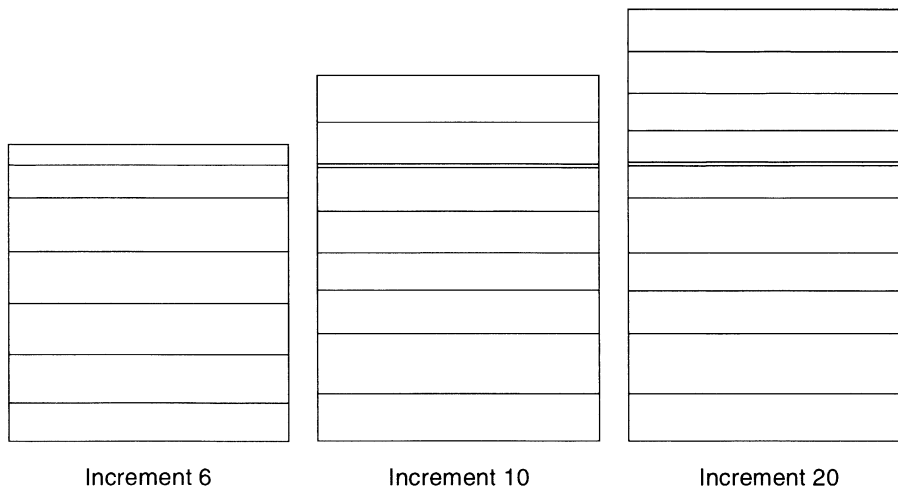


Figure 7.17-3 Deformed Meshes at Increments 6, 10, and 20

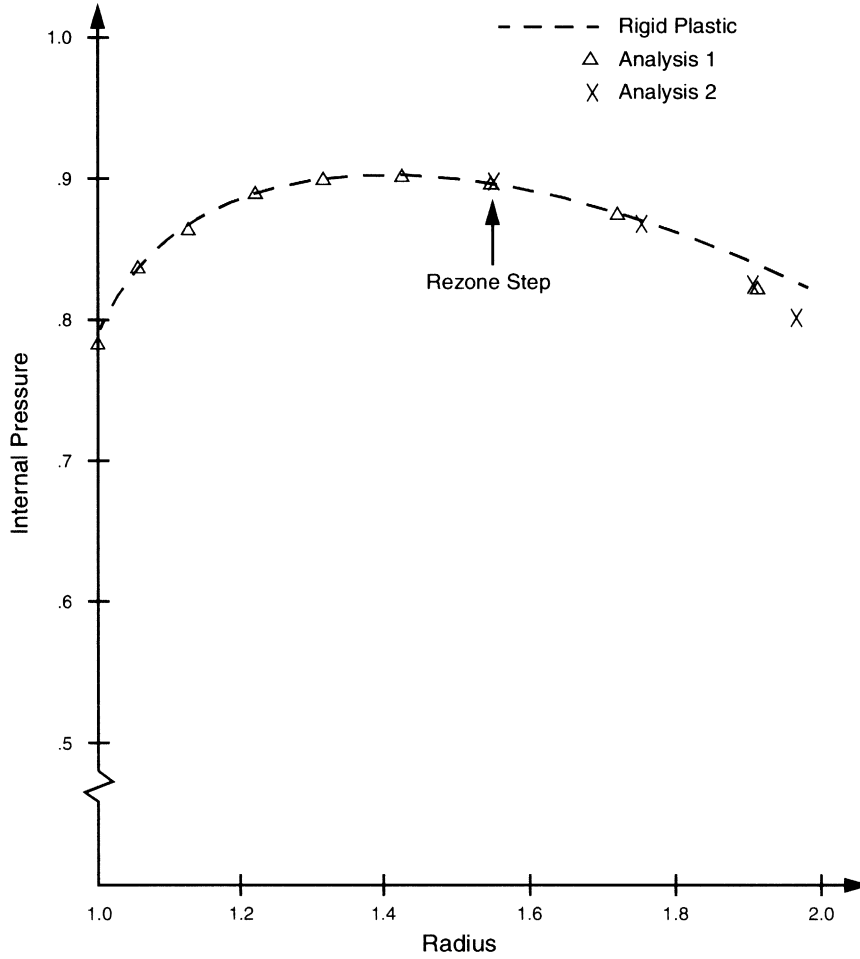


Figure 7.17-4 Internal Pressure vs. Inner Radius



7 Contact

Elastic-Plastic Finite Deformation of a Thick-Walled Cylinder

7.18 Side Pressing of a Hollow Rubber Cylinder

The behavior of a thick, hollow, rubber cylinder, compressed between two rigid plates, is analyzed. The cylinder is long; hence, a condition of plane strain in the cross section is assumed. For reasons of symmetry, only one-quarter of the cylinder needs to be modeled. No friction is assumed between cylinder and plates. The VISCELMOONEY material behavior is used to represent the viscoelastic rubber. The LARGE DISPLACEMENT option is used.

Element

The quarter cylinder is modeled by using 8-node hybrid plane strain elements (MARC element type 32). This element can be used in conjunction with the Mooney material model. Element type 12 is used to model the contact conditions.

Model

Twelve elements are used for the mesh, with two elements specified over the thickness. The geometry of the cylinder and a mesh are shown in Figure 7.18-1.

Material Properties

The MOONEY model definition option is used to specify the rubber properties; the GAP DATA option is used for the input of the gap data. The GAP closure distance is defined as the relative distance before contact occurs, which in this problem equals the initial nodal distance between cylinder and plate. The instantaneous response of the rubber material (MOONEY) can be modeled as a Mooney-Rivlin material with $C_{10} = 8 \text{ N/mm}^2$, $C_{01} = 2 \text{ N/mm}^2$. The time dependent response (VISCELMOONEY) is modeled by a single exponential decay function, with a decay factor of 0.5 at infinite time and a relaxation time of 0.3 seconds.

Loading

The AUTO LOAD option is used to apply five displacement increments to the plate at time $t = 0$. The increment is equal to the one applied in the increment 0. Subsequently, 15 time-steps (AUTO LOAD) of 0.1 seconds (TIME STEP) are applied with zero displacement increments (DISP CHANGE). The applied displacement is reversed and five steps are carried out without change in time, followed by a relaxation period of two seconds applied in 20 increments.

Boundary Conditions

Boundary conditions are along the line $r = 0$ and $z = 0$ due to symmetry and to apply the prescribed motion of the plate.

Tying

The TYING option establishes the connections between the nodal degrees of freedom of the cylinder and that of the gaps. This is necessary as the degrees of freedom of these two elements are not the same.

Results

The cylinder diameter is reduced from 6 mm to 4 mm in five increments. The cylinder is in contact with the plate at four nodes (four gaps have been closed). The incremental displacements have become very small, and the equilibrium is satisfied with high accuracy. The incremental full Newton-Raphson method was used to solve the nonlinear system. The total force on the plate can either be calculated by summing up the gap forces, or can be directly obtained from the reaction force on node 75. In both cases, this leads to a total force $F = 1.9098$ N. A plot of the deformed cylinder is shown in Figure 7.18-2.

After relaxation for 1.5 seconds, the load is reduced by almost 50%, as predicted by the equation $F_1 = F_0(1 - 0.5e^{-t/0.3})$. During that period, all properties are scaled down proportionally and the displacements do not change. The same is true for the second relaxation period.

Parameters, Options, and Subroutines Summary

Example e7x18.dat:

Parameters	Model Definition Options	History Definition Options
ELEMENT	CONNECTIVITY	AUTO LOAD
END	CONTROL	CONTINUE
LARGE DISP	COORDINATE	DISP CHANGE
SIZING	END OPTION	TIME STEP
TITLE	FIXED DISP	
	GAP DATA	
	MOONEY	
	POST	
	PRINT CHOICE	
	RESTART	
	TYING	
	VISCELMOON	

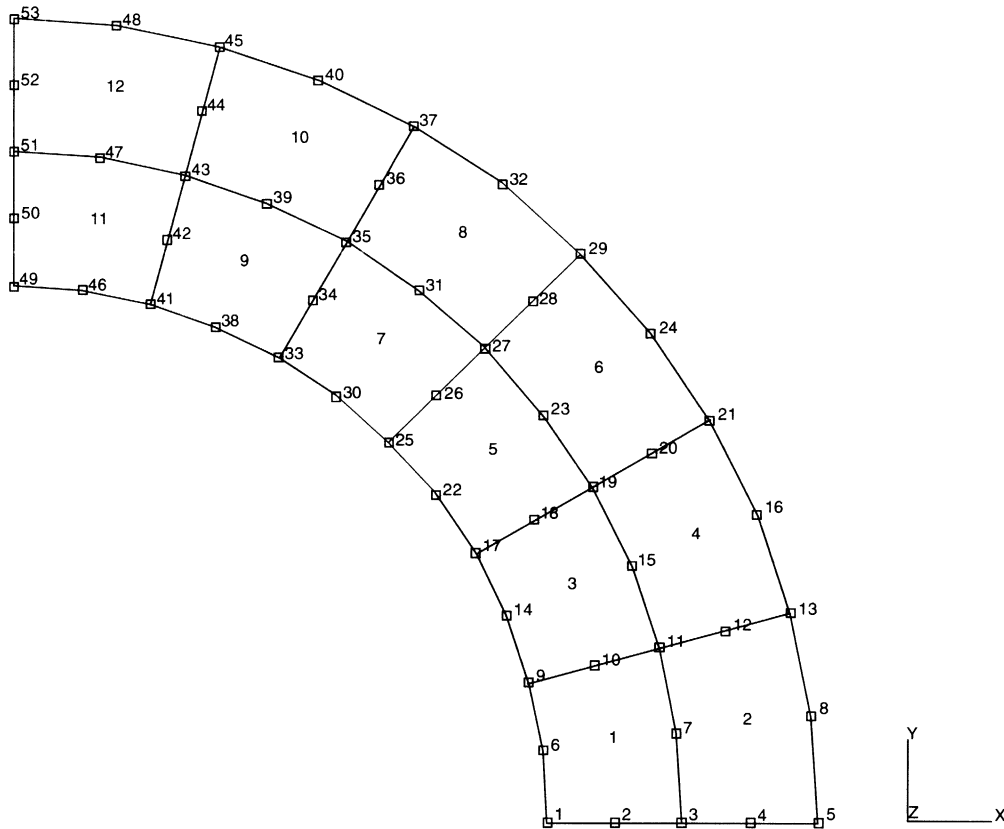
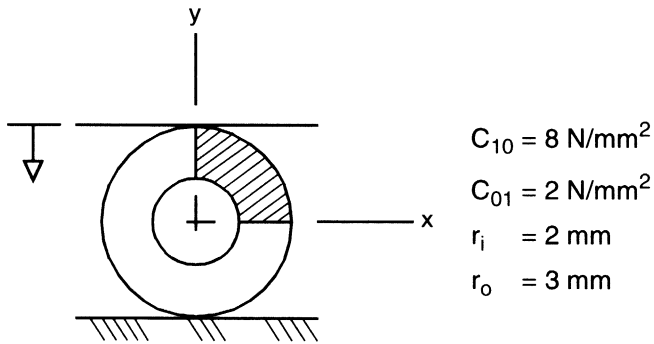
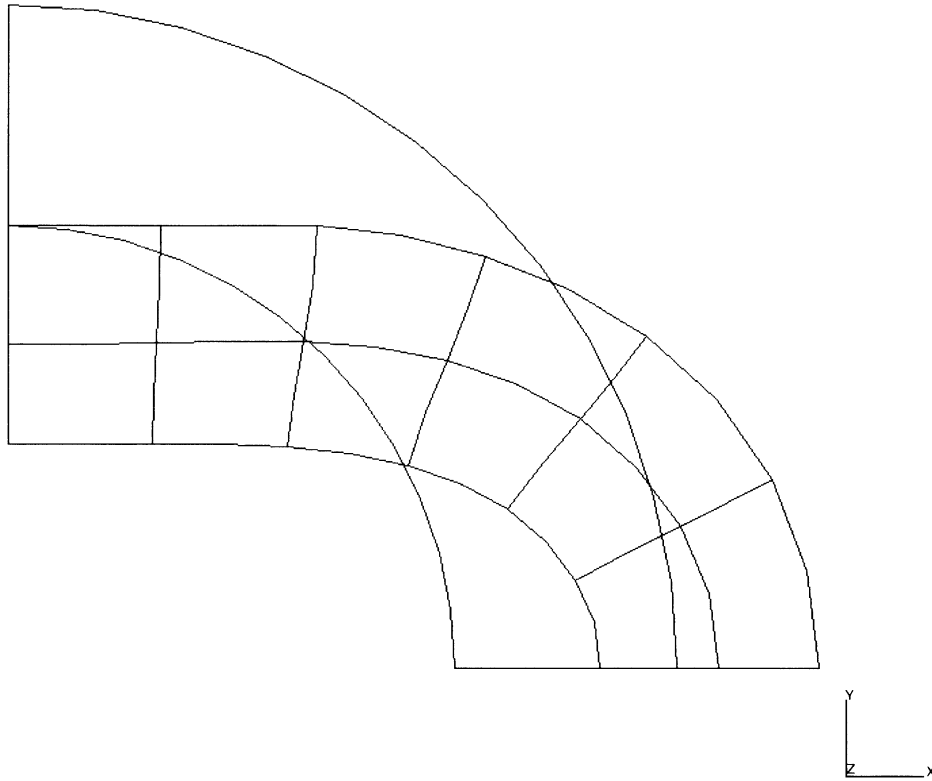


Figure 7.18-1 Rubber Cylinder and Mesh

INC : 5
SUB : 0
TIME : 0.000e+00
FREQ : 0.000e+00



prob e7.18 special topics - visc mooney
Displacements y

Figure 7.18-2 Deformed Mesh Plot

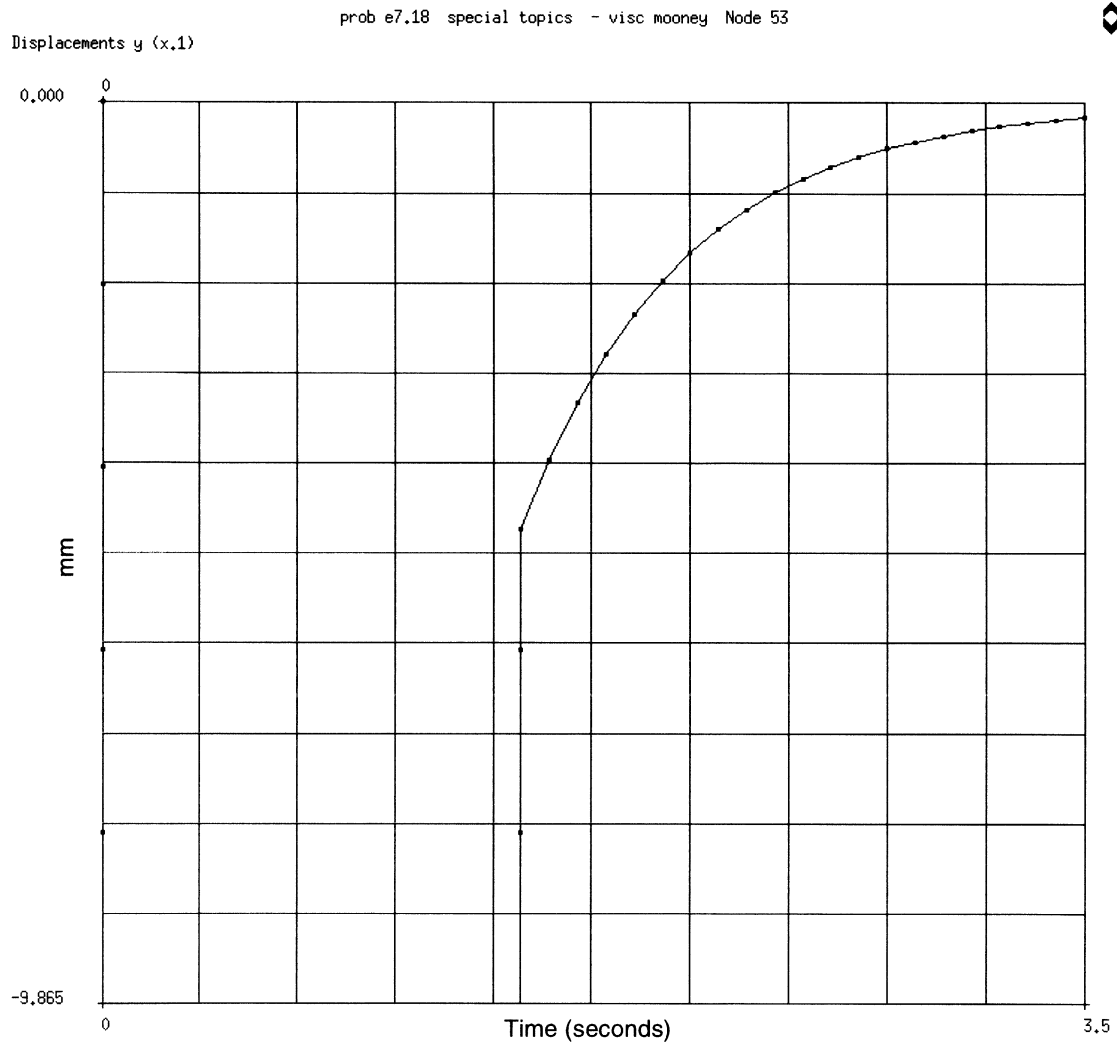


Figure 7.18-3 Displacement History of Node 53

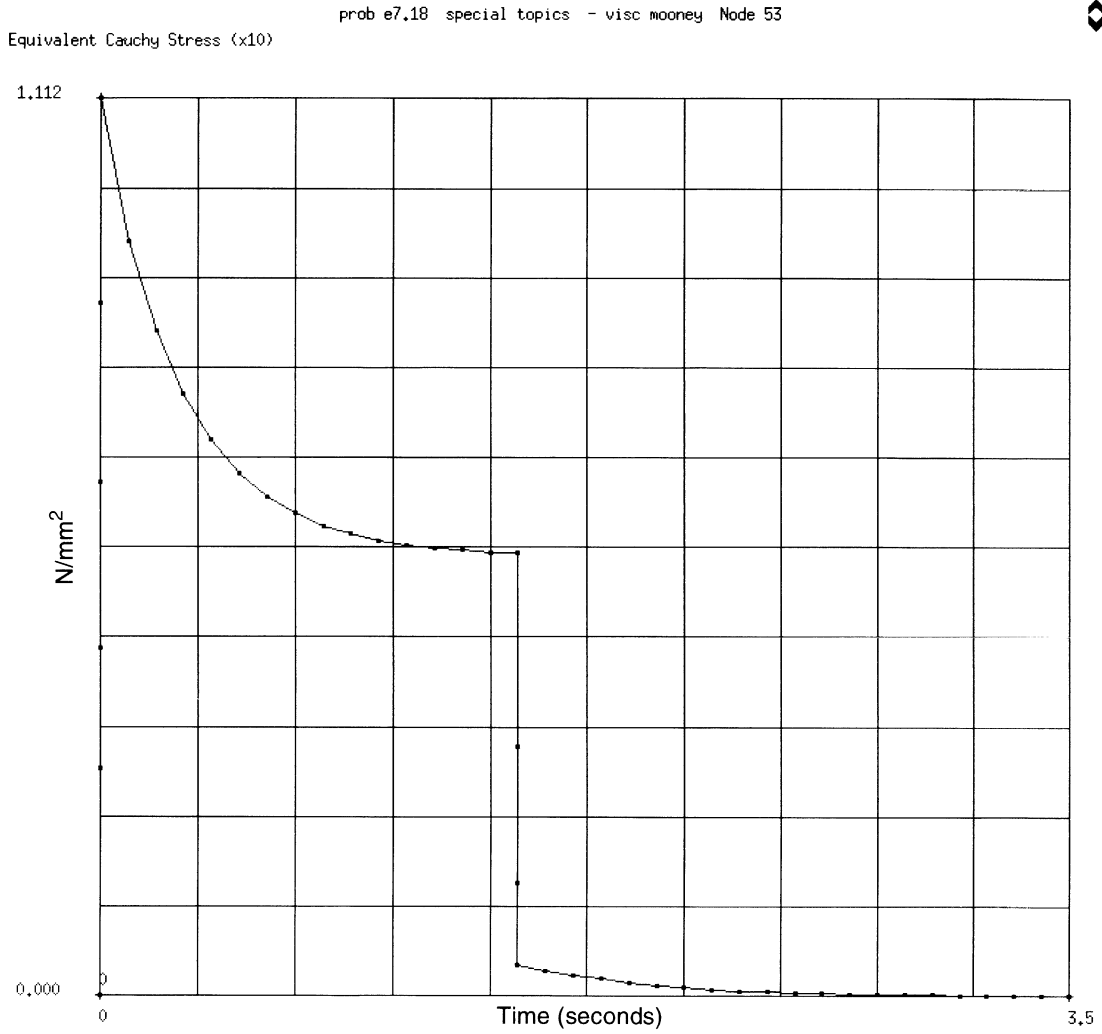


Figure 7.18-4 Stress Relaxation

7.19 Stretching of a Rubber Sheet with a Hole

This example demonstrates the use of the Mooney-Rivlin and Foam material model for a thin rubber sheet analysis with a hole.

This problem is modeled using the two techniques summarized below.

Data Set	Element Type(s)	Number of Elements	Number of Nodes	Differentiating Features
e7x19	26	80	277	Mooney Model
e7x19b	26	80	277	Foam Model

Model

A square sheet of 6.5 cm x 6.5 cm with a hole of radius 0.25 cm is to be analyzed. One quarter of the model is represented due to symmetry. The mesh shown in Figure 7.19-1 has 80 elements and 277 nodes. Element 26, the conventional displacement formulation 8-node quadrilateral, is used. When using the Mooney-Rivlin in compressible material mold, you normally use Herrmann elements. Because this is a plane-stress analysis, the use of Herrmann elements is not necessary. When using the Foam model, conventional elements should always be used. The thickness of the sheet is 0.079 which is entered through the GEOMETRY option.

Material Properties

The material is modeled using the general third-order deformation model with:

$$C_{10} = 20.300 \text{ N/cm}^2$$

$$C_{01} = 5.810 \text{ N/cm}^2$$

$$C_{11} = 0.000 \text{ N/cm}^2$$

$$C_{20} = -0.720 \text{ N/cm}^2$$

$$C_{30} = 0.046 \text{ N/cm}^2$$

for all elements. This data is entered through the MOONEY option.

The material of problem e7.19b is modeled using the three-term rubber-foam model:

Term	μ (N/cm)	α	β
1	1.48269	7.56498	-10.4156
2	-1.48269	-0.504321	-10.4155
3	$\frac{1}{4}0.0041819$	12.1478	-5.67921

for all elements. This data is entered through the OGDEN option.

Boundary Conditions

The nodes along $x = 0$ (edge 1) are fixed in the x-direction. The nodes along $y = 3.25$ (edge 2) and along $y = 0$ (edge 4) are fixed in the y-direction. The nodes which are originally along $x = 3.25$ (edge 3) are all tied to node 277. This will allow you to keep this edge straight and easily calculate the total pulling force. The displacement of node 277 is first set to 0 in the x-direction and then changed through the DISP CHANGE option. The incremental displacement will be 0.325 cm/increment. A total of 10 increments are executed. Hence, the dimension in the x-direction doubles.

Results**For the Incompressible Model:**

The deformed mesh is shown in Figure 7.19-2. The load-deflection curve for node 277 is shown in Figure 7.19-3. There is substantial thinning of the sheet.

For the Foam Model:

The deformed mesh is shown in Figure 7.19-4. The load deflection curve for node 277 is shown in Figure 7.19-4. Note that the deformation is significantly different near the hole.

Parameters, Options, and Subroutines Summary

Example e7x19.dat:

Parameters	Model Definition Options	History Definition Options
ELEMENT	CONNECTIVITY	AUTO LOAD
END	CONTROL	CONTINUE
SIZING	COORDINATES	DIST CHANGE
TITLE	END OPTION	
	DEFINE	
	FIXED DISP	
	GEOMETRY	
	MOONEY	
	POST	
	PRINT CHOICE	
	TYING	



Example e7x19b.dat:

Parameters

ELEMENTS
END
LARGE DISP
SIZING
TITLE

Model Definition Options

CONNECTIVITY
COORDINATE
DEFINE
END OPTION
FIXED DISP
FOAM
GEOMETRY
POST
PRINT CHOICE
TYING

History Definition Options

AUTO LOAD
CONTINUE
DIST CHANGE

MARC

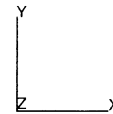
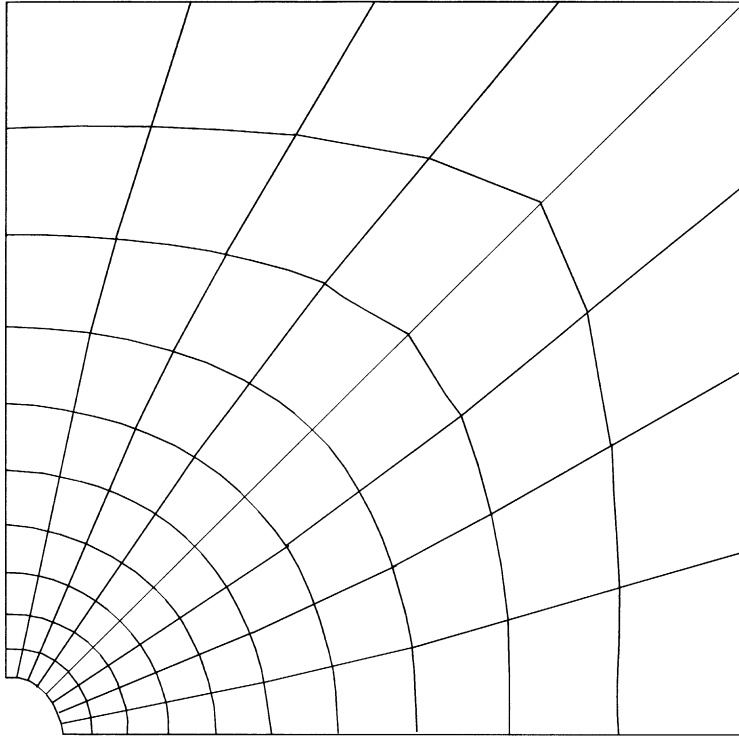
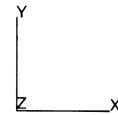
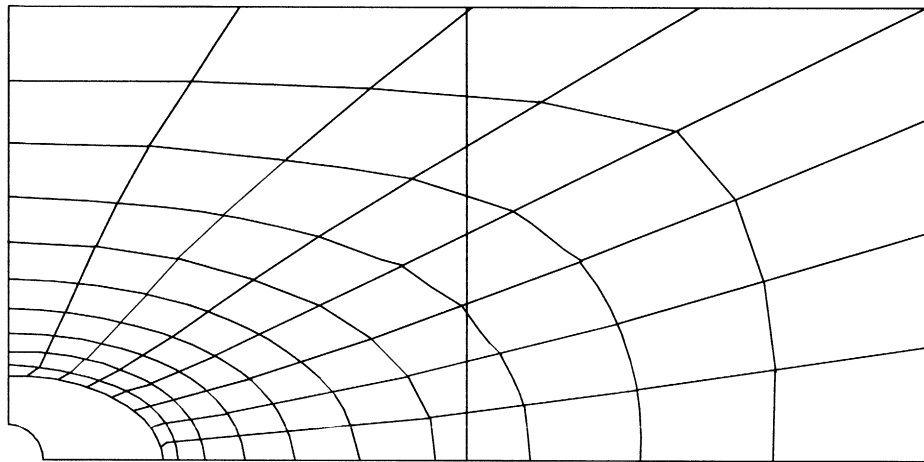


Figure 7.19-1 Finite Element Mesh

INC : 10
SUB : 0
TIME : 0.000e+00
FREQ : 0.000e+00



prob e7.19 plane stress rubber analysis – element 26
Displacement y

Figure 7.19-2 Incompressible Model Deformed Mesh

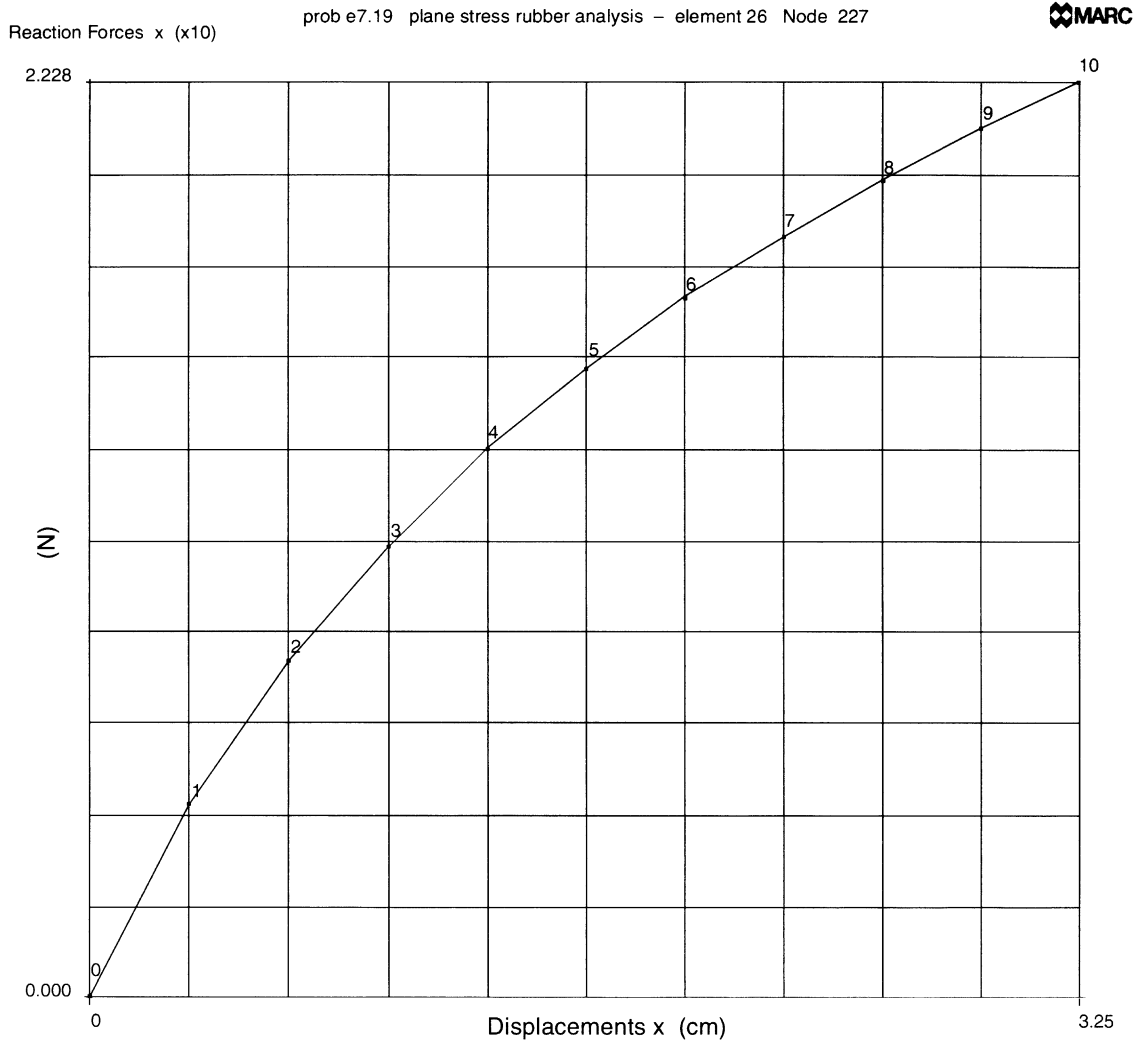
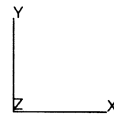
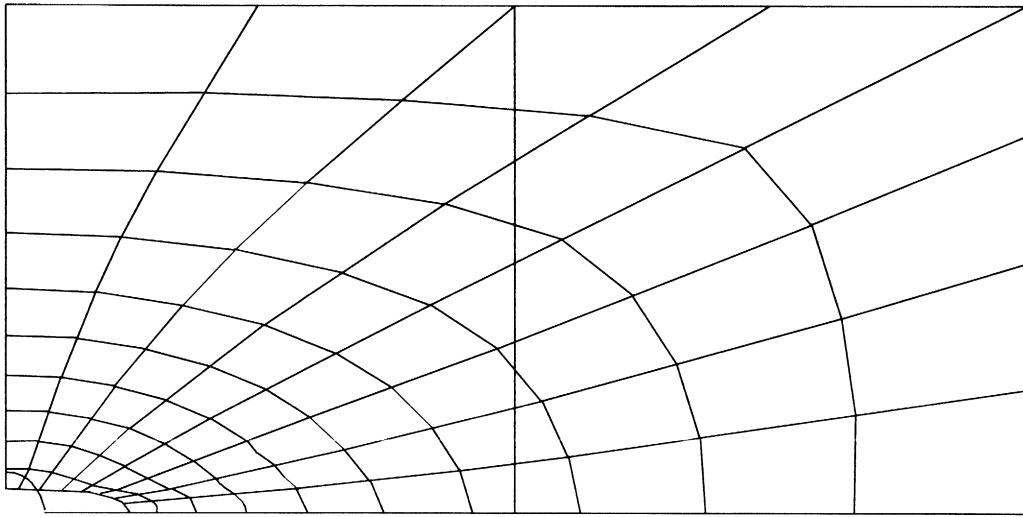


Figure 7.19-3 Incompressible Model Load Deflection Curve at Node 277



INC : 10
SUB : 0
TIME : 0.000e+00
FREQ : 0.000e+00



using foam model

Figure 7.19-4 Foam Model Deformed Mesh

INC : 10
SUB : 0
TIME : 0.000e+00
FREQ : 0.000e+00

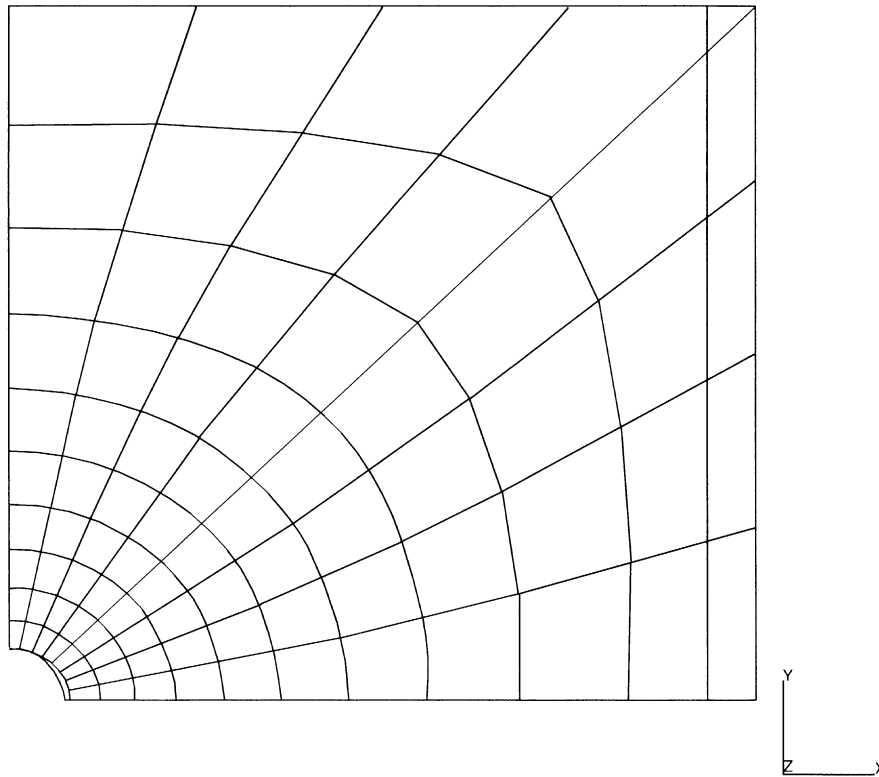


plate with hole using foam model

Figure 7.19-5 Foam Model Load Deflection Curve at Node 277

7.20 Compression of an O-Ring using Ogden Model

This example demonstrates the use of the Ogden rubber model for the high compression of an O-ring. The ring is compressed into a rigid channel. The second analysis is of the same problem, but the follower force stiffness is included. The third analysis uses a simpler mesh to begin with and then demonstrates the adaptive meshing capability. The last analysis demonstrates the use of conventional displacement based elements in an updated Lagrange framework of elasticity.

This problem is modeled using the four techniques summarized below.

Data Set	Element Type(s)	Number of Elements	Number of Nodes	Differentiating Features
e7x20	82	544	605	No Follower Force Stiffness
e7x20b	82	544	605	Follower Force Stiffness
e7x20c	82	29	40	Adaptive Meshing
e7x20d	10	544	605	Updated Lagrange, Follower Force Stiffness

Element

Library element 82, a 5-node axisymmetric element using the Herrmann formulation, is used for the first 3 data sets. In the first two analyses, there are 544 elements and 605 nodes as shown in Figure 7.20-1. Three rigid bodies are used to simulate the channel. The ring has a mean radius of 12 cm and the loading radius is 1.5 cm. In the third analysis, the coarse mesh shown in Figure 7.20-2 is used. This mesh begins with 29 elements and 40 nodes.

In the last analysis, the conventional displacement element type 10 is used. The incompressibility is treated using the same framework as the plasticity using $F^c F^p$ formulation where the elemental pressure degrees-of-freedom are condensed out before element assembly. The output stresses is Cauchy by default while the output strain is the logarithmic or true strain in the current configuration.

The rigid surface at the outside radius is first moved inwards a distance of 0.5 cm in a period of 50 seconds. The surface is then frozen and an external pressure of 18.8 N/cm² is applied onto the left face during 47 increments. The FOLLOW FOR option is used to insure that the load is applied on the deformed geometry. In the second analysis, the follower force stiffness is included. This should improve the convergence behavior.

Material Properties

The O-ring can be described using the Ogden material model using a three term series. The stress-strain curve for this model is shown in Figure 7.20-3. The data was fit such that:

Term	μ (N/cm ²)	α
1	6.30	1.3
2	0.12	5.0
3	-0.10	-2.0

and the bulk modulus was 1.0E9 N/cm².

Contact/Boundary Conditions

All of the kinematic constraints are provided using rigid contact surfaces. Coulomb friction with a coefficient of friction of 0.1 is specified.

Controls

The full Newton-Raphson iterative method is used with a convergence tolerance of 10% on residuals requested. Because of the large compressive stresses that are generated, the solution of nonpositive definite systems is forced. Additionally, a flag is set that tells MARC to only use the deviatoric stresses in the initial stress stiffness matrix. While this can slow convergence, it tends to improve stability. The PRINT,5 option is used to obtain more information regarding the contact behavior. The NO PRINT option is used to suppress the printout.

Adaptive Meshing

In the third analysis, the adaptive meshing technique is demonstrated. The mean strain energy criteria is used with a factor of 0.9. The maximum number of subdivisions allowed is two. As the O-ring initially is round, this additional information is provided using the SURFACE option. A circle at origin (1.5, 12.0 cm) and a radius of 1.5 cm is defined. The ATTACH NODE option is used to associate the original nodes with this geometry.

Results

The deformed mesh at increments 10, 30, and 50 are shown in Figure 7.20-4 through Figure 7.20-6. One observes that at increment 50, the ring almost completely fills the corner regions. The mean second Piola-Kirchhoff stresses are shown in Figure 7.20-7. One should note that in all these plots, the free surface to which the pressure is applied remains almost perfectly circular. Finally, the contact forces are shown in Figure 7.20-8 for the total Lagrange formulation which, as expected, are identical to the ones obtained with the updated Lagrange formulation as shown in Figure 7.20-13.

The progression of meshes using the adaptive meshing is shown in Figure 7.20-9 through Figure 7.20-12. At the end of the analysis, the total number of elements is 104 and the number of nodes is 148.

Parameters, Options, and Subroutines Summary

Example e7x20.dat, e7x20b.dat, and e7x20d.dat:

Parameters	Model Definition Options	History Definition Options
ELEMENT	CONNECTIVITY	CONTINUE
END	CONTACT	DIST LOADS
FOLLOW FOR	CONTROL	MOTION CHANGE
LARGE DISP	COORDINATES	TIME STEP
PRINT	DEFINE	
SIZING	DIST LOADS	
TITLE	END OPTION	
	OGDEN	
	OPTIMIZE	
	POST	

Example e7x20c.dat:

Parameters	Model Definition Options	History Definition Options
ADAPTIVE	ADAPTIVE	AUTO LOAD
ELEMENT	ATTACH NODE	CONTINUE
END	CONNECTIVITY	DIST LOADS
FOLLOW FOR	CONTACT	MOTION CHANGE
LARGE DISP	CONTROL	TIME STEP
PRINT	COORDINATES	
SETNAME	DEFINE	
SIZING	DIST LOADS	
TITLE	END OPTION	
	OGDEN	
	OPTIMIZE	
	POST	

INC : 0
SUB : 0
TIME : 0.000e+00
FREQ : 0.000e+00

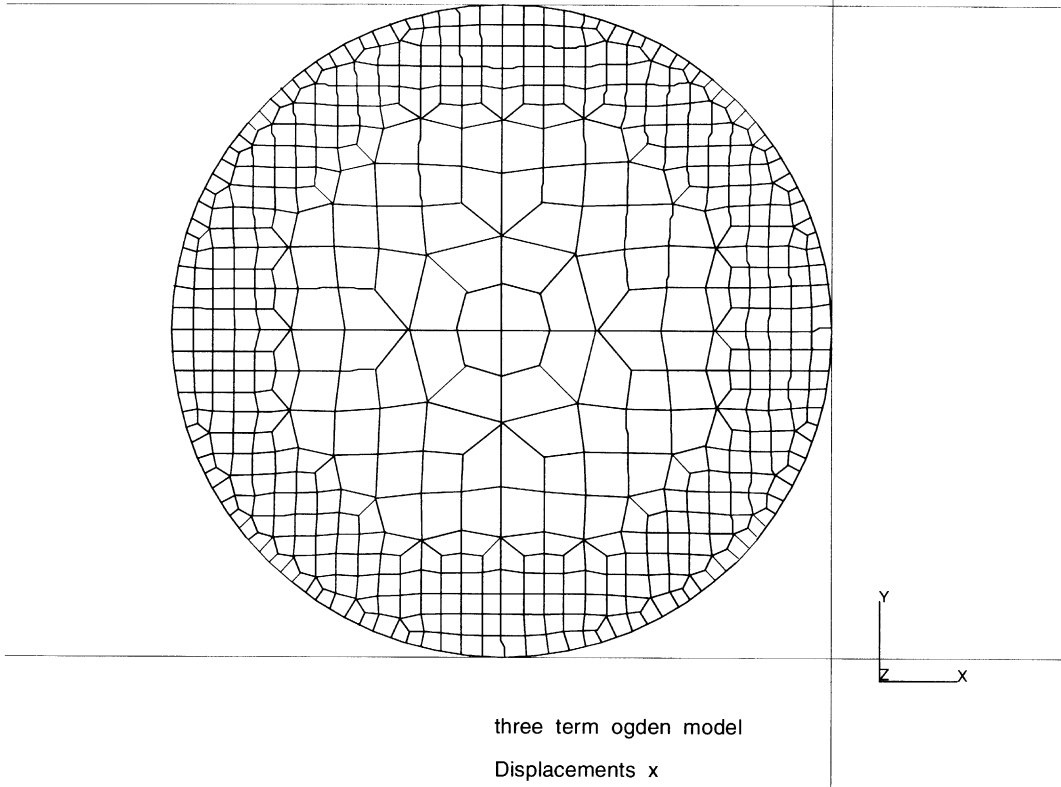


Figure 7.20-1 O-Ring Mesh

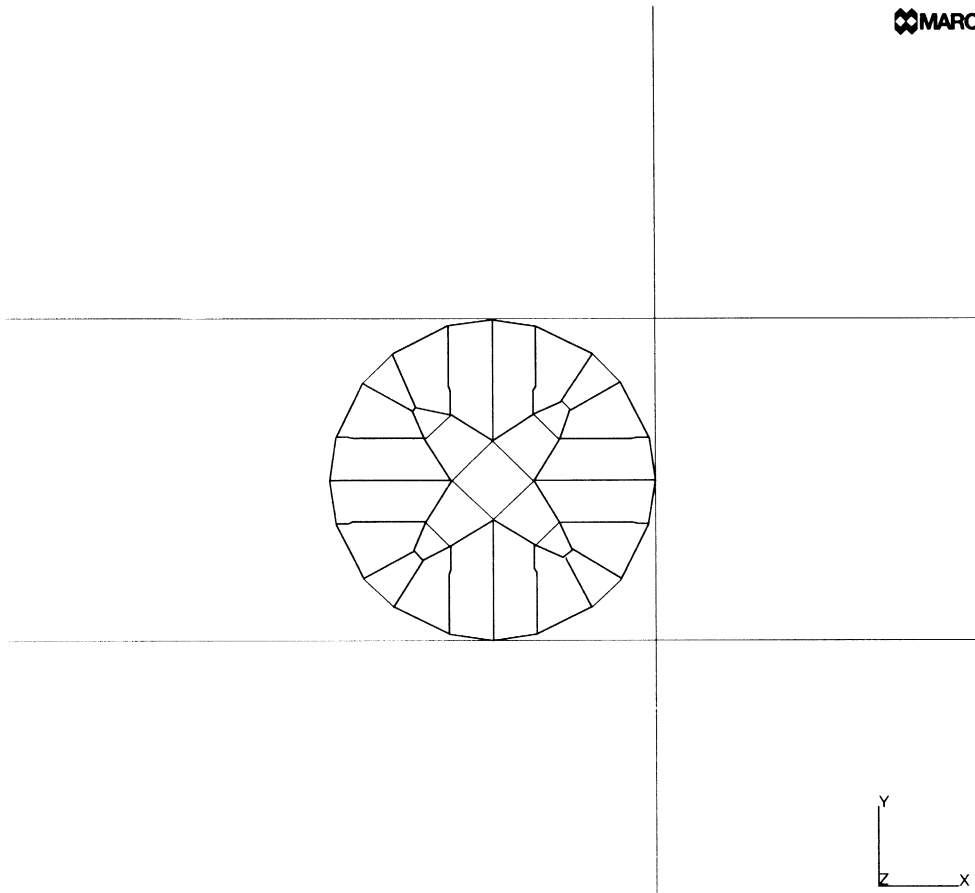


Figure 7.20-2 Coarse O-Ring Initial Mesh for Data Set e7x20c

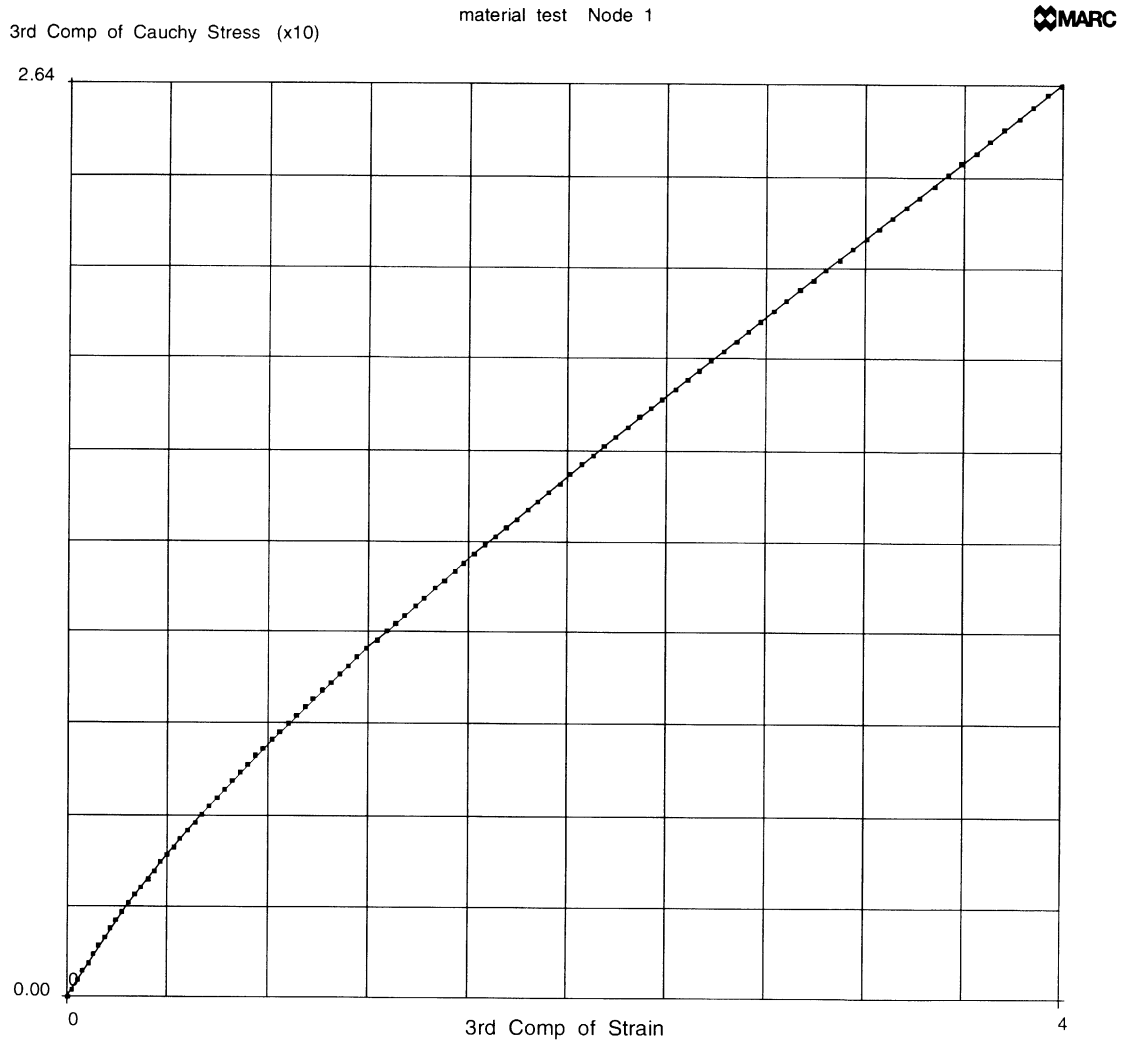


Figure 7.20-3 Stress-Strain Curve

INC : 10
SUB : 0
TIME : 2.500e+01
FREQ : 0.000e+00

MARC

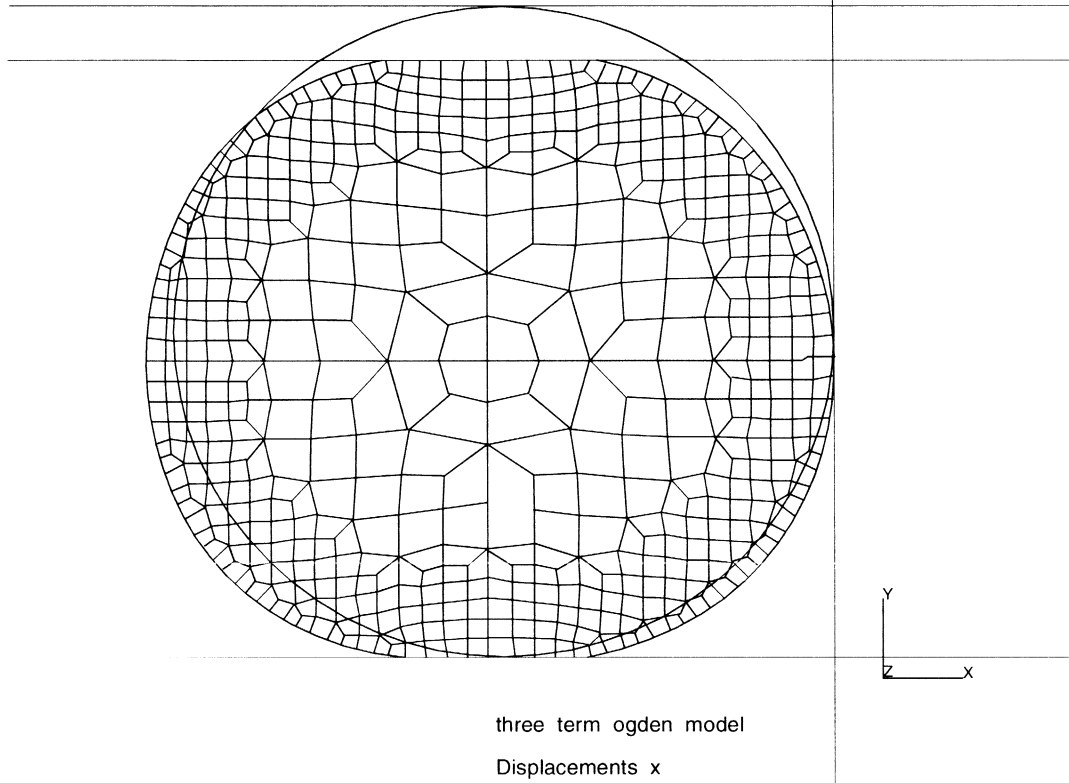


Figure 7.20-4 Deformed Mesh, Increment 10

INC : 30
SUB : 0
TIME : 6.000e+01
FREQ : 0.000e+00

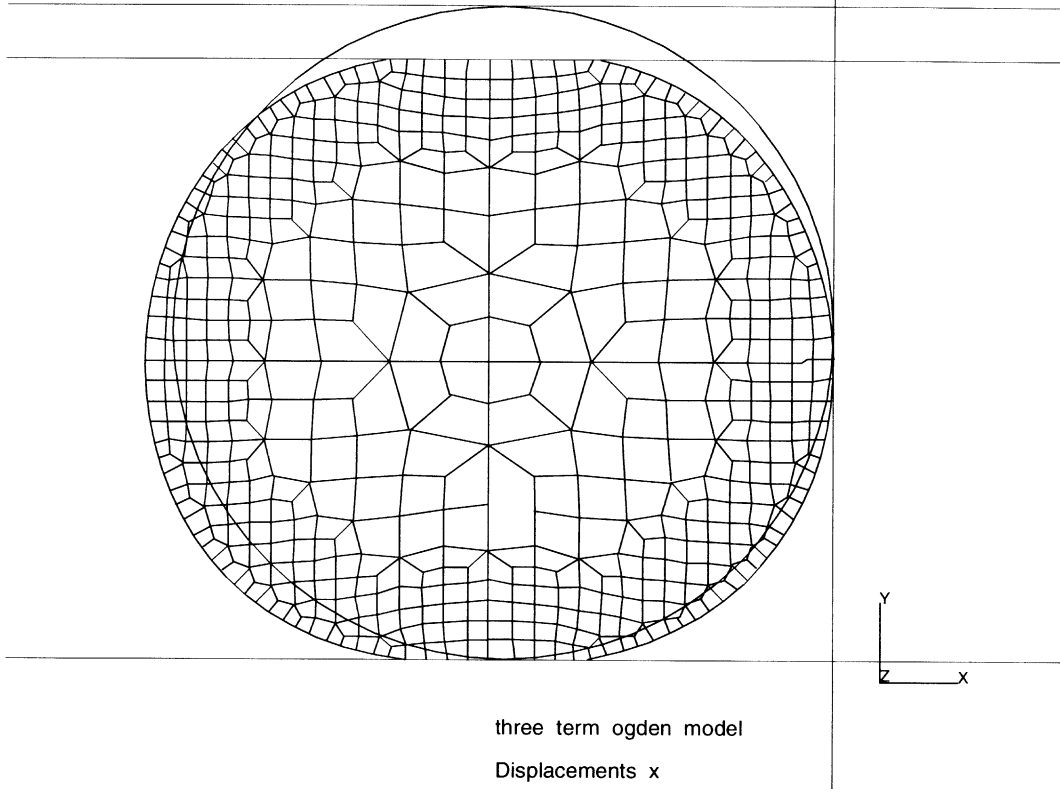


Figure 7.20-5 Deformed Mesh, Increment 30

INC : 50
SUB : 0
TIME : 8.000e+01
FREQ : 0.000e+00

MARC

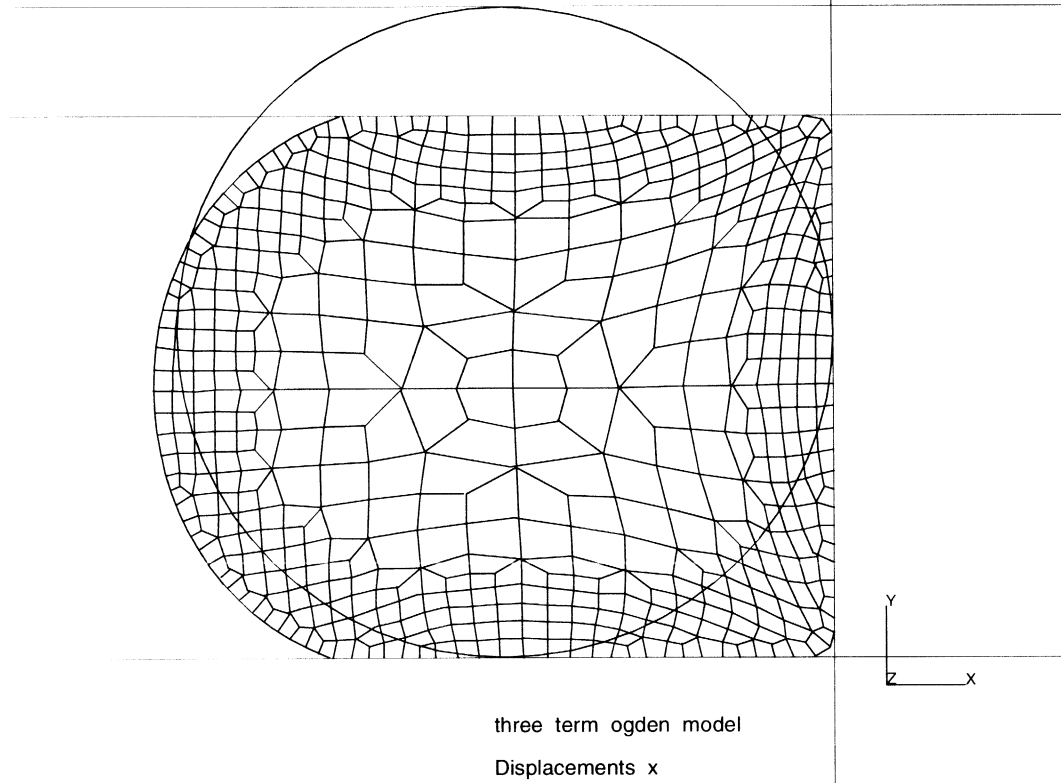


Figure 7.20-6 Deformed Mesh, Increment 50

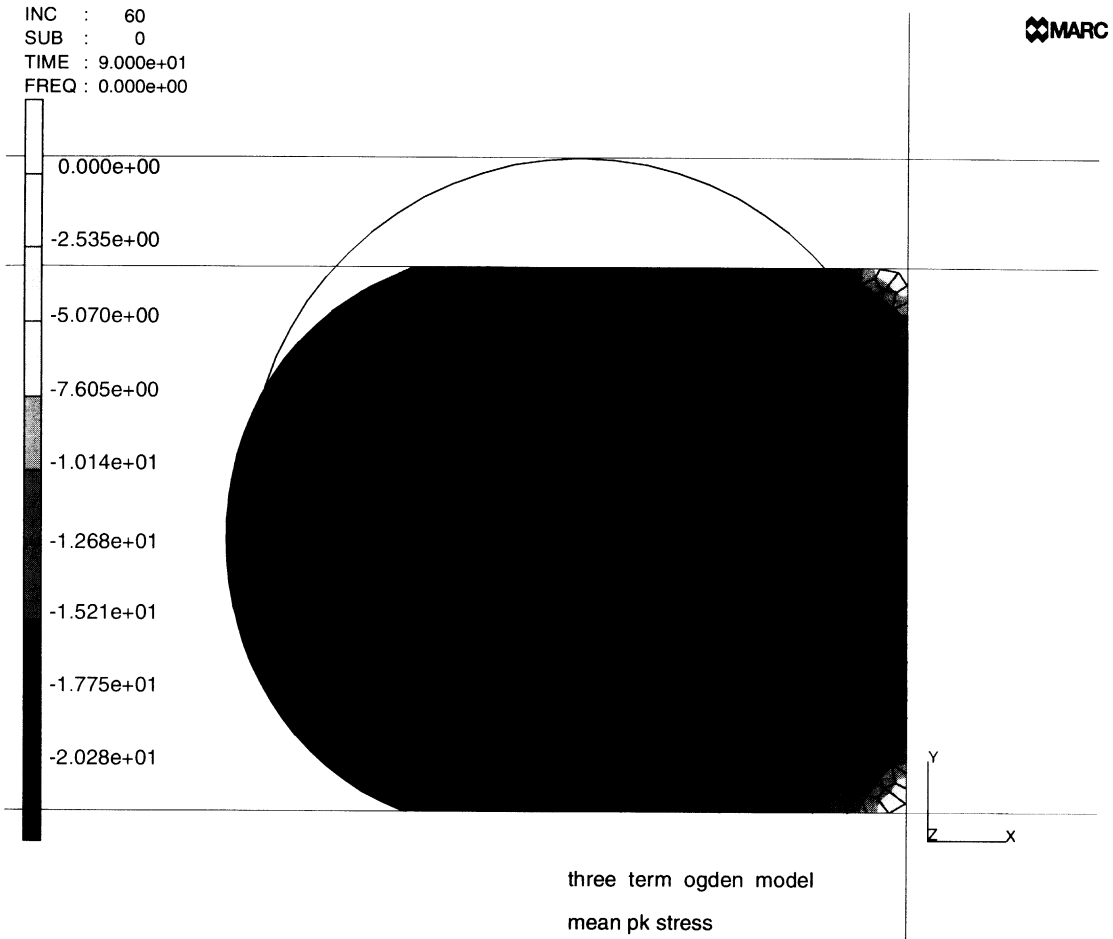


Figure 7.20-7 Mean Stress Distribution

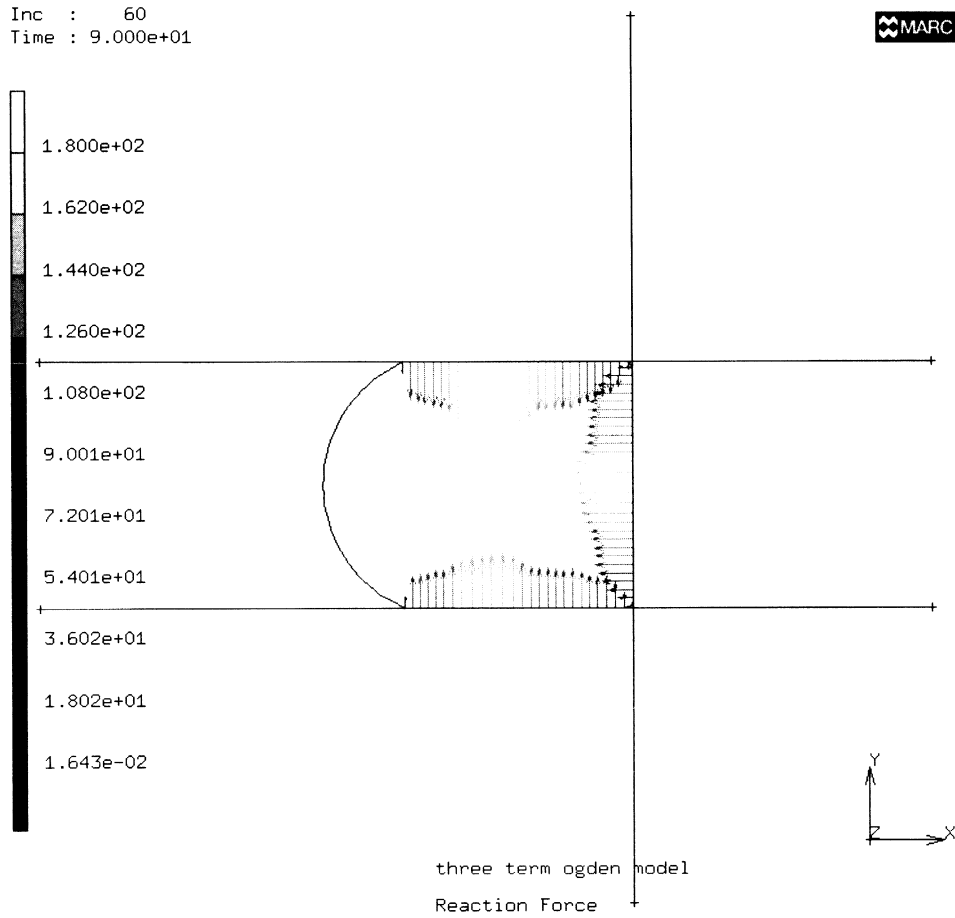


Figure 7.20-8 Contact Forces

INC : 10
SUB : 0
TIME : 2.500e+01
FREQ : 0.000e+00

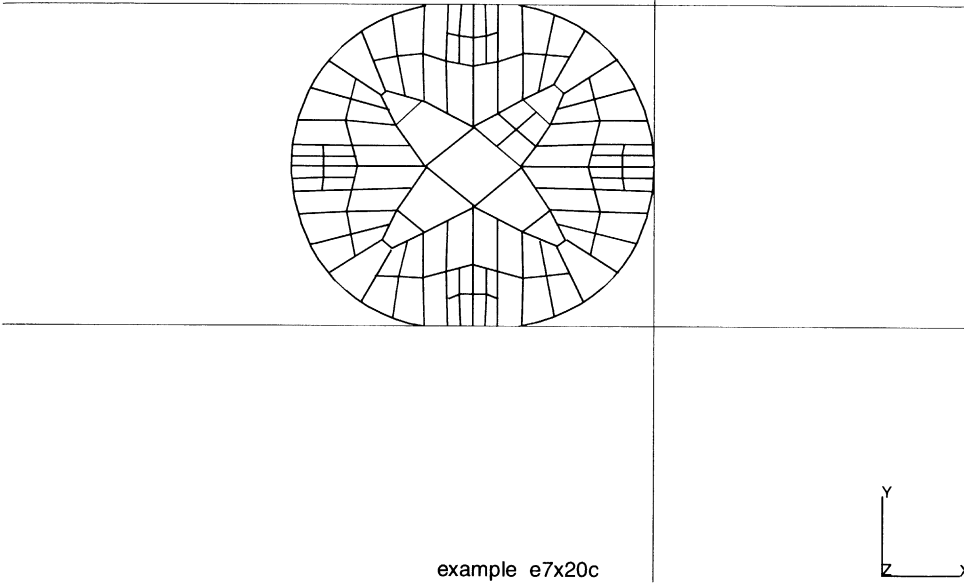


Figure 7.20-9 Adaptive Mesh at Increment 10

INC : 20
SUB : 0
TIME : 5.000e+01
FREQ : 0.000e+00

MARC

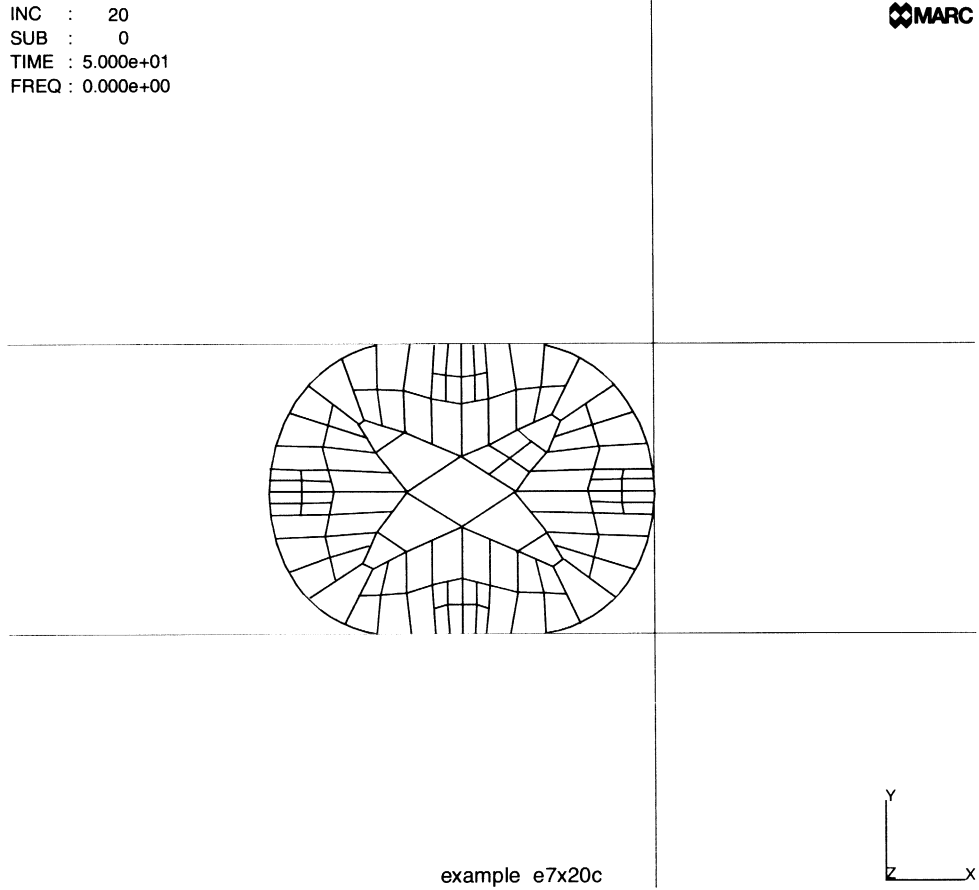


Figure 7.20-10 Adaptive Mesh at Increment 20

INC : 40
SUB : 0
TIME : 7.000e+01
FREQ : 0.000e+00

MARC

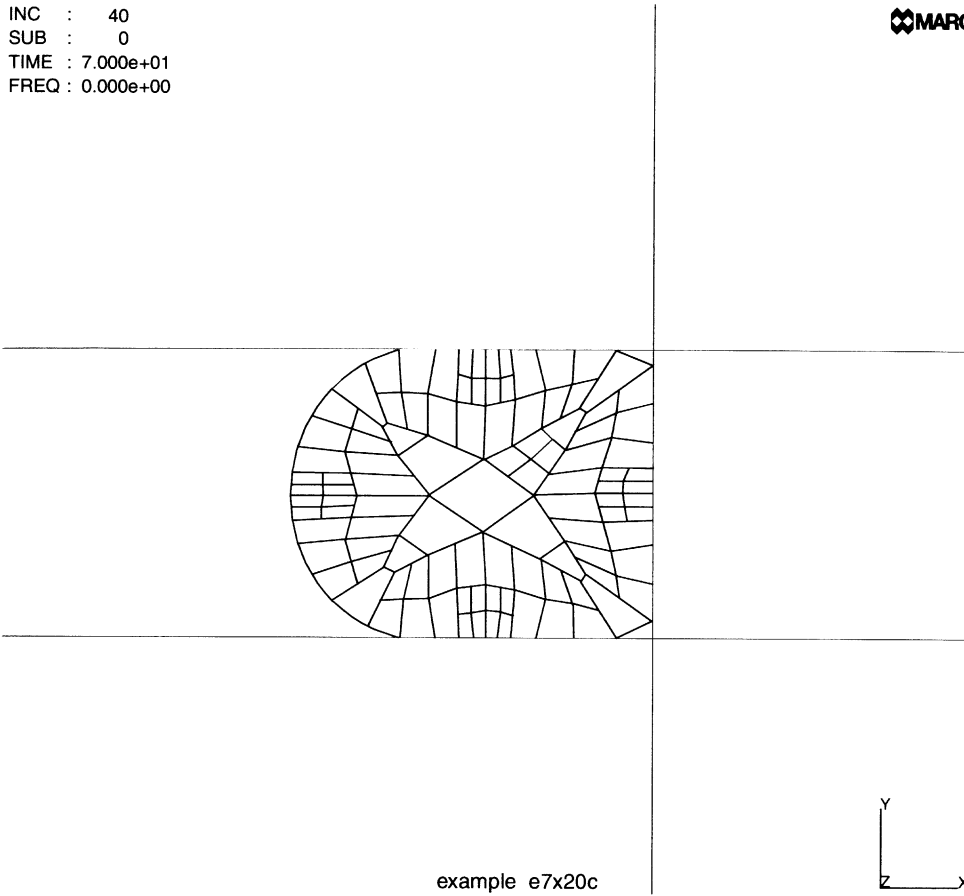


Figure 7.20-11 Adaptive Mesh at Increment 40

INC : 67
SUB : 0
TIME : 9.700e+01
FREQ : 0.000e+00

MARC

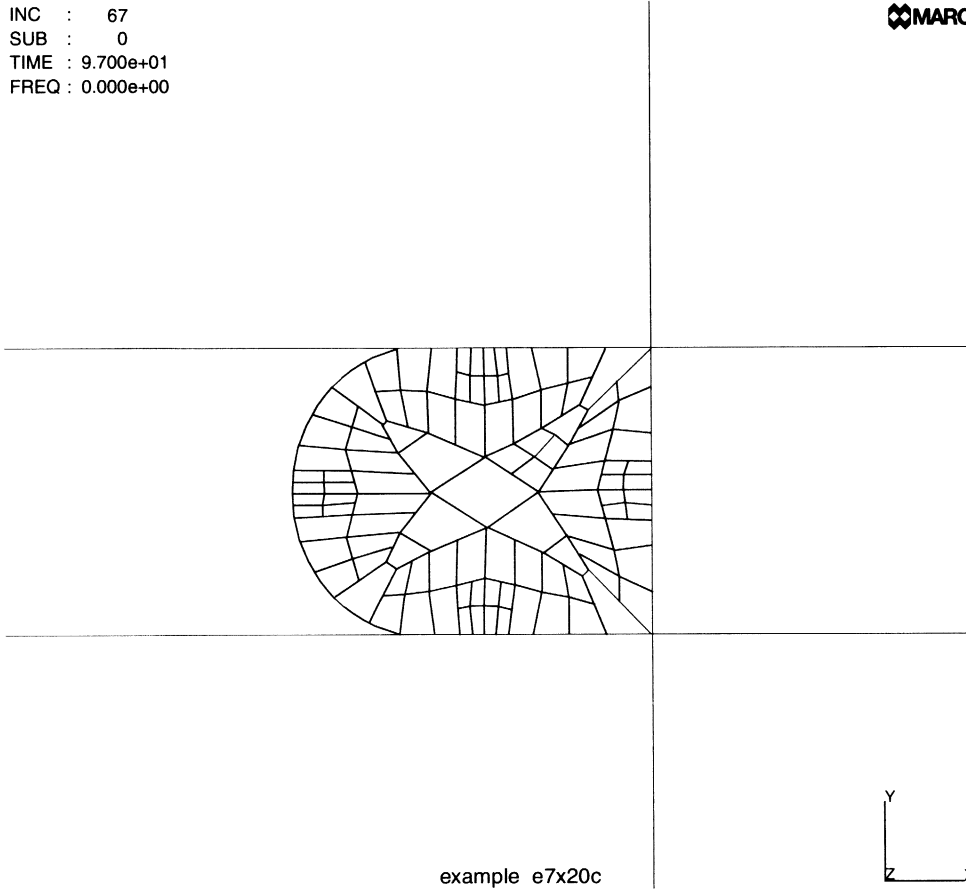


Figure 7.20-12 Adaptive Mesh at Increment 67

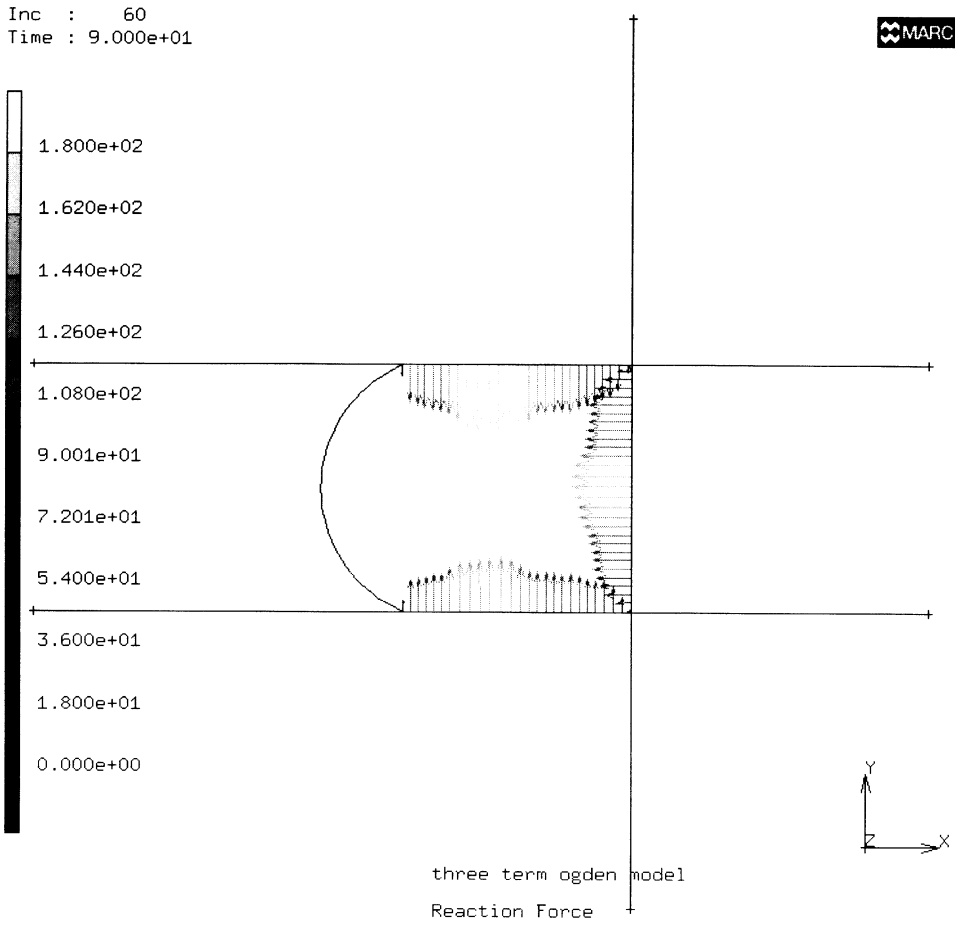


Figure 7.20-13 Contact Forces for the Updated Lagrange Formulation

7.21 Stretching of a Rubber Plate with Hole

This example demonstrates the use of the Ogden material model for a rubber sheet analysis.

Element

Element type 26 is an eight-node plane stress element. The plate is 10 cm x 10 cm, and the hole has a radius of 1. Due to symmetry, only one quarter of the model is used. The mesh is shown in Figure 7.21-1.

Loading

The $x = 0$ and $y = 0$ are symmetry planes. The line at $x = 5$ cm is being pulled with a uniform displacement of 2.5 cm over 5 increments through the DISP CHANGE and AUTO LOAD options.

Material Properties

The sheet is represented using the Ogden material model using a three-term series. The stress-strain curve for this model is shown in Figure 7.21-2. The data was fit such that:

Term	μ (N/cm ²)	α
1	19.7	1.3
2	0.038	5.0
3	-0.32	-2.0

The bulk modulus is 1×10^8 N/cm².

Geometry

The plate thickness is 1.0.

Controls

The full Newton-Raphson procedure is used with a convergence tolerance of one percent of residuals. Typically, one iteration was required to achieve convergence.

Results

The final deformed mesh is shown in Figure 7.21-3. The stress contours and the strain contours are shown in Figure 7.21-4 and Figure 7.21-5, respectively. One can observe that the strain was 250% in the vicinity of the hole.



Parameters, Options, and Subroutines Summary

Example e7x21.dat:

Parameters

ELEMENT
END
LARGE DISP
SIZING
TITLE

Model Definition Options

CONNECTIVITY
CONTROL
COORDINATES
END OPTION
FIXED DISP
GEOMETRY
OGDEN
OPTIMIZE
POST

History Definition Options

AUTO LOAD
CONTINUE
DISP CHANGE

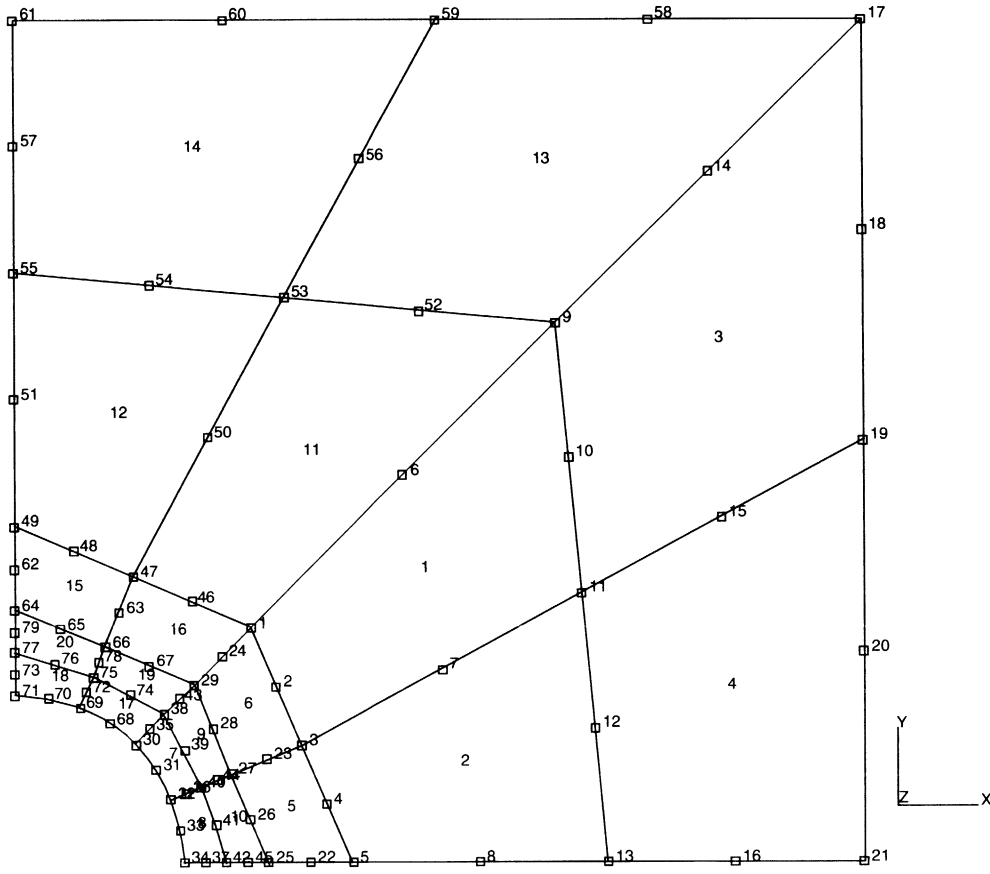


Figure 7.21-1 Finite Element Mesh

3rd Comp of Cauchy Stress (x10)

material test Node 1

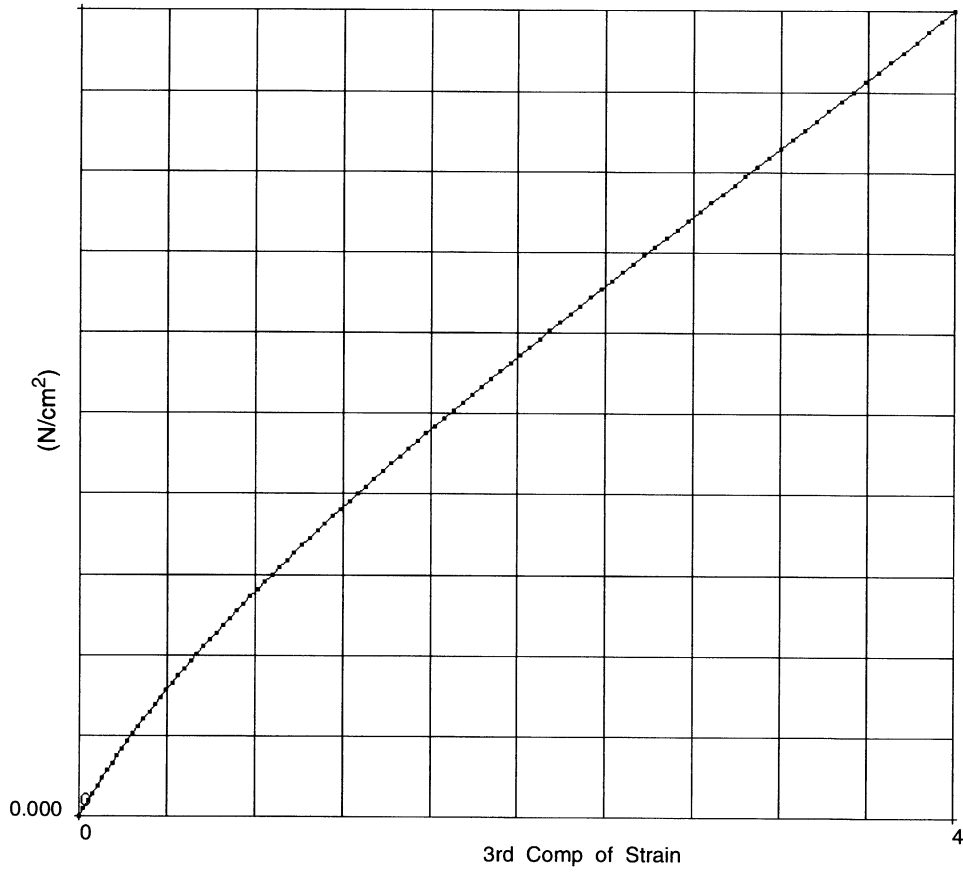
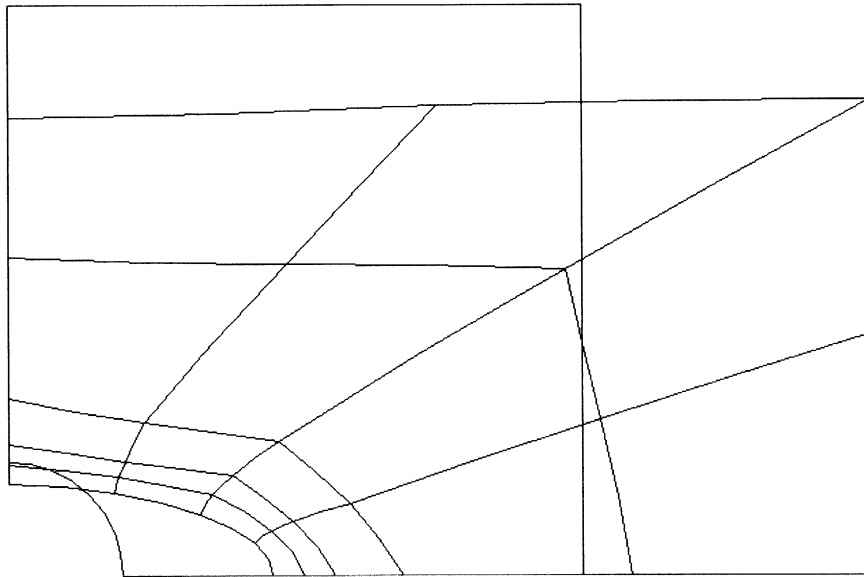


Figure 7.21-2 Stress-Strain Curve

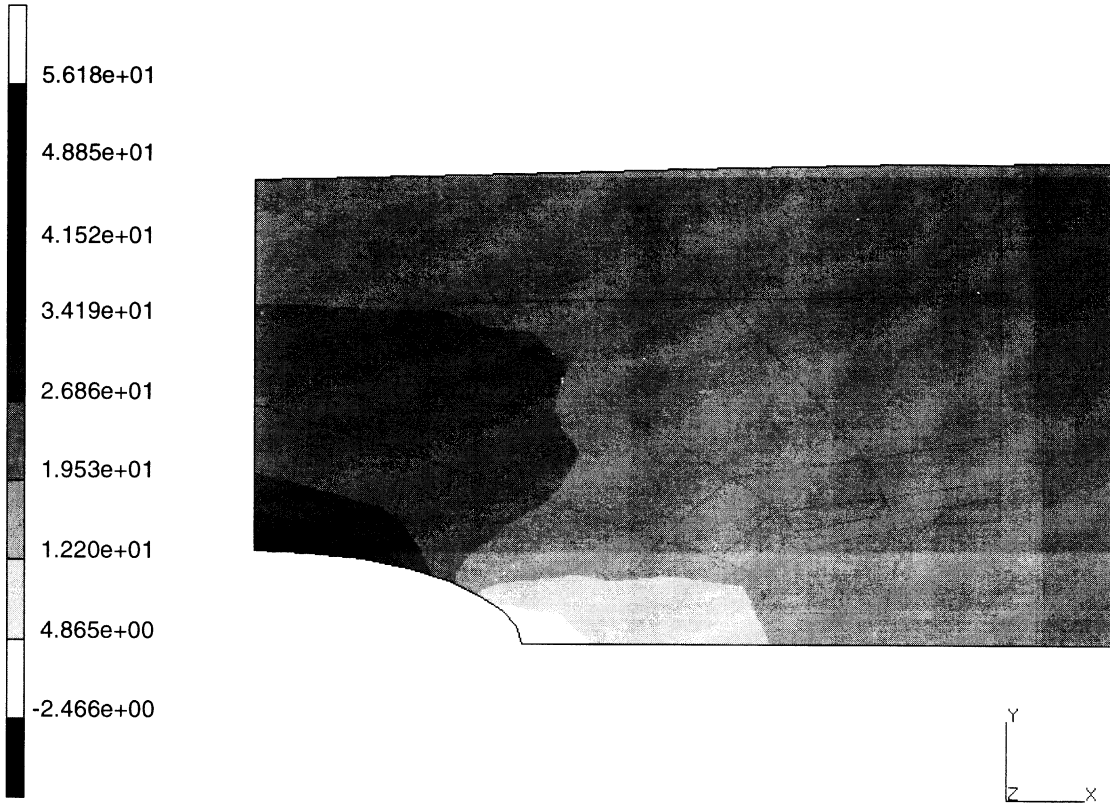
INC : 5
SUB : 0
TIME : 0.000e+00
FREQ : 0.000e+00



prob e7.21 ogden analysis plate with hole – elmt 26
cauchy sigma-zz

Figure 7.21-3 Deformed Mesh

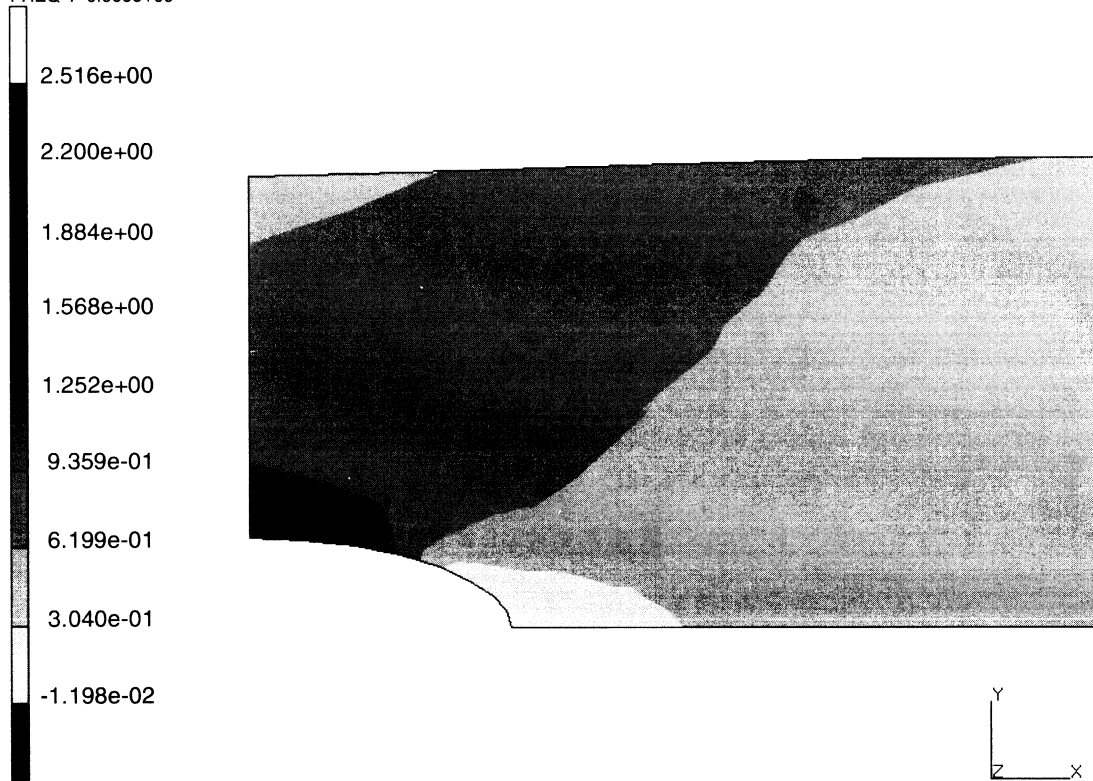
INC : 5
SUB : 0
TIME : 0.000e+00
FREQ : 0.000e+00



prob e7.21 ogden analysis plate with hole – elmt 26
1st Comp of Cauchy Stress

Figure 7.21-4 Stress Distribution

INC : 5
SUB : 0
TIME : 0.000e+00
FREQ : 0.000e+00



prob e7.21 ogden analysis plate with hole – elmt 26
1st Comp of Strain

Figure 7.21-5 Strain Distribution



7 Contact

Stretching of a Rubber Plate with Hole

7.22 Loading of a Rubber Plate

This example illustrates the analysis of a rubber plate under cyclic loading. The analysis uses three different material models. The first analysis uses simply a three-term Ogden series; the second model incorporates damage; the third and most complex model incorporates both damage and viscoelasticity.

This problem is modeled using the three techniques summarized below.

Data Set	Element Type(s)	Number of Elements	Number of Nodes	Differentiating Features
e7x22a	75	25	36	Ogden
e7x22b	75	25	36	Ogden with damage
e7x22c	75	25	36	Ogden with visco and damage

Element

Element type 75 is a 4-node shell element used for this analysis. A 60 cm x 60 cm simply-supported plate is to be modeled. Because of symmetry, only one-quarter of the plate is represented using 25 elements as shown in Figure 7.22-1. The SHELL SECT option is used to prescribe three layers. This is adequate because it is a linear analysis. The thickness of 3 cm is specified in the GEOMETRY option.

Loading

The first and second models are rate insensitive. Two increments are taken to apply a distributed load of 0.004 on the complete plate followed by two increments to remove the load. In the third analysis, the initial load is also applied in two increments instantaneously; that is, the time step is zero. Hence, creep (viscoelasticity) does not occur. This is followed by a period of one second in which relaxation occurs in which no additional load is applied. Then, two increments follow during which the load is removed again and instantaneously followed by a final relaxation period of five seconds.

Material Properties

The rubber material is defined as a three-term Ogden series with a finite compressibility. The bulk modulus = 6000 N/cm² and the coefficients are:

Term	μ (N/cm ²)	α
1	6.300	1.3
2	0.012	5.0
3	-0.100	-2.0

The stress-strain law is shown in Figure 7.22-2.

The rubber damage model is used in the second and third analyses. Only deviatoric damage are considered with the damage rate being 0.050 and the maximum damage factor = 0.90. This is specified through the DAMAGE option.

The third model includes viscoelastic deviatoric behavior. Two terms are included in the Prony series to express the strain energy relaxation function:

Series	Multiplier	Relaxation Time (Seconds)
1	0.6	1.0
2	0.1	10.0

Notice that the total time of the analysis falls within the relaxation times specified.

Boundary Conditions

Displacements are prescribed such that nodes 1 to 6 and 1 to 31 by 6 have no normal displacement or rotations about the edge, and nodes 31 to 36 and 6 to 36 by 6 are symmetric boundary conditions. The in-plane rotation is constrained at all nodes.

Controls

The full Newton-Raphson method is used in this analysis. In those increments where the total applied load is nonzero, a five percent tolerance on residuals is required. When the applied load is zero, we would be attempting to measure residual/noise so the convergence is changed to displacement control. This is very important to insure efficient convergence to a meaningful accuracy.

Results

Figure 7.22-3 shows the displacement of the center node (36) as a function of the increment number for the first model. You can observe that the material goes back to the original configuration when the load has been removed. Displacement is of the order 10^{-6} . In Figure 7.22-4, one observes the displacement history when damage is included. Note that the maximum displacement is larger and the slope of the loading and unloading curve is substantially different. Upon unloading, there is a permanent deformation of the order 2.5×10^{-2} . Finally, Figure 7.22-5 shows the displacement history when both damage and viscoelasticity occur. You observe that there are four different regions: loading, creep, unloading and creep. Figure 7.22-6 is the same information but now plotted as a function of time.

Parameters, Options, and Subroutines Summary

Example e7x22a:

Parameters	Model Definition Options	History Definition Options
ELEMENT	CONNECTIVITY	AUTO LOAD
END	CONTROL	CONTINUE
LARGE DISP	COORDINATES	DIST LOADS
SHELL SEC	DIST LOADS	
SIZING	END OPTION	
TITLE	FIXED DISP	
	GEOMETRY	
	OGDEN	
	OPTIMIZE	
	POST	



Example e7x22b:

Parameters	Model Definition Options	History Definition Options
ELEMENT	CONNECTIVITY	AUTO LOAD
END	CONTROL	CONTINUE
LARGE DISP	COORDINATES	DIST LOADS
SHELL SECT	DAMAGE	
SIZING	DIST LOADS	
TITLE	END OPTION	
	FIXED DISP	
	GEOMETRY	
	OGDEN	
	OPTIMIZE	
	POST	

Example e7x22c:

Parameters	Model Definition Options	History Definition Options
ELEMENT	CONNECTIVITY	AUTO LOAD
END	CONTROL	CONTINUE
LARGE DISP	COORDINATES	DIST LOADS
SHELL SECT	DAMAGE	
SIZING	DIST LOADS	
TITLE	END OPTION	
	FIXED DISP	
	GEOMETRY	
	OGDEN	
	OPTIMIZE	
	POST	
	VISCELOGDEN	

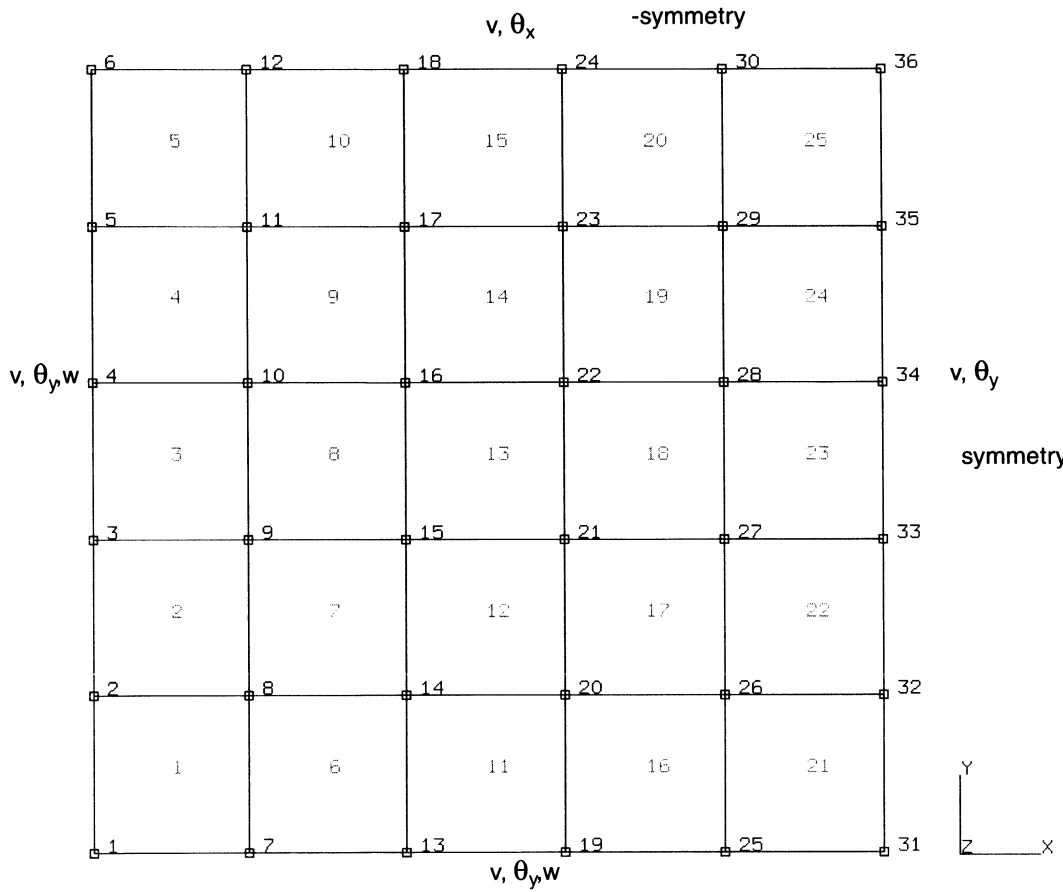


Figure 7.22-1 Finite Element Mesh

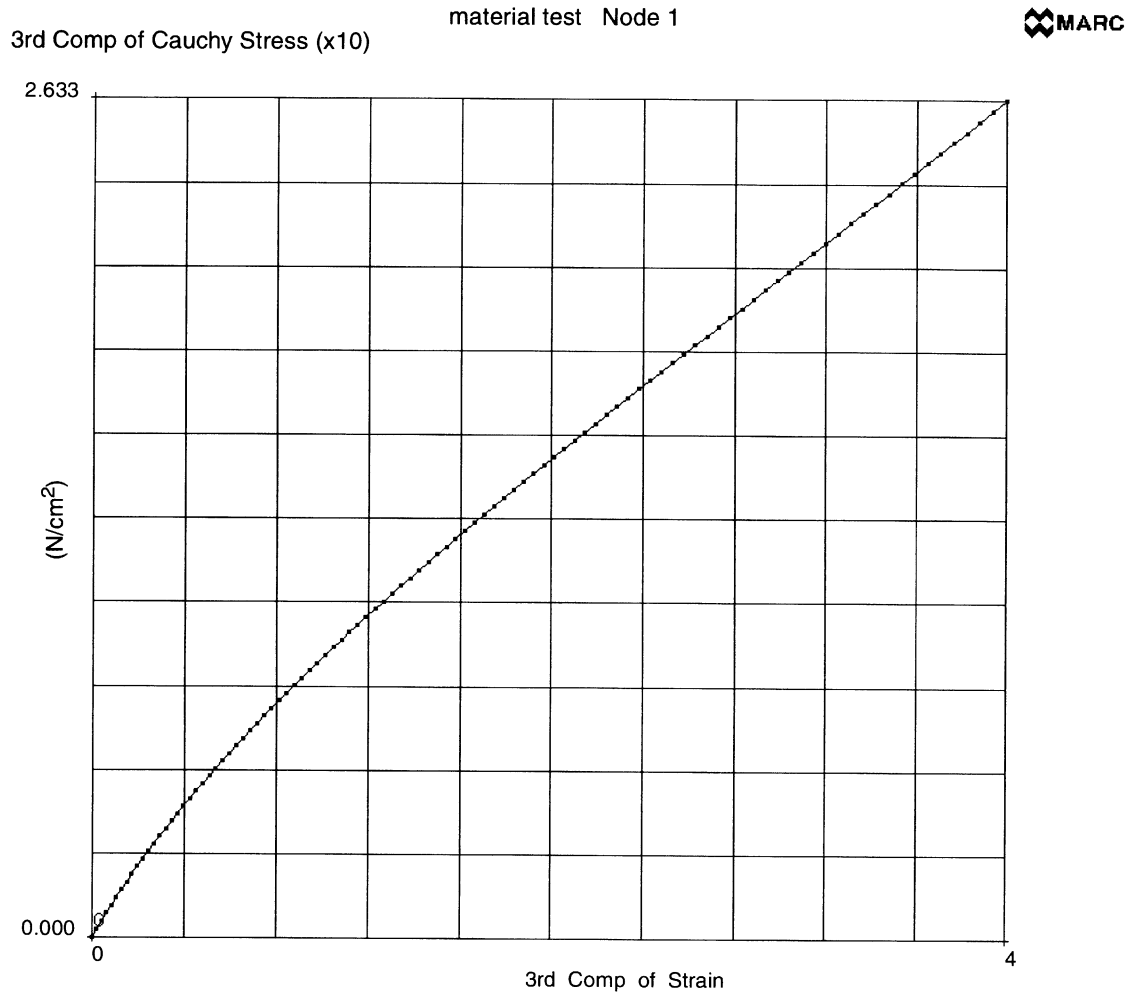


Figure 7.22-2 Stress-Strain Curve

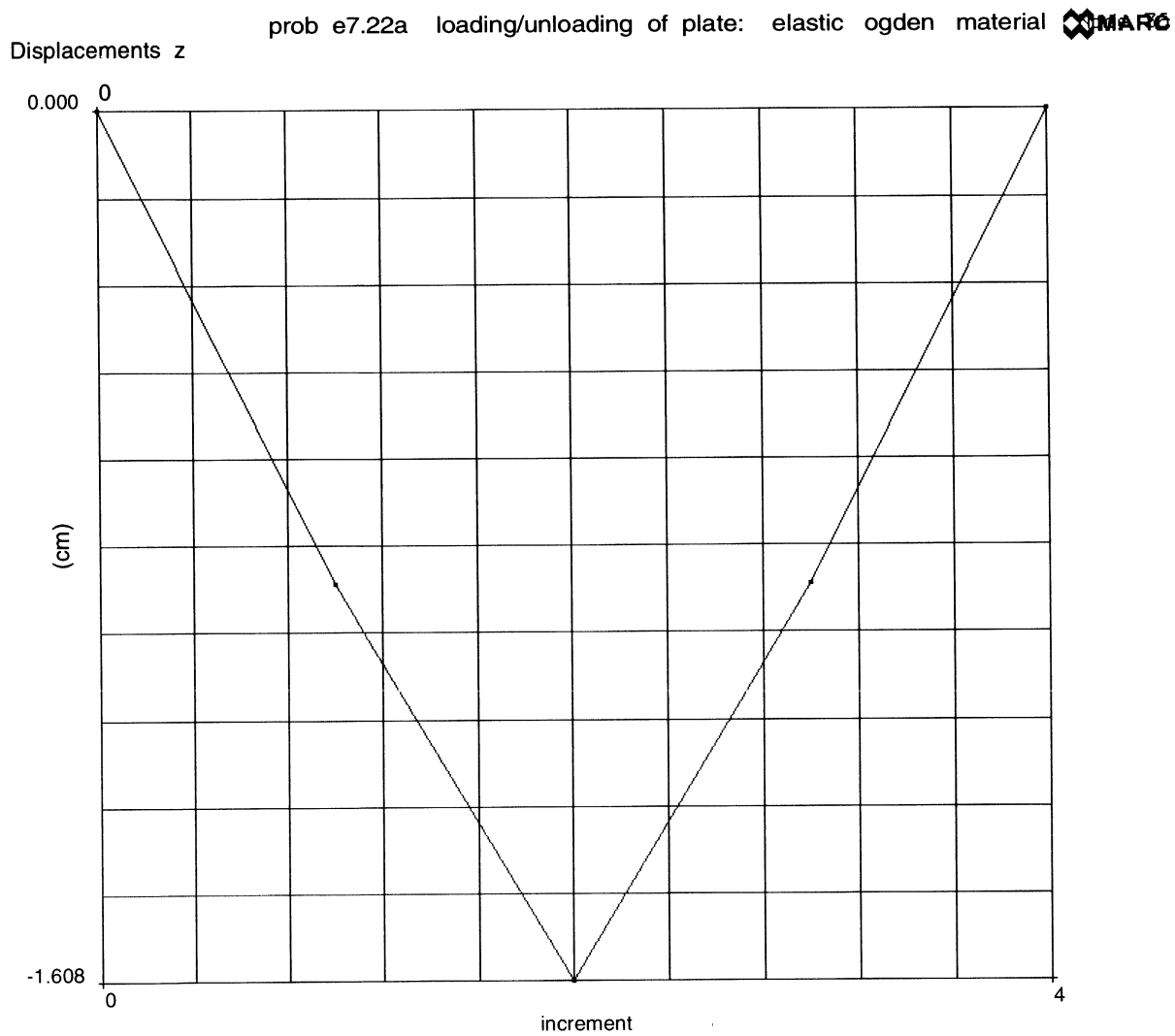


Figure 7.22-3 Displacement History of Center Node – Elastic Effects Only

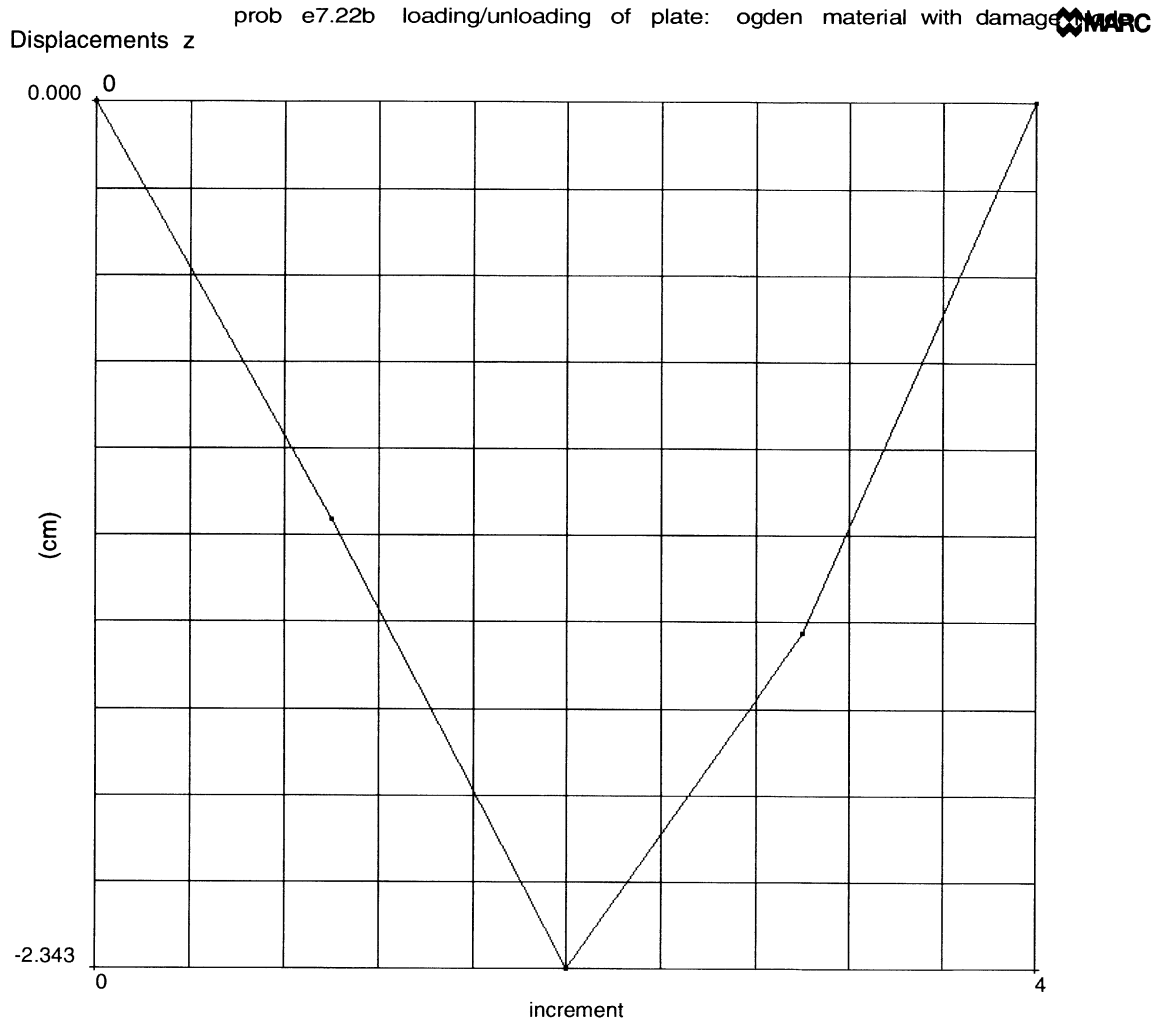


Figure 7.22-4 Displacement History of Center Node – Including Damage Effects

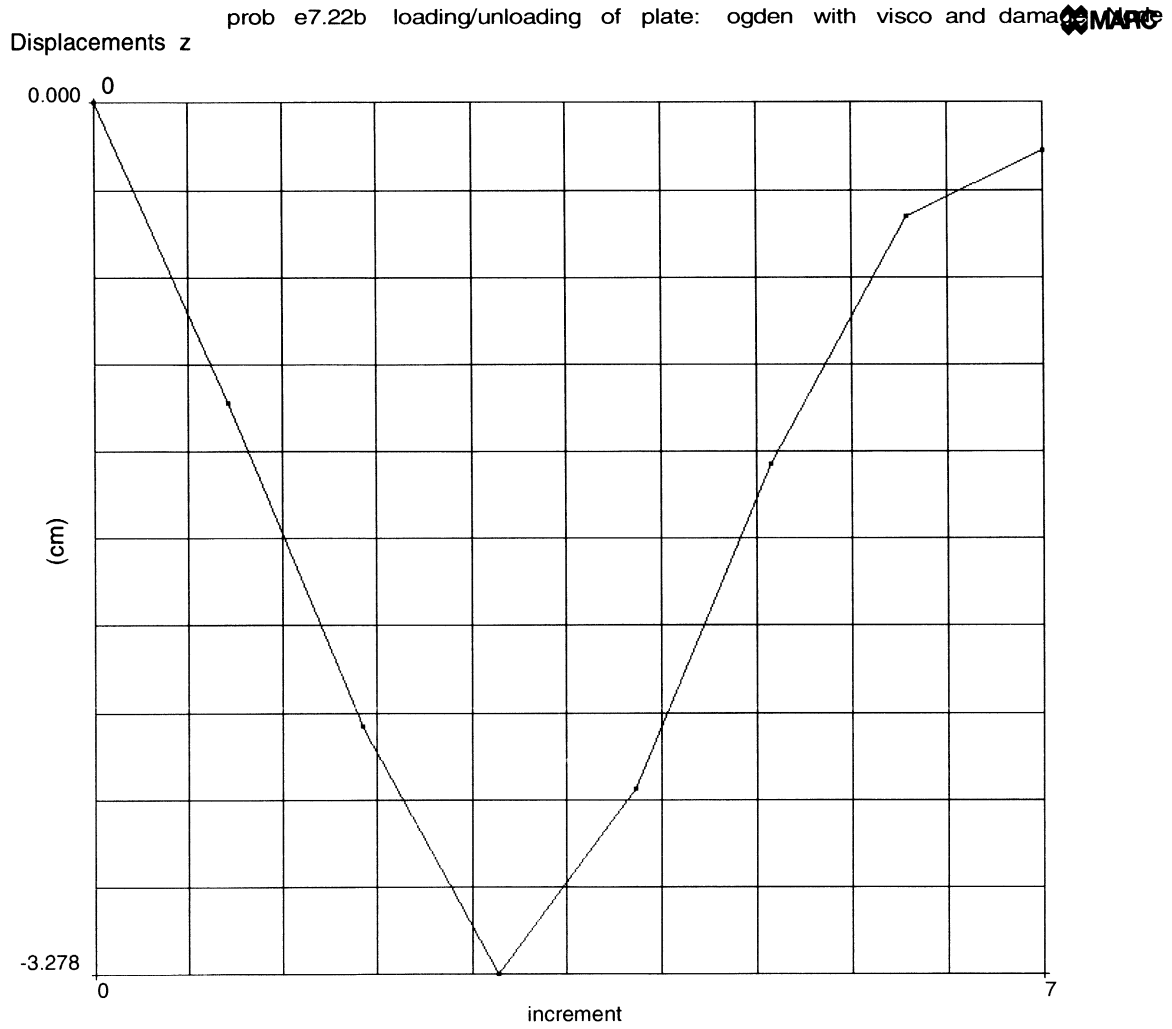


Figure 7.22-5 Displacement History of Center Node – Including Damage and Viscoelastic Effects

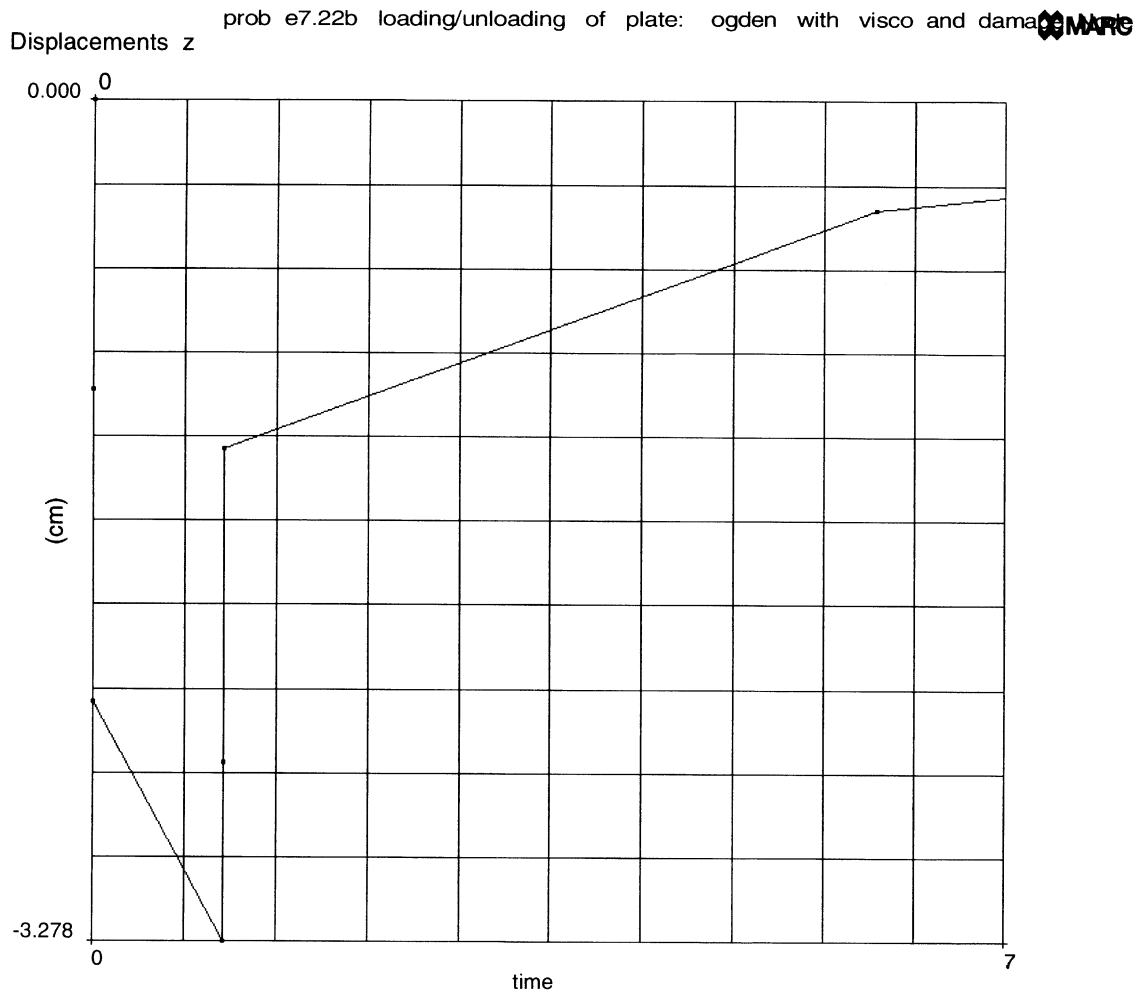


Figure 7.22-6 Displacement History as a Function of Time – Including Damage and Viscoelastic Effects

7.23 Compression of a Foam Tube

This example demonstrates the use of the generalized Ogden rubber foam model for the high compression of a tube.

Element

Library element 11, the plane strain, is used for this analysis. There are 140 elements and 175 nodes in the model as shown in Figure 7.23-1. Two rigid plates are moving toward the tube. The tube has an inner radius of 20 cm and an outer radius of 10 cm. Because of symmetry, only half of the tube of modeled.

Material Properties

The foam tube can be described using the foam material model using a two term series. The data was fixed such that:

Term	μ (N/cm)	α	β
1	0.0	2.0	-1.0
2	-32.0	-2.0	1.0

Contact/Boundary Conditions

All of the kinematic constrains are provided using rigid contact surfaces. The contact tolerance and the bias factor are set to 0.2 cm and 0.99 cm, respectively.

The rigid surface at the bottom and top move at a speed of 1.5 cm/second in a period of 8.15 seconds toward the tube.

Control

The full New-Raphson iterative method is used with a convergence tolerance of 1% on residuals requested.

Results

The deformed mesh at increments 10, 16, and 29 are shown in Figure 7.23-2 through Figure 7.23-4. The shear strain distribution is shown in Figure 7.23-5. Using Mentat, you can determine that the initial area is 469.90 cm² and the final area is 421.05 cm²; hence, there is a 10% reduction in volume.



Parameters, Options, and Subroutines Summary

Example e7x23.dat:

Parameters	Model Definition Options	History Definition Options
ALL POINTS	CONNECTIVITY	AUTO LOAD
ELEMENTS	CONTACT	CONTINUE
END	CONTROL	TIME STEP
LARGE DISP	COORDINATE	
PRINT	DEFINE	
SETNAME	END OPTION	
SIZING	FIXED DISP	
TITLE	FOAM	
	NO PRINT	
	OPTIMIZE	
	POST	
	SOLVER	

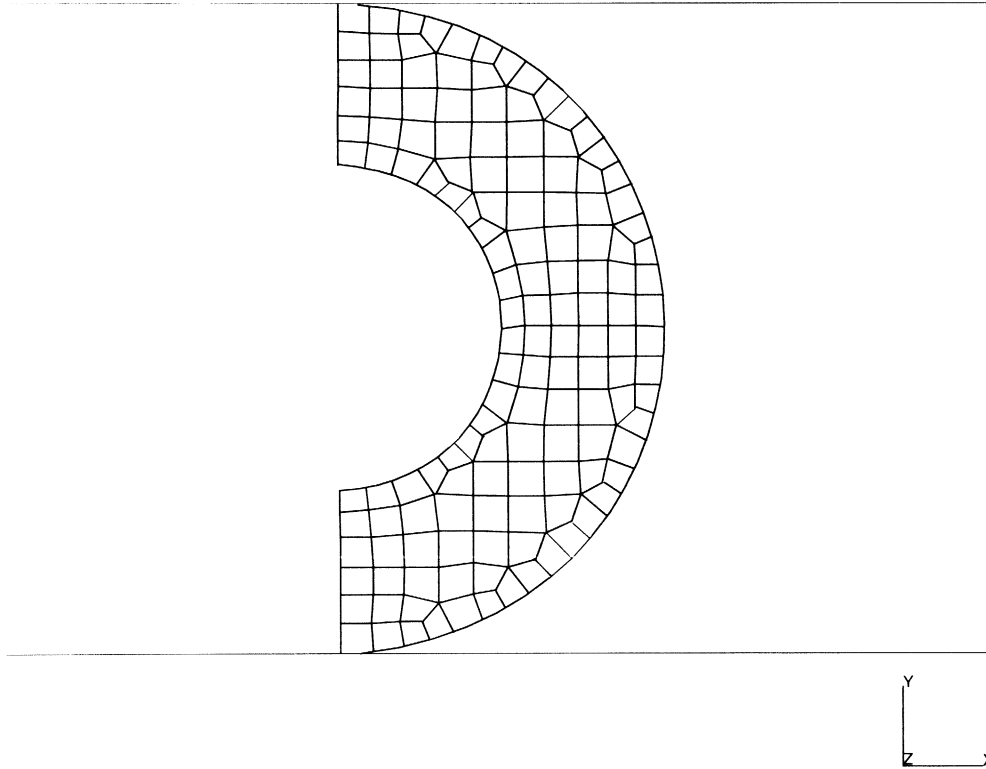
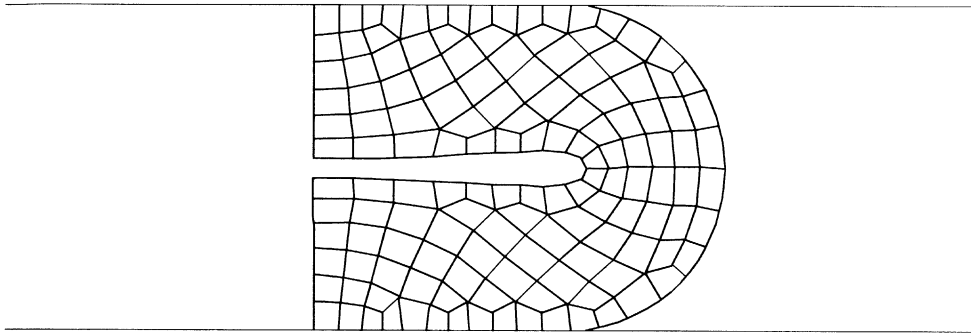


Figure 7.23-1 Finite Element Mesh of Tube

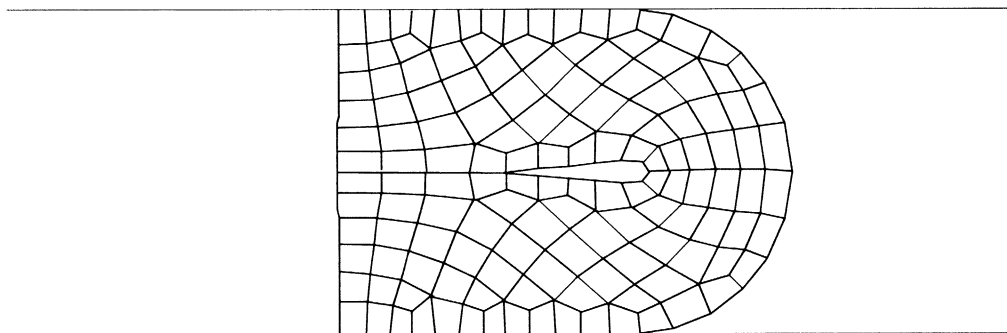
INC : 10
SUB : 0
TIME : 6.400e+00
FREQ : 0.000e+00



prob e7x23 compression of a foam tube

Figure 7.23-2 Deformed Mesh at Increment 10

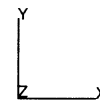
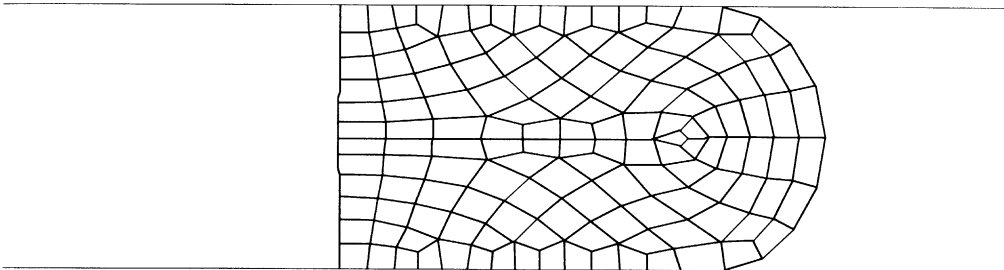
INC : 16
SUB : 0
TIME : 7.000e+00
FREQ : 0.000e+00



prob e7x23 compression of a foam tube

Figure 7.23-3 Deformed Mesh at Increment 16

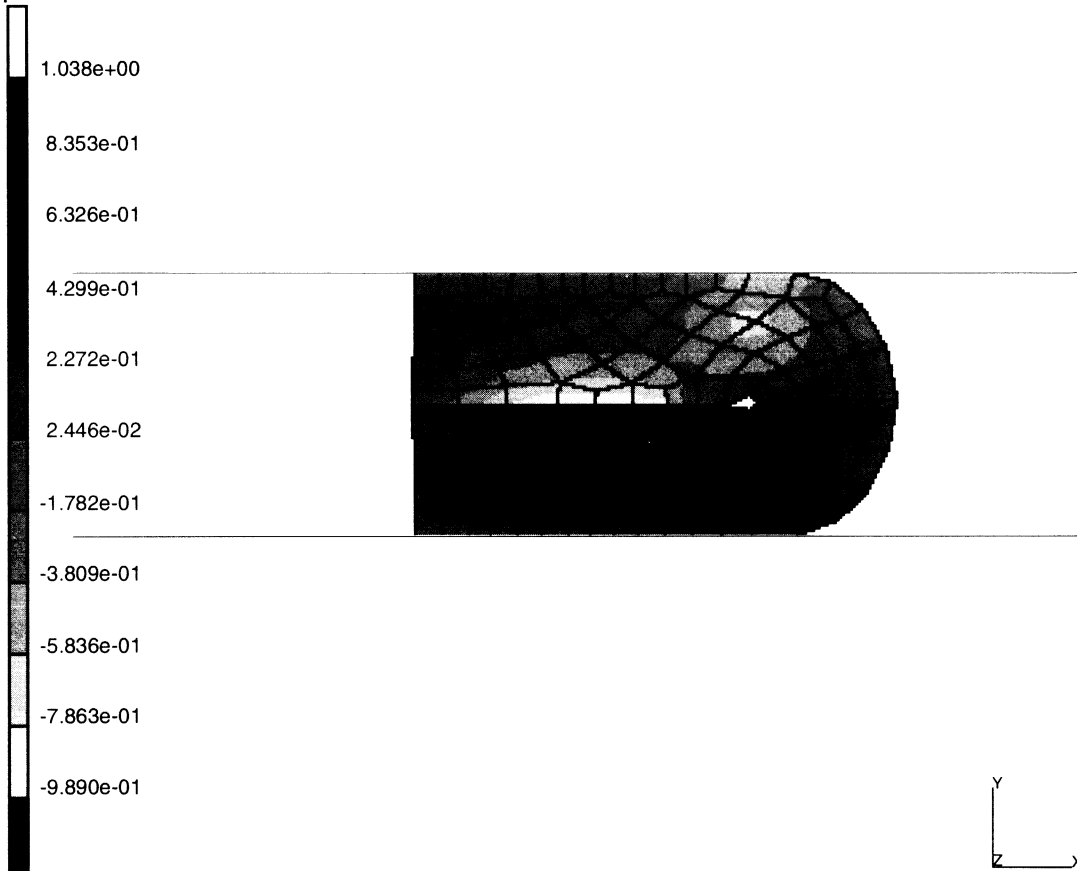
INC : 29
SUB : 0
TIME : 8.150e+00
FREQ : 0.000e+00



prob e7x23 compression of a foam tube

Figure 7.23-4 Deformed Mesh at Increment 29

INC : 29
SUB : 0
TIME : 8.150e+00
FREQ : 0.000e+00



prob e7x23 compression of a foam tube
e_12

Figure 7.23-5 Shear Strain in Compressed Tube



7 Contact

Compression of a Foam Tube

7.24 Constitutive Law for a Composite Plate

This example provides an analytic qualification of the constitutive law existing in a composite laminated plate. The model is made of a single finite element.

Model

The plate is made of a single shell element (element 75 in MARC). The element has four nodes with bilinear interpolation of displacement and rotation components.

Material Properties

The plate is made of eight laminae of boron-epoxy set to produce an equilibrated and symmetric laminate with the angles:

$$/+45/-45/+45/-45/S$$

Each lamina in boron-epoxy has the following properties of orthotropic material:

$$E_{11} = 29.7 \text{ E6 psi}$$

$$E_{22} = 2.97 \text{ E6 psi}$$

$$\nu_{12} = 0.33$$

$$G_{12} = 1. \text{ E psi}$$

Geometry

The plate has total thickness $THT = 0.4$ inches. The thickness in every lamina is thus $THL = 0.05$ inches.

Orientation

The orientation of the lamina is given by assigning the reference axis E_1 to be side 1-2 of the element (see Figure 7.24-1) The angles assigned to the fibers imply rotations of $+45^\circ$ or -45° with respect to the normal E_3 to the plate. The rotation starts from E_1 , positive if counterclockwise.

Boundary Conditions

The plate is loaded with a constant membrane strain in the x-direction. $\epsilon_{mx} = 1$ is obtained by assigning to nodes 1 and 3 displacements $u_x = 2$, $u_y = 0$. While this would produce large strains, small strain theory is used here so you can easily compare the calculations with the analytical solution.

Results

By assigning a displacement $u_x = 2$ to a plate with $H = B = 2$ inches, you obtain for all laminae:

$$\begin{aligned}\varepsilon_x &= 1 \\ \varepsilon_y = \gamma_{xy} &= 0\end{aligned}$$

The strains and stresses in a lamina at $+45^\circ$ are computed as:

$$\begin{aligned}\varepsilon'_{45} &= T_{45} \cdot \varepsilon = \begin{bmatrix} 0.5 & 0.5 & 0.5 \\ 0.5 & 0.5 & -0.5 \\ -1. & 1. & 0 \end{bmatrix} \cdot \begin{Bmatrix} 1 \\ 0 \\ 0 \end{Bmatrix} = \begin{Bmatrix} 0.5 \\ 0.5 \\ -1. \end{Bmatrix} \\ \sigma'_{45} &= D \cdot \varepsilon'_{45} = 10^6 \begin{bmatrix} 30 & 1 & 0 \\ 1 & 3 & 0 \\ 0 & 0 & 1 \end{bmatrix} \cdot \begin{Bmatrix} 0.5 \\ 0.5 \\ -1. \end{Bmatrix} = 10^6 \begin{Bmatrix} 15.5 \\ 2. \\ -1. \end{Bmatrix}\end{aligned}$$

Shear

The plate is loaded with membrane shear by assigning to nodes 2 and 3 the displacements $u_x = 0, u_y = 2$.

Results

By assigning displacements $u_x = 0$ and $u_y = 2$ to a plate with $H = B = 2$ inches, you obtain for all the laminae:

$$\begin{aligned}v_{xy} &= 1. \\ \varepsilon_y = \varepsilon_x &= 0\end{aligned}$$

The strains and stresses in a laminae are computed as:

$$\begin{aligned}\varepsilon'_{45} &= T_{45} \cdot \varepsilon = \begin{bmatrix} 0.5 & 0.5 & 0.5 \\ 0.5 & 0.5 & -0.5 \\ -1. & 1. & 0 \end{bmatrix} \cdot \begin{Bmatrix} 0 \\ 0 \\ 1 \end{Bmatrix} = \begin{Bmatrix} 0.5 \\ -0.5 \\ 0. \end{Bmatrix} \\ \sigma'_{45} &= D \cdot \varepsilon'_{45} = 10^6 \begin{bmatrix} 30 & 1 & 0 \\ 1 & 3 & 0 \\ 0 & 0 & 1 \end{bmatrix} \cdot \begin{Bmatrix} 0.5 \\ -0.5 \\ 0. \end{Bmatrix} = 10^6 \begin{Bmatrix} 14.5 \\ -1. \\ 0. \end{Bmatrix}\end{aligned}$$

Bending

The plate is loaded in bending by assigning to nodes 2 and 3 a rotation $\phi_y = 2$. You obtain a constant curvature $\chi_x = 1$.

Nodes 1 and 4 are clamped. Nodes 2 and 3 are free in the remaining degree of freedom.

Results

Assigning a rotation $\phi_y = 2$ to a plate with $H = B = 2$ inches, you obtain:

$$\begin{aligned}\chi_x &= 1. \\ \chi_y &= \chi_z = 0\end{aligned}$$

The first lamina, at $z = 0.175$ from midspan, has $\epsilon_x = z \cdot \chi_x = 0.175$ in local axes.

The strains and stresses in the first lamina at $+45^\circ$ are computed as:

$$\begin{aligned}\epsilon'_{45} &= T_{45} \cdot \epsilon = \begin{bmatrix} 0.5 & 0.5 & 0.5 \\ 0.5 & 0.5 & -0.5 \\ -1. & 1. & 0 \end{bmatrix} \cdot \begin{Bmatrix} 0.175 \\ 0 \\ 0 \end{Bmatrix} = \begin{Bmatrix} 0.875 \\ -0.875 \\ 0.175 \end{Bmatrix} \\ \sigma'_{45} &= D \cdot \epsilon'_{45} = 10^6 \begin{bmatrix} 30 & 1 & 0 \\ 1 & 3 & 0 \\ 0 & 0 & 1 \end{bmatrix} \cdot \begin{Bmatrix} 0.875 \\ -0.875 \\ 0.175 \end{Bmatrix} = 10^6 \begin{Bmatrix} 2.175 \\ 0.35 \\ 0.175 \end{Bmatrix}\end{aligned}$$

Parameters, Options, and Subroutines Summary

Example e7x24a.dat:

Parameters	Model Definition Options
ELEMENTS	COMPOSITE
END	CONNECTIVITY
SHELL SECT	COORDINATE
SIZING	END OPTION
TITLE	FIXED DISP
	ORIENTATION
	ORTHOTROPIC
	PRINT ELEMENT

Example e7x24b.dat:

Parameters	Model Definition Options
ELEMENTS	COMPOSITE
END	CONNECTIVITY
SHELL SECT	COORDINATE
SIZING	END OPTION
TITLE	FIXED DISP
	ORIENTATION
	ORTHOTROPIC
	PRINT ELEMENT

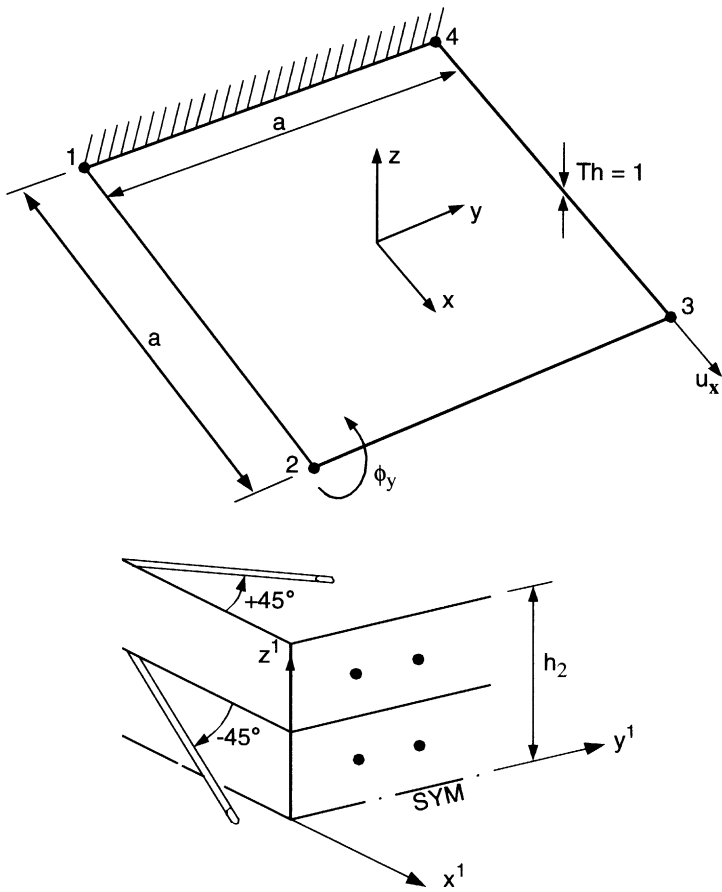


Figure 7.24-1 Geometry and Lamination of a Composite Plate

7.25 Progressive Failure of a Composite Strip

This problem tests the capability of MARC to performing progressive failure of composite structures. The test structure modeled here is a strip with a rectangular cross section clamped at both ends and loaded by concentrated forces at midspan.

The material is a laminate, with eight laminae alternating the fiber direction between 0° and 90°. The fiber failure stress in tension is taken here to be the same as in compression.

Under linear elastic behavior, the strip behaves like a beam clamped at both ends. The largest (bending) stresses occur at midspan and at the supports. The load is increased in 126 increments until the fibers are broken and only the matrix bears the load. Correspondingly, the deformed shape of the strip moves from that of a beam to a 3-hinged arch.

Model

Due to symmetry, only half of the strip is modeled. The FEM mesh includes 30 elements and 153 nodes. Element 22, (8-noded shell) is used. LARGE DISP and UPDATE are active for geometrically nonlinear analysis. The strip has length $l = 200$ mm, width $b = 10$ mm, and thickness $t = 1$ mm. The mesh is shown in Figure 7.25-1.

Material Properties

The material is a laminated carbon-epoxy. Two outer skins, with a thickness of 0.25 mm, have the fibers in the longitudinal direction (global X axis). They confine a “core”, thick 0.5 mm, with fibers in the transverse direction. The laminae have 0.125 mm thickness. Therefore, eight laminae make up the strip.

$$E_{11} = 2140000 \text{ N/mm}^2$$

$$E_{22} = 9700 \text{ N/mm}^2$$

$$\nu_{12} = 0.28$$

$$G_{12} = 5400 \text{ N/mm}^2$$

$$G_{23} = 3600 \text{ N/mm}^2$$

$$G_{31} = 5400 \text{ N/mm}^2$$

A lamina fails for maximum stress with the following limit values:

$$\sigma_1 = 1020 \text{ N/mm}^2 \quad \text{in the direction of the fibers, tension or compression}$$

$$\sigma_2 = 59 \text{ N/mm}^2 \quad \text{in the direction orthogonal to the fibers, tension or compression}$$

$$\tau = 95 \text{ N/mm}^2 \quad \text{shear}$$

Supports

Nodes 1, 2, and 3 at the strip end are clamped allowing for transverse dilation.

Nodes 151, 152, and 153 at midspan have symmetry conditions.

All midspan nodes undergo the same vertical deflection.

Loads

A concentrated load is applied at midspan. The magnitude is increased to $p = 3000$ N in 125 load increments.

Results

The time history of the tip deflection is shown in Figure 7.25-2. You can easily observe when plies failed in the system by the jump in the deflection. The first failure occurs in increment 10.

Figure 7.25-3 and Figure 7.25-4 show the time history of the stresses in layers 1 and 5. The final figure, Figure 7.25-5, shows the axial reaction force at the clamped end. Notice the sudden decrease in stress level. The strip deformation has already moved to that of a three-hinged arch.

Parameters, Options, and Subroutines Summary

Example e7x25.dat:

Parameters	Model Definition Options	History Definition Options
ELEMENTS	COMPOSITE	AUTO LOAD
END	CONNECTIVITY	CONTINUE
LARGE DISP	CONTROL	NO PRINT
SHELL SECT	COORDINATE	POINT LOAD
SIZING	END OPTION	POST INCREMENT
TITLE	FAIL DATA	PRINT ELEMENT
UPDATE	FIXED DISP	PROPORTIONAL INCREMENT
	ORIENTATION	
	ORTHOTROPIC	
	POST	
	TYING	

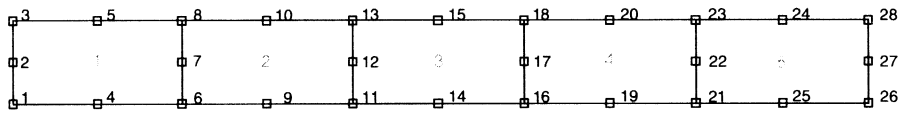


Figure 7.25-1 Finite Element Mesh of Strip

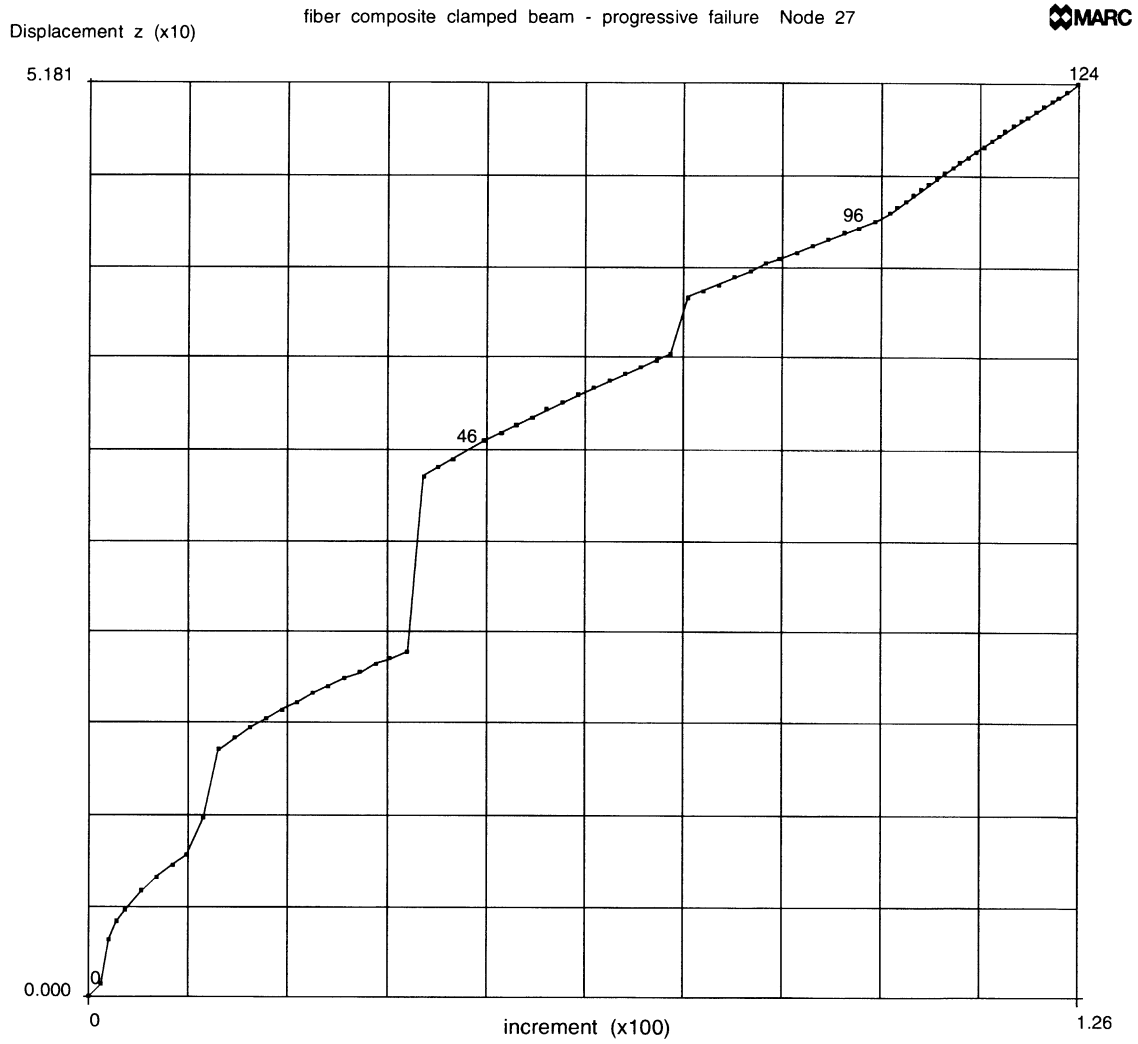


Figure 7.25-2 History of Deflection of the Tip

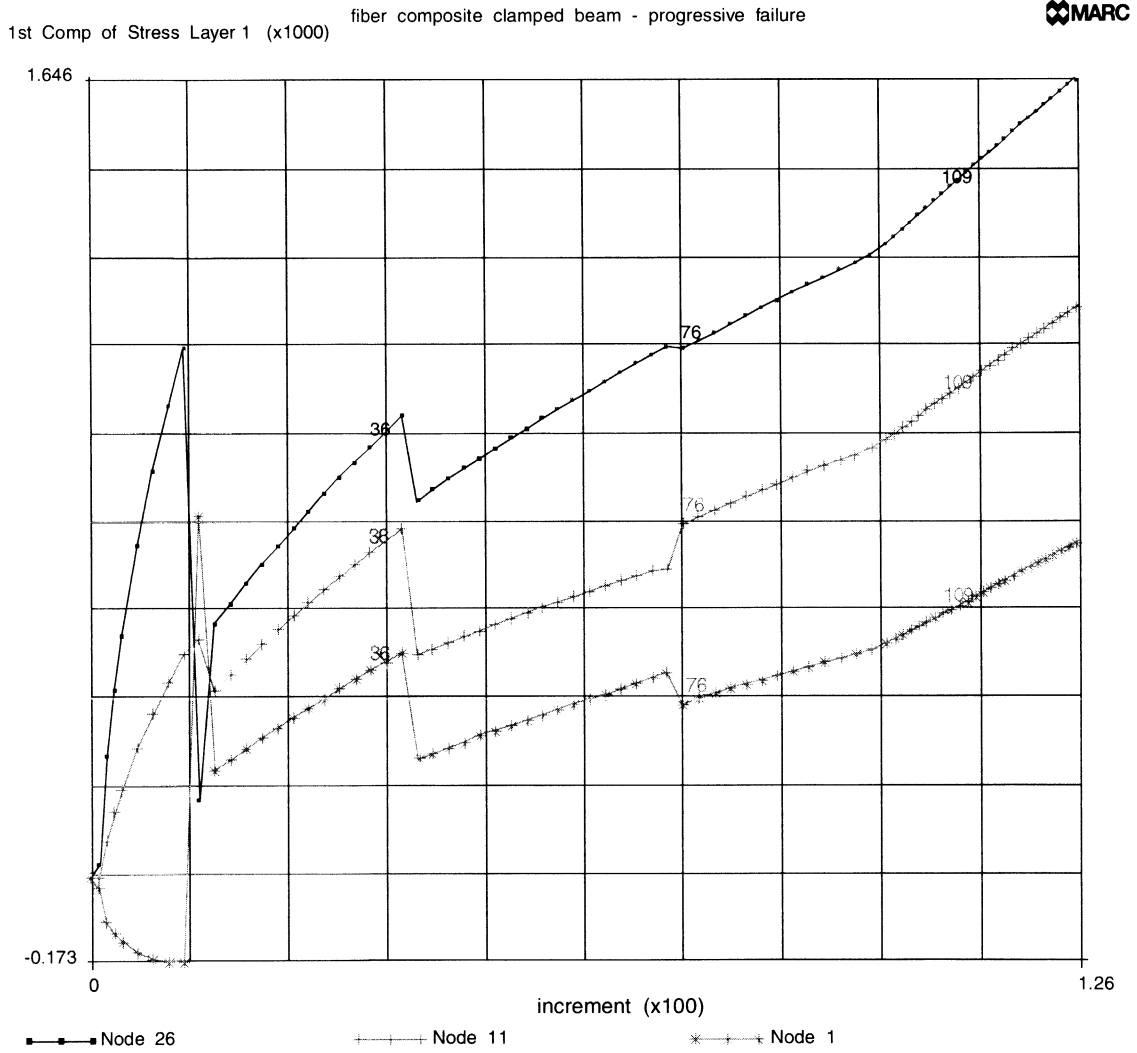


Figure 7.25-3 History of First Component of Stress in Layer 1

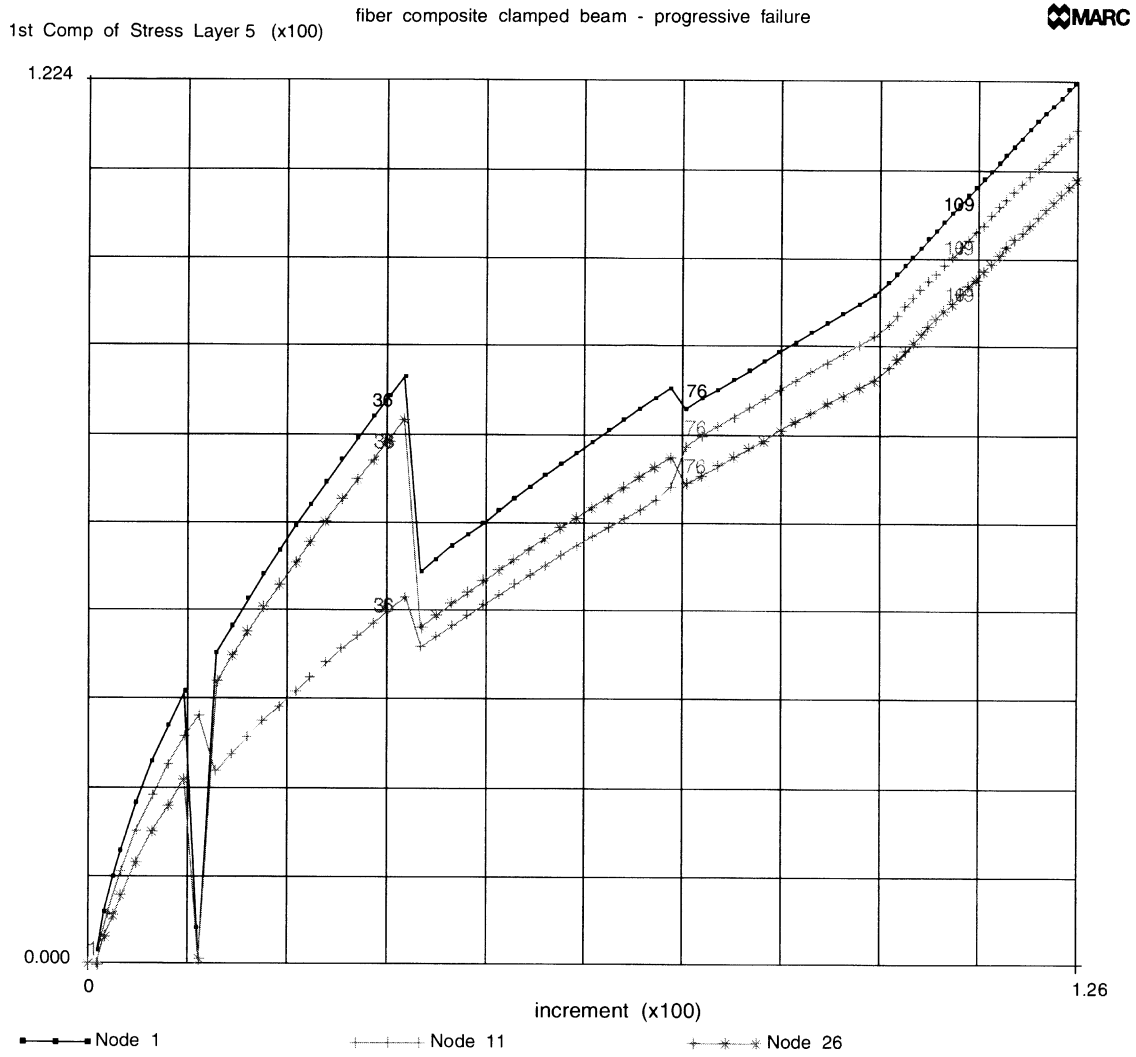


Figure 7.25-4 History of First Component of Stress in Layer 5

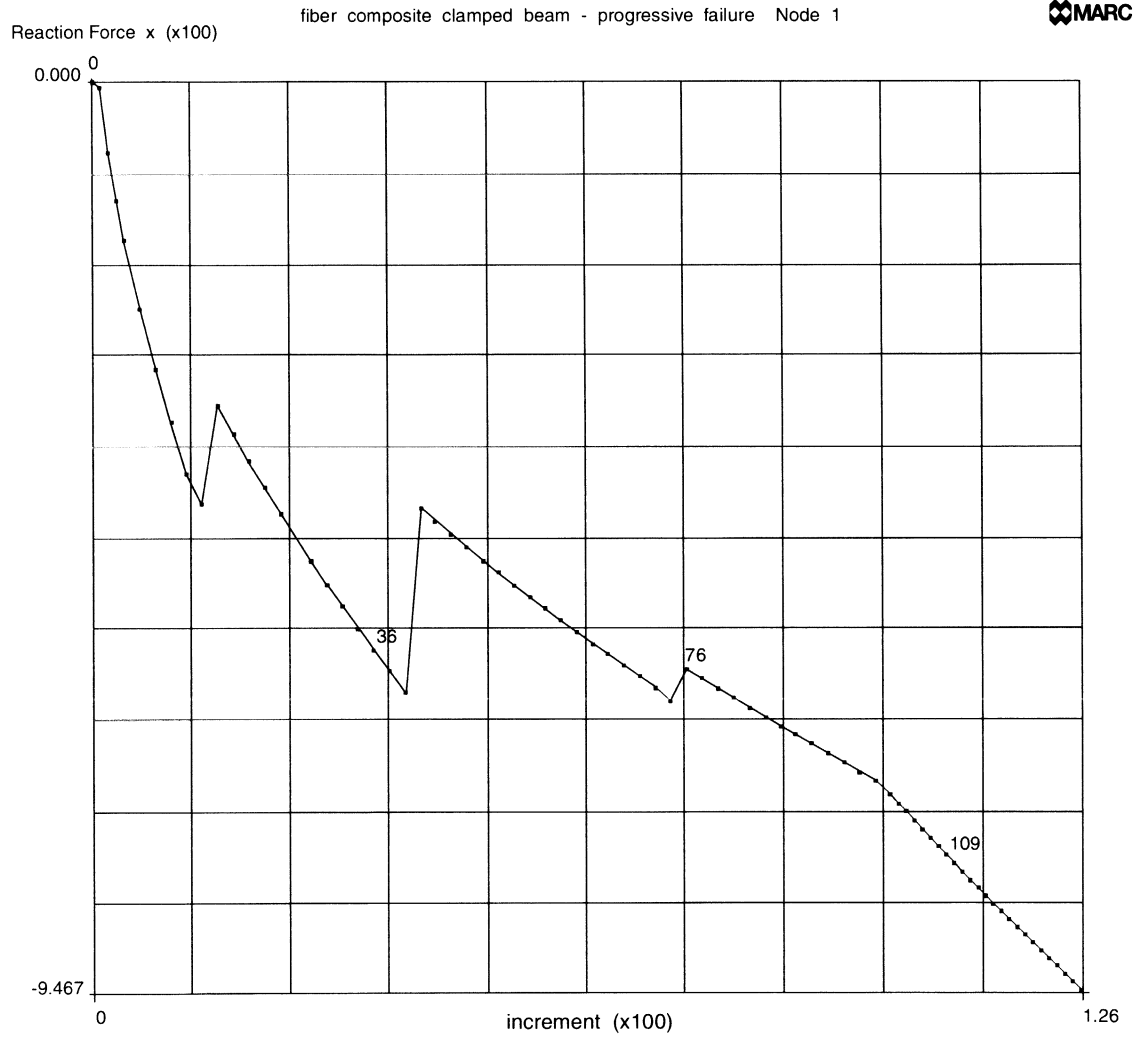


Figure 7.25-5 History of the Reaction Force at Clamped End



7 Contact

Progressive Failure of a Composite Strip

7.26 Pipe Collars in Contact

This problem demonstrates the plastic strain capability of the axisymmetric element 95 together with the non-axisymmetric gap element 97. Two pipes are connected under bending loads.

The quadrilateral element 95 represents the cross-section of a ring in the z,r symmetry plane at $\theta = 0^\circ$. A pure axisymmetric deformation induces displacements u,v in the z,r plane. These remain constant for θ ranging from 0° to 360° . A flexural deformation in the z,r plane induces different displacements u,v at opposite sections, $\theta = 0^\circ$ and $\theta = 180^\circ$, along the ring. A twist in the ring induces a circumferential displacement w , equal at every θ , and assigned to the position $\theta = 90^\circ$.

The gap element 97 works in the flexural mode. Extra degrees of freedom have been included to account for independent contact and friction between facing sides of element 95 ($q = 0^\circ - 180^\circ$). Motion can only occur in the z,r plane.

Element

In element 95, five degrees of freedom are associated with each node:

u,v displacements at 0° and 180° , respectively

w circumferential displacement at 90° angle

Element 95 is integrated numerically in the circumferential direction. The number of integration points (odd number) is given in the SHELL SECT parameter. The points are equidistant on the half circumference (see Figure 7.26-1 and Figure 7.26-2)

Here, nine integration points along the half circumference are chosen via the SHELL SECT parameter.

Element 97 is a 4-node gap and friction link with double contact and friction ($0^\circ - 180^\circ$). It is designed to be used with element type 95.

Model

The FEM model represents the longitudinal section of the pipe junction in the z,r plane. The mesh consists of 248 elements, type 95 and 9 elements type 97 for a total of 330 nodes. The mesh is shown in Figure 7.26-2.



Material Properties

The two pipes are made with the same material:

$$\begin{aligned} E \text{ (Young modulus)} &= 2E5 \text{ N/mm}^2 \\ \nu \text{ (Poisson ratio)} &= .3 \\ \sigma_y &= 200. \text{ N/mm}^2 \end{aligned}$$

A workhardening curve is assigned as follows:

σ [N/mm ²]	ϵ_p
200.	0
250.	.3
300.	.6

Loads

The bending load is applied as shown in Figure 7.26-1. The loads acts in the longitudinal direction (z-direction)

Results

The results produces by MARC for the pipe junction with gaps can be seen in the following figures.

- Figure 7.26-3 The deformed section at 0°.
- Figure 7.26-4 and Figure 7.26-5 The von Mises stress at 0° and 180° (layer 1 and 9, respectively)
- Figure 7.26-6 The plastic strain at 0°. No plastic strain appears at 180°.

Note: Only the deformed shape at 0° can be visualized with the Mentat graphics program even if all the element variables can be visualized. The displacements and all the nodal quantities referring to 180° can be seen on the output file.

Parameters, Options, and Subroutines Summary

Example e7x26.dat:

Parameters	Model Definition Options	History Definition Options
ELEMENTS	CONNECTIVITY	CONTINUE
END	CONTROL	DIST LOADS
LARGE DISP	COORDINATES	
SHELL SECT	END OPTION	
SIZING	FIXED DISP	
TITLE	GAP DATA	
UPDATE	ISOTROPIC	
	OPTIMIZE	
	POST	

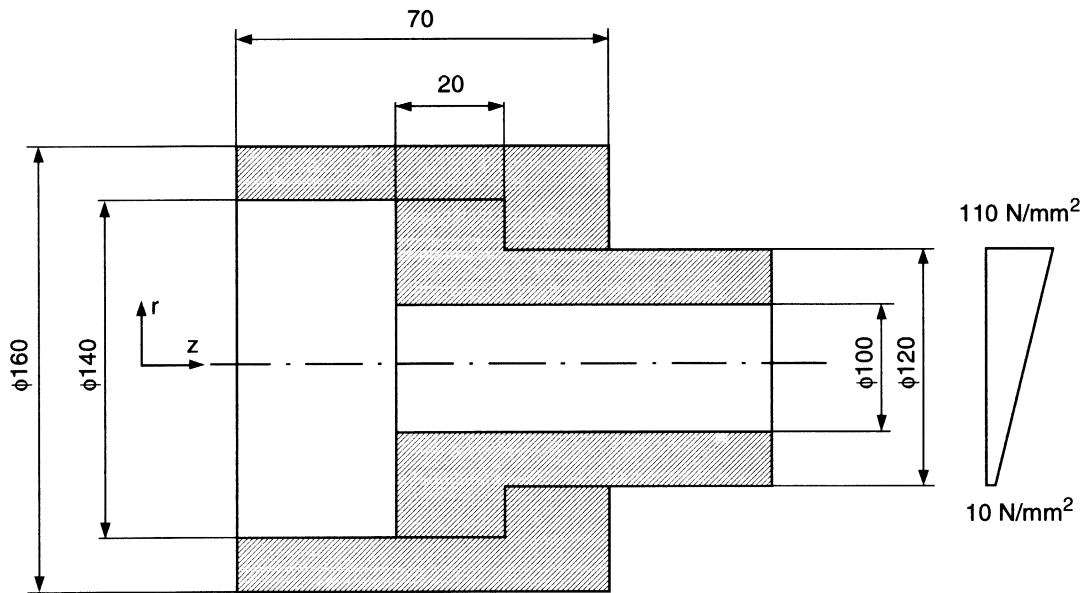


Figure 7.26-1 Geometric Dimension and Bending Loads

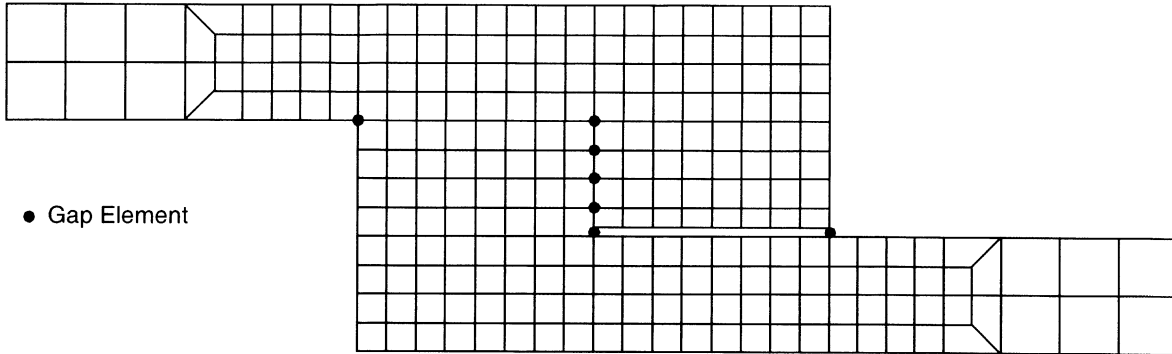


Figure 7.26-2 FEM Model

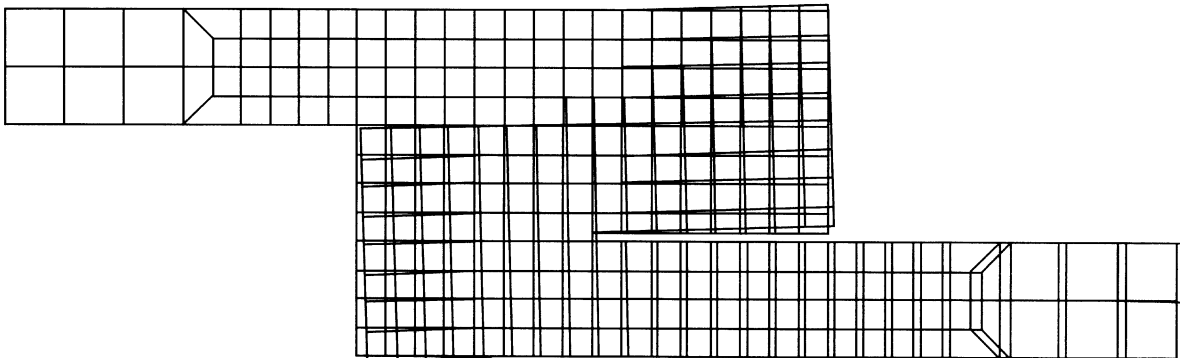


Figure 7.26-3 Deformed Shape at 0°

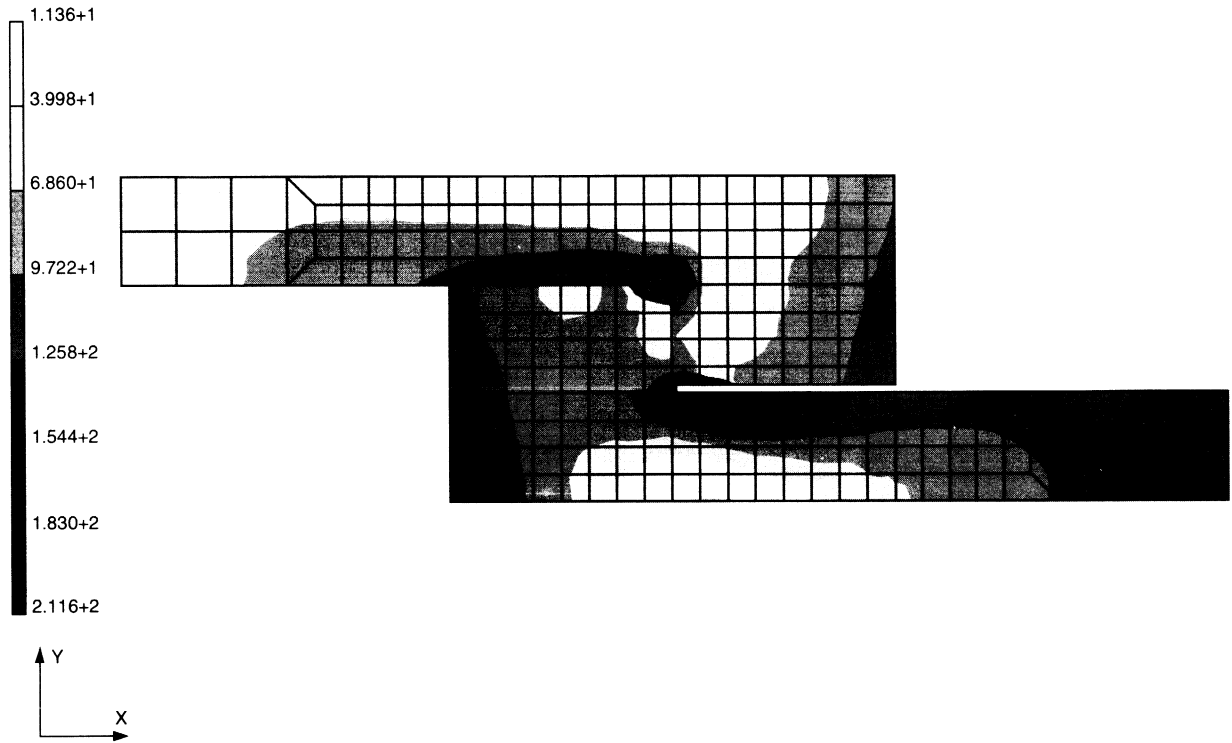


Figure 7.26-4 von Mises Stress Contour at 0°, Layer 1

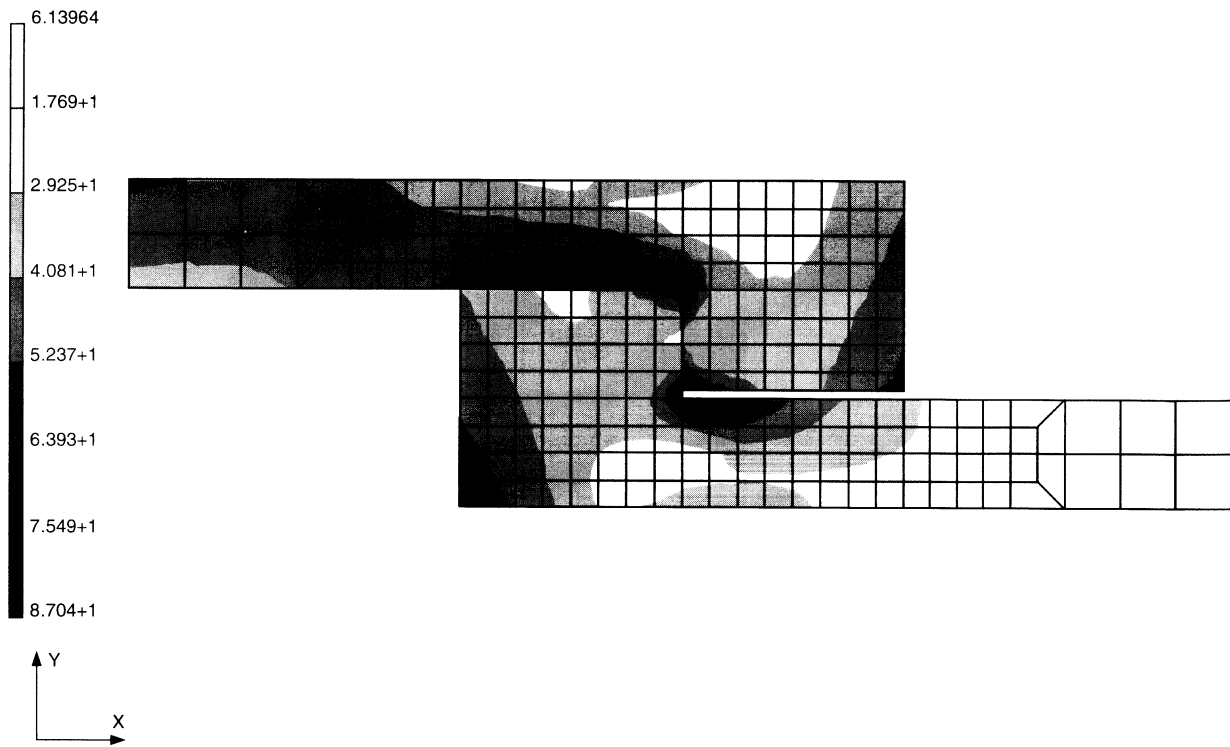


Figure 7.26-5 von Mises Stress Contour at 180°, Layer 9

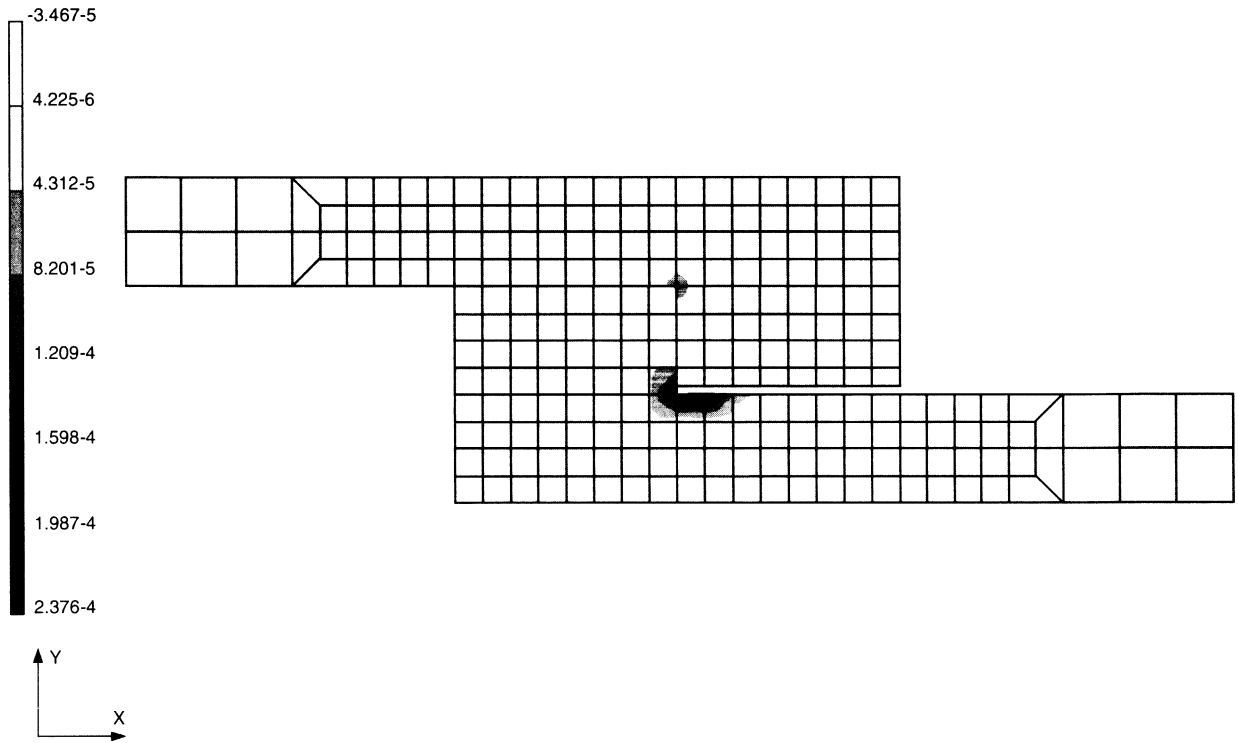


Figure 7.26-6 Plastic Strain Contour at 0° , Layer 1



7.27 Twist and Extension of Circular Bar of Variable Thickness at Large Strains

This problem illustrates the use of MARC element 67, higher order axisymmetric with twist element, for a large strain elastic analysis of a circular bar of variable thickness. The bar is subjected to both a twist moment and an axial force at the free end of the circular bar. The tying constraint option is used to insure that the cross section at the small end of the bar remains flat. The material is modeled using Ogden model. The ELASTICITY,2 option is used to activate the updated Lagrangian formulation.

Element

Element type 67, an 8-node axisymmetric element with twist, is used in this example.

Model

There are 12 elements, with a total of 53 nodes. Dimensions of the circular bar and the finite element mesh are shown in Figure 7.27-1.

Material Properties

Ogden material properties are given as:

$$\mu_1 = 16 \text{ lb/in}^2, \alpha_1 = 2, \mu_2 = -4 \text{ lb/in}^2, \alpha_2 = -2.$$

Boundary Conditions

Degrees of freedom u and w are 0 at the fixed end (nodes 1-5). Symmetry conditions are imposed at $r = 0$ ($v = 0$).

Loading

In each increment, a 10 pound point load in the positive x -direction and a 4 inch per pound torque is applied at node 49. Due to the applied tying, the point load is distributed over the whole cross section.

Tying

Tying type 1 is used at the free end to simulate a generalized plane-strain condition in the z -direction. The tied nodes are 50, 51, 52, and 53 and the retained node is 49.

Results

The deformed mesh and the distribution of Equivalent von Mises stress is depicted in Figure 7.27-2.



Parameters, Options, and Subroutines Summary

Example e7x27.dat:

Parameters

ALIAS
ELASTICITY
ELEMENTS
END
LARGE DISP
SIZING
TITLE

Model Definition Options

CONNECTIVITY
COORDINATE
END OPTION
FIXED DISP
ISOTROPIC
OGDEN
POINT LOAD
POST
TYING

History Definition Options

AUTO LOAD
CONTINUE
CONTROL
POINT LOAD

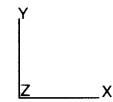
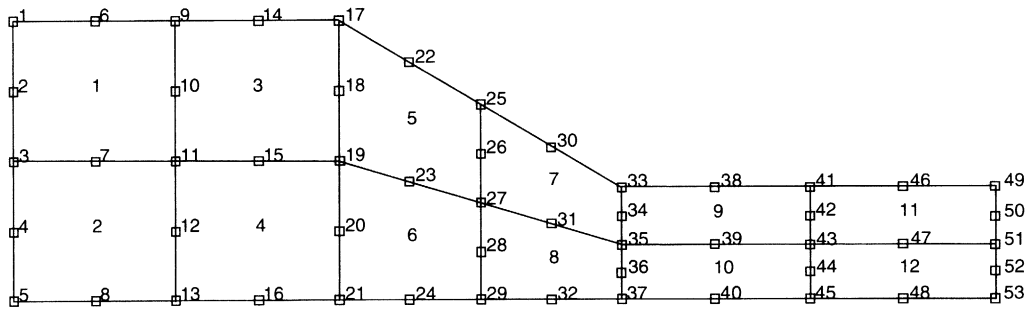
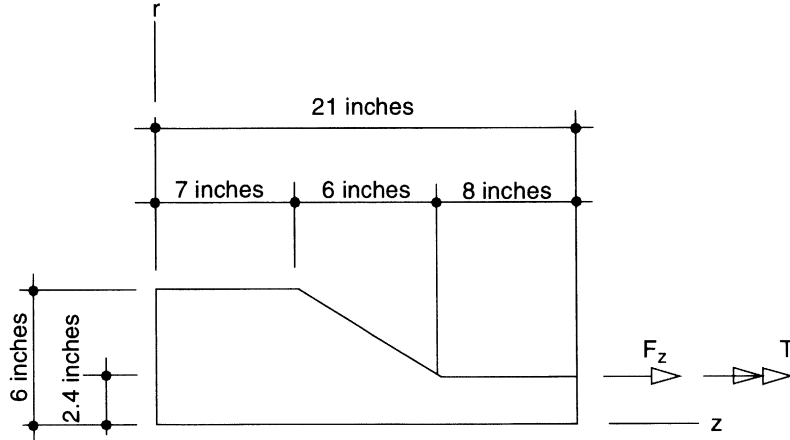
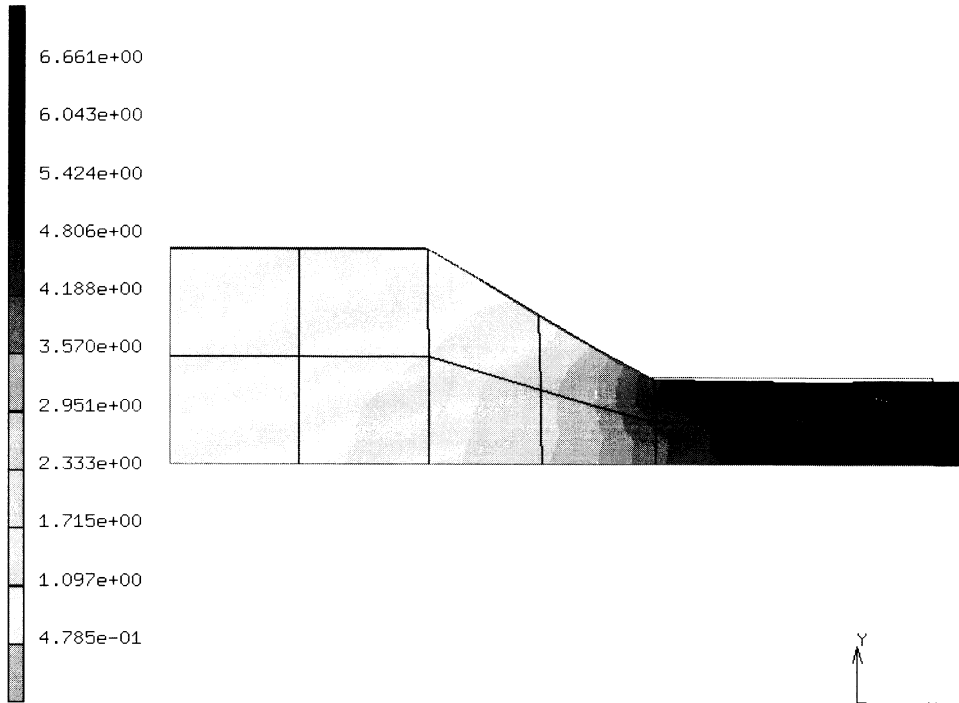


Figure 7.27-1 Circular Bar and Mesh

Inc : 8
Time : 0.000e+00



prob e7.27 nonlinear elastic analysis - elmt 6
Equivalent Von Mises Stress

Figure 7.27-2 Deformed Mesh and Distribution of Equivalent von Mises Stress

7.28 Analysis of a Thick Rubber Cylinder under Internal Pressure

In this example, the deformation of a thick rubber cylinder under internal pressure is modeled. This problem illustrates the use of MARC elements types 10, 28, 55, and 116 (4- and 8-node axisymmetric elements with only displacement degrees of freedom at nodes) for rubber materials. Option ELASTICITY,2 is invoked to activate MARC updated Lagrangian formulation. The rubber material is modeled with either the Ogden or Mooney material models.

Data Set	Element Type(s)	Number of Elements	Number of Nodes	Differentiating Features
e7x28a	10	4	20	Ogden
e7x28b	116	4	10	Mooney
e7x28c	28	4	23	Ogden
e7x28d	55	4	23	Ogden

Element

Library element 10 is a 4-node bilinear axisymmetric element with displacements in radial and axial directions as degrees of freedom. Library element 116 is a 4-node bilinear, reduced integration, axisymmetric element with displacements in radial and axial directions as degrees of freedom. Library element 28 is a 8-node axisymmetric element with displacements in radial and axial directions as degrees of freedom. Library element 55 is a 8-node, reduced integration, axisymmetric element with displacements in radial and axial directions as degrees of freedom.

Model

The cylinder has an internal radius of 1 mm and an external radius of 2 mm. Figure 7.28-1 shows the initial mesh for the data sets using 8-noded elements.

Material Properties

The Mooney material properties are given as:

$$C_1 = 8 \text{ N/mm}^2, C_2 = 2 \text{ N/mm}^2;$$

The Ogden material properties are given as:

$$\mu_1 = 16 \text{ N/mm}^2, \alpha_1 = 2, \mu_2 = 4 \text{ N/mm}^2, \alpha_2 = -2.$$

The bulk modulus is chosen as 200000 N/mm^2 , resulting in the ratio of K/G being 10000. The material is therefore highly incompressible. Both materials are equivalent.

Loads

A uniformly distributed internal pressure of 11.5 N/mm^2 is applied on element number 1. This load is applied in increment zero. In MARC, increment zero is treated as linear. So an additional increment, with no additional load, is used to bring the solution to the correct nonlinear state.

Boundary Conditions

$u = 0$ on the planes $z = 0$ and $z = 1.0$ to simulate a plane strain condition.

Results**A. 8-Node Model (Element Type 28 and 55)**

After the linear elastic step (increment 0), the radial displacements of the inside nodes for both elements 28 and 55 are 0.3833 mm.

They are the same as the analytical solution which predicts a radial displacement of 0.3833 mm.

After ten iterations, the radial displacement at the inside node is 1.0086 mm and the corresponding pressure can be computed from the following expression:

$$P = (C_1 + C_2) \left[\log \left(\frac{B^2 a^2}{A^2 (B^2 - A^2 + a^2)} \right) + \frac{(a^2 - A^2)(B^2 - A^2)}{a^2 (B^2 - A^2 + a^2)} \right]$$

where A and B are the inner and outer radii of the cylinder in the undeformed state, “ a ” is the inner radius in the deformed state, and C_1 and C_2 are material constants.

The computed pressure of 11.5 N/mm^2 is in very good agreement with the prescribed value of 11.5 N/mm^2 .

B. 4-Node Model (Element Type 10 and 116)

After the linear elastic step (increment 0), the radial displacements of the inside nodes (nodes 1 and 6) are 0.3817 mm (for element type 10) and 0.3834 mm (for element type 116) respectively.

Agreement with analytical solution of 0.3833 mm is good. After ten iterations, the radial displacement at inside node is 1.0068 mm, and the corresponding pressure is 11.5 N/mm^2 for element 10. For element 116, the displacement at the inside node is 1.0063 mm and the corresponding pressure is 11.5 N/mm^2 . Agreement with prescribed value of 11.5 N/mm^2 is excellent.



Parameters, Options, and Subroutines Summary

Example e7x28a.dat:

Parameters	Model Definition Options	History Definition Options
ALIAS	CONNECTIVITY	CONTINUE
ELASTICITY	CONTROL	DIST LOAD
ELEMENTS	COORDINATES	
END	DIST LOAD	
FOLLOW FOR	END OPTION	
LARGE DISP	FIXED DISP	
SIZING	OGDEN	
TITLE	POST	

Example e7x28b.dat:

Parameters	Model Definition Options	History Definition Options
ALIAS	CONNECTIVITY	CONTINUE
ELASTICITY	CONTROL	DIST LOAD
ELEMENTS	COORDINATES	
END	DIST LOAD	
FOLLOW FOR	END OPTION	
LARGE DISP	FIXED DISP	
SIZING	MOONEY	
TITLE	POST	



Example e7x28c and e7x28d.dat:

Parameters

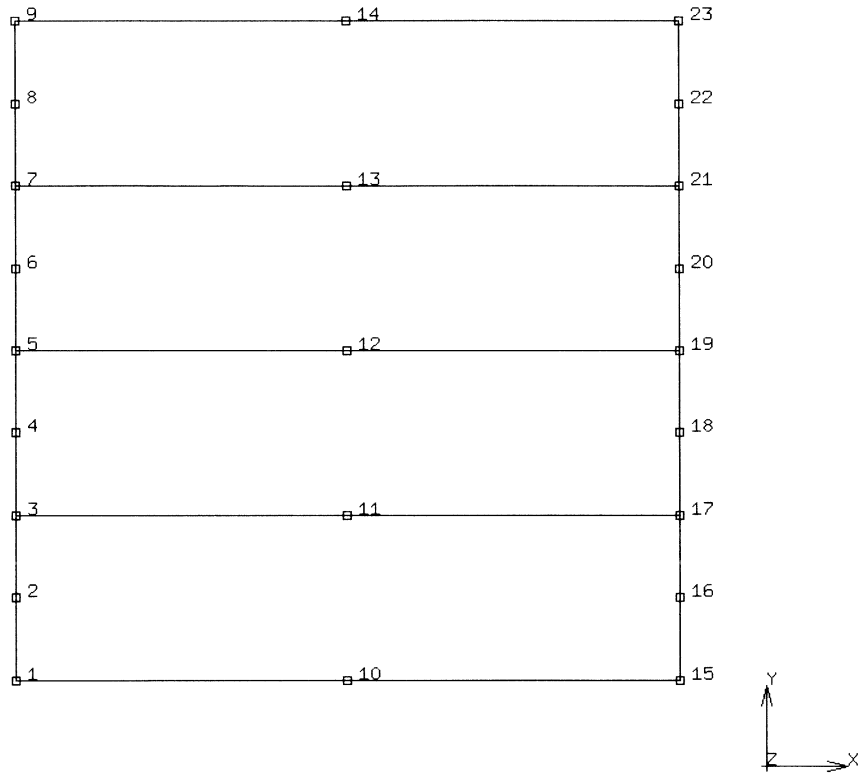
ALIAS
ELASTICITY
ELEMENTS
END
FOLLOW FOR
LARGE DISP
SIZING
TITLE

Model Definition Options

CONNECTIVITY
CONTROL
COORDINATES
DIST LOAD
END OPTION
FIXED DISP
OGDEN
NODE FILL
POST

History Definition Options

CONTINUE
DIST LOAD



prob e7.28d ogden analysis of a thick rubber cylinder

Figure 7.28-1 Cylinder Mesh (8-Node Model)

7.29 3D Analyses of a Plate with a Hole at Large Strains

This problem simulates the tensile loading of a plate with a hole at large strains. In e7x29a.dat, the HYPOELASTIC option and the user subroutine HYPELA2 are used to define constitutive behavior. Element type 7 is used and the material here is compressible. This job demonstrates the use of kinematics in defining user-defined material behavior. In e7x29b.dat, Element type 117 is used to model the plate (with the user-defined defaults file). The material in e7x29b.dat is modeled using Ogden model and is nearly incompressible.

This problem is modeled using the two techniques summarized below.

Data Set	Element Type(s)	Number of Elements	Number of Nodes	Differentiating Features
e7x29a	7	92	218	HYPOELASTIC HYPELA2
e7x29b	117	92	218	user default file

Element

Library element 7 is a 8-node trilinear brick element with global displacements as degrees of freedom. Library element 117 is a 8-node trilinear brick element with reduced integration and global displacements as degrees of freedom.

Model

Due to symmetry of the geometry and loading, a quarter of the actual model is simulated. The finite element model is made up of 92 elements and 218 nodes. The finite element mesh is shown in Figure 7.29-1.

Geometry

The model is assumed to be a square of side 2 mm from which a quarter of a circle of radius 0.6 mm has been cut out. The initial thickness is 0.2 mm.

Material Properties

In e7x29a.dat, a quadratic-logarithmic, nonlinear elastic model with the initial bulk modulus of 21666.67 N/mm² and the initial shear modulus of 10000.00 N/mm² is defined using the HYPOELASTIC option and the user subroutine HYPELA2. In e7x29b.dat, the Ogden parameters are given as $\mu_1=0.586$ N/mm², $\alpha_1=2.0$, $\mu_2=-0.354$ N/mm², and $\alpha_2=-2.0$. The initial bulk modulus is 666666.667 N/mm².

Boundary Conditions and Loading

In addition to the boundary conditions due to symmetry, the third degree of freedom of the nodes located on the edges of the lower surface are fixed to avoid the rigid body motion in z-direction.

The loading is tensile. In e7x29a.dat, a uniform displacement of 1 mm is applied to one of the plate edges using 20 increments. The macroscopic total logarithmic strain is 40%. In e7x29b.dat, a uniform displacement of 2.5 mm is applied to one of the plate edges using 10 increments. The macroscopic total logarithmic strain is 81%.

Results

The distribution of equivalent von Mises stress and the deformed model for e7x29a.dat after 20 increments is shown in Figure 7.29-2. The distribution of equivalent von Mises stress and the deformed model for e7x29b.dat after 10 increments is shown in Figure 7.29-3.

Parameters, Options, and Subroutines Summary

Example e7x29a.dat:

Parameters	Model Definition Options	History Definition Options
ELEMENTS	CONNECTIVITY	AUTO LOAD
END	CONTROL	CONTINUE
LARGE DISP	COORDINATES	DISP CHANGE
PROCESS	END OPTION	
SETNAME	FIXED DISP	
SIZING	GEOMETRY	
TITLE	HYPOELASTIC	
UPDATE	OPTIMIZE	
	POST	

User Subroutine u7x29a.f

HYPELA2



Example e7x29b.dat:

Parameters

ELEMENTS
END
SETNAME
SIZING
TITLE

Model Definition Options

CONNECTIVITY
CONTROL
COORDINATES
END OPTION
FIXED DISP
GEOMETRY
OGDEN
OPTIMIZE
POST

History Definition Options

AUTO LOAD
CONTINUE
DISP CHANGE

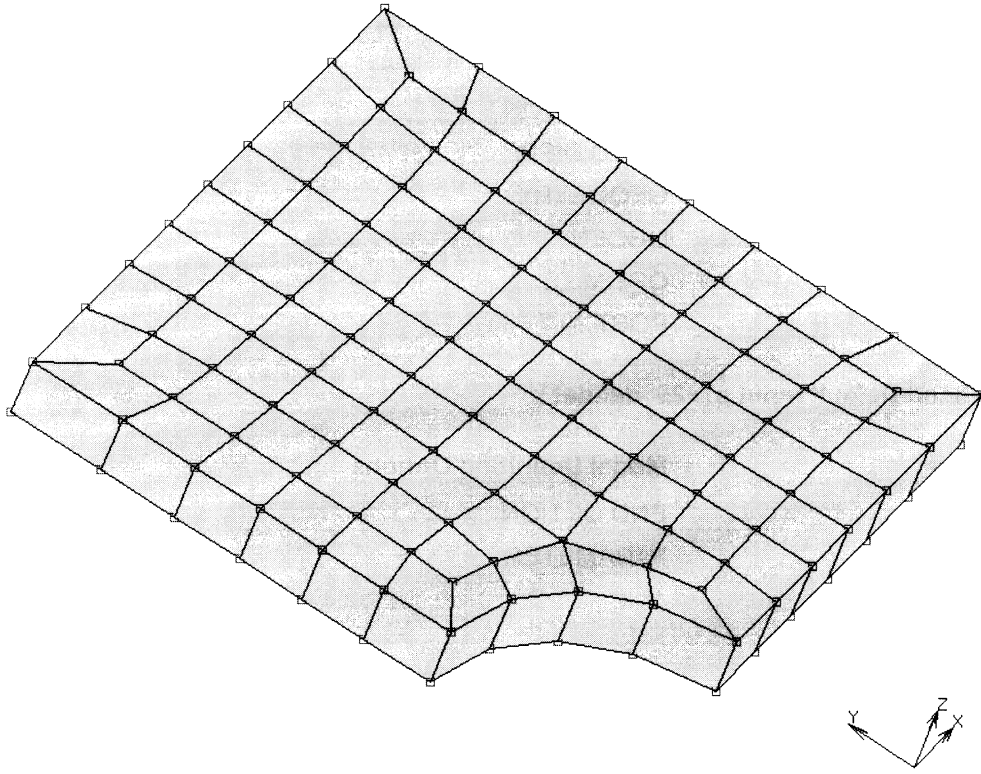
User Defined Default Input e7x29_def.dat

Parameters

ALL POINTS
ELASTICITY
END
LARGE DISP
PRINT
PROCESS

Model Definition Options

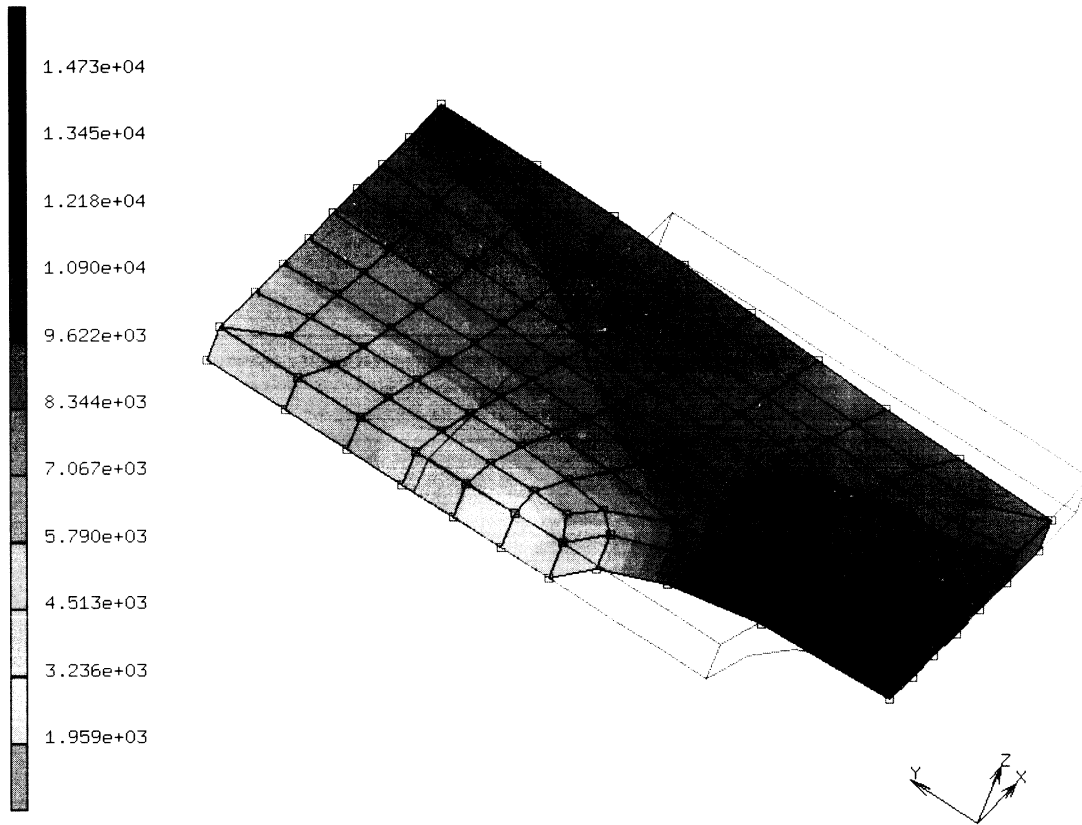
END OPTION
PARAMETER



hole in the plate : example of hypela2

Figure 7.29-1 Initial Mesh

Inc : 20
Time : 0.000e+00



hole in the plate : example of hypela2
Equivalent Von Mises Stress

Figure 7.29-2 Deformed Model and Distribution of Equivalent von Mises Stress for e7x29a

Inc : 10
Time : 0.000e+00

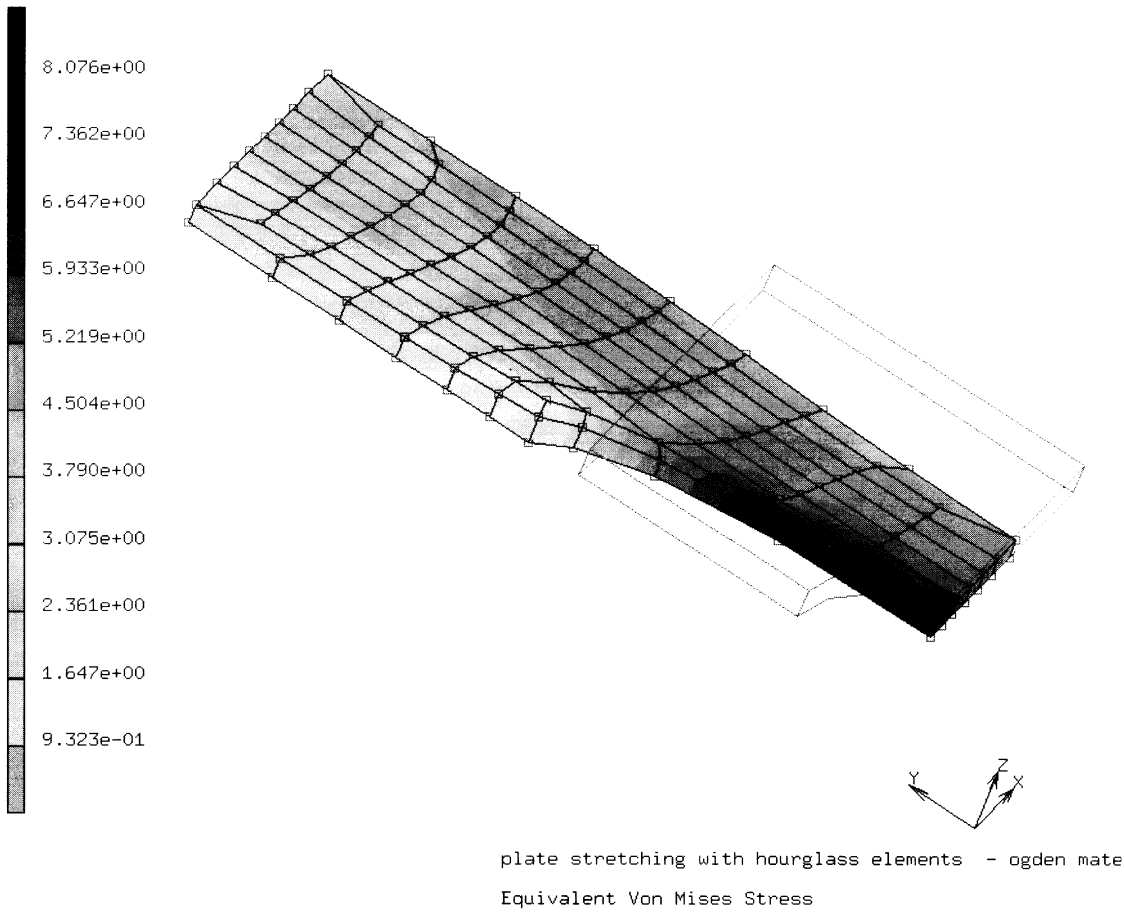


Figure 7.29-3 Deformed Model and Distribution of Equivalent von Mises Stress for e7x29b

7.30 Damage in Elastomeric Materials

Two phenomena observed in continuum damage have been evaluated in this example using continuous and discontinuous damage models. The discontinuous damage model essentially simulates the Mullins effect while the continuous damage model is able to capture the stiffness degradation (fatigue) due to cyclic loading.

This problem is modeled using the two techniques summarized below.

Data Set	Element Type(s)	Number of Elements	Number of Nodes	Differentiating Features
e7x30a	7	1	8	Discontinuous Damage Model
e7x30b	7	1	8	Continuous Damage Model

Model

A single element rubber cube, comprised of element 7, is subjected to tensile loading. The example is in itself very simple but demonstrates the two phenomena very effectively.

Material Properties

The material can be described using the Ogden material model using a three term series. The data was fit such that:

Term	μ (N/cm ²)	α
1	11.0	2.35
2	5.8e-4	7.03
3	0.73	1.28

and the bulk modulus was 1.0E9 N/cm².

The damage parameters for problem e7x30a.dat are:

	Discontinuous	Continuous
1st scale factor	0.4	0.0
1st relaxation factor	10.0	1.0
1st scale factor	0.1	0.0
2nd relaxation factor	100.0	1.0

The damage parameters for problem e7x30b.dat are:

	Discontinuous	Continuous
1st scale factor	0.0	0.40
1st relaxation factor	1.0	100.0
1st scale factor	0.0	0.1
2nd relaxation factor	1.0	100.0

Loads

The loading is applied as displacement boundary condition. The discontinuous damage is simulated by application of six loadcases while in the case of continuous damage, ten loadcases are applied. For the discontinuous damage, the applied loading increases with each set of tension and compression while for the continuous damage the applied loading is kept the same. The auto-increment option is used to apply the extension and compression in sets of 100 loading steps for each loadcase.

Results

It can be noticed from Figure 7.30-1 that the Mullin's effect is very well captured by the model, where three sets of loading and unloading show hysteresis, which increases in magnitude as the maximum applied strain in the model exceeds the previously applied level of strain. Also, once the material is reloaded past its previously applied maximum load, the loading continues on the previous loading path.

The progressive degradation of material stiffness with constant maximum applied strain level, namely fatigue, is simulated next. Figure 7.30-2 demonstrates that five sets of loading and unloading show hysteresis with a continuous loss of stiffness in the loading curve. The model implemented in MARC to simulate this behavior is due to C. Miehe.

Parameters, Options, and Subroutines Summary

Example e7x30a.dat and e7x30b.dat:

Parameters	Model Definition Options	History Definition Options
ELEMENT	CONNECTIVITY	AUTO INCREMENT
END	CONTACT	CONTINUE
ELASTICITY	CONTROL	DISP CHANGE
LARGE DISP	COORDINATES	CONTROL
PRINT	DEFINE	
SIZING	FIXED DISP	
TITLE	END OPTION	
	OGDEN	
	DAMAGE	
	POST	



Figure 7.30-1 Discontinuous Damage

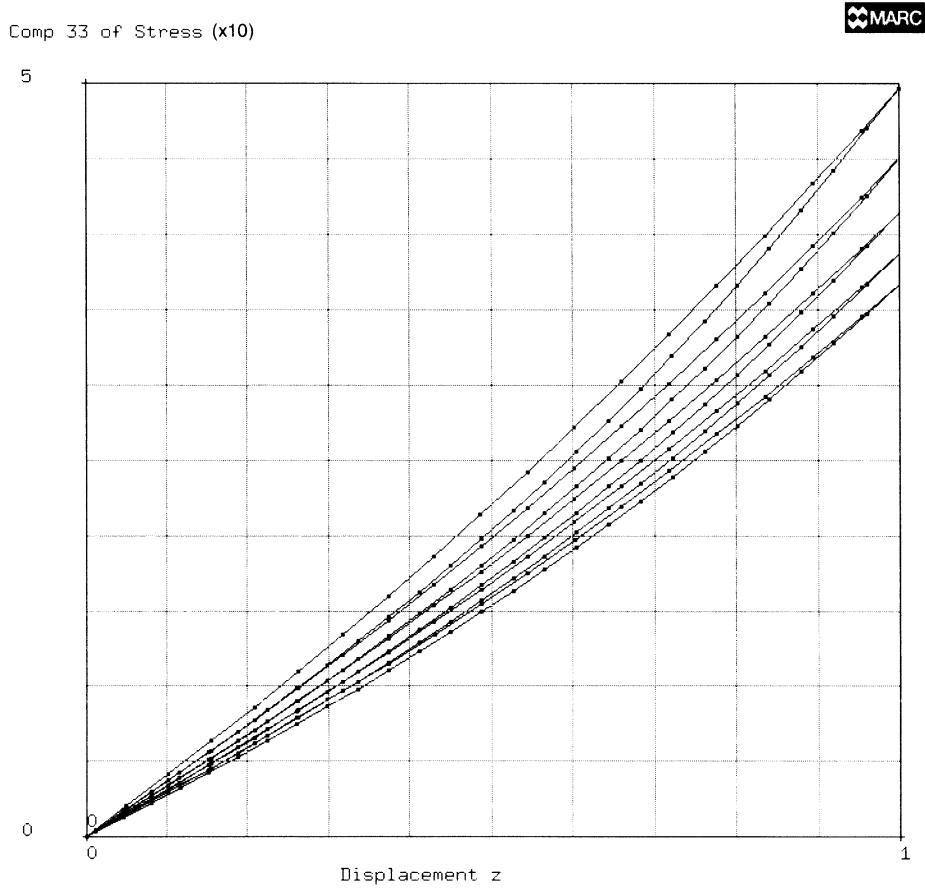


Figure 7.30-2 Continuous Damage

7.31 Rezoning in an Elastomeric Seal

This example demonstrates the capability of rezoning in an elastomeric seal. A rubber seal is being formed into its final shape by application of die pressure. Although the geometry itself is simple, the severely deformed configuration at an intermediate stage leads to a premature termination of the analysis due to excessive distortion in the elements. A new mesh via rezoning operation is clearly required for a successful completion of the analysis.

This problem is modeled using two data sets summarized below.

Data Set	Element Type(s)	Number of Elements	Number of Nodes	Differentiating Features
e7x31	11	382	433	Before Rezoning
e7x31b	11	633	692	After Rezoning

Model

The original model, i.e., before the rezoning step, consists of 382 4-node quadrilateral elements with 433 nodes. After the rezoning, the number of elements in the mesh increased to 633 while the number of nodes increased to 692. Displacement based plane strain element 11, is chosen to simulate the seal. For finite strain elasticity and plasticity material models, this element has special treatment for incompressibility.

Material Properties

The rubber seal can be described using the two term Ogden material model. The data was fit such that:

Term	μ (N/cm ²)	α
1	+0.324922	2.0
2	-0.568008	-2.0

and the bulk modulus was 8929.3 N/cm²

Contact

The contact is modeled as frictionless and the contact bodies are modeled as NURBS. Default tolerances are taken in the run with the original mesh but in the run after the rezoning, the contact zone tolerance is increased to 0.007. The reason for this is that after the rezoning step,

there are some nodes that may be outside the default contact zone of 0.00680325. As a result, in the step after rezoning, there may be increment splitting which may sometimes lead to non-convergent solutions.

Results

The deformed meshes at increments 0, 7, 14, 15, and 29 are shown in Figure 7.31-1 to Figure 7.31-5. The sudden change in the mesh between the increments 14 and 15 reflects rezoning. Also, Figure 7.31-6 gives the plot of contact force distribution in the body.

When the analysis involves rezoning with updated Lagrange elasticity, the following items must be considered:

- a. Drive down the residuals to a low value in the last one or two steps of the first analysis (before restart)
- b. Take very small steps in the beginning of the second analysis (i.e. after restart)

Parameters, Options, and Subroutines Summary

Example e7x31a.dat:

Parameters	Model Definition Options	History Definition Options
ALIAS	CONNECTIVITY	AUTO LOAD
ELASTICITY	CONTACT	CONTINUE
ELEMENT	CONTACT TABLE	CONTROL
END	CONTROL	TIME STEP
LARGE DISP	COORDINATES	
PRINT	END OPTION	
REZONE	NO PRINT	
SIZING	OGDEN	
TITLE	POST	
	RESTART	



Example e7x31b.dat:

Parameters

ALIAS
ELASTICITY
ELEMENT
END
LARGE DISP
PRINT
REZONE
SIZING
TITLE

Model Definition Options

CONNECTIVITY
CONNECTIVITY CHANGE
CONTACT
CONTACT CHANGE
CONTACT TABLE
CONTROL RESTART
COORDINATE CHANGE
COORDINATES
END OPTION
END REZONE
NO PRINT
OGDEN
POST
REAUTO
RESTART

History Definition Options

AUTO LOAD
CONTINUE
CONTROL
TIME STEP

Inc : 0
Time : 0.000e+00

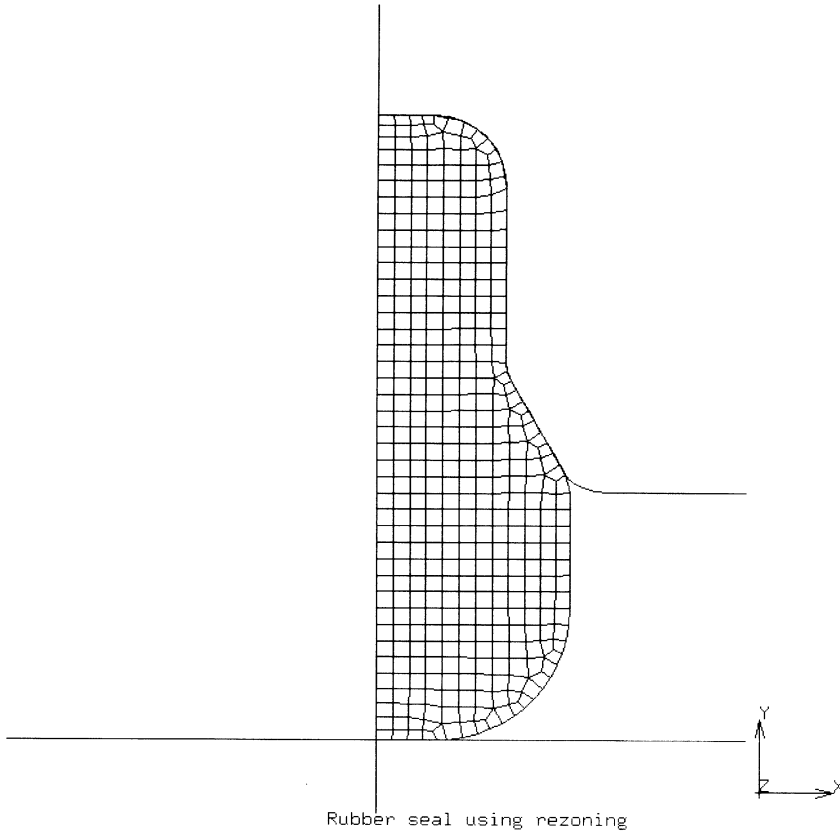


Figure 7.31-1 Deformed Mesh at Increment 0

Inc : 7
Time : 7.000e+00

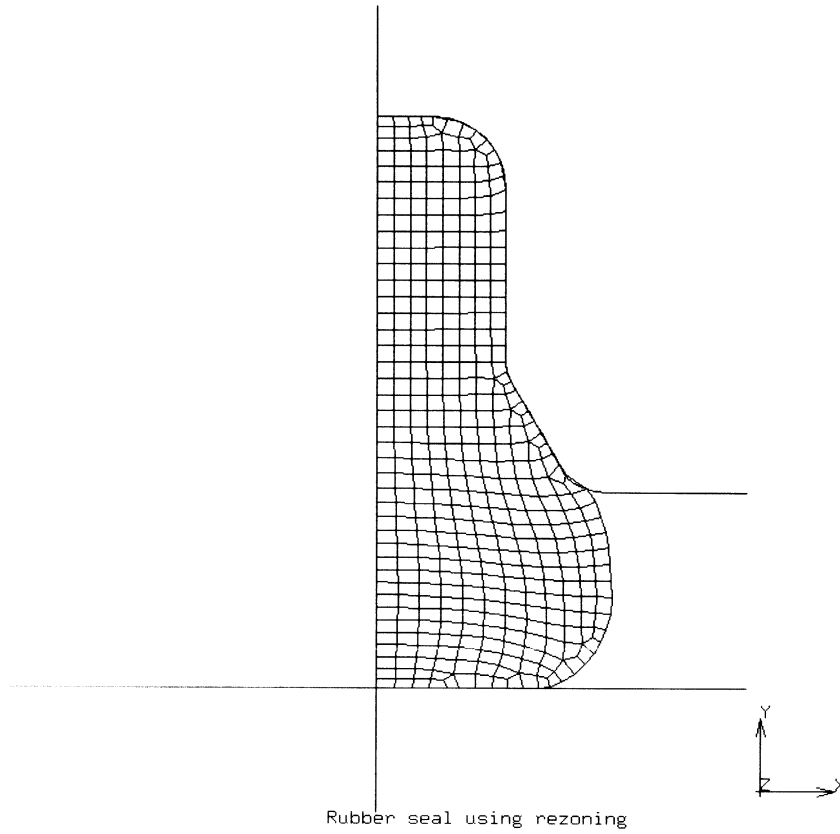


Figure 7.31-2 Deformed Mesh at Increment 7

Inc : 14
Time : 1.400e+01

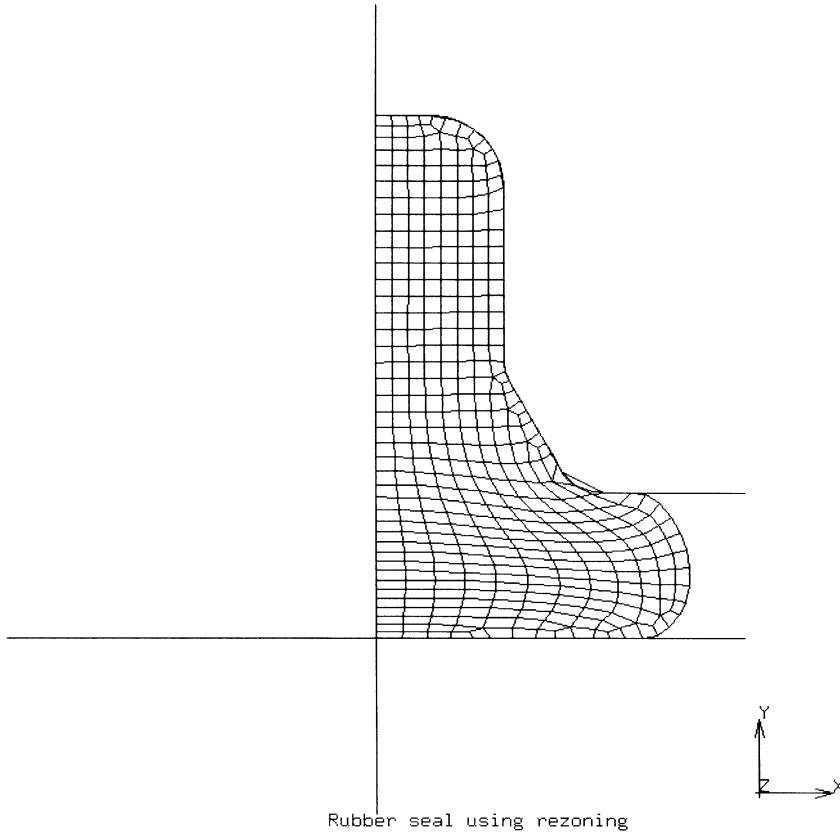


Figure 7.31-3 Deformed Mesh at Increment 14

Inc : 15
Time : 1.400e+01

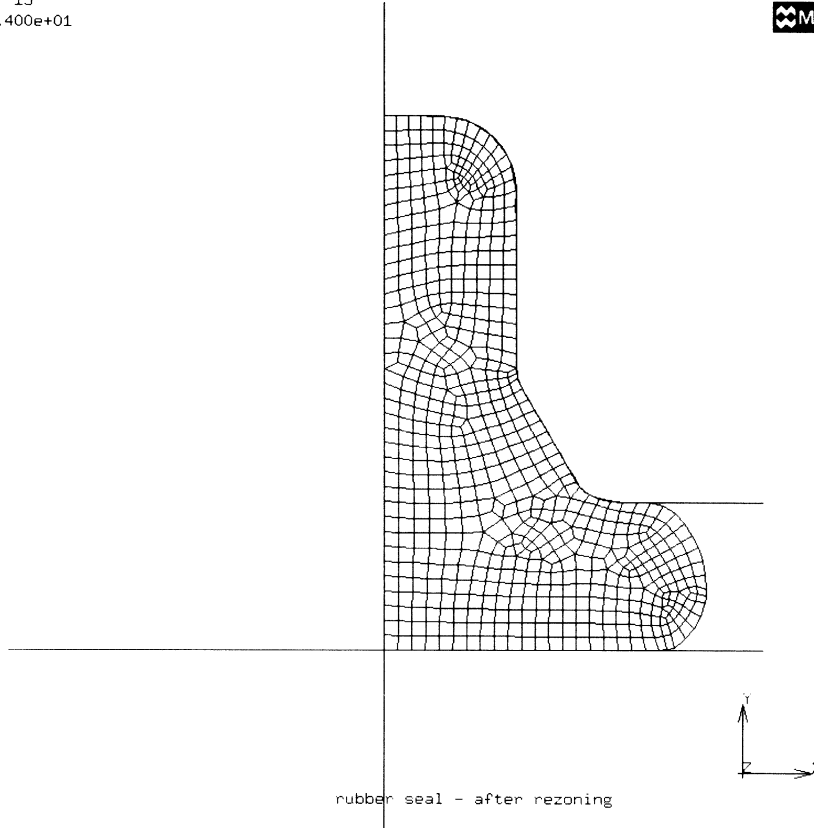


Figure 7.31-4 Deformed Mesh at Increment 15

Inc : 29
Time : 1.810e+01

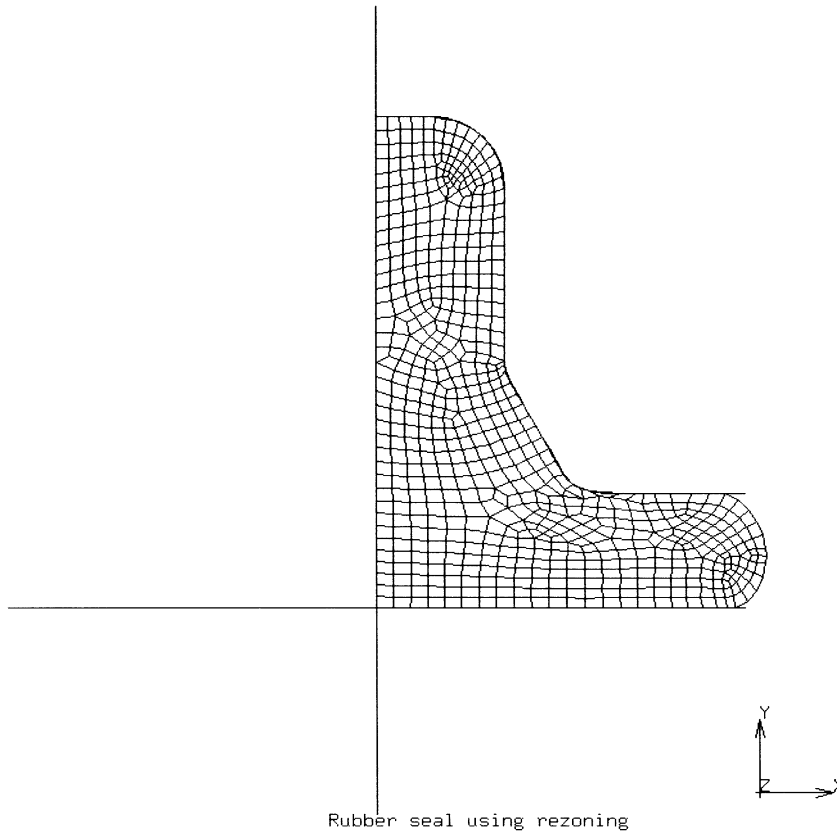


Figure 7.31-5 Deformed Mesh at Increment 29

Inc : 29
Time : 1.810e+01

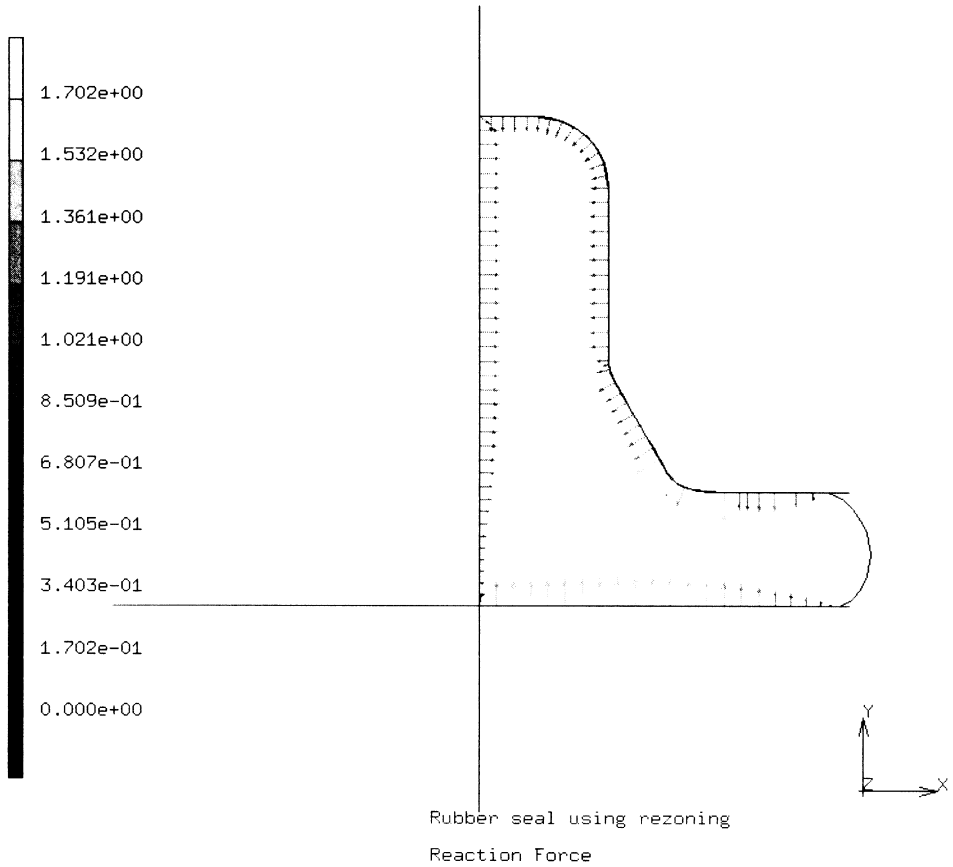


Figure 7.31-6 Contact Force Distribution

7.32 Structural Relaxation of a Glass Cube

Free structural relaxation of a glass cube subjected a cyclic temperature history, is simulated using Narayanaswamy model. This problem is modeled by means of element type 7.

The annealing of flat glass requires that the residual stresses be of an acceptable magnitude, while the specification for optical glass components usually includes a homogenous refractive index. The design of heat treated processes (for example, annealing) can be accomplished using the Narayanaswamy model. This allows you to study the time dependence of physical properties (for example, volumes) of glass subjected to a change in temperature.

The glass transition is a region of temperature in which molecular rearrangements occur on a scale of minutes or hours, so that the properties of a liquid change at a rate that is easily observed. Below the glass transition temperature, T_g , the material is extremely viscous and a solidus state exists. Above T_g the equilibrium structure is arrived at easily and the material is in liquidus state. Hence, the glass transition is revealed by a change in the temperature dependence of some property of a liquid during cooling. If a mechanical stress is applied to a liquid in the transition region, a time-dependent change in dimensions results due to the phenomenon of visco-elasticity.

If a liquid in the transition region is subjected to a sudden change in temperature, a time-dependent change in volume occurs. The latter process is called structural relaxation. Hence, structural relaxation governs the time-dependent response of a liquid to a change of temperature.

Element

Library element 7 is a 8-node trilinear brick element with global displacements as degrees of freedom.

Model

The side length of the glass cube is 2 mm. Because of the symmetry, only one eighth of the cube is modeled with one brick element.

Material Properties

The instantaneous moduli are given via ISOTROPIC option as: Young's modulus is 5.58E4 N/mm²; Poisson's ratio is 0.0814. The time dependent values are entered using VISCEPROP option as:



Term No.	Shear Constant	Relaxation Time
1	1.08876E4	9.97000E-2
2	1.09134E4	9.40000E-3
3	3.97320E4	3.00000E-4

The solid and the liquid coefficients of the thermal expansion are chosen as $5.50E-7$ and $1.93E-6$, respectively. The weights and the reference relaxation times, used to define the response function, for each term in the series are input through SHIFT FUNCTION as:

Term No.	Weight	Reference Relaxation Time
1	1.0800E-1	1.4780E+0
2	4.4300E-1	3.2970E-1
3	1.6600E-1	1.2130E-1
4	1.6100E-1	4.4600E-2
5	4.6000E-2	1.6400E-2
6	7.6000E-2	3.7000E-3

Loads

An initial temperature of $6.20E2$ is applied to the glass cube at increment 0. A cyclic temperature history is then applied: At first, the cube is gradually cooled down to $0.20E2$ in 100 equal increments; Afterwards, it is heated up to the initial temperature at the equal incremental size.

Boundary Conditions

Boundary conditions are applied to the glass cube according to the symmetry.

Results

Suppose a glass is equilibrated at temperature T_1 , and suddenly cooled to T_2 at t_0 . The instantaneous change in volume is $\alpha_g(T_2 - T_1)$, followed by relaxation towards the equilibrium value $V(\infty, T_2)$. The total change in volume due to the temperature change is $\alpha_l(T_2 - T_1)$ as shown in Figure 7.32-1b. The rate of volume change depends on a characteristic time called the relaxation time.

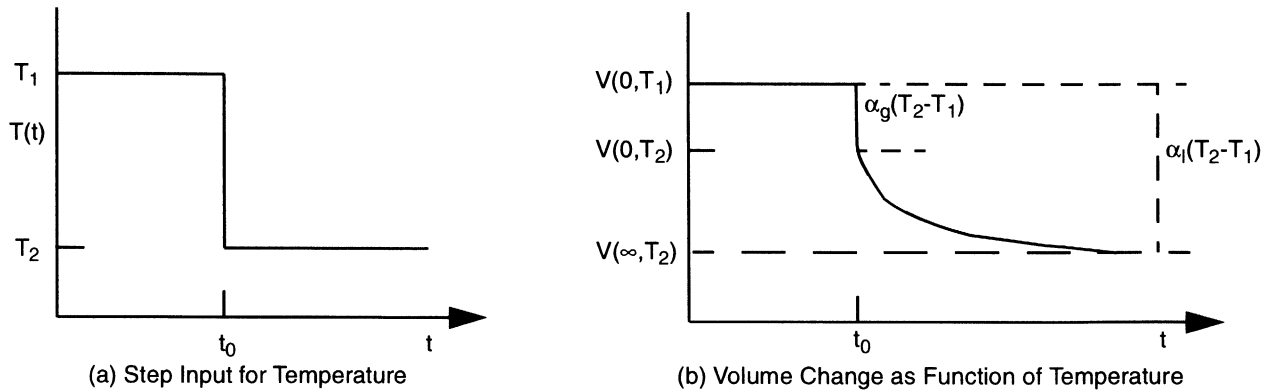


Figure 7.32-1 Structural Relaxation Phenomenon

The slope of dV/dT changes from the high value characteristic of the fluid α_l to the low characteristic of the glass α_g as shown in Figure 7.32-2. The glass transition temperature T_g is a point in the center of the transition region. The low-temperature slope α_g represents the change in volume V caused by vibration of the atoms in their potential wells. In the (glassy) temperature range, the atoms are frozen into a particular configuration. As the temperature T increases, the atoms acquire enough energy to break bonds and rearrange into new structures. That allows the volume to increase more rapidly, so $\alpha_l > \alpha_g$. The difference $\alpha = \alpha_l - \alpha_g$ represents the structural contribution to the volume.

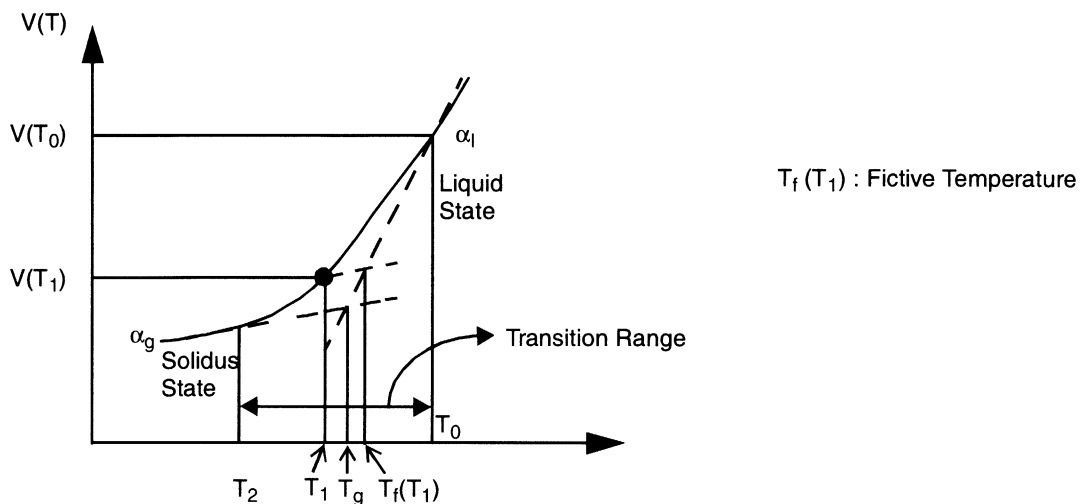


Figure 7.32-2 Property (Volume) – Temperature Plot

When a liquid is cooled and reheated, a hysteresis is observed.

The volume change of the glass cube with the change of the temperature 1 as calculated by MARC, is illustrated in Figure 7.32-3. The hysteresis shown in Figure 7.32-3 indicates the calculations are in a good qualitative agreement with experimental observations.

Parameters, Options, and Subroutines Summary

Example e7x32.dat:

Parameters	Model Definition Options	History Definition Options
ALL POINTS	CHANGE STATE	AUTO LOAD
ELEMENTS	CONNECTIVITY	CHANGE STATE
END	COORDINATES	CONTINUE
SETNAME	END OPTIONS	CONTROL
SIZING	FIXED DISP	TIME STEP
STATE VARS	ISOTROPIC	
TITLE	OPTIMIZE	
	PRINT CHOICE	
	POST	
	SHIFT FUNCTION	
	SOLVER	
	VISCEL EXP	
	VISCELPROP	
	\$NO PRINT	

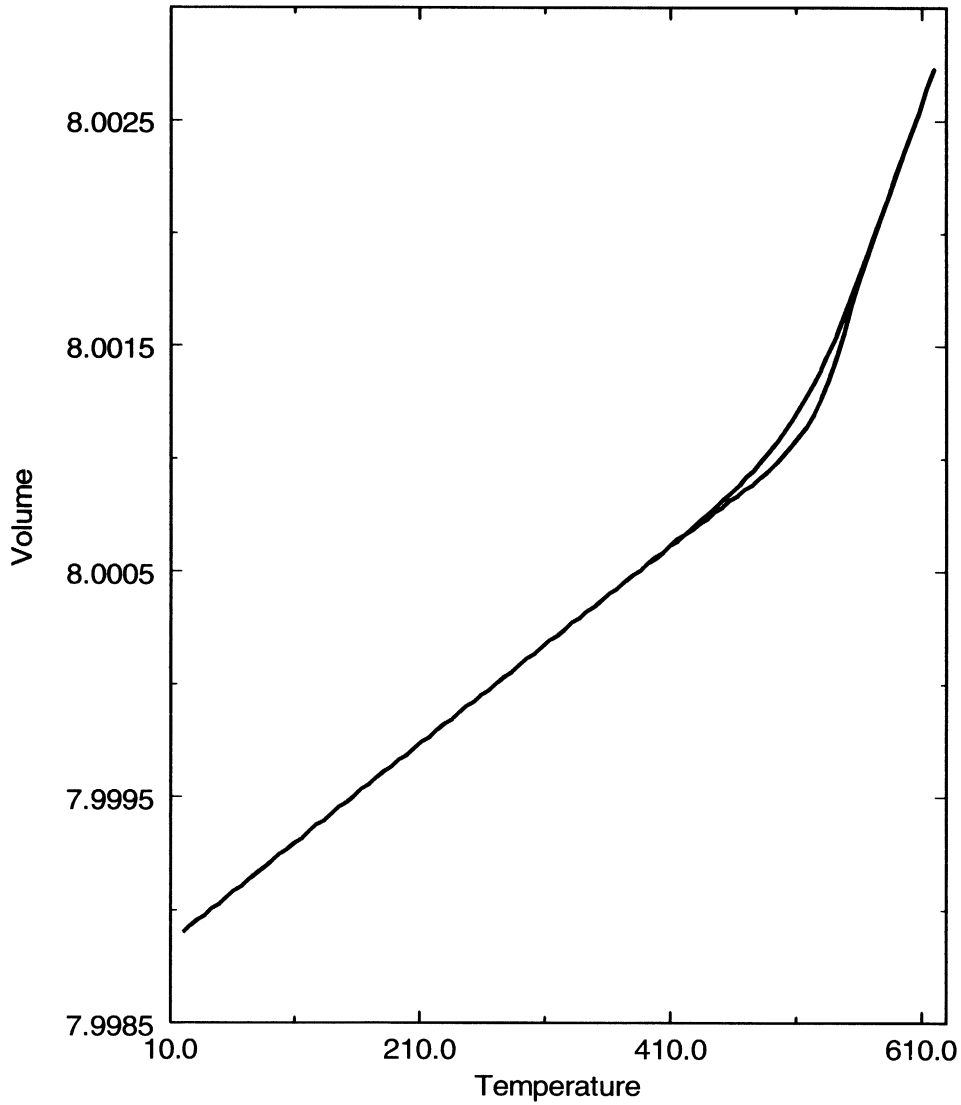
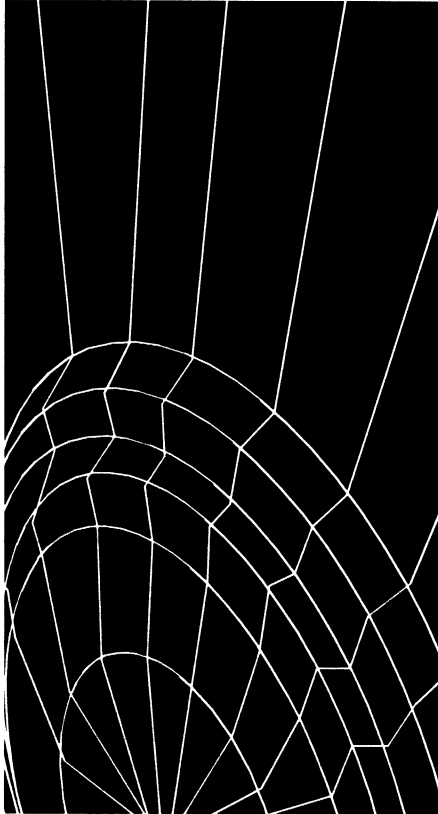
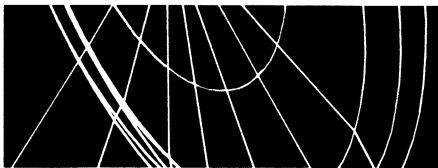


Figure 7.32-3 Volume Change during Cyclic Temperature History



MARC



Volume E

Demonstration Problems

Version K7

Chapter 8
Advanced Topics





Advanced Topics Contents



Description	Problem
Plate with Circular Hole using Substructures	8.1
Double-Edge Notch Specimen using Substructures	8.2
End-Plate-Aperture Breakaway	8.3
Collapse of a Notched Concrete Beam	8.4
Cracking Behavior of a One-way Reinforced Concrete Slab using Shell Elements	8.5
Cracking Behavior of a One-way Reinforced Concrete Slab	8.6
Compression of a Block	8.7
Simply-supported Thick Plate under Uniform Pressure with Anisotropic Properties.	8.8
Failure Criteria Calculation for Plane Stress Orthotropic Sheet.	8.9
Beam Element 52 with Nonlinear Elastic Stress-Strain Relation	8.10
Element Deactivation/Activation and Error Estimate in the Analysis of a Plate with Hole	8.11
Forging of the Head of a Bolt	8.12
Coupled Analysis of Ring Compression.	8.13
3D Contact with Various Rigid Surface Definitions.	8.14
Double-Sided Contact	8.15
Demonstration of Springback	8.16
3D Extrusion Analysis with Coulomb Friction	8.17
3D Forming of a Circular Blank Using Shell or Membrane Elements and Coulomb Friction	8.18
3D Indentation and Rolling without Friction	8.19
2D Electrostatic Analysis of a Circular Region	8.20



Description	Problem
3D Electrostatic Analysis of a Circular Region	8.21
2D Magnetostatic Analysis of a Circular Region	8.22
3D Magnetostatic Analysis of a Coil	8.23
2D Nonlinear Magnetostatic Analysis.	8.24
Acoustic Problem: Eigenvalue Analysis of a Circular Cavity.	8.25
Acoustic Problem: Eigenvalue Analysis of a Rectangular Cavity.	8.26
Progressive Failure of a Plate with a Hole.	8.27
Linear Distribution of Dipoles.	8.28
Magnetic Field around Two Wires carrying Opposite Currents.	8.29
Harmonic Electromagnetic Analysis of a Wave Guide	8.30
Transient Electromagnetic Analysis around a Conducting Sphere	8.31
Cavity Resonator.	8.32
Electromagnetic Analysis of an Infinite Wire	8.33
Triaxial Test on Normally Consolidated Weald Clay	8.34
Soil Analysis of an Embankment	8.35
Interference Fit of Two Cylinders	8.36
Interference Fit Analysis.	8.37
Deep Drawing of a Box using NURB Surfaces	8.38
Contact of Two Beams using AUTO INCREMENT	8.39
Circular Disk under Point Loads Using Adaptive Meshing	8.40
Stress Singularity Analysis using Adaptive Meshing	8.41
Contact Analysis with Adaptive Meshing	8.42
Rubber Seal Analysis using Adaptive Meshing	8.43
Simplified Rolling Example with Adaptive Meshing	8.44
Use of the SPLINE Option for Deformable-Deformable Contact	8.45
Use of the EXCLUDE Option for Contact Analysis	8.46



Description	Problem
Simulation of Contact with Stick-Slip Friction	8.47
Simulation of Deformable-Deformable Contact with Stick-Slip Friction.	8.48
Rolling of a Compressed Rubber Bushing with Stick-Slip Friction.	8.49
Compression Test of Cylinder with Stick-Slip Friction	8.50
Modeling of a Spring	8.51
Deep Drawing of Sheet	8.52
Shell-Shell Contact and Separation	8.53
Self Contact of a Shell Structure.	8.54
Deep Drawing of Copper Sheet	8.55
2D Contact Problem - Load Control and Velocity Control	8.56
The ADAPTIVE Capability with Shell Elements	8.57
Adaptive Meshing in Multiply Connected Shell Structures	8.58
Not Available	8.59
Simulation of Sheet Bending	8.60



8 *Advanced Topics Contents*



Advanced Topics List of Figures



Figure		Page
8.1-1	Hole in Plate	8.1-4
8.1-2	Substructure 1,1	8.1-5
8.2-1	Double-Edge Notch Specimen.	8.2-4
8.2-2	Mesh for Double-Edge Notch Specimen Cross-Hatched Area Indicates Substructures	8.2-5
8.2-3	(A) Elements in Substructure 1-1	8.2-6
8.2-3	(B) Nodes in Substructure 1-1	8.2-7
8.2-4	(A) Elements at Highest Level.	8.2-8
8.2-4	(B) Nodes at Highest Level	8.2-9
8.2-5	Workhardening Slopes.	8.2-10
8.3-1	Geometry and Mesh of End Plate-Aperture	8.3-4
8.3-2	Transient Normal Force in Bolts	8.3-5
8.3-3	Transient Shear Force in Bolt	8.3-6
8.3-4	Radial Displacement at Outside Top (Node 46).	8.3-7
8.4-1	Geometry and Element Mesh	8.4-4
8.4-2	Element Numbering Detail of Mesh.	8.4-5
8.4-3	Node Numbering Detail of Mesh	8.4-6
8.4-4	Material Properties.	8.4-7
8.4-5	Comparison of Calculated and Experimental Load Deflection Curve Notched Beam Test.	8.4-7
8.5-1	Geometry of One-Way Reinforced Slab.	8.5-4
8.5-2	Element Mesh with Node Numbering	8.5-5
8.5-3	Element Mesh with Element Numbering	8.5-6
8.5-4	Load-Deflection Relationship for One-Way Reinforced Slab.	8.5-7



Figure		Page
8.6-1	One-Way Reinforced Slab	8.6-4
8.6-2	Element Types used in Analysis.	8.6-4
8.6-3	Node Numbering.	8.6-5
8.6-4	Element Numbering Concrete Elements.	8.6-6
8.6-5	Element Numbering Rebar Elements	8.6-7
8.6-6	Load/Deflection Relationship for One-Way Reinforced Slab.	8.6-8
8.7-1	Mesh	8.7-5
8.7-2	Equivalent Stress, Increment 30	8.7-6
8.7-3	Temperature, Increment 30	8.7-7
8.7-4	Equivalent Stress, Increment 40	8.7-8
8.7-5	Temperature, Increment 40	8.7-9
8.7-6	Equivalent Stress, Increment 50	8.7-10
8.7-7	Temperature, Increment 50	8.7-11
8.7-8	Equivalent Stress, Increment 60	8.7-12
8.7-9	Temperature, Increment 60	8.7-13
8.7-10	Equivalent Stress, Increment 70	8.7-14
8.7-11	Temperature, Increment 70	8.7-15
8.7-12	Total Displacement, Increment 70.	8.7-16
8.8-1	Thick Plate Mesh	8.8-5
8.8-2	Anisotropic Behavior Stress Contours.	8.8-6
8.8-3	Isotropic Behavior Stress Contours	8.8-7
8.9-1	Orthotropic Square Plate.	8.9-4
8.9-2	Point Load ($\times 10^6$) and Support	8.9-5
8.10-1	Cantilever Beam with Prescribed Tip Displacement	8.10-4
8.11-1	Mesh Layout for Plate with Hole	8.11-4
8.12-1	Model	8.12-8
8.12-2	Initial Mesh	8.12-9
8.12-3	Initial Mesh with Modified Rigid Body 3 for Adaptive Analysis	8.12-10
8.12-4	Rezoning Mesh	8.12-11
8.12-5	Equivalent Plastic Strain until Rezoning	8.12-12
8.12-6	Equivalent Mises Tensile Stress at Bolt Height = 22.68	8.12-13



Figure	Page
8.12-7 Mean Normal Stress Until Rezoning	8.12-14
8.12-8 Final Equivalent Plastic Strain.	8.12-15
8.12-9 Final Equivalent von Mises Tensile Stress	8.12-16
8.12-10 Final Mean Normal Stress	8.12-17
8.12-11 Adapted Mesh at Increment 20	8.12-18
8.12-12 Adapted Mesh at Increment 40	8.12-19
8.12-13 Adapted Mesh at Increment 60	8.12-20
8.12-14 Equivalent Mises Tensile Stress at Bolt Height = 22.7 ($F^e F^P$)	8.12-21
8.13-1 Original Mesh	8.13-6
8.13-2 Deformed Mesh (50% Height Reduction).	8.13-7
8.13-3 Equivalent Plastic Strain.	8.13-8
8.13-4 Equivalent von Mises Tensile Stress	8.13-9
8.13-5 Total Nodal Temperature	8.13-10
8.14-1 Undeformed Block.	8.14-5
8.14-2 Block and Indentor.	8.14-6
8.14-3 Ruled Surface	8.14-7
8.14-3 Ruled Surface (Continued)	8.14-8
8.14-3 Ruled Surface (Continued)	8.14-9
8.14-4 Deformed Block	8.14-10
8.15-1 Mesh	8.15-6
8.15-2 Nodal Configuration, Element Type 11	8.15-7
8.15-3 Nodal Configuration, Element Type 27	8.15-8
8.15-4 Nodal Displacements at Increment 10, Element Type 11	8.15-9
8.15-5 Nodal Displacements at Increment 20, Element Type 11	8.15-10
8.15-6 Nodal Displacements at Increment 30, Element Type 11	8.15-11
8.15-7 Equivalent Plastic Strain at Increment 30, Element Type 11	8.15-12
8.15-8 Nodal Displacements at Increment 10, Element Type 27	8.15-13
8.15-9 Nodal Displacements at Increment 20, Element Type 27	8.15-14
8.15-10 Nodal Displacements at Increment 30, Element Type 27	8.15-15
8.15-11 Equivalent Plastic Strain at Increment 30, Element Type 27	8.15-16
8.15-12 Load History for Both Element Types.	8.15-17
8.15-13 Deformed Geometry at Increment 25 for Data Set e8x15d	8.15-18



Figure		Page
8.15-14	Deformed Geometry at Increment 50 for Data Set e8x15d	8.15-19
8.15-15	Contours of Total Equivalent Plastic Strain on Final Geometry for Data Set e8x15d	8.15-20
8.16-1	Original Configuration.	8.16-4
8.16-2	Deformed Mesh	8.16-5
8.16-3	Equivalent Stress.	8.16-6
8.16-4	Initial and Deformed Geometry 53 Increments for Data Set e8x16b	8.16-7
8.16-5	Contours of Equivalent von Mises Stress at 53 Increments for Data Set e8x16b	8.16-8
8.17-1	Rigid Surfaces Defining Extrusion Die	8.17-4
8.17-2	Deformed Mesh, Increment 35	8.17-5
8.17-3	Deformed Mesh, Increment 35	8.17-6
8.17-4	Deformed Mesh, Increment 70	8.17-7
8.17-5	Deformed Mesh, Increment 70	8.17-8
8.17-6	Equivalent Plastic Strain, Increment 70	8.17-9
8.17-7	Equivalent Stress, Increment 70	8.17-10
8.17-8	Equivalent Plastic Strain at Increment 199 for Data Set e8x17b	8.17-11
8.17-9	Equivalent von Mises Effective Stress at Increment 199 for Data Set e8x17b .	8.17-12
8.18-1	Circular Blank Holder and Punch	8.18-6
8.18-2	Deformed Sheet at Increment 40	8.18-7
8.18-3	Plastic Strain at Increment 40	8.18-8
8.18-4	Equivalent Stress at Increment 40	8.18-9
8.18-5	Analytical Form of Rigid Contact Surfaces	8.18-10
8.18-6	Final Deformed Geometry for Data Set e8x18c.	8.18-11
8.18-7	Final Deformed Geometry for Data Set e8x18d.	8.18-12
8.19-1	Initial Geometry for both Data Sets	8.19-4
8.19-2	Deformed Mesh at Increment 12 for Data Set e8x19	8.19-5
8.19-3	Deformed Mesh at Increment 24 for Data Set e8x19	8.19-6
8.19-4	Deformed Mesh at Increment 36 for Data Set e8x19	8.19-7
8.19-5	Equivalent Total Plastic Strain at Increment 36 for Data Set e8x19	8.19-8
8.19-6	Equivalent Total Plastic Strain at Increment 164 for Data Set e8x19b	8.19-9
8.19-7	Equivalent von Mises Stress for Data Set e8x19	8.19-10
8.19-8	von Mises for Data Set e8x19b	8.19-11



Figure		Page
8.20-1	Node Numbers in Circular Region	8.20-2
8.20-2	Element Numbers in Circular Region	8.20-3
8.20-3	Electric Potential Along Diameter.	8.20-4
8.20-4	First Component of Electric Field	8.20-5
8.21-1	Node Numbers in Mesh	8.21-2
8.21-2	Element Numbers in Mesh	8.21-3
8.21-3	Scalar Potential Through Radius	8.21-4
8.22-1	Node Numbers in Circular Region	8.22-2
8.22-2	Element Numbers in Circular Region	8.22-3
8.22-3	Magnetic Scalar Potential along Radial Line	8.22-4
8.22-4	Magnetic Flux Distribution	8.22-5
8.23-1	Mesh and Applied Current.	8.23-3
8.23-2	Third Component of Magnetic Flux along Radial Line	8.23-4
8.23-3	Magnetic Potential Vector	8.23-5
8.24-1	Mesh with Node Numbers	8.24-3
8.24-2	Mesh with Element Numbers	8.24-3
8.24-3	Magnetic Scalar Potential Linear Material Behavior	8.24-4
8.24-4	Magnetic Scalar Potential Nonlinear Material Behavior	8.24-5
8.25-1	Acoustic Cavity Mesh with Node Numbers	8.25-3
8.25-2	Acoustic Cavity Mesh with Element Numbers	8.25-4
8.25-3	Outline Plot Showing Internal Barrier.	8.25-5
8.25-4	Second Mode	8.25-6
8.25-5	Third Mode	8.25-7
8.25-6	Fourth Mode	8.25-8
8.25-7	Fifth Mode	8.25-9
8.25-8	Sixth Mode.	8.25-10
8.25-9	Acoustic Pressure at Time = 0.000001	8.25-11
8.25-10	Acoustic Pressure at Time = 0.005	8.25-12
8.25-11	Acoustic Pressure at Time = 0.01	8.25-13



Figure		Page
8.26-1	Acoustic Cavity Mesh	8.26-3
8.26-2	Time History of Pressure Pulse	8.26-4
8.27-1	Finite Element Mesh – Nodes	8.27-4
8.27-2	Finite Element Mesh – Nodes	8.27-5
8.27-3	Failure Index, Increment 0.	8.27-6
8.27-4	Failure Index, Increment 5.	8.27-7
8.27-5	Failure Index – No Failure Allowed.	8.27-8
8.27-6	First Component of Stress in Preferred Direction	8.27-9
8.27-7	Second Component of Stress in the Preferred Direction	8.27-10
8.28-1	Finite Element Mesh with Dipole	8.28-3
8.28-2	Scalar Potential	8.28-4
8.28-3	Vector Plot of Electric Field.	8.28-5
8.28-4	Scalar Potential Distribution.	8.28-6
8.29-1	Finite Element Mesh and Parallel Wires	8.29-3
8.29-2	Magnetic Scalar Potential	8.29-4
8.29-3	Magnetic Flux Density.	8.29-5
8.29-4	Magnetic Flux Distribution	8.29-6
8.30-1	Finite Element Mesh with Node Numbers	8.30-3
8.30-2	Finite Element Mesh with Element Numbers	8.30-4
8.30-3	Third Component of Electric Field at 20 MHz	8.30-5
8.31-1	Finite Element Mesh.	8.31-3
8.31-2	Third Component of Magnetic Potential, Time = 2 Microseconds	8.31-4
8.31-3	Third Component of Magnetic Potential, Time = 25 Microseconds	8.31-5
8.31-4	Time History of Magnetic Potential	8.31-6
8.31-5	Current Density, Time = 25 Microseconds	8.31-7
8.32-1	Finite Element Mesh of Resonator	8.32-4
8.33-1	Sector of Circular Region	8.33-3
8.33-2	Third Component of Magnetic Potential using Harmonic Procedure	8.33-4
8.33-3	Time History of Magnetic Potential of Node 1, Transient Procedure.	8.33-5



Figure		Page
8.34-1	One-Element Model	8.34-3
8.34-2	Time History of Axial Stress	8.34-4
8.34-3	Time History of Void Ratio	8.34-5
8.34-4	Time History of Preconsolidation Pressure	8.34-6
8.35-1	Mesh of Embankment with Sets used for Material Definition and Initial Preconsolidation	8.35-4
8.35-2	Boundary Conditions	8.35-5
8.35-3	Contour of Settlement	8.35-6
8.35-4	Vertical Stresses	8.35-7
8.35-5	Mean Pressure in Soil	8.35-8
8.35-6	Void Ratio	8.35-9
8.35-7	Preconsolidation Pressure	8.35-10
8.35-8	Fluid Pore Pressure	8.35-11
8.36-1	Two Cylinders	8.36-3
8.36-2	Radial and Hoop Stresses through Radius.	8.36-4
8.37-1	Finite Element Mesh with Symmetry Surfaces	8.37-3
8.37-2	Reaction and Contact (Interference) Forces	8.37-4
8.38-1	Plate with Rigid Surfaces	8.38-4
8.38-2	Male Punch Consisting of Seven NURBS.	8.38-5
8.38-3	Blank Holder.	8.38-6
8.38-4	Deformed Plate at Increment 20.	8.38-7
8.38-5	Deformed Plate at Increment 50.	8.38-8
8.38-6	Deformed Plate at Increment 80.	8.38-9
8.38-7	Deformed Plate at Increment 110	8.38-10
8.38-8	Equivalent Stress at Midsurface at Increment 110	8.38-11
8.38-9	Equivalent Plastic Strain at Midsurface at Increment 110.	8.38-12
8.39-1	Mesh of Two Beams.	8.39-3
8.39-2	Initial Contact of Beams	8.39-4
8.39-3	Deformed Mesh at Increment 20	8.39-5
8.39-4	Deformed Mesh at Increment 30	8.39-6
8.39-5	Deformed Mesh at Increment 39	8.39-7
8.39-6	Load Deflection Curve.	8.39-8



Figure		Page
8.40-1	Original Mesh	8.40-3
8.40-2	First Adaptive Mesh	8.40-4
8.40-3	Second Adaptive Mesh	8.40-5
8.40-4	Third Adaptive Mesh	8.40-6
8.40-5	Fourth Adaptive Mesh	8.40-7
8.41-1	Original Finite Element Mesh	8.41-4
8.41-2	First Adaptive Mesh	8.41-5
8.41-3	Second Adaptive Mesh	8.41-6
8.41-4	Third Adaptive Meshing	8.41-7
8.41-5	Fourth Adaptive Mesh	8.41-8
8.41-6	Fifth Adaptive Mesh	8.41-9
8.42-1	Original Mesh	8.42-3
8.42-2	Deformed New Mesh at Increment 30.	8.42-4
8.42-3	Deformed New Mesh at Increment 60.	8.42-5
8.42-4	Deformed New Mesh at Increment 120	8.42-6
8.42-5	Deformed New Mesh at Increment 180	8.42-7
8.43-1	Close-up of Original Finite Element Mesh	8.43-5
8.43-2	Seal with Prescribed Boundary Conditions	8.43-6
8.43-3	Deformed Mesh showing New Elements	8.43-7
8.43-4	Deformed Mesh at Initial Contact	8.43-8
8.43-5	Adaptivity Due to Contact	8.43-9
8.43-6	Adaptivity Due to Contact (Updated Lagrange Formulation).	8.43-10
8.44-1	Original Finite Element Mesh for all 3 Data Sets	8.44-5
8.44-2	Adaptive Criteria Box for Data Set e8x44 and e8x44c	8.44-6
8.44-3	Deformed Mesh at Increment 48 for Data Set e8x44	8.44-7
8.44-4	Deformed Mesh at Increment 75 for Data Set e8x44	8.44-8
8.44-5	Deformed Mesh at Increment 100 for Data Set e8x44	8.44-9
8.44-6	Deformed Mesh at Increment 3 for Data Set e8x44b	8.44-10
8.44-7	Deformed Mesh at Increment 50 for Data Set e8x44b	8.44-11
8.44-8	Deformed Mesh at Increment 80 for Data Set e8x44b	8.44-12
8.44-9	Deformed Mesh at Increment 48 for Data Set e8x44c	8.44-13
8.44-10	Deformed Mesh at Increment 75 for Data Set e8x44c	8.44-14



Figure		Page
8.44-11	Deformed Mesh at Increment 100 for Data Set e8x44c	8.44-15
8.44-12	Deformed Mesh at Increment 155 for Data Set e8x44c	8.44-16
8.45-1	Geometry for Problem 8.45 to show the SPLINE Option	8.45-3
8.45-2	Initial Model for this Example.	8.45-4
8.45-3	Contours of Effective von Mises Stress	8.45-5
8.46-1	Initial Model	8.46-3
8.46-2	Final Deformed Shape after 10 Increments	8.46-4
8.47-1	Initial Model for Stick-Slip Problem	8.47-3
8.47-2	Distributed Load Boundary Conditions	8.47-3
8.47-3	Loading History for the Distributed Loads	8.47-4
8.47-4	First Slipping Motion (Increment 21)	8.47-5
8.47-5	First Slipping Motion (Increment 21)	8.47-6
8.47-6	Final Slip occurring in Increment 51	8.47-7
8.47-7	X Displacement History for Node 1	8.47-8
8.48-1	Initial Model for Stick-Slip Problem	8.48-3
8.48-2	Loading History - Y Axis is Load Per Unit Area divided by 10^6	8.48-3
8.48-3	First Slip occurs in Increment 13	8.48-4
8.48-4	Final Deformed Shape in Increment 20	8.48-5
8.48-5	History Plot of x Displacement for Node 51	8.48-6
8.49-1	Initial Model	8.49-3
8.49-2	Deformed Shape of Bushing at the End of Increment 25	8.49-4
8.49-3	Deformed Shape of Bushing at the End of Increment 27	8.49-5
8.49-4	Deformed Shape of Bushing at the End of Increment 40	8.49-6
8.49-5	Deformed Shape of Bushing at the End of Increment 51	8.49-7
8.50-1	Initial Model	8.50-3
8.50-2	Deformed Shape at End of 25 Increments.	8.50-4
8.50-3	Deformed Shape at End of 50 Increments.	8.50-5
8.50-4	Load Stroke Curve for the Deformation.	8.50-6
8.51-1	Initial Model for Both Data Sets.	8.51-4
8.51-2	Boundary Condition Definition for Both Data Sets	8.51-5



Figure		Page
8.51-3	Deformed Shell Structure at Increment 5 for Data Set e8x51a	8.51-6
8.51-4	Deformed Shell Structure at Increment 10 for Data Set e8x51a	8.51-7
8.51-5	Deformed Shell Structure at Increment 20 for Data Set e8x51a	8.51-8
8.51-6	Deformed Shell Structure at Increment 25 for Data Set e8x51a	8.51-9
8.51-7	Deformed Shell Structure at Increment 5 for Data Set e8x51b	8.51-10
8.51-8	Deformed Shell Structure at Increment 10 for Data Set e8x51b	8.51-11
8.51-9	Deformed Shell Structure at Increment 20 for Data Set e8x51b	8.51-12
8.51-10	Deformed Shell Structure at Increment 25 for Data Set e8x51b	8.51-13
8.52-1	Initial Geometry - Only One Quarter is Modeled due to Symmetry	8.52-4
8.52-2	Deformed Geometry at the End of 10 Increments.	8.52-5
8.52-3	Deformed Geometry at the End of 20 Increments.	8.52-6
8.52-4	Deformed Geometry at the End of 30 Increments.	8.52-7
8.52-5	Effective Plastic Strain Distribution at the End of 30 Increments.	8.52-8
8.53-1	Initial Geometry for both Data Sets	8.53-3
8.53-2	End View of Original and Deformed Geometry after 14 Increments for Data Set e8x53a 8.53-4	
8.53-3	Original and Deformed Geometry after 20 Increments for Data Set e8x53a . .	8.53-5
8.53-4	Original and Deformed Geometry after 14 Increments for Data Set e8x53b - End View	8.53-6
8.53-5	Original and Deformed Geometry after 20 Increments for Data Set e8x53b . .	8.53-7
8.53-6	History Plot of the Variation of the y Reaction Force at Node 405 for Data Set e8x53a	8.53-8
8.53-7	History Plot of the Variation of the y Reaction Force at Node 405 for Data Set e8x53b	8.53-9
8.54-1	Side View of Initial Geometry.	8.54-3
8.54-2	Initial Model of Structure	8.54-4
8.54-3	Deformed Shape of the Structure at Increment 5	8.54-5
8.54-4	Deformed Shape of the Structure at Increment 10.	8.54-6
8.54-5	Displacement x versus Reaction Force X for Node 26	8.54-7
8.55-1	Initial Model	8.55-4
8.55-2	Elements to which Clamp Down Pressure is Applied.	8.55-5
8.55-3	The Final Deformed Geometry for Data Set e8x55a	8.55-6
8.55-4	The Final Deformed Geometry for Data Set e8x55b	8.55-7



Figure		Page
8.56-1	Initial Model for both Data Sets	8.56-3
8.56-2	The Final Deformed Shape for Data Set e8x56a	8.56-4
8.56-3	The Final Deformed Shape for Data Set e8x56b	8.56-5
8.57-1	Initial Model with Point Load applied on Node 1	8.57-3
8.57-2	Initial and Deformed Shape for Data Set e8x57a	8.57-4
8.57-3	Equivalent von Mises Stress for Data Set e8x57a	8.57-5
8.57-4	Equivalent von Mises Stress for Data Set e8x5c	8.57-6
8.58-1	Initial Model	8.58-2
8.58-2	Deformed Geometry with the Adapted Mesh	8.58-3
8.60-1	Initial Model	8.60-3
8.60-2	Deformed Geometry for Increment 25	8.60-4
8.60-3	Deformed Geometry for Increment 50	8.60-5
8.60-4	Deformed Geometry for Increment 100	8.60-6
8.60-5	Deformed Geometry for Increment 120	8.60-7
8.60-6	Deformed Geometry for Increment 130	8.60-8
8.60-7	Magnified View of Contours of Total Effective Plastic Strain for Increment 130	8.60-9



8 *Advanced Topics List of Figures*



Advanced Topics List of Tables



Table	Page
8-1 Recent Analysis Capabilities in MARC	8-2
8.2-1 J-Integral Evaluation Results	8.2-3
8.9-1 Comparison of Results.	8.9-3
8.10-1 Comparison of MARC Results vs. Analytical.	8.10-3
8.11-1 σ_{yy} vs. Load Increment.	8.11-3
8.28-1 Comparison of MARC Results	8.28-2
8.29-1 Comparison of MARC Results	8.29-2
8.30-1 Electric Field as a Function of Frequency	8.30-2
8.32-1 Electric Field as a Function of Frequency	8.32-2



8 *Advanced Topics List of Tables*



Advanced Topics



This chapter demonstrates capabilities that have been added to MARC in the last few releases. These capabilities include substructures, cracking, composites, contact, electrostatics, magnetostatics, and acoustics capabilities among others. Discussions of these capabilities can be found in *MARC Volume A: Theory and User Information* and a summary of the various capabilities is given below:

Substructures

- Linear analysis
- Nonlinear analysis
- Cracking analysis

Thermal-mechanical coupled analysis

Composite analysis

- Failure criteria
- Progressive failure

Activate and deactivate

Contact analysis

- Two-dimensional
- Three-dimensional
- Springback
- Friction

Electrostatic analysis

Magnetostatic analysis

Acoustic analysis

Adaptive Meshing

- Linear analysis
- Nonlinear analysis

Compiled in this chapter are a number of solved problems. Table 8-1 shows the MARC elements and options used in these demonstration problems.



Table 8-1 Recent Analysis Capabilities in MARC

Problem Number	Element Type(s)	Parameters	Model Definition	History Definition	User Subroutines	Problem Description
8.1	26	ELASTIC SUBSTRUCT NEWDB SUPER	SUBSTRUCTURE DIST LOAD SUPERINPUT RESTART	BACK TO SUBS	SSTRAN	Hole in plate. Generate substructure (1-1) and 1-2). Combine substructures, perform analysis. Read RESTART tape, Go back to substructures to obtain results.
8.2	27	SUBSTRUCT NEWDB SUPER J-INT SCALE	SUBSTRUCTURE DIST LOADS SUPERINPUT J-INTEGRAL WORK HARD	AUTO LOAD PROPORTIONAL INC	WKSLP	Double-edge notch specimen using substructure. Elastic region away from the crack is treated as a substructure.
8.3	10 12	SUBSTRUCT NEWDB SUPER	SUBSTRUCTURE SUPERINPUT POINT LOADS GAP DATA	POINT LOADS AUTO LOAD BACK TO SUBS	—	End plate aperture breakaway problem. The rate is treated as a substructure leaving the contact elements to be at highest level.
8.4	26	—	ISOTROPIC CRACK DATA TYING	PROPORTIONAL INC AUTO LOAD	—	Collapse of a notched concrete beam.
8.5	75	PRINT	CONN GENER COMPOSITE ISOTROPIC ORTHOTROPIC	POINT LOADS AUTO INCREMENT	—	Cracking of a plate one-way reinforced using shell elements.
8.6	27 46	PRINT	CONN GENER NODE FILL CRACK DATA ISOTROPIC	POINT LOADS AUTO INCREMENT	REBAR	Cracking of a one-way reinforced plate using rebar elements.

Table 8-1 Recent Analysis Capabilities in MARC (Continued)

Problem Number	Element Type(s)	Parameters	Model Definition	History Definition	User Subroutines	Problem Description
8.7	11 12 39	FINITE UPDATE LARGE DISP COUPLE MESH PLOT	CONTROL FIXED DISP FIXED TEMP INITIAL TEMP ISOTROPIC GAP DATA CONVERT WORK HARD TEMP EFFECTS RESTART DIST FLUXES	TRANSIENT	—	Thermal-mechanically coupled analysis of the compression of a block.
8.8	21	—	ORTHOTROPIC DIST LOADS	—	HOOPLW ANELAS	Bending of a thick anisotropic plate.
8.9	3	—	DEFINE ORTHOTROPIC ORIENTATION FALL DATA PRINT ELEM	—	—	Failure criteria calculation of an orthotropic plate.
8.10	52	—	HYPOELASTIC	—	UBEAM	Nonlinear beam bending.
8.11	26	—	ERROR ESTIMATE	DEACTIVATE ACTIVATE	—	Example of Activate, Deactivate and error estimates.
8.12	10	PRINT,5 FINITE LARGE DISP UPDATE REZONING	WORK HARD CONTACT	AUTO LOAD TIME STEP REZONE CONTACT CHANGE ISOTROPIC CHANGE CONNECTIVITY CHANGE COORDINATE CHANGE END REZONE AUTO TIME	—	Forging of the head of a bolt.
8.13	10 116	PRINT,5 FINITE LARGE DISP UPDATE COUPLE	POST FIXED TEMP FIXED DISP TEMP EFFECTS WORK HARD DIST FLUXES CONTACT INITIAL TEMP CONVERT	TRANSIENT DISP CHANGE AUTO TIME	—	Coupled analysis of ring compression.



Table 8-1 Recent Analysis Capabilities in MARC (Continued)

Problem Number	Element Type(s)	Parameters	Model Definition	History Definition	User Subroutines	Problem Description
8.14	7	UPDATE FINITE LARGE DISP PRINT,5	—	AUTO LOAD TIME STEP	—	3D indentation problem demonstrating how rigid surfaces are defined.
8.15	11 27	UPDATE FINITE LARGE DISP PRINT,5	CONTACT CONTACT TABLE DEFINE RESTART LAST	AUTO LOAD TIME STEP	—	Double-sided contact between deformable bodies.
8.16	11	UPDATE FINITE LARGE DISP PRINT,5	SPRINGS CONTACT WORK HARD	AUTO LOAD TIME STEP RELEASE MOTION CHANGE	MOTION	Formation of a metal part and the examination of springback.
8.17	7	REZONING UPDATE FINITE LARGE DISP PRINT,8	CONTACT RESTART LAST	AUTO LOAD TIME STEP	—	Metal extrusion analysis using the CONTACT option. Coulomb friction.
8.18	75	SHELL SET,7 LARGE DISP UPDATE FINITE PRINT,8	CONTACT	AUTO LOAD TIME STEP MOTION CHANGE	WKSLP	Stretch forming of a circular sheet. Coulomb friction between sheet and punch.
8.19	7	UPDATE FINITE LARGE DISP PRINT,8 SIZING	CONTACT UMOTION	AUTO LOAD TIME STEP	MOTION	Three dimensional indentation rolling of elastic-perfectly plastic material.
8.20	39	SIZING ELECTRO	POINT CHARGE FIXED POTENTIAL	STEADY STATE	—	Point charge in a circular region.
8.21	43	SIZING ELECTRO	FIXED POTENTIAL POINT CHARGE	STEADY STATE	—	Point charge in a circular cylinder.
8.22	39	SIZING\ MAGNET	POINT CURRENT FIXED POTENTIAL	STEADY STATE	—	Point current in a circular region.
8.23	109	MAGNET	FIXED POTENTIAL POINT CURRENT	STEADY STATE	—	3D analysis of a magnetic field in a coil.
8.24	39	MAGNET	ISOTROPIC FIXED POTENTIAL POINT CURRENT B-H RELATION	STEADY STATE	—	2D nonlinear magnetostatic analysis.

Table 8-1 Recent Analysis Capabilities in MARC (Continued)

Problem Number	Element Type(s)	Parameters	Model Definition	History Definition	User Subroutines	Problem Description
8.25	39	ACOUSTIC PRINT,3	ISOTROPIC	DYNAMIC CHANGE	—	2D acoustic problem demonstrating the eigenvalue analysis in a circular cavity with barrier.
8.26	39	ACOUSTIC	ISOTROPIC FIXED PRESSURE	DYNAMIC CHANGE	FORCDT	2D acoustic problem demonstrating the eigenvalue analysis of a rectangular cavity.
8.27	26	INPUT TAPE	FIXED DISP ORTHOTROPIC	AUTO LOAD PROPORTIONAL CONTROL	—	Progressive failure of a plate with a hole.
8.28	41 103	ELECTRO	POINT CHARGE FIXED POTENTIAL	STEADY STATE	—	Linear distribution of dipoles.
8.29	41 103	MAGNET	POINT CHARGE FIXED POTENTIAL	STEADY STATE	—	Magnetic field around two wires carrying opposite currents.
8.30	111	EL-MA HARMONIC PRINT, 3	DIST CURRENT FIXED POTENTIAL	DIST CURRENT HARMONIC POINT CURRENT	—	Harmonic electromagnetic analysis of a waveguide.
8.31	112	EL-MA PRINT, 3	FIXED POTENTIAL	DYNAMIC CHANGE POTENTIAL CHANGE	—	Transient electromagnetic analysis around a conducting sphere.
8.32	113	EL-MA HARMONIC	FIXED POTENTIAL	DIST CURRENT HARMONIC	—	Calculate the resonance in a cavity.
8.33	111	EL-MA HARMONIC	FIXED POTENTIAL	POINT CURRENT CURRENT DYNAMIC CHANGE HARMONIC	—	Steady state analysis of an infinitely long wire using both harmonic and transient analysis.
8.34	28	PORE UPDATE ISTRESS	SOIL INITIAL PC INITIAL VOID INITIAL STRESS DIST LOADS	DIST LOADS TIME STEP DISP CHANGE AUTO LOAD	—	Drained triaxial test on normally consolidated clay.



Table 8-1 Recent Analysis Capabilities in MARC (Continued)

Problem Number	Element Type(s)	Parameters	Model Definition	History Definition	User Subroutines	Problem Description
8.35	32	PORE ISTRESS	SOIL SOLVER INITIAL PC INITIAL STRESS INITIAL VOID DIST LOADS DEFINE	DIST LOADS TIME STEP AUTO TIME CONTROL	—	Coupled pore-pressure calculation of stratified soil embankment.
8.36	116	PRINT, 5	SPRINGS CONTACT DEFINE	CONTACT TABLE AUTO LOAD TIME STEP	—	Interference fit of two cylinders.
8.37	11	PRINT, 8	CONTACT SPRINGS DEFINE	CONTACT TABLE AUTO LOAD TIME STEP	—	Interference fit between sectors of two cylinders. Demonstrates symmetry surfaces.
8.38	75	LARGE DISP UPDATE FINITE	CONTACT WORK HARD CONTACT TABLE	AUTO LOAD TIME STEP	—	Deep drawing of a box using rigid punch described as NURBS.
8.39	5	LARGE DISP	CONTACT POINT LOAD	AUTO INCREMENT POINT LOAD	—	Contact of two beams by a point load.
8.40	11	ADAPT ELASTIC	ADAPTIVE ATTACH NODES SURFACE POINT LOAD	—	—	Adaptive meshing of a disk subjected to point loads.
8.41	3	ADAPT ELASTIC	ADAPTIVE ERROR ESTIMATES	—	—	Adaptive meshing of a stress concentration.
8.42	11	ADAPT LARGE DISP FOLLOW FOR	CONTACT ATTACH NODE SURFACE DIST LOADS	MOTION CHANGE AUTO LOAD TIME STEP	—	Double-sided contact analysis with adaptive meshing.
8.43	119	LARGE DISP FOLLOW FOR ADAPT	ADAPTIVE MOONEY CONTACT	AUTO LOAD TIME STEP DISP CHANGE	—	Modeling a rubber seal with adaptive meshing.
8.44	11	UPDATE LARGE DISP FINITE ADAPT	WORK HARD ADAPTIVE CONTACT CONTACT TABLE	MOTION CHANGE TIME STEP AUTO LOAD	—	Rolling example with adaptive meshing.
8.45	11	EXTENDED	CHANGE STATE INITIAL STATE SPLINE CONTACT	AUTO LOAD TIME STEP MOTION CHANGE CHANGE STATE	—	Use of the SPLINE option for deformable-deformable contact.



Table 8-1 Recent Analysis Capabilities in MARC (Continued)

Problem Number	Element Type(s)	Parameters	Model Definition	History Definition	User Subroutines	Problem Description
8.46	3	EXTENDED DIST LOADS	CONTACT EXCLUDE FIXED DISP	AUTO LOAD DISP CHANGE DIST LOADS	—	Use of EXCLUDE option for contact analysis.
8.47	3	DIST LOADS	DIST LOADS FIXED DISP SPRINGS CONTACT	AUTO LOAD DIST LOADS TIME STEP	—	Simulation of contact with stick-slip friction.
8.48	3	LARGE DISP DIST LOADS	FIXED DISP SOLVER SPRINGS GEOMETRY	AUTO LOAD DISP CHANGE DIST LOADS TIME STEP	—	Simulation of deformable-deformable contact with stick-slip friction.
8.49	80	DIST LOADS LARGE DISP	CONTACT MOONEY	AUTO LOAD MOTION CHANGE TIME STEP	—	Rolling of a compressed rubber bushing with stick-slip friction.
8.50	10	UPDATE FINITE LARGE DISP	GEOMETRY WORK HARD	AUTO LOAD MOTION CHANGE TIME STEP	—	Compression test of cylinder with stick-slip friction.
8.51	139 75	FINITE LARGE DISP UPDATE SHELL SECT	CONTACT CONTACT TABLE FIXED DISP WORK HARD GEOMETRY	AUTO LOAD MOTION CHANGE TIME STEP	—	Modeling of a spring.
8.52	75	FINITE LARGE DISP UPDATE SHELL SECT	GEOMETRY CONTACT CONTACT TABLE WORK HARD	AUTO LOAD DISP CHANGE TIME STEP	—	Deep drawing of a sheet.
8.53	75 49	DIST LOADS LARGE DISP SHELL SECT	DIST LOADS GEOMETRY FIXED DISP	AUTO LOAD DIST LOADS DISP CHANGE TIME STEP	—	Shell-shell contact and separation.
8.54	75	LARGE DISP SHELL SECT UPDATE	CONTACT FIXED DISP	AUTO LOAD DISP CHANGE TIME STEP	—	Self contact of a shell structure.
8.55	75	FINITE LARGE DISP UPDATE SHELL SECT	CONTACT POINT LOAD WORK HARD	AUTO LEAD POINT LOAD TIME STEP	—	Deep drawing of copper sheet (velocity and load controlled dies).
8.56	10	FINITE LARGE DISP UPDATE	CONTACT WORK HARD	AUTO LOAD DISP CHANGE TIME STEP	—	2D contact problem (load and velocity controlled dies).



Table 8-1 Recent Analysis Capabilities in MARC (Continued)

Problem Number	Element Type(s)	Parameters	Model Definition	History Definition	User Subroutines	Problem Description
8.57	75 138 139 140	ADAPTIVE ELASTIC SHELL SECT	ADAPTIVE POINT LOAD	—	—	The adaptive capability with shell elements.
8.58	75	ADAPTIVE ELASTIC SHELL SECT	GEOMETRY DIST LOADS ADAPTIVE	—	—	Adaptive meshing in multiple connected shell structures.
8.59						Not Available at this Time.
8.60	11	PLASTICITY	CONTACT WORD HARD FIXED DISP	AUTO LOAD MOTION CHANGE TIME STEP	—	Simulation of sheet bending.



8.1 Plate with Circular Hole using Substructures

In this problem, the substructuring capability is demonstrated to solve an elastic problem of a square plate with a circular hole (see Figure 8.1-1). This example demonstrates the three aspects of using substructures:

1. Generate superelement
2. Combine superelements, obtaining results for external nodes
3. Obtain solution within the substructure.

Element

Element type 26 is an 8-node plane stress quadrilateral.

Model

Due to symmetry, only one quarter of the specimen is modeled. Because of symmetry about a 45° line, this quarter plate is modeled using two identical substructures.

Geometry

A unit thickness is used.

Boundary Conditions

Boundary conditions are used to enforce symmetry about the x-axis. When the 1,1 superelement is mirrored about the 45° line, this boundary condition will effectively be about the y-axis.

Material Properties

The material is elastic. Values for Young's modulus, Poisson's ratio are 30×10^6 psi and 0.3, respectively.

DIST LOADS

A uniform pressure of 0 psi is applied to substructure 1,1. A uniform pressure of -1 psi is applied to substructure 1,2.

Substructure Procedure

In the first part of the first analysis, superelement level 1 number 1 is formed. On the SUBSTRUC parameter, it is requested that the substructure database be written to unit 31. Unit 16 is used to write the stiffness matrix. The NEWDB parameter indicates this is the first superelement created and, hence, the data base should be initialized. The SUBSTRUCTURE model definition option indicates which nodes are the external nodes. There are 11 external nodes.



In the second part of the first analysis, substructure level 1 number 1 is copied to substructure level 1 number 2. This is performed using the SUBSTRUC parameter. This new substructure is placed on unit 17. This substructure is given a different load factor than the previous one. When using substructures, the load can be modified using the AUTO LOAD option or the PROPORTIONAL increment option.

While forming substructures, multiple substructure formations can be performed during the same run. This is achieved by putting the MARC input “decks” back-to-back to create one large input.

In the second analysis, the two previous superelements are combined and the solution obtained for the external degrees-of-freedom. The SUPER parameter is used to indicate that superelements are used in this analysis. It also indicates the maximum number of nodes and degrees-of-freedom associated with a superelement. The SUPERINPUT model definition option is used to enter a correspondence table between previously defined external nodes and the nodes used in this analysis. In this problem, the externals lie along the 45° diagonal (see Figure 8.1-2). As there are no normal elements, there are no stresses or strains calculated here. A restart file is written. In addition, the calculated displacements are written back to the database.

User subroutine SSTRAN is used to reflect substructure level 1 number 2 by 90°. In the third analysis, the displacements calculated at the external nodes are used to calculate the internal degrees of freedom, the strains and the stresses. This is performed using the BACKTOSUBS option.

If desired, after the results are obtained in the subelement, plots could be obtained. In addition, if the POST option was used, the results would have been written for both substructures.

Parameters, Options, and Subroutines Summary

Example e8x1a.dat:

Parameters	Model Definition Options	History Definition Options
ELASTIC	CONNECTIVITY	CONTINUE
ELEMENT	COORDINATE	DIST LOADS
END	DIST LOADS	
MESH PLOT	END OPTION	
NEWDB	FIXED DISP	
SIZING	GEOMETRY	
SUBSTRUCTURE	ISOTROPIC	
TITLE	SUBSTRUCTURE	



Example e8x1b.dat:

Parameters

END
PRINT
SIZING
SUPER ELEMENT
TITLE

Model Definition Options

END OPTION
RESTART
SUPERINPUT

User subroutine in u8x1.f:

SSTRAN

Example e8x1c.dat:

Parameters

END
MESH PLOT
PRINT
SIZING
SUPER ELEMENT
TITLE

Model Definition Options

END OPTION
RESTART
SUPERINPUT

History Definition Options

BACKTOSUBS
CONTINUE

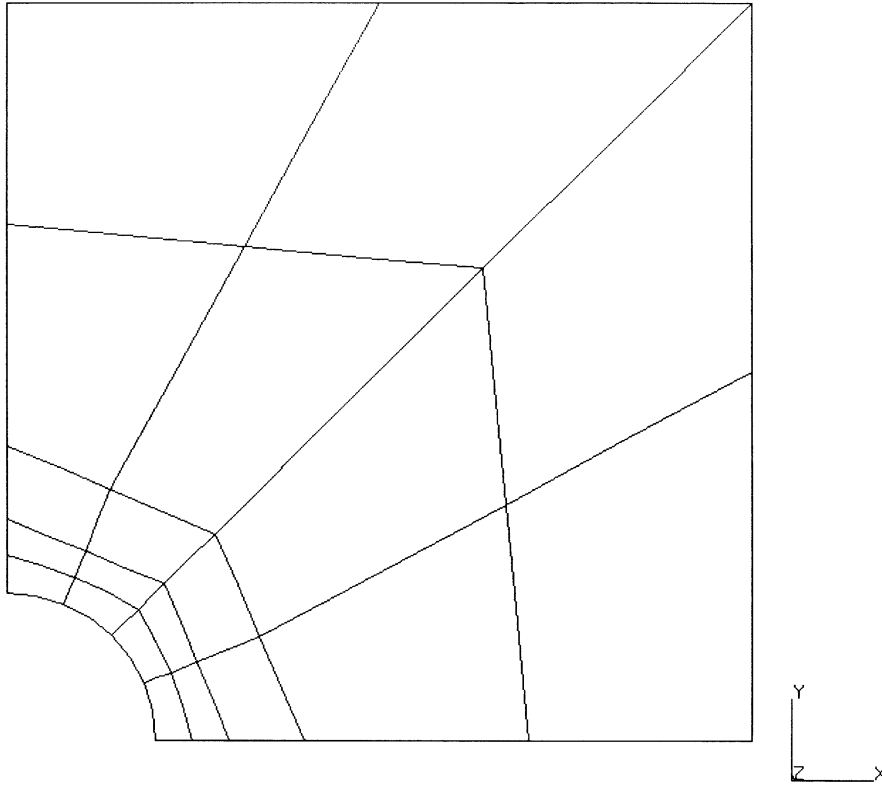


Figure 8.1-1 Hole in Plate

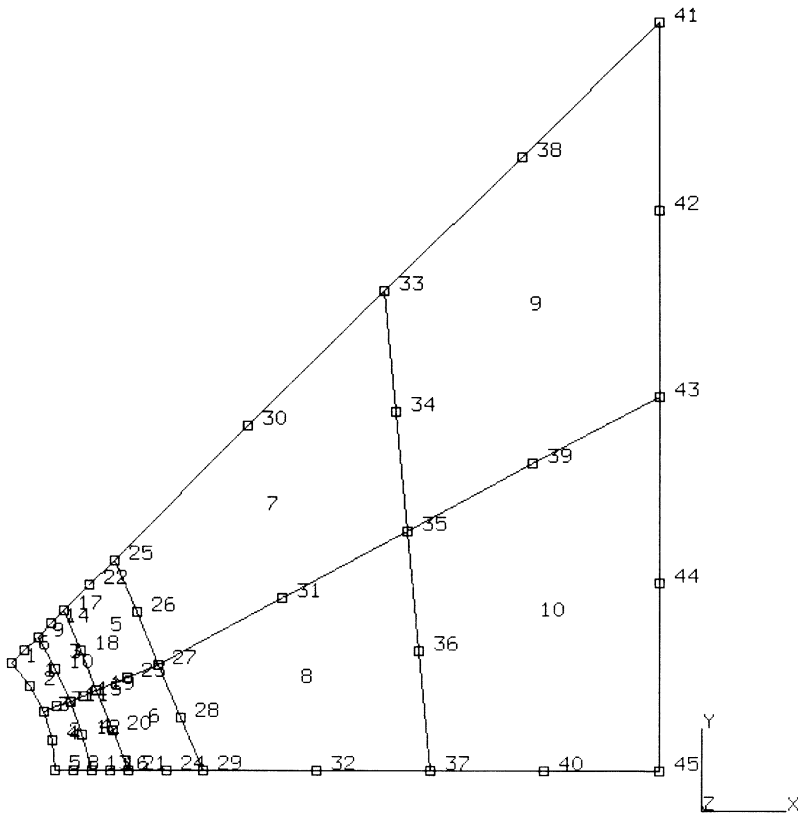


Figure 8.1-2 Substructure 1,1



8 *Advanced Topics*

Plate with Circular Hole using Substructures

8.2 Double-Edge Notch Specimen using Substructures

In this problem, the J-integral is evaluated for an elastic-plastic double-edge notch specimen under axial tension. The use of substructures for a nonlinear problem is demonstrated. Two different paths are used for the J-integral evaluation. The variation in the value of J between the two paths indicates the accuracy of the solution. This problem is identical to problem 3.8 with the exception that substructures are used. Substructures can be used in a nonlinear analysis as long as the area that is in the superelement remains linear elastic.

Element

Element type 27 is an eight-node plane strain quadrilateral.

Model

The full double-edge specimen with loading is shown in Figure 8.2-1. Due to symmetry, only one-quarter on the specimen is modeled. Figure 8.2-2 shows the mesh with 32 elements and 107 nodes.

Geometry

The option is not required for this element as a unit thickness is considered.

Boundary Conditions

Boundary conditions are used to enforce symmetry about the x- and y-axes.

Material Properties

The material is elastic-plastic with strain hardening. Values for Young's modulus, Poisson's ratio and yield stress used here are 30×10^6 psi, 0.3, and 50×10^3 psi, respectively.

Workhard

User subroutine WKSLP is used to input the workhardening slope. The workhardening curve is shown in Figure 8.2-5.

$$\bar{\sigma}(\bar{\epsilon}^p) = \sigma_o (1 + E\bar{\epsilon}^p / \sigma_o)^{0.2}$$

$$\frac{\partial \bar{\sigma}}{\partial \bar{\epsilon}^p} = 0.2 \times E (1 + E\bar{\epsilon}^p / \sigma_o)^{-0.8}$$

J-Integral

The J-integral is evaluated numerically by moving nodes within a certain ring of elements around the crack tip and measuring the change in strain energy. (This node movement represents a differential crack advance.) This mesh has two obvious "rings" of elements around the crack tip,



so that two evaluations of J are provided. A differential movement of 10^{-2} is used in all three evaluations. In problem 3.8, three paths were used. Because of the use of substructures, only two paths are possible at the highest level.

Loading

An initial uniform pressure of 100 psi is applied using the DIST LOAD option. The SCALE parameter is used to raise this pressure to a magnitude such that the highest stressed element (element 20 here) is at first yield. The pressure is scaled to 3,047 psi. The pressure is then incremented for five steps until the final pressure is 3,308 psi.

Substructure Technique

In performing a nonlinear analysis using substructures, it is important that the area included in the substructure remains elastic. In this analysis, the portion of Figure 8.2-2 that is cross-hatched is considered one substructure. Figure 8.2-2 and Figure 8.2-4 show the elements in the substructure and the highest level, respectively. It is far enough removed from the crack tip that plasticity is unlikely to occur there.

In the first part of the analysis, the superelement is created. It is written to the direct access database on unit 31. In this problem, no auxiliary sequential file is used. The SUBSTRUCTURE model definition option lists those nodes which are external. There are 17 external nodes along the thick line as shown. The distributed load is applied to the superelement. This is incremented in the second part. In the second part, the previously generated substructure is combined with the 16 elements nearest to the crack tip. The SUPER parameter indicates that file 31 is to be used; the number of super elements is 1 and there are 17 externals with two degrees of freedom. The SUPERINPUT model definition gives a correspondence table between the external node numbers and the node numbers used in this analysis. In this analysis, they are the same. After the END option is the load incrementation data. AUTO LOAD and/or PROPORTIONAL INC options can be used to modify loads in the SUBSTRUCTURE.

Results

MARC provides an output of the strain energy differences. This must be normalized by the crack opening area to obtain the value of J . Since this specimen is of unit thickness, the crack opening area is $\frac{3}{4} \Delta$, where $\frac{3}{4} \Delta$ is the differential crack motion. The mesh uses symmetry about the crack line, so that the strain energy change in the actual specimen is twice that printed out. These results are summarized in Table 8.2-1. It is clear that these results do demonstrate the path independence for the J -integral evaluation. Because of the use of substructures, this analysis was executed in 66% the time of problem 3.8. If the J -integrals are not evaluated, the run time is 50%. This shows the advantage of using substructures for locally nonlinear analysis.

**Table 8.2-1** J-Integral Evaluation Results

	Move Tip Only	Move First Ring of Elements
Strain Energy Change for increment 0 (Δu)	6.23×10^{-2}	6.212×10^{-2}
J-Integral $\left(\frac{2\Delta u}{\Delta l}\right)$	12.46	12.424
Strain Energy Change for increment 1 (Δu)	6.869×10^{-2}	6.849×10^{-2}
J-Integral $\left(\frac{2\Delta u}{\Delta l}\right)$	13.738	13.698
Strain Energy Change for increment 2 (Δu)	7.539×10^{-2}	7.517×10^{-2}
J-Integral $\left(\frac{2\Delta u}{\Delta l}\right)$	15.078	15.034
Strain Energy Change for increment 3 (Δu)	8.241×10^{-2}	8.217×10^{-2}
J-Integral $\left(\frac{2\Delta u}{\Delta l}\right)$	16.482	16.434
Strain Energy Change for increment 4 (Δu)	8.974×10^{-2}	8.948×10^{-2}
J-Integral $\left(\frac{2\Delta u}{\Delta l}\right)$	17.948	17.896
Strain Energy Change for increment 5 (Δu)	9.738×10^{-2}	9.711×10^{-2}
J-Integral $\left(\frac{2\Delta u}{\Delta l}\right)$	19.476	19.422



Parameters, Options, and Subroutines Summary

Example e8x2.dat:

Parameters	Model Definition Options	History Definition Options
ELEMENT	CONNECTIVITY	AUTO LOAD
END	COORDINATE	BOUNDARY CHANGE
NEWDB	DIST LOADS	CONTINUE
SIZING	END OPTION	PROPORTIONAL INCREMENT
SUBSTRUCTURE	FIXED DISP	
TITLE	ISOTROPIC	

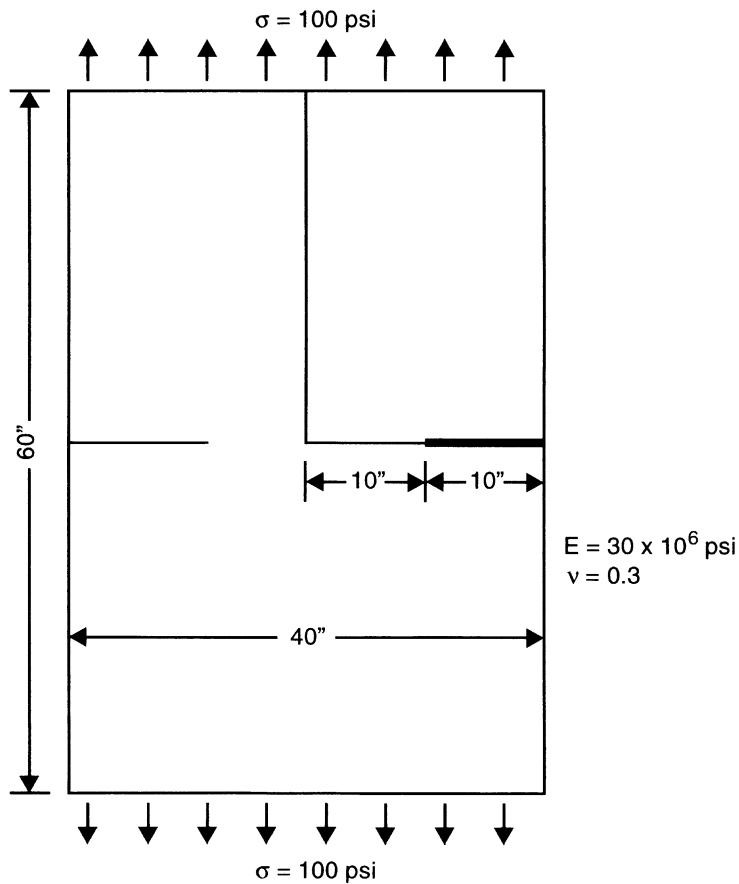


Figure 8.2-1 Double-Edge Notch Specimen

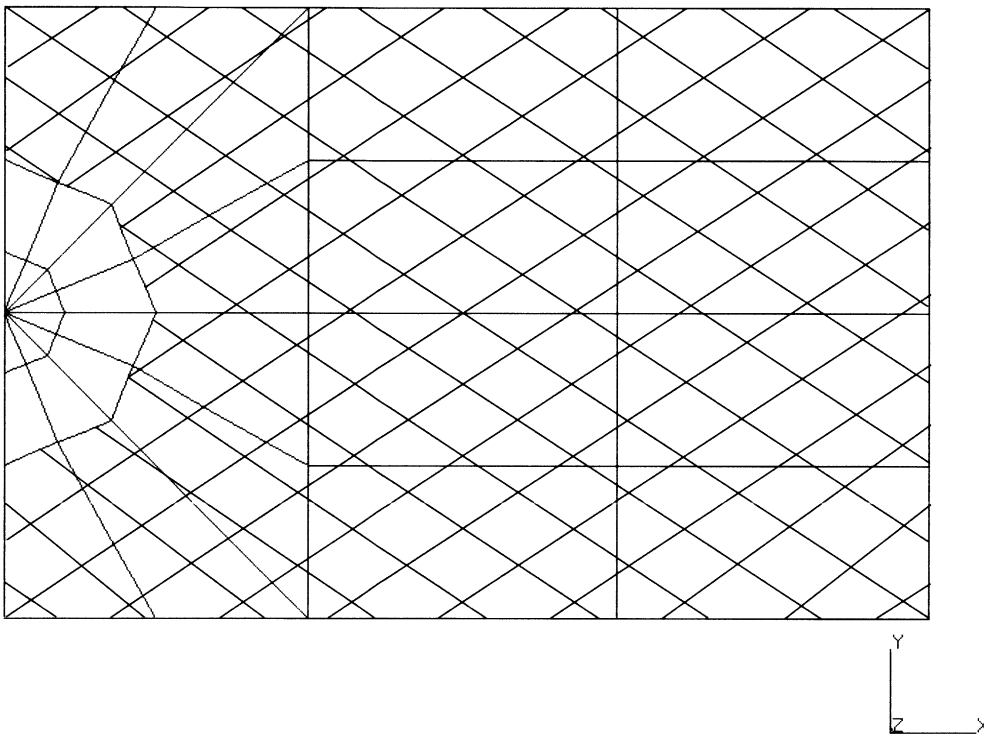


Figure 8.2-2 Mesh for Double-Edge Notch Specimen Cross-Hatched Area Indicates Substructures

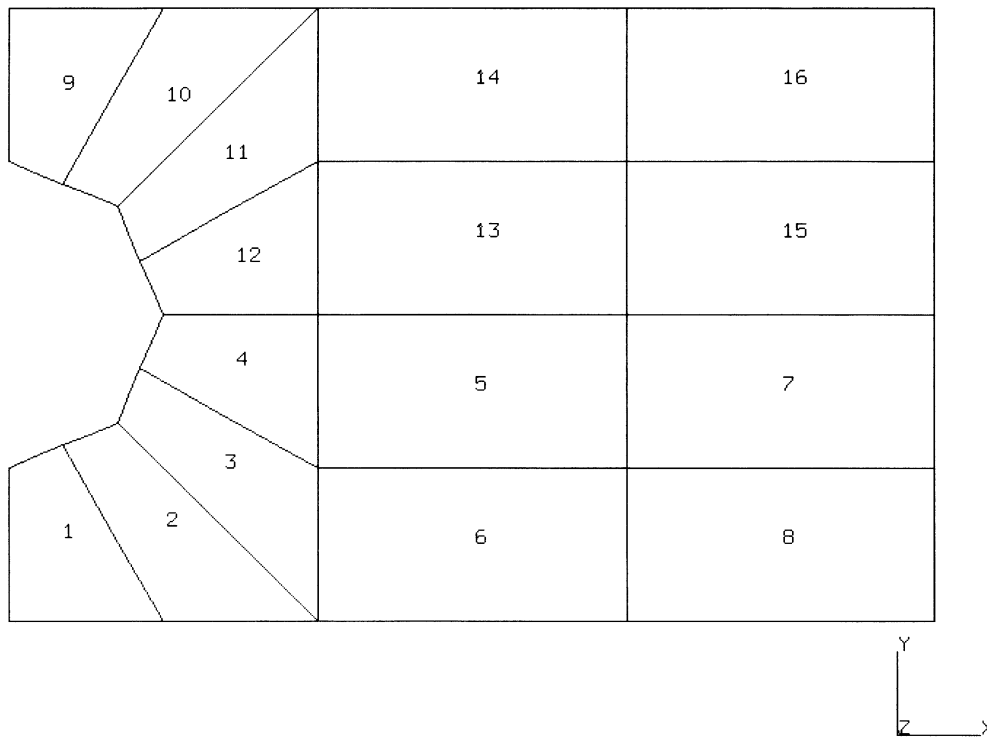


Figure 8.2-3 (A) Elements in Substructure 1-1

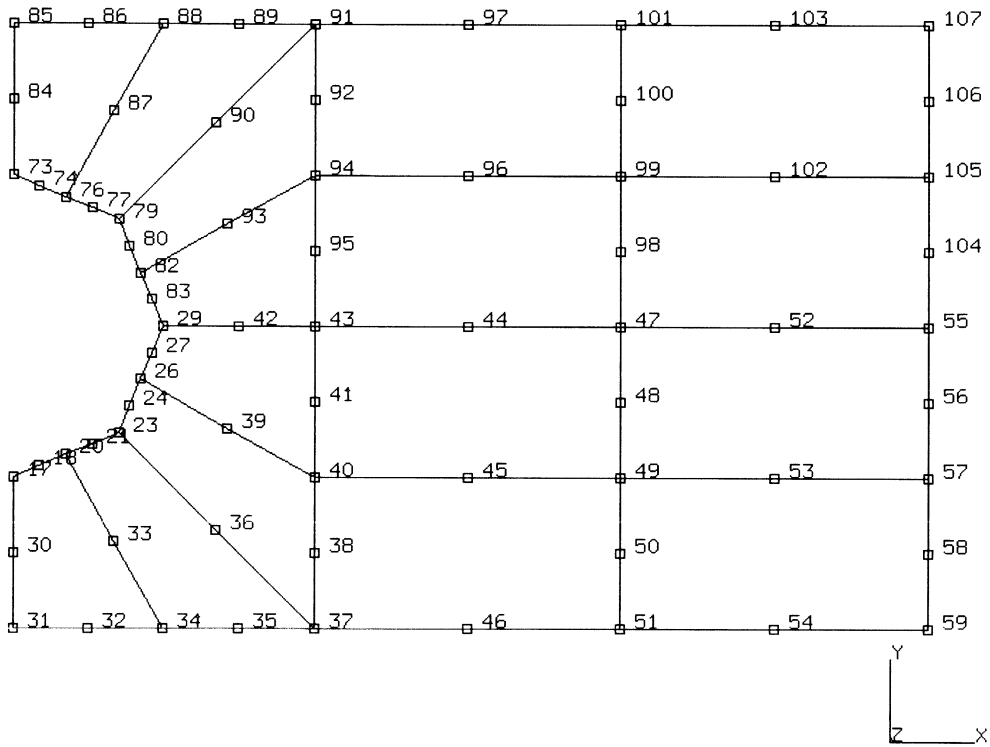


Figure 8.2-3 (B) Nodes in Substructure 1-1

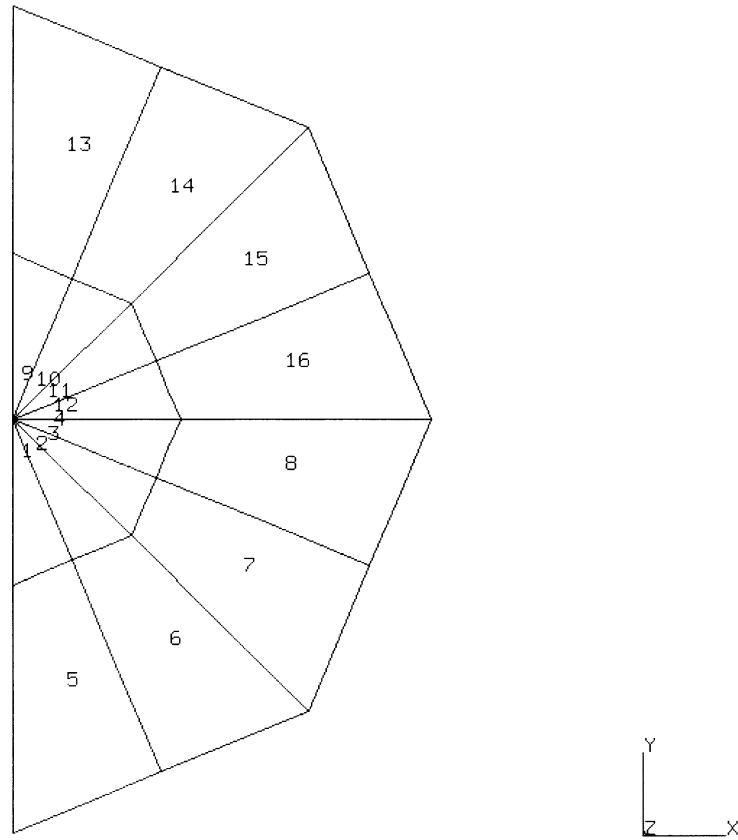


Figure 8.2-4 (A) Elements at Highest Level

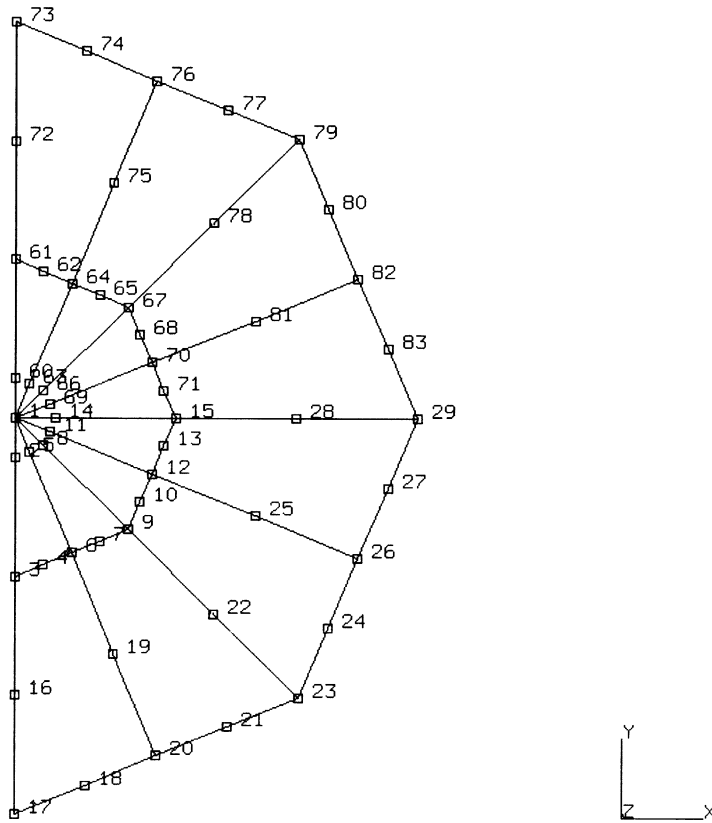


Figure 8.2-4 (B) Nodes at Highest Level

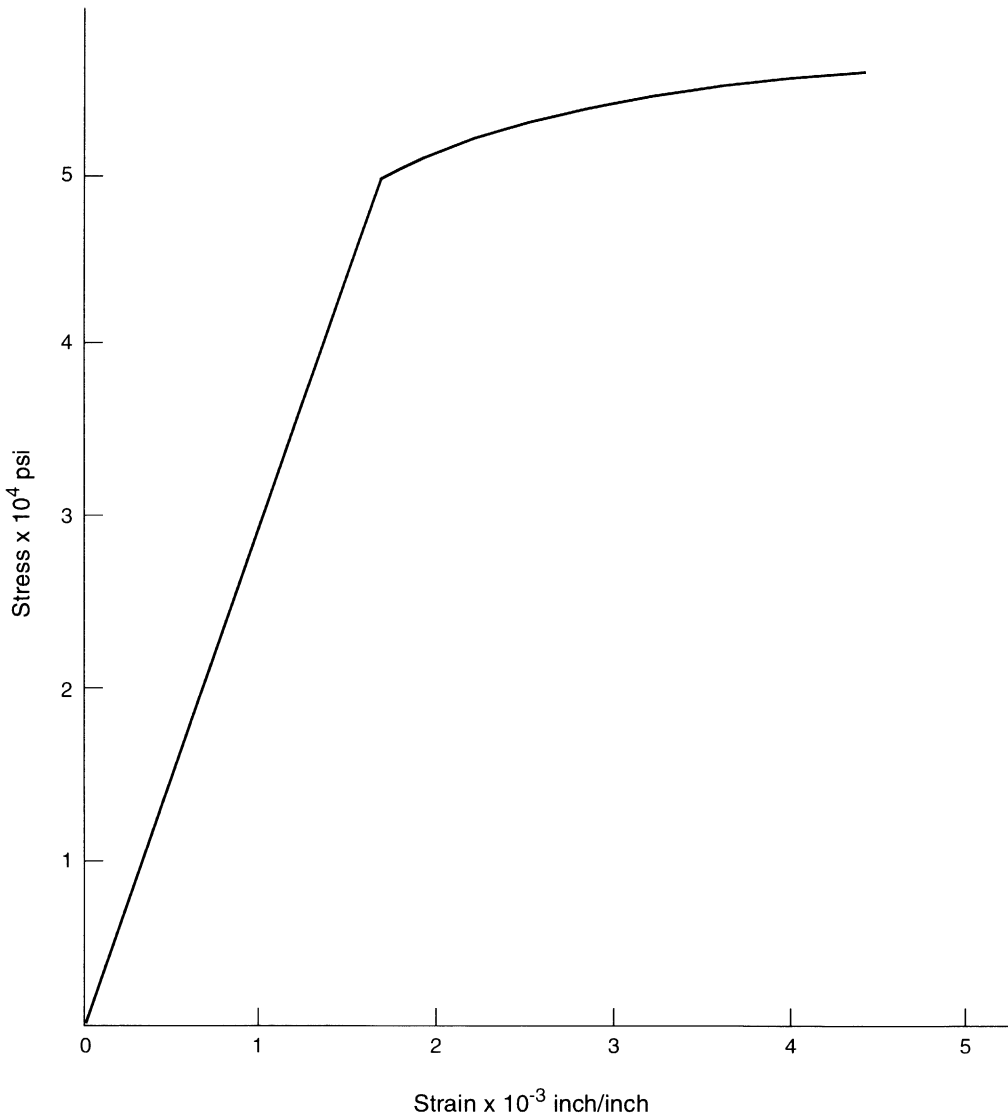


Figure 8.2-5 Workhardening Slopes



8.3 End-Plate-Aperture Breakaway

This example illustrates the use of substructures in an elastic contact problem. All of the elastic region is combined into one substructure. The gap elements which are inherently nonlinear are included in the highest level. This problem is identical to problem 7.2 with the exception that substructures are used.

This example illustrates the use of the gap and friction link, element type 12. This element allows surface friction effects to be modeled. This example is a simple model of a manhole cover in a pressure vessel. The axisymmetric mesh is shown in Figure 8.3-1. The objective of this analysis is to establish the response of the bolted joint between the manhole cover (elements 1-12) and the vessel (elements 13-27). The elements are combined into substructure level 1,1. The first bolts are tightened, and then the main vessel expands radially (as might occur due to thermal or internal pressure effects). You should be aware that this problem is presented only as a demonstration. The mesh is too coarse for accurate results.

Elements

Element 12 is a friction and gap element. It is based on the imposition of a gap closure constraint and/or a frictional constraint via Lagrange multipliers. The element has four nodes: nodes 1 and 4 are the end nodes of the link and each has two degrees of freedom (u, v) in the global coordinate direction; node 2 gives the gap direction cosines (n_x, n_y) and has γ_n , the force in the gap direction, as its one degree of freedom; node 3 gives the friction direction cosines (t_{1_x}, t_{1_y}) and has γ_1 , the frictional shear forces, and p , the net frictional slip, as its two degrees of freedom.

Model

Twenty-seven type 10 elements are used for the two discrete structures: the end cap and the aperture. These are then joined by four type 12 elements. There are 54 nodes.

Substructure Strategy

A substructure consisting of all of the axisymmetric elements is formed. The external nodes are those where the bolt load is applied (4,5,32,32), where the gap interfaces with the end cap and aperture (15 to 18 and 22 to 25) and where the radial load is applied (43 to 46). This is performed in the first part of the analysis.

In the second part of the analysis, the previously generated superelement is combined with the four gap elements.

**Loading**

The load history consists of applying bolt loads (that is, tightening down the bolts), then pulling out the outer perimeter of the main vessel model. Bolt loads are modeled here as point loads applied in opposite directions (self-equilibrating) on node pairs 4 and 32, 5 and 33. Since there is a possibility of gaps developing between the facing surfaces of the cover and vessel, the bolt load is initially applied as a small magnitude, then incremented up to the total value of 2000 lbs per bolt ring. This usually requires two runs of the problem: an initial run with a “small” load to see the pattern developing, from which some judgment can be made about the load steps which can be used to apply the total bolt force. In this actual run, the full bolt loads are applied in one increment.

The radial expansion of the main vessel is modeled as point loads on the outside circumference nodes (43 to 46). As there are no elements when performing the analysis, point loads rather than distributed loads are applied. Again, the purpose of the analysis is to watch the development of slippage between the main vessel and the cover plate, and the analyst cannot easily estimate the appropriate load increments to apply to model this nonlinearity. For this purpose, the RESTART option can be used effectively. A restart is written at the point where full bolt load is applied, and then a trial increment of pull-out force is applied. Based on the response to this (in the friction links), a reasonable size for the sequence of loading increments can be determined. This procedure is frequently necessary in such problems. For brevity, this example shows only the final load sequence obtained as a result of such trials.

Boundary Conditions

The nodes on the axis of symmetry are constrained radially, and the rigid body mode in the axial direction is suppressed at node 46.

Gap Data

In this example, a small negative closure distance of -.001 is given for the gaps. This indicates that the gaps are closed initially allowing an interference fit solution is to be obtained in increment 0. The coefficient of friction, μ , is input as 0.8.

Results

The results of the analysis are shown in Figure 8.3-2 through Figure 8.3-4. First of all, it is observed in Figure 8.3-2 that the link elements never go into tension.

In this case, the initial bolt load is carried quite uniformly (A in Figure 8.3-2), but as the pull-out increases, the inner two links take more of the stress and the outer link (element 31) sheds stress. The shear stress development is followed in Figure 8.3-3 – initially (bolt load only), all shear stresses are essentially zero. The two outer links slip first, but then the additional forces required to resist the pull develop in the inner two elements until the shear stress pattern follows the normal stress pattern, when the shear in the pair of links also slip ($\tau = \mu\sigma$). Figure 8.3-4 shows a plot of



the radial displacement of the outer perimeter against the pull-out force – notice the small loss of stiffness caused by slip developing, as the vessel model has to resist the extra force along without any further force transfer to the cover.

Convergence

Because the only ‘nodes’ in this structure are external nodes during the analysis phase, a different convergence path is followed than in problem 7.2. Displacement testing is automatically invoked by MARC. The gap forces at any increment are within one percent of those calculated in 7.2.

Computational Costs

Because of the use of substructures, this analysis was performed in 30% of the time of problem 7.2, which is a considerable computational savings.

Parameters, Options, and Subroutines Summary

Example e8x3.dat:

Parameters	Model Definition Options	History Definition Options
ELEMENT	CONNECTIVITY	AUTO LOAD
END	COORDINATE	BACKTOSUBS
NEWDB	END OPTION	CONTINUE
SIZING	FIXED DISP	CONTROL
SUBSTRUCTURE	ISOTROPIC	POINT LOAD
TITLE	SUBSTRUCTURE	

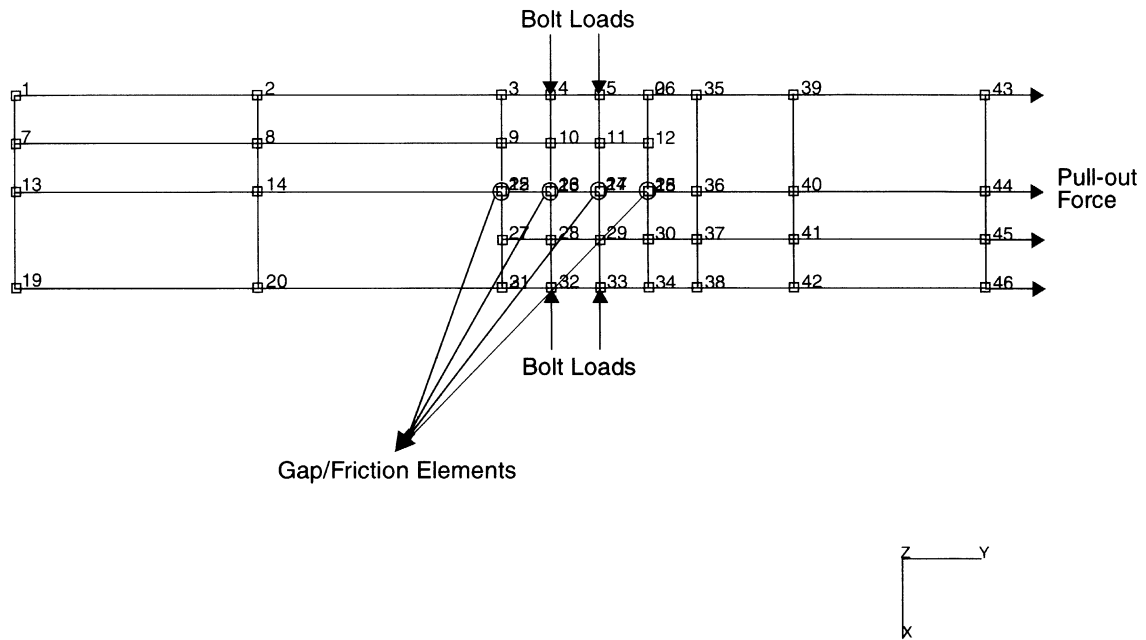


Figure 8.3-1 Geometry and Mesh of End Plate-Aperture

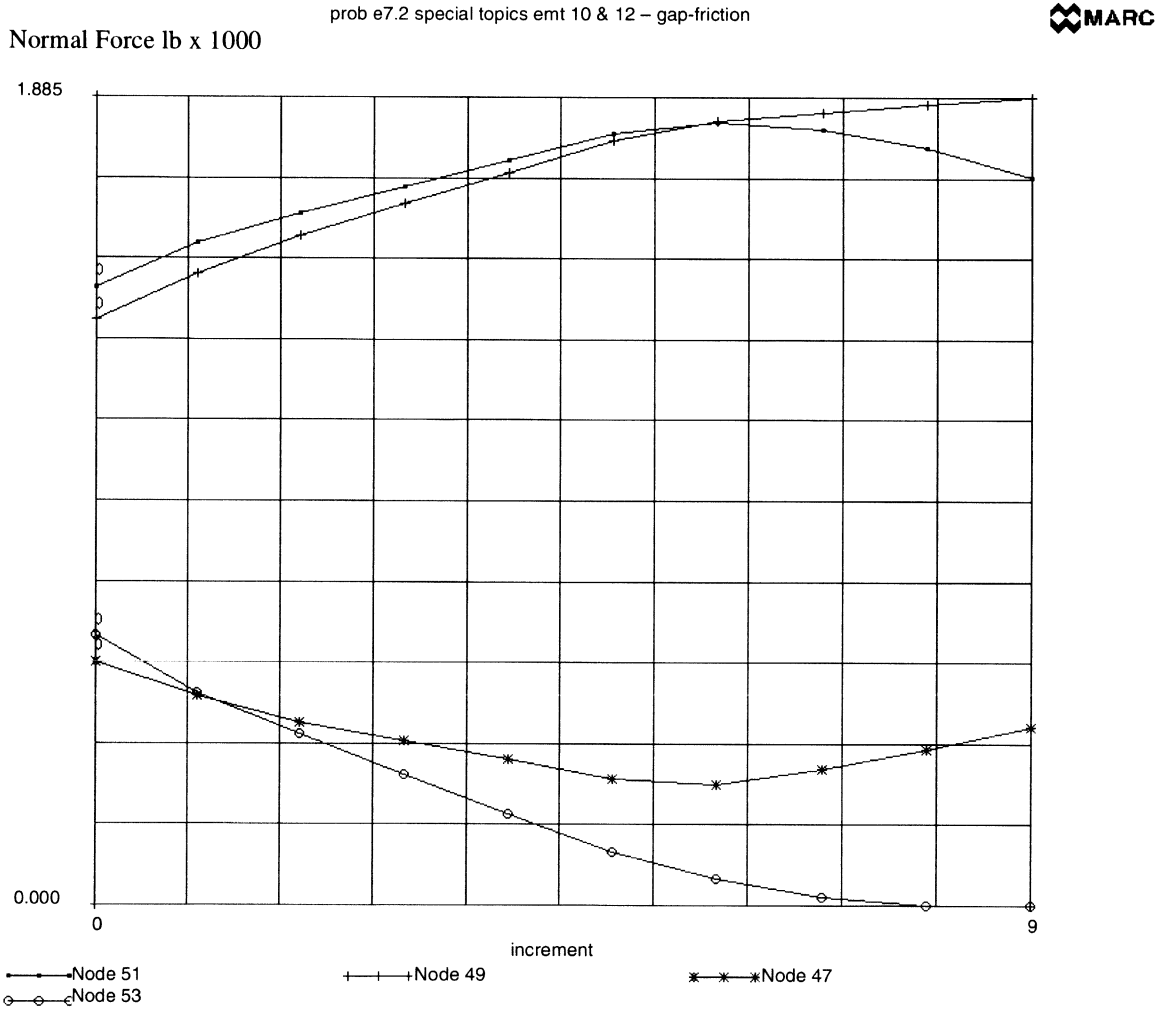


Figure 8.3-2 Transient Normal Force in Bolts

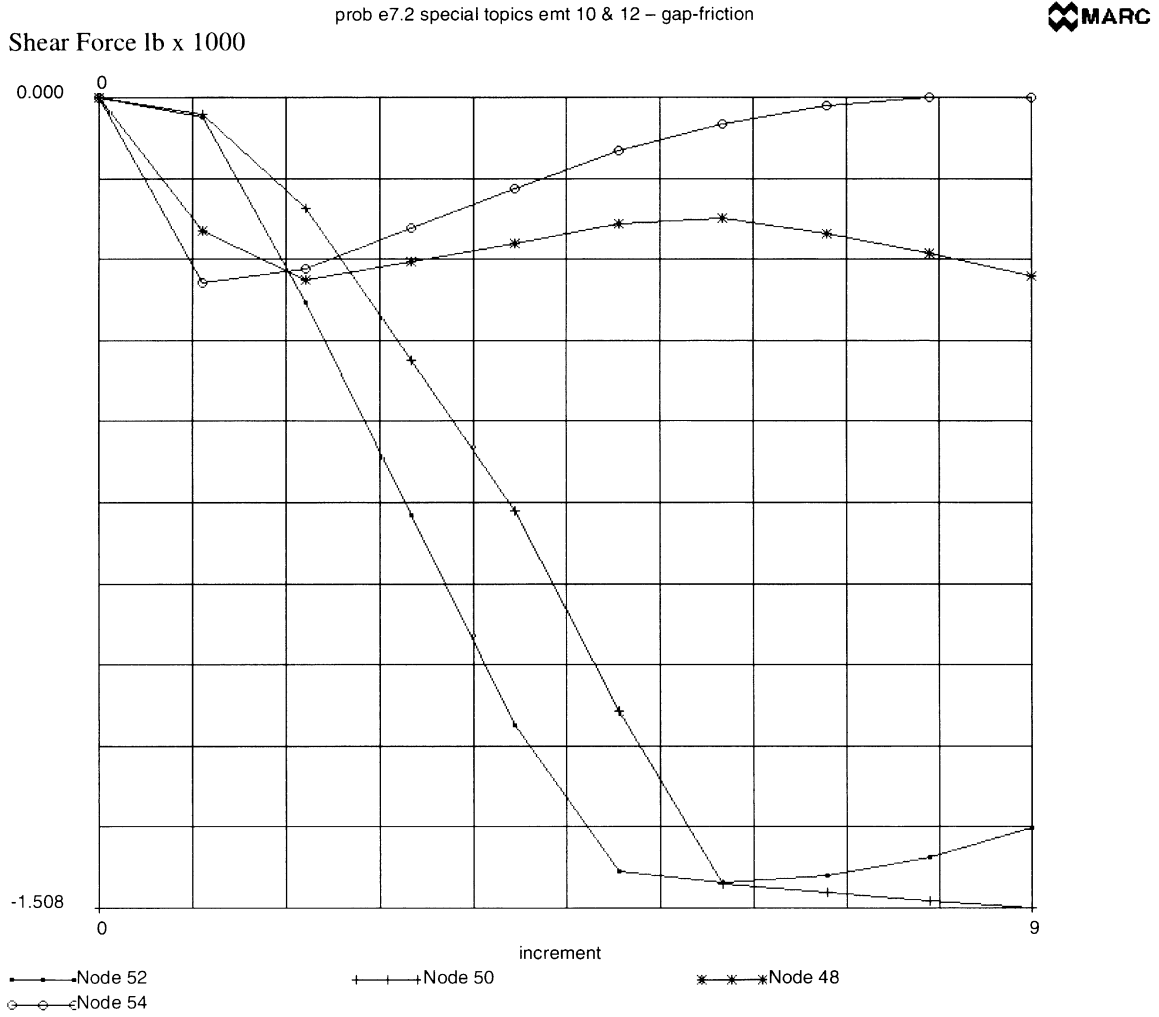


Figure 8.3-3 Transient Shear Force in Bolt

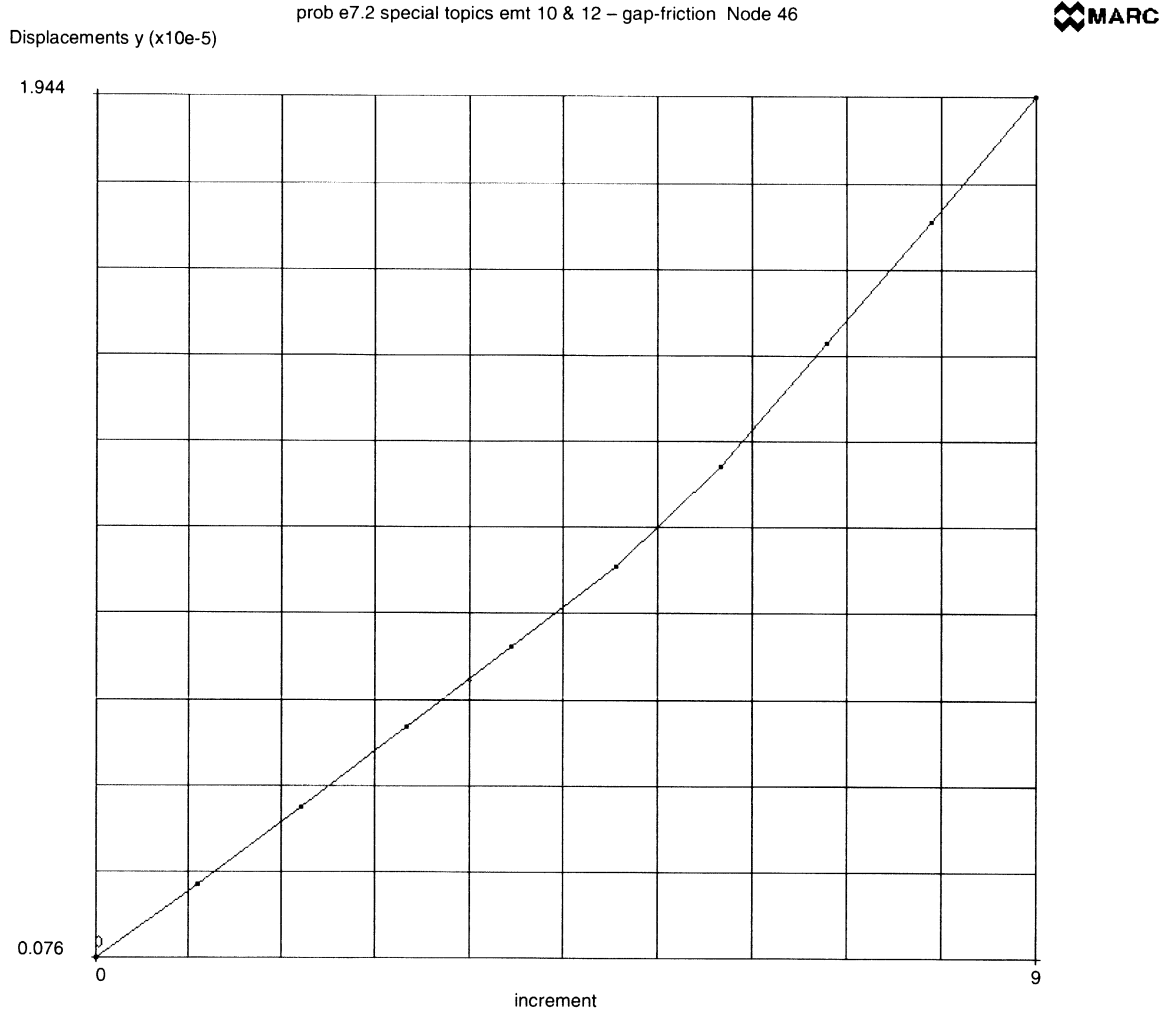


Figure 8.3-4 Radial Displacement at Outside Top (Node 46)





8.4 Collapse of a Notched Concrete Beam

A quasi static collapse analysis is carried out for a notched concrete beam. This analysis demonstrates the use of the cracking option for plane stress elements. An elastic tension softening material has been used in this analysis and the results obtained have been compared with experimental data (1).

Element

Element type 26 is an eight-node quadrilateral plane stress element with a nine point integration scheme.

Model

This notched beam (dimensions and element mesh in Figure 8.4-3) has been divided in 26 elements with a refinement near the notch. The beam is supported at its ends and loaded by a force applied just above the notch.

Tying

Tying type 32 is used to ensure a consistent displacement behavior near the mesh refinement. With this tying, the interior nodes of the elements of the refined side are coupled to the three retained nodes of the element on the coarse side. Eight tying equations of this type are needed.

Tying type 2 is needed to ensure equal displacements in the y-direction of the three nodes of the element above the notch on which the loads have to be applied.

Boundary Conditions

Simply supported and sliding conditions have been prescribed at the left and right bottom corners, respectively. At the midnode of the element above the notch, displacement increment in negative y-direction is prescribed. In the analysis, initially two displacement increments of -0.5 mm have been applied. With proportional increment, the displacement is scaled to 0.002 mm and 30 increments of this size have been applied.

Isotropic

An elastic isotropic material with Young's modulus $E = 30000 \text{ N/mm}^2$ and a Poisson's ratio $\nu = 0.2$ has been specified through the ISOTROPIC option. In addition, the cracking flag is turned on for material id 1.

Crack Data

In this block, the cracking data needs to be specified for each material group. The critical cracking stress is set to 3.33 N/mm^2 . A linear tension softening behavior has been specified with a softening modulus $E_s = 1790 \text{ N/mm}^2$ and is assumed to be independent of the element



size. The choice of a value of the tension softening modulus can be related to on the fracture energy G_f . Assuming that the micro-cracks are uniformly distributed over the specimen length l_s , the fracture energy is related to $G_f = l_s \int \sigma d\epsilon^{cr}$, which results for a linear tension softening behavior in $G_f = \frac{1}{2} l_s \sigma_c \epsilon_u$. For this particular analysis, it can be assumed that cracking only occurs in the elements just above the notch with a width h and in the energy expression, G_f can be expressed by $G_f = \frac{1}{2} h \sigma_c \epsilon_u$. It is clear, that depending on the width of the notch, the value ϵ_u needs to be adapted and the tension softening modulus $E_s = \sigma_c / \epsilon_u$ needs to be a function of the width of the notch.

The critical crushing strain is not set, and default a high value 10^{11} is used (crushing occurs at a critical value of the plastic strain and since no plasticity is allowed in the analysis, crushing does not occur). The shear retention factor is set to zero; hence, no shear stiffness is present at an integration point once a crack occurs.

Control

A maximum number of 32 loadsteps have been specified. In each step, maximal 5 iterations are allowed. The default full Newton-Raphson iterative technique has been used with tolerance checking on the residual forces (10% of the maximum reaction force).

Results

In increment 1, the first cracks initiate in the element just above the notch. At this increment, three cycles are needed to reach convergence. In the subsequent increments, no new cracks initiate and no cycles are needed. In increment 7, new cracks initiate with recycling followed by a number of steps with only back substitution. In subsequent increments, new cracks occur in increment 14, 20, 27 and 29. Cracks occur only in the elements above the notch (width 40 mm). The assumption needed in the choice of the tension softening modulus was correct. The calculated load-deflection curve is shown in Figure 8.4-5 and is compared with the experimental result (1). It is seen that the experimental result is overestimated. The reason for this overly stiff behavior can probably be found in the choice of the linear tension softening behavior.

Reference

1. Petersen, P. E., "Crack growth and development of fracture zones in plain concrete and similar materials," Report TVM-1006, Lund Institute of Technology, Lund, Sweden, 1981.



Parameters, Options, and Subroutines Summary

Example e8x4.dat:

Parameters

ELEMENT
END
PRINT
SIZING
TITLE

Model Definition Options

CONNECTIVITY
CONTROL
COORDINATE
CRACK DATA
END OPTION
FIXED DISP
GEOMETRY
ISOTROPIC
POST
PRINT CHOICE
TYING

History Definition Options

AUTO LOAD
CONTINUE
PROPORTIONAL INCREMENT

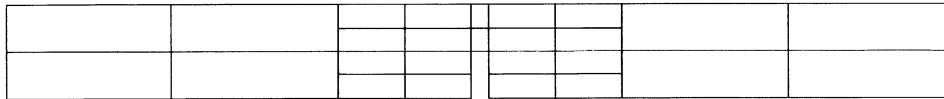


Figure 8.4-1 Geometry and Element Mesh



11	12	14	21	22
9	10	13	19	20
7	8		17	18
5	6		15	16



Figure 8.4-2 Element Numbering Detail of Mesh

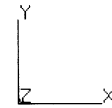
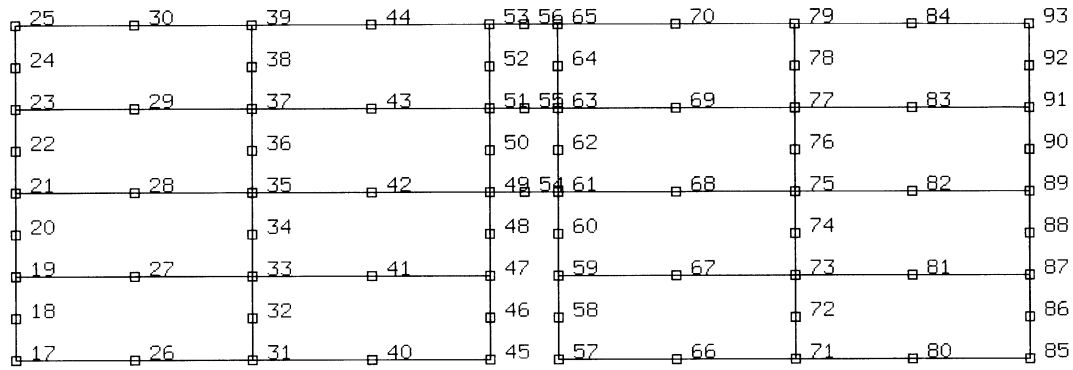


Figure 8.4-3 Node Numbering Detail of Mesh

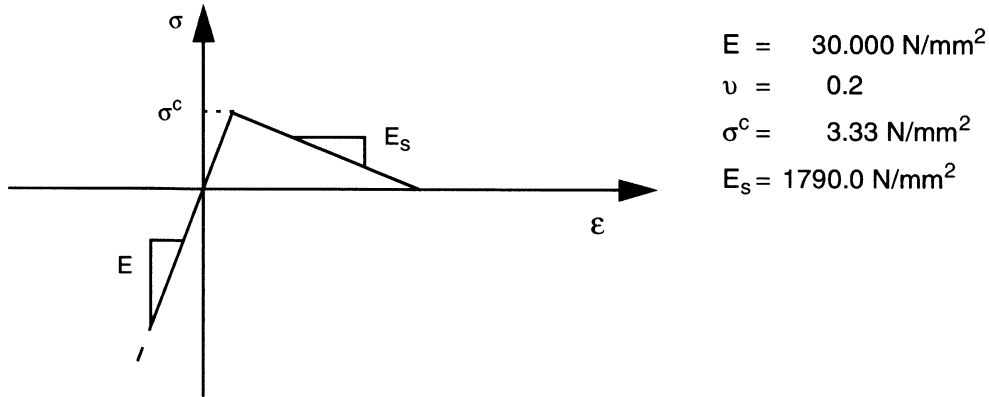


Figure 8.4-4 Material Properties

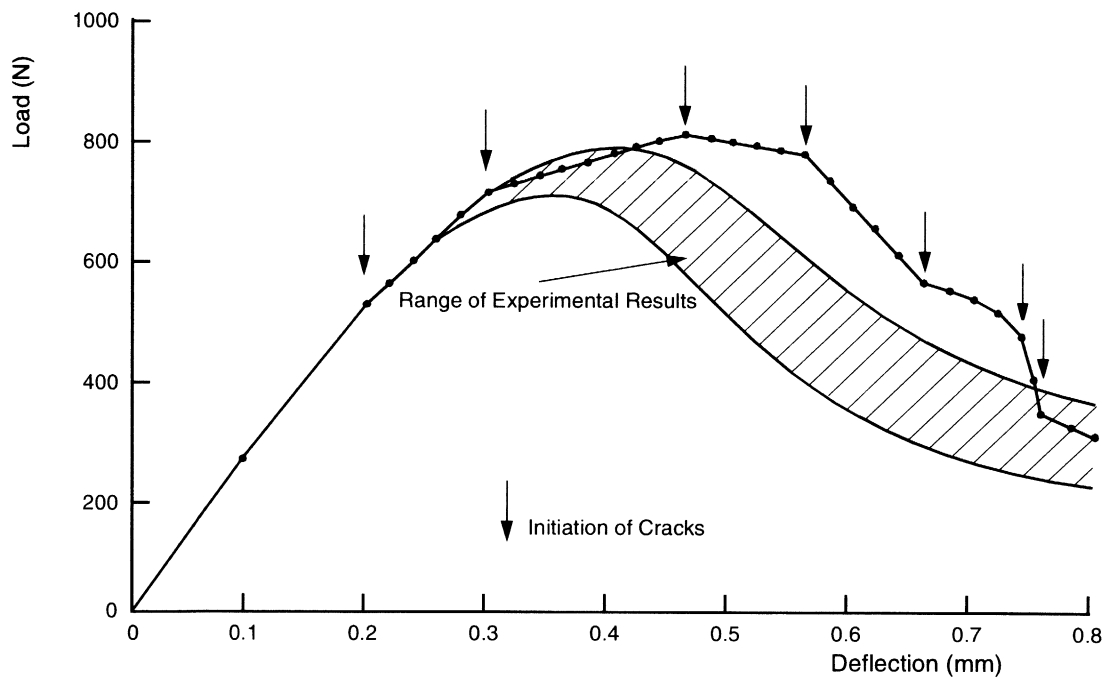


Figure 8.4-5 Comparison of Calculated and Experimental Load Deflection Curve Notched Beam Test





8.5 Cracking Behavior of a One-way Reinforced Concrete Slab using Shell Elements

This example demonstrates the analysis of a one-way reinforced concrete slab, which was tested by Jain and Kennedy [1] and material data for this problem can be found [2]. The slab is line supported at its ends (Figure 8.5-1) and loaded by a line load. The elastic cracking behavior with tension softening of the concrete and the elastic-plastic behavior of the steel reinforcement is demonstrated.

Element

Element type 75 is a 4-node thick shell element with six global degrees of freedom at each node.

Model

The slab, with dimensions shown in Figure 8.5-1, is divided into six shell elements. In these shell elements, integration of the material properties over the thickness is performed using nine layers; one layer represents the (smeared) steel reinforcement, while the other eight layers represent the concrete behavior. The mesh (Figure 8.5-2) is generated using the CONN GENER and NODE FILL option. Only one-half of the plate is modeled.

Material Properties

The concrete material is defined using the ISOTROPIC and the CRACK DATA options. First the ISOTROPIC option is defined to have a material ID of 1, and the cracking option is flagged. The properties are Young's modulus of 28960 N/mm^2 , Poisson's ratio of 0.2 and initial yield stress of 31.6 N/mm^2 . The CRACK DATA option indicates that the concrete has a ultimate stress of 2 N/mm^2 and a shear retention of 0.5. In the first analysis, no tension softening is specified. In the second analysis, a tension softening of 3620 N/mm^2 is specified.

The steel reinforcement is modeled as a uniaxial material in a single layer of the shell element. This is done using the ORTHOTROPIC option, specifying an $E_{xx} = 20,000 \text{ N/mm}^2$ and $E_{yy} = E_{zz} = 0.01 \text{ N/mm}^2$. The associated shear moduli are $G_{xy} = 10,000 \text{ N/mm}^2$ and $G_{yz} = G_{zx} = G_{zy} = 0.005 \text{ N/mm}^2$. The steel has an initial yield stress of 221 N/mm^2 .

COMPOSITE

The COMPOSITE option is used to indicate that there are nine layers of materials. The first six are of equal thickness of 5.166 mm each and are composed of material 1 (concrete). The seventh layer is the very thin steel layer, thickness of 0.272 mm and material ID = 2. Finally, layers 8 and 9 are concrete with a thickness of 3.364 mm.

**Boundary Conditions**

Symmetry conditions are specified on node 1 and 2 of the element mesh. On the line $Y = 0, Z = 0$, no translation in y-direction is allowed, and at nodes 13 and 14, a sliding support (no displacement in z-direction) is prescribed.

Control

On the control block, a maximum of 25 load steps is specified with a maximum of seven cycles per load increment. The default Newton-Raphson iterative procedure with testing on the relative residual forces (tolerance 10%) is used. The solution of nonpositive definite systems is forced by the PRINT,3 option.

Loading

On node 9 and 10, a point load with magnitude -1500 in z-direction is applied. This is the estimated maximum value of the collapse load. Via the AUTO INCREMENT option, the automatic load stepping procedure, using Riks algorithm, starts with 10% of the total load and a desired number of three cycles (must be smaller than the maximum number specified on the CONTROL block). The maximum numbers of steps in this load incrementation set is 20 and the maximum step size is 10% of the load.

Results

The calculated load center-deflection response is shown in Figure 8.5-4 for the run with and without tension softening. Without tension softening, an unstable behavior, present in the response, is caused by the loss of stiffness between reinforcement and concrete once a crack occurs. With tension softening, some artificial interaction is introduced and usually results in a more stable solution procedure. In the run with tension softening, fewer cycles are needed to reach convergence. Compared with the experimental result [1], [2], the effect of tension softening is clearly indicated. Best agreement is obtained with tension softening.

References

1. Jain, S.C. and Kennedy, J.B., "Yield criterion for reinforced concrete slabs," *J. Struct. Div.*, Am. Soc. Civ. Engrs., 100, 513, March 1974, pp. 631-644
2. Crisfield, M.A. "Variable step lengths for non-linear structural analysis," Report 1049, Transport and Road Research Lab., Crowthorne, England, 1982.



Parameters, Options, and Subroutines Summary

Example e8x5a.dat:

Parameters	Model Definition Options	History Definition Options
ELEMENT	COMPOSITE	AUTO INCREMENT
END	CONN GENER	CONTINUE
PRINT	CONNECTIVITY	POINT LOAD
SIZING	CONTROL	
TITLE	COORDINATE	
	CRACK DATA	
	END OPTION	
	FIXED DISP	
	ISOTROPIC	
	NODE FILL	
	ORIENTATION	
	ORTHOTROPIC	
	POST	
	PRINT CHOICE	
	RESTART	

Example e8x5b.dat:

Parameters	Model Definition Options	History Definition Options
ELEMENT	COMPOSITE	AUTO INCREMENT
END	CONN GENER	CONTINUE
PRINT	CONNECTIVITY	POINT LOAD
SIZING	CONTROL	
TITLE	COORDINATE	
	CRACK DATA	
	END OPTION	
	FIXED DISP	
	ISOTROPIC	
	NODE FILL	
	ORIENTATION	
	ORTHOTROPIC	
	POST	
	PRINT CHOICE	
	RESTART	

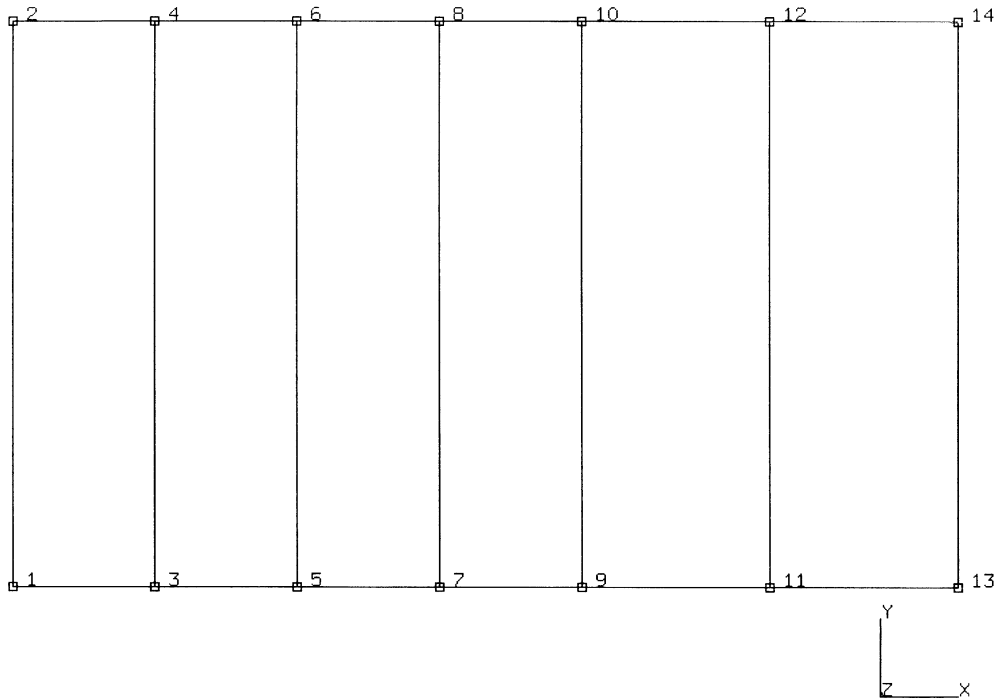


Figure 8.5-1 Geometry of One-Way Reinforced Slab

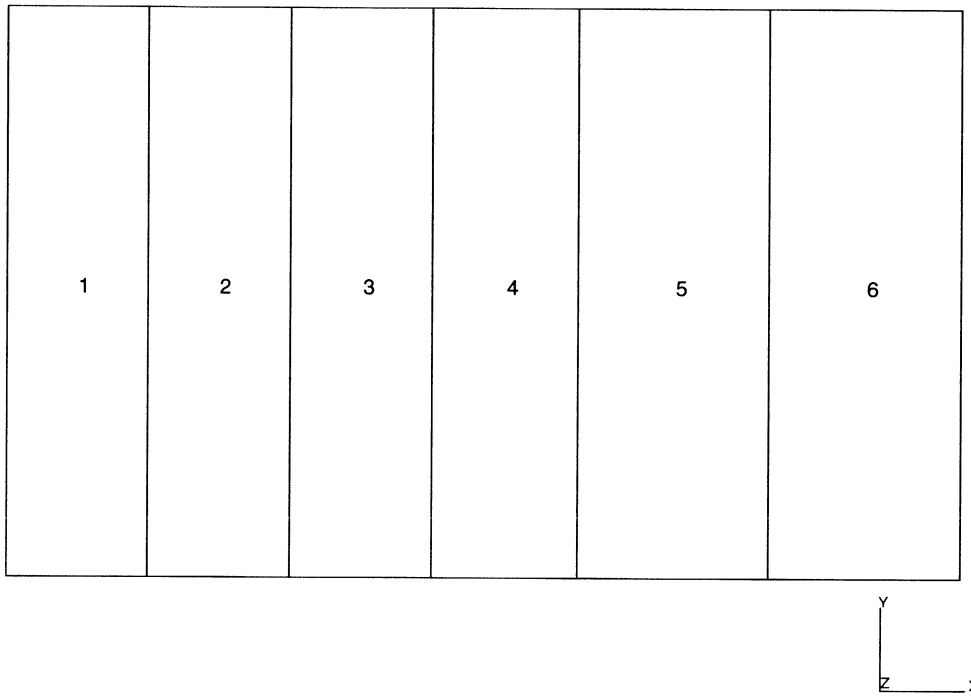


Figure 8.5-2 Element Mesh with Node Numbering

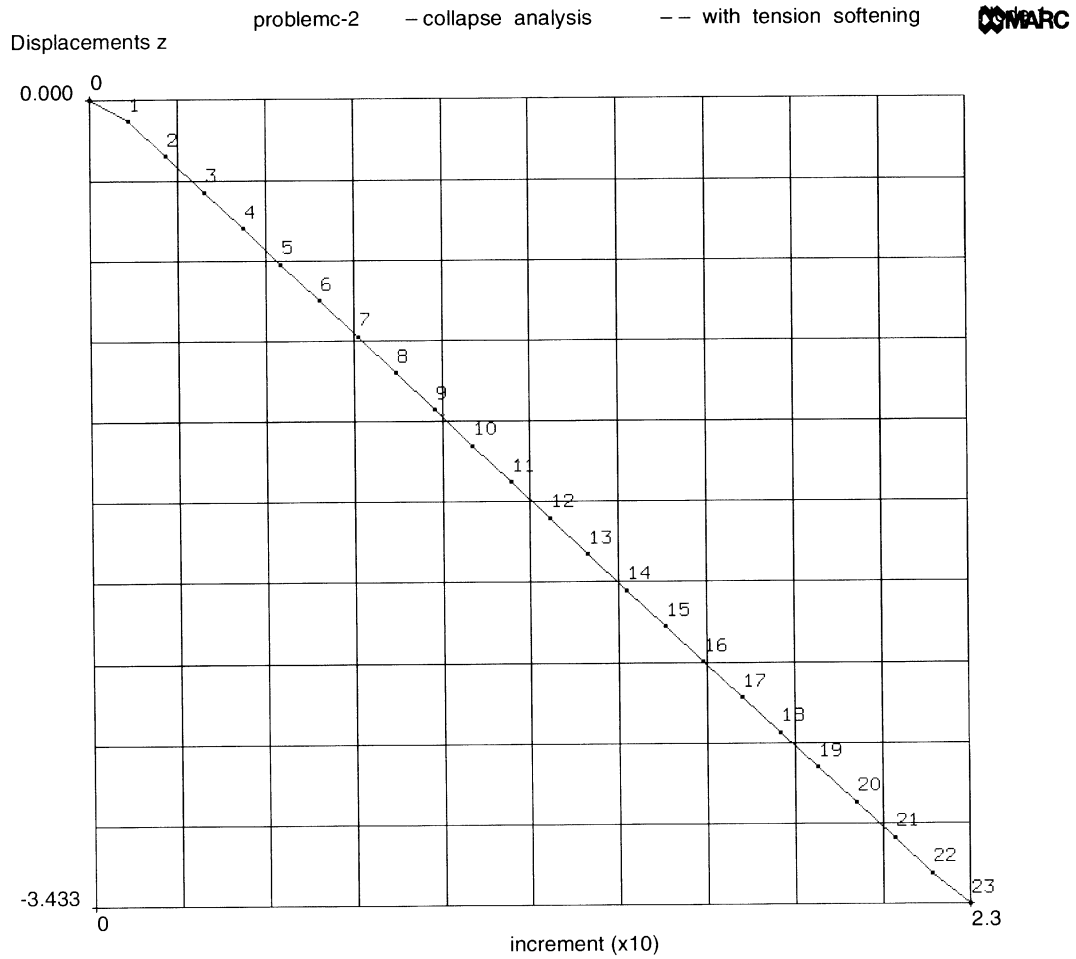


Figure 8.5-3 Element Mesh with Element Numbering

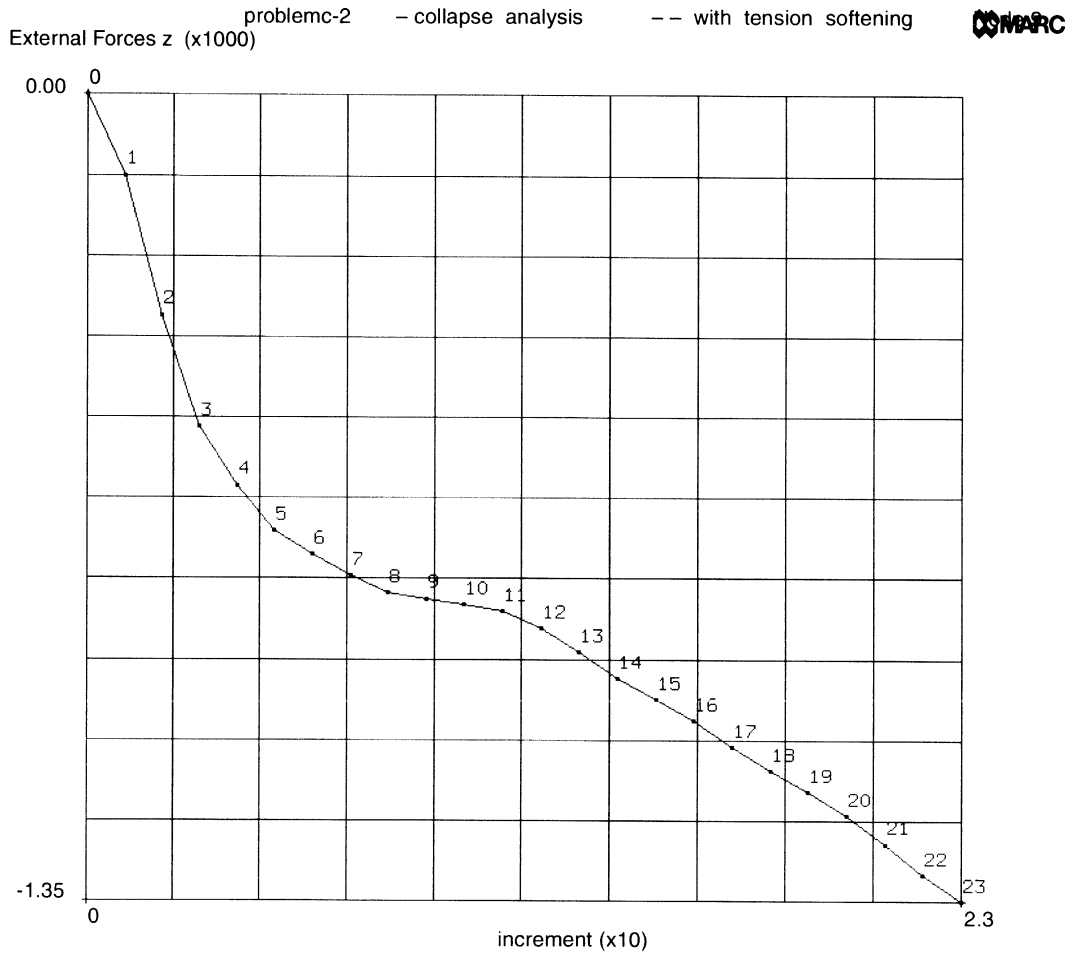


Figure 8.5-4 Load-Deflection Relationship for One-Way Reinforced Slab



8 Advanced Topics

Cracking Behavior of a One-way Reinforced Concrete Slab using Shell Elements



8.6 Cracking Behavior of a One-way Reinforced Concrete Slab

This example is the same type of analysis as described in problem 8.5 (Figure 8.6-1). Instead of shell elements, however, continuum plane strain elements and rebar elements have been used, which is allowed since the problem is essentially two-dimensional. For the concrete, an elastic-cracking behavior with tension softening and shear retention is specified. In the rebar elements, an elastic-plastic behavior is possible.

Element

Element type 27 is an eight-node plane quadrilateral strain element with two degrees of freedom per node is used to model the concrete. This element is preferred over element 11 (four-node plane strain) since considerable shear is present in the beam. Element type 46 is an eight-node plane strain rebar element compatible with element 27 and is used to specify the reinforcement (Figure 8.6-2).

Model

The concrete is modeled with 10 plane strain elements (Figure 8.6-3 and Figure 8.6-4). At least two elements over the thickness are needed for accurate analysis of the bending of the beam. In each element, nine integration points are present, resulting in a six-point integration scheme over the thickness. Over the concrete elements below the neutral line (1 to 5), an overlay of rebar elements is used (elements 11 to 15). The position, thickness, and orientation of the reinforcement layers in this element needs to be specified via user subroutine REBAR.

The mesh is generated using the CONN GENER and NODE FILL option.

Material Properties

The elastic properties of the concrete (material identification number 1) is taken as:

Young's modulus	$E = 28,960 \text{ N/mm}^2$
Poisson's ratio	$\nu = 0.3$

The cracking flag is turned on for material number 1.

The following properties for the steel reinforcement (material identification number 2) is taken:

Young's modulus	$E = 200,000 \text{ N/mm}^2$
Poisson's ratio	$\nu = 0.2$
Yield stress	$\sigma_y = 221 \text{ N/mm}^2$

**Crack Data**

Only one set of cracking data needs to be specified since cracking is only possible in the concrete elements (specified via the ISOTROPIC option). The following values have been taken:

Critical cracking stress	$\sigma_c = 2 \text{ N/mm}^2$
Tension softening modulus	$E = 3620 \text{ N/mm}^2$
Shear retention factor	0.5

Boundary Conditions

Symmetry conditions are specified for nodes 1 to 5 and a sliding condition for node 41.

Control

On the CONTROL option, a maximum of 25 load steps is specified with a maximum of seven cycles per load increment. The default Newton-Raphson iterative procedure with testing on the relative residual forces (tolerance 10%) is used. The solution of nonpositive definite systems is forced by the PRINT,3 option.

Loading

On node 29, a point load with magnitude -1500 in y-direction is applied. This is the estimated maximum value of the collapse load. Via the AUTO INCREMENT option, the automatic load stepping algorithm, using the Riks algorithm, starts with 10% of the total load and a desired number of three cycles (must be smaller than the maximum number specified in the CONTROL option). The maximum numbers of steps in this load incrementation set is 20 and the maximum step size is 10% of the load.

Results

The calculated load-deflection response is shown in Figure 8.6-6 and compared with the experimental result. Compared with the results of tension softening using shell elements (problem 8.5), a nearly identical load-deflection curve is obtained. In the run with shell elements, no shear retention factor is used but sufficient shear stiffness is present even if large scale cracking occurs. In the run with plane strain elements, the absence of shear retention (meaning there is no shear stiffness if a crack occurs) results in an unstable behavior and very poor convergence. With shear retention, a stable behavior is obtained. The shear retention factor can be specified as a function of the crack length via user subroutine UCRACK.



Parameters, Options, and Subroutines Summary

Example e8x6.dat:

Parameters

ELEMENT
END
PRINT
TITLE

Model Definition Options

CONN GENER
CONNECTIVITY
COORDINATES
CONTROL
CRACK DATA
END OPTION
FIXED DISP
GEOMETRY
ISOTROPIC
NODE FILL
POST
RESTART

History Definition Options

AUTO INCREMENT
CONTINUE
POINT LOAD

User subroutine in u8x6.f:

REBAR

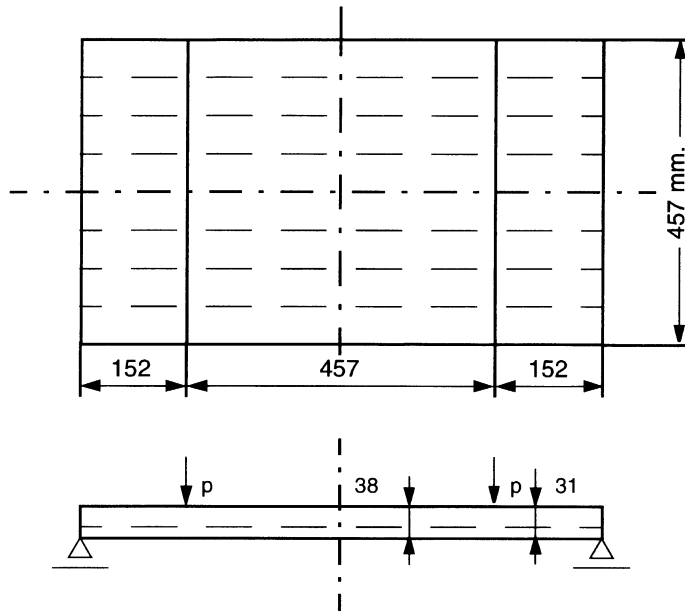
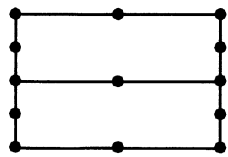
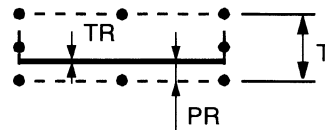


Figure 8.6-1 One-Way Reinforced Slab



Continuum Element
Type 27



Rebar Element
Type 476

T = 19.
PR = 6.864
TR = .272

Figure 8.6-2 Element Types used in Analysis

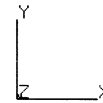
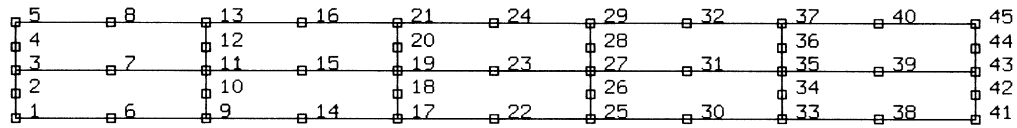


Figure 8.6-3 Node Numbering



6	7	8	9	10
1	2	3	4	5

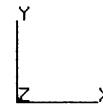


Figure 8.6-4 Element Numbering Concrete Elements

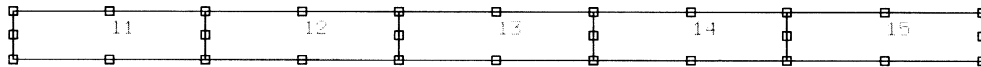


Figure 8.6-5 Element Numbering Rebar Elements

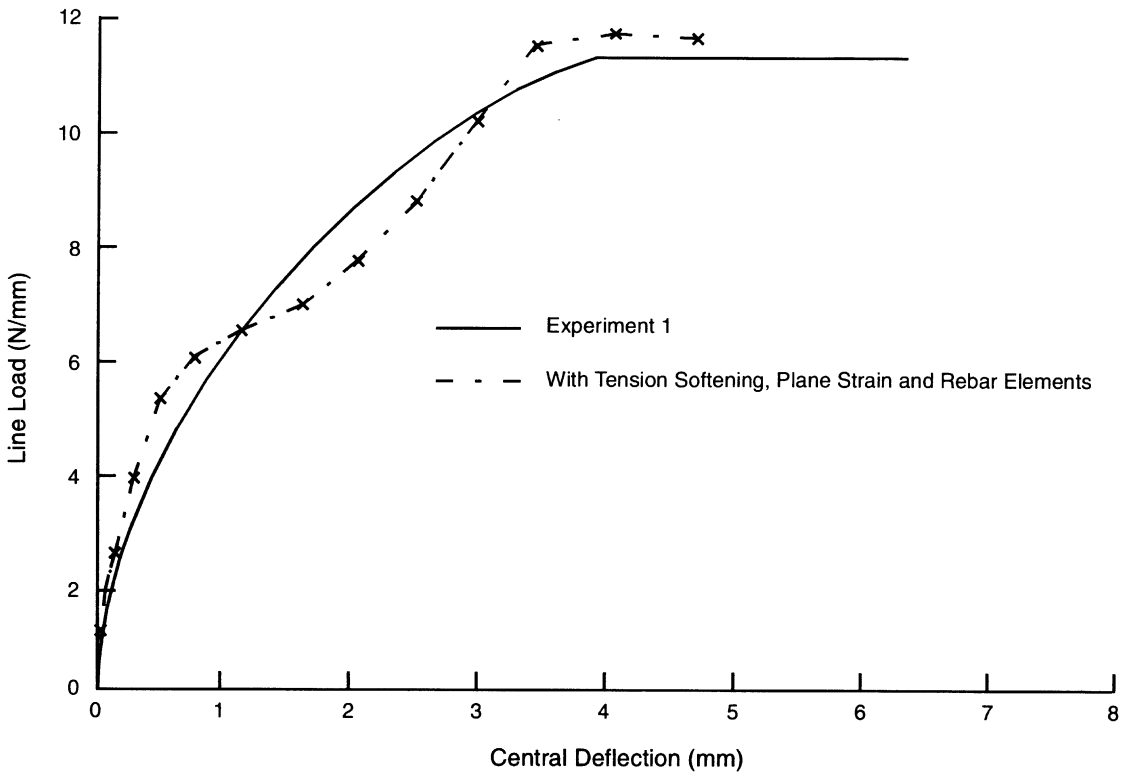


Figure 8.6-6 Load/Deflection Relationship for One-Way Reinforced Slab



8.7 Compression of a Block

This example demonstrates MARC's capability to perform a large deformation contact problem which incorporates thermal mechanical coupling. The block is considered an elastic-plastic deformable material, and both the deformations and temperatures are calculated. The platen is treated as a rigid region and only temperatures are calculated. Gap elements are used to insure that the contact condition is properly accounted for.

Coupling

There are four sources of coupling in this analysis:

1. As the temperature changes, thermal strains are developed; this is due to nonzero coefficient of thermal expansion.
2. As the temperature changes, the mechanical properties change because of the temperature-dependent elasticity.
3. As the geometry changes, the heat transfer problem changes.
4. As plastic work is performed, internal heat is generated.

Parameters

The UPDATE, FINITE, and LARGE DISP are included in the parameter section as this is a finite deformation analysis. The COUPLE option is used to indicate that a couple thermal-mechanical analysis is being performed.

Mesh Definition

Due to symmetry, only one quarter of the region is modeled. The mesh is shown in Figure 8.7-1. The deformable block is modeled using Element type 11 (4-node quadrilateral), while the platen is modeled with Element type 39 (4-node quadrilateral). In a coupled analysis, if the element type is a displacement element, a coupled (displacement-temperature) formulation will be used. If the element type is a thermal element, only a heat transfer analysis will be performed in that region; that is, rigid.

Two gap elements are used between the platen and the block. In a coupled analysis, when the gap elements are open, there is no load transmitted across the gap and the gap acts as a perfect insulator. When the gap closes, load is transmitted and the gap acts as a perfect conductor.

Geometry

A unit thickness is used. A '1' is placed in the second field which indicates that the constant dilatation formulation is used.

**Boundary Conditions**

Symmetry displacement boundary conditions are imposed on two surfaces. An applied displacement is used to model the plate. The intention is to compress the block to 60% of its original height. The displacement boundary conditions are entered via the FIXED DISP option. On the outside surface of the platen, the temperature is constrained to 70° by using the FIXED TEMP option. Because of an ambiguity in type, the BOUNDARY CONDITION option should not be used in a coupled analysis.

Initial Conditions

The block is given an initial temperature of 300°, and the platen an initial temperature of 70°.

Material Properties

The block is treated as an elastic plastic material with a Young's modulus of $1. \times 10^6$ psi, Poisson's ratio of 0.3, mass density of 0.1 lb/in^3 , coefficient of thermal expansion of $1.3 \times 10^{-5} \text{ in/in}^\circ\text{F}$ and a yield stress of 50,000 psi. The material is given an initial workhardening slope of 10,000 psi which reduces to 1000 psi at an equivalent plastic strain of 0.01.

The thermal properties are a conductivity of $21.6 \text{ in-lb/in}^\circ\text{F}$ and the specific heat of $2147 \text{ in-lb/lb}^\circ\text{F}$. In the platen, no mechanical properties are given as it is rigid. The thermal properties are the same as the block. In a coupled analysis, the mass density must be entered on the first property.

Gap Data

For the two gap elements, the only property necessary is the closure distance. This is the original distance between the gap nodes attached to the block and the platen.

Temperature Effects

The elastic modulus is assumed to be a linear function of temperature such that:

$$E(T) = 1 \times 10^7 - (T - T_0) \times 1 \times 10^4,$$

where the reference temperature T_0 is 0°F.

Distributed Flux

This distributed flux block is used to indicate that internal heat is generated due to plastic deformation.

**Convert**

This option is used to give the conversion factor between the mechanical energy and the thermal energy.

The internal volumetric flux per unit volume becomes:

$$f = c \cdot W^P$$

where W^P is the plastic strain energy density.

Control Options

The Cuthill-McKee optimizer is used to minimize the bandwidth. A formatted post file containing only nodal variables is written every ten increments. In a coupled analysis, the nodal variables are the total displacements, applied forces, reaction forces, temperatures, and applied flux. The restart file is written each increment. The PRINT CHOICE option is used to minimize the amount of output.

Two lines are used to enter the control tolerances. These are the default values.

Load Control

This problem is performed with a fixed time step, fixed increment size. This is specified with a time step of 1 second, and a total of 80 seconds is requested. As no proportional increment is used, each increment imposes a displacement of 0.2 inches.

In a coupled analysis, if an adaptive time-stepping is required, the AUTO TIME option should be invoked.

Results

Figure 8.7-2 through Figure 8.7-11 show the contour plots of the equivalent stress and the temperatures on the deformed body. The body folds over onto the platen at increment 45. The figures are shown until increment 70. At approximately increment 75 (depends on machine accuracy), the analysis stops because of very large distortion. A rezoning step should have been performed in increment 60.

The analysis shows in increment 30 that there is a small rigid region stress below yield under the platen, which remains for the entire analysis. The highest stress at increment 70 occurs where the material is folded over and is 10% above yield. This is an indication of the minimal amount of workhardening in the material. The final highest temperature of 340°F, an increment of 10°F above initial conditions, is due to the plastic deformation.

The printed results for a coupled analysis give the stress, total strain, plastic strain, thermal strain, and temperature for each integration point requested. In the platen (rigid region), only the temperatures are given. The nodal variables printed are the incremental and total displacements, temperatures, nodal forces and reaction forces.



Parameters, Options, and Subroutines Summary

Example e8x7.dat:

Parameters

COUPLE
ELEMENT
END
FINITE
LARGE DISP
SIZING
TITLE
UPDATE

Model Definition Options

CONNECTIVITY
CONTROL
CONVERT
COORDINATE
DIST FLUXES
END OPTION
FIXED DISP
FIXED TEMPERATURE
GAP DATA
GEOMETRY
INITIAL TEMPERATURE
ISOTROPIC
POST
PRINT CHOICE
RESTART
TEMPERATURE EFFECTS
WORK HARD

History Definition Options

CONTINUE
TRANSIENT

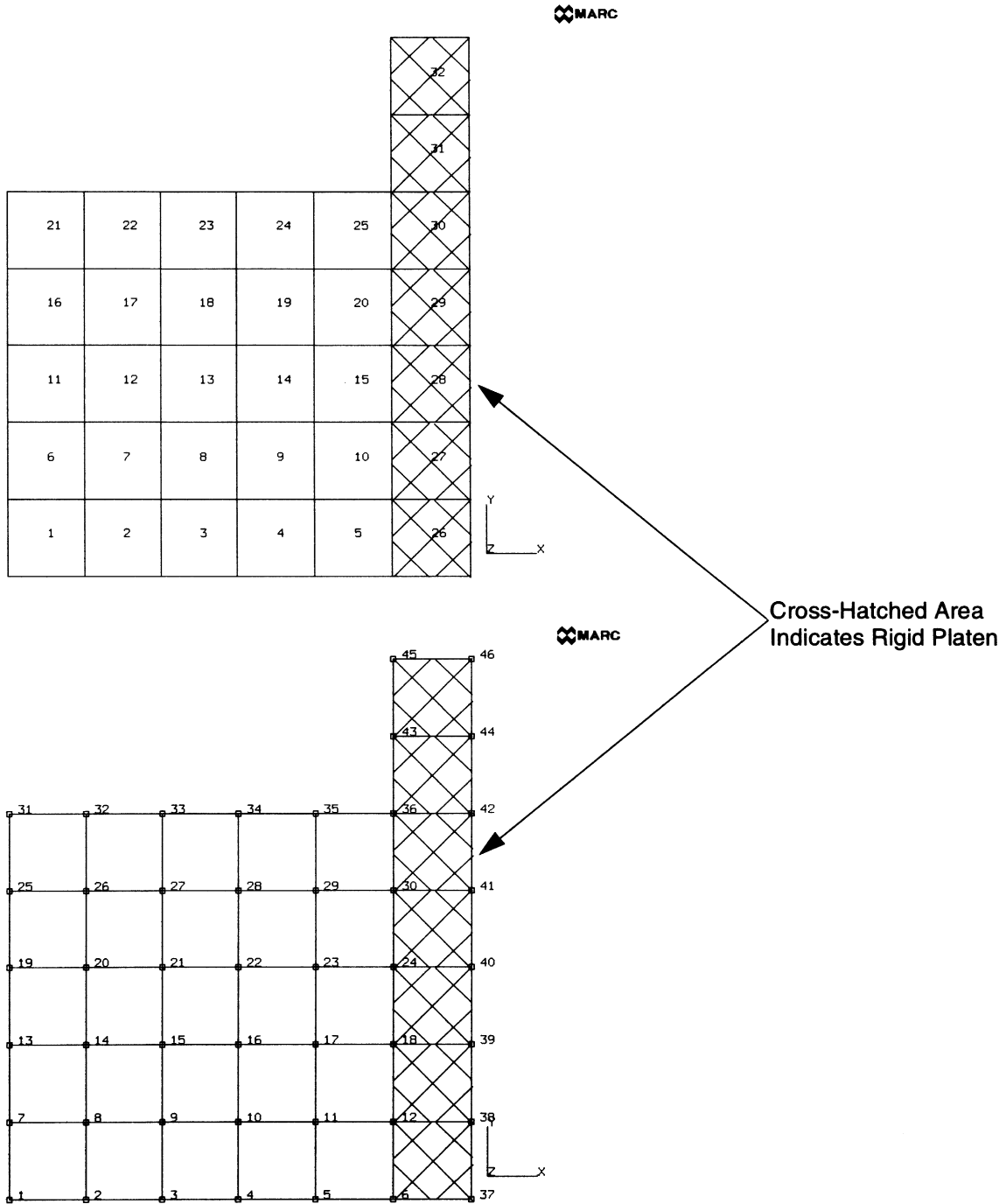
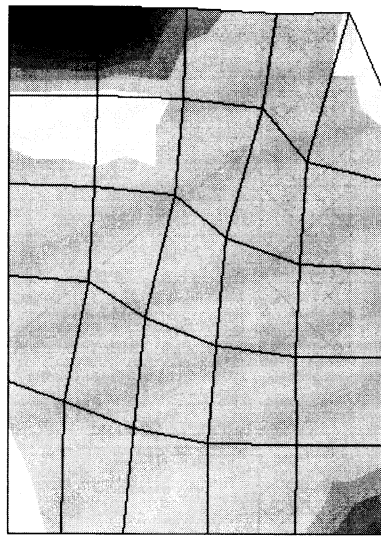
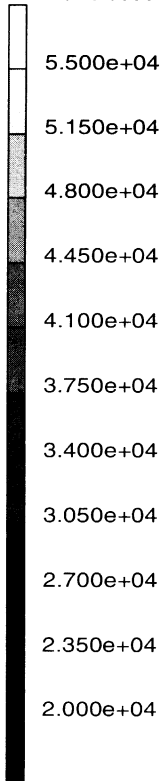


Figure 8.7-1 Mesh

INC : 30
SUB : 0
TIME : 3.000e+01
FREQ : 0.000e+00

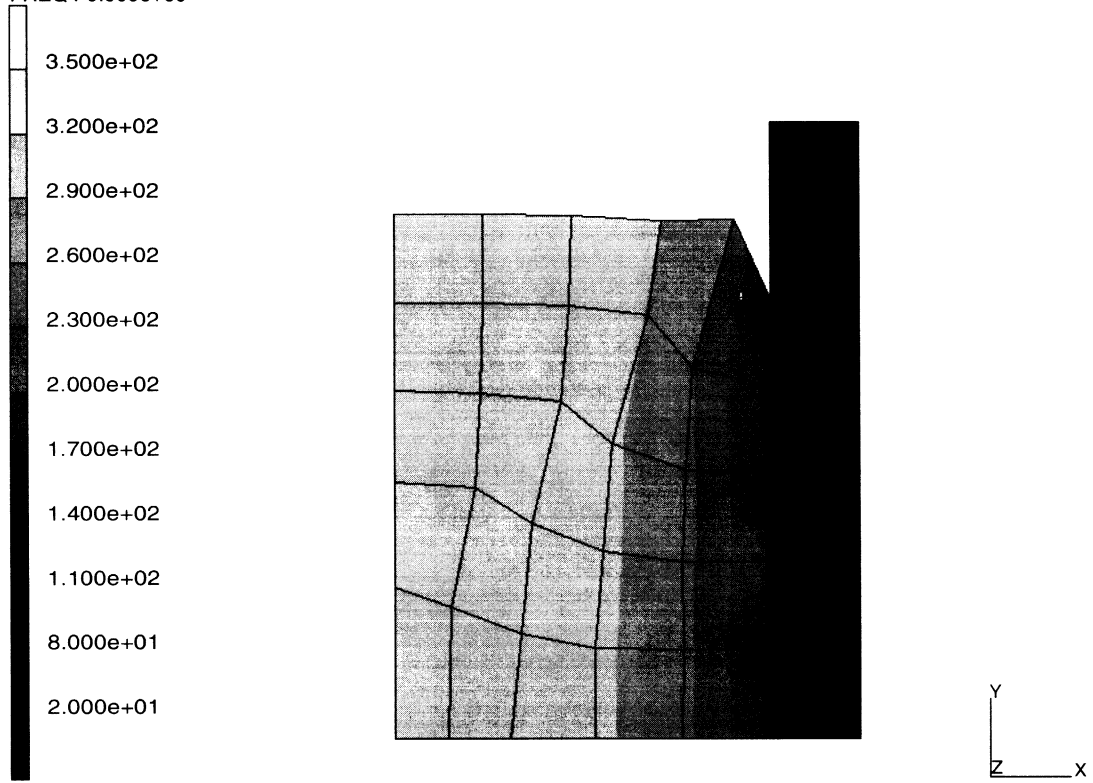


compression of block
Equivalent von Mises Stress

Figure 8.7-2 Equivalent Stress, Increment 30



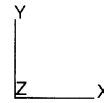
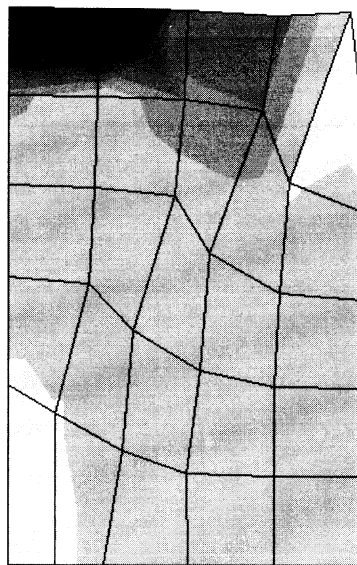
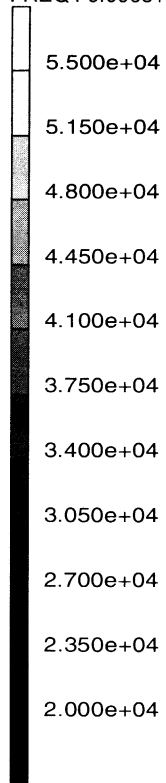
INC : 30
SUB : 0
TIME : 3.000e+01
FREQ : 0.000e+00



compression of block
Temperature

Figure 8.7-3 Temperature, Increment 30

INC : 40
SUB : 0
TIME : 4.000e+01
FREQ : 0.000e+00

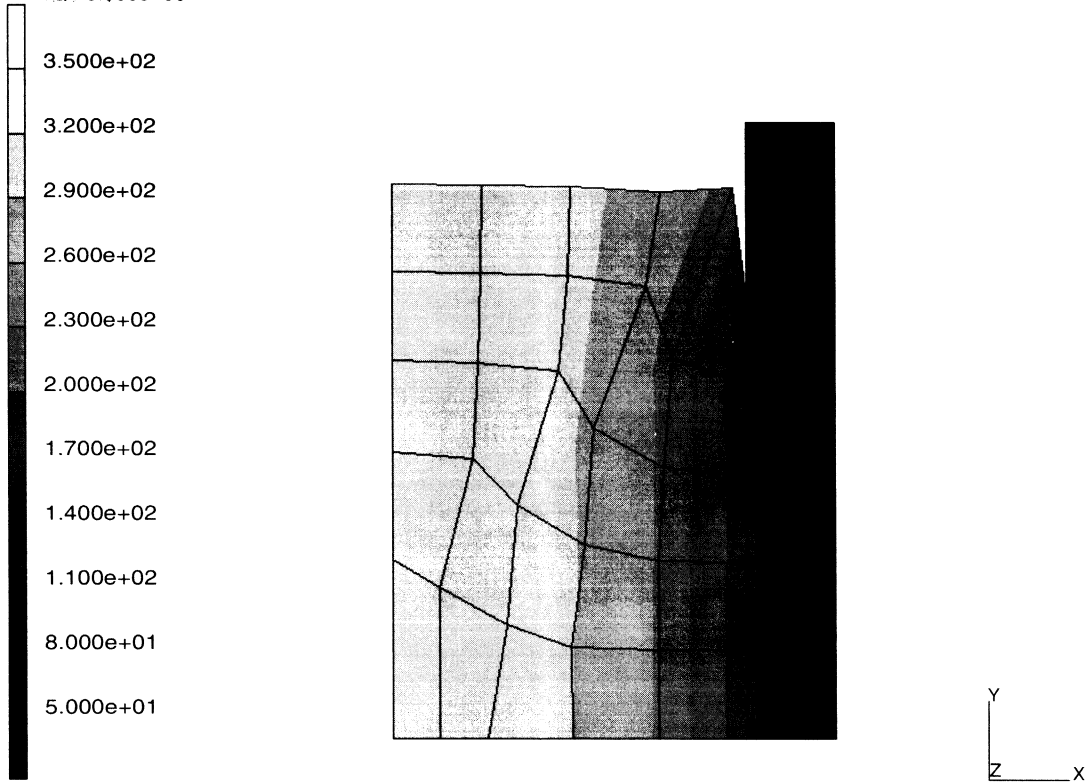


compression of block
Equivalent von Mises Stress

Figure 8.7-4 Equivalent Stress, Increment 40



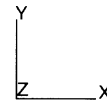
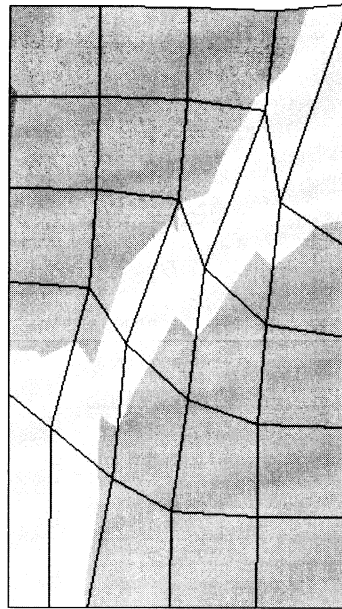
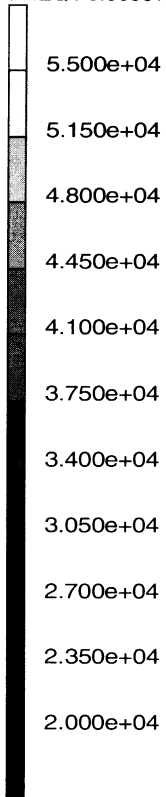
INC : 40
SUB : 0
TIME : 4.000e+01
FREQ : 0.000e+00



compression of block
Temperature

Figure 8.7-5 Temperature, Increment 40

INC : 50
SUB : 0
TIME : 5.000e+01
FREQ : 0.000e+00

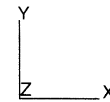
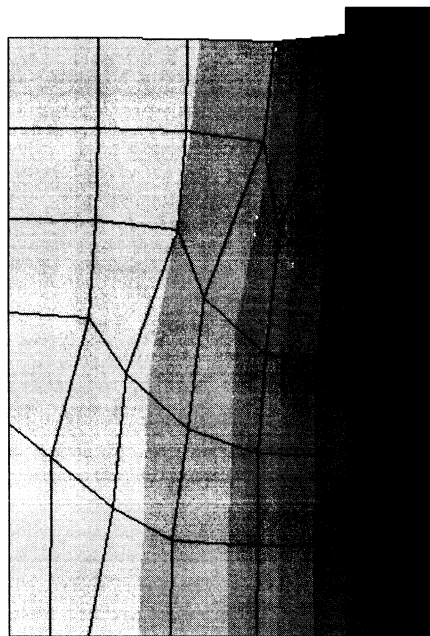
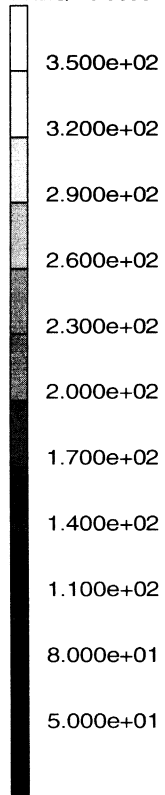


compression of block
Equivalent von Mises Stress

Figure 8.7-6 Equivalent Stress, Increment 50



INC : 50
SUB : 0
TIME : 5.000e+01
FREQ : 0.000e+00

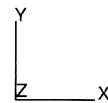
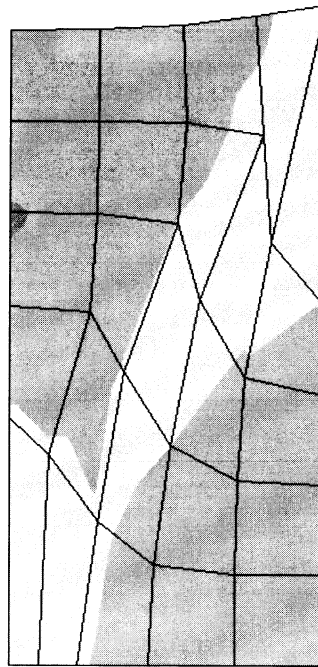
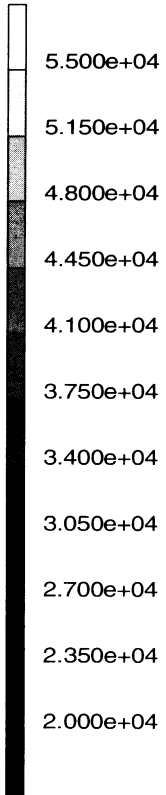


compression of block
Temperature

Figure 8.7-7 Temperature, Increment 50



INC : 60
SUB : 0
TIME : 6.000e+01
FREQ : 0.000e+00

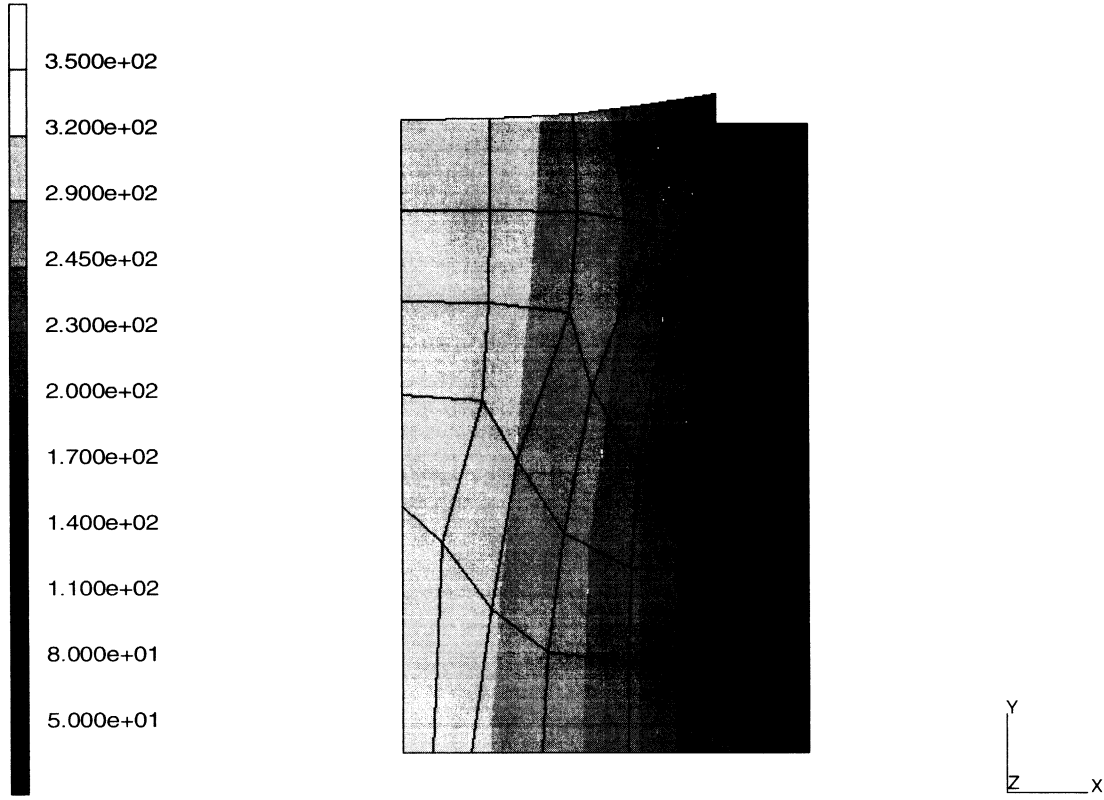


compression of block
Equivalent von Mises Stress

Figure 8.7-8 Equivalent Stress, Increment 60



INC : 60
SUB : 0
TIME : 6.000e+01
FREQ : 0.000e+00

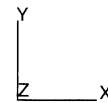
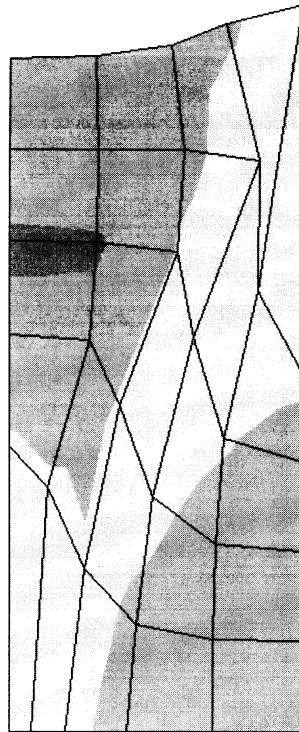
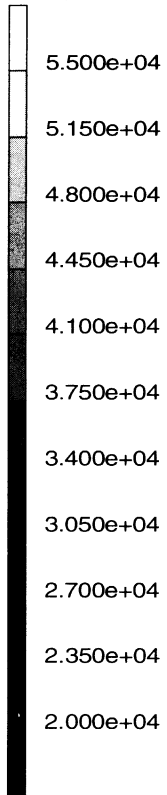


compression of block
Temperature

Figure 8.7-9 Temperature, Increment 60



INC : 70
SUB : 0
TIME : 7.000e+01
FREQ : 0.000e+00

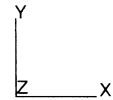
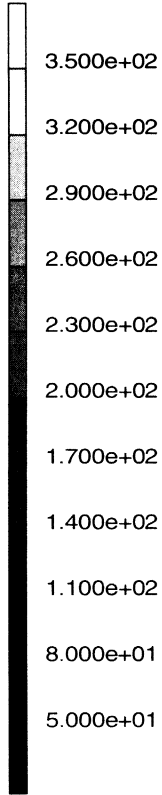


compression of block
Equivalent von Mises Stress

Figure 8.7-10 Equivalent Stress, Increment 70



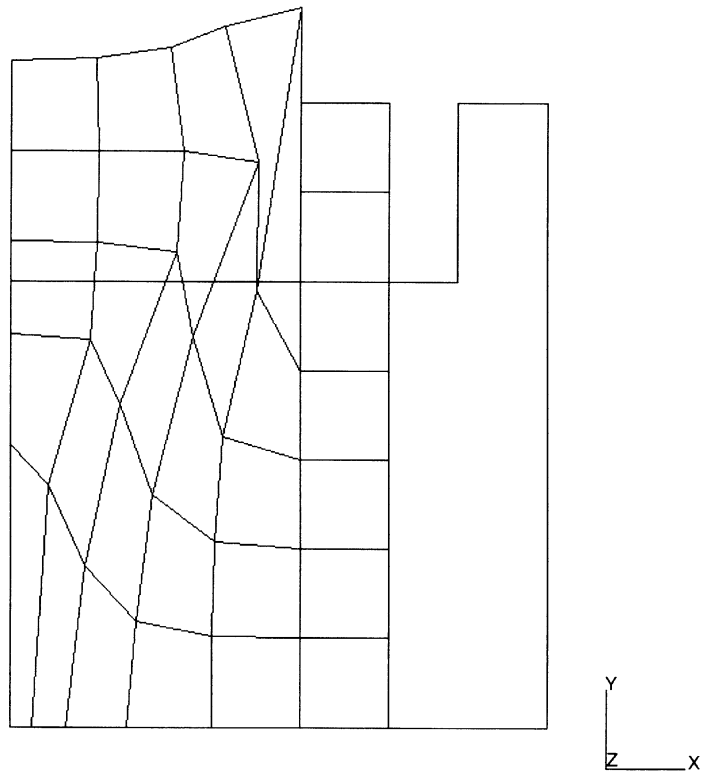
INC : 70
SUB : 0
TIME : 7.000e+01
FREQ : 0.000e+00



compression of block
Temperature

Figure 8.7-11 Temperature, Increment 70

INC : 70
SUB : 0
TIME : 7.000e+01
FREQ : 0.000e+00



compression of block
Displacements x

Figure 8.7-12 Total Displacement, Increment 70



8.8 Simply-supported Thick Plate under Uniform Pressure with Anisotropic Properties

A thick plate, simply-supported around its perimeter, is analyzed with a pressure load normal to the plate surface. This problem demonstrates the use of various options for the input of anisotropic properties.

Element

Element type 21 is a 20-node isoparametric brick. There are three displaced degrees of freedom at each node; eight are corner nodes, 12 midside. Each edge of the brick can be parabolic; a curve is fitted through the midside node. Numerical integration is accomplished with 27 points using Gaussian quadrature. See *MARC Volume B: Element Library* for further details.

Model

Taking advantage of symmetry, only one-quarter of the plate is modeled. One element is used through the thickness; two in each direction in the plane of the plate. There are 51 nodes for a total of 153 degrees of freedom. See Figure 8.8-1.

Anisotropic Properties

Material properties in this problem are assumed to be anisotropic. The Young's moduli, Poisson's ratios, and shear moduli are:

$$\begin{aligned} E_x &= 30 \times 10^6, & E_y &= 20 \times 10^6, & E_z &= 10 \times 10^6 \\ \nu_{xy} &= 0.3, & \nu_{yz} &= 0.25, & \nu_{zx} &= 0.2 \\ G_{xy} &= 10 \times 10^6, & G_{yz} &= 5 \times 10^6, & G_{zx} &= 1 \times 10^6 \end{aligned}$$

The preferred directions of the material are aligned with the global x-, y-, z-axes, which are also the basis for the continuum element. Three input options are demonstrated in this example for the input of anisotropic properties. These options are: model definition block ORTHOTROPIC, user subroutine HOOKLW, and user subroutine ANELAS.

ORTHOTROPIC (Model Definition Block)

The anisotropic material properties can be directly entered through the model definition block ORTHOTROPIC. As shown in the input list e8.8A, this data block consists of seven lines. The keyword ORTHOTROPIC is on line series 1; the number of data sets is 1 on line series 2. On line series 3, the material identification number is entered as 1; on line series 4, 5, 6, the anisotropic properties (E_x , E_y , etc.) are sequentially entered. Finally, an element list (1 to 4) is entered on line series 7. In this example, the ORTHOTROPIC model definition block is used for entering the material data. The ORTHOTROPIC block can also be used for entering isotropic properties.



In such a case, the material constants must be set to the same constant:

$$E_x = E_y = E_z; \quad \nu_{xy} = \nu_{yz} = \nu_{zx}, \text{ etc.}$$

HOOKLW (User Subroutine)

The user subroutine HOOKLW allows for the input of stress-strain relation [B] at each integration point of an element. For MARC element 21 (20-node brick) used in this problem, the strain-stress relation [B]⁻¹ is expressed as:

$$\begin{Bmatrix} \epsilon_{xx} \\ \epsilon_{yy} \\ \epsilon_{zz} \\ \gamma_{xy} \\ \gamma_{yz} \\ \gamma_{zx} \end{Bmatrix} = \begin{bmatrix} 1/E_{xx} & -\nu_{yx}/E_{yy} & -\nu_{zx}/E_{zz} & 0 & 0 & 0 \\ -\nu_{xy}/E_{xx} & 1/E_{yy} & -\nu_{zy}/E_{zz} & 0 & 0 & 0 \\ -\nu_{xz}/E_{xx} & -\nu_{yz}/E_{yy} & 1/E_{zz} & 0 & 0 & 0 \\ 0 & 0 & 0 & 1/G_{xy} & 0 & 0 \\ 0 & 0 & 0 & 0 & 1/G_{yz} & 0 \\ 0 & 0 & 0 & 0 & 0 & 1/G_{zx} \end{bmatrix} \begin{Bmatrix} \sigma_{xx} \\ \sigma_{yy} \\ \sigma_{zz} \\ \sigma_{xy} \\ \sigma_{yz} \\ \sigma_{zx} \end{Bmatrix}$$

or $\{\epsilon\} = [B]^{-1} \{\sigma\}$.

As shown in the subroutine list HOOKLW, the matrix [B]⁻¹ is first evaluated directly from the anisotropic material data (E_x, E_y, E_z, ν_{xy}, ν_{yz}, ν_{zx}, G_{xy}, G_{yz}, and G_{zx}) and a MARC matrix inversion subroutine INVERT is called to invert the strain-stress matrix [B]⁻¹. The stress-strain matrix [B] is returned to MARC for the evaluation of element stiffness matrix. In order to activate the user subroutine HOOKLW, the model definition block ORTHOTROPIC must be used to indicate anisotropic material behavior as well as the use of HOOKLW user subroutine.

ANELAS (User Subroutine)

The user subroutine ANELAS allows for the input of anisotropy-to-isotropy ratios in the stress-strain relation at an integration point of an element. For MARC element 21 (20-node brick) used in this problem, the isotropic strain-stress relation is expressed as:

$$\begin{Bmatrix} \epsilon_{xx} \\ \epsilon_{yy} \\ \epsilon_{zz} \\ \gamma_{xy} \\ \gamma_{yz} \\ \gamma_{zx} \end{Bmatrix} = \begin{bmatrix} 1/E & -\nu/E & -\nu/E & 0 & 0 & 0 \\ -\nu/E & 1/E & -\nu/E & 0 & 0 & 0 \\ -\nu/E & -\nu/E & 1/E & 0 & 0 & 0 \\ 0 & 0 & 0 & 1/G & 0 & 0 \\ 0 & 0 & 0 & 0 & 1/G & 0 \\ 0 & 0 & 0 & 0 & 0 & 1/G \end{bmatrix} \begin{Bmatrix} \sigma_{xx} \\ \sigma_{yy} \\ \sigma_{zz} \\ \sigma_{xy} \\ \sigma_{yz} \\ \sigma_{zx} \end{Bmatrix}$$



or $\{\epsilon\} = [E]^{-1} \{\sigma\}$

and for anisotropic material as:

$$\begin{Bmatrix} \epsilon_{xx} \\ \epsilon_{yy} \\ \epsilon_{zz} \\ \gamma_{xy} \\ \gamma_{yz} \\ \gamma_{zx} \end{Bmatrix} = \begin{bmatrix} 1/E_{xx} & -\nu_{yx}/E_{yy} & -\nu_{zx}/E_{zz} & 0 & 0 & 0 \\ -\nu_{xy}/E_{xx} & 1/E_{yy} & -\nu_{zy}/E_{zz} & 0 & 0 & 0 \\ -\nu_{xz}/E_{xx} & -\nu_{yz}/E_{yy} & 1/E_{zz} & 0 & 0 & 0 \\ 0 & 0 & 0 & 1/G_{xy} & 0 & 0 \\ 0 & 0 & 0 & 0 & 1/G_{yz} & 0 \\ 0 & 0 & 0 & 0 & 0 & 1/G_{zx} \end{bmatrix} \begin{Bmatrix} \sigma_{xx} \\ \sigma_{yy} \\ \sigma_{zz} \\ \sigma_{xy} \\ \sigma_{yz} \\ \sigma_{zx} \end{Bmatrix}$$

or $\{\epsilon\} = [B]^{-1} \{\sigma\}$.

As shown in the subroutine list ANELAS, the matrices $[E]^{-1}$ and $[B]^{-1}$ are first evaluated from the isotropic material data (E and ν) and anisotropic material data ($E_x, E_y, E_z, \nu_{xy}, \nu_{yz}, \nu_{zx}, G_{xy}, G_{yz},$ and G_{zx}). Then, the MARC matrix inversion subroutine INVERT is called to obtain the stress-strain relations $[E]$ and $[B]$ for isotropic and anisotropic properties, respectively. The anisotropy-to-isotropy ratios to be defined in the subroutine ANELAS are:

```
DRATS(I,J) = B(I,J)/E(I,J)
I,J = 1,...,3
DRATS(L,L) = B(L,L)/E(L,L)
L = 4,...,6
```

In order to activate the user subroutine ANELAS, the model definition block ORTHOTROPIC must be used to indicate anisotropic material behavior. In addition, the isotropic properties $[E_x = E_y = E_z = E; \nu_{xy} = \nu_{yz} = \nu_{zx} = \nu; G_{xy} = G_{yz} = G_{zx} = E/2(1+\nu)]$ must also be entered through ORTHOTROPIC block.

Geometry

No geometry specification is used.

Loading

A uniform pressure of 1.00 psi is applied in the DIST LOADS block. Load type 4 is specified for uniform pressure on the 6-5-8-7 face of all four elements.

Boundary Conditions

On the symmetry planes, $x = 30$ and $y = 30$, in-plane movement is constrained. On the $x = 30$ plane, $u = 0$, and on the $y = 30$ plane, $v = 0$. On the plate edges, $x = 0$ and $y = 0$; the plate is simply supported, $w = 0$.



Results

A contour plot of the equivalent stress for all four elements is shown in Figure 8.8-3. A comparison of the contours (Figure 8.8-3 and Figure 8.8-3) between isotropic and anisotropic behavior clearly shows the effect of anisotropy on stress distributions.

Parameters, Options, and Subroutines Summary

Example e8x8a.dat:

Parameters	Model Definition Options
ELEMENT	CONNECTIVITY
END	COORDINATE
SIZING	DIST LOADS
TITLE	END OPTION
	FIXED DISP
	ORTHOTROPIC

Example e8x8b.dat:

Parameters	Model Definition Options
ELEMENT	CONNECTIVITY
END	COORDINATE
SIZING	DIST LOADS
TITLE	END OPTION
	FIXED DISP
	ORTHOTROPIC

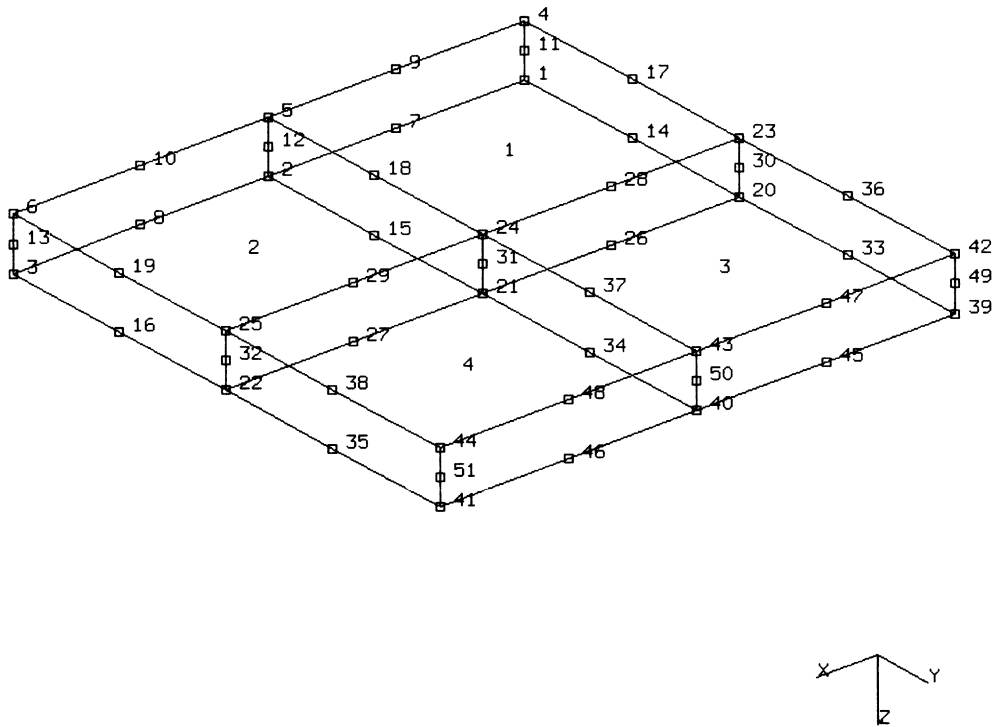
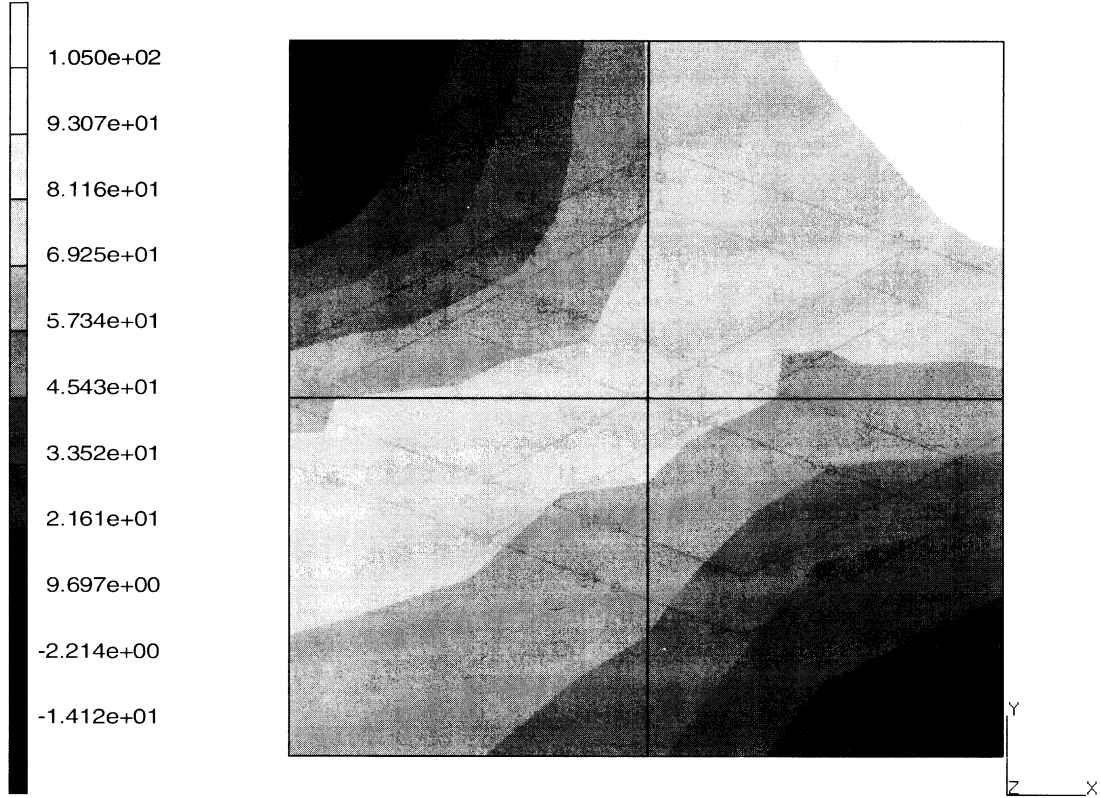


Figure 8.8-1 Thick Plate Mesh



INC : 0
SUB : 0
TIME : 0.000e+00
FREQ : 0.000e+00

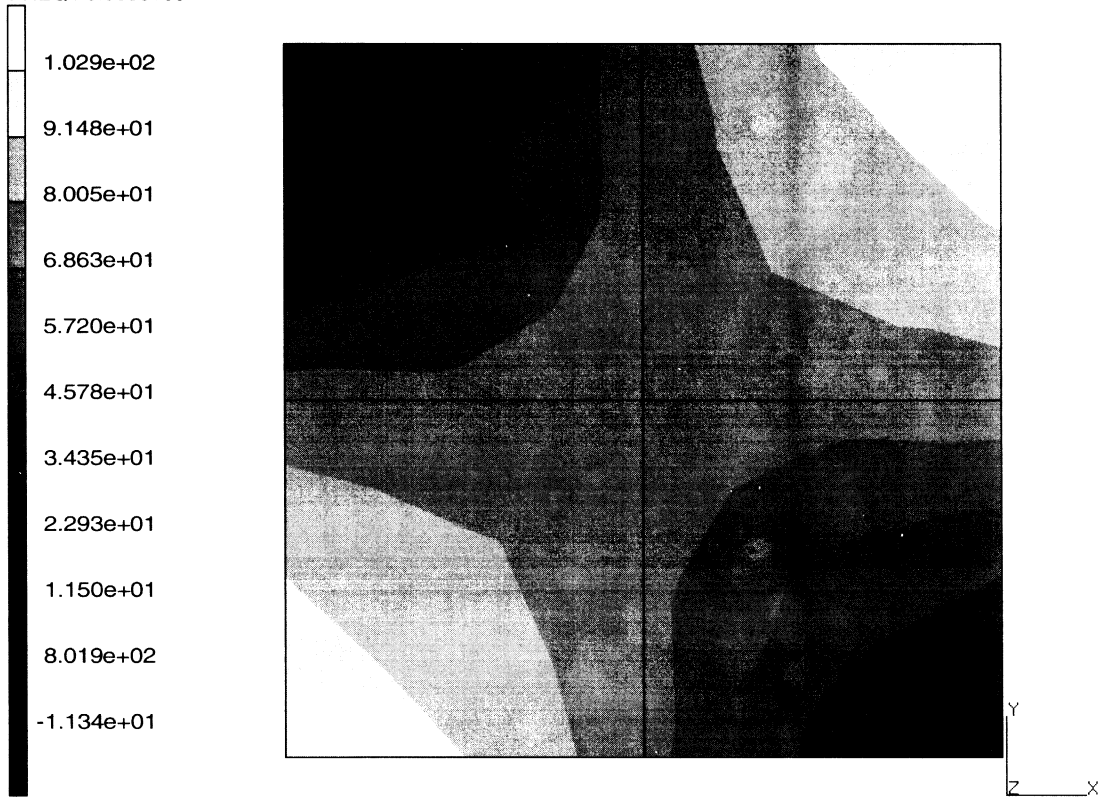


prob e8.8a elastic analysis – elmt 21
Equivalent von Mises Stress

Figure 8.8-2 Anisotropic Behavior Stress Contours



INC : 0
SUB : 0
TIME : 0.000e+00
FREQ : 0.000e+00



prob e8.8b elastic analysis – elmt 21
Equivalent von Mises Stress

Figure 8.8-3 Isotropic Behavior Stress Contours



8 Advanced Topics

Simply-supported Thick Plate under Uniform Pressure with Anisotropic Properties



8.9 Failure Criteria Calculation for Plane Stress Orthotropic Sheet

This problem illustrates the use of the FAIL DATA model definition block to supply data used by MARC to calculate failure criteria based on the current state of stress in a material. In this problem, an orthotropic square plate is subjected to a biaxial state of stress. The resulting program calculated failure criteria is compared with a textbook solution of this problem.

Element

Element type 3, a two-dimensional plane stress quadrilateral is used to model the square plate. This element is a 4-node isoparametric arbitrary quadrilateral element with two translational (u,v) degrees-of-freedom at each node. See *MARC Volume B: Element Library* for a detailed discussion of this element.

Model

As shown in Figure 8.9-1, a square plate of $4 \times 4 \text{ m}^2$ is subjected to a biaxial state of stress. The applied stresses are: $\sigma_x = -3.5 \times 10^6 \text{ N/m}^2$; $\sigma_y = +7.0 \times 10^6 \text{ N/m}^2$; and $\tau_{xy} = -1.4 \times 10^6 \text{ N/m}^2$. The plate is assumed to be made of an orthotropic material with a preferred direction (LOCAL 1-DIRECTION) of 60 degrees from the global x-axis. Sixteen elements are used to model this plate. Both the element and the nodal numbers are purposely set to be nonconsecutive. For the purpose of preventing rigid body motion, roller and hinge supports are prescribed at one side of the plate. Set names are used for boundary nodes as well as elements in the mesh.

Orthotropic

The orthotropic material properties of the plate are:

$$E_{11} = 14.0E9, \quad E_{22} = E_{33} = 3.5E9$$

$$\nu_{12} = 0.4 \quad \nu_{23} = \nu_{31} = 0.0$$

$$G_{12} = G_{23} = G_{31} = 4.2E9$$

Orientation

The preferred material direction (LOCAL 1-DIRECTION) of 60 degrees from the global x-axis, is entered through the PGLOBAL X option.

Fail Data

Five program calculated failure criteria provided in MARC are as follows:

1. maximum stress
2. maximum strain



3. Hill
4. Tsai-Wu
5. Hoffman

A user-defined criterion is also available through user subroutine UFAIL. The five preprogrammed criteria are valid only for states of plane stress, while user subroutine UFAIL can be used for a general 3D state of stress using the FAIL DATA block. You specify on a material basis your failure data. Up to three failure criteria can be calculated per material. Failure criterion output appears along with other element output. The failure data is given in the material principal coordinate system. These are the preferred coordinates in MARC and are specified by the ORIENTATION block.

Both the maximum stress (MX STRESS) and the Hill (HILL) failure criteria are requested in this analysis. The maximum stresses used for this criteria are:

MAX. X-TENSILE STRESS = 250.0E6

MAX. ABSOLUTE X-COMPRESSIVE STRESS = 0

MAX. Y-TENSILE STRESS = 0.5E6

MAX. ABSOLUTE Y-COMPRESSIVE STRESS = 10.0E6

MAX. ABSOLUTE SHEAR STRESS = 8.0E6

For Hill's criterion, a default failure index of 1.0 is used.

Fixed Disp

Roller supports ($u = 0$) are prescribed at nodes 2, 3, 4, 5 (LEFT EXCEPT 1); hinge ($u = v = 0$) support is prescribed at node 1, for the prevention of rigid body motion.

Point Load

Both the direct (σ_x, σ_y) and shear (τ_{xy}) stresses are represented by point loads acted at boundary nodal points. A distribution of the points loads is shown in Figure 8.9-2.

Nodal Thickness

In this problem, the plate thickness is specified in the NODAL THICKNESS block. A thickness of 1.0 is assumed for all nodal points in the mesh.

Results

In the reference, a solution to this problem is given. These results along with MARC output is summarized in Table 8.9-1. The comparison is favorable.



Table 8.9-1 Comparison of Results

Criterion	Reference	MARC
Max σ_2	1.26%*	1.3%
Max σ_2	68.0%	67.5%
Max τ_{12}	65.6%	65.6%
Hill	89.0%	88.6%

Note: * = 100% means failure occurs

References

Argarwal, B.D., and Broutman, L.J., *Analysis and Performance of Fiber Composites*, Wiley, 1980.

Parameters, Options, and Subroutines Summary

Example e8x9.dat:

Parameters

ELEMENT
END
SIZING
TITLE

Model Definition Options

CONNECTIVITY
COORDINATE
DEFINE
END OPTION
FAIL DATA
FIXED DISP
NODAL THICKNESS
ORIENTATION
ORTHOTROPIC
POINT LOAD
POST
PRINT ELEM

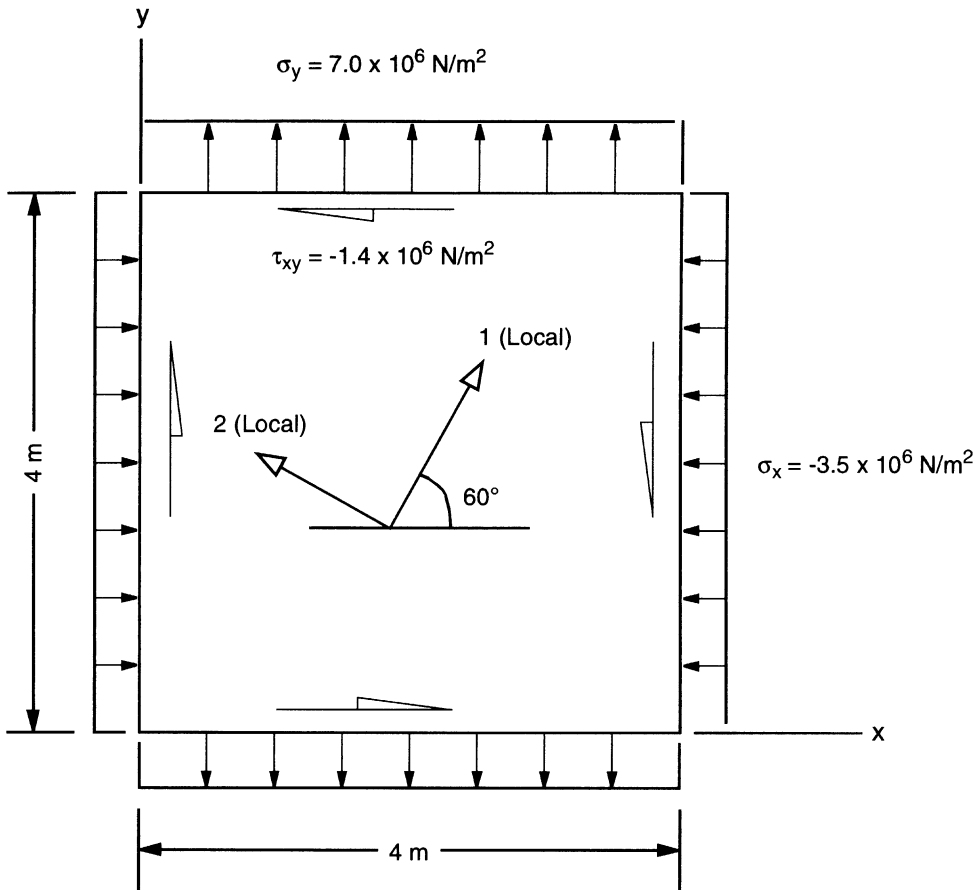


Figure 8.9-1 Orthotropic Square Plate

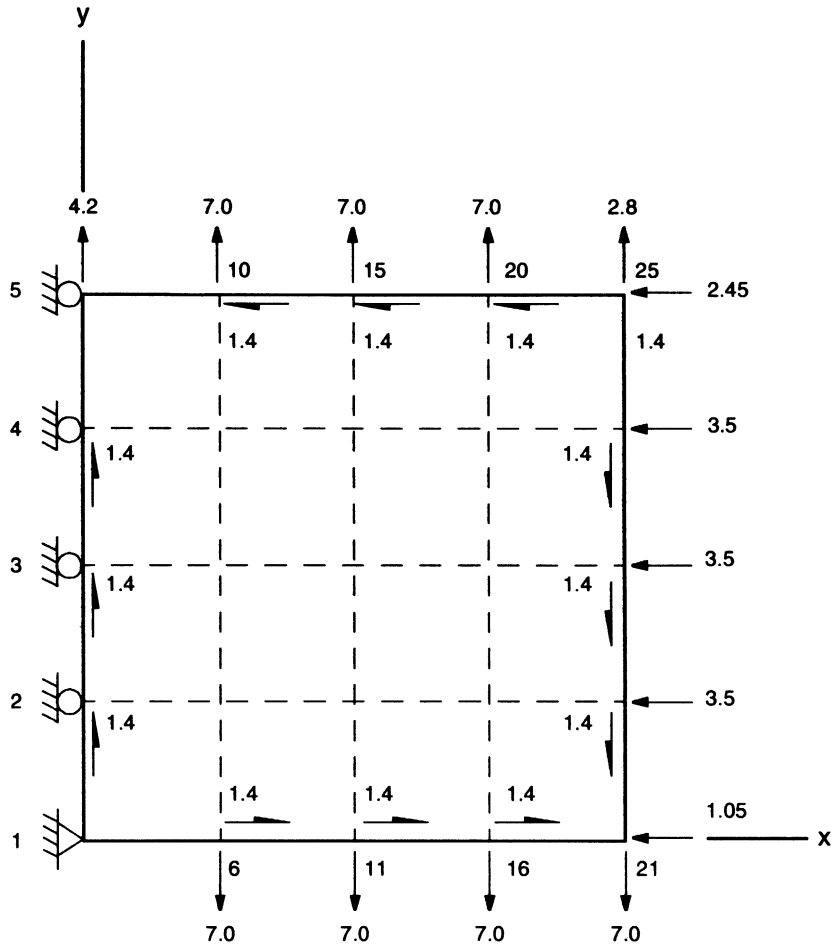


Figure 8.9-2 Point Load ($\times 10^6$) and Support



8 *Advanced Topics*

Failure Criteria Calculation for Plane Stress Orthotropic Sheet



8.10 Beam Element 52 with Nonlinear Elastic Stress-Strain Relation

As described in *MARC Volume B: Element Library*, the beam element 52 can be used for nonlinear elastic material. This problem demonstrates the use of model definition option HYPOELASTIC and user subroutine UBEAM for the nonlinear elastic behavior of a cantilever beam, modeled by element type 52, subjected to prescribed tip displacements.

Element

Element type 52 is a straight, Euler-Bernoulli beam in space with three translations and three rotations as degrees of freedom at each node of the element. The element is defined by nodal coordinates in global coordinate system and by section properties such as area, bending stiffnesses, as well as torsional stiffness. See *MARC Volume B: Element Library* for further detail.

Model

As shown in Figure 8.10-1, the cantilever beam is modeled by five beam elements with a fixed end at node 1, and prescribed displacements at node 6. The section and material properties are entered through GEOMETRY and HYPOELASTIC options; however, the user subroutine UBEAM is used for the description of nonlinear elastic stress-strain relation of the beam. The stress-strain relation is assumed to be dependent on strain quantities.

Geometry

A beam with a square cross section of length 0.2 inch is modeled. The area of the beam section is 0.04 in.² and moments of inertia are $I_x = I_y = 0.000133333$ in.⁴.

HYPOELASTIC

The HYPOELASTIC model definition option is used to indicate that all of the elements use this formulation. User subroutine UBEAM defines the material behavior.

The initial Young's modulus is 1,000,000 psi and the Poisson's ratio is 0.2, which are given in the user subroutine.

FIXED DISP and DISP CHANGE

All degrees of freedom at node 1 are fixed for the simulation of a fixed-end condition. A 0.2 incremental displacement is prescribed at node 6, for degrees of freedom 1, 4, 5, and 6 (axial displacement and rotations). The same incremental displacements are repeated for increments 1 through 3, using DISP CHANGE history definition option.



Nonlinear Stress-Strain Relation (User Subroutine UBEAM)

The generalized stress-generalized strain relation for element 52 can be expressed as follows:

$$\begin{Bmatrix} F \\ M_x \\ M_y \\ T \end{Bmatrix} \begin{bmatrix} D_{11} & & & \\ & D_{22} & & \\ & & D_{33} & \\ & & & D_{44} \end{bmatrix} \begin{Bmatrix} \epsilon \\ K_x \\ K_y \\ \theta \end{Bmatrix} \tag{EQ 1}$$

where F , M_x , M_y , and T are axial force, bending and twist moments (generalized stress components); ϵ , K_x , K_y , and θ are axial stretch, curvatures and twist (generalized strain components), respectively.

For the purpose of demonstration, the terms D_{11} , D_{22} , D_{33} , and D_{44} in the stress-strain matrix are assumed to have the following dependence on strains:

$$\begin{aligned} D_{11} &= (EA)\text{EXP}(-C|\epsilon|) \\ D_{22} &= (EA)\text{EXP}(-C|K_x|) \\ D_{33} &= (EA)\text{EXP}(-C|K_y|) \\ D_{44} &= (EA)\text{EXP}(-C|\theta|) \end{aligned} \tag{EQ 2}$$

In EQ 2, E is the Young's modulus, A is the area, I_x , I_y are moments of inertia; $G = E/2(1+\nu)$ and $J = (I_x + I_y)$. The constant C is assumed to be 13.8.

The incremental generalized stress-generalized strain relation $D(I,I)$, the incremental generalized stress $DF(I)$, and the total generalized stress at the end of increment $GS(I)$, $I = 1, \dots, 4$, are respectively computed in the subroutine and returned to MARC for further computations.

Results

Table 8.10-1 shows a comparison of MARC results with analytical solution computed from equations (EQ 1) and (EQ 2). The comparison is excellent.

**Table 8.10-1** Comparison of MARC Results vs. Analytical

Tip Displacements (in.)	F (lb.)		M _x (in-lb.)		M _y (in-lb.)		T (in-lb.)	
	MARC	Analytical	MARC	Analytical	MARC	Analytical	MARC	Analytical
0.2	9.21275E2	9.2127E2	3.07901E0	3.0709E0	3.07091E0	3.0709E0	2.55909E0	2.5591E0
0.4	1.06093E3	1.0609E2	3.53644E0	3.5364E0	3.53644E0	3.5364E0	2.94703E0	2.9470E0
0.6	9.16324E2	9.1632E2	3.05442E0	3.0544E0	3.05458E0	3.0544E0	2.54533E0	2.5453E0
0.8	7.03489E2	7.0349E2	2.34496E0	2.3450E0	2.34494E0	2.3450E0	1.95413E0	1.9541E0

Parameters, Options, and Subroutines Summary

Example e8x10.dat:

ParametersELEMENT
END
SIZING
TITLE**Model Definition Options**CONNECTIVITY
CONTROL
COORDINATE
END OPTION
FIXED DISP
GEOMETRY
HYPOELASTIC**History Definition Options**CONTINUE
DISP CHANGE

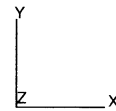
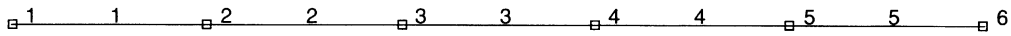


Figure 8.10-1 Cantilever Beam with Prescribed Tip Displacement



8.11 Element Deactivation/Activation and Error Estimate in the Analysis of a Plate with Hole

The problem of a plate with hole subjected to an in-plane tensile force (problem 2.9) is analyzed with the options DEACTIVATE, ACTIVATE, and ERROR ESTIMATE. These options allow for the deactivation or activation of elements during the analysis, and the estimation of errors on stress continuity and geometric measures (aspect and skew ratios).

During analysis, after the elements are deactivated, they retain the stress state in effect at the time of deactivation. At a later stage in the analysis, the elements can again be activated with the ACTIVATE history definition option. Elements which were deactivated before analysis have zero internal stress upon activation. Elements which were used earlier and deactivated during analysis have an internal stress which is equal to the state when they were deactivated.

The ERROR ESTIMATE option provides information regarding the error associated with the finite element discretization. There are two measures. The first evaluates the stress discontinuity between elements. A large value implies that the stresses gradients are not accurately represented in the finite element mesh.

The second error measure examines geometric distortion in the model. It first examines the aspect ratios and warpage of the elements and, in subsequent increments, measures how much these ratios change. This measure can be used to indicate the adequacy of the original mesh.

Element

Element type 26 is a second-order, isoparametric two-dimensional element for plane stress. There are eight nodes with two degrees of freedom at each node.

Model

The example uses a coarse mesh for demonstration purposes only. The mesh generated by MARC is shown in Figure 8.11-1.

Geometry

The plate thickness of one inch is entered in EGEOM1.

Property

Young's modulus is 30×10^6 psi, with Poisson's ratio as 0.3. These quantities are sufficient to define the material as isotropic linear-elastic.

Loading

To simulate a tension acting at infinity, a negative 1-psi load is applied to the top edge of the mesh.

**FIXED DISP**

The boundary conditions are determined by symmetry considerations. No displacement is permitted on the axis of symmetry perpendicular to the applied force direction. On the axis of symmetry parallel to the force direction, only parallel displacements are permitted.

Optimize

The Cuthill-McKee algorithm is chosen in this example. Ten iterations are sufficient to obtain a reasonably optimal bandwidth.

Error Estimates

Both the stress continuity and geometry measures are requested by inputting 1, 1, on the second card of this data block.

DEACTIVATE/ACTIVATE

After END OPTION, two DEACTIVATE increments and one ACTIVATE increment are provided for the deactivation of elements 7, 8, 17, 18 at the first increment; elements 9, 10, 19, 20 at the second increment; and the activation of all eight elements at the third increment.

Results

Table 8.11-1 shows σ_{yy} at element 8, integration point 6 and element 10, integration point 6, at increments 0 through 3. The effects of deactivation/activation of elements are clearly demonstrated. In addition, the stress discontinuity and geometry measures at increment 0 (ERROR ESTIMATE option) are as follows:

WORST ORIGINAL ASPECT RATIO IS 3.343 AT ELEMENT 1

WORST ORIGINAL WARPAGE RATIO IS 1.957 AT ELEMENT 3

WORST CURRENT ASPECT RATIO IS 3.343 AT ELEMENT 1

WORST CURRENT WARPAGE RATIO IS 1.957 AT ELEMENT 3

LARGEST CHANGE IN ASPECT RATIO IS 1.000 AT ELEMENT 7

LARGEST CHANGE IN WARPAGE RATIO IS 1.000 AT ELEMENT 8

GENERALIZED STRESSES

LARGEST NORMALIZED STRESS JUMP IS:

0.11152E 02 AT NODE 17 COMPONENT 1 MEAN VALUE IS 0.28047E-02

LARGEST STRESS JUMP IS:

0.23227E 00 AT NODE 76 COMPONENT 2 MEAN VALUE IS 0.23237E 01



Table 8.11-1 σ_{yy} vs. Load Increment

Inc. No.	EL 8, INT 6	EL 10, INT 6
0	2.62	1.89
1	2.62 (D)	6.24
2	2.62 (D)	6.24 (D)
3	2.88 (A)	5.68 (A)

Note: (D) – element DEACTIVATED

(A) – element ACTIVATED

Parameters, Options, and Subroutines Summary

Example e8x11.dat:

Parameters

ELEMENT
END
SIZING
TITLE

Model Definition Options

CONNECTIVITY
COORDINATE
DIST LOADS
END OPTION
ERROR ESTIMATES
FIXED DISP
GEOMETRY
ISOTROPIC
PRINT NODE

History Definition Options

ACTIVATE
CONTINUE
DEACTIVATE

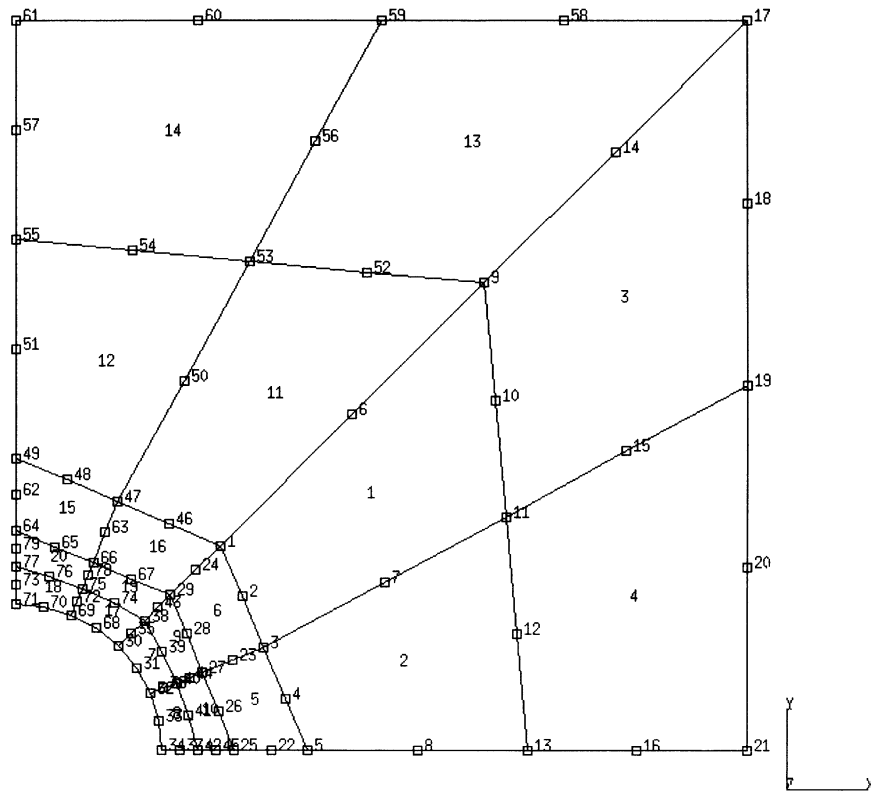


Figure 8.11-1 Mesh Layout for Plate with Hole



8.12 Forging of the Head of a Bolt

This example demonstrates the contact capability of MARC, using rigid surfaces for a simple forging analysis. An original cylindrical block is sitting in a surface with the shape of a cavity, and is deformed by another rigid surface which has the shape of the bolt head and moves at constant speed (Figure 8.12-2). The block is considered an elastic-plastic deformable material.

This problem is modeled using the six techniques summarized below.

Data Set	Element Type(s)	Number of Elements	Number of Nodes	Differentiating Features
e8x12	10	70	90	AUTO LOAD, REZONING
e8x12b	10	70	90	AUTO TIME
e8x12c	10	70	90	ADAPTIVE MESH, AUTO LOAD
e8x12d	10	70	90	AUTO STEP
e8x12e	10	70	90	F [°] FP, AUTO TIME
e8x12r	10	70	90	RESTART, REZONING

This analysis is done using three different approaches. In the first method (e8x12.dat), a fixed time step approach is used and the rezoning capability is used to improve the mesh when distortion occurs. In the second approach (e8x12b.dat), a variable time step approach is used by requesting the AUTO TIME option. In the third approach (e8x12c.dat), a fixed time step method is again used, but here the adaptive meshing capability is utilized. The restart capability is demonstrated based upon the first analysis (e8x12r.dat), which is typically used in rezoning analyses.

Parameters

The UPDATE, FINITE, and LARGE DISP options are included to trigger a finite deformation analysis for the first four analyses. Element 10, a 4-node bilinear axisymmetric element is used. The PRINT,5 block requests printed information on change in contact status of boundary nodes. In the first analysis, the SIZING parameter reserves space for 120 elements, 150 nodes, and 60 boundary conditions. The amounts are larger than the starting model which contains 70 elements and 90 nodes. This is done so that there is freedom to increase the size of the model later using the REZONING option. The REZONING parameter is included to indicate that this may be required.

In the second analysis, the same SIZING parameter is used even though rezoning is not performed. This results in an over allocation of memory, but is insignificant for this small problem.



In the third analysis, the number of elements and nodes is not specified on the SIZING parameter, but an upper bound is defined on the ADAPTIVE option. Here, the analysis initially starts with 70 elements and 90 nodes and re-allocates memory as the adaptive meshing process occurs. Two levels of refinement are allowed; so if all elements refine, the total would be 1120 which is less than the number specified on the ADAPTIVE parameter. Note that the SIZING option specifies an upper bound on the number of boundary conditions and distributed loads.

Mesh Definition

CONNECTIVITIES and COORDINATES were brought from a preprocessor. The mesh depicted in Figure 8.12-2 is quite regular over the rectangular block. Due to symmetry, only half of the cylinder needs to be modeled.

No gap elements are used in this problem, as the contact with the rigid surfaces are governed by the CONTACT option.

Geometry

A '1' is placed in the second field to indicate that the constant dilatation formulation is used for all of the analyses, except the analysis using F^cF^p . This is not necessary using the F^cF^p procedure as a mixed variational principal is automatically used.

Boundary Conditions

Symmetry displacement boundary conditions are applied to all nodes on the axis.

Material Properties

The bolt is treated as an elastic plastic material with a Young's modulus of 17,225., Poisson's ratio of 0.35, mass density of 1., and initial yield stress of 34.45. The material workhardens from the initial yield stress up to 150 at a strain of 400% according to the piecewise linear curve entered in WORK HARD DATA.

Control Options

A formatted post file is requested every twenty increments, as well a restart file. PRINT CHOICE is used to minimize the amount of output. In the third analysis, the print out is suppressed using the NO PRINT option. Convergence control is done by relative residuals, with a tolerance of 10%.

Contact

This option defines three bodies with no friction between them. The code is expected to determine by itself a contact tolerance. (See Figure 8.12-1.)

The first body is deformable and is made out of all the elements in the model.



The second body is the top rigid surface, defined by three sets of geometrical entities. It has a reference point along the axis, and is given a translational velocity of 1 parallel to the axis of symmetry. The first geometrical entity is a straight line, the second is a concave arc of a circle, and the third is another straight line. The last line was added so that the top node on the axis would not encounter the end of the rigid surface definition.

The third body is the bottom rigid surface, defined by one set of geometrical entities. It does not need a reference point and is not given any motion. The geometrical entities are three straight lines, defined by four points.

Note how the sequence of entering the geometrical data of the second and third bodies corresponds to following the profiles of such bodies in a counterclockwise direction.

Based upon information obtained in the first two analyses, a redesign of the third body was performed such that a circular fillet was placed between what was the second and third entities. This can be seen in Figure 8.12-3. The third body now consists of three entities:

First entity is a line segment with three points

Second entity is a circle using method 2 (starting point, end point, center, and radius)

Third entity is a straight line

Load Control

The first part of the analysis was performed with a fixed TIME STEP of 0.1 in a sequence of 100 increments.

As an alternative in the second input file (e8x12b), the AUTO TIME option was used to control the time step procedure. The initial time step was 0.1 second and a maximum of 150 steps were allowed to reach a total time of 10 seconds. Only 51 increments were necessary using this procedure.

In the third analysis (e8x12c), only 60 increments using a fixed TIME STEP of 0.2 were used.

In the fourth (e8x12d) and fifth (e8x12e) analyses, the AUTO STEP option is used. The period of 12 seconds was covered. The plasticity criteria was used to control the loading as shown below:

Allowable Plasticity Change	Range
1%	$0 < \epsilon^P < 1\%$
1%	$1\% < \epsilon^P < 10\%$
3%	$10\% < \epsilon^P$



Rezoning

The next increment performs a rezoning operation. A new mesh is created with a preprocessor, which covers the profile of the previously deformed mesh (Figure 8.12-4). This mesh is defined by means of CONNECTIVITY CHANGE and COORDINATE CHANGE. Both the number of elements and the number of nodes are increased. The ISOTROPIC CHANGE option is also used to extend material properties to the new elements. Similarly, the CONTACT option is repeated to account for the new element definition of the deformable body; the contact tolerance is decreased because much thinner elements were created.

One increment of deformation, with a TIME STEP of 0.05, is then executed. At this point, it is necessary to include the DISPLACEMENT CHANGE to account for the new node numbers that are located along the axis of symmetry. An extra node at the convex corner of surface 3 is fixed. This is done to allow a very coarse mesh to represent a sharp corner without cutting it.

The rest of the deformation proceeded. Twenty increments with five steps of 0.04 are completed first, followed by seventy increments of time step 0.02. The reason for decreasing the time step is that as the deformation proceeds, the height of the bolt head becomes smaller and a constant movement of the second surface would produce larger and larger strains per increment.

Adaptive

In the third problem, the adaptive meshing technique is demonstrated. Such that the first 50 elements are enriched based upon the contact criteria. That is, if nodes associated with these elements come into contact, the element is refined. A limit of two levels of refinement is prescribed.

Results

Figure 8.12-5 through Figure 8.12-7, show the contour plots of the equivalent plastic strain, the equivalent von Mises stress, and the average stress in the deformed configuration before rezoning. The block completely fills the bottom surface and is folding into the top surface. The need to rezone stems from the fact that soon there will be too few nodes in the free surface that have to fit in the narrow gap between the two rigid bodies. The rezoning method allows us to represent the material flash. Comparison of Figure 8.12-6 with the results obtained using the F^cF^p method in Figure 8.12-14 indicate a very close agreement between the von Mises stresses obtained from the two theories as expected since the elasticity is small.

Virtually all the deformation takes place in the part of the block above the bottom surface.

Figure 8.12-8 through Figure 8.12-10 show the same contour plots in the final deformed configuration. At this stage, the full shape of the head of the bolt has been acquired by the original block and flash formed in the gap between surfaces. The strains are very concentrated in the part which folded on the bottom surface. The von Mises stress shows that the bottom cavity is elastic at the end of deformation.



The progression of the deformed adaptive mesh is shown in Figure 8.12-11 through Figure 8.12-13, for increments 20, 40, and 60, respectively. You can observe that, based upon the adaptive criteria, additional elements are formed as the workpiece comes into contact with the dies. At the end of the analysis, there are 187 elements and 250 nodes. Based upon this analysis, perhaps you would perform the analysis also with an adaptive criteria based upon strain energies or plastic strains.

The printed results of an analysis with the contact option include general information about rigid surfaces, such as the updated position of the reference point, the velocity of the surface, the loads on the surface, as well as the moment with respect to the reference point.

Parameters, Options, and Subroutines Summary

Example e8x12.dat:

Parameters	Model Definition Options	History Definition Options	Rezone Options
END	CONNECTIVITY	AUTO LOAD	CONNECTIVITY CHANGE
FINITE	CONTACT	CONTINUE	CONTACT CHANGE
LARGE DISP	CONTROL	DISPLACEMENT CHANGE	CONTINUE
PRINT	COORDINATES	TIME STEP	COORDINATE CHANGE
REZONE	END OPTION		END REZONE
SIZING	FIXED DISP		ISOTROPIC CHANGE
TITLE	GEOMETRY		REZONE
UPDATE	ISOTROPIC		
	POST		
	PRINT CHOICE		
	RESTART		
	WORK HARD		



Example e8x12b.dat:

Parameters	Model Definition Options	History Definition Options
END	CONNECTIVITY	AUTO TIME
FINITE	CONTACT	CONTINUE
LARGE DISP	CONTROL	
PRINT	COORDINATES	
SIZING	END OPTION	
TITLE	FIXED DISP	
UPDATE	GEOMETRY	
	ISOTROPIC	
	POST	
	PRINT CHOICE	
	WORK HARD	

Example e8x12c.dat:

Parameters	Model Definition Options	History Definition Options
ADAPTIVE	ADAPTIVE	AUTO LOAD
END	CONNECTIVITY	CONTINUE
FINITE	CONTACT	TIME STEP
LARGE DISP	CONTROL	
PRINT	COORDINATES	
TITLE	END OPTION	
UPDATE	FIXED DISP	
	GEOMETRY	
	ISOTROPIC	
	POST	
	PRINT CHOICE	
	WORK HARD	



Example e8x12d.dat:

Parameters

END
FINITE
LARGE DISP
PRINT
TITLE
UPDATE

Model Definition Options

CONNECTIVITY
CONTACT
CONTROL
COORDINATES
END OPTION
FIXED DISP
GEOMETRY
ISOTROPIC
POST
PRINT CHOICE
WORK HARD

History Definition Options

AUTO STEP
CONTINUE

Example e8x12e.dat:

Parameters

END
PLASTICITY
PRINT
TITLE

Model Definition Options

CONNECTIVITY
CONTACT
CONTROL
COORDINATES
END OPTION
FIXED DISP
ISOTROPIC
POST
WORK HARD

History Definition Options

AUTO STEP
CONTINUE



Example e8x12r.dat:

Parameters	Model Definition Options	History Definition Options	Rezone Options
END	CONNECTIVITY	CONTINUE	CONNECTIVITY CHANGE
FINITE	CONTACT	DISP CHANGE	CONTACT CHANGE
LARGE DISP	CONTROL		CONTINUE
PRINT	COORDINATE		COORDINATE CHANGE
REZONE	END OPTION		END REZONE
TITLE	FIXED DISP		ISOTROPIC CHANGE
UPDATE	GEOMETRY		
	ISOTROPIC		
	POST		
	PRINT CHOICE		
	RESTART		
	WORK HARD		

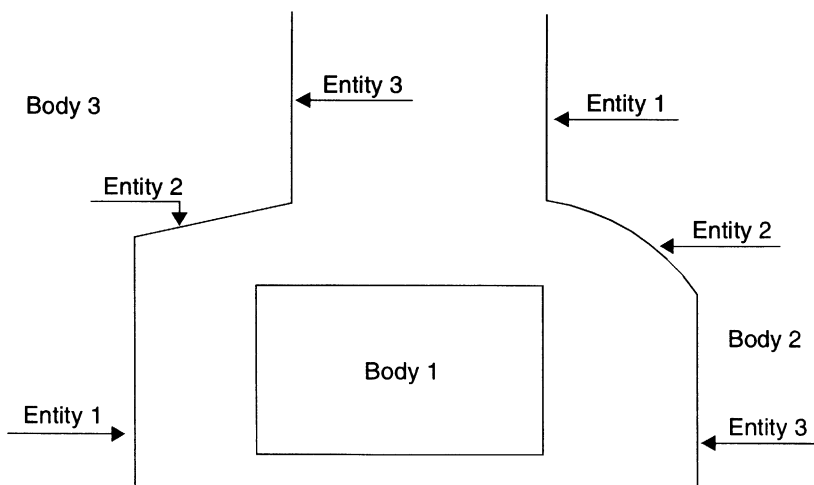


Figure 8.12-1 Model

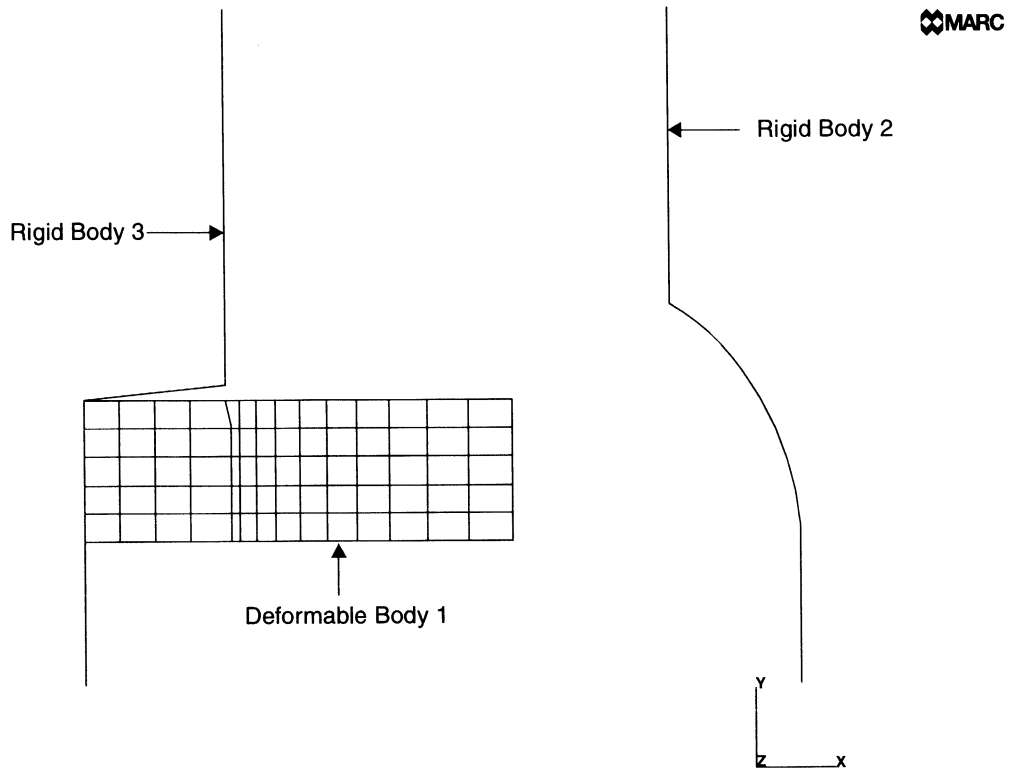


Figure 8.12-2 Initial Mesh

INC : 0
SUB : 0
TIME : 0.000e+00
FREQ : 0.000e+00

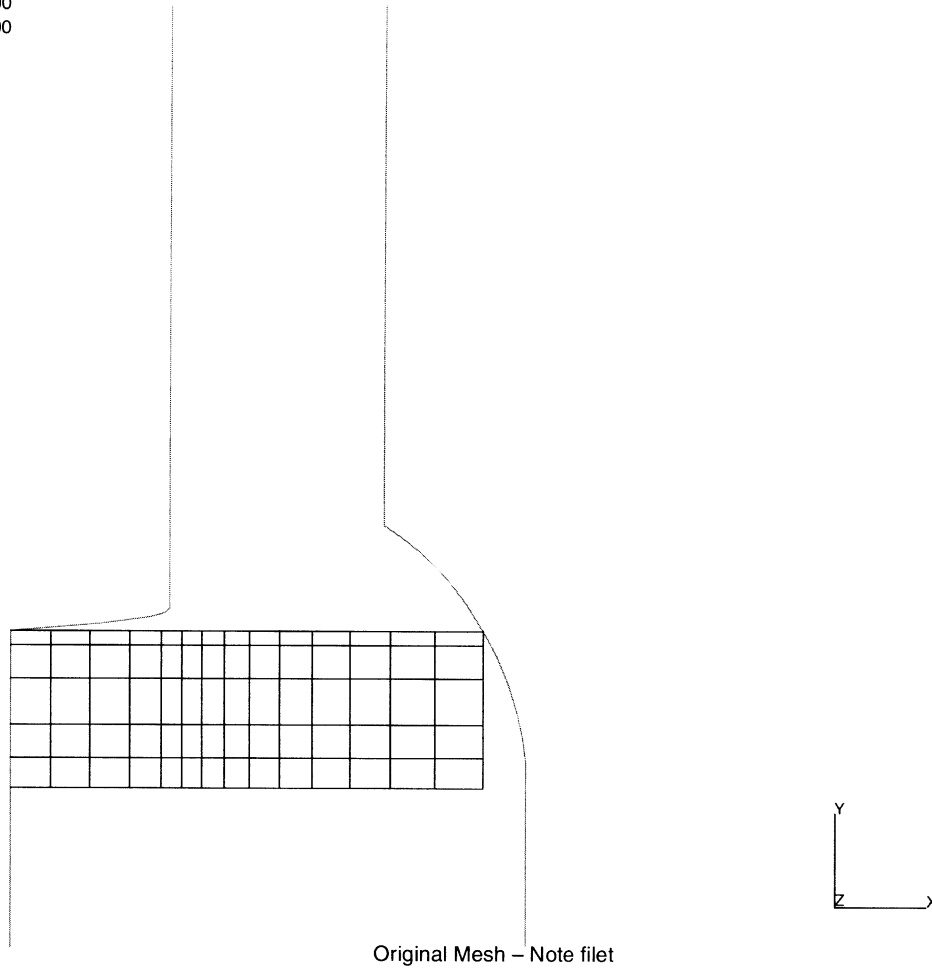


Figure 8.12-3 Initial Mesh with Modified Rigid Body 3 for Adaptive Analysis



INC : 101
SUB : 0
TIME : 2.730e+01
FREQ : 0.000e+00

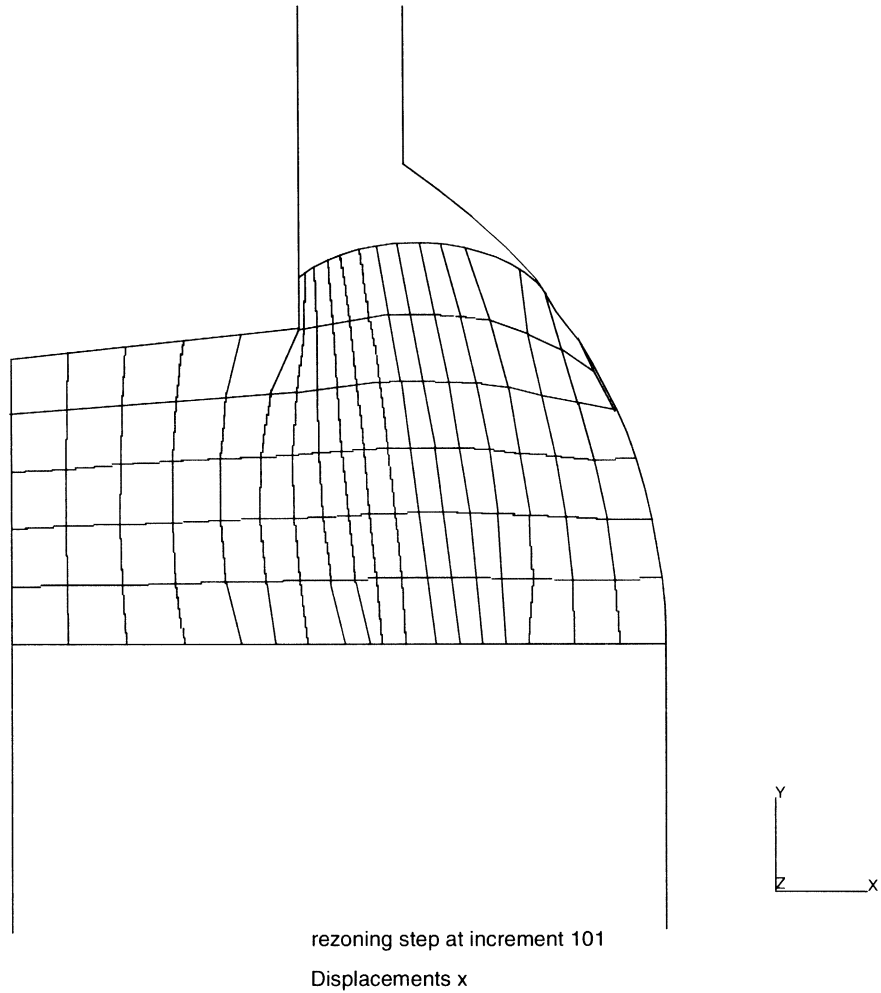


Figure 8.12-4 Rezoning Mesh

INC : 100
SUB : 0
TIME : 2.730e+01
FREQ : 0.000e+00

MARC

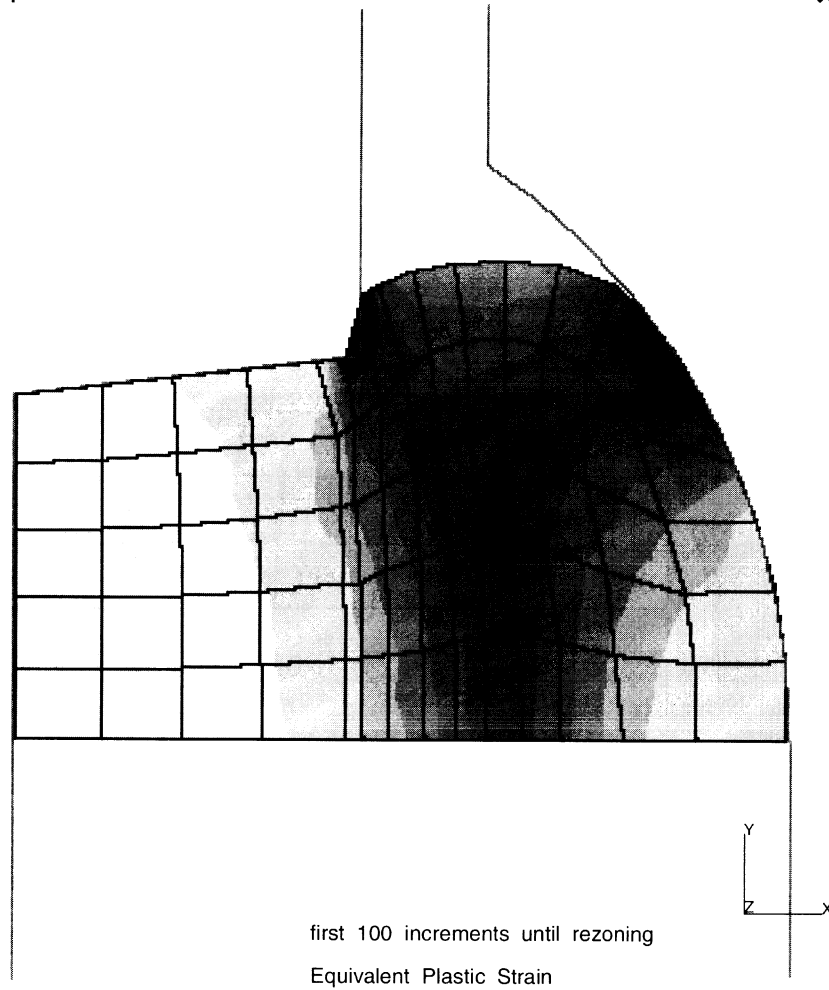
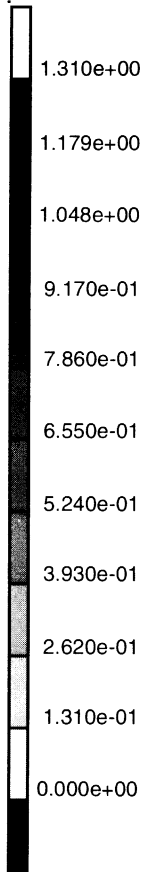


Figure 8.12-5 Equivalent Plastic Strain until Rezoning

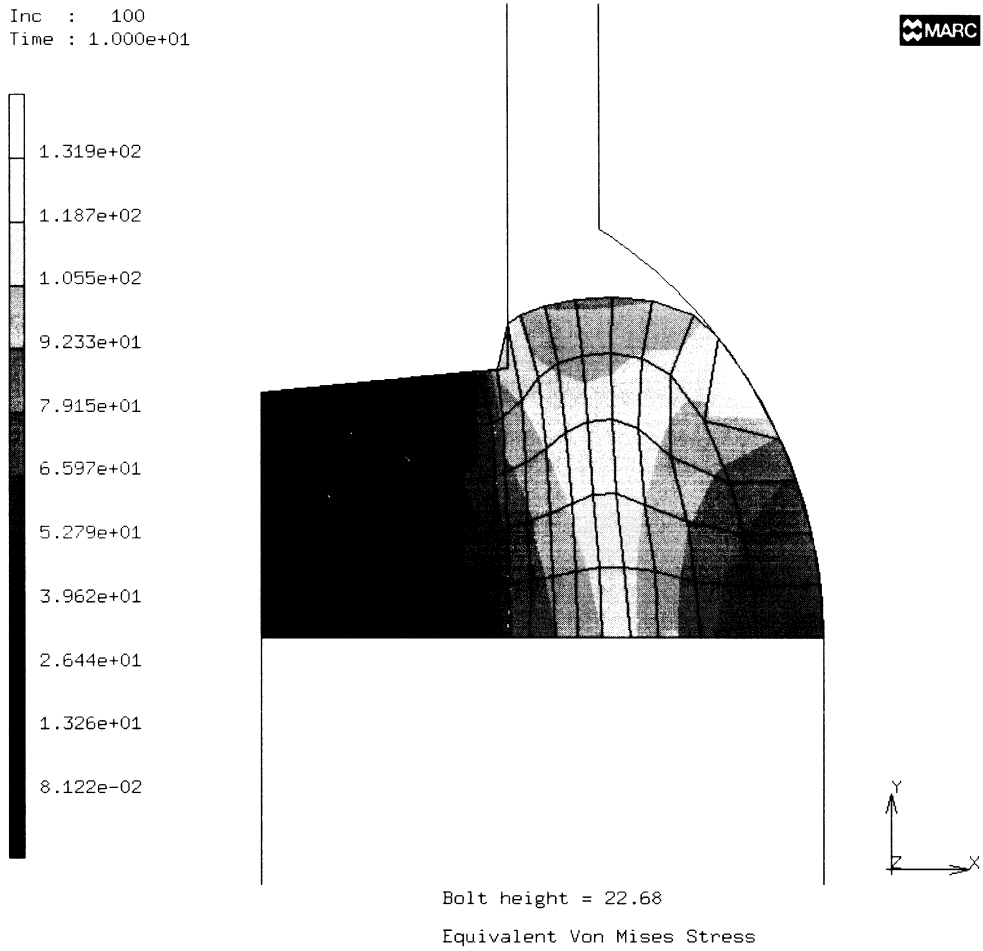


Figure 8.12-6 Equivalent Mises Tensile Stress at Bolt Height = 22.68



INC : 100
SUB : 0
TIME : 2.730e+01
FREQ : 0.000e+00

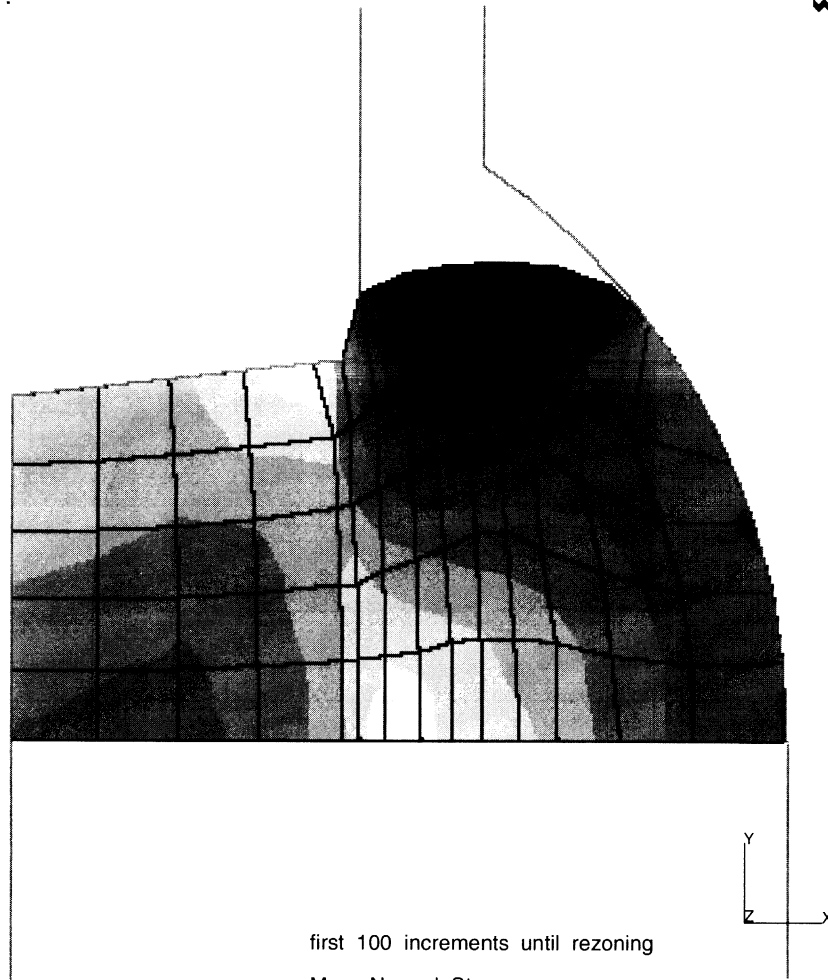
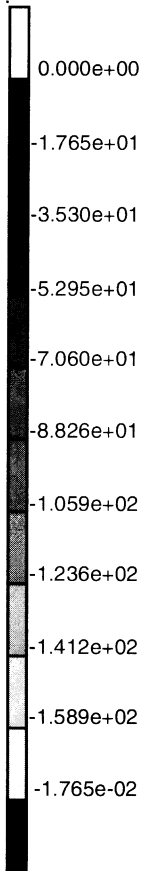


Figure 8.12-7 Mean Normal Stress Until Rezoning



INC : 180
SUB : 0
TIME : 2.931e+01
FREQ : 0.000e+00

MARC

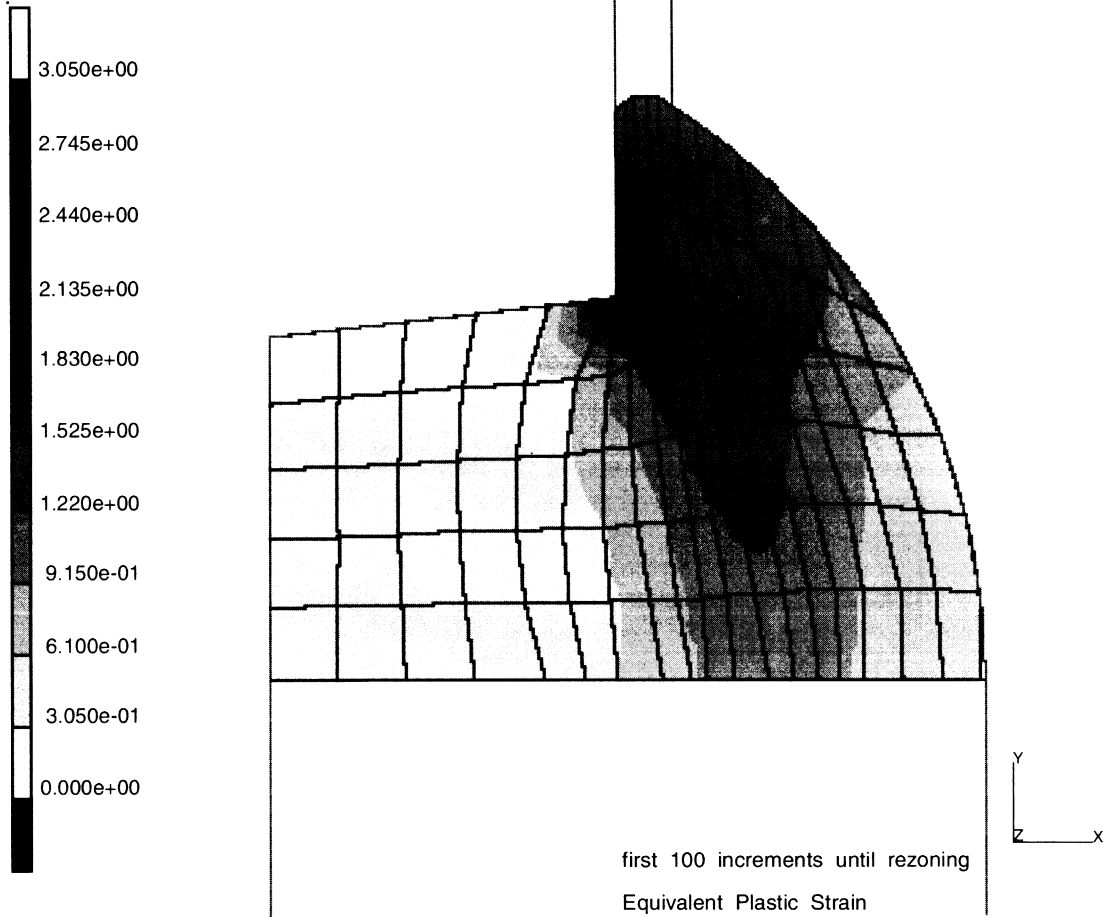


Figure 8.12-8 Final Equivalent Plastic Strain

INC : 180
SUB : 0
TIME : 2.931e+01
FREQ : 0.000e+00

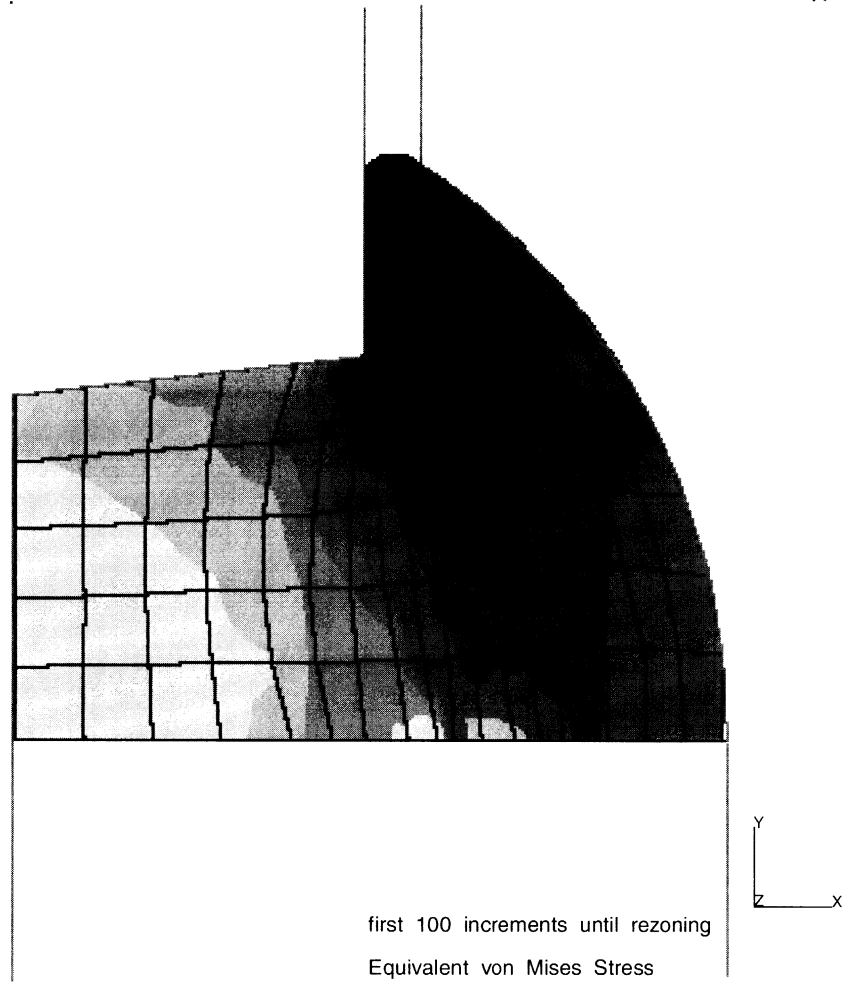
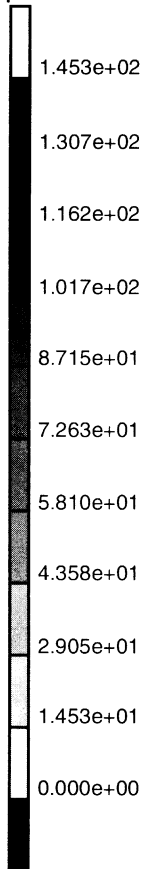


Figure 8.12-9 Final Equivalent von Mises Tensile Stress



INC : 180
SUB : 0
TIME : 2.931e+01
FREQ : 0.000e+00

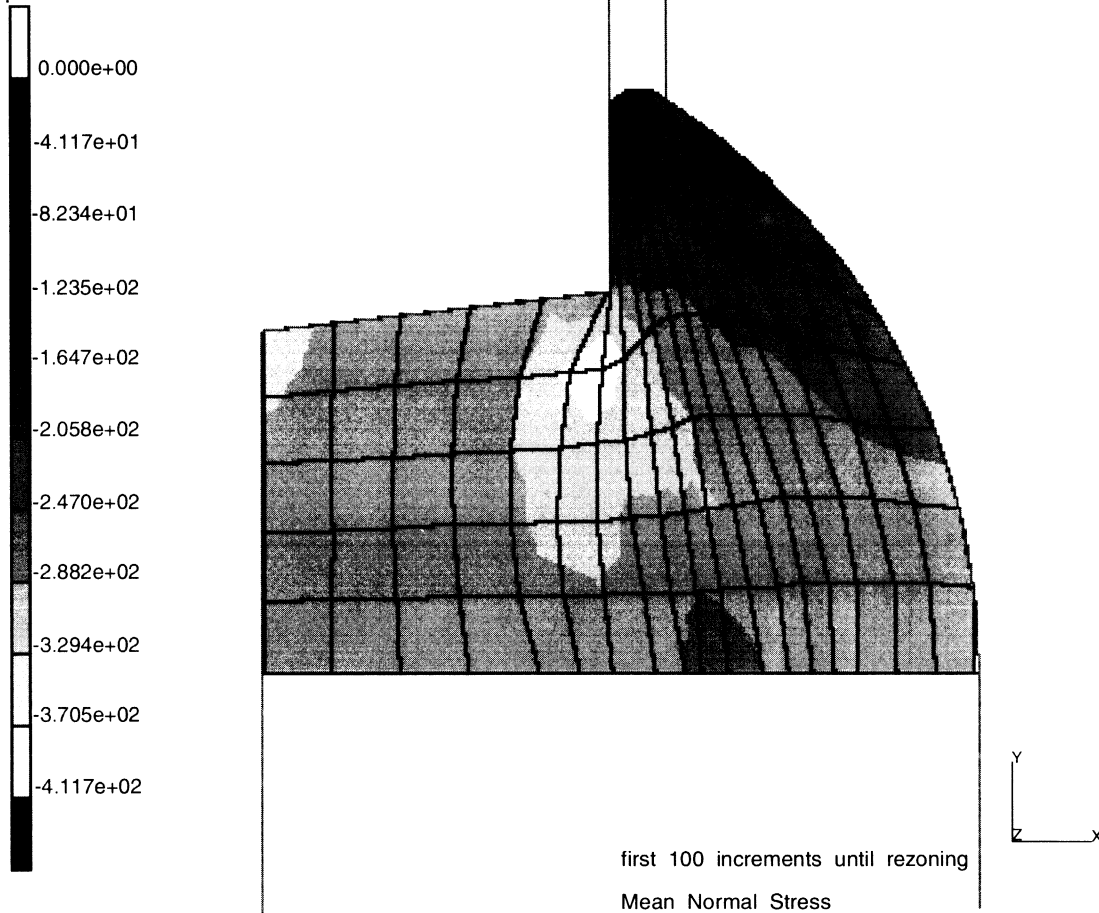


Figure 8.12-10 Final Mean Normal Stress

INC : 20
SUB : 0
TIME : 4.000e+00
FREQ : 0.000e+00

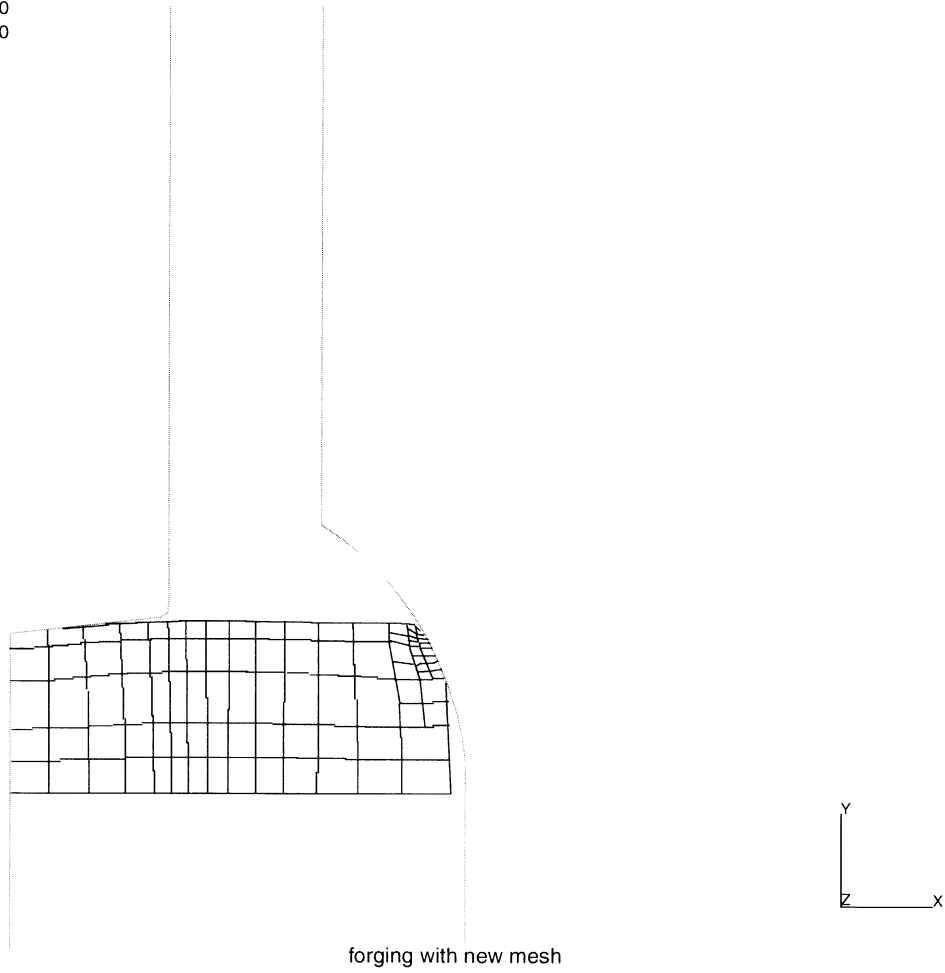


Figure 8.12-11 Adapted Mesh at Increment 20

INC : 40
SUB : 0
TIME : 8.000e+00
FREQ : 0.000e+00

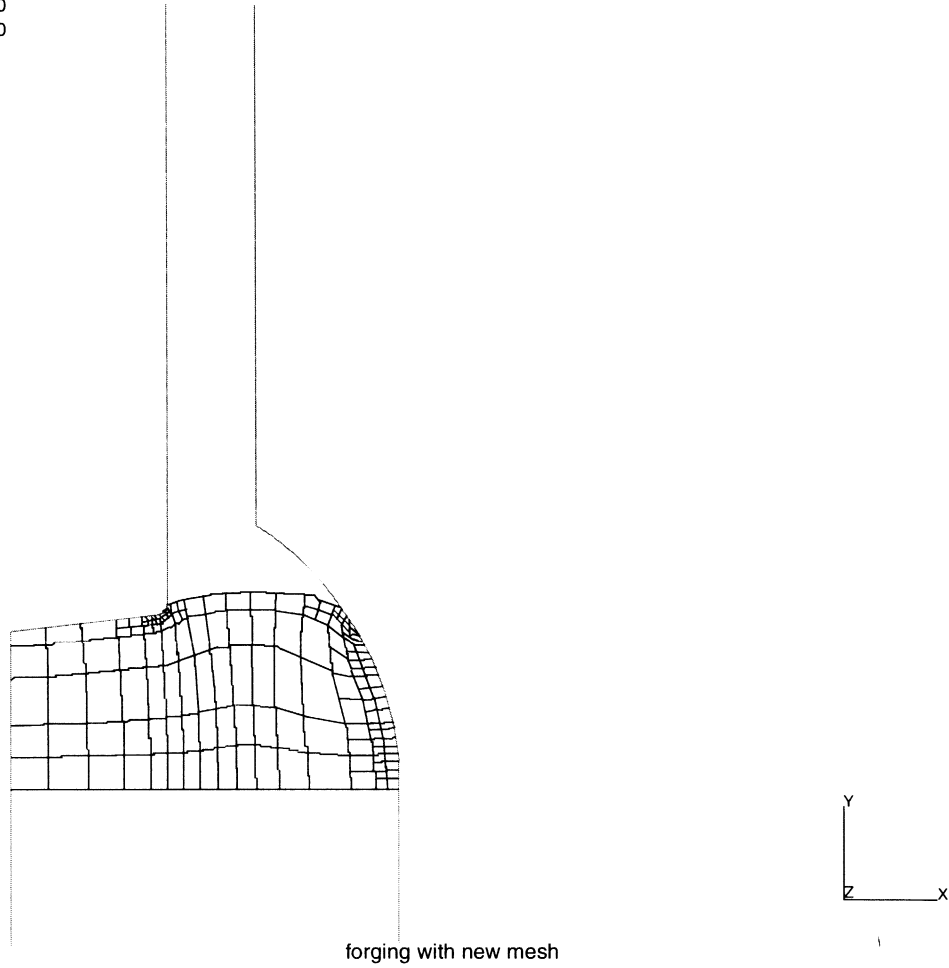


Figure 8.12-12 Adapted Mesh at Increment 40

INC : 60
SUB : 0
TIME : 1.200e+01
FREQ : 0.000e+00

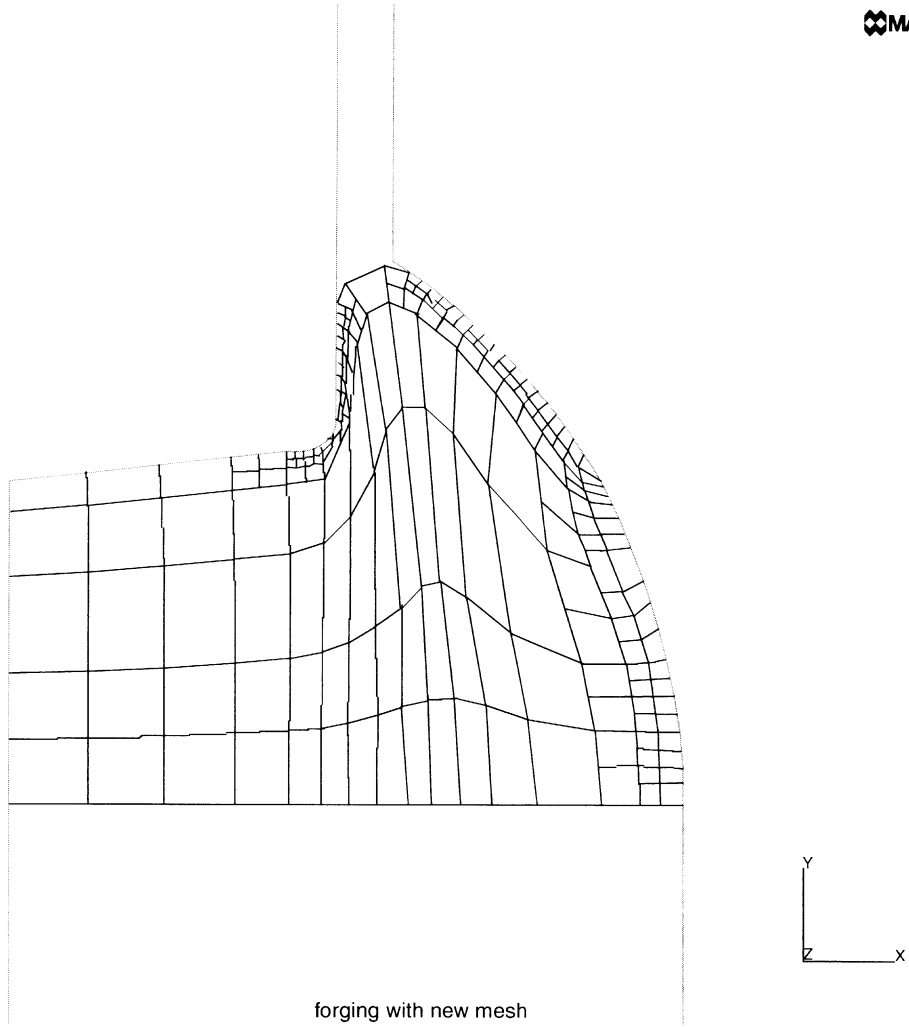


Figure 8.12-13 Adapted Mesh at Increment 60

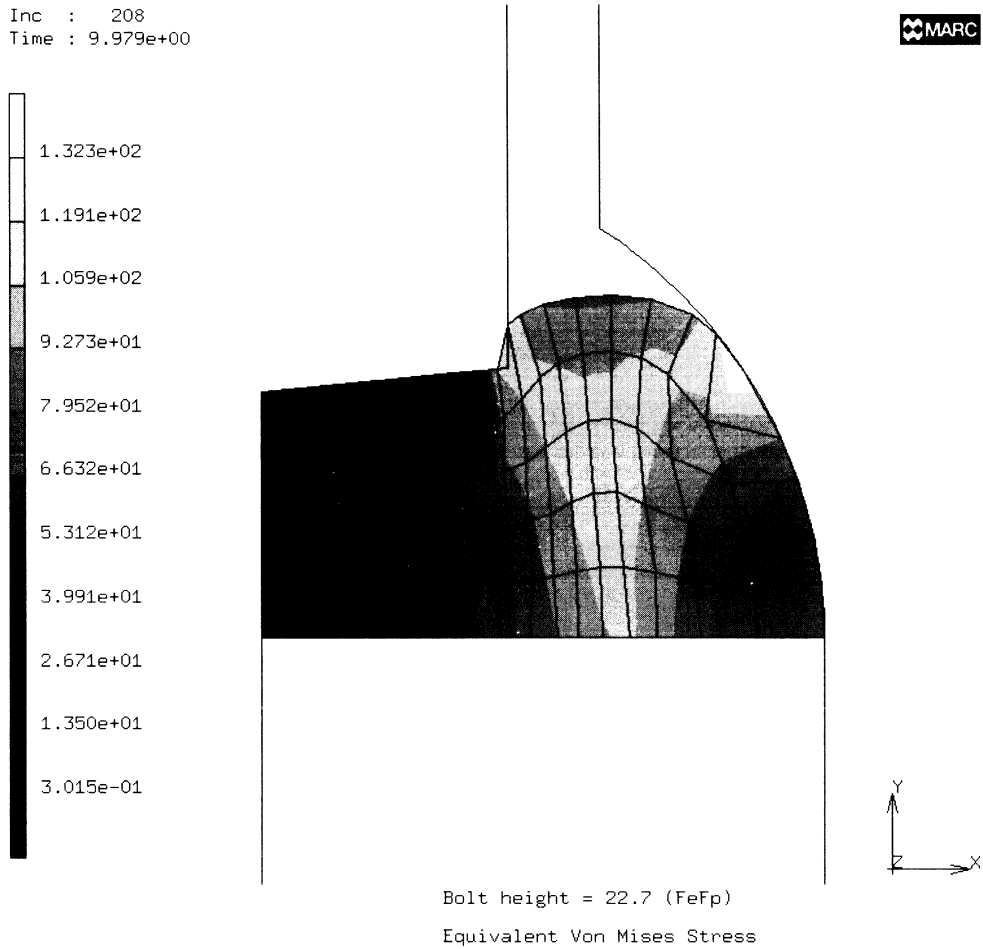


Figure 8.12-14 Equivalent Mises Tensile Stress at Bolt Height = 22.7 (F^eF^p)



8 *Advanced Topics*

Forging of the Head of a Bolt

8.13 Coupled Analysis of Ring Compression

This example demonstrates MARC's ability to perform a large deformation problem, incorporating thermal mechanical coupling and automated contact.

A ring of aluminum is deformed by a block of steel. Both have the capacity to deform, and possibly, slide between each other.

Coupling

There are several sources of coupling in this analysis.

1. As the temperature changes, thermal stresses are developed due to nonzero coefficient of thermal expansion.
2. As the temperature changes, the mechanical properties change. It happens in this case because of the temperature-dependent flow stress.
3. As the geometry changes, the heat transfer problem changes. This includes changes in the contacting interface.
4. As plastic work is performed, internal heat is generated.
5. As the bodies slide, friction generates heat.

Parameters

The UPDATE, FINITE, and LARGE DISP parameters indicate this is a finite deformation analysis. The COUPLE option is used to indicate that a coupled thermal-mechanical analysis is being performed. A four-node bilinear axisymmetric element is used. The PRINT,5 option requests additional information in the output regarding nodes acquiring or losing contact.

Mesh Definition

Mentat was used to determine the CONNECTIVITY and COORDINATES of the mesh. There are separate nodes along both sides of the contact interface so that sliding is possible. Due to symmetry, only one quarter of the region is modeled. The mesh is shown (with the units in mm) in Figure 8.13-1. In a coupled analysis, a displacement element automatically produces the coupled (displacement-temperature) formulation to be used.

This analysis is performed using both element type 10 and element type 116. Both elements are four-node axisymmetric elements. Element type 116 uses a single integration point and an hourglass stiffness stabilization procedure.

No gap elements are used. Free surfaces can have convection heat transfer to the environment. As soon as contact is detected, a contact thermal barrier, defined by means of a film coefficient, starts operating.

**Geometry**

A '1' is placed in the second field to indicate that the constant dilatation formulation is used. This is not necessary for the analysis using element type 116.

Boundary Conditions

Symmetry displacement boundary conditions are imposed on the ring meridian plane and on the block axis. The block is moved down by application of displacement boundary conditions to the face opposite to the contact face. Space for such boundary conditions is reserved in the model definition section. The displacement boundary conditions are entered in the **FIXED DISPLACEMENT** option. On the outside surface of the block, the temperature is constrained to 20°C, to simulate a much larger size block. This is done with the **FIXED TEMPERATURE** option.

Control Options

A formatted post file containing stress components and effective plastic strain is written at the end of 50 increments. The **NO PRINT** option limits the amount of output to a minimum. Displacement control is used in the deformation part of the analysis with a relative error of 15%. As far as the heat transfer part of the analysis is concerned, a 10°C maximum error in temperature estimate is entered. Even if thermal material properties are not temperature-dependent, this provides a means of forcing recycling when heat transfer between two bodies produces large variations of temperature per increment.

Initial Conditions

The ring is given an initial temperature of 427°C, and the block is given an initial temperature of 20°C.

Material Properties

The ring is treated as an elastic-plastic material with a Young's modulus of 1000 N/mm², a Poisson's ratio of 0.33, a mass density of 1.0g/mm³, a coefficient of thermal expansion of 1.3×10^{-5} mm/mm°C, and an initial yield stress of 3.4 N/mm², corresponding to a reference temperature of 200°C. The material workhardens from the initial yield stress to a yield stress of 5.78 N/mm² for strains above 70%, according to a piecewise linear function entered via **WORK HARD DATA**. The flow stress decreases with temperature increases at a rate of 0.007 N/mm² per degree. The thermal properties are conductivity of 242.0 N/s°C and specific heat of 2.4255 Nmm/g°C.

The block is treated as an elastic material with a Young's modulus of 100,000 N/mm², a Poisson's ratio of 0.33 and a mass density of 1 g/mm³. The thermal properties are conductivity of 19.0 N/s°C and specific heat of 3.77 Nmm/g°C.

**Distributed Flux**

This distributed flux block is used to indicate that internal heat is generated due to plastic deformation.

Convert

The option is used to give the conversion factor between the mechanical energy and the thermal energy.

The internal volumetric flux per unit volume becomes:

$$\phi = cw^P$$

where w^P is the plastic strain energy density.

Contact

The CONTACT option declares that there are two bodies with adhesive friction between them. MARC calculates both the contact tolerance and the sticking tolerance.

The first body is deformable and is made of the elements of the ring. There is no need to specify any motion. The ring's free surfaces have convection heat transfer defined by a film coefficient of 0.01, and a sink temperature of 20°C. The second body is also deformable and made out of the elements of the block. A reference point and an axial velocity are given, although they are not used in the calculations; this is done as a reminder of what the imposed boundary conditions are simulating. A friction factor of 1.0 defines the interface friction conditions, based on the cohesive model. The block's free surfaces have convection heat transfer defined by a film coefficient of 0.01 N/s-mm°C, and a sink temperature of 20°C. The contact surfaces have a thermal barrier defined by a film coefficient of 35.

This ordering of the two bodies results in imposing the constraint so that the nodes of the ring do not penetrate the surface of the block. Friction and thermal barrier at the interface use data taken from the body defining the block.

Load Control

This problem is performed with a fixed time step and fixed increment size. It is specified with a time step of 0.0003 seconds with a total of 0.03 seconds requested. Each increment imposes a displacement of 0.045mm to the nodes of the block in the plane opposed to the contact surface. This displacement increment is declared in DISP CHANGE and not in the original boundary conditions because the CONTACT option always bypasses increment zero.

In a coupled analysis, if an adaptive time stepping is required, the AUTO TIME option should be invoked. This option is demonstrated in the second analysis. Using AUTO TIME, it is requested that a maximum of 100 increments be used. The analysis used only 26 increments as there are very few changes in the contact surface.



Results

Figure 8.13-2 shows the deformed body at the end of 100 increments compounding to 50% reduction in height of the ring. Due to the high friction, the ring folds several times into the block on both sides, and there is an increase of the outer diameter as well as a decrease of the inner diameter. It can be seen that the amount of interface sliding is very small, also due to the high friction. Elastic deformations on the block are not visible, therefore it looks like the block had a rigid body translation.

Figure 8.13-3 shows equivalent plastic strain contours produced on the ring. They range from small amounts in the middle of the contact area (neutral zone) and in the free surface, to very large amounts at the corners where folding took place, and in the center of the middle plane.

In Figure 8.13-4, the equivalent von Mises stresses give an idea of the stresses produced in the block, which are higher than in the ring. They increase from low values in the free standing areas towards the center. Local peaks in the friction shearing zones also appear.

The thermal part of the analysis produces the temperatures of Figure 8.13-5. The total time for the deformation is only 0.03 seconds. Therefore, all the effects are confined to the contact region. Aluminum's high temperature, low flow stress produces no noticeable heating due to plastic deformation. On the ring side, the temperature decreases about 75°C at the interface, while the block heats around 50°C. Steel's lower conductivity produces steeper temperature gradients.

Parameters, Options, and Subroutines Summary

Example e8x13.dat:

Parameters	Model Definition Options	History Definition Options
COUPLE	CONNECTIVITY	CONTINUE
ELEMENT	CONTACT	DISP CHANGE
END	CONTROL	TRANSIENT
FINITE	CONVERT	
LARGE DISP	COORDINATE	
PRINT	DIST FLUXES	
SIZING	END OPTION	
TITLE	FIXED DISP	
UPDATE	FIXED TEMPERATURE	
	GEOMETRY	
	INITIAL TEMPERATURE	
	ISOTROPIC	
	NO PRINT	
	POST	
	TEMPERATURE EFFECTS	
	WORK HARD	



Example e8x13b.dat:

Parameters

COUPLE
ELEMENT
END
FINITE
LARGE DISP
PRINT
SIZING
TITLE
UPDATE

Model Definition Options

CONNECTIVITY
CONTACT
CONTROL
CONVERT
COORDINATE
DIST FLUXES
END OPTION
FIXED DISP
FIXED TEMPERATURE
GEOMETRY
INITIAL TEMPERATURE
ISOTROPIC
NO PRINT
POST
TEMPERATURE EFFECTS
WORK HARD

Example e8x13c.dat:

Parameters

ALIAS
COUPLE
ELEMENT
END
FINITE
LARGE DISP
PRINT
SIZING
TITLE
UPDATE

Model Definition Options

CONNECTIVITY
CONTACT
CONTROL
CONVERT
COORDINATE
DIST FLUXES
END OPTION
FIXED DISP
FIXED TEMPERATURE
GEOMETRY
INITIAL TEMPERATURE
ISOTROPIC
NO PRINT
POST
TEMPERATURE EFFECTS
WORK HARD

History Definition Options

CONTINUE
DISP CHANGE
TRANSIENT

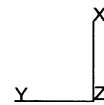
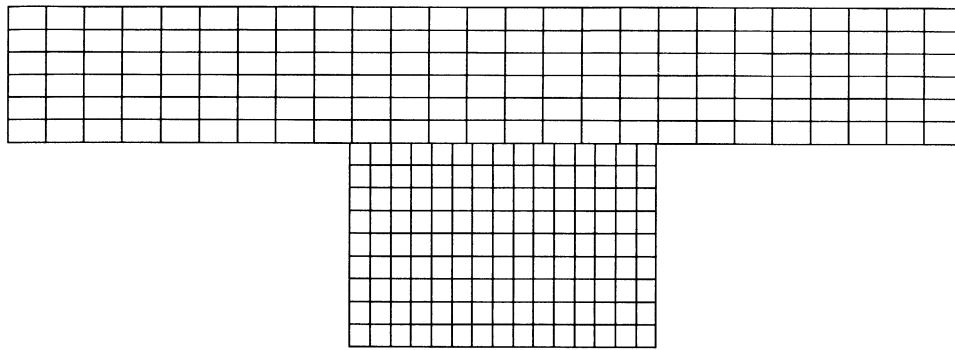
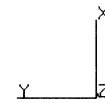
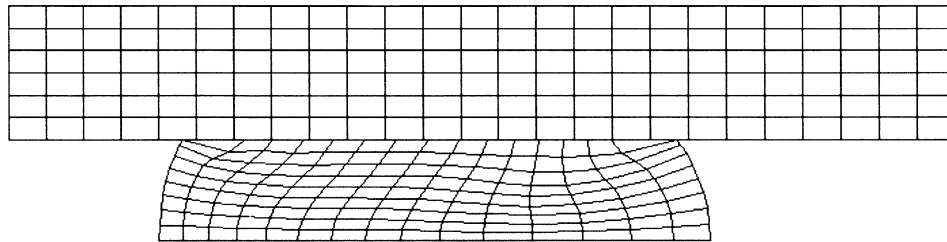


Figure 8.13-1 Original Mesh



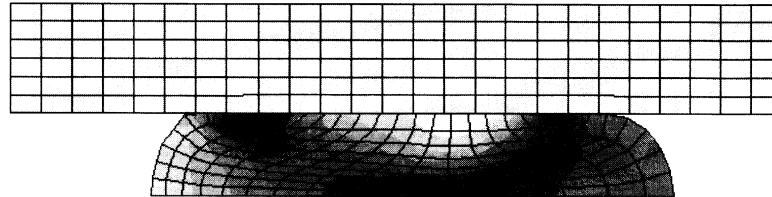
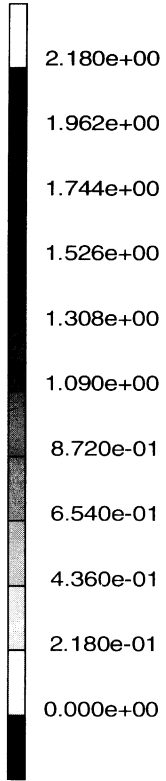
INC : 100
SUB : 0
TIME : 3.000e-02
FREQ : 0.000e+00



prob e8.13 coupled analysis of ring compression
Displacements x

Figure 8.13-2 Deformed Mesh (50% Height Reduction)

INC : 100
SUB : 0
TIME : 3.000e-02
FREQ : 0.000e+00

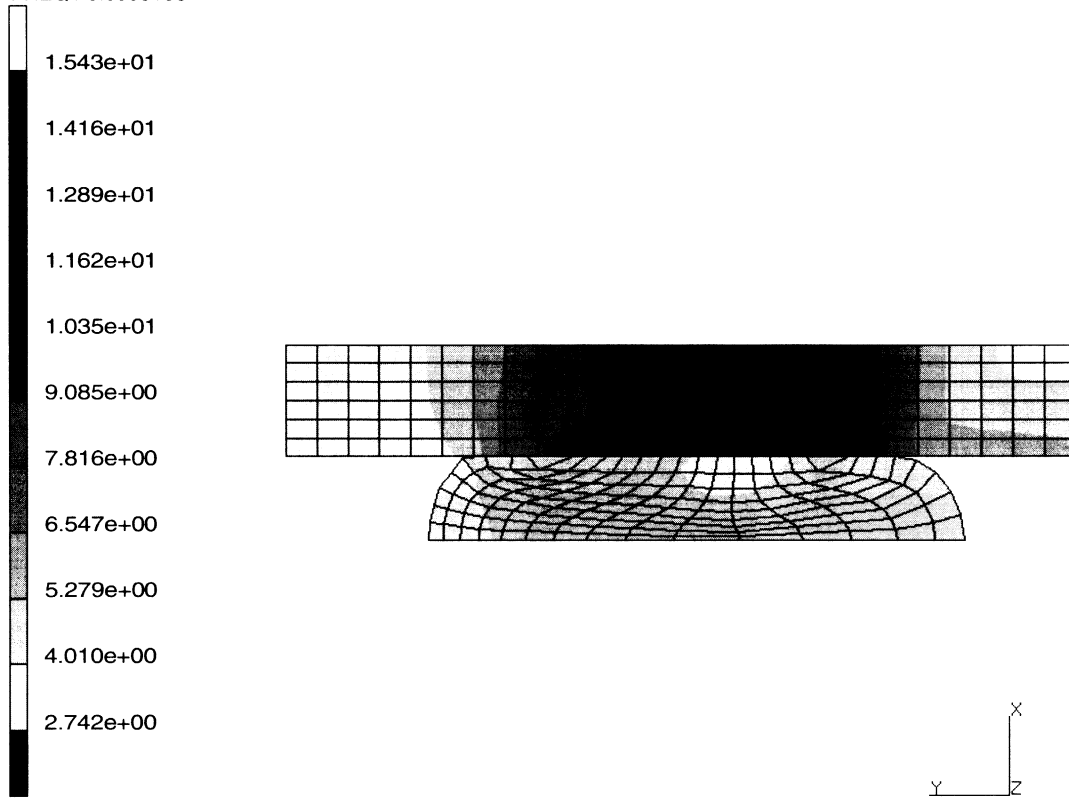


prob e8.13 coupled analysis of ring compression
Equivalent Plastic Strain

Figure 8.13-3 Equivalent Plastic Strain



INC : 100
SUB : 0
TIME : 3.000e-02
FREQ : 0.000e+00

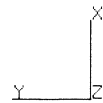
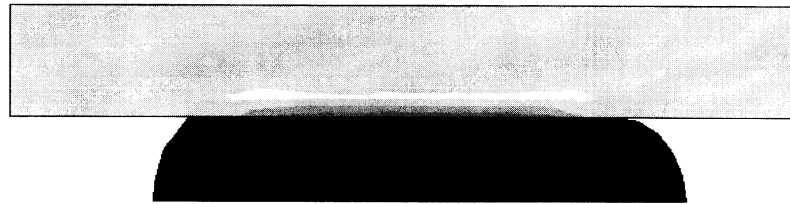
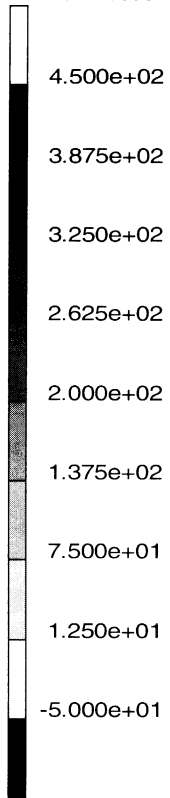


prob e8.13 coupled analysis of ring compression
Equivalent von Mises Stress

Figure 8.13-4 Equivalent von Mises Tensile Stress



INC : 100
SUB : 0
TIME : 3.000e-02
FREQ : 0.000e+00



prob e8.13 coupled analysis of ring compression
Temperatures t

Figure 8.13-5 Total Nodal Temperature



8.14 3D Contact with Various Rigid Surface Definitions

This problem demonstrates MARC's ability to perform contact analysis between a deformable body and a rigid die described through various surface definitions. It also demonstrates MARC's ability to perform contact analysis between a flexible body and a rigid die described through the NURBS definition.

Parameters

The UPDATE, FINITE, and LARGE DISP parameters are included in the parameter section to indicate that this is a finite deformation analysis. The PRINT,5 option requests additional information in the output regarding nodes acquiring or losing contact.

Geometry

A '1' is placed in the second data field to indicate that the constant dilatation formulation is used. This is particularly useful for analysis of approximately incompressible materials and for structures in the fully plastic range.

Boundary Conditions

To prevent rigid body motions, several nodes are restrained from displacing in the global x-, y-, z-directions. These constraints are given through the FIXED DISP option.

POST/PRINT Control

It is requested that the E_{xx} strain (post code 1) be written onto a formatted post file. The NO PRINT option limits the amount of printed output to a minimum.

Control

A maximum of 200 increments is allowed, with no more than 20 recycles per increment. Displacement control is used, with a relative error of 10%. However, keep in mind that control parameters under the CONTACT option set generally govern the convergence of the problem.

Material Properties

The material for all elements is treated as an elastic-perfectly plastic material, with Young's modulus of 1.75E+07 psi, Poisson's ratio of .3, and an initial yield stress of 35,000 psi.

Contact

The CONTACT option declares that there are two bodies in contact with no friction between them. The distance tolerance is specified as 0.005 inches. The reaction and velocity tolerances is computed by MARC. A die velocity of -0.3 in/sec in the global z-direction constitutes the driving motion for this problem.

**Load Control**

This problem is loaded by the application of number of increments specified in the AUTO LOAD option of the prescribed die velocities in the CONTACT option. The load increment is applied once.

Die Surface Definitions

The only difference between problems e8x14a, b, c, d, and e is the type of surface defined for the rigid die. In data set 14a, it is a 3D ruled surface with straight line generators. In 14b, it is again a ruled surface with circular arc generators. In 14c, it is a surface of revolution. In 14d, it is a 4-node patch. Finally, in 14e, a 3D polysurface defines the rigid die.

In e8x14f, the second body is described by NURBS. The '1' in the fifth field (surface definition) indicates the analytical form of NURBS is used to implement contact conditions. If '0' is entered in the field, the surface is still divided into 4-node patches and uses the piecewise linear approach to do the analysis.

The NURBS is defined by 9 x 5 control points with four cubic degrees along the u- and v-directions. The surface is divided into 20 x 5 patches for visualization.

Results

Figure 8.14-2 shows the deformed body at the end of increment one with the deformation at the same scale as the coordinates.

Parameters, Options, and Subroutines Summary

Example e8x14a.dat:

Parameters	Model Definition Options	History Definition Options
ELEMENT	CONNECTIVITY	AUTO LOAD
END	CONTACT	CONTINUE
FINITE	CONTROL	TIME STEP
LARGE DISP	COORDINATE	
PRINT	END OPTION	
SIZING	FIXED DISP	
TITLE	GEOMETRY	
UPDATE	ISOTROPIC	
	NO PRINT	
	POST	



Example e8x14b.dat:

Parameters

ELEMENT
END
FINITE
LARGE DISP
PRINT
SIZING
TITLE
UPDATE

Model Definition Options

CONNECTIVITY
CONTACT
CONTROL
COORDINATE
END OPTION
FIXED DISP
GEOMETRY
ISOTROPIC
NO PRINT
POST

History Definition Options

AUTO LOAD
CONTINUE
TIME STEP

Example e8x14c.dat:

Parameters

ELEMENT
END
FINITE
LARGE DISP
PRINT
SIZING
TITLE
UPDATE

Model Definition Options

CONNECTIVITY
CONTACT
CONTROL
COORDINATE
END OPTION
FIXED DISP
GEOMETRY
ISOTROPIC
NO PRINT
POST

History Definition Options

AUTO LOAD
CONTINUE
TIME STEP

Example e8x14d.dat:

Parameters

ELEMENT
END
FINITE
LARGE DISP
PRINT
SIZING
TITLE
UPDATE

Model Definition Options

CONNECTIVITY
CONTACT
CONTROL
COORDINATE
END OPTION
FIXED DISP
GEOMETRY
ISOTROPIC
NO PRINT
POST

History Definition Options

AUTO LOAD
CONTINUE
TIME STEP



Example e8x14e.dat:

Parameters	Model Definition Options	History Definition Options
ELEMENT	CONNECTIVITY	AUTO LOAD
END	CONTACT	CONTINUE
FINITE	CONTROL	TIME STEP
LARGE DISP	COORDINATE	
PRINT	END OPTION	
SIZING	FIXED DISP	
TITLE	GEOMETRY	
UPDATE	ISOTROPIC	
	NO PRINT	
	POST	

Example e8x14f.dat:

Parameters	Model Definition Options	History Definition Options
ELEMENTS	CONNECTIVITY	AUTO LOAD
END	CONTACT	CONTINUE
FINITE	CONTROL	TIME STEP
LARGE DISP	COORDINATE	
PRINT	END OPTION	
SIZING	FIXED DISP	
TITLE	GEOMETRY	
UPDATE	ISOTROPIC	
	NO PRINT	
	POST	

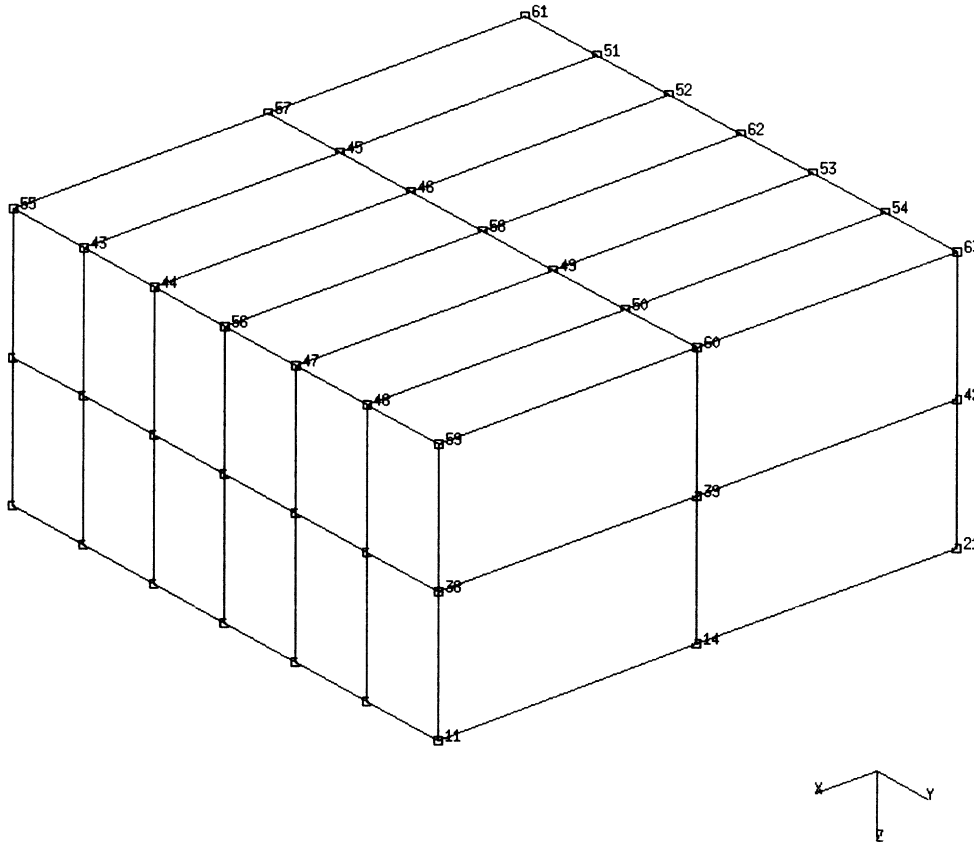


Figure 8.14-1 Undeformed Block

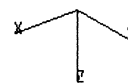
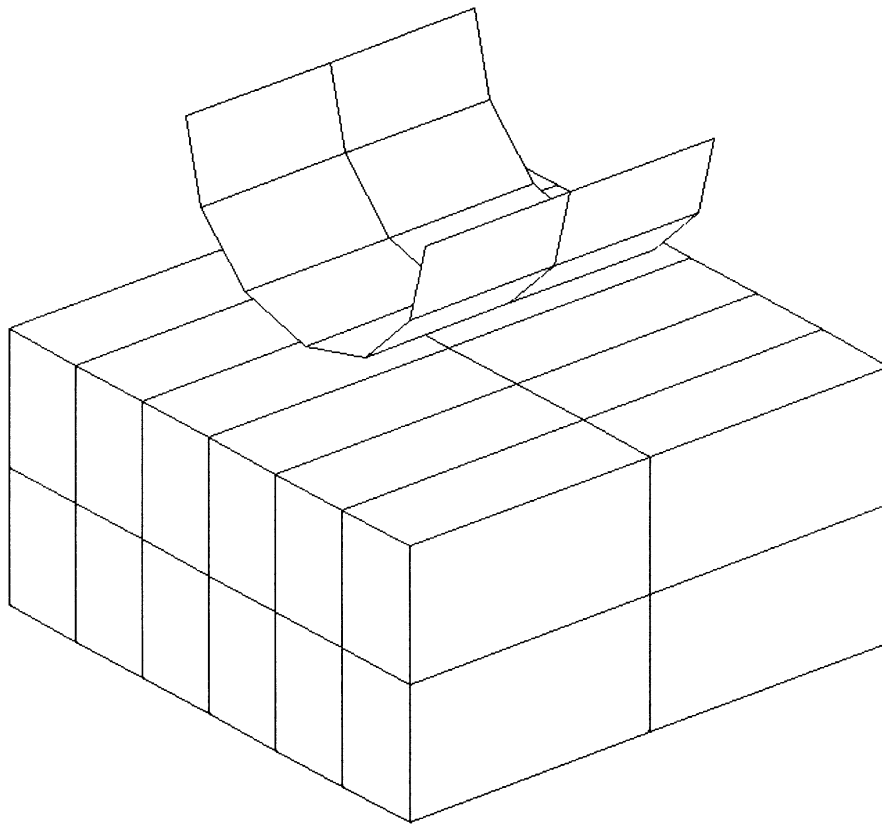


Figure 8.14-2 Block and Indentor

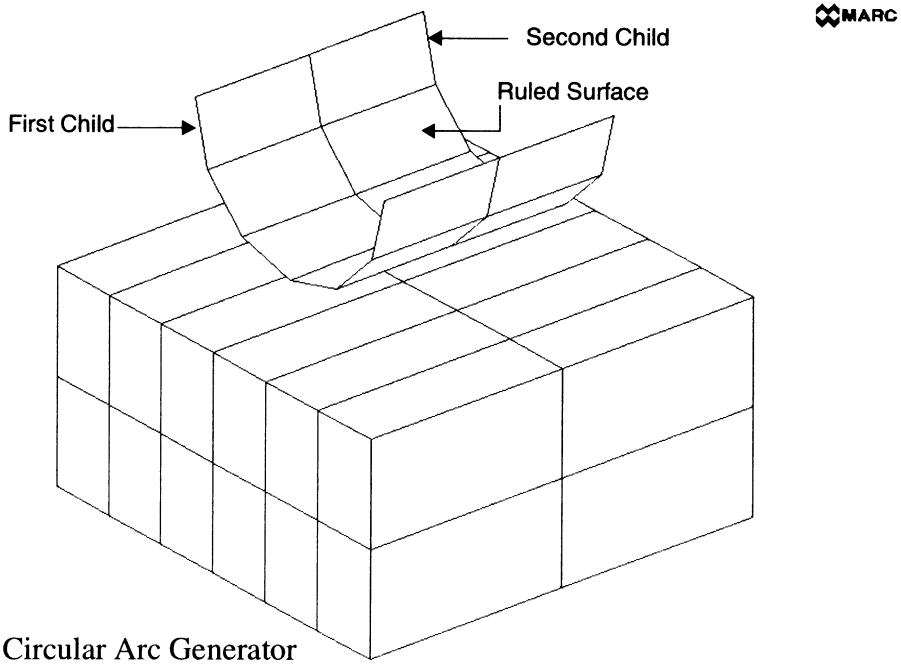
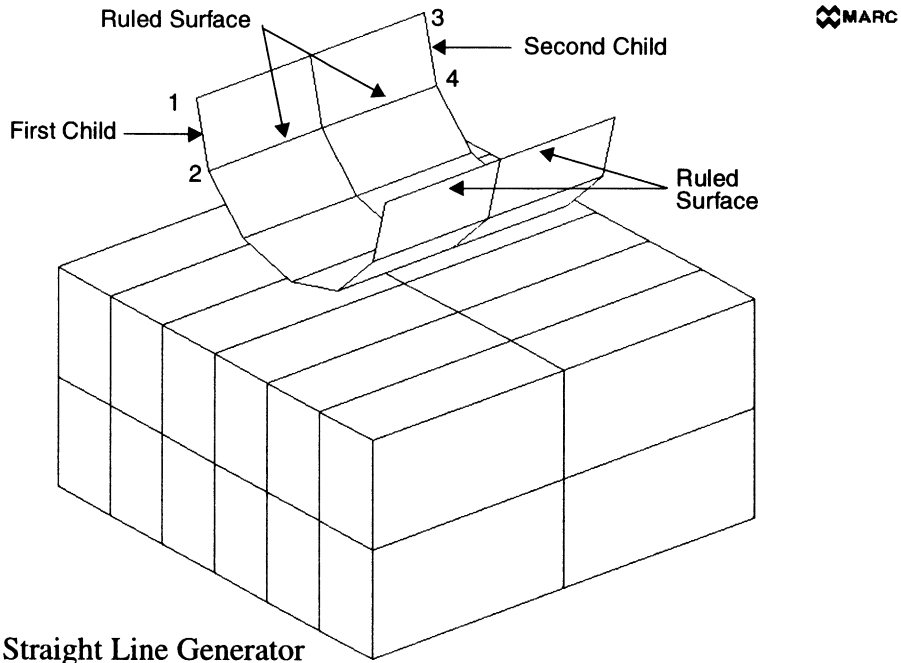
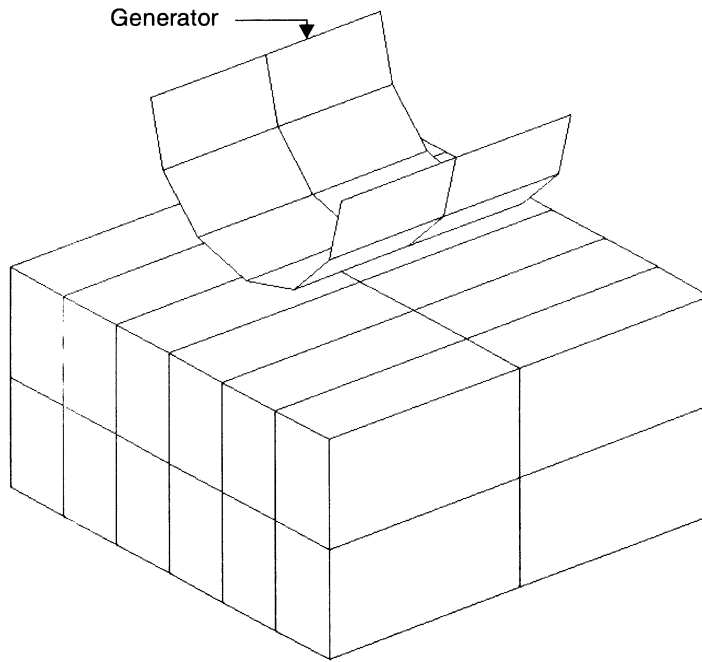
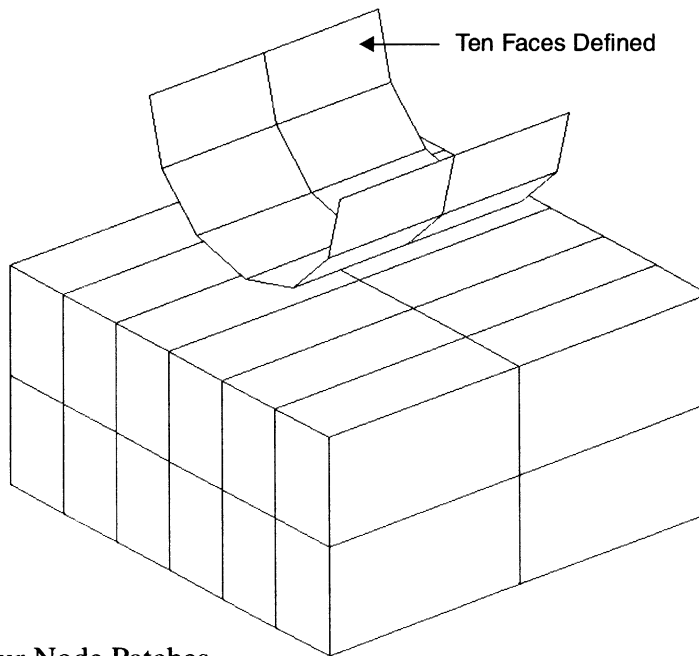


Figure 8.14-3 Ruled Surface



MARC

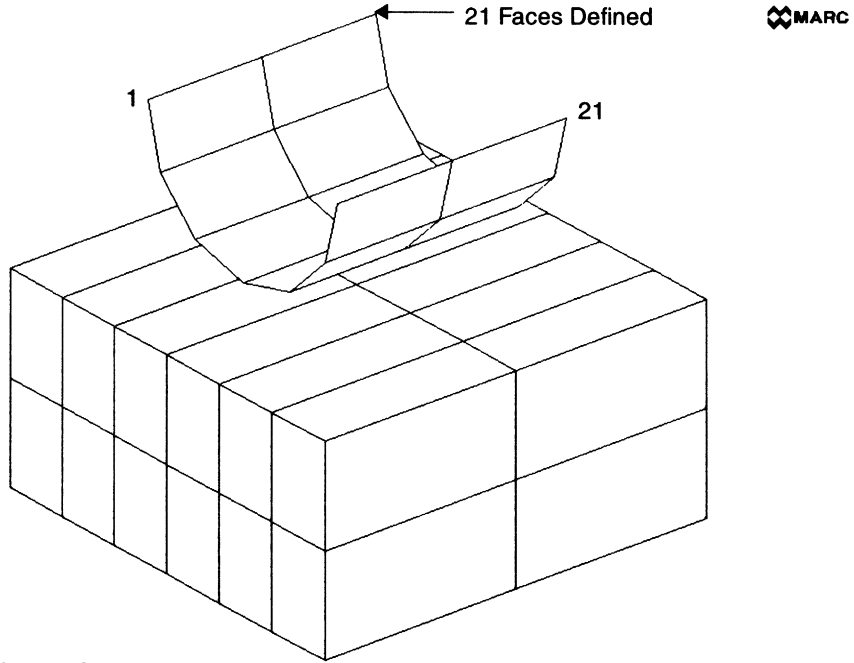
(c) Surface of Revolution



MARC

(d) Four Node Patches

Figure 8.14-3 Ruled Surface (Continued)



(d) Poly Surface

Figure 8.14-3 Ruled Surface (Continued)

**Geometry**

A '1' is placed in the second data field to indicate that the constant dilatation formulation is used when the additive decomposition procedure is used. This is particularly useful for analysis of approximately incompressible materials and for structures in the fully plastic range. This is not necessary when the multiplicative decomposition procedure is used. The '1.0' placed in the first data field indicates the thickness of 1 inch.

Boundary Conditions

The nodes on the top surface ($y = 3$) are moved uniformly downward. The left ($x = 0$) and bottom ($y = 0$) side are constrained.

Material Properties

The material for all elements is treated as an elastic-plastic material, with Young's modulus of $31.75\text{E}+06$ psi, Poisson's ratio of 0.268, a mass density of $7.4\text{E}-04$ lbf-sec²/in⁴, a coefficient of thermal expansion of $5.13\text{E}-06$ in/(in-deg F), corresponding reference temperature of 70°F, and an initial yield stress of 80,730 psi. The material work-hardens from the initial yield stress to a final yield stress of 162,747 psi at a strain of 1.0 in the WORK HARD DATA block.

Contact

The CONTACT option declares that there are two bodies in contact with adhesive friction between them. The relative slip velocity is defined as 0.01 in/second. The contact tolerance distance is 0.01 inches. The coefficient of friction associated with each body is 0.7. The reaction tolerance will be computed by the program.

The CONTACT TABLE is used to indicate that body 1 will potentially come in contact with body 2. Because the contact table is used, no contact between body 1 and itself or body 2 and itself is checked.

Load Control

This problem is loaded by the repeated application of the load increment created by the prescribed boundary conditions in the AUTO LOAD option. The load increment is applied 20 times. The TIME STEP option allows you to enter the time variable for static analysis. All contact analyses are time driven and require the definition of a time step. A formatted post file contains the equivalent plastic strain, the first two stress components, von Mises equivalent stress, and the mean normal stress. The NO PRINT option limits the amount of printed output to a minimum. Displacement control is used with a relative error of 20%. The RESTART LAST option is used to save the last increment of data if a later restart is required.



For data set e8x15d, the load incrementation is done using the AUTO STEP option. The initial time step is chosen to be 0.01 sec while the total time period is chosen to be 1 sec. The AUTO STEP option is chosen to control the maximum allowed effective plastic strain increment in each load increment. This is summarized in the table below:

Plastic Strain Range	Maximum Plastic Strain Increment
0.0 – 0.10	0.02
0.10 – 0.25	0.05
0.25 – 0.75	0.10
0.75 – 2.0	0.20

Results

Figure 8.15-1 shows the original mesh with the elements labeled of double-sided contact problem for both element types. Figure 8.15-2 and Figure 8.15-3, respectively, show the nodal labels for element types 11 and 27. Figure 8.15-4, Figure 8.15-5, and Figure 8.15-6 show the deformed body at the end of 10, 20 and 30 increments with the deformation at the same scale as the coordinates. Figure 8.15-8, Figure 8.15-9, and Figure 8.15-10 show the deformed body at the end of 10, 20 and 30 increments for element type 27. Due to the high level of friction, significant transverse deformation is shown along the contact surfaces. Figure 8.15-7 and Figure 8.15-11 show the equivalent plastic strain at the end of increment 30. The peak values of equivalent plastic strain are 137% and 151% for element types 11 and 27, respectively. The additional degrees of freedom in the model using element type 27 makes the structure more flexible. The larger plastic strain found for the higher degrees of freedom model is on the high side of convergence tolerance.

A user-written subroutine, IMPD, is used in conjunction with the UDUMP model definition option to sum the nodal loads across the $y = 3$ (top) surface and print the nodal load and displacement for each increment into the output file. This information is plotted and shown in Figure 8.15-12 for both element types. The overall force-displacement behavior of the two element types is in good agreement with all differences occurring in the early portion of the contact.

In the third analysis, a flag is set to indicate that increment splitting is not to be used. Also the CONTACT NODE option is used to only check contact for the corner nodes for the parabolic element, type 27.

For the fourth analysis (data set e8x15d), the deformed geometry at increments 25 and 50 are shown in Figure 8.15-13 and Figure 8.15-14 respectively. The final deformed shape after 53 increments is shown in Figure 8.15-15 with contours of total effective plastic strain superimposed.



Parameters, Options, and Subroutines Summary

Example e8x15.dat:

Parameters	Model Definition Options	History Definition Options
ELEMENT	CONNECTIVITY	AUTO LOAD
END	CONTACT	CONTINUE
FINITE	CONTACT TABLE	TIME STEP
LARGE DISP	CONTROL	
PRINT	COORDINATES	
SIZING	DEFINE	
TITLE	END OPTION	
UPDATE	FIXED DISP	
	GEOMETRY	
	ISOTROPIC	
	NO PRINT	
	POST	
	RESTART LAST	
	WORK HARD	

Example e8x15b.dat:

Parameters	Model Definition Options	History Definition Options
ELEMENT	CONNECTIVITY	AUTO LOAD
END	CONTACT	CONTINUE
FINITE	CONTACT TABLE	TIME STEP
LARGE DISP	CONTROL	
PRINT	COORDINATES	
SIZING	DEFINE	
TITLE	END OPTION	
UPDATE	FIXED DISP	
	GEOMETRY	
	ISOTROPIC	
	NO PRINT	
	POST	
	RESTART LAST	
	WORK HARD	



E8x15c.dat:

Parameters

ELEMENT
END
FINITE
LARGE DISP
PRINT
SIZING
TITLE
UPDATE

Model Definition Options

CONNECTIVITY
CONTACT
CONTACT NODE
CONTACT TABLE
CONTROL
COORDINATES
DEFINE
END OPTION
FIXED DISP
GEOMETRY
ISOTROPIC
NO PRINT
POST
RESTART LAST
WORK HARD

History Definition Options

AUTO LOAD
CONTINUE
TIME STEP

Example e8x15d.dat:

Parameters

ELEMENT
END
PRINT
SIZING
TITLE
PLASTICITY

Model Definition Options

CONNECTIVITY
CONTACT
CONTACT TABLE
CONTROL
COORDINATES
DEFINE
END OPTION
FIXED DISP
GEOMETRY
ISOTROPIC
NO PRINT
POST
RESTART LAST
WORK HARD

History Definition Options

CONTINUE
AUTO STEP

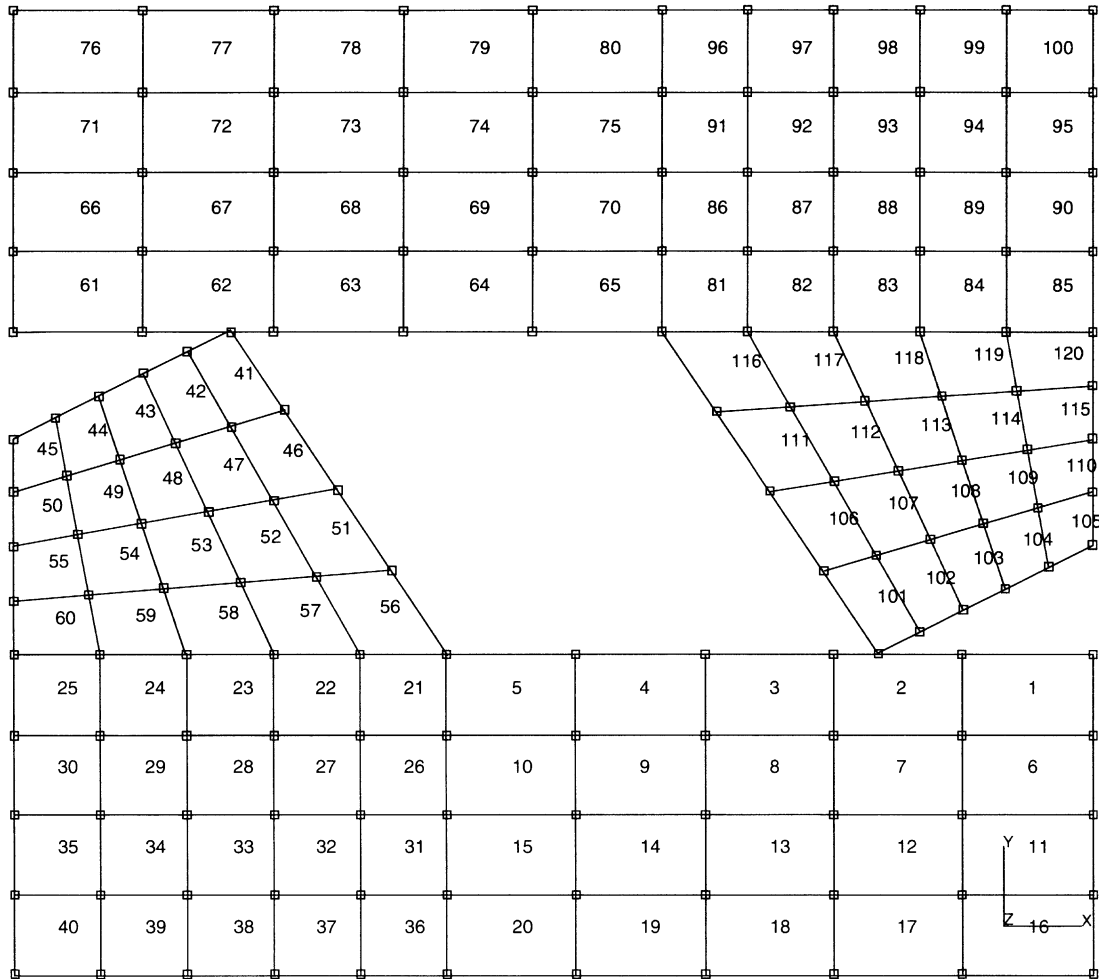


Figure 8.15-1 Mesh

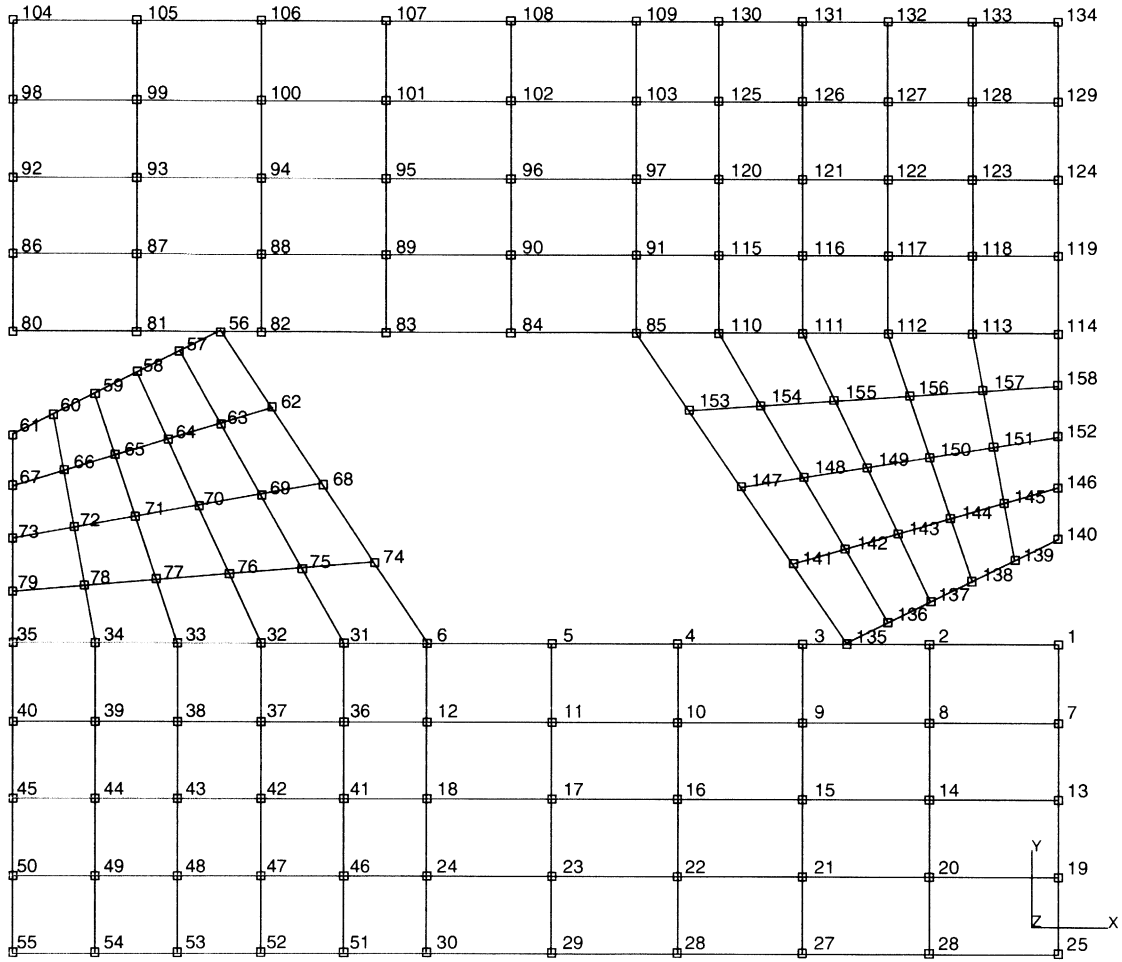


Figure 8.15-2 Nodal Configuration, Element Type 11

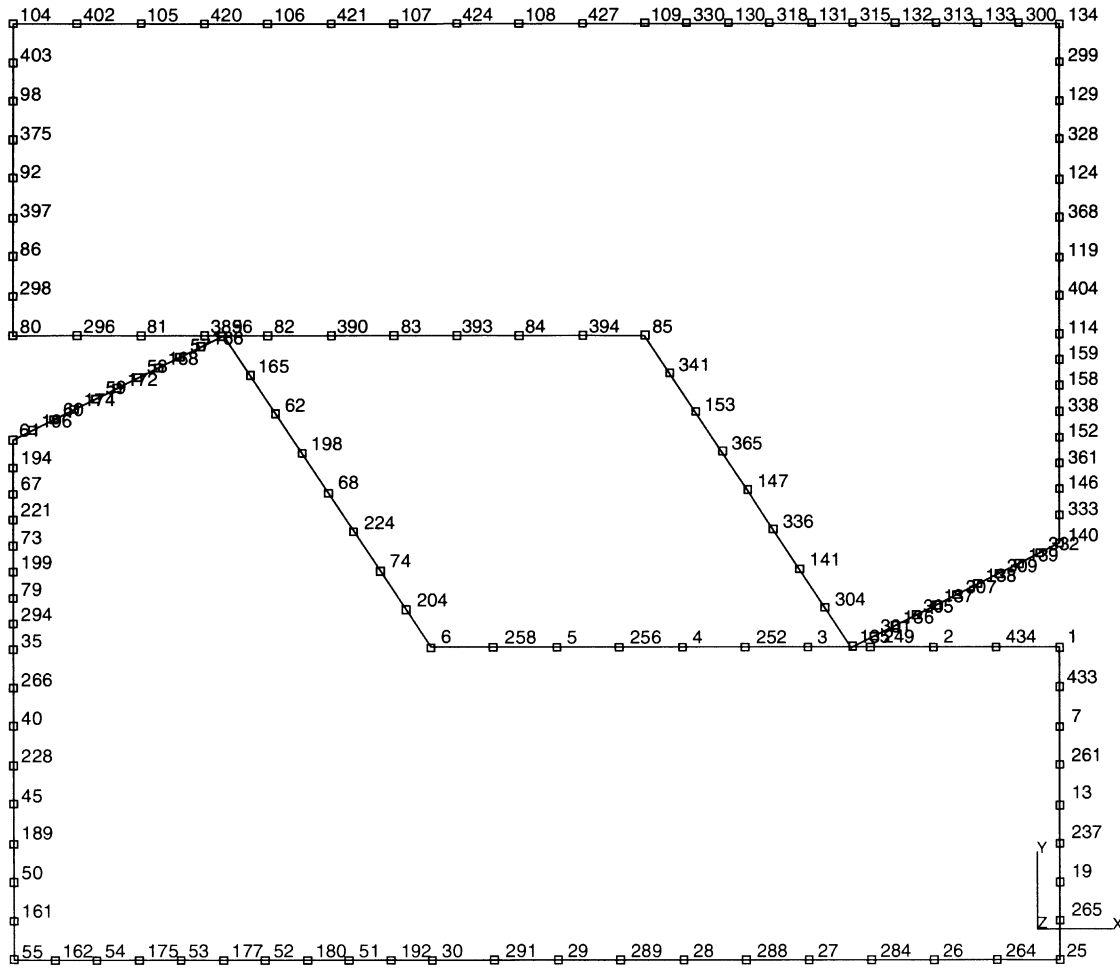
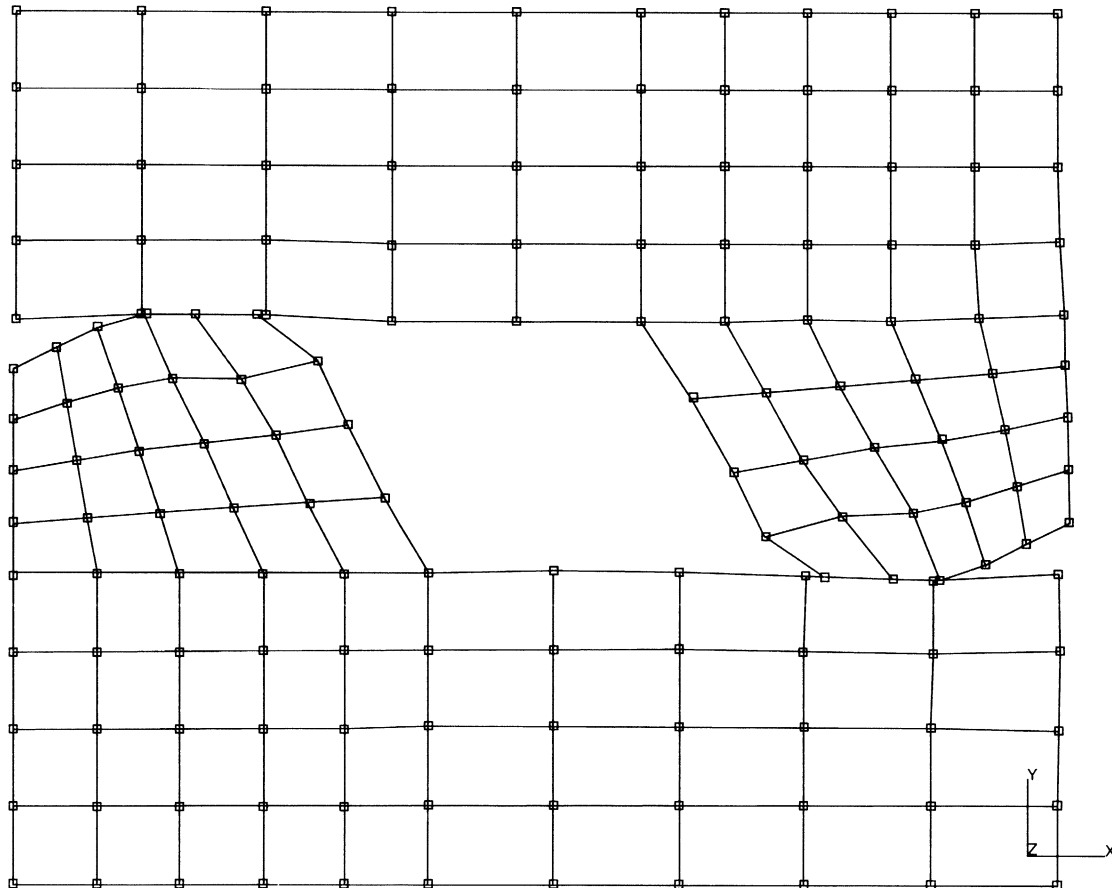


Figure 8.15-3 Nodal Configuration, Element Type 27



INC : 10
SUB : 0
TIME : 3.000e-01
FREQ : 0.000e+00

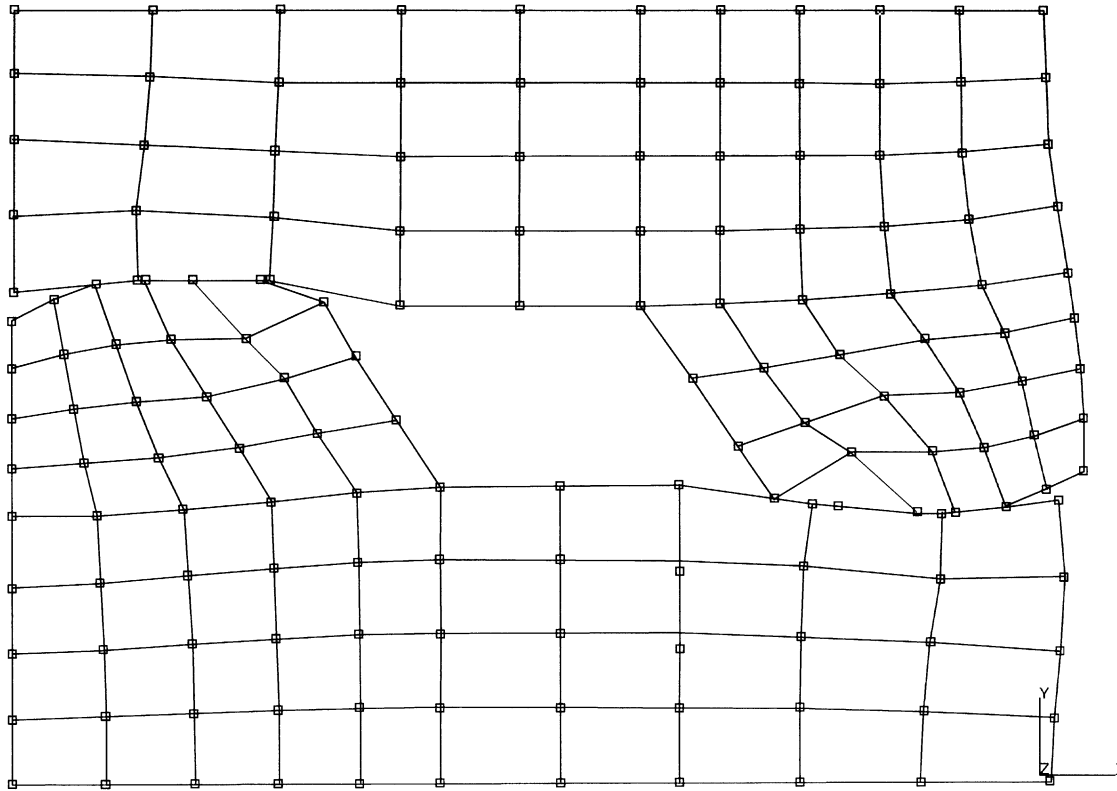


prob e8.15 double sided contact elem 11

Reaction Forces y

Figure 8.15-4 Nodal Displacements at Increment 10, Element Type 11

INC : 20
SUB : 0
TIME : 6.000e-01
FREQ : 0.000e+00



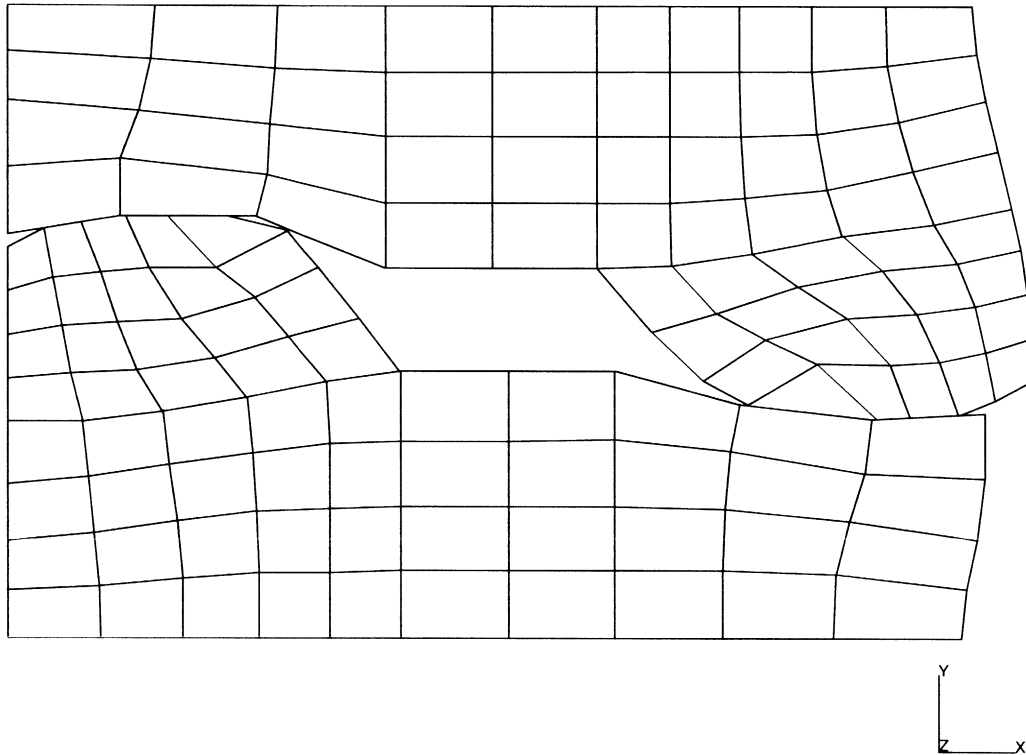
prob e8.15 double sided contact elem 11

Reaction Forces y

Figure 8.15-5 Nodal Displacements at Increment 20, Element Type 11



INC : 30
SUB : 0
TIME : 9.000e-01
FREQ : 0.000e+00



prob e8.15 double sided contact elem 11

Equivalent Plastic Strain

Figure 8.15-6 Nodal Displacements at Increment 30, Element Type 11

Inc : 30
Time : 9.000e-01

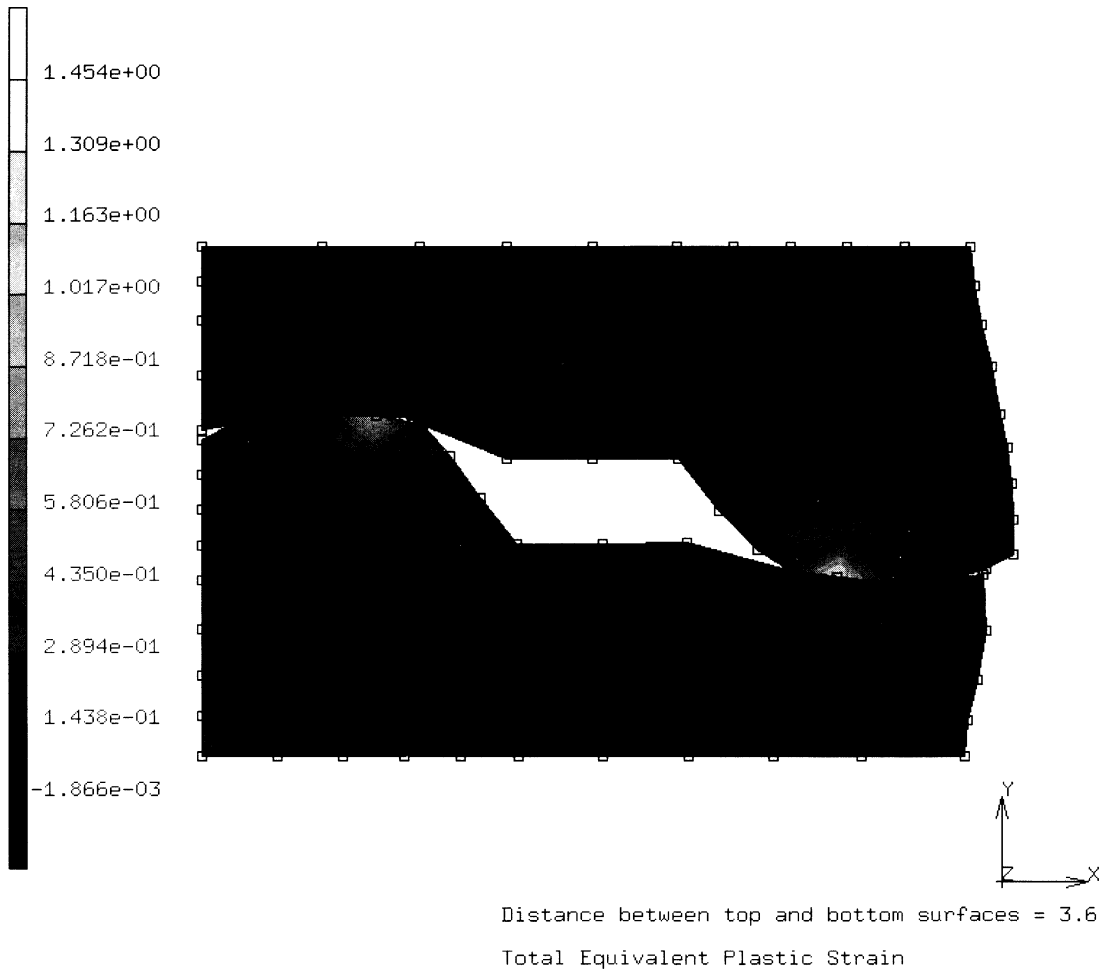
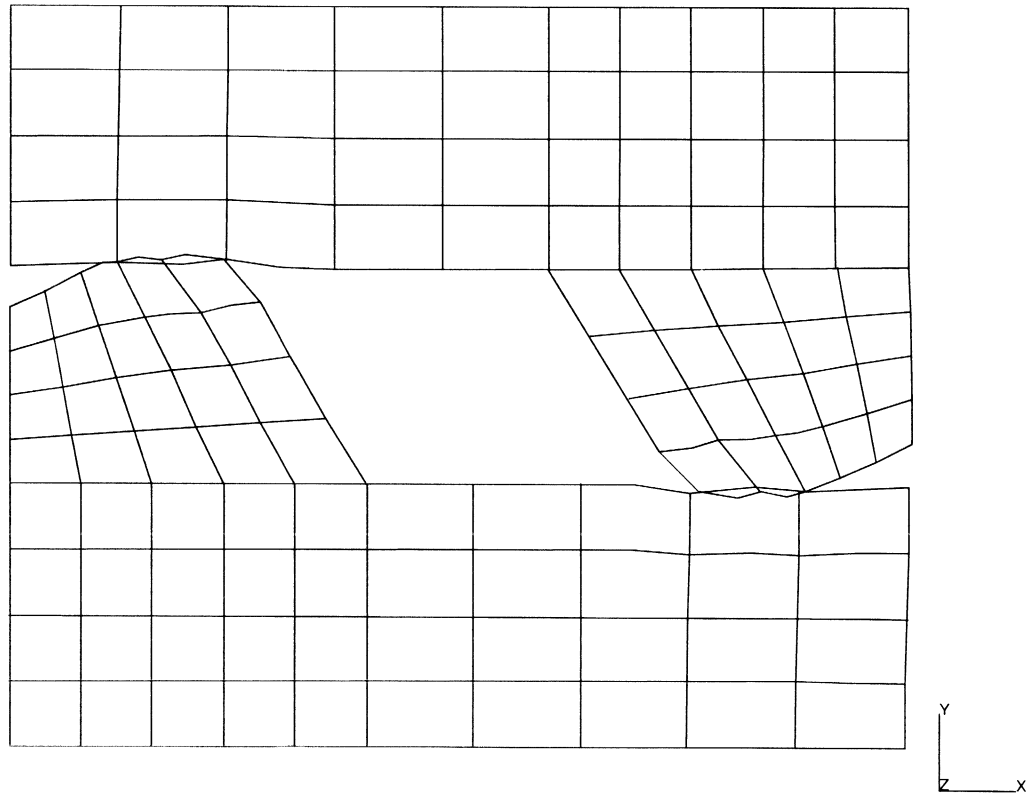


Figure 8.15-7 Equivalent Plastic Strain at Increment 30, Element Type 11



INC : 10
SUB : 0
TIME : 3.000e-01
FREQ : 0.000e+00



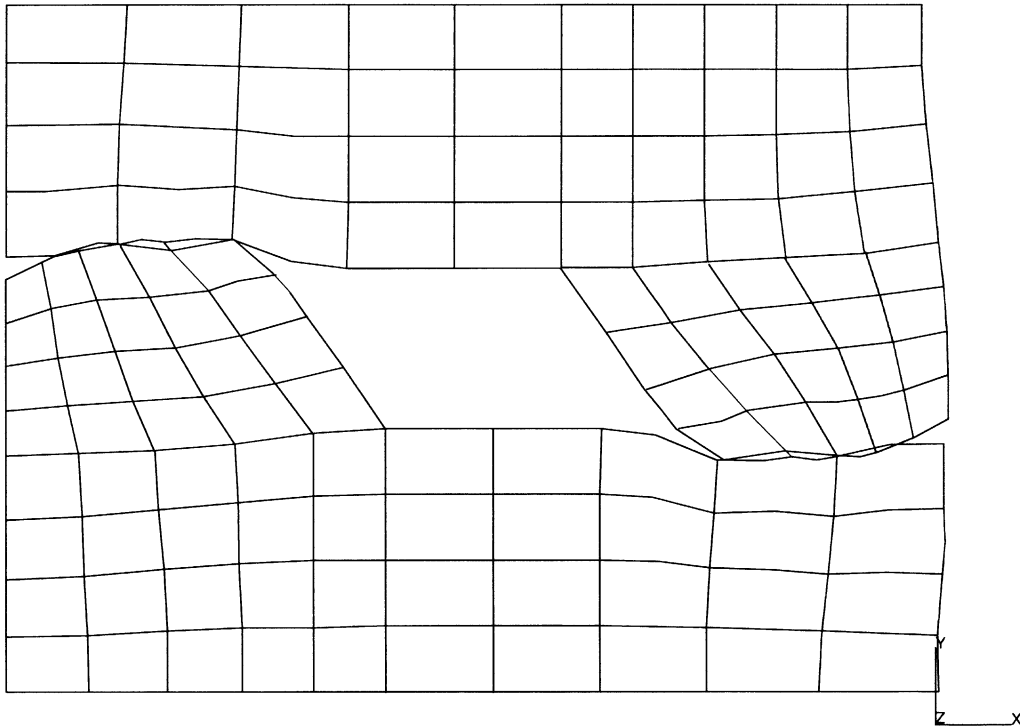
prob e8.15b double sided contact elem 27

Displacement x

Figure 8.15-8 Nodal Displacements at Increment 10, Element Type 27



INC : 20
SUB : 0
TIME : 6.000e-01
FREQ : 0.000e+00



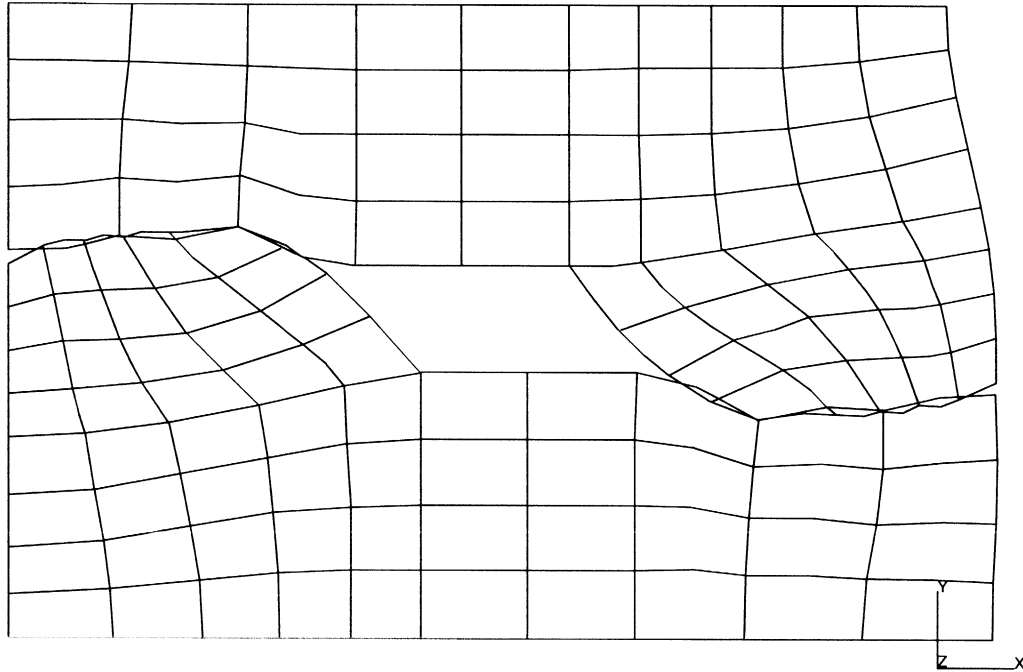
prob e8.15b double sided contact elem 27

Displacement x

Figure 8.15-9 Nodal Displacements at Increment 20, Element Type 27



INC : 30
SUB : 0
TIME : 9.000e-01
FREQ : 0.000e+00

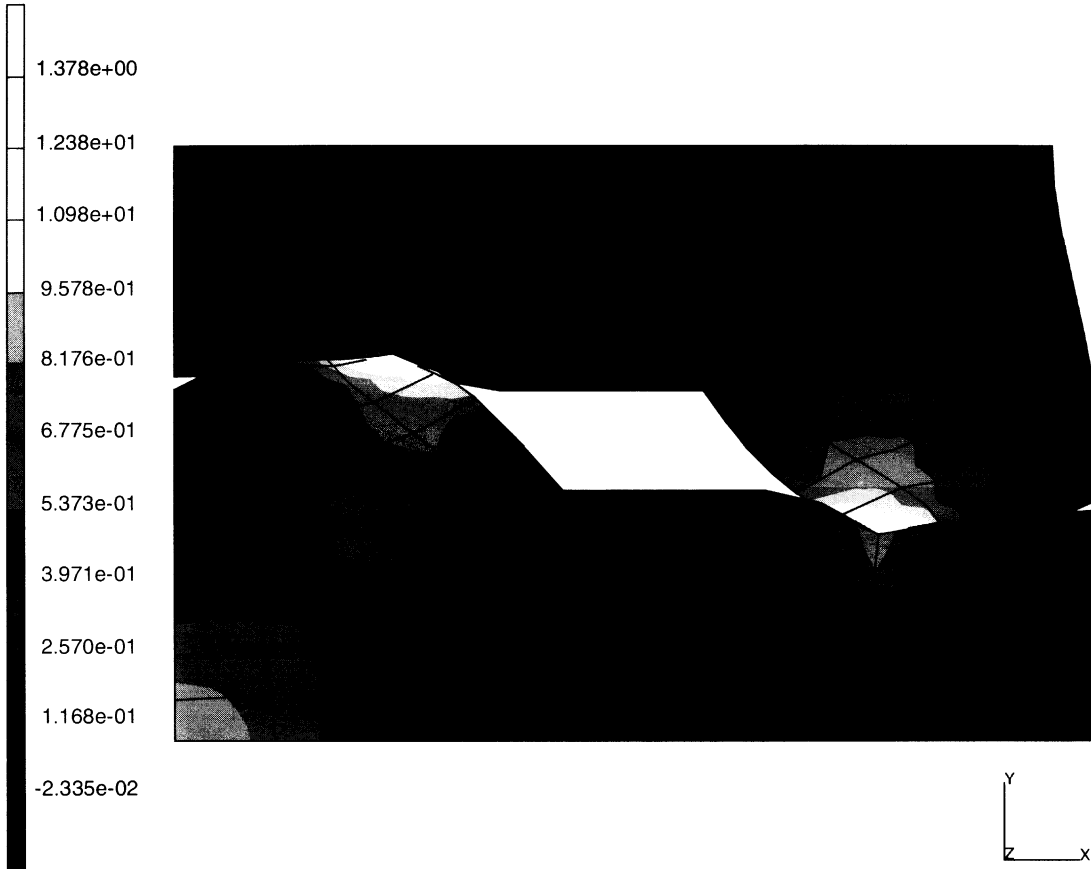


prob e8.15b double sided contact elem 27
Displacement x

Figure 8.15-10 Nodal Displacements at Increment 30, Element Type 27



INC : 30
SUB : 0
TIME : 9.000e-01
FREQ : 0.000e+00



prob e8.15b double sided contact elem 11

equivalent plastic strain

Figure 8.15-11 Equivalent Plastic Strain at Increment 30, Element Type 27



Disp (x-1e+0)	Load (x-1e+5)		Disp (x-1e+0)	Load (x-1e+5)	
	Type 11	Type 27		Type 11	Type 27
0.00000E+00	0.00000E+00	0.00000E+00	4.50000E-01	5.73937E+00	5.76850E+00
3.00000E-02	1.49358E+00	9.65015E-01	4.80000E-01	5.82146E+00	5.92706E+00
6.00000E-02	1.36351E+00	1.34468E+00	5.10000E-01	5.88858E+00	6.02711E+00
9.00000E-02	1.40418E+00	1.61070E+00	5.40000E-01	5.95362E+00	6.11778E+00
1.20000E-01	3.59213E+00	2.52490E+00	5.70000E-01	6.01384E+00	6.20322E+00
1.50000E-01	3.26189E+00	3.02085E+00	6.00000E-01	6.28412E+00	6.28309E+00
1.80000E-01	3.31538E+00	3.35550E+00	6.30000E-01	6.35279E+00	6.35828E+00
2.10000E-01	3.52452E+00	3.70196E+00	6.60000E-01	6.39055E+00	6.42653E+00
2.40000E-01	4.55123E+00	4.33235E+00	6.90000E-01	6.43786E+00	6.52579E+00
2.70000E-01	4.74629E+00	4.63125E+00	7.20000E-01	6.56095E+00	6.55766E+00
3.00000E-01	4.89159E+00	4.88421E+00	7.50000E-01	6.72437E+00	6.52325E+00
3.30000E-01	5.03333E+00	5.07415E+00	7.80000E-01	6.77405E+00	6.70139E+00
3.60000E-01	5.16167E+00	5.23750E+00	8.10000E-01	6.70833E+00	6.79742E+00
3.90000E-01	5.39677E+00	5.41752E+00	8.40000E-01	6.89754E+00	7.02602E+00
4.20000E-01	5.51851E+00	5.60917E+00	8.70000E-01	6.97591E+00	7.14885E+00
			9.00000E-01	7.01286E+00	7.24298E+00

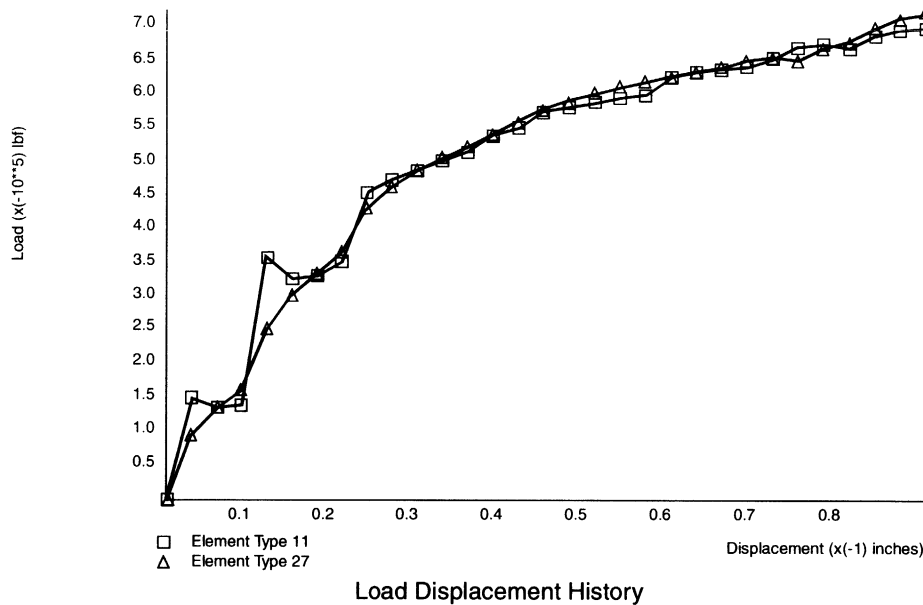
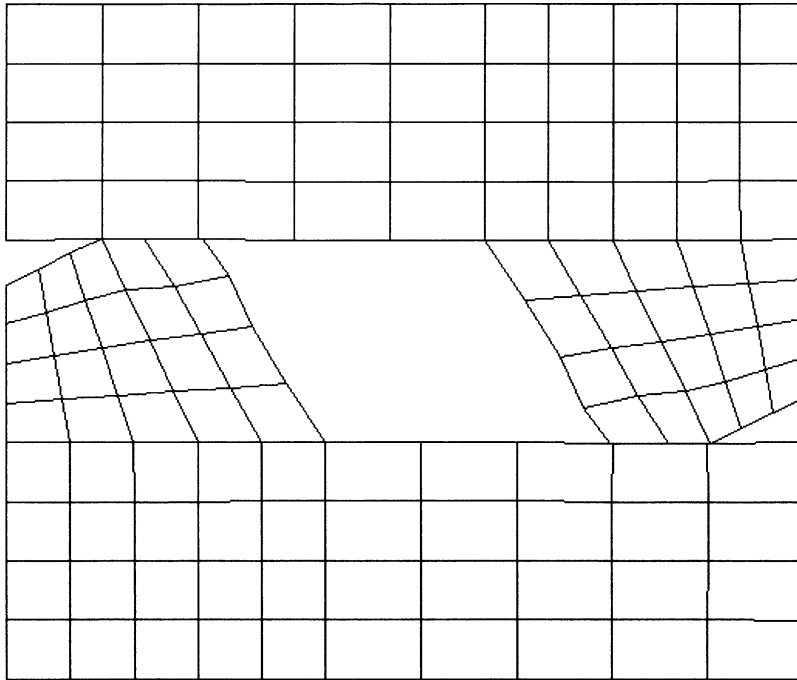


Figure 8.15-12 Load History for Both Element Types



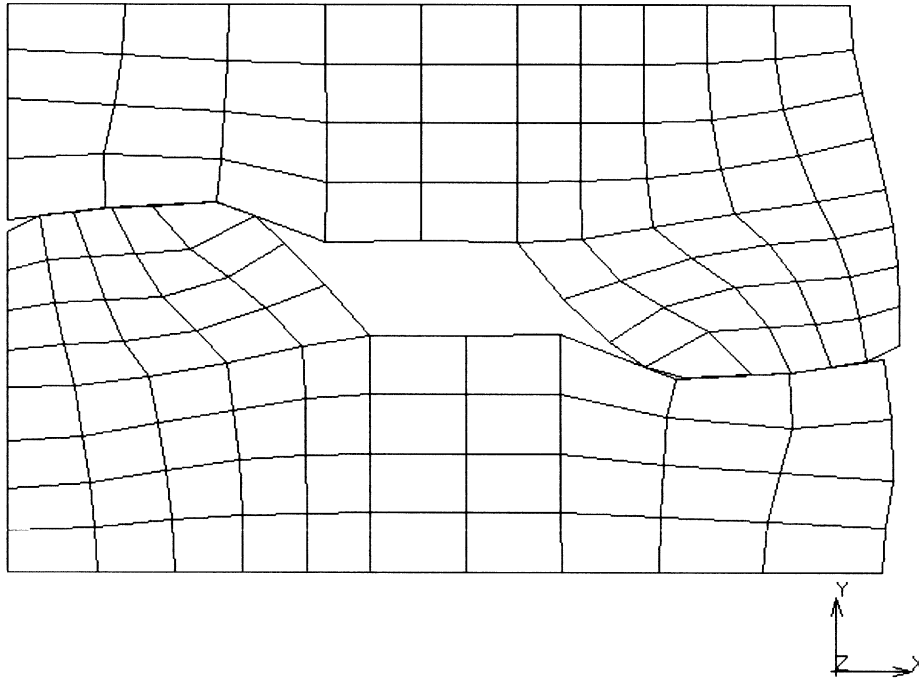
Inc : 25
Time : 2.345e-01



e8x15d - FeFp plasticity

Figure 8.15-13 Deformed Geometry at Increment 25 for Data Set e8x15d

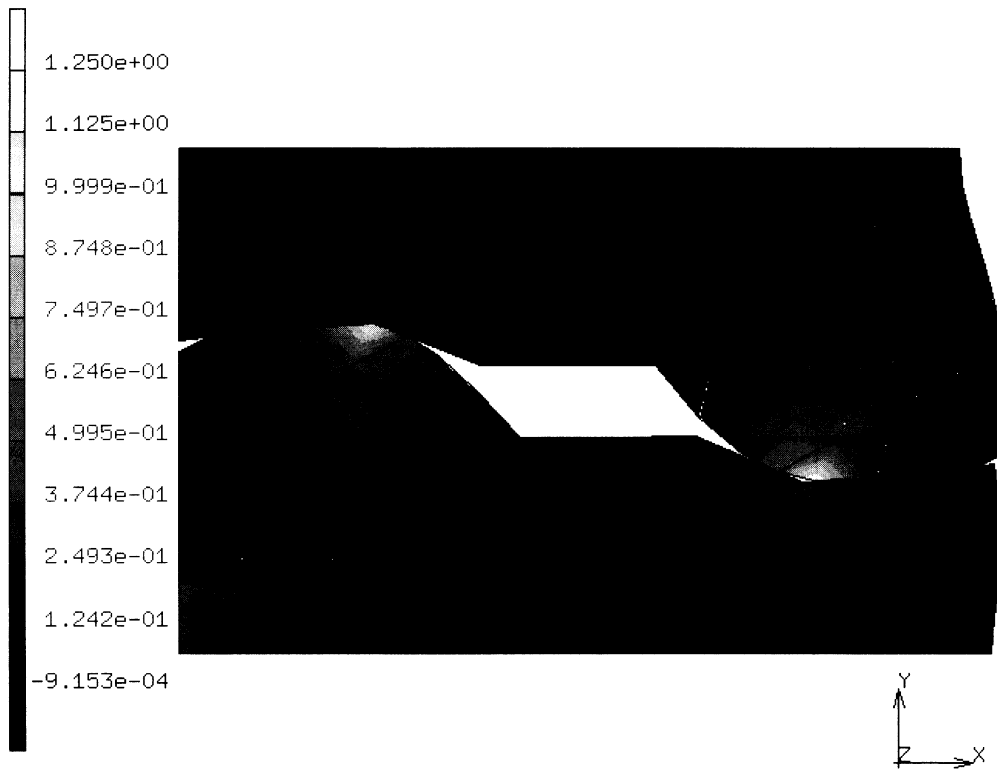
Inc : 50
Time : 9.044e-01



e8x15d - FeFp plasticity

Figure 8.15-14 Deformed Geometry at Increment 50 for Data Set e8x15d

Inc : 53
Time : 1.000e+00



e8x15d - FeFp plasticity
Total Equivalent Plastic Strain

Figure 8.15-15 Contours of Total Equivalent Plastic Strain on Final Geometry for Data Set e8x15d



8.16 Demonstration of Springback

A metal part is formed and the springback is examined. A large strain elastic plastic analysis is performed.

This problem is modeled using the two data sets summarized below.

Data Set	Element Type(s)	Number of Elements	Number of Nodes	Differentiating Features
e8x16	11	147	178	Mean Normal Additive Decomposition Plasticity
e8x16b	11	147	178	Radial Return F^cF^p Plasticity

Model

The original part is shown in Figure 8.16-1 and is composed of 197 elements type 11 plane strain quadrilaterals. A rigid cylinder is used to deform the part.

Parameters

In the first analysis, the additive decomposition procedure is used. This is activated by using the LARGE DISP, FINITE, and UPDATE parameters.

In the second analysis, the multiplicative decomposition (F^cF^p) procedure is used. The PLASTICITY option is used. The PRINT, 5 option results in additional output regarding contact.

Geometry

The '1' in the second field invokes the constant dilatation option. This gives improved behavior for nearly incompressible behavior that occurs during plastic deformation. The '1' in the third field invokes the assumed strain formulation for element type 11. This gives improved behavior in bending which is the dominant mechanism in this problem. The geometry parameters are not necessary for the F^cF^p procedure.

Boundary Conditions

The left side is constrained in the first degree of freedom. A spring is used to constrain the motion in the y-degree of freedom, so there will not be any rigid body modes.

**Material Properties**

The part is made of aluminum with a Young's modulus of 10.6E+6 psi. The material strain hardens such that at 5.8% strain the flow stress will be 50,355 psi. It is important that the first stress in the WORK HARD DATA be the same as given through the ISOTROPIC option.

Contact

Two contact bodies are defined. The first is the deformable body, consisting of 147 elements. The second body is the rigid pin, defined as four circular arcs. Each arc is subdivided into ten segments. The circular pin has a velocity of 0.2 in/second.

Control

The full Newton-Raphson procedure is used in this analysis. Displacement control is requested with a tolerance of 2%. The Cuthill-McKee method is used to minimize the bandwidth. The post file frequency is specified through the POST and POST INCREM options. For data set e8x16, the post file was written at increments 0(default), 18 and 19. For data set e8x16b, the post file is written for every increment.

For data set e8x16, the AUTO LOAD and TIME STEP options are used to use 18 increments with a time step of 0.10 seconds. At this point, the pin is removed from the model allowing the workpiece to elastically springback. For data set e8x16b, the AUTO STEP option is used to impose the loading prior to springback.

Release

After the deformation, the rigid pin is removed from the hook and springback occurs. In the first analysis, this is done in one step by using the RELEASE and MOTION CHANGE options. The RELEASE option is used to ensure that all of the nodes separate from body 2, the rigid pin. In the second analysis, the rigid body is released, but the contact forces are gradually brought to zero over five increments. This is performed by using the RELEASE and AUTO LOAD options. This procedure is often advantageous as often the contact forces are quite large and cannot be redistributed in one increment. The MOTION CHANGE option is used to move the pin away from the body, so that it will not make any further contact.

Results

The deformed shape at increment 18 is shown in Figure 8.16-2. The stresses at this point are shown in Figure 8.16-3. After release of the pin, there is a slight amount of springback. Recall that the elastic strain is, at the most, $5.4 \text{ E}4/10.6\text{E}6 = 0.5\%$ which will limit the amount of springback.

For data set e8x16b, the deformed shape in increment 53 is shown in Figure 8.16-4. The contours of equivalent von Mises stress are shown in Figure 8.16-5 for increment 53.



Parameters, Options, and Subroutines Summary

Example e8x16.dat:

Parameters	Model Definition Options	History Definition Options
ELEMENT	CONNECTIVITY	AUTO LOAD
END	CONTACT	CONTINUE
FINITE	CONTROL	POST INCREMENT
LARGE DISP	COORDINATES	RELEASE
PRINT	END OPTION	TIME STEP
SIZING	FIXED DISP	
TITLE	GEOMETRY	
UPDATE	ISOTROPIC	
	OPTIMIZE	
	POST	
	PRINT CHOICE	
	WORK HARD	

Example e8x16b.dat:

Parameters	Model Definition Options	History Definition Options
ELEMENT	CONNECTIVITY	AUTO LOAD
END	CONTACT	AUTO STEP
FINITE	CONTROL	CONTINUE
LARGE DISP	COORDINATES	MOTION CHANGE
PRINT	END OPTION	POST INCREMENT
SIZING	FIXED DISP	RELEASE
TITLE	GEOMETRY	TIME STEP
UPDATE	ISOTROPIC	
	OPTIMIZE	
	POST	
	PRINT CHOICE	
	WORK HARD	

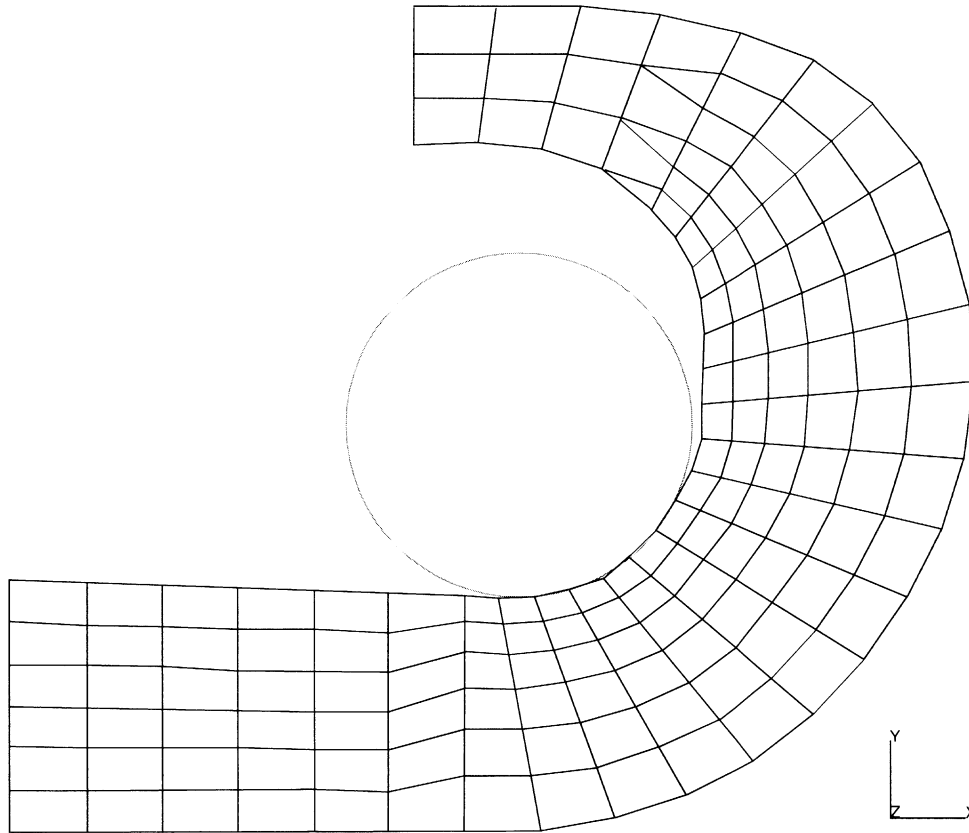
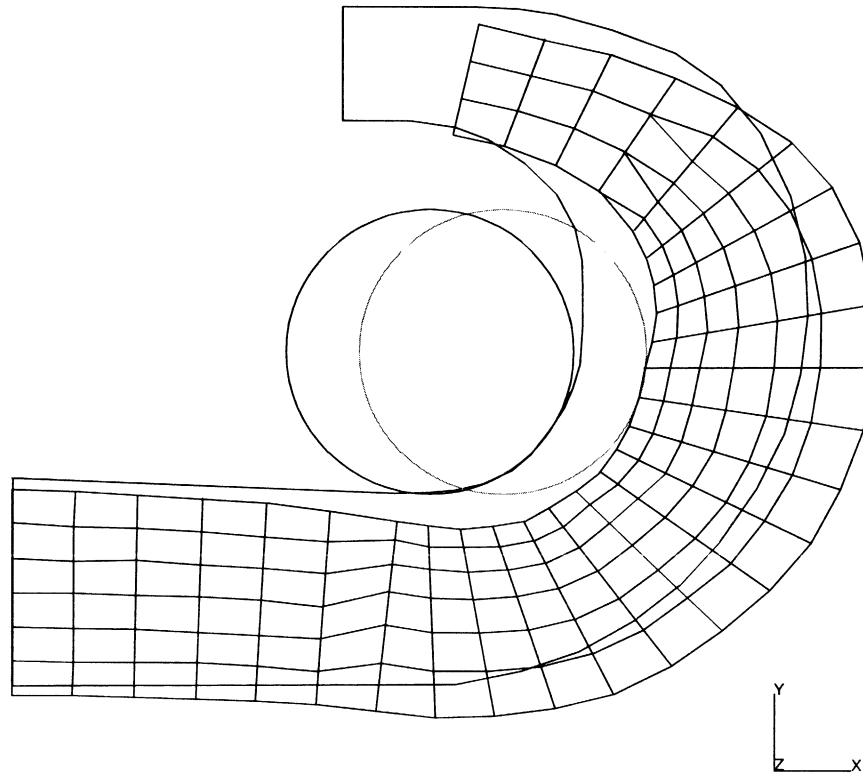


Figure 8.16-1 Original Configuration



INC : 18
SUB : 0
TIME : 1.800e+01
FREQ : 0.000e+00



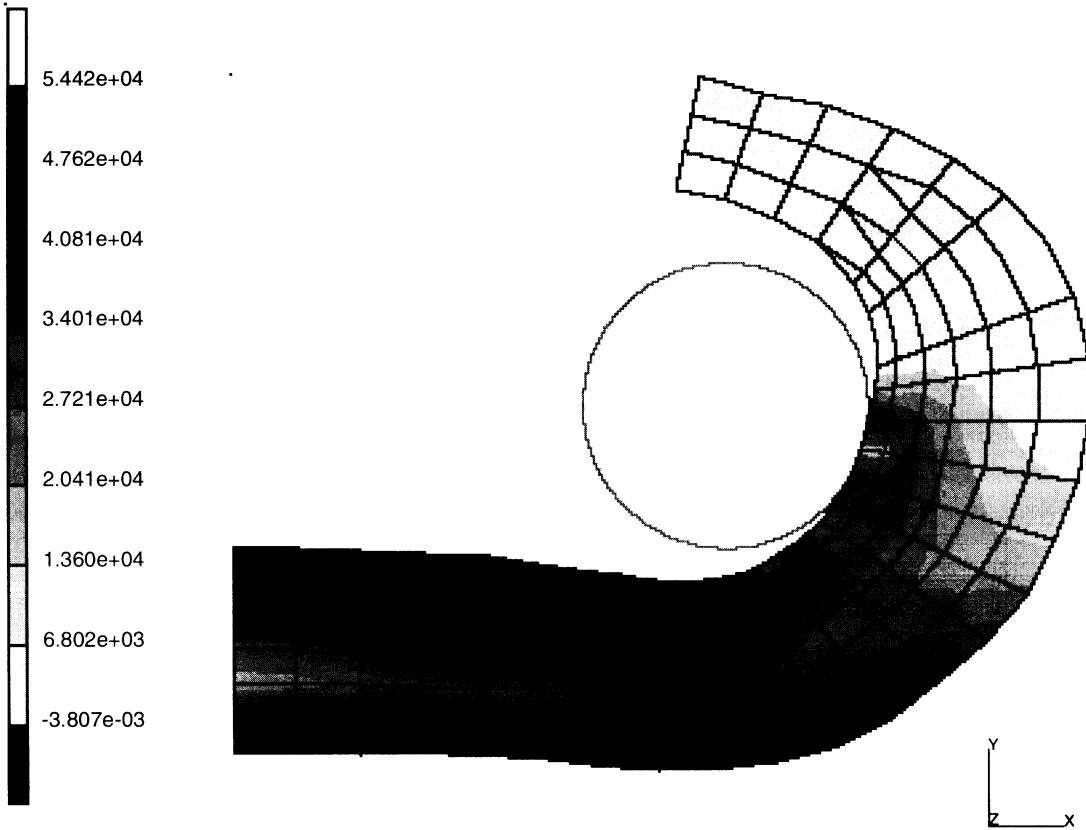
prob e8.16 double sided of spring back

Displacement x

Figure 8.16-2 Deformed Mesh



INC : 18
SUB : 0
TIME : 1.800e+00
FREQ : 0.000e+00



prob e8.16 demonstration of spring back

Equivalent von Mises Stress

Figure 8.16-3 Equivalent Stress

Inc : 53
Time : 1.800e+00

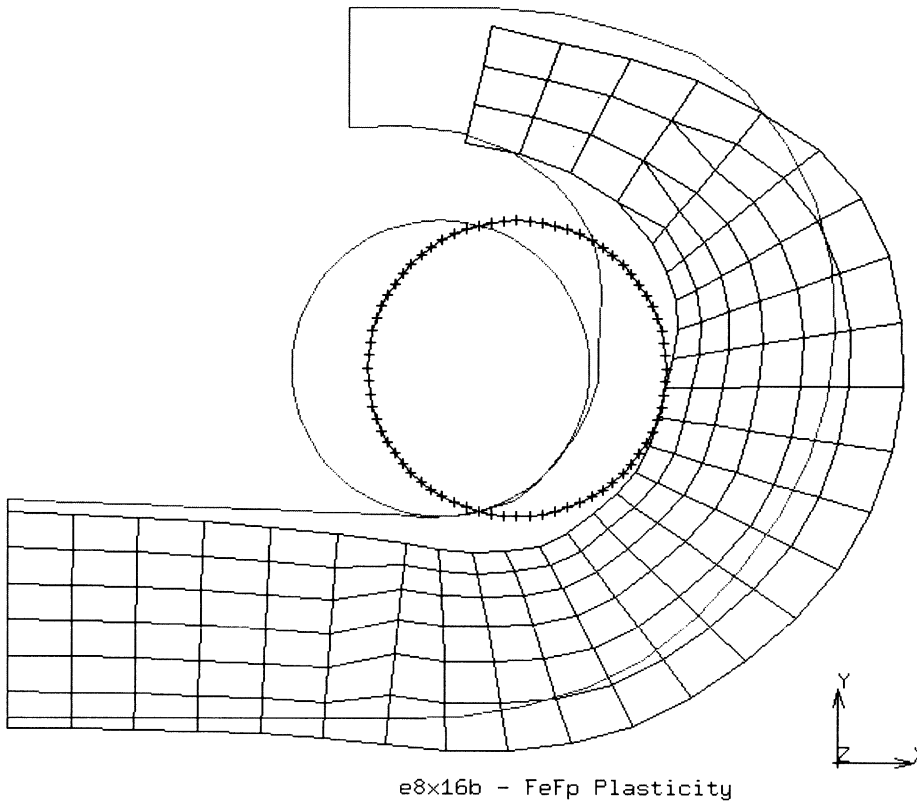


Figure 8.16-4 Initial and Deformed Geometry 53 Increments for Data Set e8x16b

Inc : 53
Time : 1.800e+00

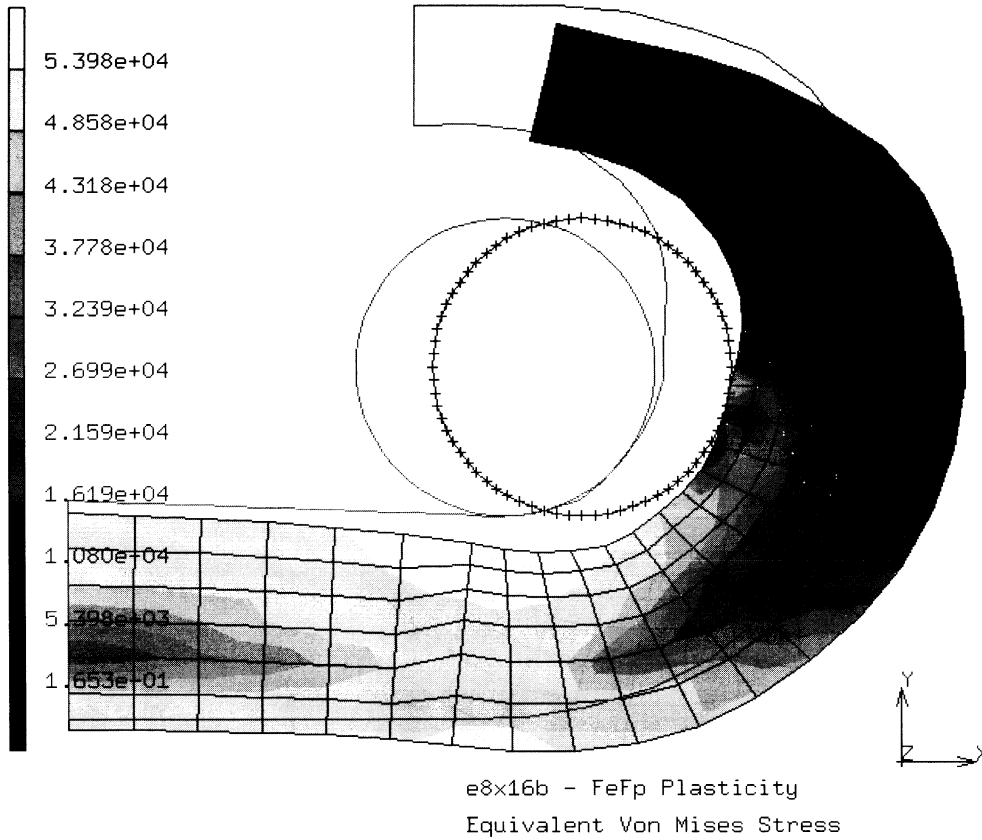


Figure 8.16-5 Contours of Equivalent von Mises Stress at 53 Increments for Data Set e8x16b



8.17 3D Extrusion Analysis with Coulomb Friction

This problem demonstrates MARC's ability to perform metal extrusion analysis using the CONTACT option. The analysis is complicated by the multiple intersecting contact surfaces.

This problem is modeled using the two data sets summarized below.

Data Set	Element Type(s)	Number of Elements	Number of Nodes	Differentiating Features
e8x17	7	16	45	Mean Normal Additive Decomposition Plasticity, CONSTANT DILATATION
e8x17b	7	16	45	Radial Return F^cF^p Plasticity

Parameters

In the first analysis, the UPDATE, FINITE, and LARGE DISP parameters are included in the parameter section to indicate this is a finite deformation analysis. The PRINT,8 option requests the output of additional information concerning contact. The REZONE parameter is included to allow the potential for future mesh rezoning to compensate for gross distortions in the original mesh.

In the second analysis, the PLASTICITY option is used to invoke the multiplicative decomposition (F^cF^p) procedure for finite strain plasticity.

Geometry

Element type 7, the eight-node brick element, is used in this analysis. For the first analysis, a '1' is placed in the second data field (EGEOM2) of the third data block of the GEOMETRY option to indicate that the constant dilatation formulation is used. This is done in recognition of the fact that metal extrusion results in large plastic deformations which are nearly incompressible. This is not necessary in the second analysis as the F^cF^p procedure used a mixed variational principal that accurately accounts for incompressibility.

Boundary Conditions

Appropriate nodal constraints are applied in the global X, Y directions to impose symmetry. The billet is extruded by having a constant velocity imposed.

POST/RESTART

The following variables are written to a formatted post file every 35 increments:

7} Equivalent plastic strain 17} Equivalent von Mises stress

The last converged increment is written to a restart file.

Control

A maximum of 200 increments are to be carried out, with no more than 20 recycles per increment. Displacement control is used, with a relative error of 10%.

Material Properties

The material for all elements is treated as an elastic-perfectly plastic material, with Young's modulus of 1.75E+07 psi, Poisson's ratio of 0.3, and an initial yield stress of 35,000 psi.

Contact

This option declares that there are three bodies in contact with Coulomb friction between them. In particular, the friction coefficient associated with each rigid die is 0.1. The relative slip velocity is 0.01 inch/second. The contact tolerance distance is 0.01 inches.

The three contact bodies are defined as follows:

Body 1: The deformable body consisting of 16 brick elements. Note that the velocity cannot be entered for a deformable body.

Body 2: A single plane is used to represent the ram and is given a velocity of -0.3 in/sec.

Body 3: Six planes are used to define the die.

Load Control

In the first analysis, the problem is loaded by the repeated application of the prescribed die velocities with the AUTO LOAD option. The load increment is applied 70 times. The TIME STEP option allows you to enter the time variable for static analysis should time dependent constitutive relations be used.

In the second analysis, the AUTO STEP option is used to adaptively change the time step.

Results

Figure 8.17-1 show the geometry configuration for the extrusion analysis. Figure 8.17-2 and Figure 8.17-3 shows the deformed body at the end of 35 increments with the deformation at the same scale as the coordinates. Due to the high level of friction, significant transverse deformation is shown along the contact surfaces.

Figure 8.17-4 and Figure 8.17-5 show the deformed body at the end of 70 increments.

Figure 8.17-6 shows the equivalent plastic strain contours on the deformed structure at increment 70 with the largest strain level at 0.705.

Figure 8.17-7 shows the equivalent von Mises stress contours on the deformed structure at increment 70 with peak values at 37,820 psi.

Figure 8.17-8 shows the contours of equivalent plastic strain at increment 199 for data set e8x17b.

Figure 8.17-9 shows the contours of von Mises effective stress at increment 199 for data set e8x17b.

The comparison of von Mises stresses and equivalent plastic strains show a very close agreement.



Parameters, Options, and Subroutines Summary

Example e8x17.dat:

Parameters	Model Definition Options	History Definition Options
ELEMENT	CONNECTIVITY	AUTO LOAD
END	CONTACT	CONTINUE
FINITE	CONTROL	TIME STEP
LARGE DISP	COORDINATE	
PRINT	END OPTION	
REZONE	FIXED DISP	
SIZING	GEOMETRY	
TITLE	ISOTROPIC	
UPDATE	POST	
	PRINT CHOICE	
	RESTART LAST	

Example e8x17b.dat:

Parameters	Model Definition Options	History Definition Options
ELEMENT	CONNECTIVITY	AUTO STEP
END	CONTACT	CONTINUE
FINITE	CONTROL	
LARGE DISP	COORDINATE	
PRINT	END OPTION	
REZONE	FIXED DISP	
SIZING	GEOMETRY	
TITLE	ISOTROPIC	
UPDATE	POST	
	PRINT CHOICE	
	RESTART LAST	

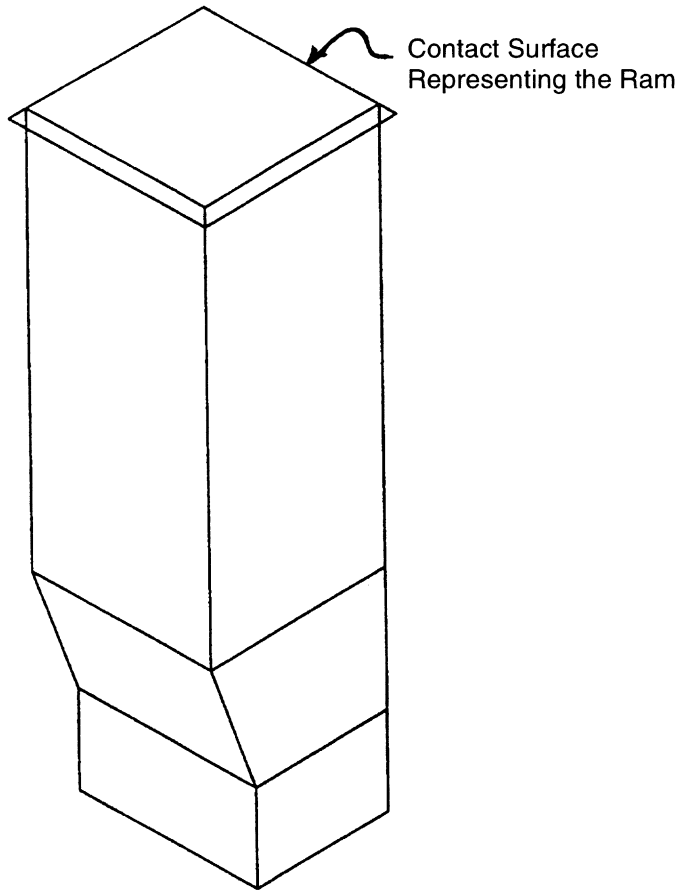
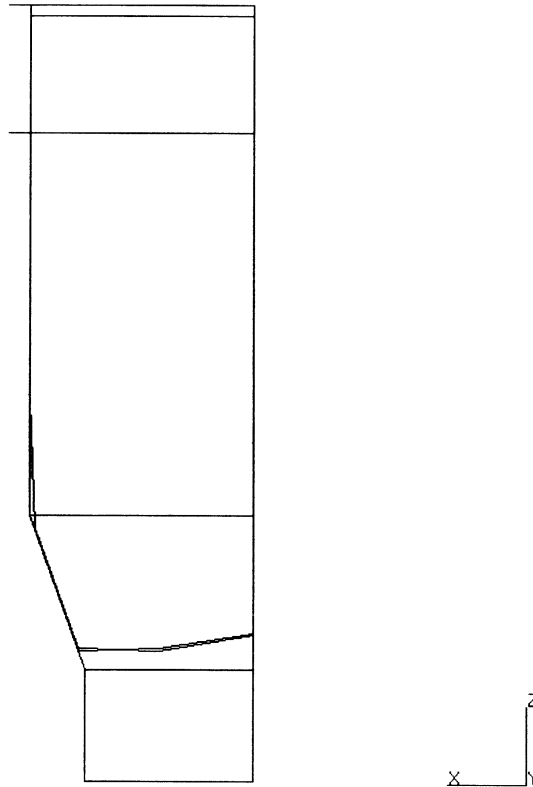


Figure 8.17-1 Rigid Surfaces Defining Extrusion Die



INC : 35
SUB : 0
TIME : 3.833e+01
FREQ : 0.000e+00

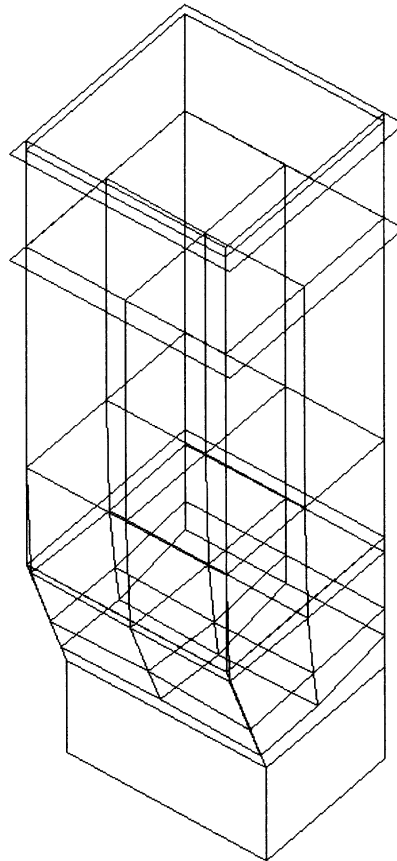


prob e8.17 extrusion analysis
Displacements z

Figure 8.17-2 Deformed Mesh, Increment 35



INC : 35
SUB : 0
TIME : 3.833e+01
FREQ : 0.000e+00



prob e8.17 extrusion analysis
Displacements z

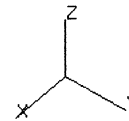
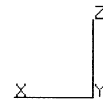
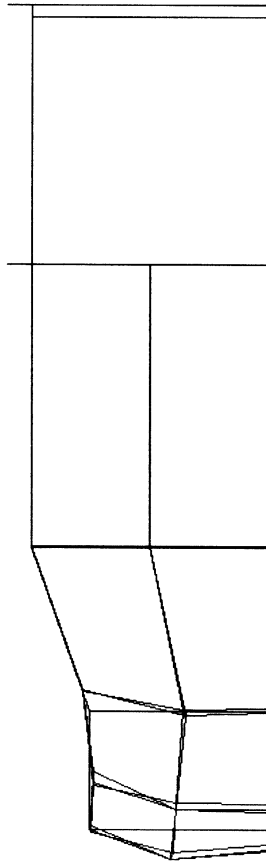


Figure 8.17-3 Deformed Mesh, Increment 35



INC : 70
SUB : 0
TIME : 7.333e+01
FREQ : 0.000e+00



prob e8.17 extrusion analysis
Displacements z

Figure 8.17-4 Deformed Mesh, Increment 70

INC : 70
SUB : 0
TIME : 7.333e+01
FREQ : 0.000e+00

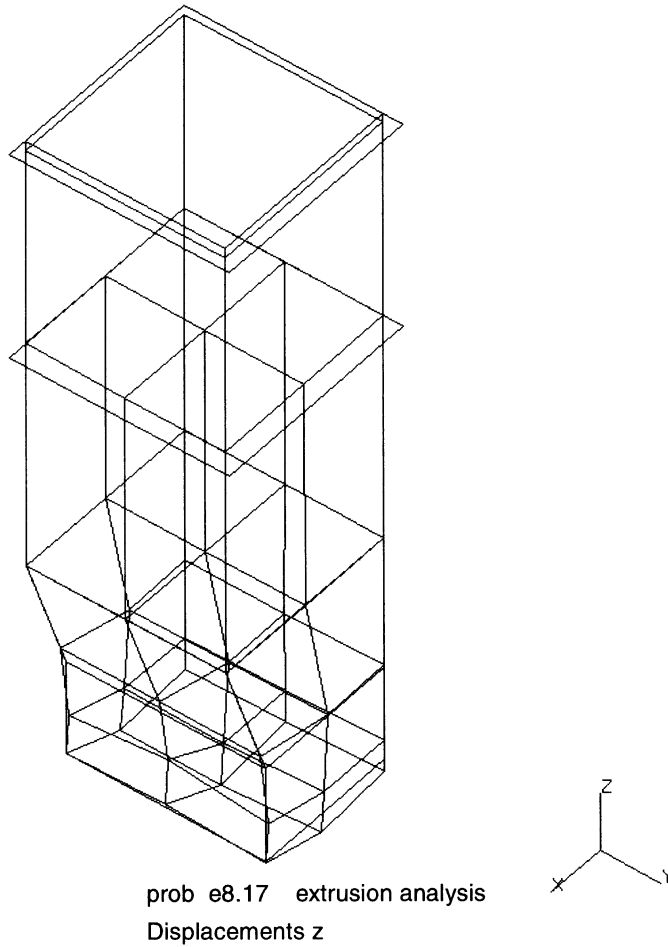


Figure 8.17-5 Deformed Mesh, Increment 70



Inc : 70
Time : 7.000e+01

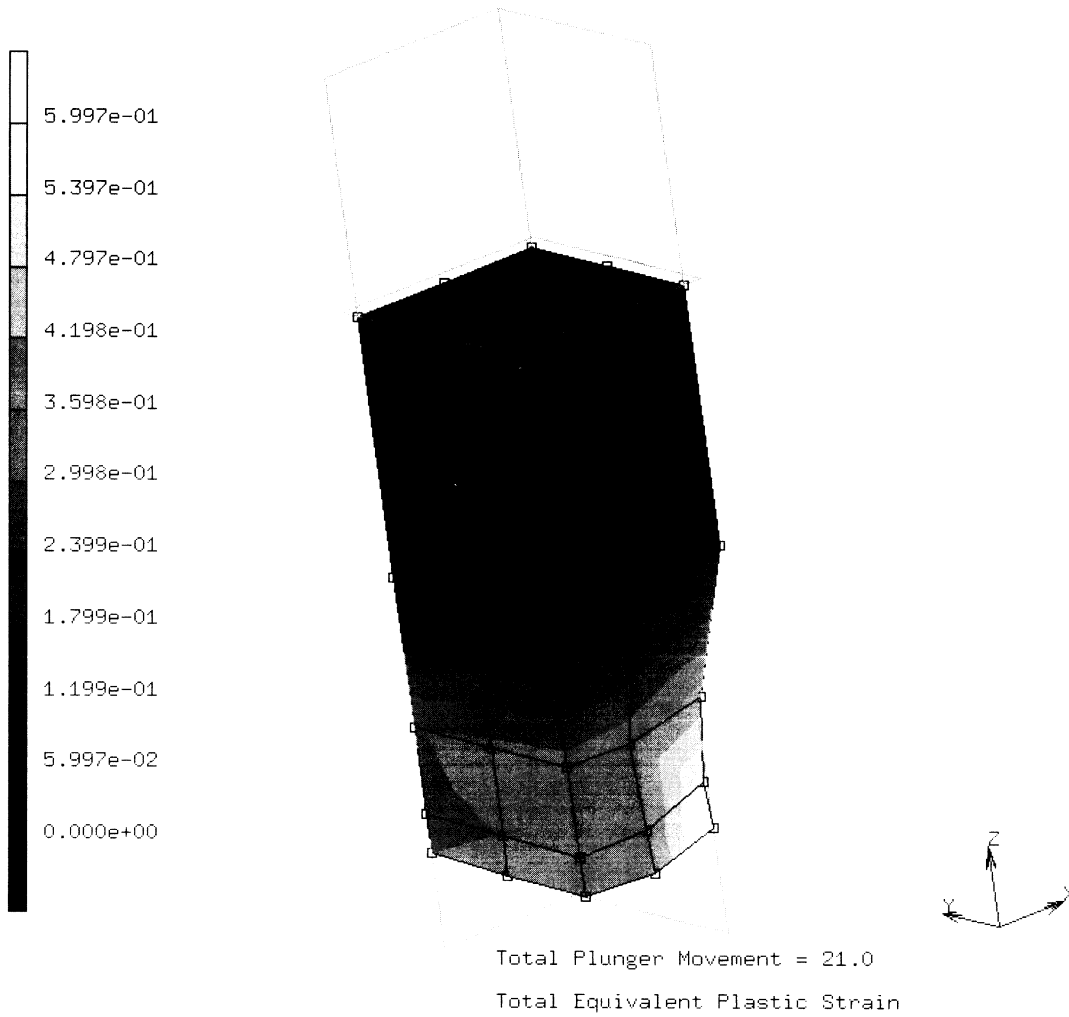


Figure 8.17-6 Equivalent Plastic Strain, Increment 70

Inc : 70
Time : 7.000e+01

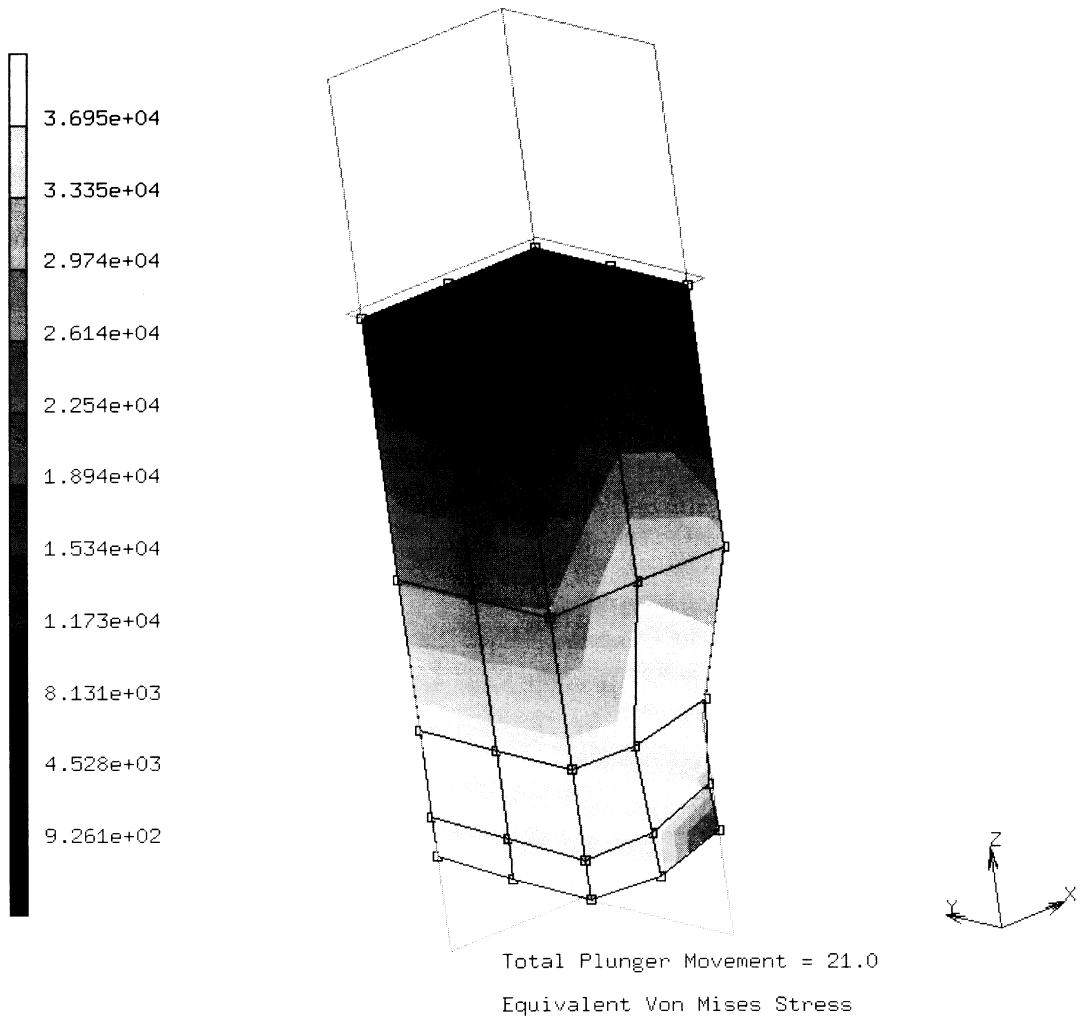


Figure 8.17-7 Equivalent Stress, Increment 70

Inc : 151
Time : 7.014e+00

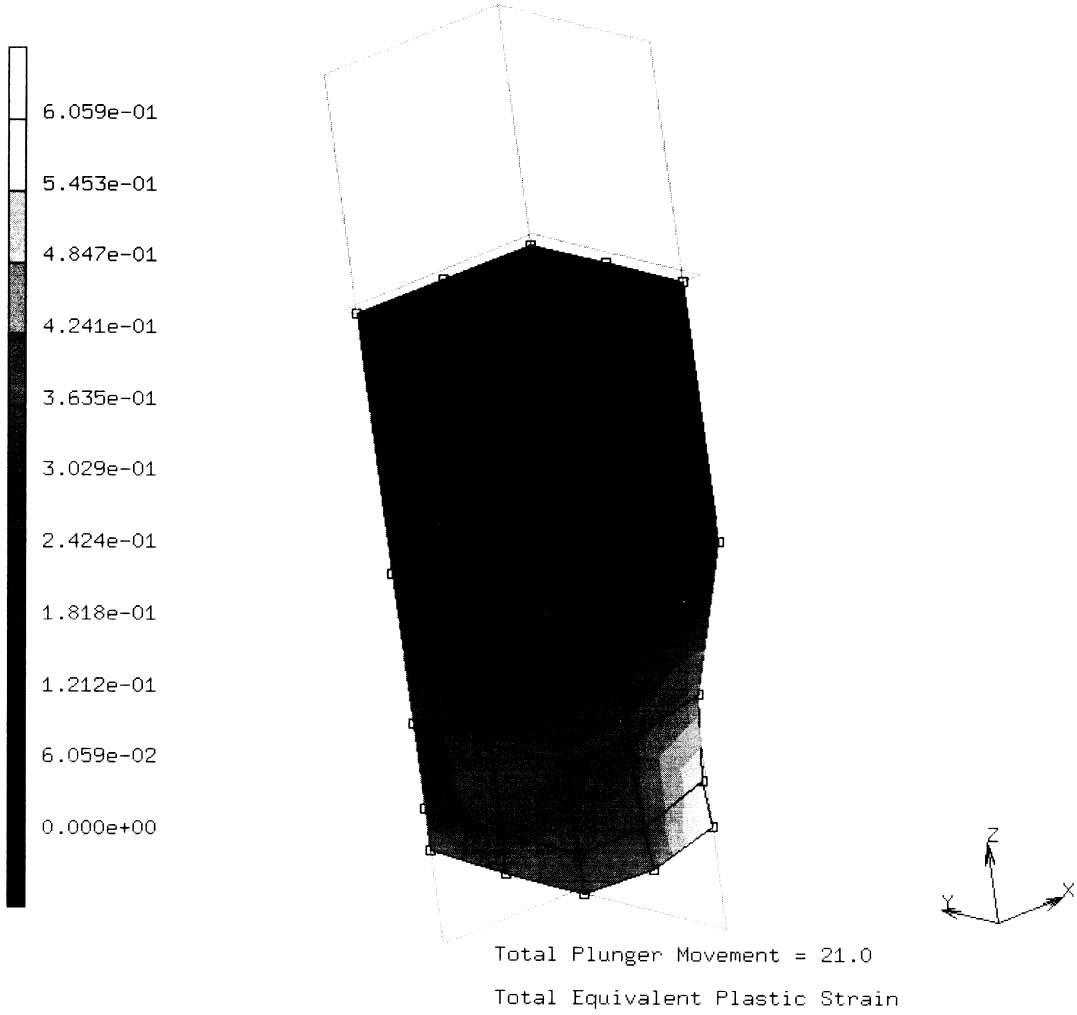


Figure 8.17-8 Equivalent Plastic Strain at Increment 199 for Data Set e8x17b

Inc : 151
Time : 7.014e+00

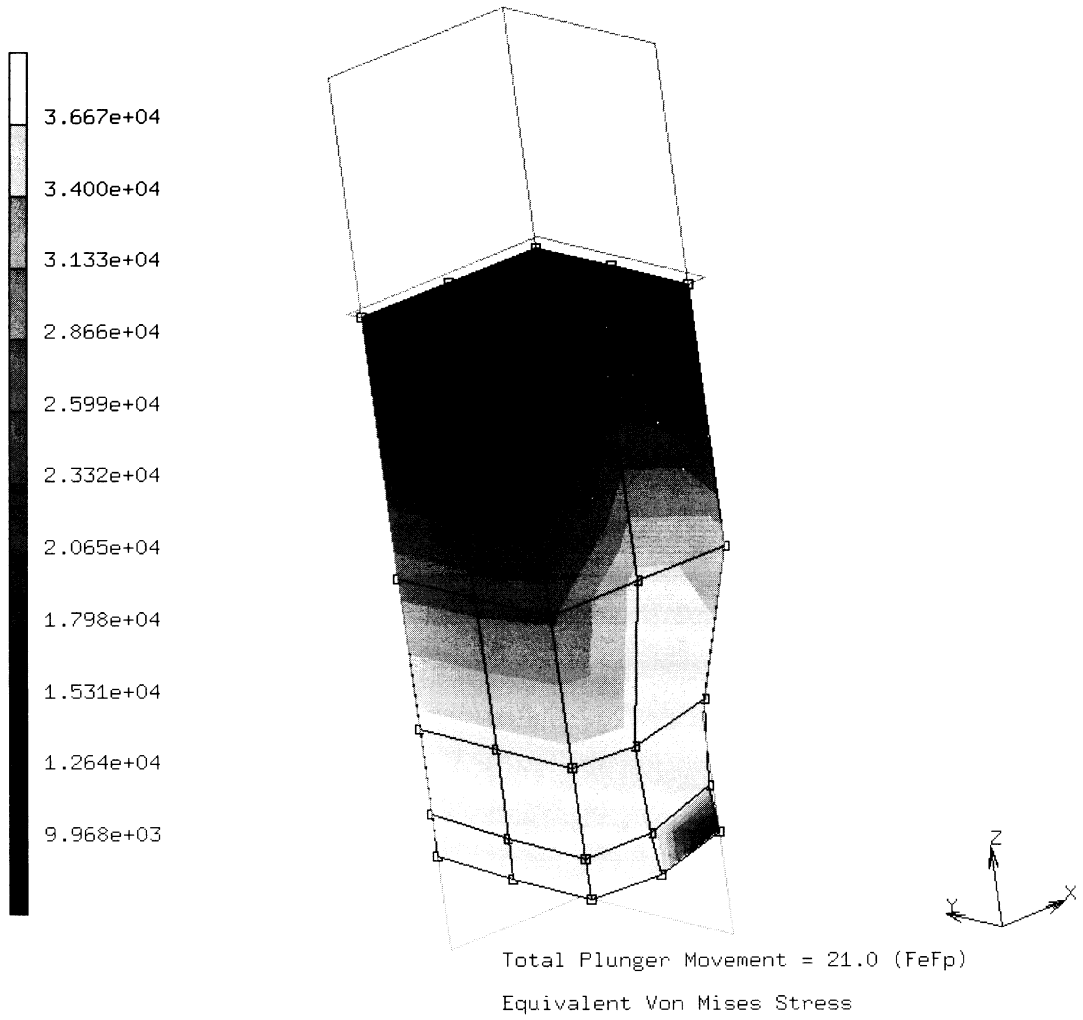


Figure 8.17-9 Equivalent von Mises Effective Stress at Increment 199 for Data Set e8x17b



8.18 3D Forming of a Circular Blank Using Shell or Membrane Elements and Coulomb Friction

This problem demonstrates MARC's ability to perform stretch forming by a spherical punch using the CONTACT option with shell or membrane elements.

This problem is modeled using the four techniques summarized below.

Data Set	Element Type(s)	Number of Elements	Number of Nodes	Differentiating Features
e8x18	75	112	127	Mean Normal Additive Decomposition Plasticity Piecewise Linear Representation of Rigid Surfaces
e8x18b	75	112	127	Mean Normal Additive Decomposition Plasticity with Analytical Representation for Rigid Surfaces
e8x18c	18	112	127	Multiplicative Decomposition $F_e F_p$ Plasticity, Membrane Elements, Piecewise Linear Representation of Rigid Surfaces
e8x18d	75	112	127	Mean Normal Additive Decomposition Plasticity, Analytical Representation for Rigid Surfaces, AUTO STEP option controls loading

Parameters

Problems e8x18a, e8x18b, and e8x18d use the UPDATE, LARGE DISP, and FINITE parameters to indicate a finite deformation analysis. These three problems also use the 4-node thick shell element, element type 75. Seven layers are used through the shell thickness. Problem e8x18c uses element 18, a 4-node membrane element. Radial return multiplicative decomposition finite strain plasticity is used in problem e8x18c.

Geometry

A shell thickness of 1 cm is specified through the GEOMETRY option in the first field (EGEOM1).

Boundary Conditions

The first boundary condition is used to model the binding in the stretch forming process. The second and third boundary conditions are used to represent the symmetry conditions.

**POST**

The following variables are written to a formatted post file:

- 7} Equivalent plastic strain
- 17} Equivalent von Mises stress
- 20} Element thickness

Furthermore, the above three variables are also requested for all shell elements at layer number 4, which is the midsurface.

Control

A full Newton-Raphson iterative procedure is requested, along with the mean normal method approach to solve plasticity equations. Displacement control is used, with a relative error of 5%. Twenty-six load steps are prescribed, with a maximum of twenty recycles (iterations) per load step.

Material Properties

The material for all shell elements is treated as an elastic-plastic material, with Young's modulus of 690,040 lbf/cm², Poisson's ratio of 0.3, and an initial yield stress of 80.6 lbf/cm². The yield stress is given in the form of a power law and is defined through the WKSLP user subroutine. For membrane element problem e8x18c, a constant workhardening modulus of 100 ksi is used.

Contact

This option declares that there are three bodies in contact with Coulomb friction between them. A coefficient of friction of 0.3 is associated with each rigid die. The first body represents the workpiece. The second body is the lower die, defined as three surfaces of revolution. The first and third surfaces of revolution use a straight line as the generator, the second uses a circle as the generator. In examples e8x18a and e8x18c, the third body (the punch) is defined as two surfaces of revolution. These surfaces are extended from -0.5 to 101.21 degrees. In examples e8x18b and e8x18d, the third body (the punch) is represented by a sphere. Its initial center is at 0, 0, 51.3 and the radius is 50. In problems e8x18 and e8x18c, the rigid surfaces are discretized into 4-node patches. This results in a piecewise-linear representation of the surface. In e8x18b and e8x18d, the analytical form is used. This results in a smooth representation of the surface. The relative slip velocity is specified as 0.01 cm/sec. The contact tolerance distance is 0.05 cm.

Load Control

This problem is displacement controlled with a velocity of 1 cm/sec applied in the negative z-direction with the AUTO LOAD option. The load increment is applied 40 times. The MOTION CHANGE option is illustrated to control the velocity of the rigid surfaces.



Results

Figure 8.18-2 shows the deformed body at the end of 40 increments with the deformation at the same scale as the coordinates. Due to the high level of friction, significant transverse deformation is shown along the contact surfaces.

Figure 8.18-3 shows the equivalent plastic strain contours on the deformed structure at increment 40, with the largest strain level at 60%.

Figure 8.18-4 shows the equivalent von Mises stress contours on the deformed structure at increment 40 with peak values at 527.4 lbf/cm².

Figure 8.18-5 shows the deformed body at the end of 40 increments. The computational performance and results are improved by using the analytical form.

Figure 8.18-6 shows the deformed geometry with contours of total effective plastic strain for data set e8x18c which uses membrane elements.

Figure 8.18-7 shows the final deformed geometry with contours of total effective plastic strain for data set e8x18d.

Parameters, Options, and Subroutines Summary

Example e8x18.dat:

Parameters	Model Definition Options	History Definition Options
ELEMENT	CONNECTIVITY	AUTO LOAD
END	CONTACT	CONTINUE
FINITE	CONTROL	MOTION CHANGE
LARGE DISP	COORDINATE	TIME STEP
PRINT	END OPTION	
SHELL SECT	FIXED DISP	
SIZING	GEOMETRY	
TITLE	ISOTROPIC	
UPDATE	POST	
	PRINT CHOICE	
	WORK HARD	



Example e8x18b.dat:

Parameters	Model Definition Options	History Definition Options
ELEMENTS	CONNECTIVITY	AUTO LOAD
END	CONTACT	CONTINUE
FINITE	CONTROL	MOTION CHANGE
LARGE DISP	COORDINATE	TIME STEP
PRINT	END OPTION	
SHELL SECT	FIXED DISP	
SIZING	GEOMETRY	
TITLE	ISOTROPIC	
UPDATE	POST	
	PRINT CHOICE	
	WORK HARD	

Example e8x18c.dat:

Parameters	Model Definition Options	History Definition Options
ELEMENTS	CONNECTIVITY	AUTO LOAD
END	CONTACT	CONTINUE
PLASTICITY	CONTROL	MOTION CHANGE
LARGE DISP	COORDINATE	TIME STEP
PRINT	END OPTION	
SIZING	FIXED DISP	
TITLE	GEOMETRY	
ALIAS	ISOTROPIC	
	POST	
	PRINT CHOICE	
	WORK HARD	



Example e8x18d.dat:

Parameters

ELEMENTS
END
FINITE
LARGE DISP
PRINT
SHELL SECT
SIZING
TITLE
UPDATE

Model Definition Options

CONNECTIVITY
CONTACT
CONTROL
COORDINATE
END OPTION
FIXED DISP
GEOMETRY
ISOTROPIC
POST
PRINT CHOICE
WORK HARD

History Definition Options

AUTO STEP
CONTINUE
MOTION CHANGE
TIME STEP

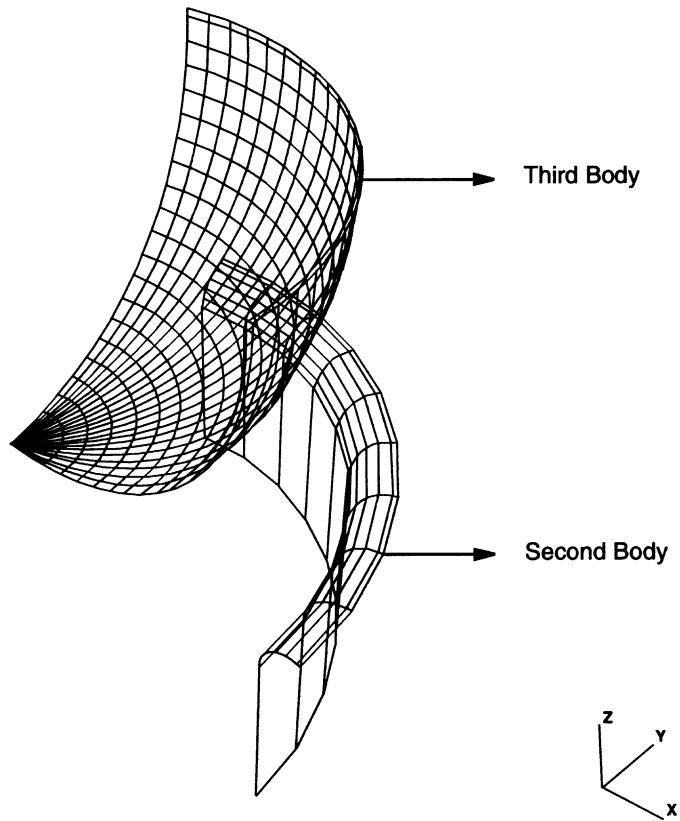


Figure 8.18-1 Circular Blank Holder and Punch



INC : 40
SUB : 0
TIME : 4.000e+01
FREQ : 0.000e+00

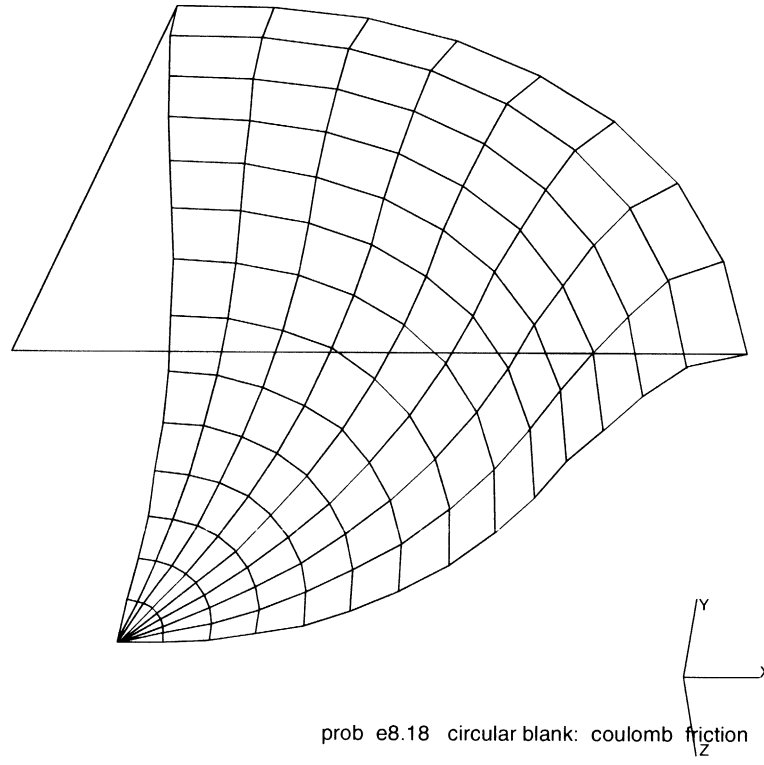
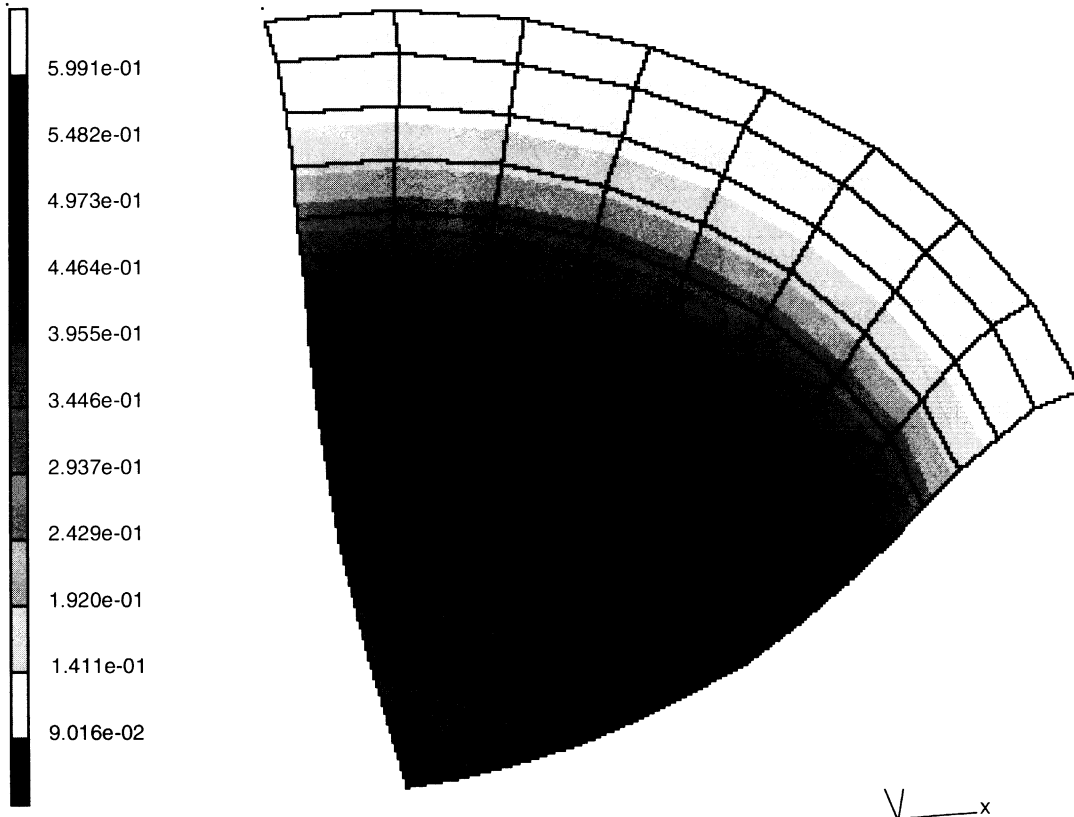


Figure 8.18-2 Deformed Sheet at Increment 40



INC : 40
SUB : 0
TIME : 4.000e+01
FREQ : 0.000e+00



prob e8.18 circular blank: coulomb friction
Equivalent Plastic Strain Layer 4

Figure 8.18-3 Plastic Strain at Increment 40



INC : 40
SUB : 0
TIME : 4.000e+01
FREQ : 0.000e+00

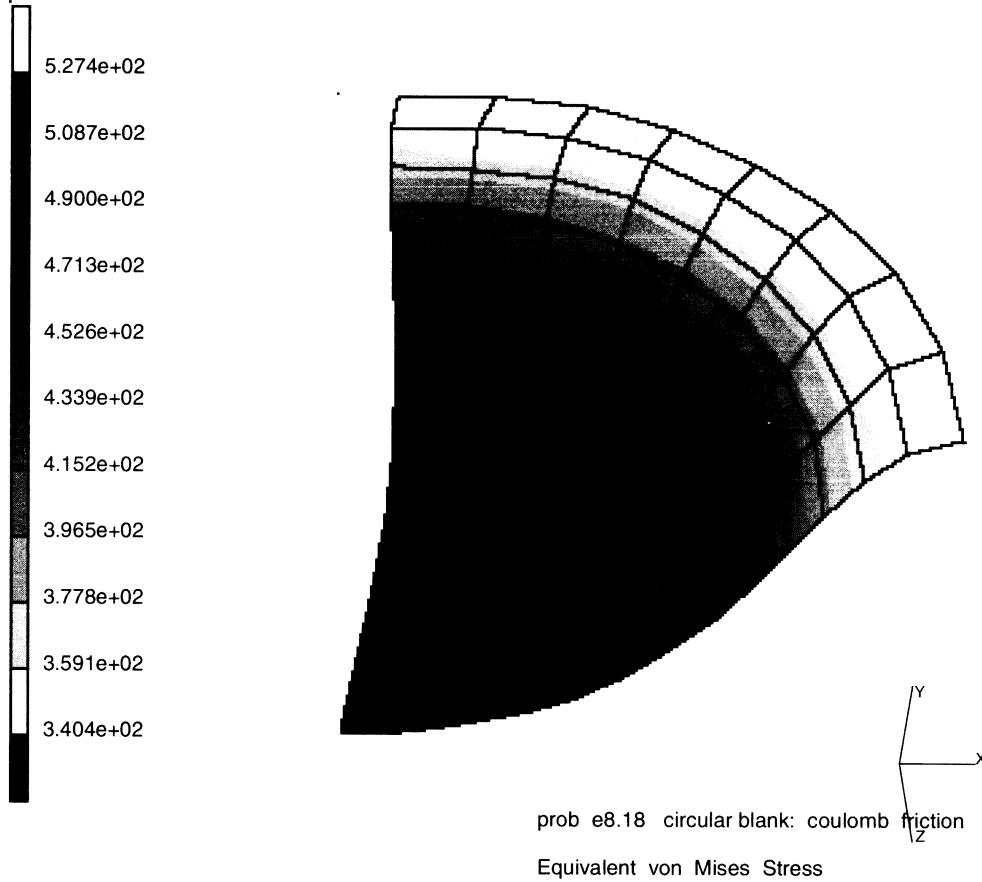


Figure 8.18-4 Equivalent Stress at Increment 40

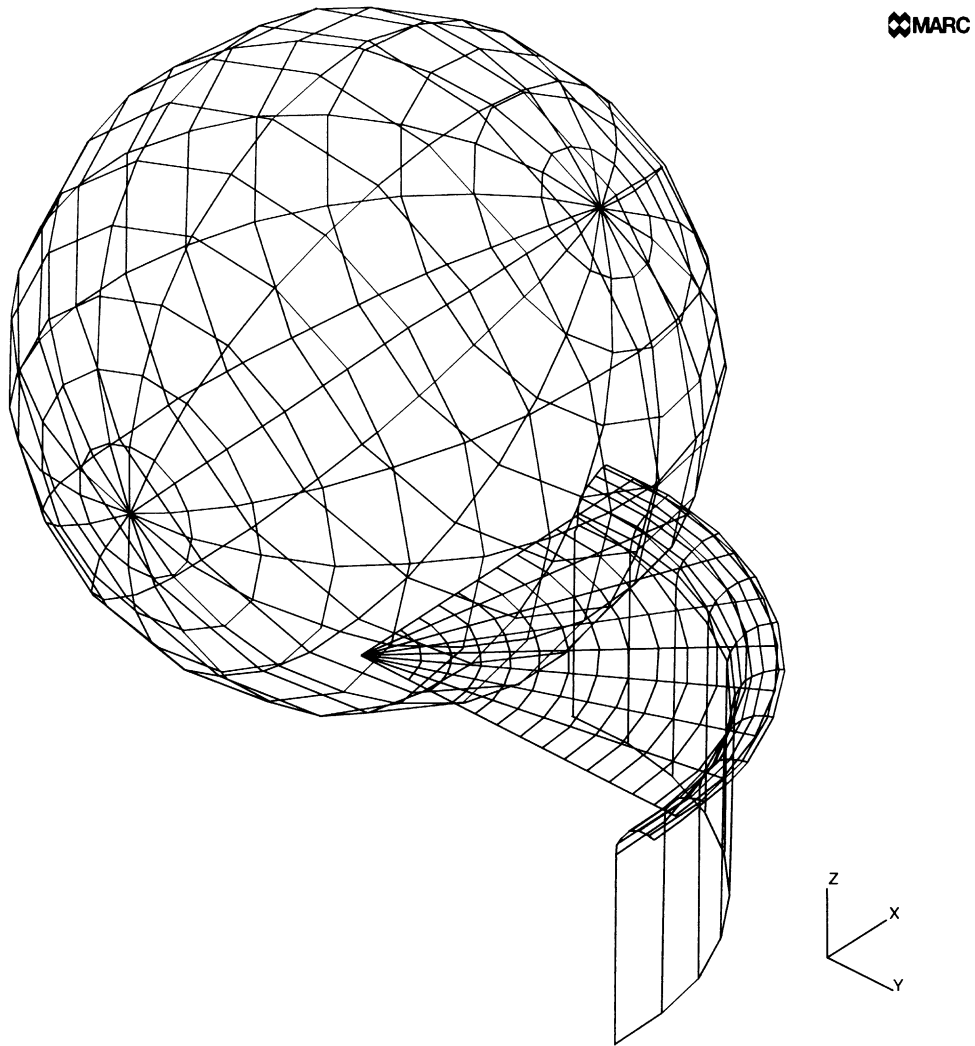


Figure 8.18-5 Analytical Form of Rigid Contact Surfaces



Inc : 110
Time : 4.000e+01

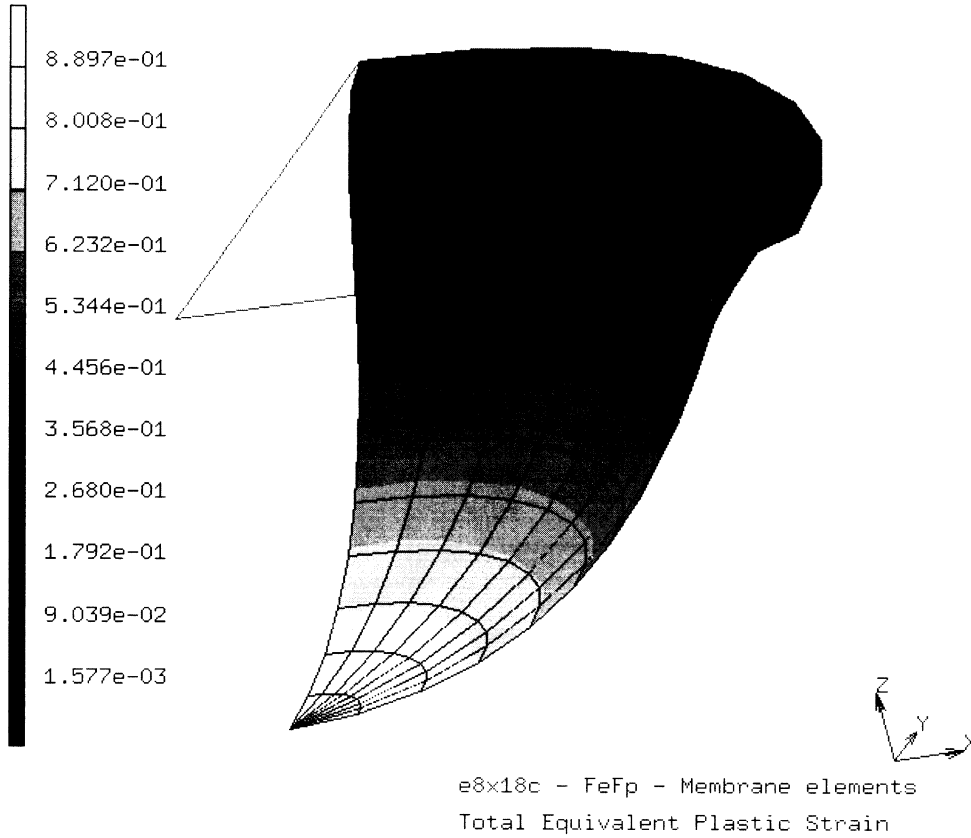


Figure 8.18-6 Final Deformed Geometry for Data Set e8x18c



Inc : 200
Time : 7.880e+01

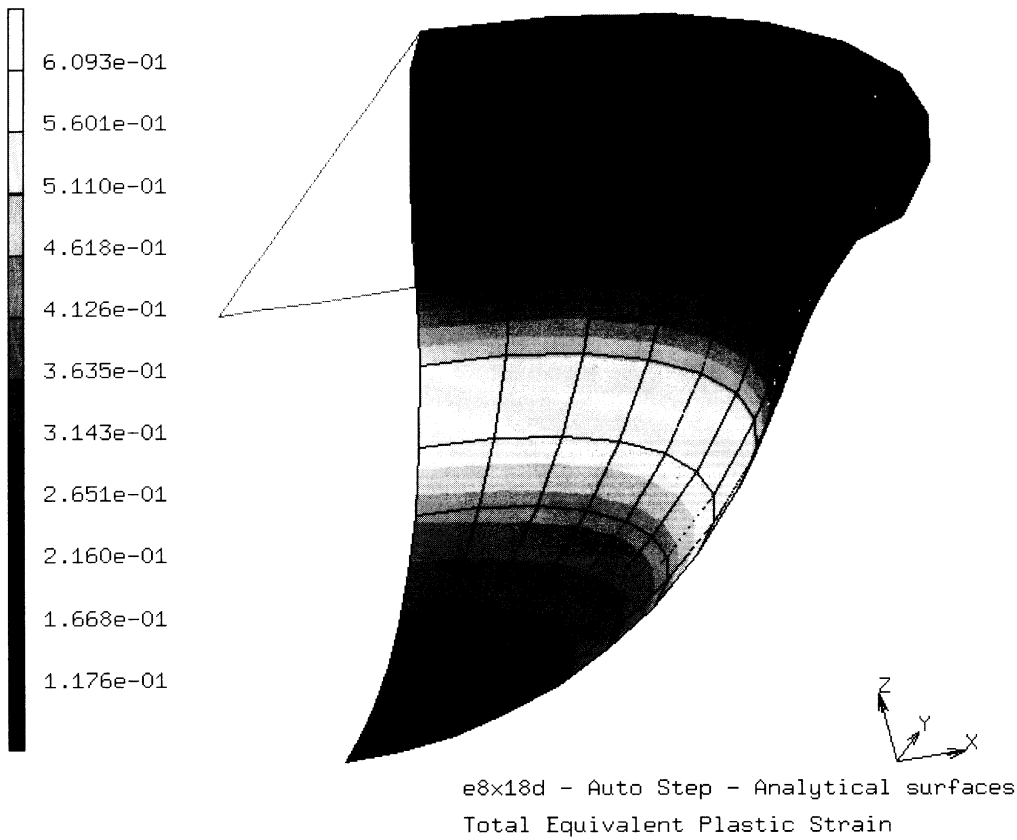


Figure 8.18-7 Final Deformed Geometry for Data Set e8x18d



8.19 3D Indentation and Rolling without Friction

This problem demonstrates the program’s ability to perform metal forming analyses (for example, rolling) using the CONTACT option. Large plastic deformation is anticipated in this analysis.

This problem is modeled using the two techniques summarized below.

Data Set	Element Type(s)	Number of Elements	Number of Nodes	Differentiating Features
e8x19	7	128	225	Additive decomposition mean normal plasticity
e8x19b	7	128	225	Multiplicative decomposition (F^cF^p) radial return plasticity

Parameters

In the first analysis, the UPDATE, FINITE, and LARGE DISP parameters are used to indicate that the additive decomposition is to be used in the finite deformation analysis. In the second analysis, the PLASTICITY parameter is used to indicate that the multiplicative (F^cF^p) procedure is used. The PRINT,8 option requests the output of additional information regarding contact.

Geometry

The model consists of 128 brick elements, type 7. For the first analysis, a ‘1’ is placed in the second data field (EGEOM2) to indicate that the constant dilatation formulation is used. This is done in recognition of the fact that metal extrusion results in large plastic deformations which are nearly incompressible.

Boundary Conditions

Appropriate nodal constraints are applied in the global X, Y directions. Since the geometry and loading are symmetric in the Z direction, no boundary conditions are applied in that direction. A contact surface is used to represent this symmetry surface.

POST/PRINT Control

The following variables are written to a formatted post file:

- 11 σ_{XX}
- 12 σ_{YY}
- 13 σ_{ZZ}
- 17 Mean normal stress
- 7 Equivalent total plastic strain.



These variables are written every 12th increment. The PRINT CHOICE option selects element number 1 as the only one which will have printed output (every 12th increment, like the post file). Such output will be for integration points 1 and 5 only.

Material Properties

The material for all elements is treated as an elastic-plastic material, with Young's modulus of $1.75\text{E}+07$ psi, Poisson's ratio of 0.3, and an initial yield stress of 35,000 psi.

Contact

The first body is the deformable workpiece; the second is the rigid roller defined using the surface of revolution method. The radius is 10 inches. The third body is the symmetry surface. The contact tolerance distance is specified as 0.02 inches.

Load Control/Restart

Data sets e8x19 and e8x19b use the MOTION subroutine to specify the motion.

For data set e8x19, the rigid roll is pushed into the workpiece with a velocity of 0.25 in/sec for the first 25 increments. No motion is specified in the 26th increment. The total indentation is 6.25 inches. Following this, the roll is given an angular velocity of 0.05 radians/sec and a forward motion of 0.5 in/sec. A restart file is written at the end of increment 26.

For data set e8x19b, the rigid roll is pushed into the workpiece with a velocity of 0.25 in/sec for the first 110 increments. No motion is specified in the 111th increment. Following this, the roll is given an angular velocity of 0.05 radians/sec and a forward motion of 0.5 in/sec.

Since the problem involves large incremental changes of motion, many iterations may be required in each increment. A maximum of 20 recycles are chosen per increment. The convergence checking specifies a displacement increment relative norm with a tolerance of 0.10.

Results

Figure 8.19-1 shows the geometry configuration for this problem. The cylindrical rigid surface will be pushed into the deformable block that is resting on the flat rigid surface.

Figure 8.19-2, Figure 8.19-3, and Figure 8.19-4 show the deformed workpiece in increments 12, 24, and 36.

Figure 8.19-5 shows the equivalent total plastic strain for final deformed geometry for data set e8x19. Figure 8.19-6 shows the equivalent total plastic strain final deformed geometry for data set e8x19b. Figure 8.19-7 shows the von Mises for final deformed geometry for data set e8x19. Figure 8.19-8 shows the von Mises for final deformed geometry for data set e8x19b.



Parameters, Options, and Subroutines Summary

Example e8x19.dat:

Parameters	Model Definition Options	History Definition Options
ELEMENT	CONNECTIVITY	AUTO LOAD
END	CONTACT	CONTINUE
FINITE	CONTROL	TIME STEP
LARGE DISP	COORDINATE	
PRINT	END OPTION	
SIZING	FIXED DISP	
TITLE	GEOMETRY	
UPDATE	ISOTROPIC	
	POST	
	PRINT CHOICE	
	UDUMP	
	UMOTION	

Example e8x19b.dat:

Parameters	Model Definition Options	History Definition Options
ELEMENT	CONNECTIVITY	AUTO LOAD
END	CONTACT	CONTINUE
PLASTICITY	CONTROL	TIME STEP
PRINT	COORDINATE	
SIZING	END OPTION	
TITLE	FIXED DISP	
	GEOMETRY	
	ISOTROPIC	
	POST	
	PRINT CHOICE	
	UDUMP	
	UMOTION	

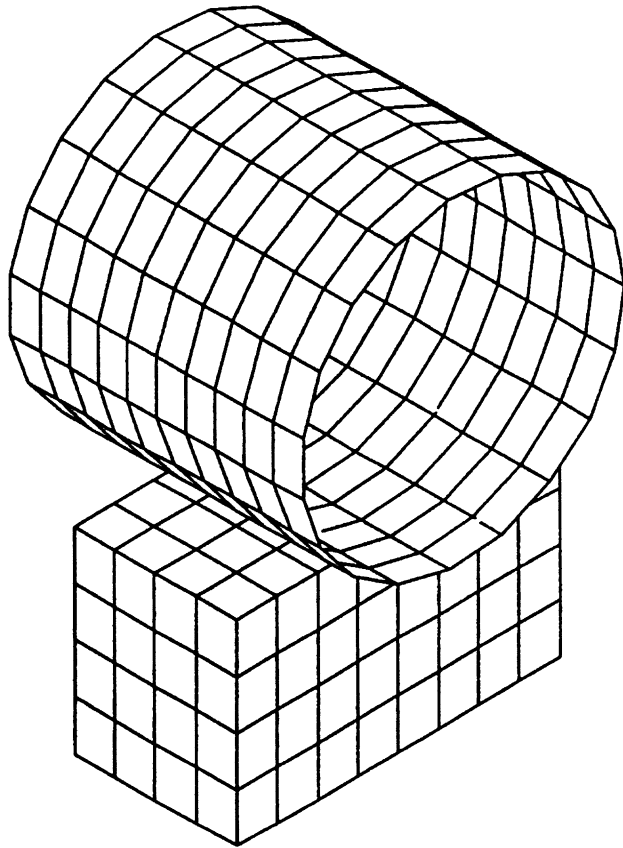


Figure 8.19-1 Initial Geometry for both Data Sets

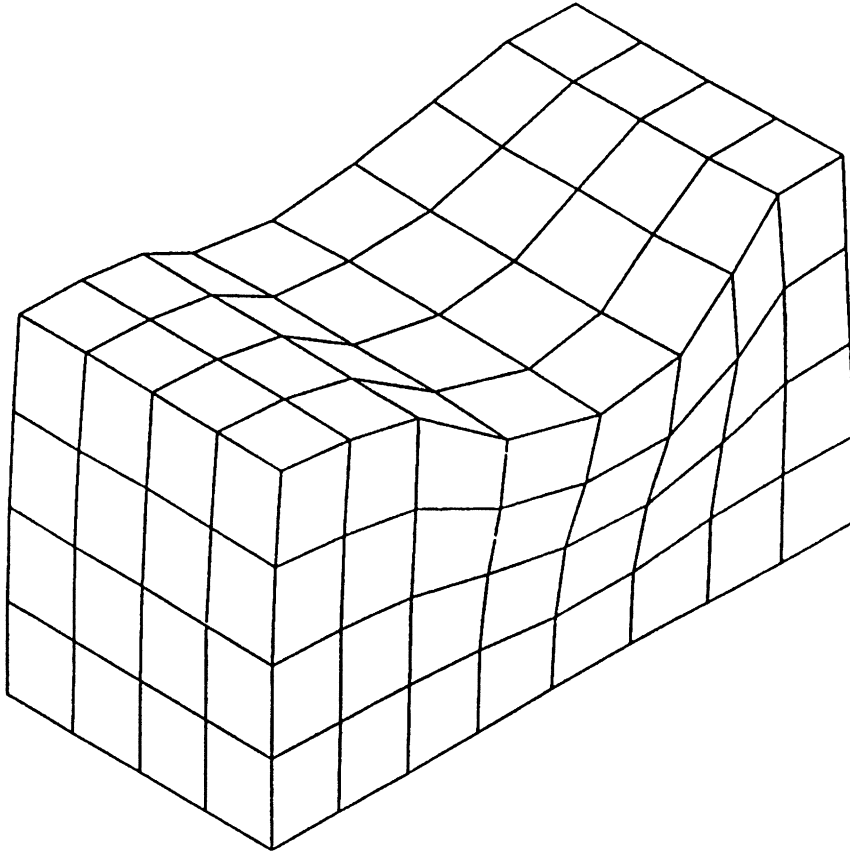


Figure 8.19-2 Deformed Mesh at Increment 12 for Data Set e8x19

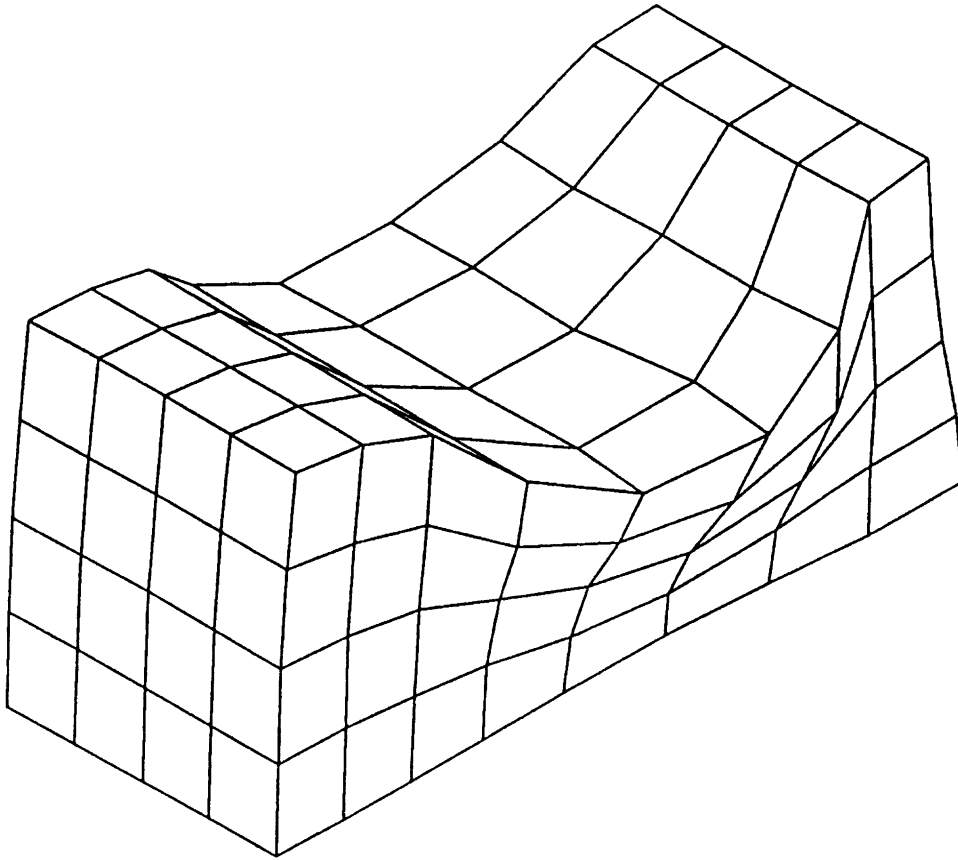


Figure 8.19-3 Deformed Mesh at Increment 24 for Data Set e8x19

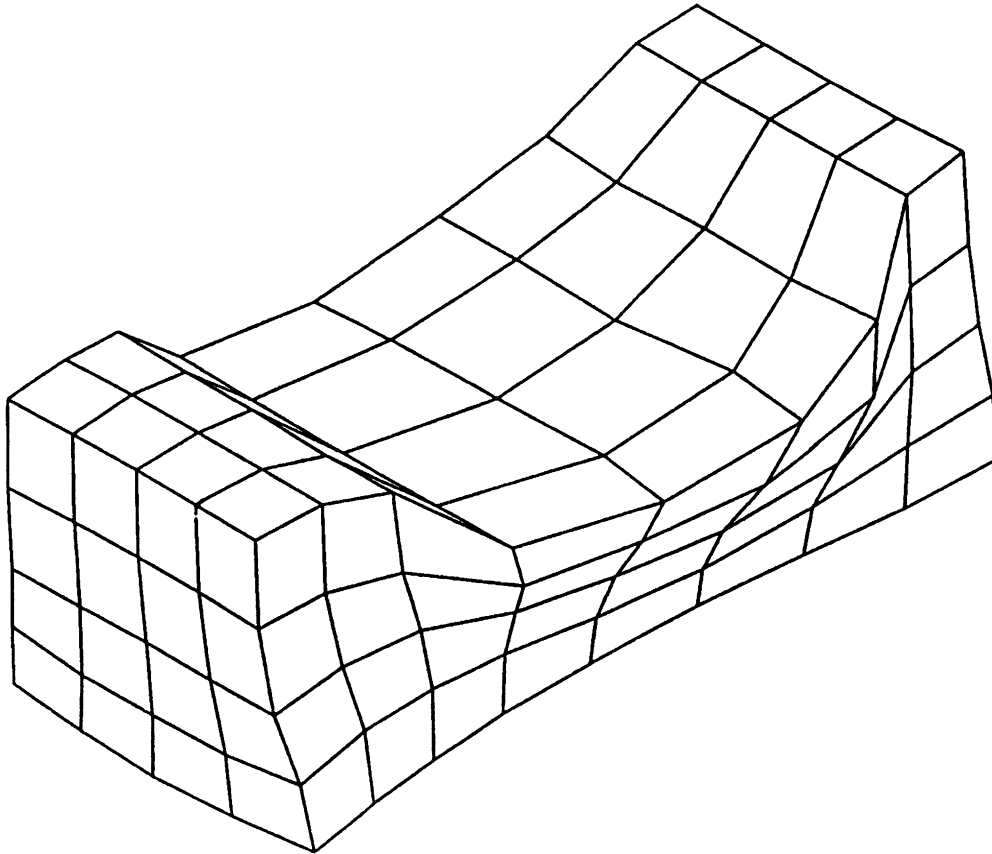


Figure 8.19-4 Deformed Mesh at Increment 36 for Data Set e8x19

Inc : 36
Time : 3.600e+01

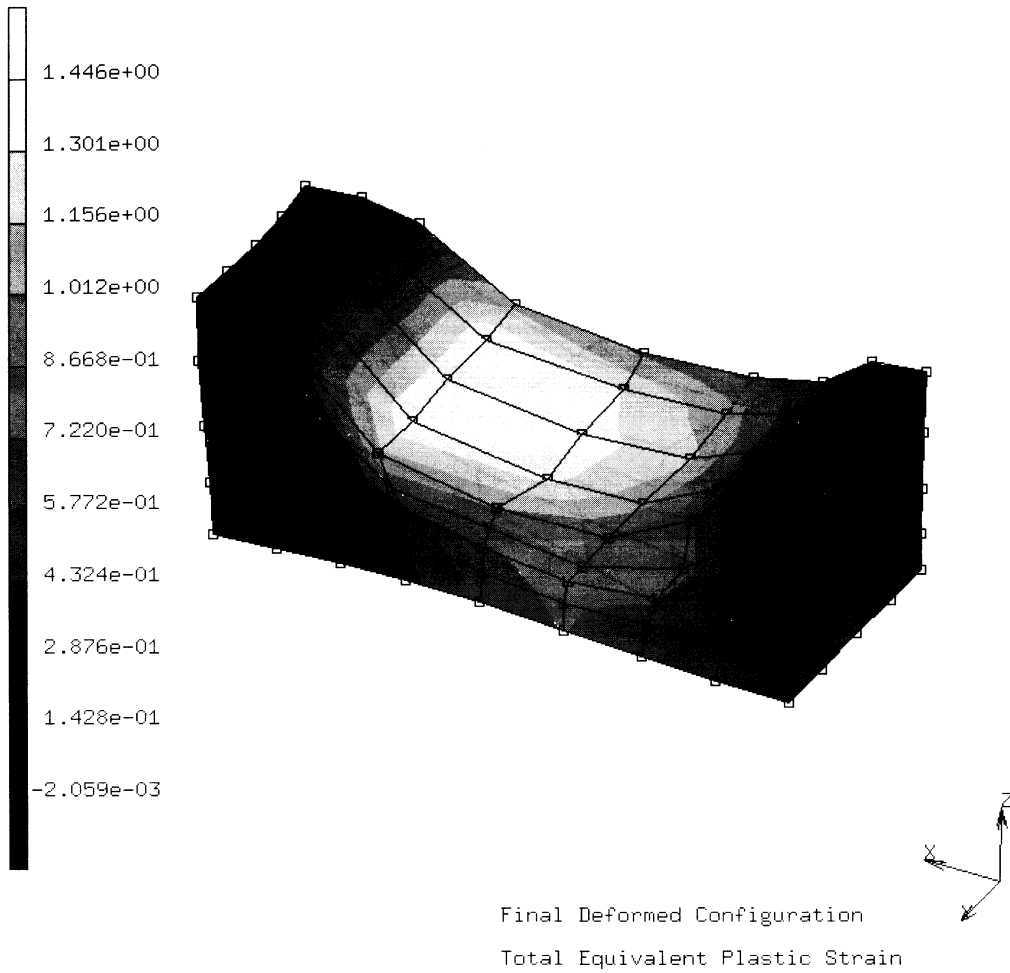


Figure 8.19-5 Equivalent Total Plastic Strain at Increment 36 for Data Set e8x19

Inc : 164
Time : 3.610e+01

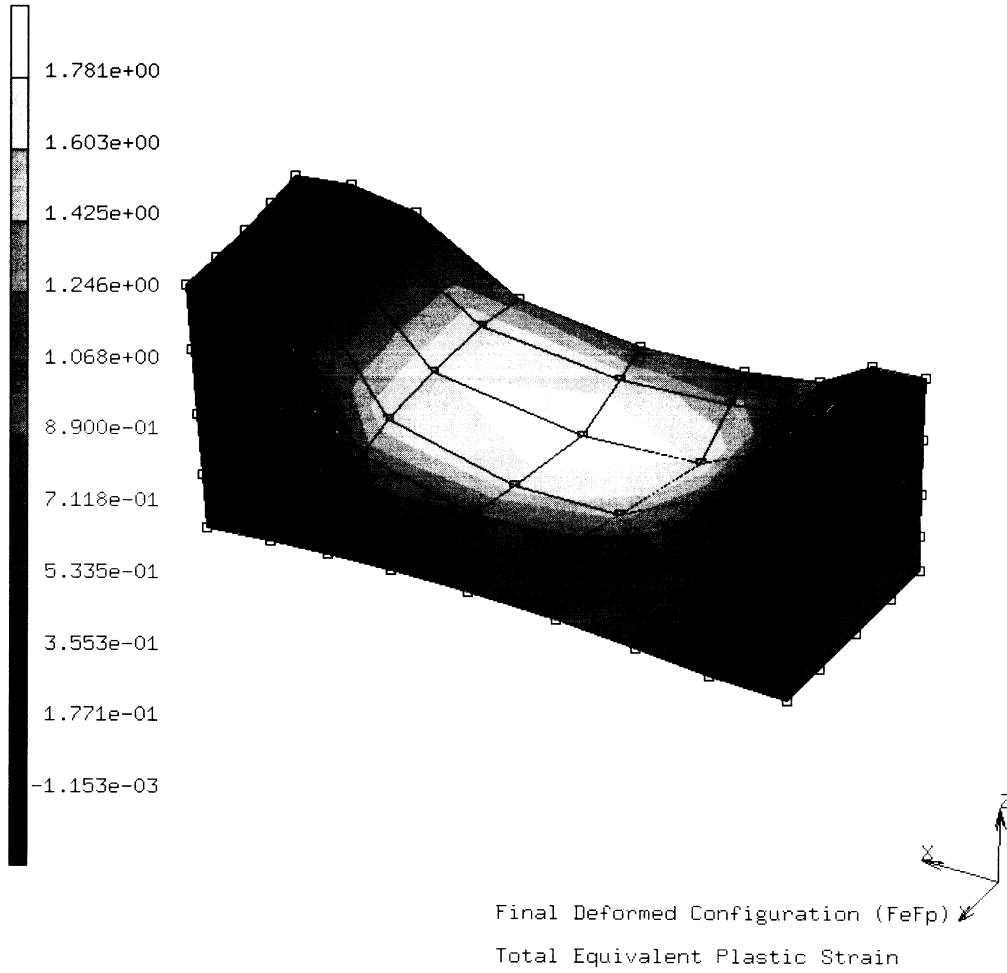


Figure 8.19-6 Equivalent Total Plastic Strain at Increment 164 for Data Set e8x19b

Inc : 36
Time : 3.600e+01

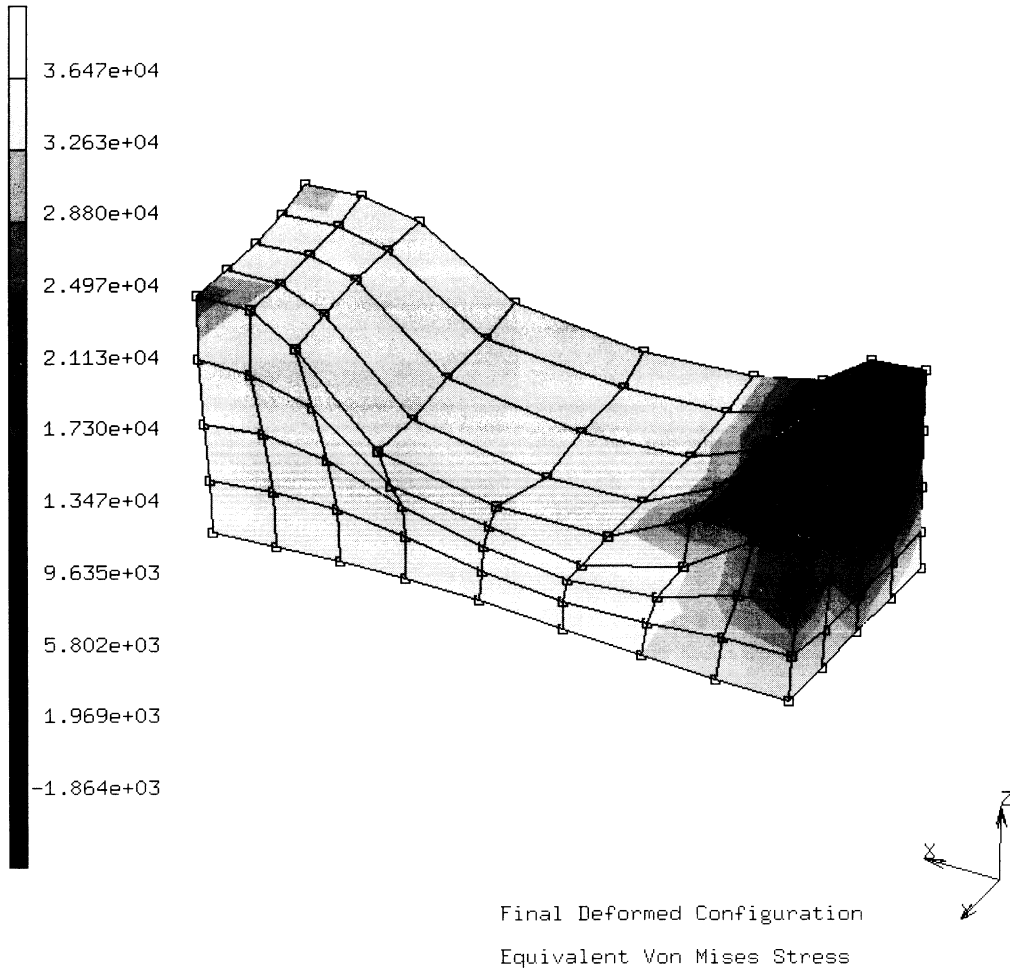


Figure 8.19-7 Equivalent von Mises Stress for Data Set e8x19

Inc : 164
Time : 3.610e+01

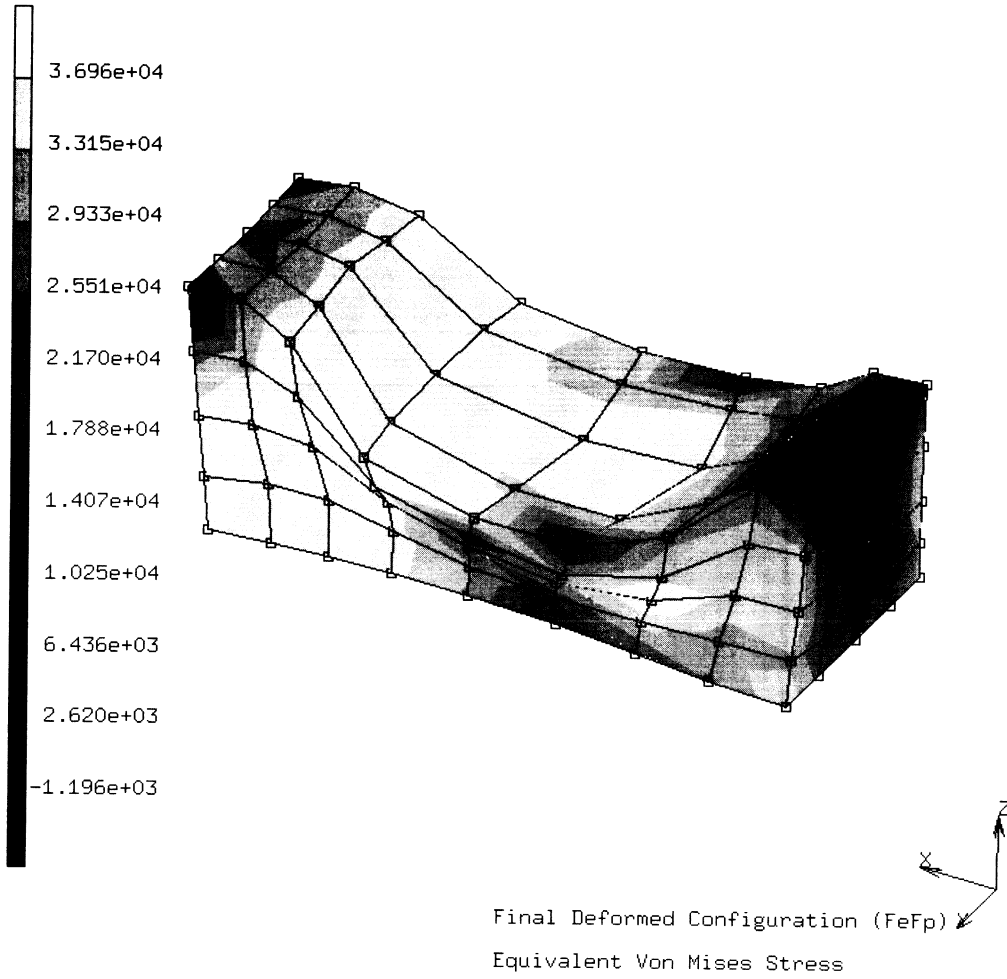


Figure 8.19-8 von Mises for Data Set e8x19b



8 *Advanced Topics*

3D Indentation and Rolling without Friction



8.20 2D Electrostatic Analysis of a Circular Region

This problem analyses a point charge in a circular region to demonstrate MARC's electrostatic analysis capability using a 2D element formulation. The electrostatic problem is governed by Poisson's equation for scalar potential, valid for heat transfer and electrostatic analyses among others. Using this duality, heat transfer elements (type 39) are used but all input and output is seen in terms of an electrical problem.

Parameters

The ELECTRO parameter is included to indicate an electrostatic analysis.

Mesh Definition

Half of the circle is modeled due to symmetry. The mesh has 100 elements and 111 nodes. Figure 8.20-1 shows the nodes, and Figure 8.20-2 shows the element configuration.

Boundary Conditions

A potential of zero volts is specified along the outer radius which is nodes 11 to 111 by 10 through the FIXED POTENTIAL option.

Material Properties

The permittivity of the medium is specified at 1.0 farad/cm in the ISOTRPOIC option.

Electrostatic Charge

A point charge of 1.0 Coulomb is applied at node 1 through the POINT CHARGE option.

POST

The following variables are requested to be written to both binary and formatted post files:

130	}	Scalar potential	131,132	}	Components of electric field vector
134,135	}	Components of electric displacement vector			

Control

The STEADY STATE option is used to initiate the analysis.

Results

Figure 8.20-3 shows the scalar potential (post code 130). Figure 8.20-4 and E8.20-5 show the first and second components of displacement the electric field (post codes 131,132). Figures E8.20-6 and E8.20-7 show the first and second components of electric displacements (post codes 134,135).

Parameters, Options, and Subroutines Summary

Example e8x20.dat:

Parameters	Model Definition Options	History Definition Options
ELECTROSTATIC	CONNECTIVITY	CONTINUE
ELEMENT	COORDINATE	STEADY STATE
END	END OPTION	
SIZING	FIXED POTENTIAL	
TITLE	ISOTROPIC	
	POINT CHARGE	
	POST	

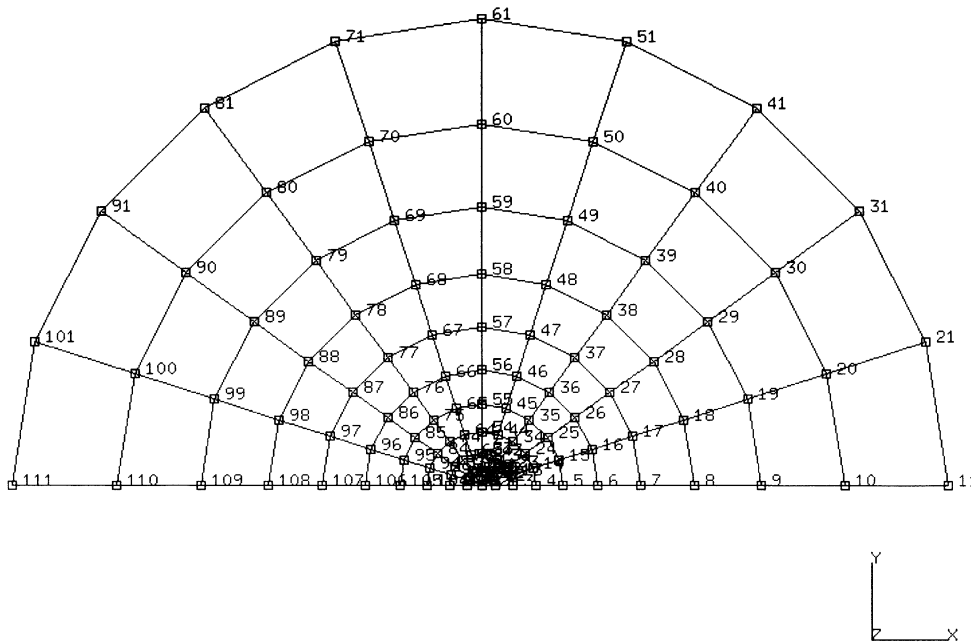


Figure 8.20-1 Node Numbers in Circular Region

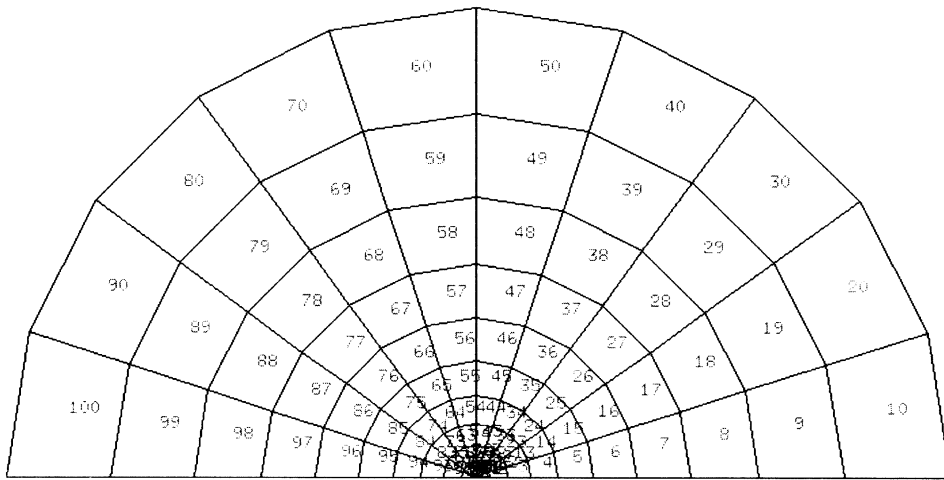


Figure 8.20-2 Element Numbers in Circular Region

INC : 1 prob e8.20 point charge on a circular region element 39
 SUB : 0
 TIME : 0.000e+00
 FREQ : 0.000e+00



Electric Potential

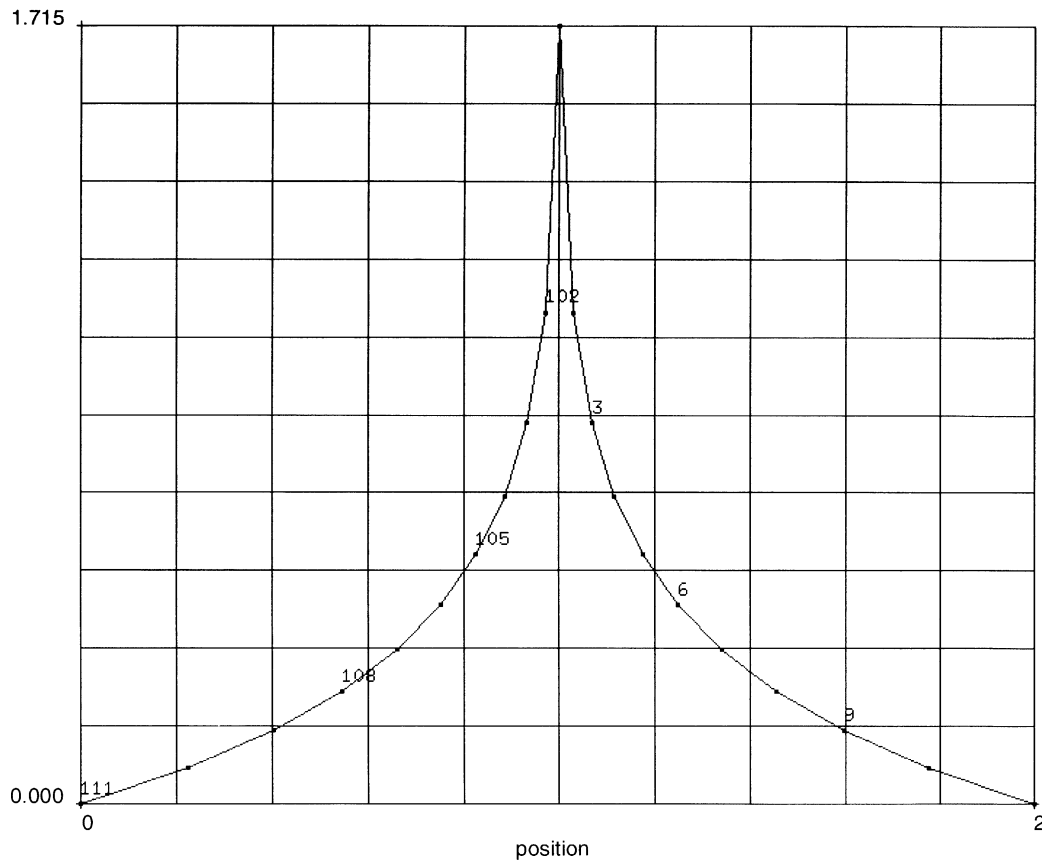


Figure 8.20-3 Electric Potential Along Diameter



INC : 1 prob e8.20 point charge on a circular region element 39
SUB : 0
TIME : 0.000e+00
FREQ : 0.000e+00



1st (Real) Comp of Electric Field (x10)

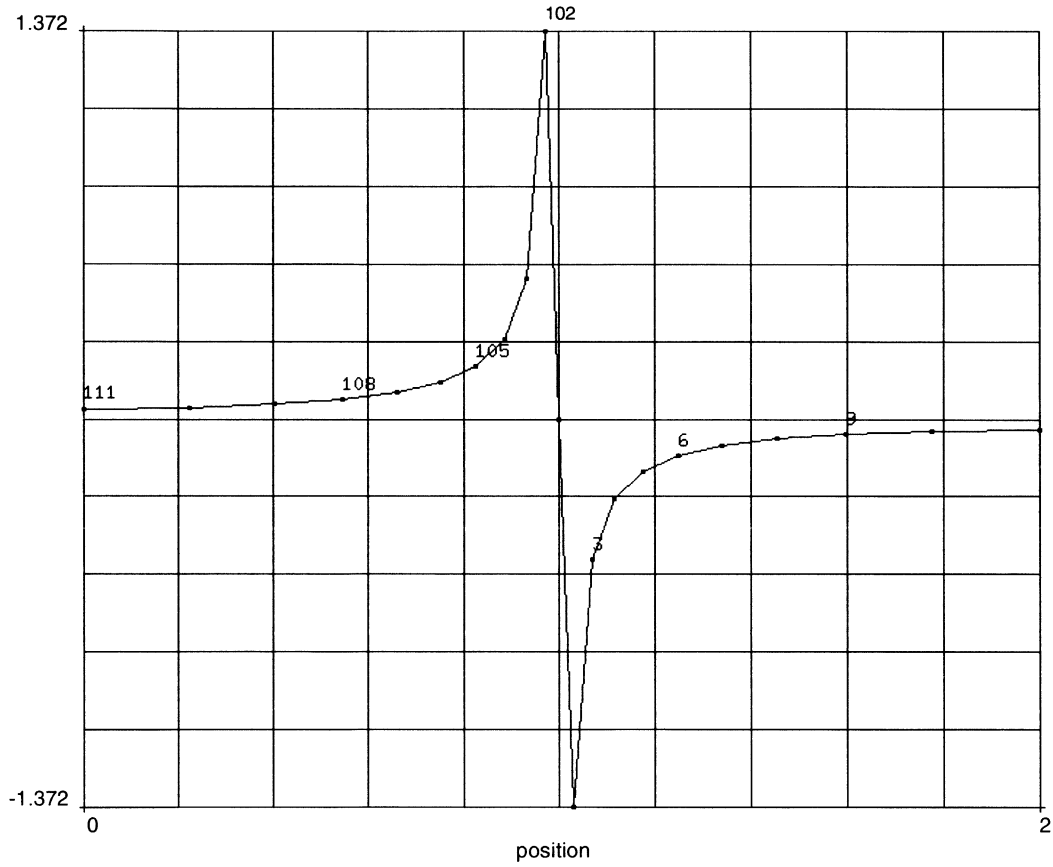


Figure 8.20-4 First Component of Electric Field



8 *Advanced Topics*

2D Electrostatic Analysis of a Circular Region



8.21 3D Electrostatic Analysis of a Circular Region

This problem analyses a point charge in a circular region to demonstrate MARC's electrostatic analysis capability using a 3D element formulation. The electrostatic problem is governed by Poisson's equation for scalar potential, valid for heat transfer and electrostatic analyses among others. Using this duality, eight-noded heat transfer elements (type 43) are used but all input and output is seen in terms of an electrical problem.

Parameters

The ELECTRO parameter is included to indicate an electrostatic analysis.

Mesh Definition

One half of the region is modeled due to symmetry. The model has 100 brick elements and 222 nodes. Figure 8.21-1 shows the mesh nodal points, and Figure 8.21-2 shows the element configuration.

Boundary Conditions

A potential of zero volts is specified along the outside radius at nodes 201 to 222.

Material Properties

The permittivity of the medium is specified at 1.0 farad/cm for all elements.

Electrostatic Charge

A point charge of 0.1 coulomb is applied at nodes 1 and 2.

POST

The following codes are requested to be output to both binary and formatted post files:

130	}	Scalar potential	131-133	}	Components of the electric field vector
134-136	}	Components of the electric displacement vector			

Control

The STEADY STATE option is used to initiate the analysis.

Results

Figure 8.21-3 shows the scalar potential (post code 130). As anticipated, the calculated potential is of the same magnitude as the two-dimensional problem E 8.20.



Parameters, Options, and Subroutines Summary

Example e8x21.dat:

Parameters	Model Definition Options	History Definition Options
ELECTROSTATIC	CONNECTIVITY	CONTINUE
ELEMENT	COORDINATE	STEADY STATE
END	END OPTION	
SIZING	FIXED POTENTIAL	
TITLE	ISOTROPIC	
	POINT CHARGE	
	POST	

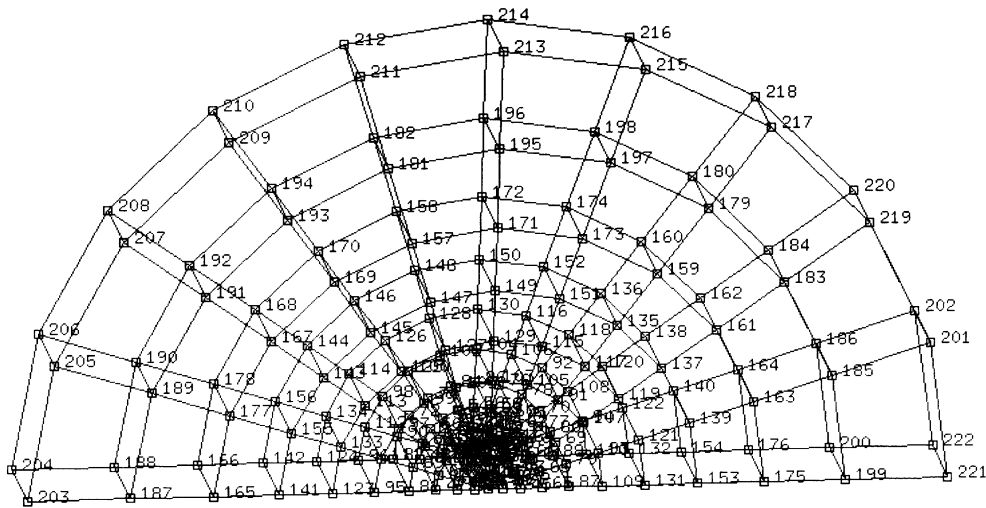


Figure 8.21-1 Node Numbers in Mesh

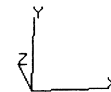
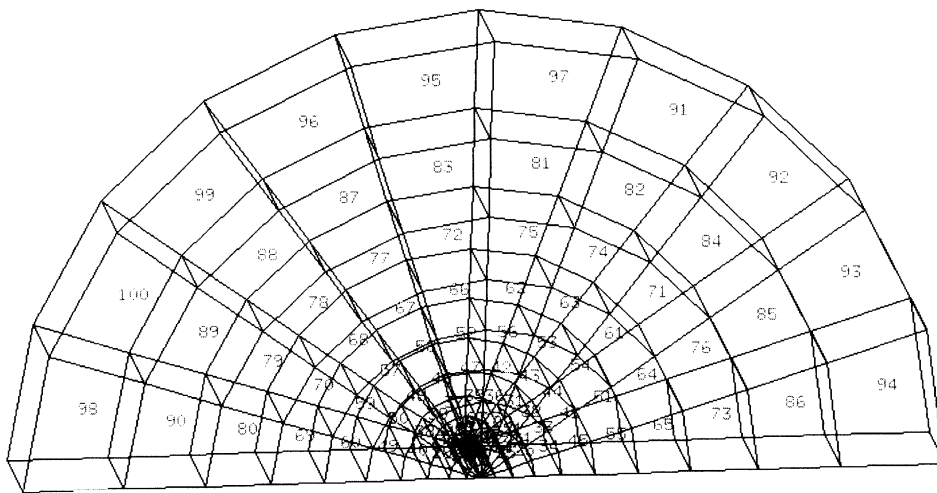


Figure 8.21-2 Element Numbers in Mesh



INC : 1 prob e8.21 point charge on a circular region element 43
SUB : 0
TIME : 0.000e+00
FREQ : 0.000e+00



Scalar Potential

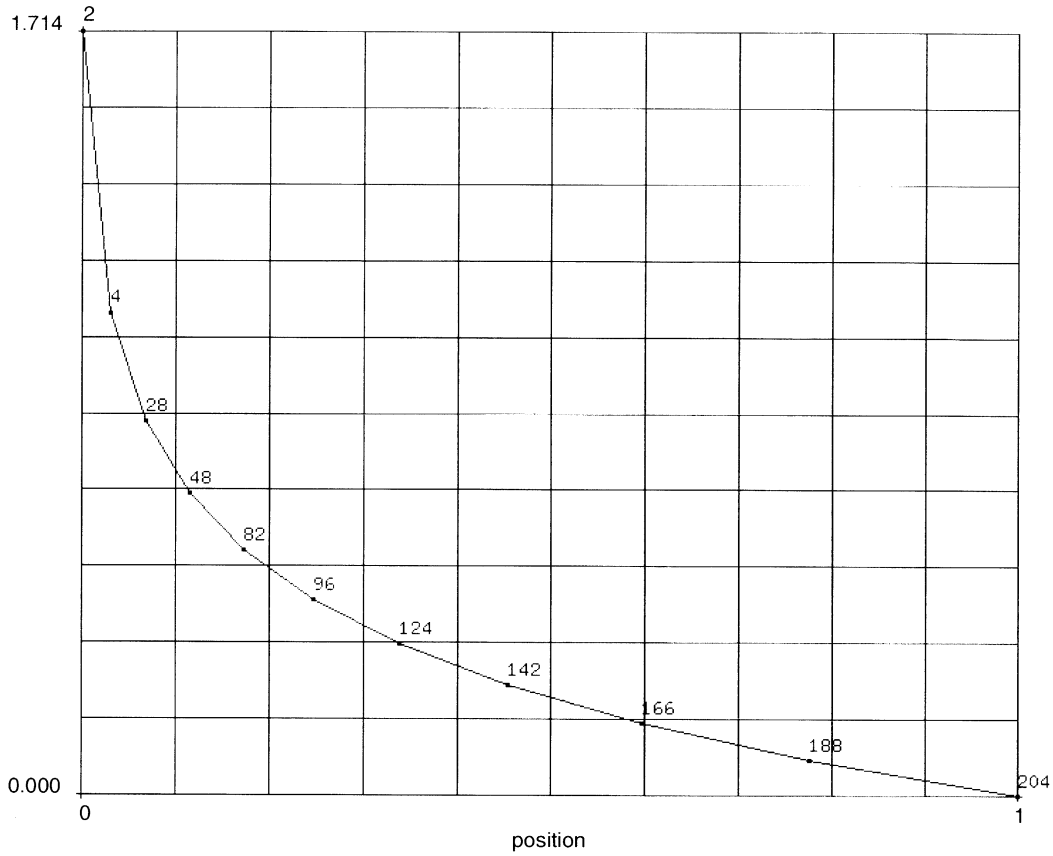


Figure 8.21-3 Scalar Potential Through Radius



8.22 2D Magnetostatic Analysis of a Circular Region

This problem shows MARC's magnetostatic analysis capability using a 2D element formulation. The two-dimensional magnetostatic problem is governed by Poisson's equation for scalar potential, valid for heat transfer, magnetostatic and electrostatic analyses among others. When using this duality, eight-noded heat transfer elements (type 39) are used, but all input and output is seen in terms of an electrical problem.

Parameters

The MAGNET parameter is included to indicate a magnetostatic analysis.

Mesh Definition

Half of the circular region is modeled due to symmetry. The mesh has 100 elements and 111 nodes. Figure 8.22-1 shows the nodal configuration of the mesh and Figure 8.22-2 shows the element configuration.

Boundary Conditions

A potential of zero volts is specified on the outside radius which is at nodes 11 to 111 by 10.

Material Properties

The magnetic permeability of the medium is specified at 1.0 Henry/cm for all elements.

Current

A point current of 1.0 amps is applied at node 1 through the POINT CURRENT option.

POST

The following variables are requested to be written to both a binary and a formatted post file:

140	}	Scalar potential	141,142	}	Components of magnetic flux
144,145	}	Components of magnetic density			

Results

Figure 8.22-3 shows the scalar potential (POST code 140). Figure 8.22-4 shows the vector plot of the magnetic flux.



Parameters, Options, and Subroutines Summary

Example e8x22.dat:

Parameters	Model Definition Options	History Definition Options
ELEMENT	CONNECTIVITY	CONTINUE
END	COORDINATE	STEADY STATE
MAGNETOSTATIC	END OPTION	
SIZING	FIXED POTENTIAL	
TITLE	ISOTROPIC	
	POINT CURRENT	
	POST	

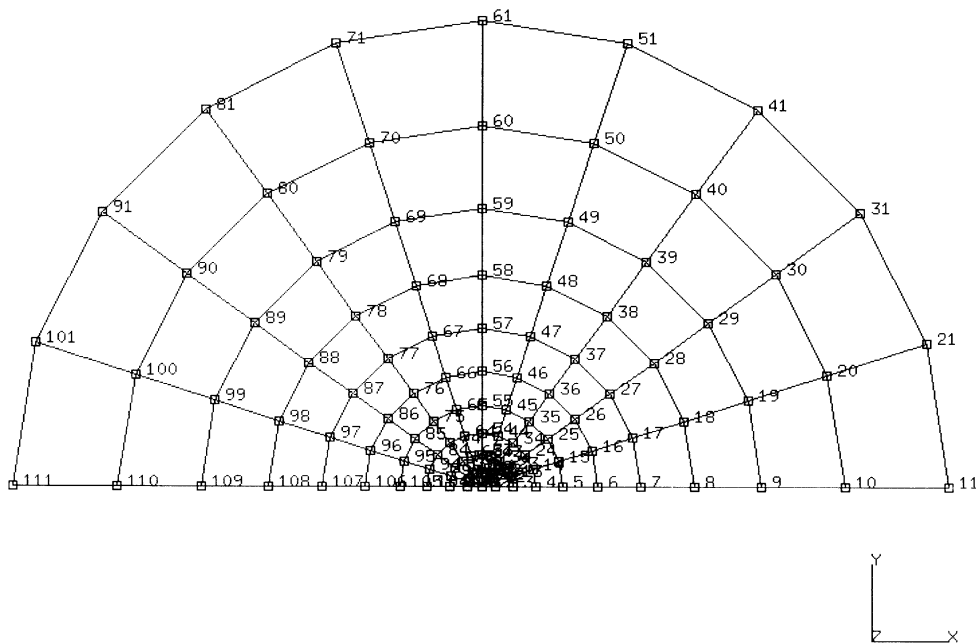


Figure 8.22-1 Node Numbers in Circular Region

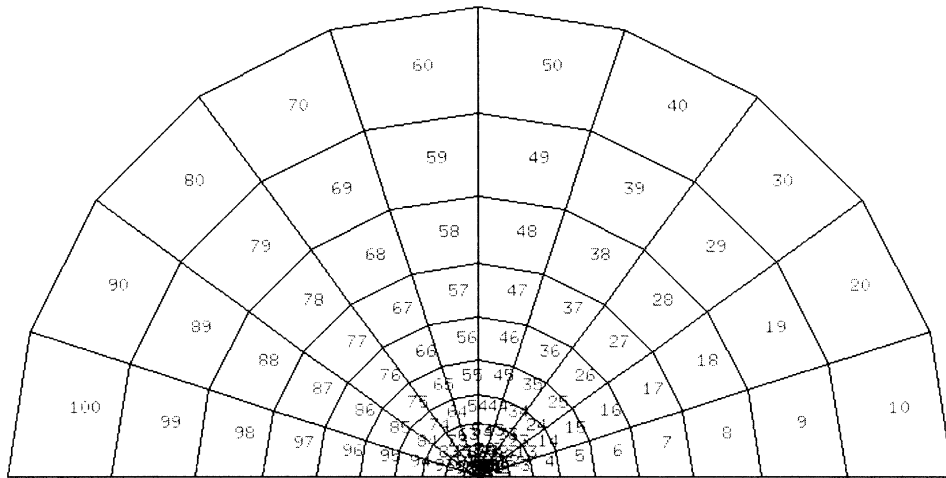


Figure 8.22-2 Element Numbers in Circular Region



INC : 1 prob e8.22 point current on a circular region element 39
SUB : 0
TIME : 0.000e+00
FREQ : 0.000e+00



Magnetic Potential

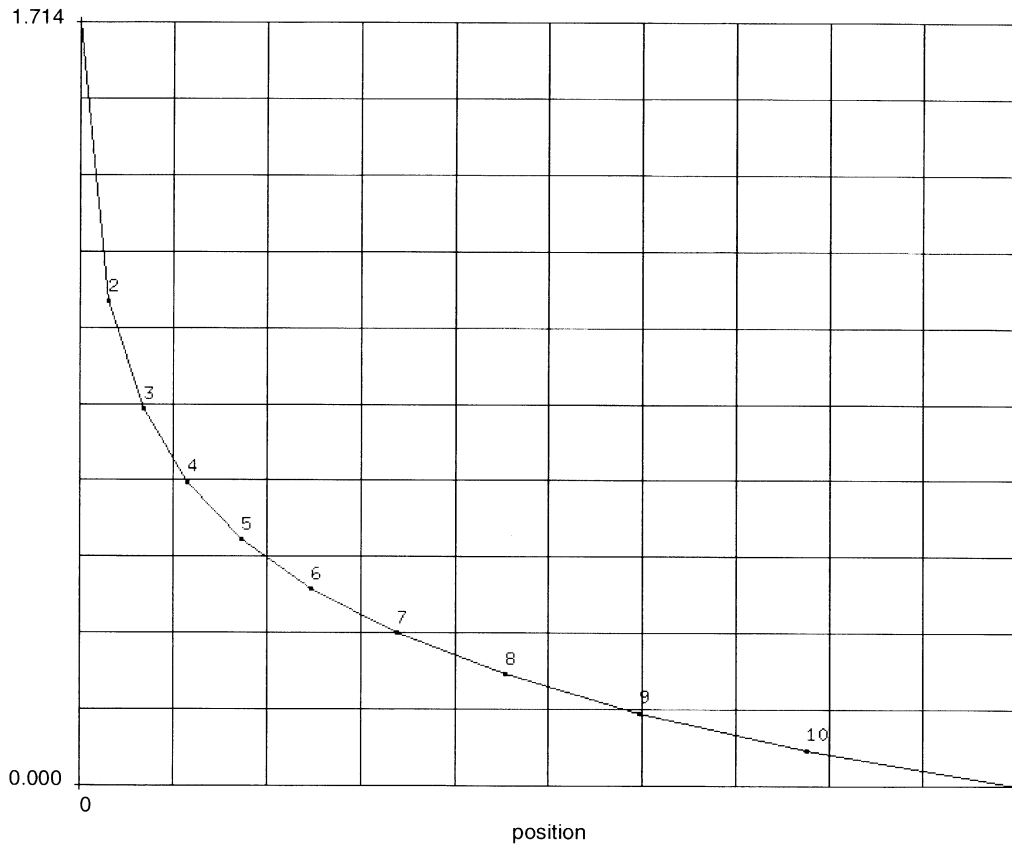


Figure 8.22-3 Magnetic Scalar Potential along Radial Line

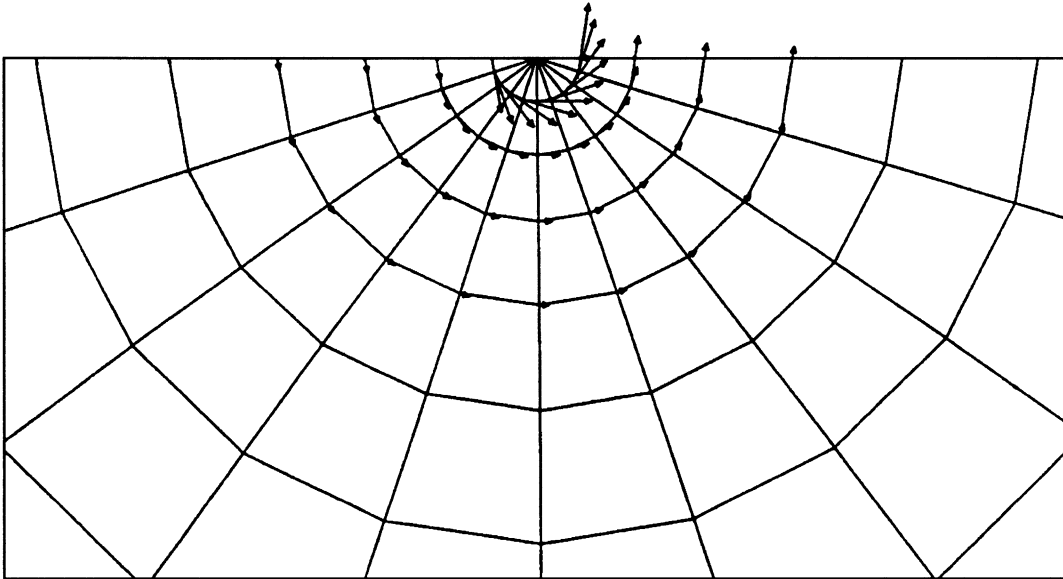


Figure 8.22-4 Magnetic Flux Distribution





8.23 3D Magnetostatic Analysis of a Coil

This problem shows magnetostatic analysis capability using a 3D element formulation in MARC. Since the potential to be solved is a new vector potential, the normal “heat transfer” approach cannot be used. Instead, an eight-noded magnetostatic element (type 109) is used for this analysis.

Parameters

The MAGNETO parameter is included to indicate a magnetostatic analysis.

Mesh Definition

One quarter of the coil is modeled using element type 109. The outside radius is 2.405 cm. Figure 8.23-1 shows the mesh and applied current.

Boundary Conditions

Along the $y = 0$ edge $A_1 = 0$. Along the $x = 0$ edge $A_2 = 0$. Along the outside radius $A_1 = A_2 = 0$. $A_3 = 0$ everywhere to simulate a two-dimensional problem.

Material Properties

The magnetic permeability of all elements is set to 1000.0 Henry/cm.

Currents

A current running in the circumferential direction at a radius of 1 cm is applied. The point currents ranging in value from -0.951 amps to +0.951 amps are applied at nodes 111 to 120.

POST

The following variables are written to both a binary and a formatted post file:

141-143 } Components of magnetic flux
144-146 } Components of magnetic intensity

Results

The third component of the magnetic flux is shown as a function of the radius in Figure 8.23-2. You can observe that a steep gradient occurs about the ring of nodes to which the current is applied. In addition, the total magnetization is zero, as:

$$\pi r_c^2 (338.5) + \pi(r_o^2 - r_c^2) (-42.32) = 2.7$$

where $r_c = 1$, and $r_o = 3$.

The vector potential A is shown in Figure 8.23-3.



Parameters, Options, and Subroutines Summary

Example e8x23.dat:

Parameters	Model Definition Options	History Definition Options
ELEMENT	CONNECTIVITY	CONTINUE
END	COORDINATE	STEADY STATE
MAGNETOSTATIC	END OPTION	
SIZING	FIXED POTENTIAL	
TITLE	ISOTROPIC	
	POINT CURRENT	
	POST	

Example e8x23b.dat:

Parameters	Model Definition Options	History Definition Options
ELEMENT	CONNECTIVITY	CONTINUE
END	COORDINATE	STEADY STATE
MAGNETOSTATIC	DEFINE	
SIZING	END OPTION	
TITLE	FIXED POTENTIAL	
	ISOTROPIC	
	POINT CURRENT	
	POST	

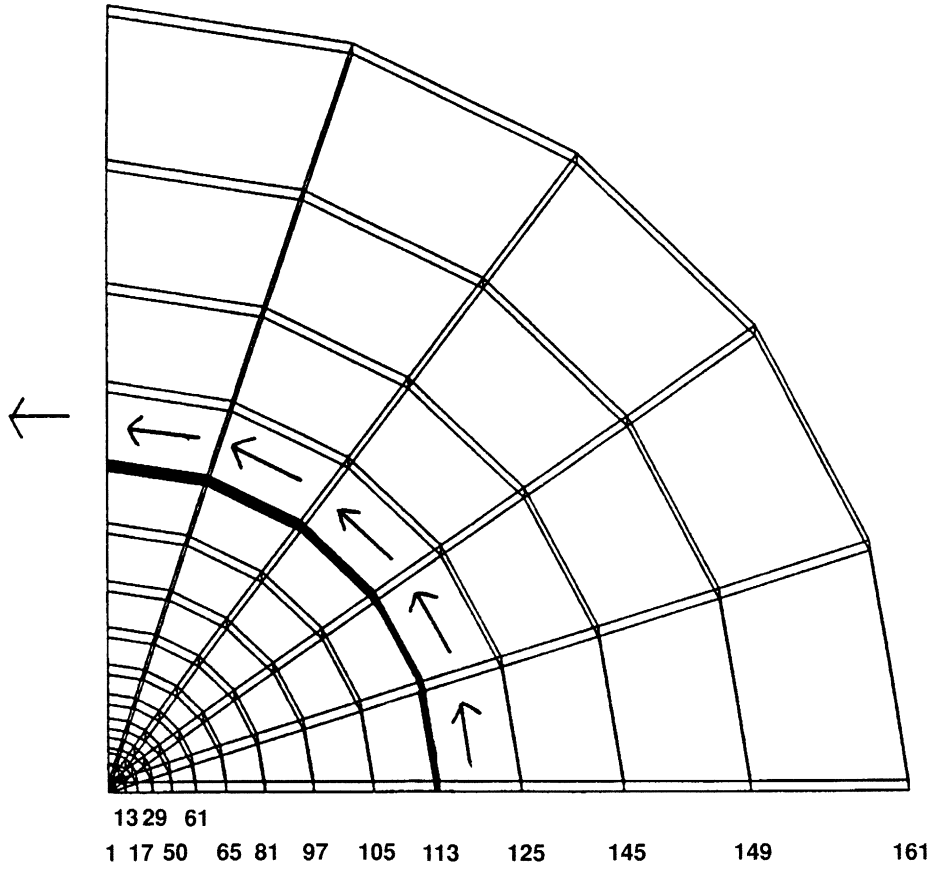


Figure 8.23-1 Mesh and Applied Current

INC : 1
 SUB : 0
 TIME : 0.000e+00
 FREQ : 0.000e+00

prob e8.23 magnetostatic-analysis of coil



3rd (Real) Comp of Magnetic Flux (x100)

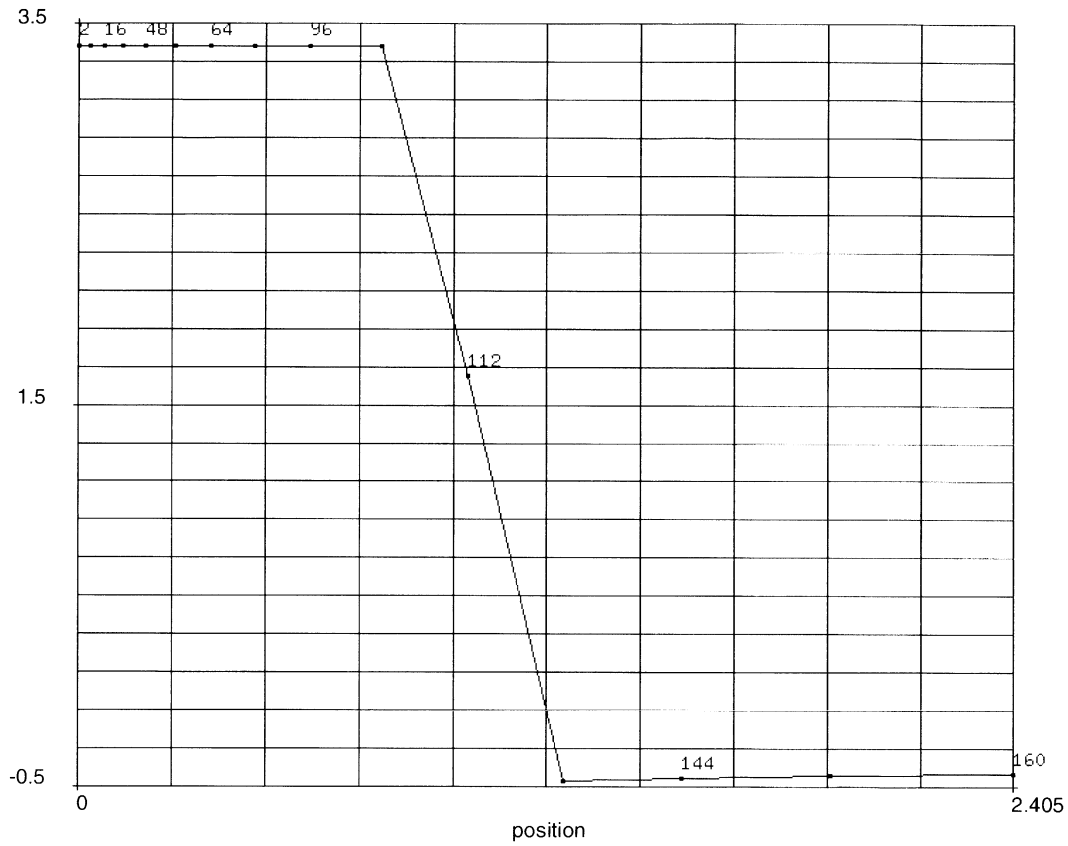
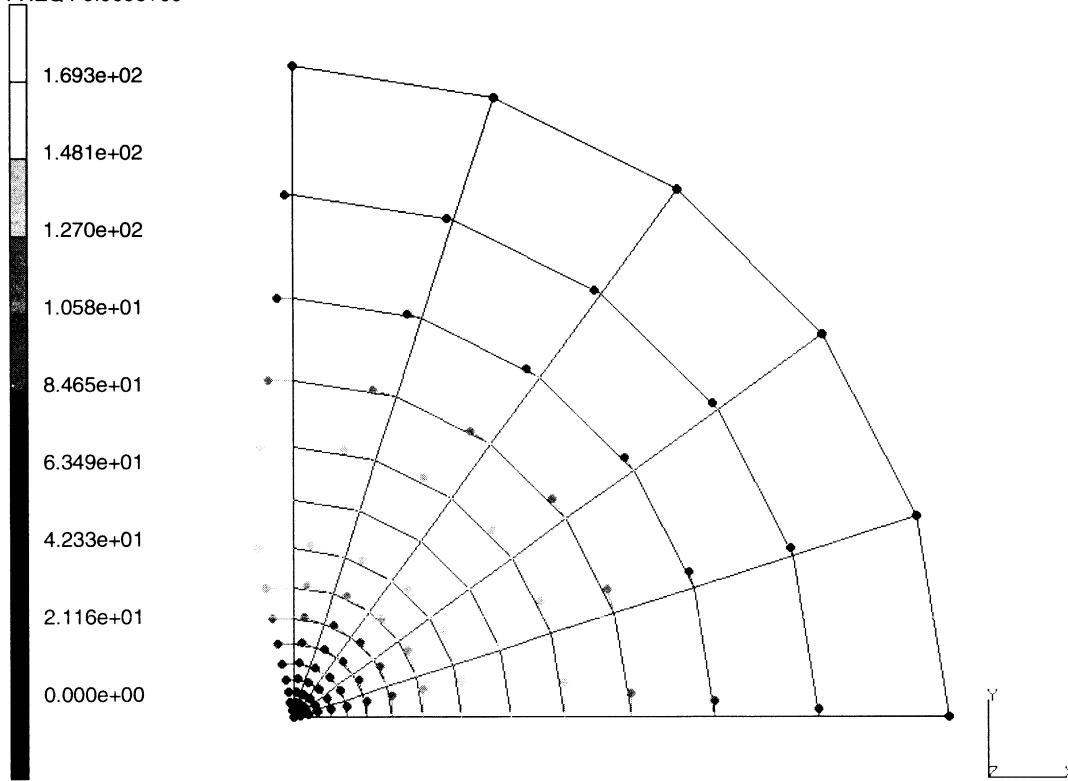


Figure 8.23-2 Third Component of Magnetic Flux along Radial Line



INC : 1
SUB : 0
TIME : 0.000e+00
FREQ : 0.000e+00



prob e8.23 magnetostatic analysis of coil
Magnetic Potential z

Figure 8.23-3 Magnetic Potential Vector





8.24 2D Nonlinear Magnetostatic Analysis

An infinite wire carries a current through a circular region.

This problem shows MARC's magnetostatic analysis capability using a 2D element formulation together with an orthotropic magnetic permeability that is a function of the magnetic flux density. The latter requires that a nonlinear problem be solved.

Parameters

The MAGNET parameter is included to indicate a magnetostatic analysis.

Mesh Definition

Only a section of the region is modeled due to symmetry. Element type 39, the 4-node heat transfer element, is used. Figure 8.24-1 shows the mesh nodal points, and Figure 8.24-2 shows the element configuration.

Boundary Conditions

A potential of zero volts is specified at nodes 20 and 21.

Material Properties

Use of the ORTHOTROPIC model definition option allows the input of the baseline magnetic permeabilities in the principal directions. These are set to 1000.0, 1200.0, and 1400.0 Henry/cm in the 1, 2, and 3 directions respectively. These permeabilities are functions of the magnetic flux density, the functionality being described through the B-H RELATION model definition option.

Current

A point current of 1.0 amps is applied at nodes 1.

POST

The following variables are written to a formatted post file:

```
140      } Scalar magnetic potential
141-142  } Components of magnetic flux
144-1465 } Components of magnetic intensity
```

Results

Figure 8.24-3 shows the scalar potential (post code 140) using linear material properties. Figure 8.24-4 shows the potential when the nonlinear material behavior is represented.



Parameters, Options, and Subroutines Summary

Example e8x24a.dat:

Parameters	Model Definition Options	History Definition Options
ELEMENT	CONNECTIVITY	CONTINUE
END	COORDINATE	STEADY STATE
MAGNETOSTATIC	END OPTION	
SIZING	FIXED POTENTIAL	
TITLE	ISOTROPIC	
	POINT CURRENT	
	POST	
	PRINT ELEM	

Example e8x24b.dat:

Parameters	Model Definition Options	History Definition Options
ELEMENT	B-H RELATION	CONTINUE
END	CONNECTIVITY	STEADY STATE
MAGNETOSTATIC	CONTROL	
SIZING	COORDINATE	
TITLE	END OPTION	
	FIXED POTENTIAL	
	ISOTROPIC	
	POINT CURRENT	
	POST	
	PRINT ELEM	

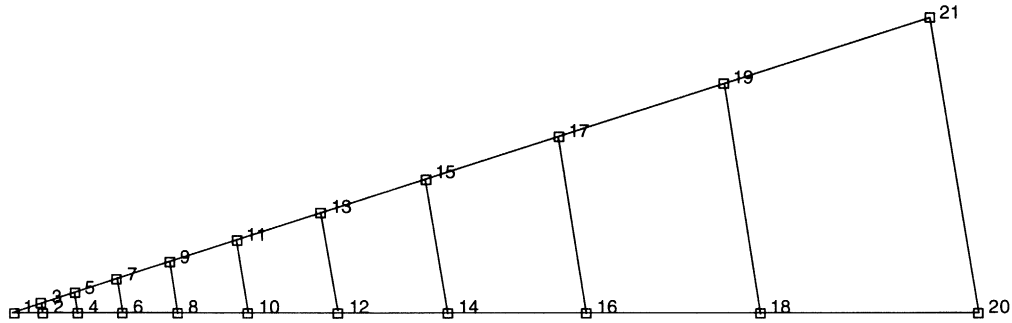


Figure 8.24-1 Mesh with Node Numbers

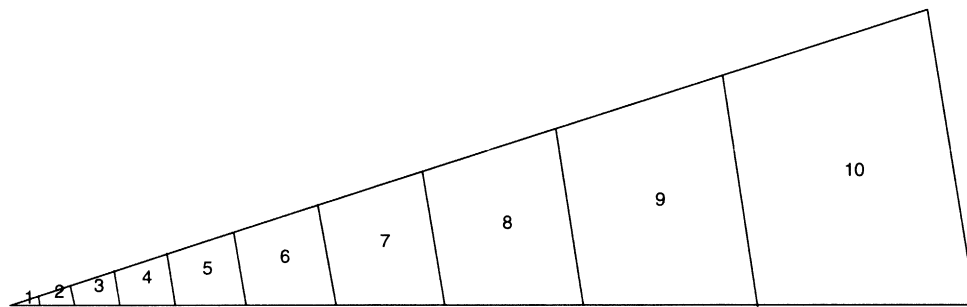


Figure 8.24-2 Mesh with Element Numbers



INC : 1
SUB : 0
TIME : 0.000e+00
FREQ : 0.000e+00

prob e8.24 linear magnetostatic analysis



Magnetic Potential (x1000)

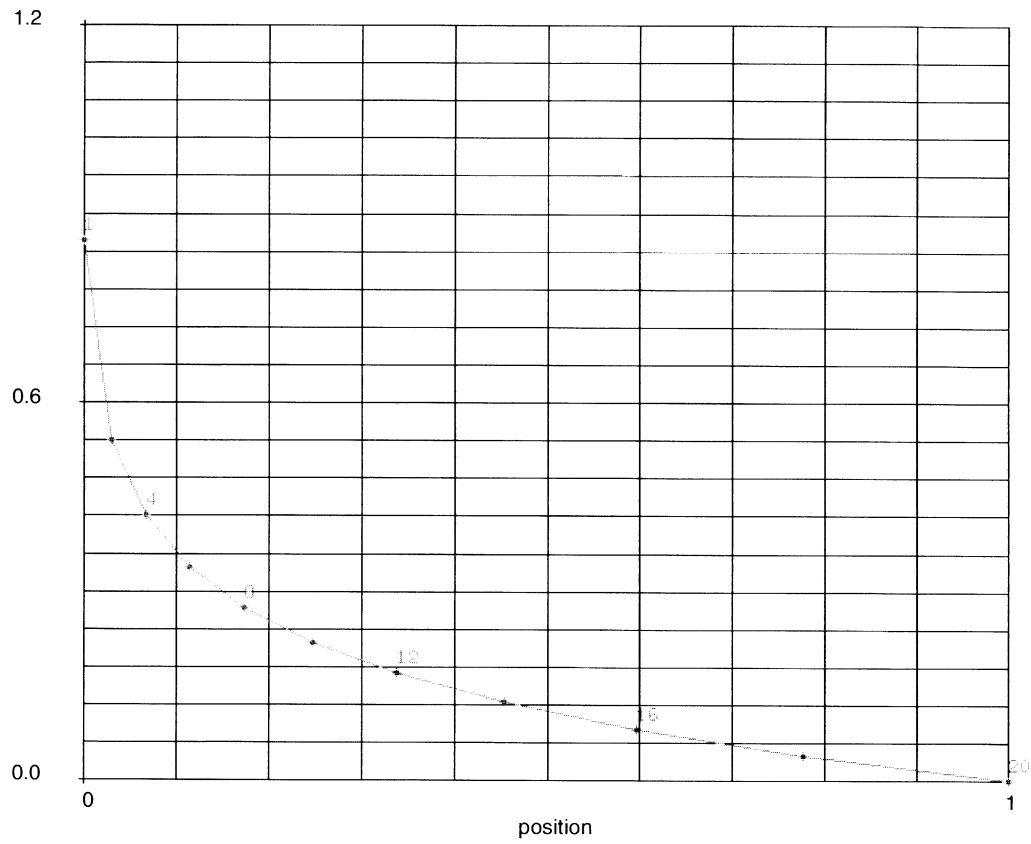


Figure 8.24-3 Magnetic Scalar Potential Linear Material Behavior



INC : 1 prob e8.24 nonlinear magnetostatic analysis
SUB : 0
TIME : 0.000e+00
FREQ : 0.000e+00



Magnetic Potential (x1000)

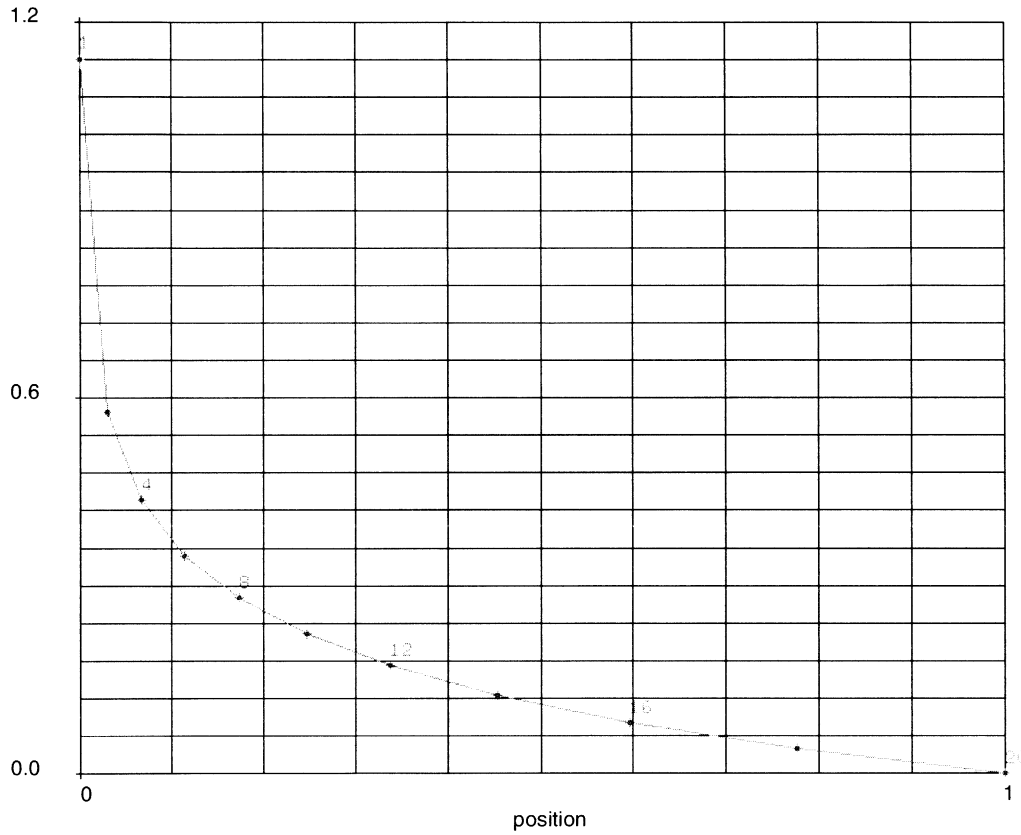


Figure 8.24-4 Magnetic Scalar Potential Nonlinear Material Behavior





8.25 Acoustic Problem: Eigenvalue Analysis of a Circular Cavity

This problem demonstrates the acoustic analysis capability using a 2D element formulation in MARC. MARC can be used to obtain the pressure distribution in a cavity with rigid reflecting boundaries. A transient analysis is then performed.

Parameters

The ACOUSTIC parameter is included to indicate an acoustic analysis. A maximum of six modes are to be used in the modal superposition. The Lanczos method is used for eigenvalue analysis, and resulting mode shapes are written onto the post file. PRINT, 3 is used to force the solution of a nonpositive definite stiffness matrix.

Elements/Mesh Definition

The input was originally created with element type 11. Using the ALIAS parameter, we can easily respecify them as element type 39. Figure 8.25-1 and Figure 8.25-2 show the node numbers and the elements in the cavity. The reflecting barrier is modeled by having a free surface. This can be seen in Figure 8.25-3 showing the double nodes. A refined mesh is used around the edges of the plate.

Boundary Conditions

No boundary conditions are applied. This will result in the first mode being the “rigid body” mode.

Material Properties

A bulk modulus of 139,000 psi and a material density of 1.2 lb/in³ are specified through the ISOTROPIC model definition option.

Loading

An acoustic source pulse is applied in increment 1 with a time step of 0.000001. Ten increments are then performed with a time step of 0.001 at node 3. The DYNAMIC CHANGE option is used to define the time step.

Print Control

Print output of mode shapes and nodal reactions is requested through the use of a PRINT NODE option with MODE and REAC subparameters. All relevant element quantities are requested for elements 1 to 20 (at all four integration points) through the use of a PRINT ELEMENT option.

**POST**

The pressure (post code 120) and the first two components of the pressure gradient (post codes 121, 122) are written to a formatted post file. In addition, by providing a RECOVER option, the first two eigenvectors are also written to this file.

Results

Figure 8.25-4 through Figure 8.25-8 show the eigenmodes in the cavity. The frequencies are as follows:

Mode	Frequency (Hz)
1	0
2	653.7
3	978.1
4	1500
5	1638
6	1985

The pressure distribution in the transient analysis is shown in Figure 8.25-9 through Figure 8.25-11. You can observe the pressure pulse propagating through the cavity.

Parameters, Options, and Subroutines Summary

Example e8x25.dat:

Parameters	Model Definition Options	History Definition Options
ACOUSTIC	CONNECTIVITY	CONTINUE
ALIAS	COORDINATE	DYNAMIC CHANGE
ELEMENT	END OPTION	MODAL SHAPE
END	GEOMETRY	POINT SOURCE
PRINT	ISOTROPIC	RECOVER
SIZING	POST	
TITLE	PRINT ELEM	
	PRINT NODE	

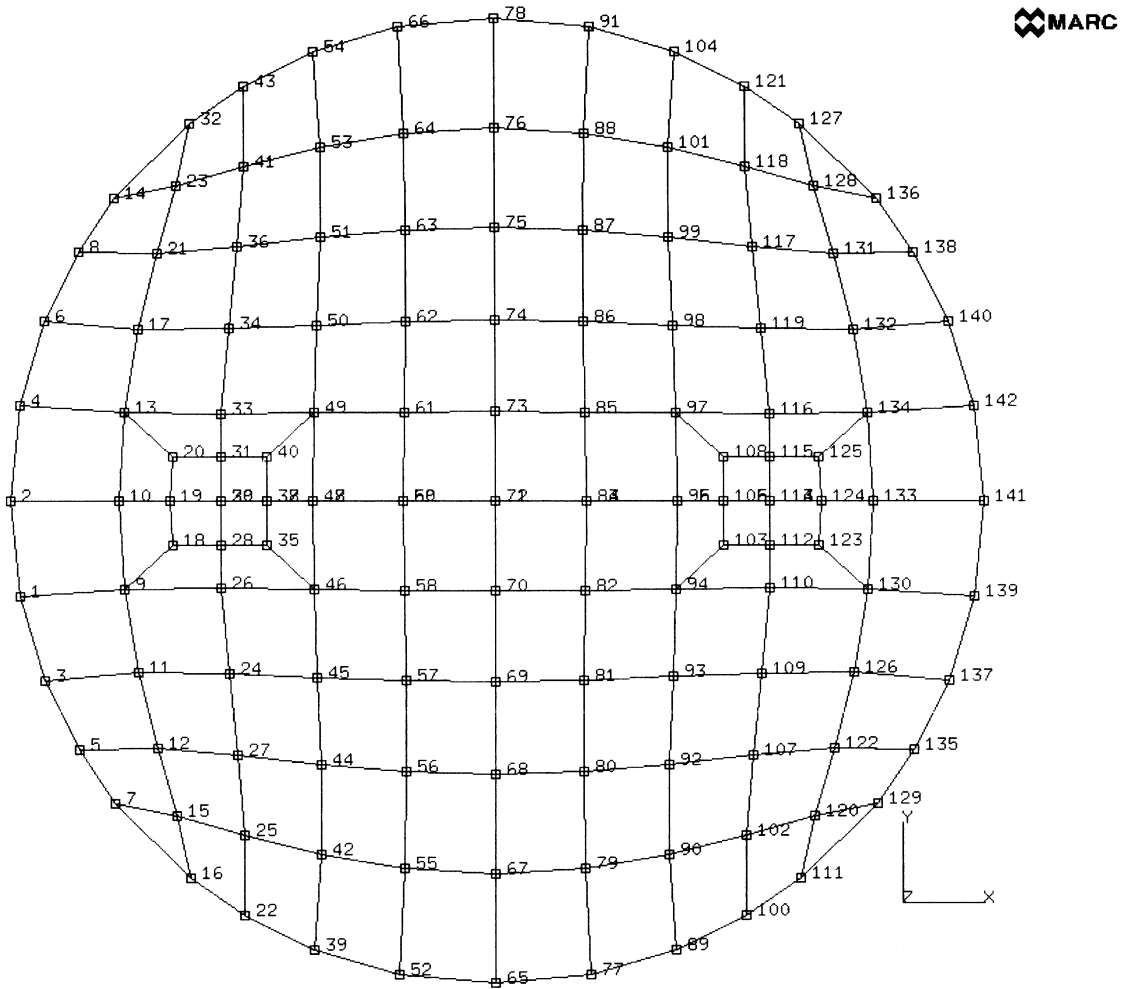


Figure 8.25-1 Acoustic Cavity Mesh with Node Numbers

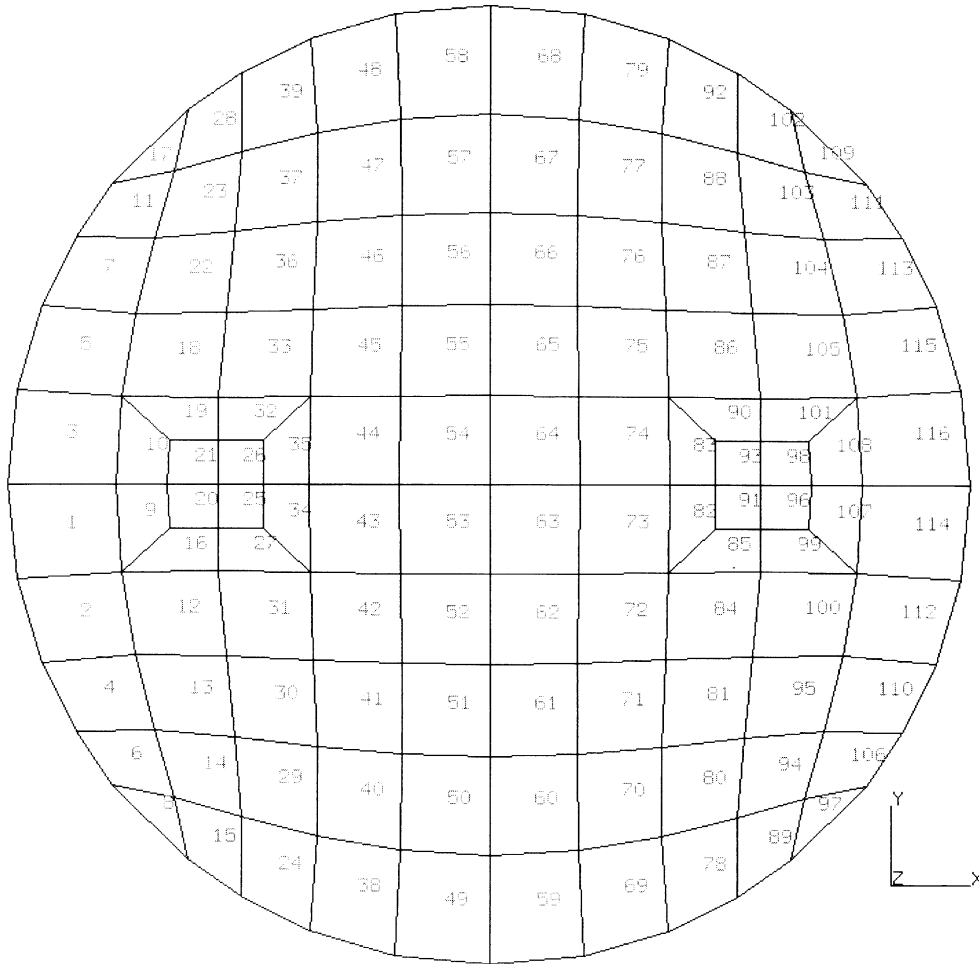


Figure 8.25-2 Acoustic Cavity Mesh with Element Numbers

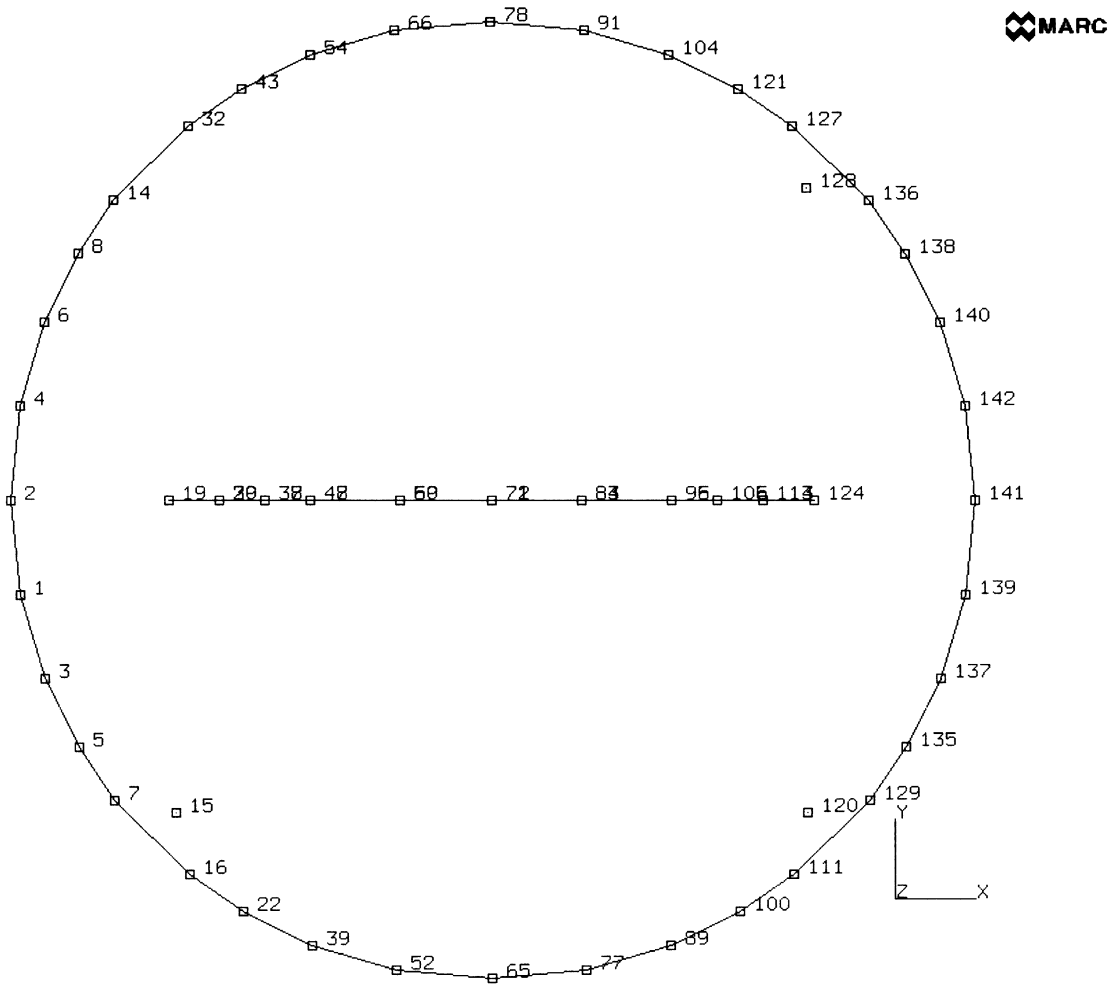
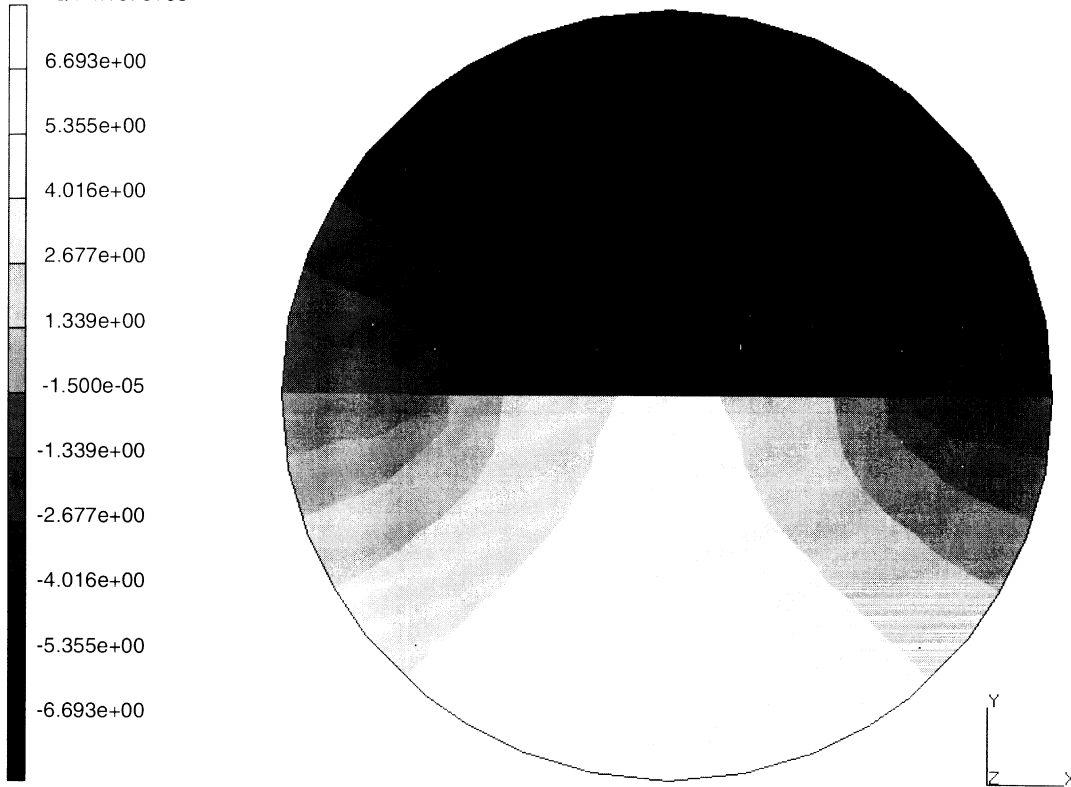


Figure 8.25-3 Outline Plot Showing Internal Barrier

INC : 0
SUB : 2
TIME : 0.000e+00
FREQ : 4.107e+03

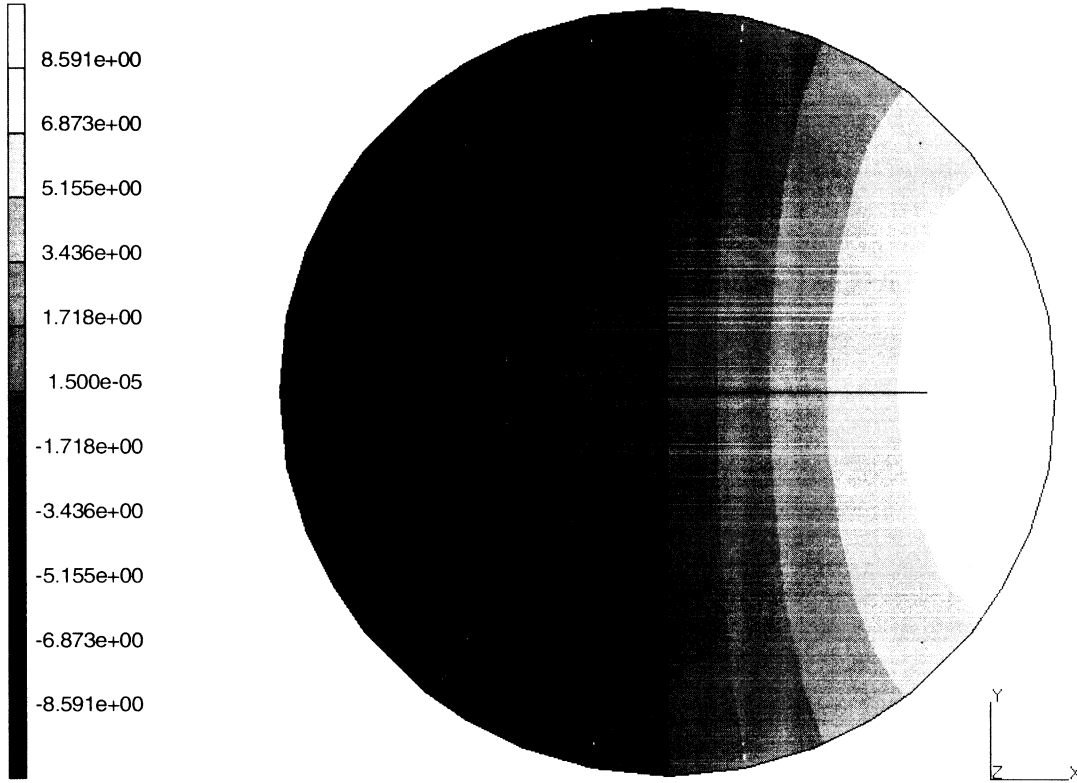


prob e8.25 acoustic problem central plate
Displacements

Figure 8.25-4 Second Mode



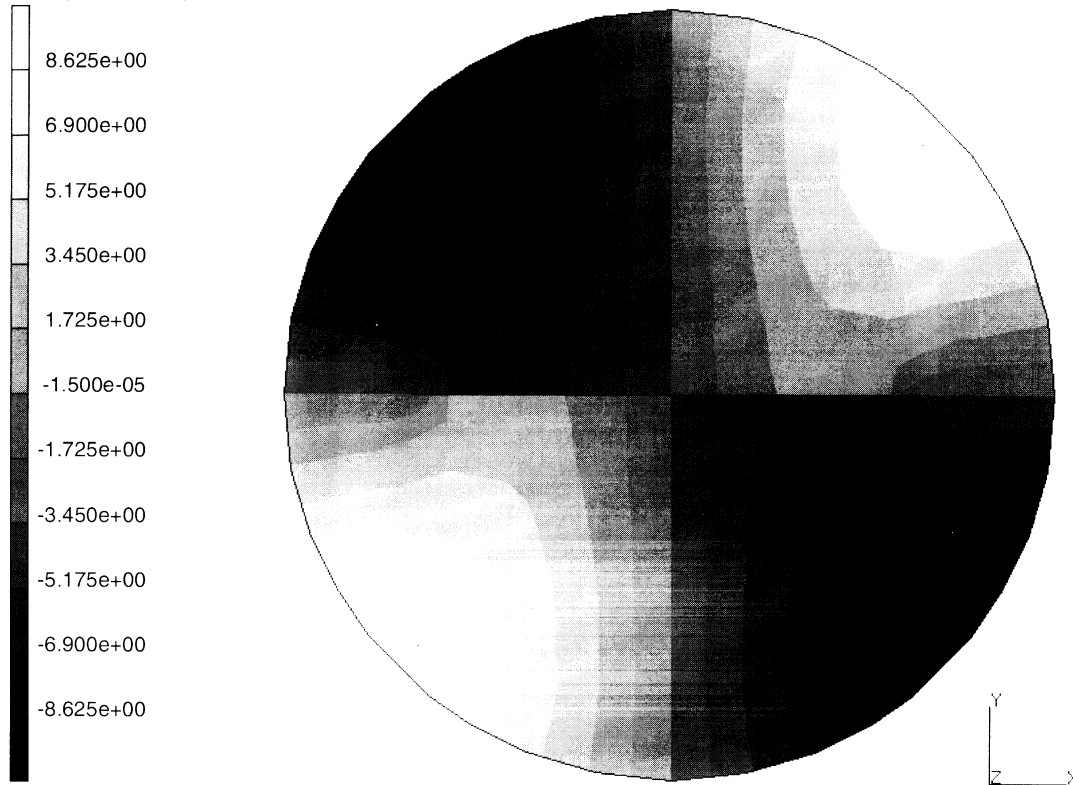
INC : 0
SUB : 3
TIME : 0.000e+00
FREQ : 6.146e+03



prob e8.25 acoustic problem central plate
Displacements

Figure 8.25-5 Third Mode

INC : 0
SUB : 4
TIME : 0.000e+00
FREQ : 9.427e+03

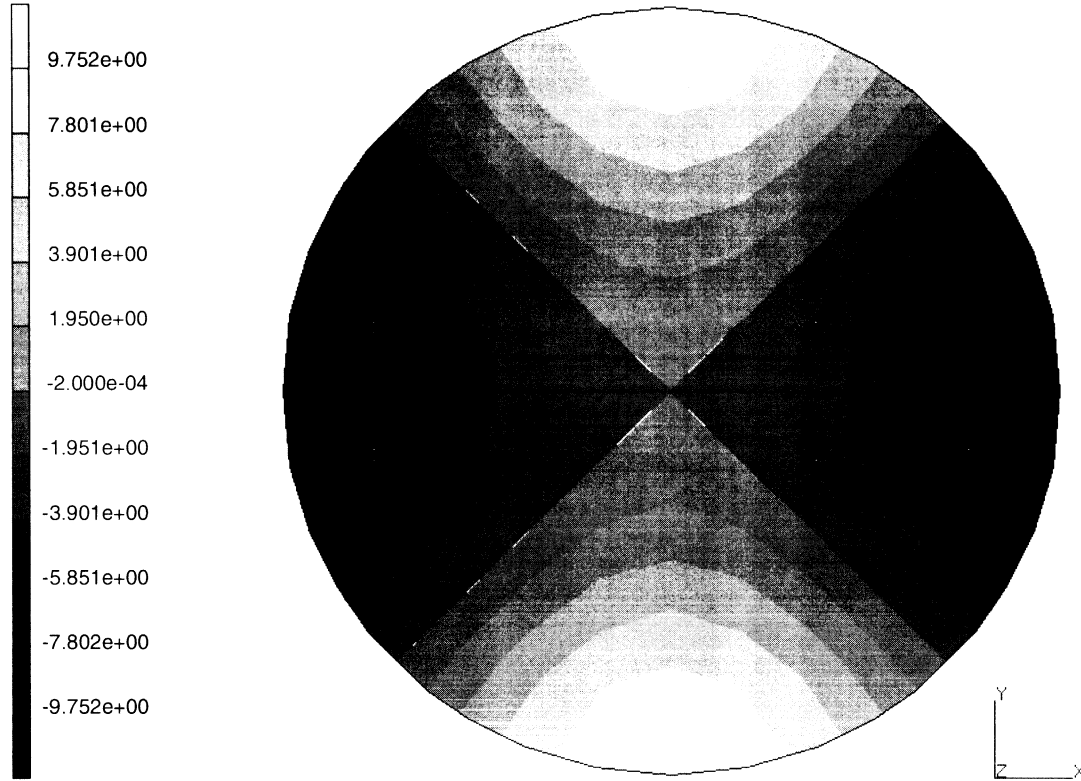


prob e8.25 acoustic problem central plate
Displacements

Figure 8.25-6 Fourth Mode



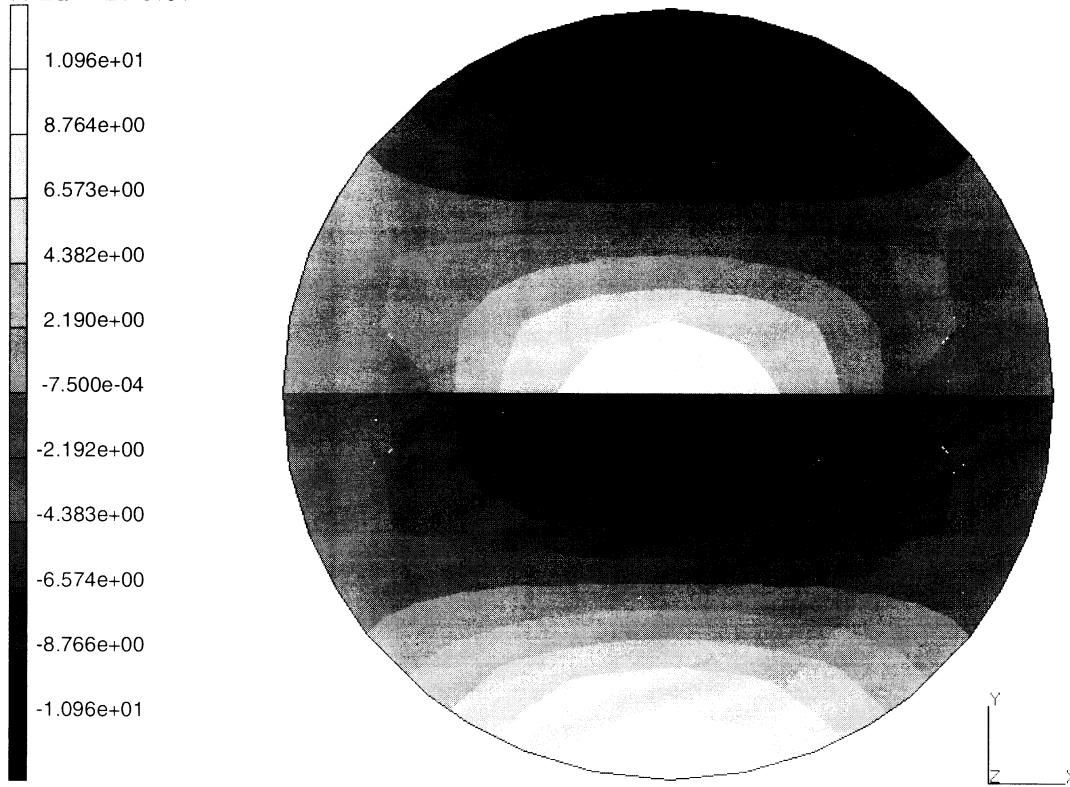
INC : 0
SUB : 5
TIME : 0.000e+00
FREQ : 1.029e+04



prob e8.25 acoustic problem central plate
Displacements

Figure 8.25-7 Fifth Mode

INC : 0
SUB : 6
TIME : 0.000e+00
FREQ : 1.247e+04

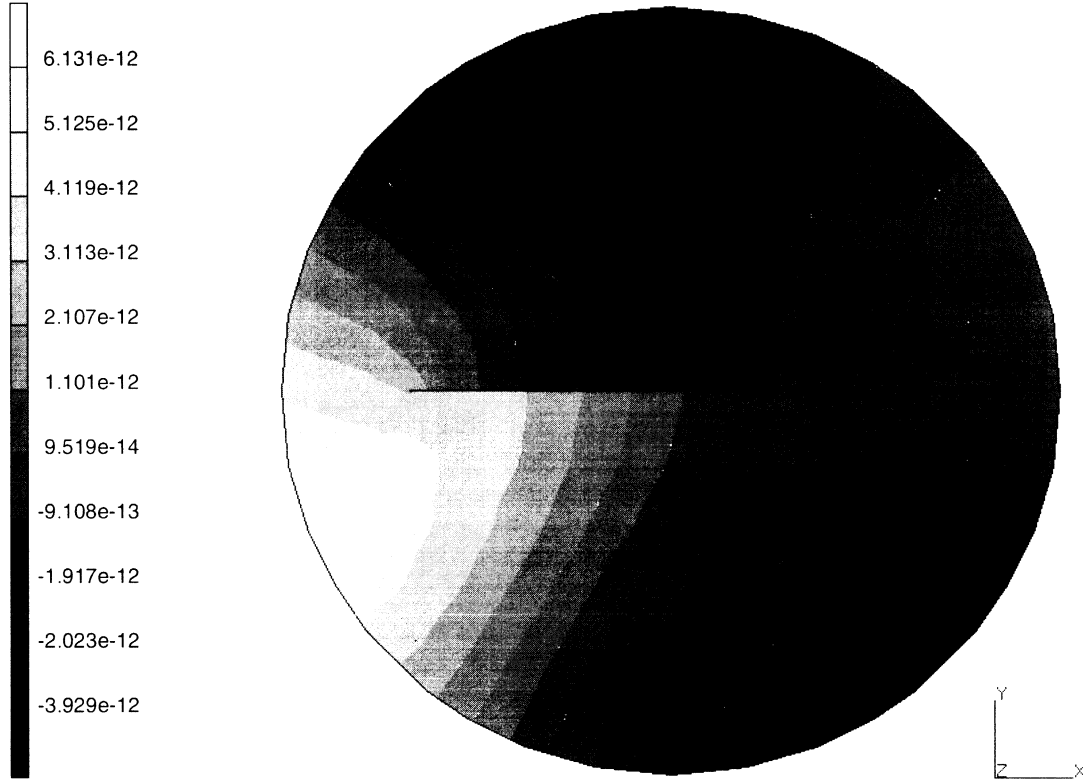


prob e8.25 acoustic problem central plate
Displacements

Figure 8.25-8 Sixth Mode



INC : 1
SUB : 0
TIME : 1.000e-06
FREQ : 0.000e+00

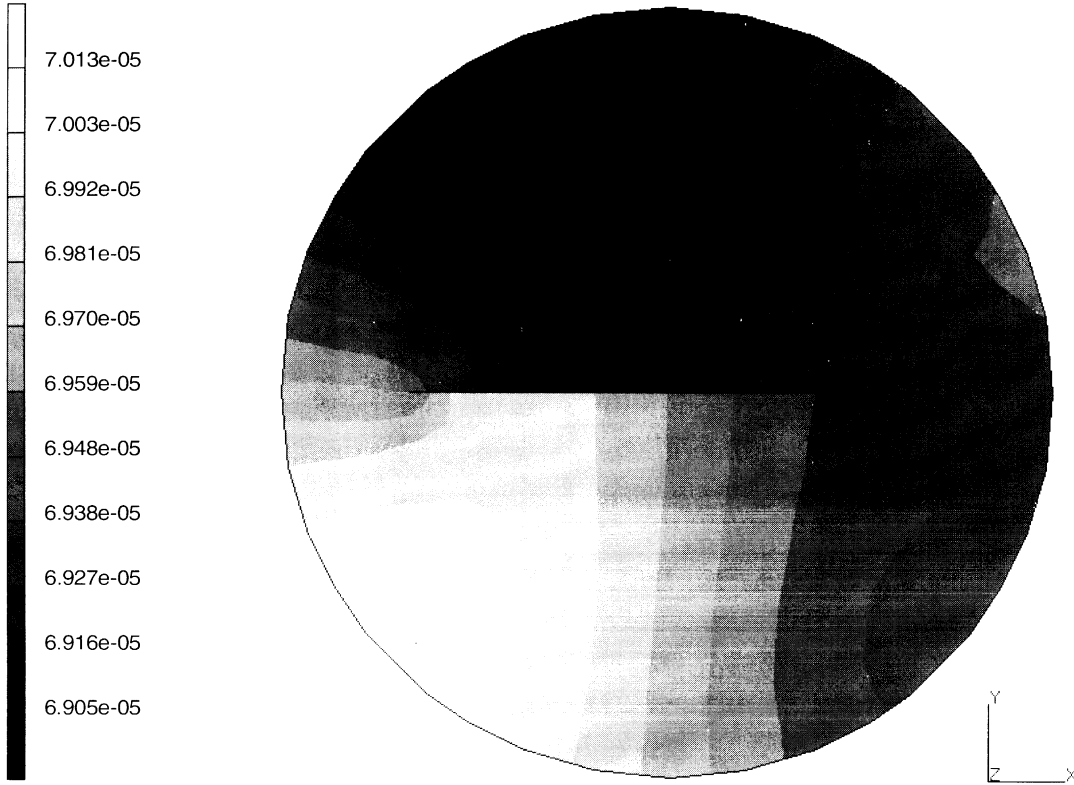


prob e8.25 acoustic problem central plate
Sound Source

Figure 8.25-9 Acoustic Pressure at Time = 0.000001



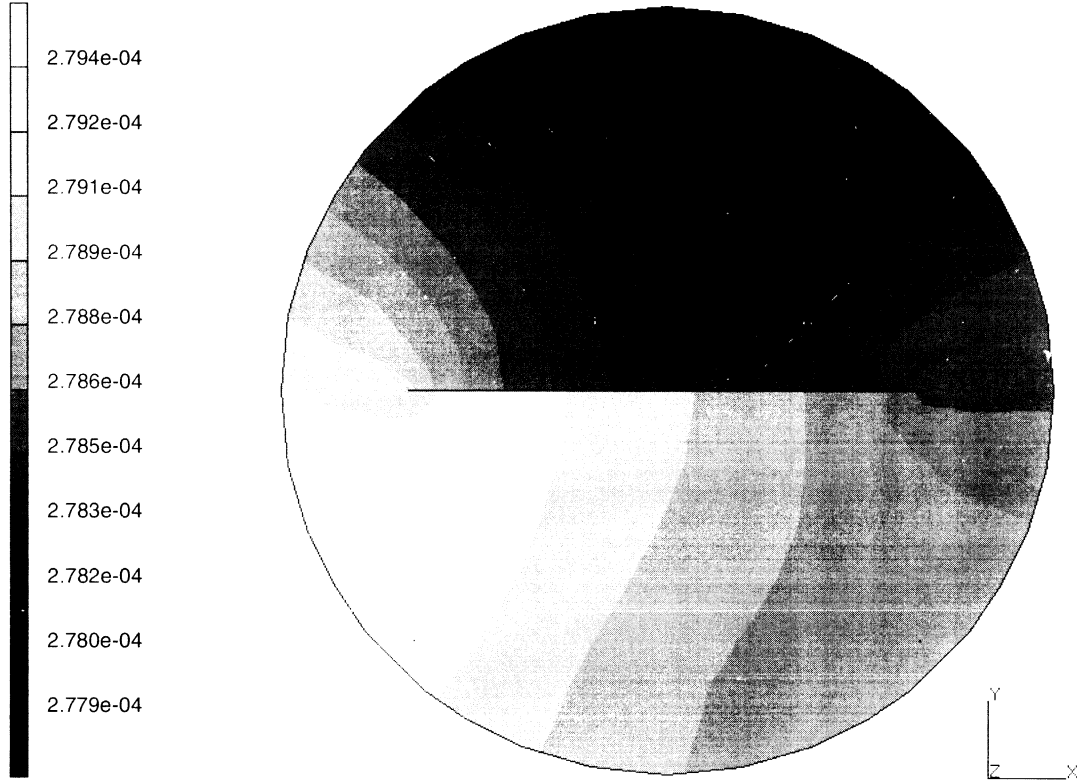
INC : 6
SUB : 0
TIME : 5.001e-03
FREQ : 0.000e+00



prob e8.25 acoustic problem central plate
Sound Source

Figure 8.25-10 Acoustic Pressure at Time = 0.005

INC : 11
SUB : 0
TIME : 1.000e-02
FREQ : 0.000e+00



prob e8.25 acoustic problem central plate
Sound Source

Figure 8.25-11 Acoustic Pressure at Time = 0.01





8.26 Acoustic Problem: Eigenvalue Analysis of a Rectangular Cavity

This problem shows MARC's acoustic analysis capability using a 2D element formulation. The acoustic pressure distribution in a rectangular cavity is to be calculated.

Parameters

The ACOUSTIC parameter is included to indicate an acoustic analysis. It further indicates that a maximum of five modes are to be used for modal superposition, that the eigenvalue problem is to be solved using the Lanczos formulation, and that the mode shapes are to be saved in the post file. PRINT, 3 is used to force the solution of a nonpositive definite stiffness matrix, which occurs due to the presence of a zero frequency (constant pressure) mode shape.

Boundary Conditions

A fixed pressure of zero psi is prescribed at nodes 1 and 2. The remaining edges have reflecting boundaries; no boundary conditions are required.

Material Properties

Through use of the ISOTROPIC option, the bulk modulus is given to be 139,000 psi, and the material density of 1.2 lbm/in³.

Loads

A sinusoidal forcing function is defined using user subroutine FORCDT of magnitude $\sin(1074t)$ on the second edge of nodes 21 and 22. Note that FORCDT must apply incremental source quantities and not total source quantities.

Dynamics

A total of five mode shapes are to be extracted using the Lanczos eigensolver. The lowest frequency is specified to be -10 Hz, which ensures the capture of zero frequency modes. The DYNAMIC CHANGE option provides the following parameters that are necessary for the integration of the modal equations of motion:

Time step size = 0.0003 seconds Duration = 0.0091 seconds
Number of time steps = 30

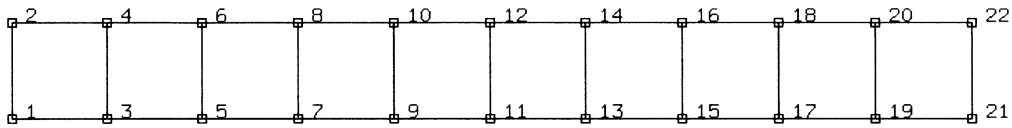


Figure 8.26-1 Acoustic Cavity Mesh

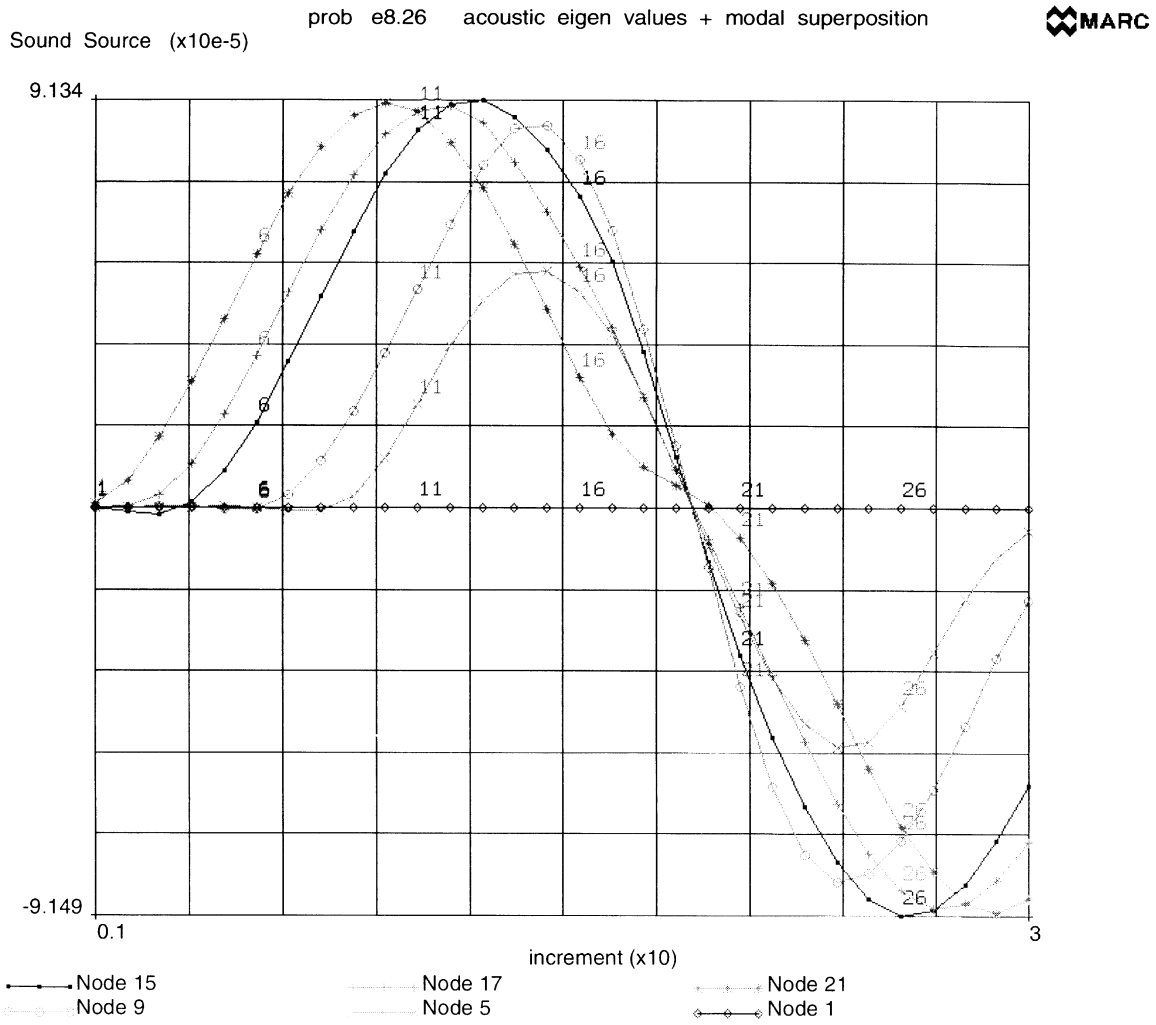


Figure 8.26-2 Time History of Pressure Pulse



8.27 Progressive Failure of a Plate with a Hole

This problem demonstrates the application of MARC's progressive failure modeling capability applied to a plane stress problem. A plate with a circular hole, made of an orthotropic material, is loaded until selective regions fail.

Parameters

The use of element 26 (8-noded plane stress quadrilateral) is specified through an ELEMENT parameter.

Mesh Definition

The square plate is 100 mm long. The radius of the hole is 10 mm. Only one-quarter of the plate is modeled due to symmetry. A thickness of 1 mm is provided through the first field in the GEOMETRY option (EGEOM1). Figure 8.27-1 shows the nodal configuration of the mesh and Figure 8.27-2 shows the element configuration.

Boundary Conditions

Constraints in the global X-, Y-directions are applied through the use of the FIXED DISP model definition option.

Material Properties

Use of the ORTHOTROPIC model definition option allows the input of directional moduli. The following values are specified:

$$E = 14.0 \times 10^9 \text{ N/mm}^2 \quad E = 3.50 \times 10^9 \text{ N/mm}^2 \quad G = 4.2 \times 10^9 \text{ N/mm}^2$$

Poisson's ratio relating strains in the 1-2 directions is 0.4. The orthotropic axes are skewed with respect to the global X,Y by an angle of sixty degrees. To take this into account, an ORIENTATION option group is given defining the material axis base vectors to be a function of the intersection of the element tangent plane and the global ZX plane. The progressive failure option is invoked through the FAIL DATA model option, specifically by entering a '1' in the third field of the third record. Two failure criteria coexist: maximum stress (MX STRESS option) and Hill (HILL). For the both stress criteria, failure is predicated on the following stress levels:

$$\sigma_X \text{ (tension)} = \text{Sigma X (compression)} = 250,000,000 \text{ N/mm}^2$$

$$\sigma_Y \text{ (tension)} = 500,000 \text{ N/mm}^2$$

$$\sigma_Y \text{ (compression)} = 10,000,000 \text{ N/mm}^2$$

$$\sigma_{XY} = 8,000,000 \text{ N/mm}^2$$

Failure occurs when the corresponding interaction equation (see *Volume A: User Information*) reaches or exceeds unity.



Loads

A distributed load of $300,000 \text{ N/mm}^2$ is applied on the 2-6-3 face of elements 13 and 14 during increment zero. Five load steps of 20% of the increment zero load are applied bringing the total distributed load magnitude to $600,000 \text{ N/mm}^2$. This is done through the use of the AUTO LOAD and PROPORTIONAL INC options.

Control

A maximum of ten load steps and four recycles per step is allowed through the CONTROL option. Furthermore, convergence is considered to be reached when the maximum residual force divided by the maximum reaction force falls below the value 0.1.

POST

A formatted post file is requested with the following variables:

code 94	Failure index
code 111	Direct stress 11 in preferred 1 direction
code 112	Direct stress 22 in preferred 2 direction
code 113	Shear stress 12

Results

Figure 8.27-3, Figure 8.27-4, and Figure 8.27-5 show the fourth failure index at increments 1, 3, and 5, respectively. The stresses in the preferred directions are shown in Figure 8.27-6 and Figure 8.27-7.



Parameters, Options, and Subroutines Summary

Example e8x27.dat:

Parameters

ELEMENT
END
SIZING
TITLE

Model Definition Options

CONNECTIVITY
CONTROL
COORDINATE
DIST LOADS
END OPTION
FAIL DATA
FIXED DISP
GEOMETRY
ORIENTATION
ORTHOTROPIC
POST
PRINT ELEM

History Definition Options

AUTO LOAD
CONTINUE
PROPORTIONAL INCREMENT

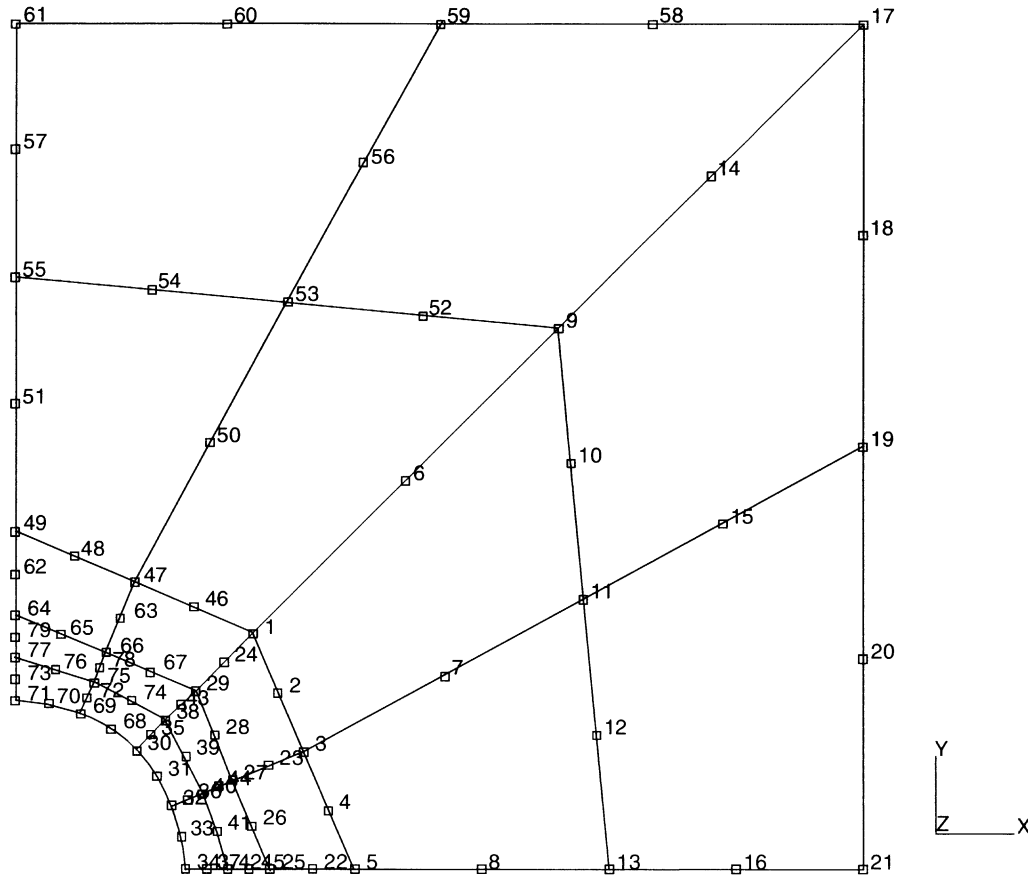


Figure 8.27-1 Finite Element Mesh – Nodes

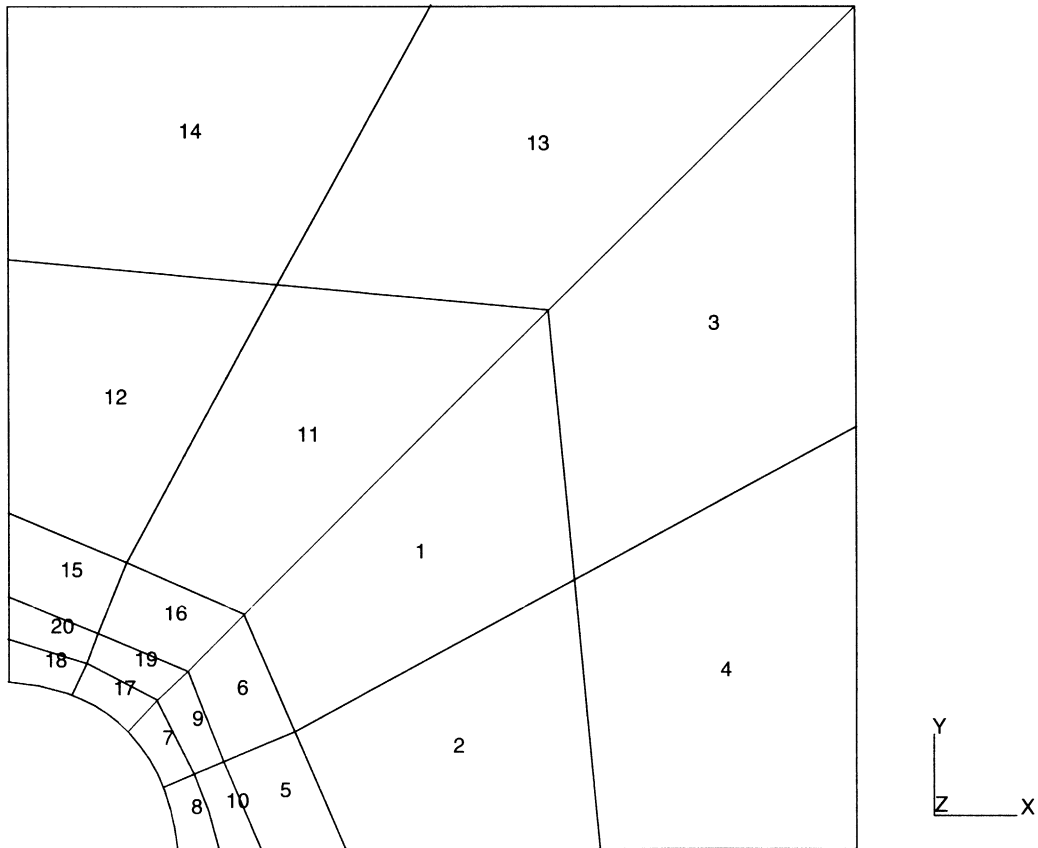
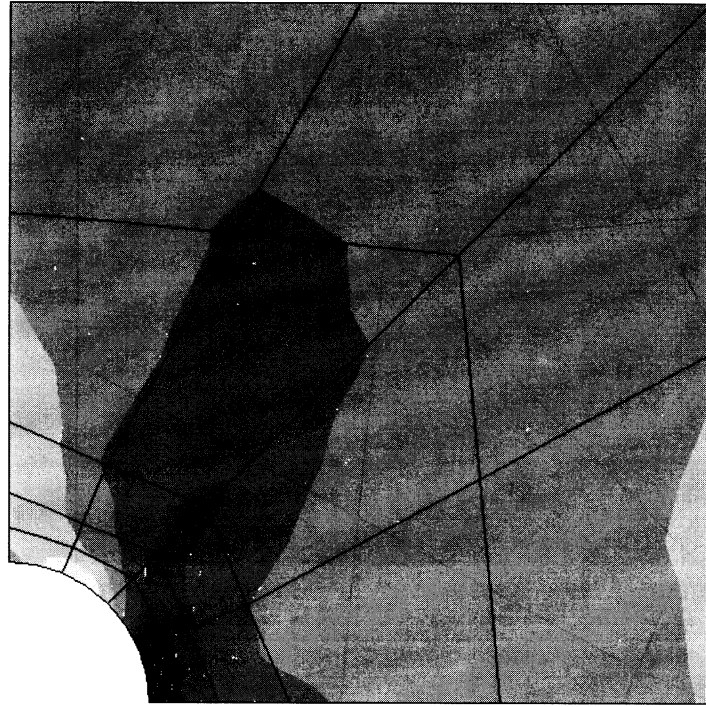
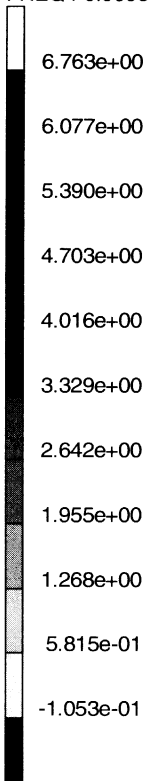


Figure 8.27-2 Finite Element Mesh – Nodes



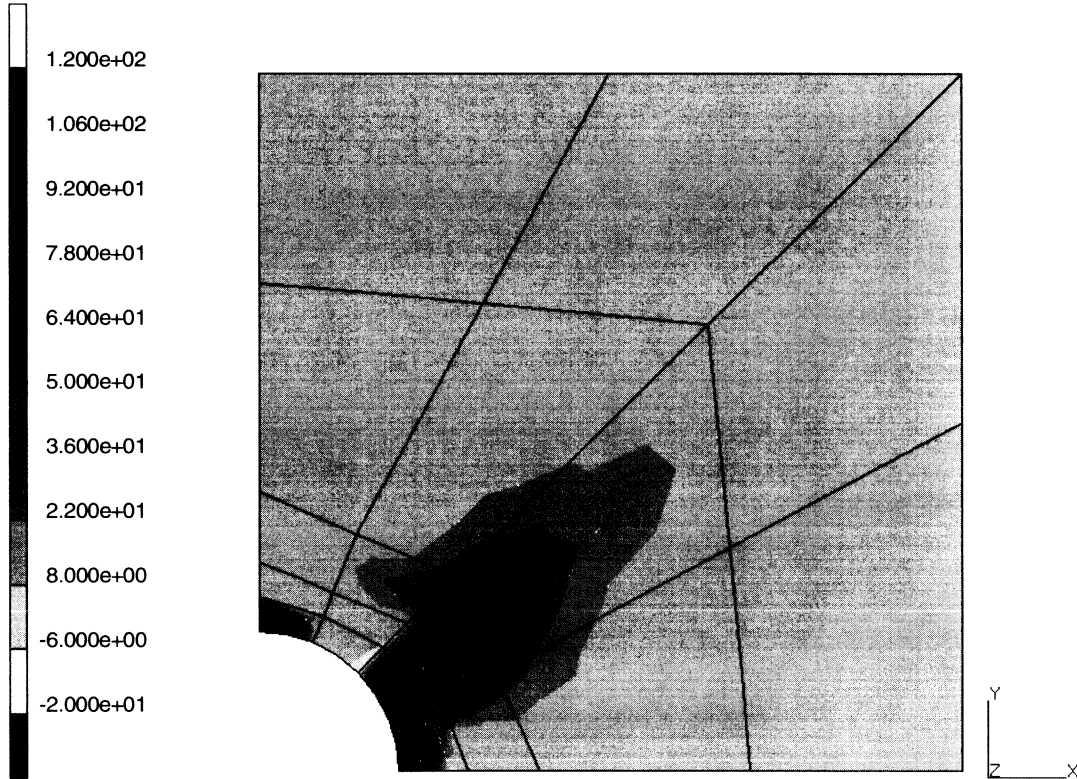
INC : 0
SUB : 0
TIME : 0.000e+00
FREQ : 0.000e+00



prob e8.27 progressive failure of a plate with hole
4th Failure Index

Figure 8.27-3 Failure Index, Increment 0

INC : 5
SUB : 0
TIME : 0.000e+00
FREQ : 0.000e+00

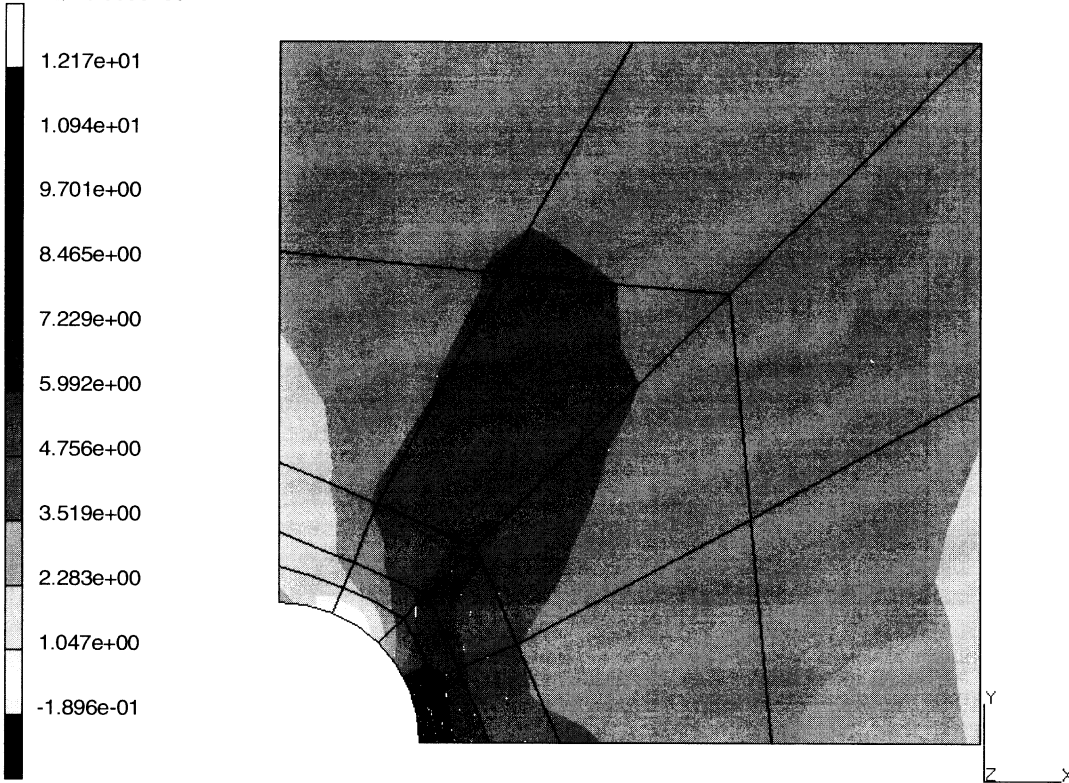


prob e8.27 progressive failure of a plate with hole
4th Failure Index

Figure 8.27-4 Failure Index, Increment 5



INC : 4
SUB : 0
TIME : 0.000e+00
FREQ : 0.000e+00



prob e8.27 progressive failure of a plate with hole
4th Failure Index

Figure 8.27-5 Failure Index – No Failure Allowed



INC : 5
SUB : 0
TIME : 0.000e+00
FREQ : 0.000e+00

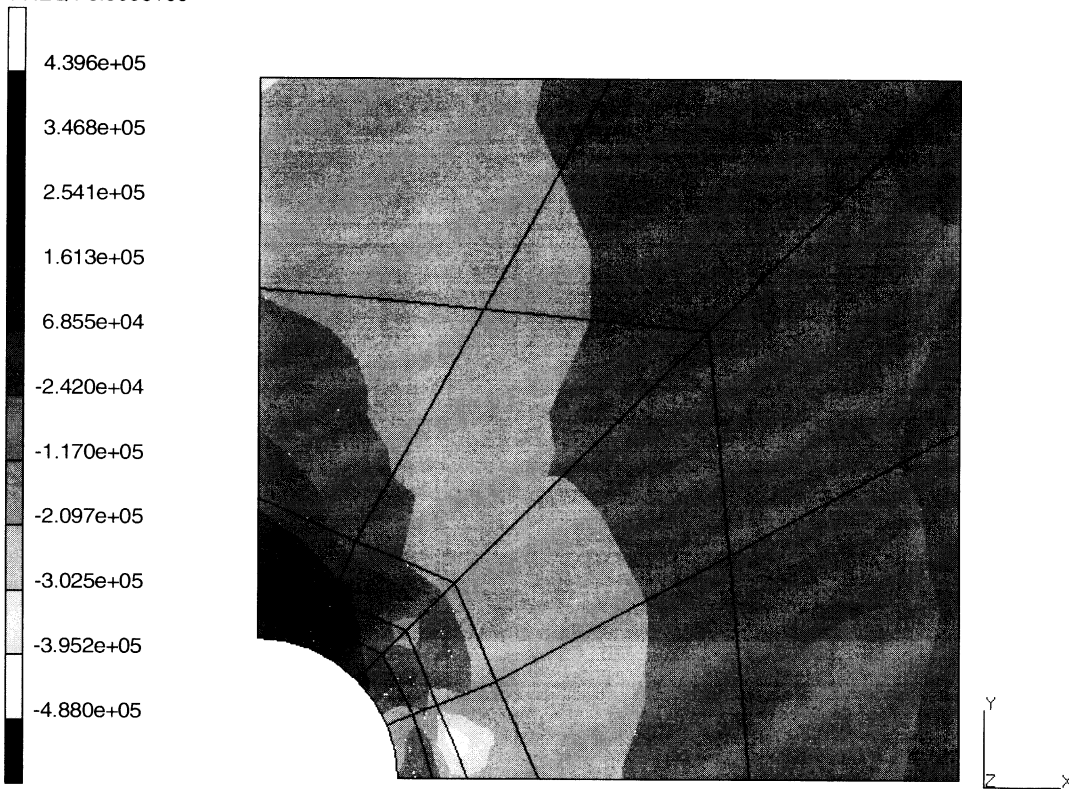


prob e8.27 progressive failure of a plate with hole
1st Comp of Stress in Preferred Coord

Figure 8.27-6 First Component of Stress in Preferred Direction



INC : 5
SUB : 0
TIME : 0.000e+00
FREQ : 0.000e+00



prob e8.27 progressive failure of a plate with hole
2nd Comp of Stress in Preferred Coord

Figure 8.27-7 Second Component of Stress in the Preferred Direction



8.28 Linear Distribution of Dipoles

The problem presented here is the determination of the two-dimensional electric field generated in a vacuum around two wires with uniform electrostatic charge of opposite signs. The numerical results are compared with the analytic solution.

Parameters

The ELECTRO parameter is included to indicate that an electrostatic analysis is being performed.

Element

Elements type 41 and 103 are used.

Element 41 is a second-order planar isoparametric quadrilateral for “quasi-harmonic” field problems. Element type 103 is a nine-node semi-infinite element. In the first direction, special interpolation functions are used which can represent exponential decay.

Model

The mesh of the plane is shown in Figure 8.28-1. The outer ring is modeled with semi-infinite elements. The outer radius is 1.5 m.

Material Properties

The permittivity of the medium (vacuum) is 8.8×10^{-12} farad/m.

Point Charge

A linear distribution normal to the plane of 10^{-12} coulomb/m is prescribed with opposite signs at nodes 80 and 81 ($X = 0$, $Y = \pm 0.21621$ m).

Fixed Potential

The potential is prescribed to be zero at the center of the plane.

Control

The STEADY STATE option initiates the analysis. A formatted post file is created.

Results

A contour plot of the electric potential is shown in Figure 8.28-2. A vector plot of the electric field is shown in Figure 8.28-3. An X-Y plot of the potential along the Y-axis is shown in Figure 8.28-4. Table 8.28-1 shows a comparison of the MARC results with the analytical solution.

**Table 8.28-1** Comparison of MARC Results

Node	Y (m.)	Potential (Volt)		Error (%)
		MARC	Analytical	
8	0.07254	1.302	1.255	+ 3.7
36	0.14435	2.729	2.900	- 5.9
165	0.29150	3.257	3.432	- 5.1
320	0.48159	1.732	1.739	- 0.4
558	1.0	0.789	0.790	- 0.1

Parameters, Options, and Subroutines Summary

Example e8x28.dat:

ParametersELECTROSTATIC
ELEMENT
END
SIZING
TITLE**Model Definition Options**CONNECTIVITY
COORDINATE
DEFINE
END OPTION
FIXED POTENTIAL
ISOTROPIC
POINT CHARGE
POST
PRINT ELEM**History Definition Options**CONTINUE
STEADY STATE

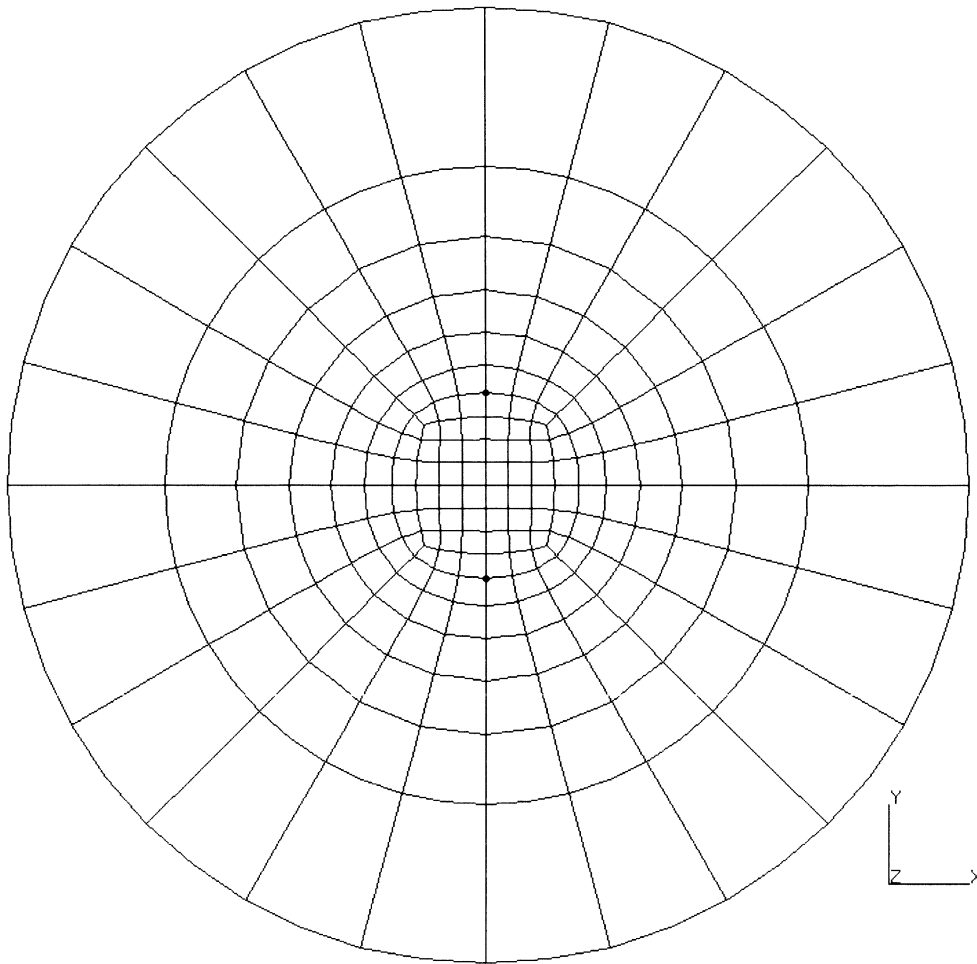
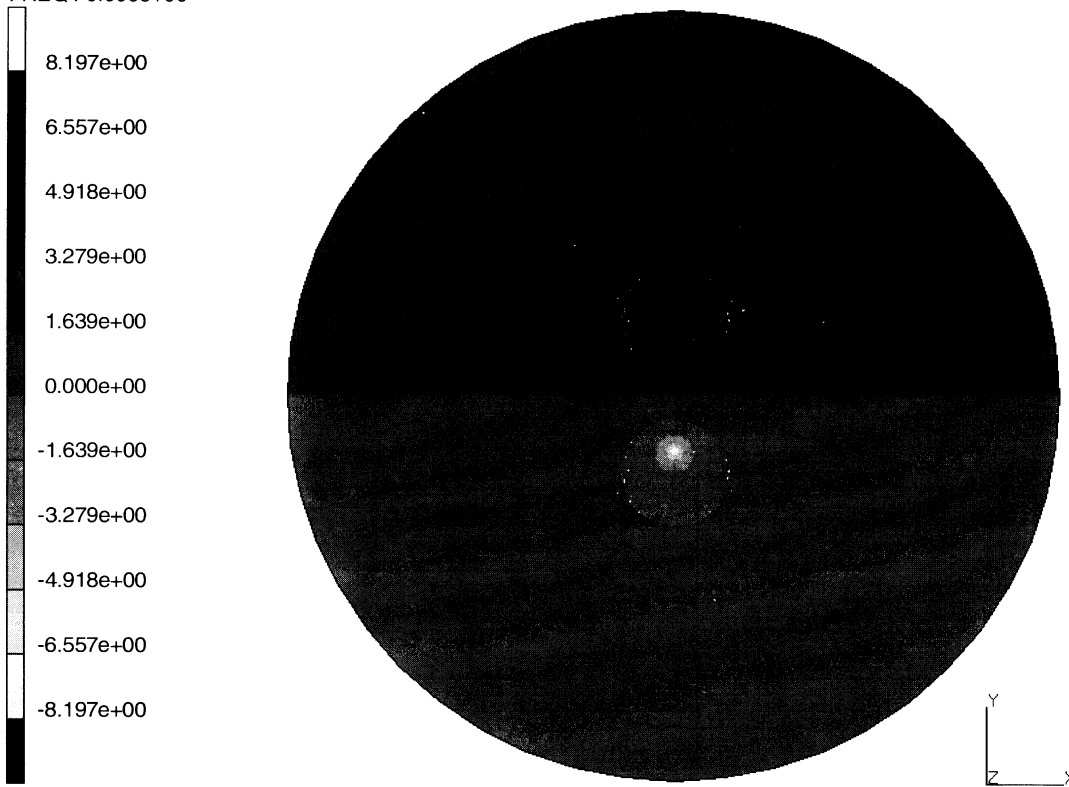


Figure 8.28-1 Finite Element Mesh with Dipole



INC : 1
SUB : 0
TIME : 0.000e+00
FREQ : 0.000e+00



prob e8.28 linear distribution of dipoles
Electric Potential

Figure 8.28-2 Scalar Potential

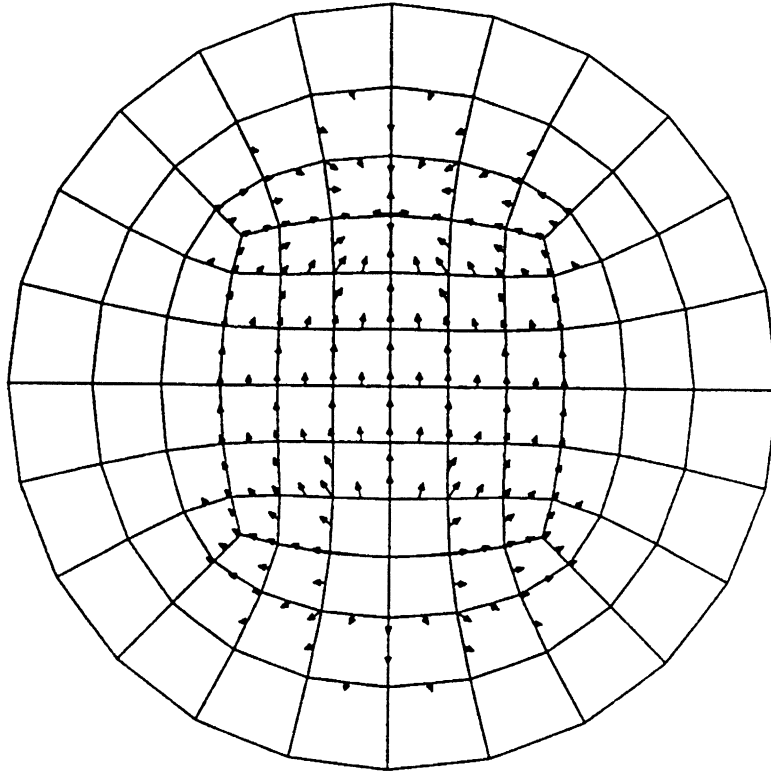


Figure 8.28-3 Vector Plot of Electric Field



INC : 1
SUB : 0
TIME : 0.000e+00
FREQ : 0.000e+00

prob e8.28 linear distribution of dipoles



Electric Potential

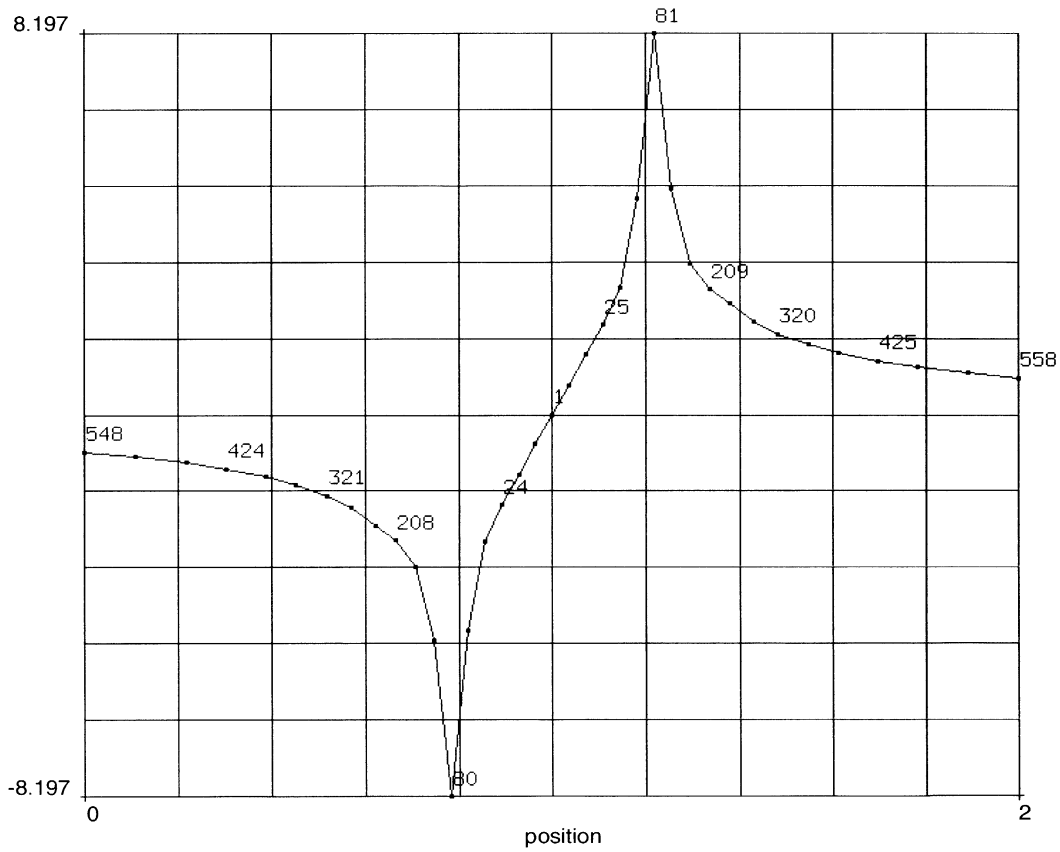


Figure 8.28-4 Scalar Potential Distribution



8.29 Magnetic Field around Two Wires carrying Opposite Currents

The problem presented here is the determination of the two-dimensional electric field generated in a vacuum around two wires carrying equal current of opposite signs. The numerical results are compared with the analytical solution.

Parameters

The MAGNETO parameter is included to indicate that a magnetostatic option is being performed.

Element

Elements type 41 and 103 are used.

Element 41 is a second-order planar isoparametric quadrilateral for “quasi-harmonic” field problems.

Element 103 is a nine-node planar semi-infinite quadrilateral for “quasi-harmonic” field problems.

Model

The mesh of the plane is shown in Figure 8.29-1. The outer ring is modeled with semi-infinite elements. The outer radius is 1.5 m.

Material Properties

The magnetic permeability of the medium (vacuum) is 1.26×10^{-6} henry/m.

Point Current

A point current of 10^{-6} amp running normal to the plane is prescribed with opposite signs at nodes 80 and 81 ($X = 0$, $Y = \pm 0.21621$ m).

Fixed Potential

The potential is prescribed to be zero at the center of the plane.

Control

The STEADY STATE option initiates the analysis. A formatted post file is created.

Results

A contour plot of the scalar potential (only available for 2D magnetostatic) is shown in Figure 8.29-2. A vector plot of the magnetic flux density is shown in Figure 8.29-3. An X-Y plot of the potential along the Y-axis is shown in Figure 8.29-4. Table 8.29-1 shows a comparison of the MARC results with the analytical solution.



Table 8.29-1 Comparison of MARC Results

Node	X (m.)	Bx (weber/m ²)		Error (%)
		MARC	Analytical	
1	0.	1.855	1.855	+ 0.0
6	0.072534	1.674	1.667	+ 0.4
34	0.14434	1.288	1.283	+ 0.4
162	0.29149	0.664	0.658	+ 0.9
319	0.48158	0.316	0.311	+ 1.6
547	1.0	0.0832	0.0828	+ 0.5

Parameters, Options, and Subroutines Summary

Example e8x29.dat:

Parameters

ELEMENT
END
MAGNETOSTATIC
SIZING
TITLE

Model Definition Options

CONNECTIVITY
COORDINATE
DEFINE
END OPTION
FIXED POTENTIAL
ISOTROPIC
POINT CURRENT
POST
PRINT ELEM

History Definition Options

CONTINUE
STEADY STATE

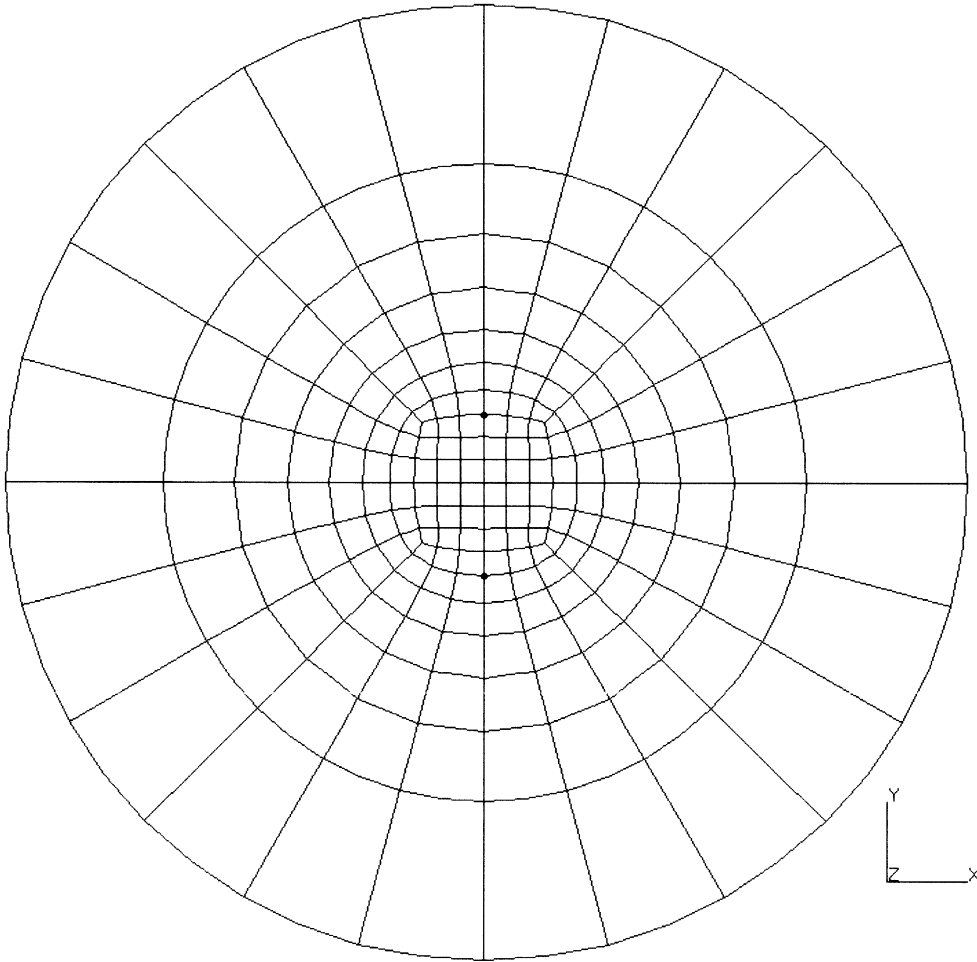


Figure 8.29-1 Finite Element Mesh and Parallel Wires



INC : 1
SUB : 0
TIME : 0.000e+00
FREQ : 0.000e+00



prob e8.29 parallel wires with opposite currents
Magnetic Potential

Figure 8.29-2 Magnetic Scalar Potential

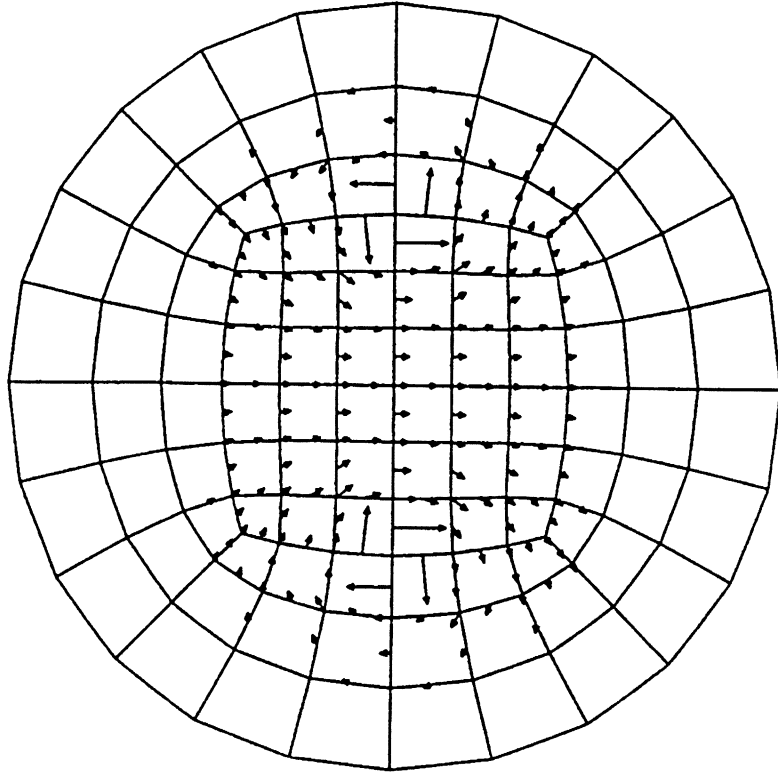


Figure 8.29-3 Magnetic Flux Density



INC : 1
SUB : 0
TIME : 0.000e+00
FREQ : 0.000e+00

prob e8.28 parallel wires with opposite currents



1st (Real) Comp of Magnetic Flux

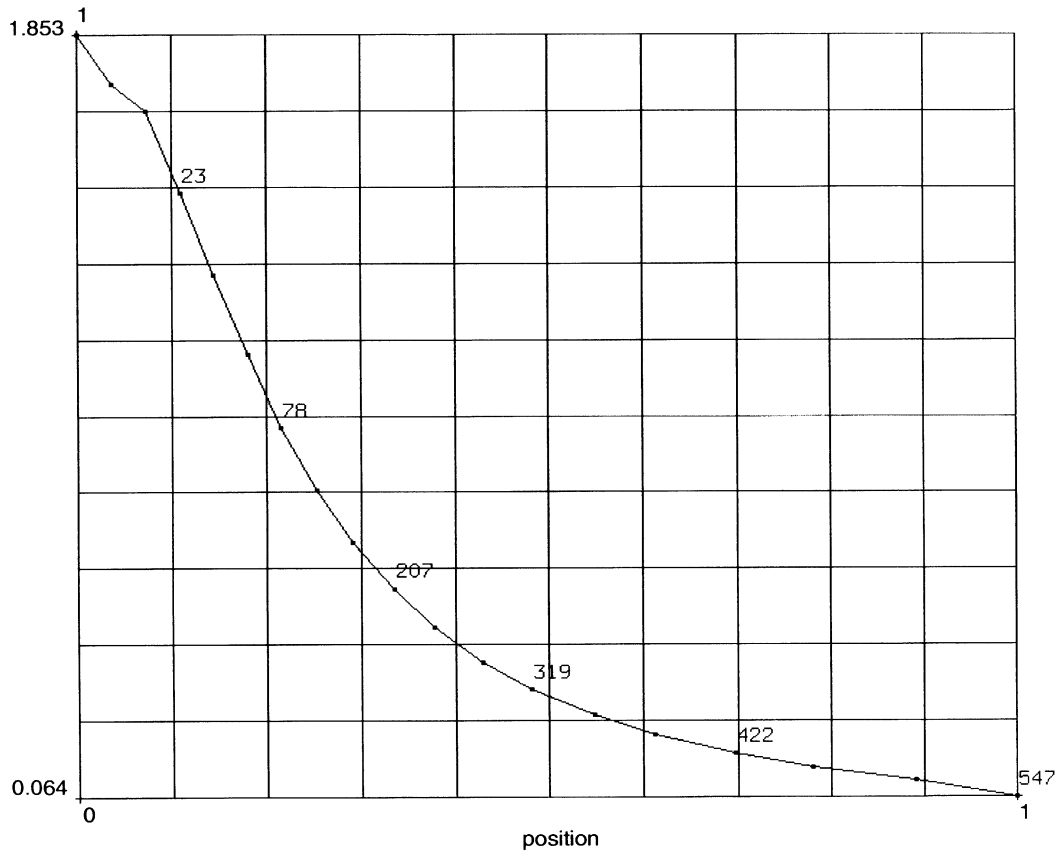


Figure 8.29-4 Magnetic Flux Distribution



8.30 Harmonic Electromagnetic Analysis of a Wave Guide

This problem demonstrates MARC’s capability to perform electromagnetic analysis of a wave guide. The harmonic procedure is utilized in this problem.

Parameters

The EL-MA, 1 parameter is used to indicate that a harmonic electromagnetic analysis is to be performed. This always results in a complex formulation. The HARMONIC parameter is used to give an upper bound to the number of harmonic boundary conditions.

Element

Element 111 is used in this problem. This element is a four-node planar element for electromagnetic analysis. There are four degrees of freedom, the vector magnetic potential A , and the scalar electrical potential ϕ .

Model

The model, as shown in Figure 8.30-1, has a length of 1 m and a width of 0.5m. A wall is placed at 0.5 m which is 0.02 m thick (elements 33 to 36).

Loading

The outside periphery labeled “metal” is held at a fixed magnetic potential of zero. The corner, node 46, is given a fixed electrical potential of zero. A distributed current is applied to element one. The current is applied at a frequency between 200 MHz to 240 MHz in 2 MHz steps.

Material Properties

There are two materials in this analysis: the air and the wall. The material properties are:

	Permeability (henry/m)	Permittivity (farad/m)	Permeability of Air (henry/m)	Conductivity (s/m)
Air	1.2566×10^{-6}	8.854×10^{-12}	1.2566×10^{-6}	1000
Wall	1.2566×10^{-6}	8.854×10^{-12}	1.2566×10^{-6}	1×10^{-8}

Control

As this is a linear analysis, no controls are required.



Results

The third component of the electric field varies in magnitude from 0.989 to 0.831 over the frequency range requested. The user can also observe that there is no distribution on the right side of the wall in Figure 8.30-3. Note that the frequency is input in cycles/time, but Mentat reports the frequency in radians/time.

Table 8.30-1 Electric Field as a Function of Frequency

Subincrement	ω x MHz	E_3
1	200	9.892
5	210	9.512
10	220	9.076
15	230	8.679
20	240	8.314

Parameters, Options, and Subroutines Summary

Example e8x30.dat:

Parameters

ELEMENT
EL-MA
END
PRINT
SIZING
TITLE

Model Definition Options

CONNECTIVITY
COORDINATE
DEFINE
END OPTION
FIXED POTENTIAL
ISOTROPIC
OPTIMIZE
POST

History Definition Options

CONTINUE
DIST CURRENT
HARMONIC

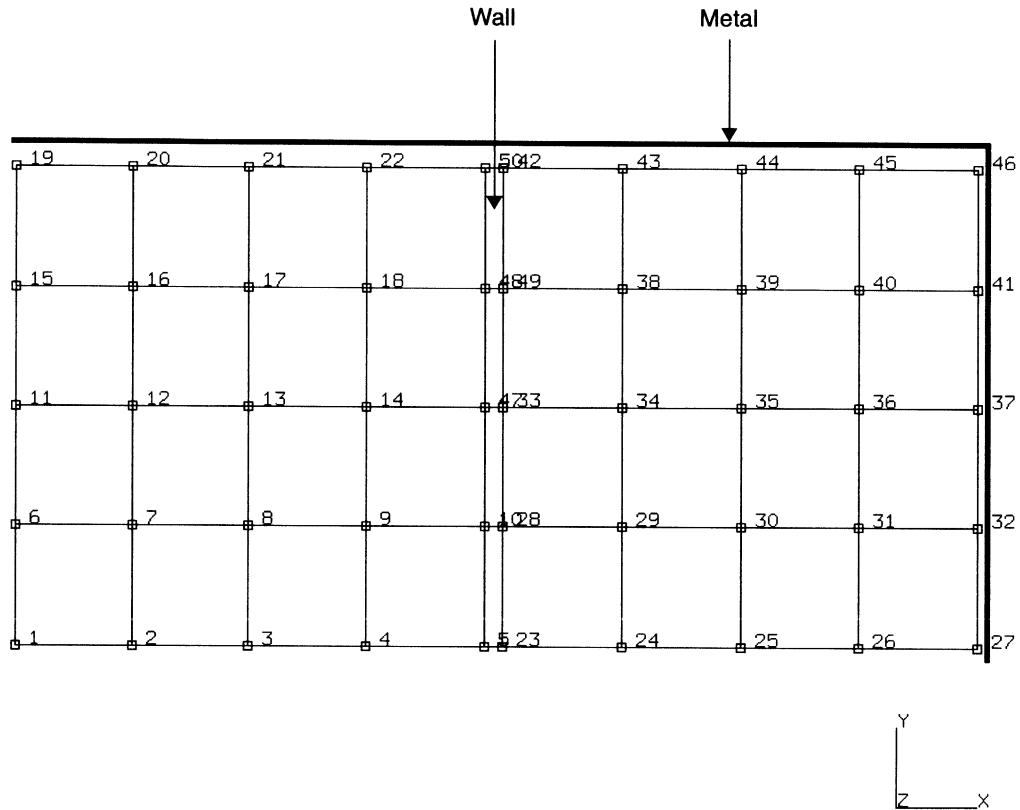


Figure 8.30-1 Finite Element Mesh with Node Numbers



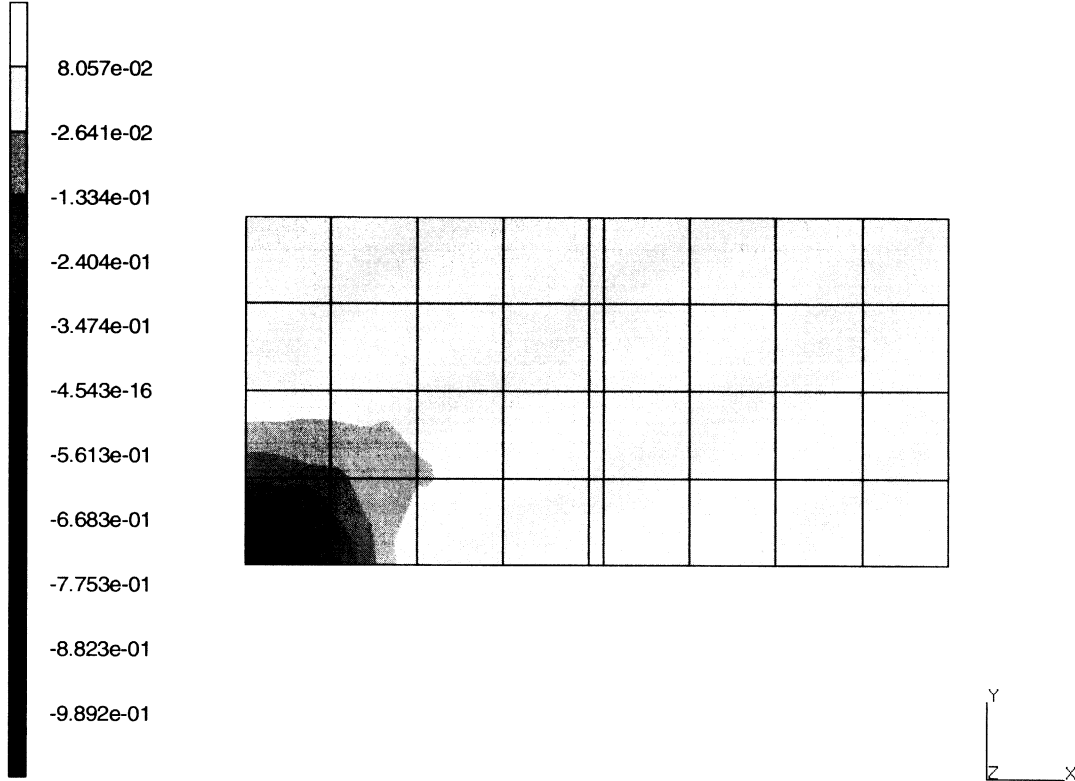
13	14	15	16	36	29	30	31	32
9	10	11	12	35	25	26	27	28
5	6	7	8	34	21	22	23	24
1	2	3	4	33	17	18	19	20



Figure 8.30-2 Finite Element Mesh with Element Numbers



INC : 0
SUB : 1
TIME : 0.000e+00
FREQ : 1.257e+09



prob e8.30 waveguide demo – elmt 111
3rd (Real) Comp of Electric Field

Figure 8.30-3 Third Component of Electric Field at 20 MHz





8.31 Transient Electromagnetic Analysis around a Conducting Sphere

This example demonstrates the transient electromagnetic analysis around a conducting sphere subjected to a planar pulse.

Parameters

The EL-MA,0 parameter is used to indicate that a transient electromagnetic analysis is to be performed.

Element

This model consists of 165 element type 112 as shown in Figure 8.31-1. Element type 112 is a four-node axisymmetric element for electromagnetic analysis. It has four degrees of freedom. The first three represent the magnetic vector potential. The last represents the scalar electrostatic potential. The spherical shell is elements 135-143 and 153. The inner radius is 5 cm and the outer radius is 5.5 cm.

Loading

The vertical symmetry line at $z = 0$ is constrained such that all components of A are zero. The nodes along $z = 15$ have $A_z = 0$. The nodes along $r = 0$ and $r = 15$ have A_x and A_z prescribed to be zero. The nodes along $z = 15$ have a ramp charge applied to the second component that varies from 0 to 25×10^{-6} coulomb over 25 microseconds. This data is entered using the DYNAMIC CHANGE and POTENTIAL CHANGE options.

Material Properties

There are two materials in this analysis: the air and the metal sphere. The material properties are as follows:

	Permeability (henry/m)	Permittivity (farad/m)	Permeability of Air (henry/m)	Conductivity (s/m)
Air	1.2566×10^{-6}	8.54×10^{-12}	1.2566×10^{-6}	5×10^8
Sphere	1.2566×10^{-6}	8.54×10^{-12}	1.2566×10^{-6}	0.0

These are specified through the ISOTROPIC option.

**Control**

The convergence tolerance requested is 10% on residuals. The POST option is used to save the magnetic flux for post processing. The DYNAMIC CHANGE option is used to specify a time period of 25 microseconds to be performed in 25 increments with a fixed time step of 1 microsecond.

Results

Figure 8.31-2 and Figure 8.31-3 show the propagation of the magnetic field with time. The time history of the magnetic field is shown in Figure 8.31-4. Finally, the current density is shown in Figure 8.31-5. As expected, most of the current is in the sphere and the magnetic field is virtually zero within the sphere.

Parameters, Options, and Subroutines Summary

Example e8x31.dat:

Parameters	Model Definition Options	History Definition Options
ELEMENT	CONNECTIVITY	CONTINUE
EL-MA	COORDINATE	DYNAMIC CHANGE
END	CONTROL	
PRINT	DEFINE	
SIZING	END OPTION	
TITLE	FIXED POTENTIAL	
	FORCDDT	
	ISOTROPIC	
	OPTIMIZE	
	POST	

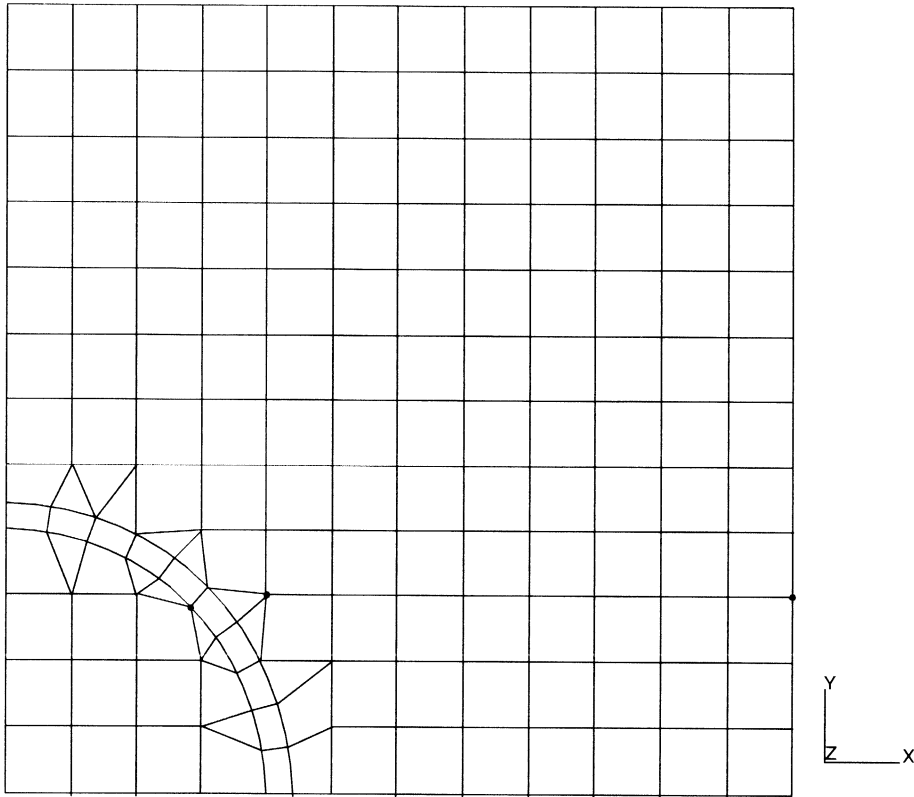
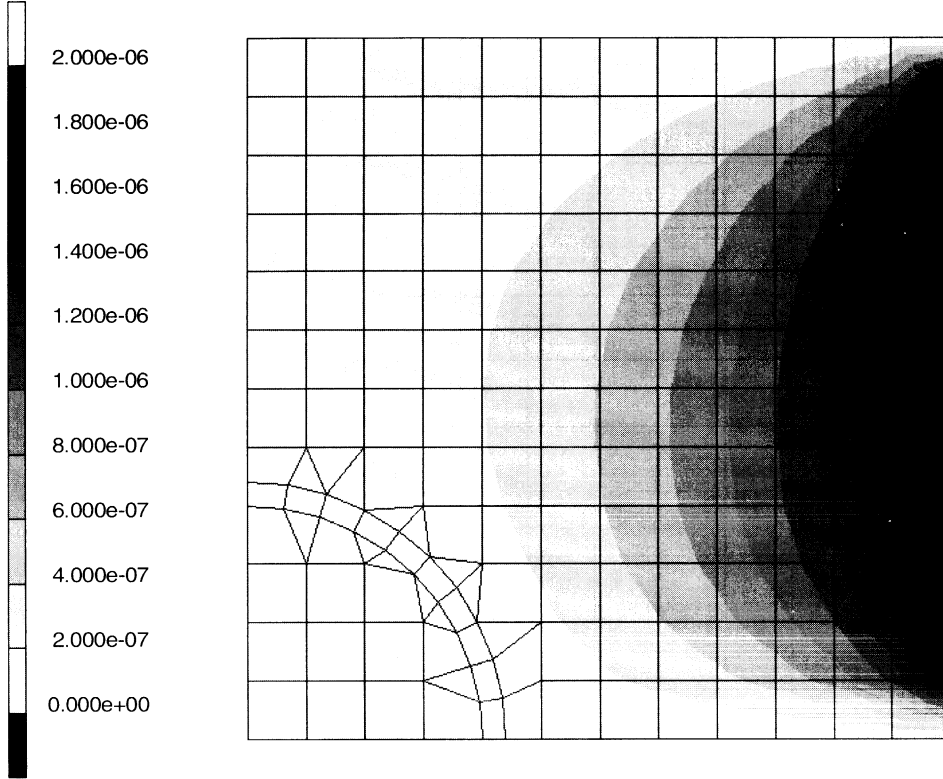


Figure 8.31-1 Finite Element Mesh



INC : 2
SUB : 0
TIME : 2.000e-06
FREQ : 0.000e+00

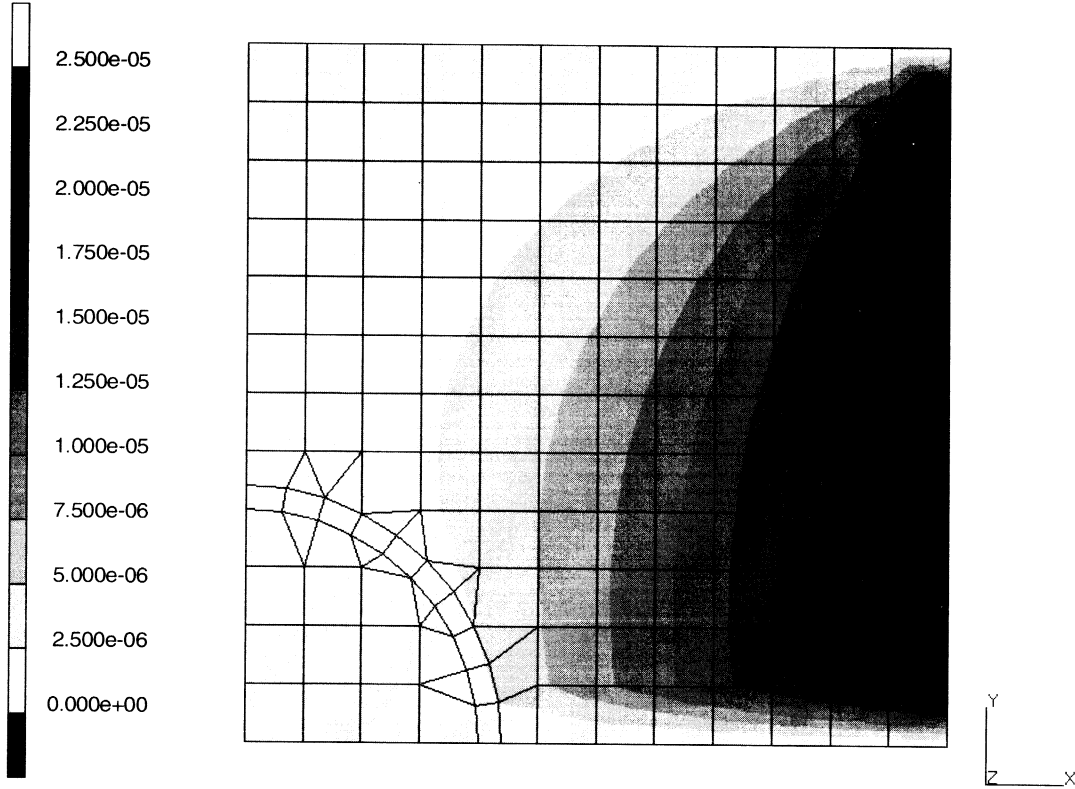


prob e8.31 transient magnetic field in a conducting sph
Magnetic Potential z

Figure 8.31-2 Third Component of Magnetic Potential, Time = 2 Microseconds




INC : 25
SUB : 0
TIME : 2.500e-05
FREQ : 0.000e+00



prob e8.31 transient magnetic field in a conducting sph
Magnetic Potential z

Figure 8.31-3 Third Component of Magnetic Potential, Time = 25 Microseconds

prob e8.31 transient magnetic field in a conducting sphere elm 
 Magnetic Potential z (x10e-5)

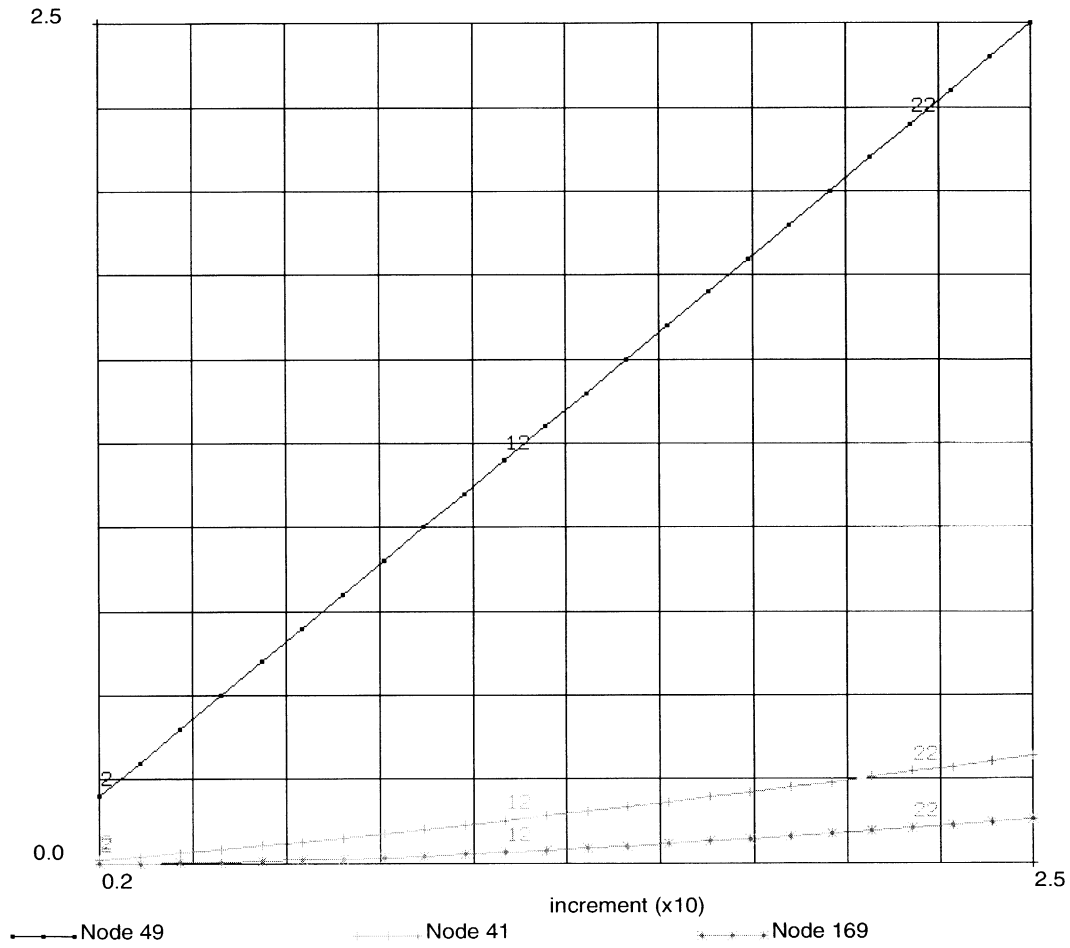
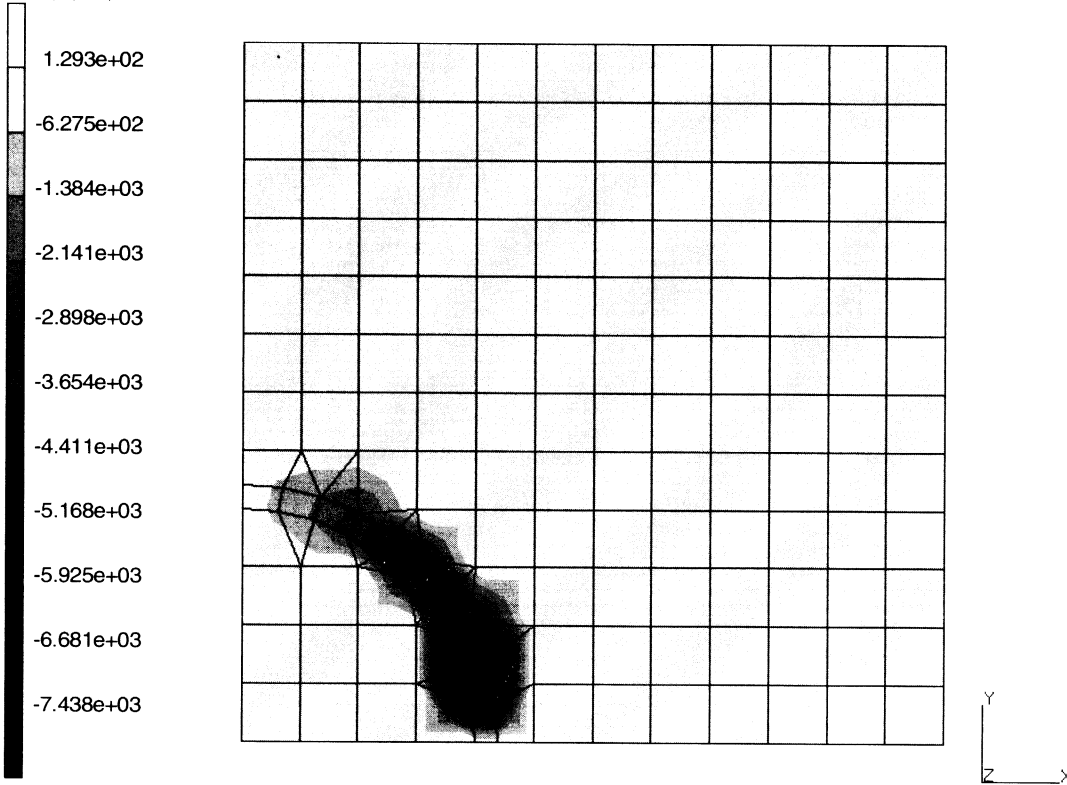


Figure 8.31-4 Time History of Magnetic Potential



INC : 25
SUB : 0
TIME : 2.500e-05
FREQ : 0.000e+00



prob e8.31 transient magnetic field in a conducting sph
3rd (Real) Comp of Current Density

Figure 8.31-5 Current Density, Time = 25 Microseconds





8.32 Cavity Resonator

This problem demonstrates the use of the harmonic electromagnetic capability for a prismatic resonator.

Parameters

The EL-MA,1 parameter indicates that a harmonic electromagnetic analysis is to be performed. The HARMONIC option gives an upper bound to the number of harmonic boundary conditions.

Element

Element 113, an eight-node electromagnetic brick, is used in this example. The cavity is 0.5 x 0.25 x 1 meter long. The mesh of 12 elements is shown in Figure 8.32-1.

Loading

Along the surfaces $x = 0$ and $x = 0.5$ $A_y = A_z = 0$.

Along the surfaces $y = 0$ and $y = 1.0$ $A_x = A_z = 0$.

Along the surfaces $z = 0$ and $z = 0.25$ $A_x = A_y = 0$.

A current is placed on element 1. This is applied for a frequency range of 200 MHz to 250 MHz.

Material Properties

The material properties of the air in the cavity is permeability = 1.2566×10^{-6} henry/m, permittivity = 8.854×10^{-12} farad/m, and conductivity = 1×10^{-4} s/m.

Control

The POST option is used to save the electric field and magnetic flux (both real and imaginary components). As this is a linear problem, no additional controls are necessary. The PRINT option is used to force the solution of the nonpositive definite system.

Results

Table 8.32-1 gives the electric field as a function of frequency. The user observes that MARC indicates that the resonance occurs at 230 MHz.

**Table 8.32-1** Electric Field as a Function of Frequency

Frequency (MHz)	$E_x \times 10^2$	$E_y \times 10^2$	$E_z \times 10^2$
200	-4.57	-3.42	-9.13
202	-4.38	-3.28	-8.76
204	2.43	1.82	4.87
206	5.45	4.09	10.90
208	-1.56	-1.17	-3.12
210	-14.52	-10.89	-2.90
212	-1.35	-1.02	-2.71
214	2.75	2.07	5.51
216	-5.14	-3.86	-10.29
218	-16.05	-12.04	-32.11
220	2.39	1.80	4.77
222	-0.32	-0.24	-0.60
224	-5.07	-3.80	-10.14
226	0.69	0.51	1.37
228	4.32	3.24	8.64
230	56.29	42.22	112.60
232	5.24	3.93	10.48
234	-0.82	0.61	-1.63
236	-16.15	-12.11	-32.30
238	-1.96	-1.47	-3.93
240	0.89	0.67	1.79
242	-1.15	0.86	-2.30
244	0.02	0.02	0.05
246	1.95	1.46	3.90
248	-4.14	-3.10	-8.27



Parameters, Options, and Subroutines Summary

Example e8x32.dat:

Parameters

ELEMENT
EL-MA
END
HARMONIC
PRINT,3
SIZING
TITLE

Model Definition Options

CONNECTIVITY
COORDINATE
DEFINE
END OPTION
FIXED POTENTIAL
ISOTROPIC
OPTIMIZE
POST

History Definition Options

CONTINUE
DIST CURRENT
HARMONIC

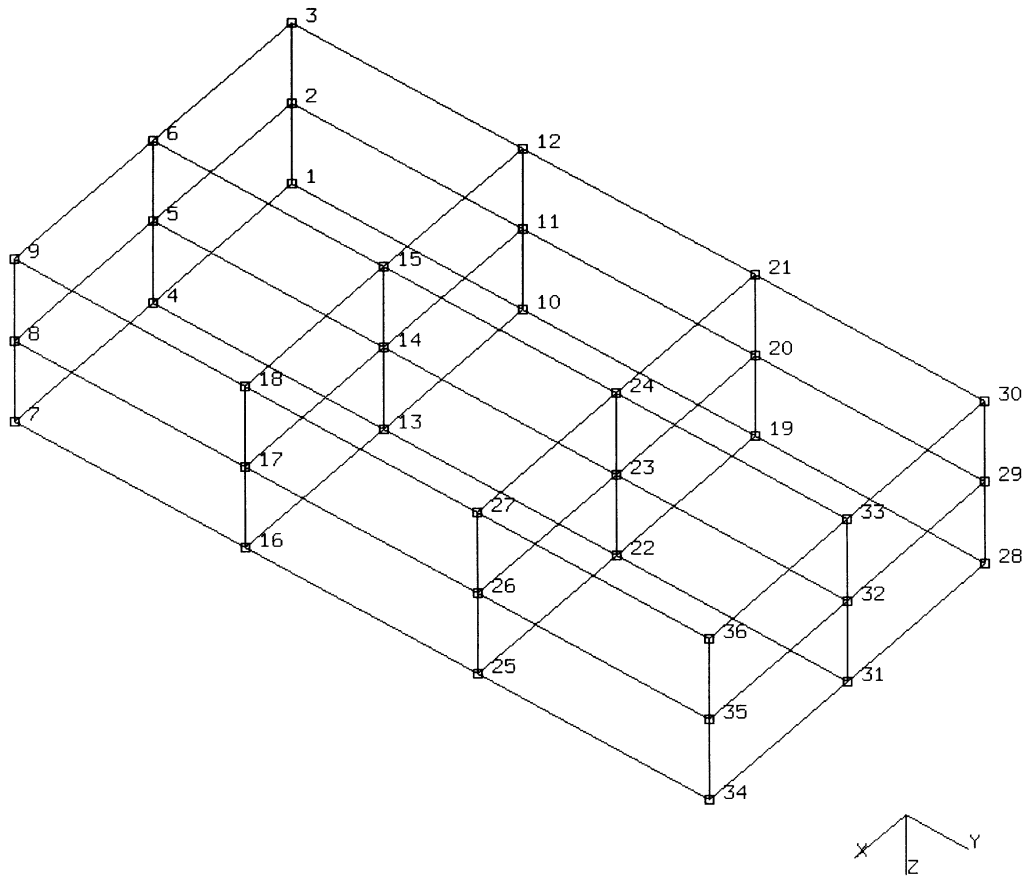


Figure 8.32-1 Finite Element Mesh of Resonator



8.33 Electromagnetic Analysis of an Infinite Wire

In this example, the harmonic and transient electromagnetic capabilities are used to predict the steady state magnetic field distribution due to a wire. This is the same as problem 8.24 where the MAGNETOSTATIC procedure is used.

Parameters

The EL-MA parameter option indicates that an electromagnetic analysis is being performed. The '0' option indicates a transient analysis while a '1' indicates a harmonic analysis.

Element

Element type 111, a four node planar electromagnetic element, is chosen. This element has the vector potential A and the scalar potential ϕ as its degrees of freedom.

Only a sector of a circular region is modeled as shown in Figure 8.33-1. The outer radius is 1 cm.

Loading

In both analyses, the magnetic potential and scalar at the outside radius is prescribed to be zero. A harmonic point charge of 0.05 amps is applied at node 1 at a frequency of 1×10^{-6} Hz in the harmonic analysis. In the transient analysis, a point charge of 0.05 amps is applied at node 1 during the first step of 0.01 seconds. This is then held constant for ten steps of 1×10^{-6} second each. The load is applied using the POINT CURRENT-CHARGE option.

Material Properties

The magnetic permeability of 1000 henry/cm is entered through the ISOTROPIC option.

Results

When using the harmonic procedure, the z component of the magnetic potential is shown in Figure 8.33-2. It is virtually identical to Figure 8.24-3. When using the transient procedure, the solution oscillates about the correct solution. This is shown in Figure 8.33-3.



Parameters, Options, and Subroutines Summary

Example e8x33a.dat:

Parameters	Model Definition Options	History Definition Options
ELEMENT	CONNECTIVITY	CONTINUE
EL-MA	COORDINATE	HARMONIC
END	END OPTION	POINT CURRENT-CHARGE
HARMONIC	FIXED POTENTIAL	
SIZING	ISOTROPIC	
TITLE	POST	
	PRINT ELEMENT	

Example e8x33b.dat:

Parameters	Model Definition Options	History Definition Options
ELEMENT	CONNECTIVITY	CONTINUE
END	CONTROL	DYNAMIC CHANGE
PRINT	COORDINATE	POINT CURRENT-CHARGE
SIZING	END OPTION	
TITLE	FIXED POTENTIAL	
	ISOTROPIC	
	POST	
	PRINT ELEMENT	

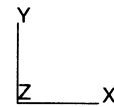
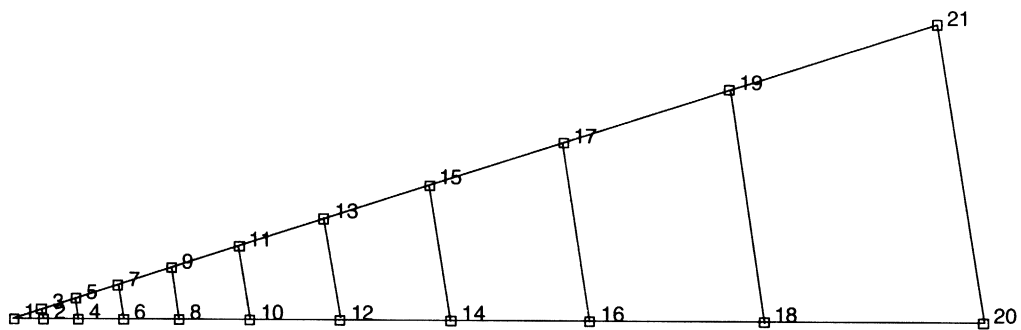


Figure 8.33-1 Sector of Circular Region



INC : 0 prob e8.33a mag2d test one (inf long filamentary current)
SUB : 1
TIME : 0.000e+00
FREQ : 6.283e-06



Displacements z (x100)

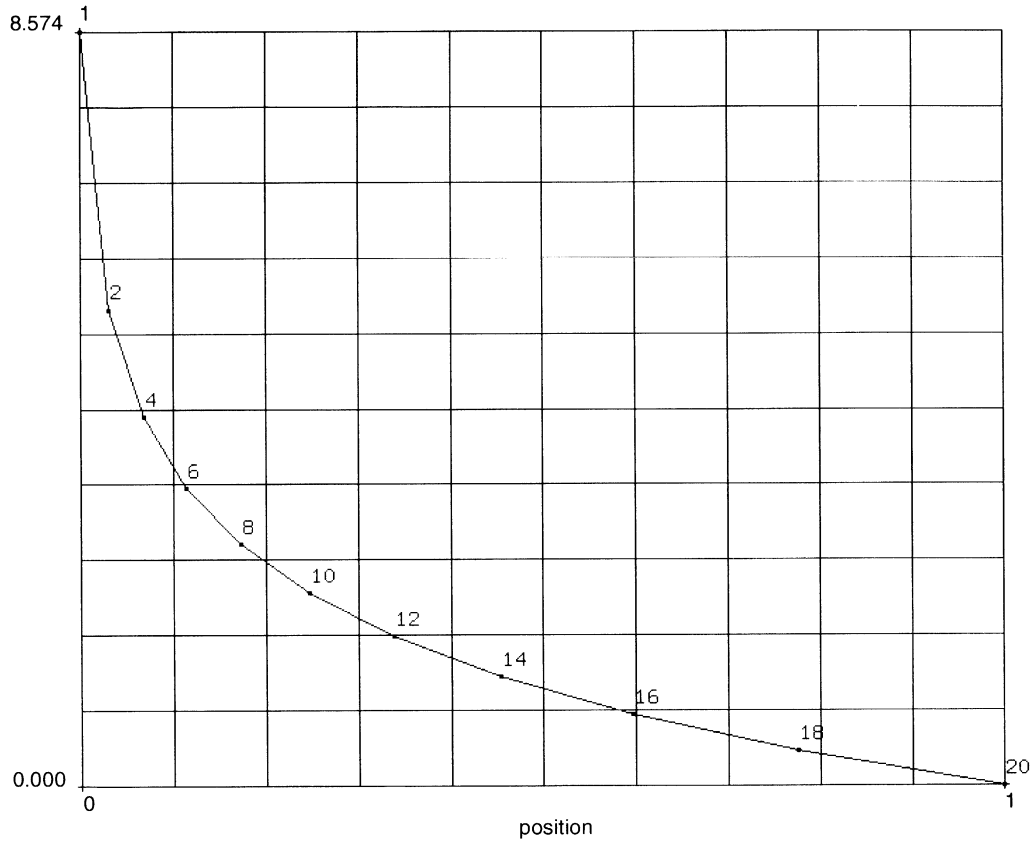


Figure 8.33-2 Third Component of Magnetic Potential using Harmonic Procedure

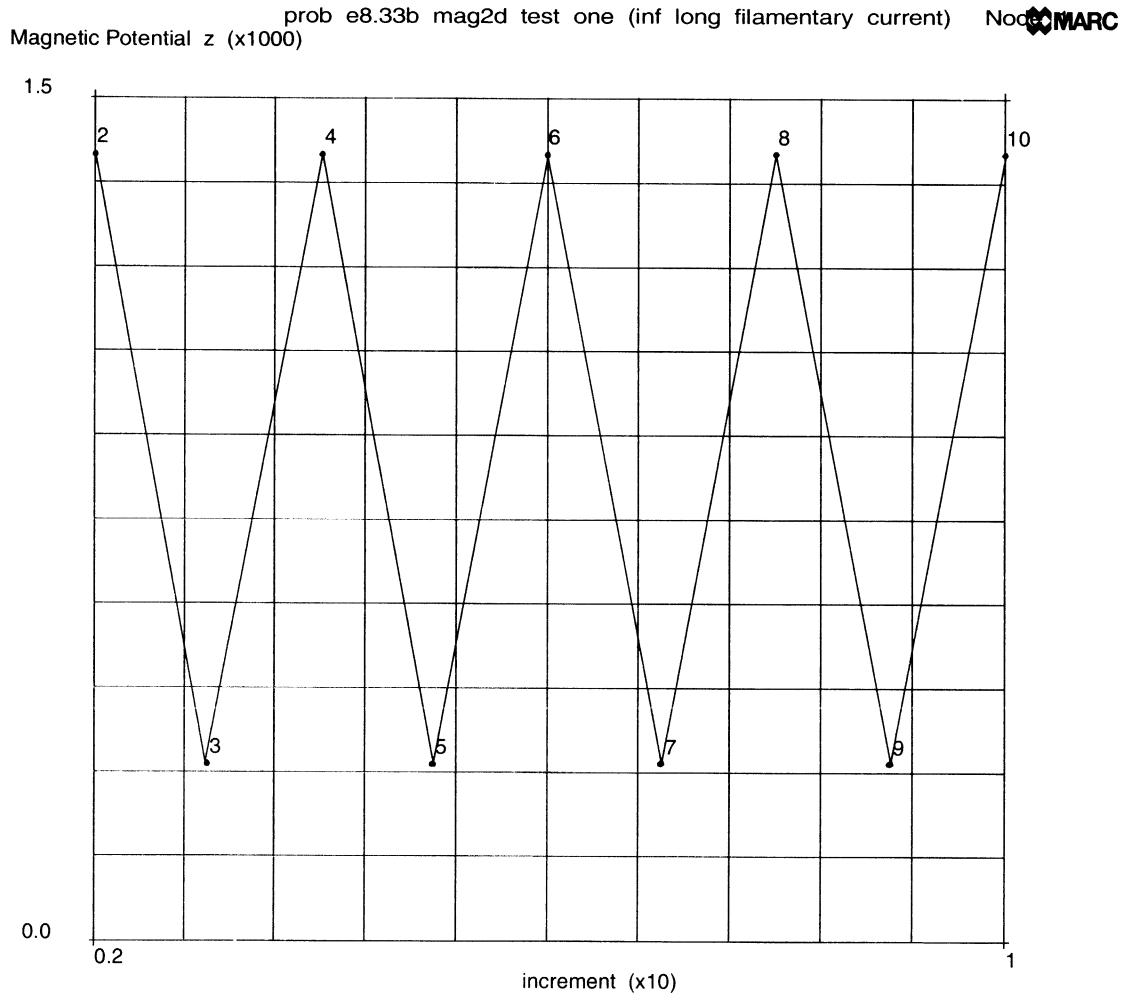


Figure 8.33-3 Time History of Magnetic Potential of Node 1, Transient Procedure





8.34 Triaxial Test on Normally Consolidated Weald Clay

This problem demonstrates the uncoupled pore plasticity analysis of a homogeneous specimen. A drained triaxial test on a normally consolidated clay is simulated.

Parameters

The PORE, 0, 1 parameter indicates that a stress analysis is to be performed, but the fluid pore pressure is not calculated. The ISTRESS parameter indicates that an initial stress is defined as is usually the case in soil analysis. The UPDATE parameter indicates that the analysis is to perform the calculation using the current (deformed) geometric configuration. As the Cam-Clay soil model involves volumetric plastic behavior, a different procedure is used as compared to metal plasticity.

Model

A single axisymmetric element, type 28, is used in the analysis. The specimen is 4 inches long and has a radius of 0.75 inch as shown in Figure 8.34-1.

Material Properties

The Cam-Clay model is invoked using the SOIL model definition option. The material data is:

$E = 100$ psi	Young's modulus
$\nu = 0.4$	Poisson's ratio
$\sigma_y = 200$ psi	Yield stress
$K_{\text{Fluid}} = 100$ psi	Bulk modulus of fluid
$\nu = 0.3982$	Dynamic viscosity of fluid
$= 0.0$	Permeability of soil
$\lambda = 0.88$	Virgin compression ratio
$\kappa = 0.031$	Recompression ratio
$M_{cs} = 0.882$	Slope of critical state line

In the Cam-Clay model, the Young's modulus and the Poisson's ratio are not actually used.

The initial void density, $e_0 = 0.7977$, is entered through the INITIAL VOID option. It is assumed to be homogeneous over all nine integration points.

Loading

The initial confining pressure is 30 psi. This is entered in two places. First, the INITIAL PC option is used to define the initial preconsolidation pressure to be 30 psi. The INIT STRESS is then used to enter the value of the initial stress to be -30 psi (remember that compressive stresses are negative).



In increment 0, no deformation occurs.

In increment 1, a pressure of 30 psi is applied on the outside radius and the right side. This is to ensure that equilibrium exists.

This is followed by an axial compression of 0.004 inch per increment for 200 increments. The total axial compression is then 0.8 or an engineering axial strain of about 20%. The time step is two seconds per increment.

Results

The time history of the axial stress is shown in Figure 8.34-2. The time history of the void ratio is shown in Figure 8.34-3. We can observe that the void ratio decreases from the original value of 0.7977 to 0.7202. The preconsolidation pressure history is shown in Figure 8.34-4. The value increases from 30 psi to 87.78 psi.

Parameters, Options, and Subroutines Summary

Example e8x34.dat:

Parameters	Model Definition Options	History Definition Options
ELEMENT	CONNECTIVITY	AUTO LOAD
END	CONTROL	CONTINUE
ISTRESS	COORDINATES	DISP CHANGE
PORE	DIST LOADS	DIST LOADS
SIZING	END OPTION	TIME STEP
TITLE	FIXED DISP	
UPDATE	INIT STRESS	
	INITIAL PC	
	INITIAL VOID	
	POST	
	SOIL	

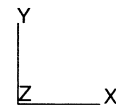
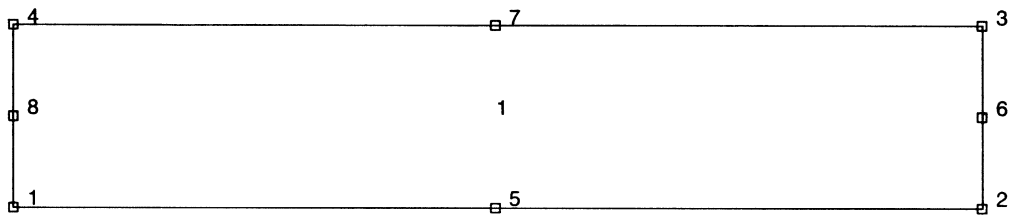


Figure 8.34-1 One-Element Model

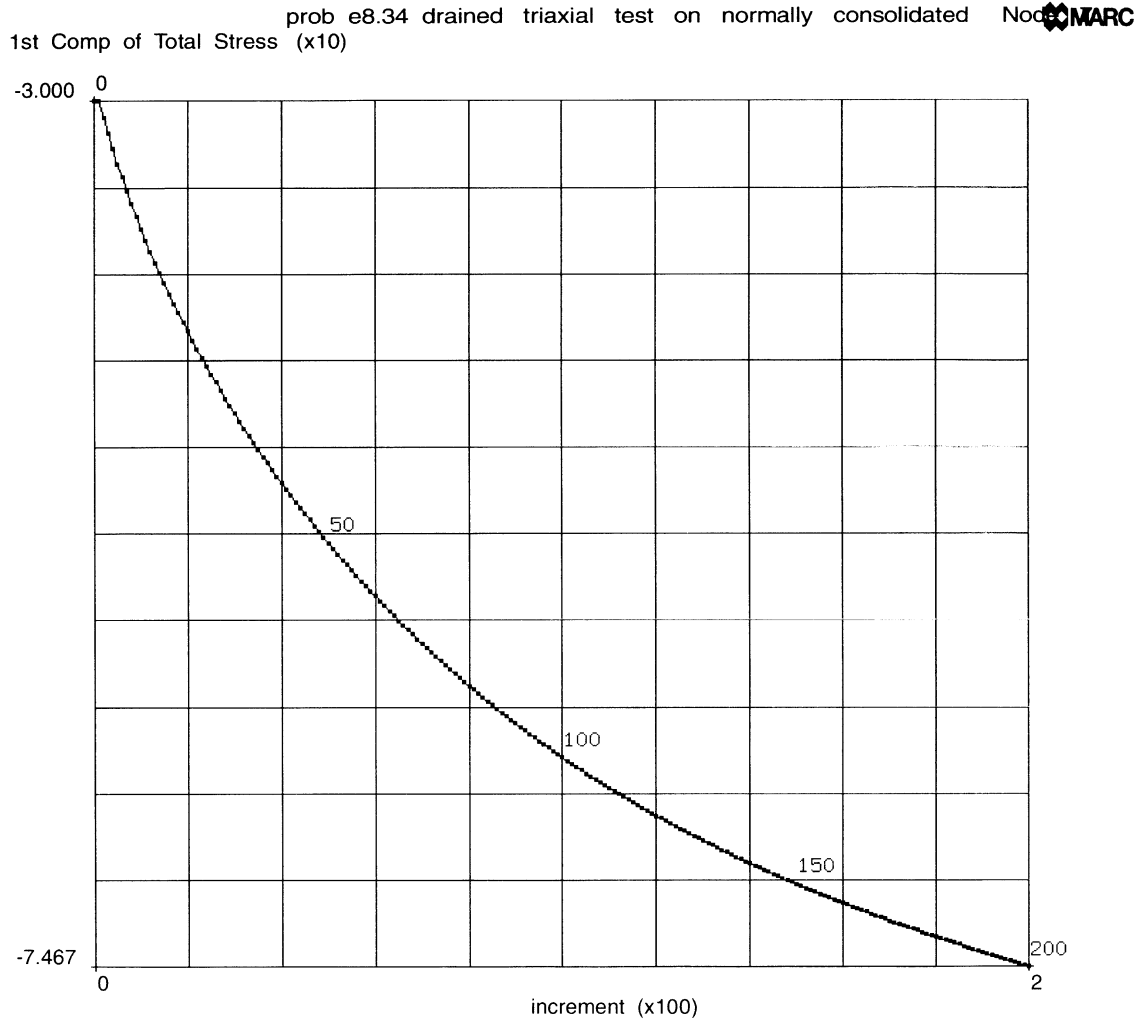


Figure 8.34-2 Time History of Axial Stress

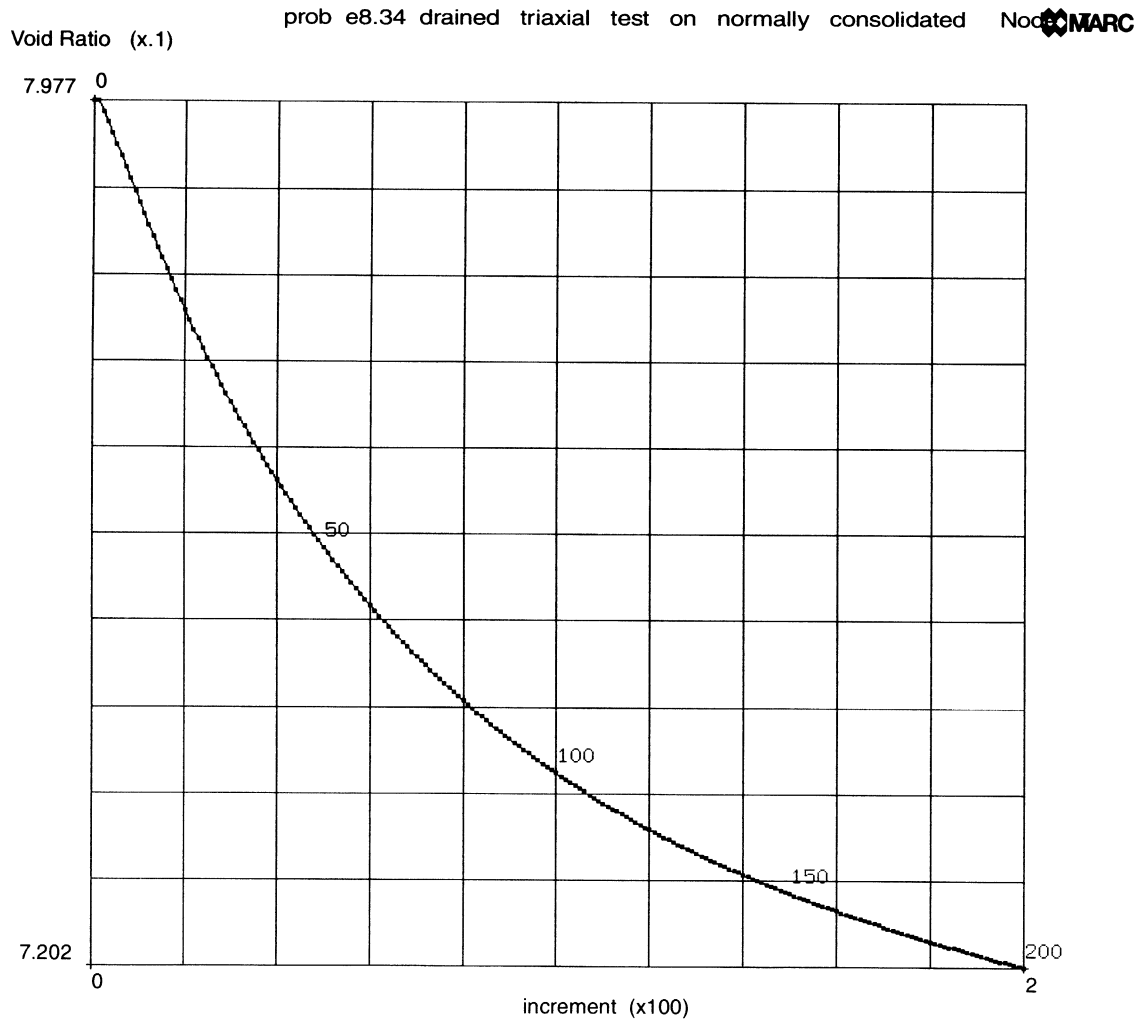


Figure 8.34-3 Time History of Void Ratio

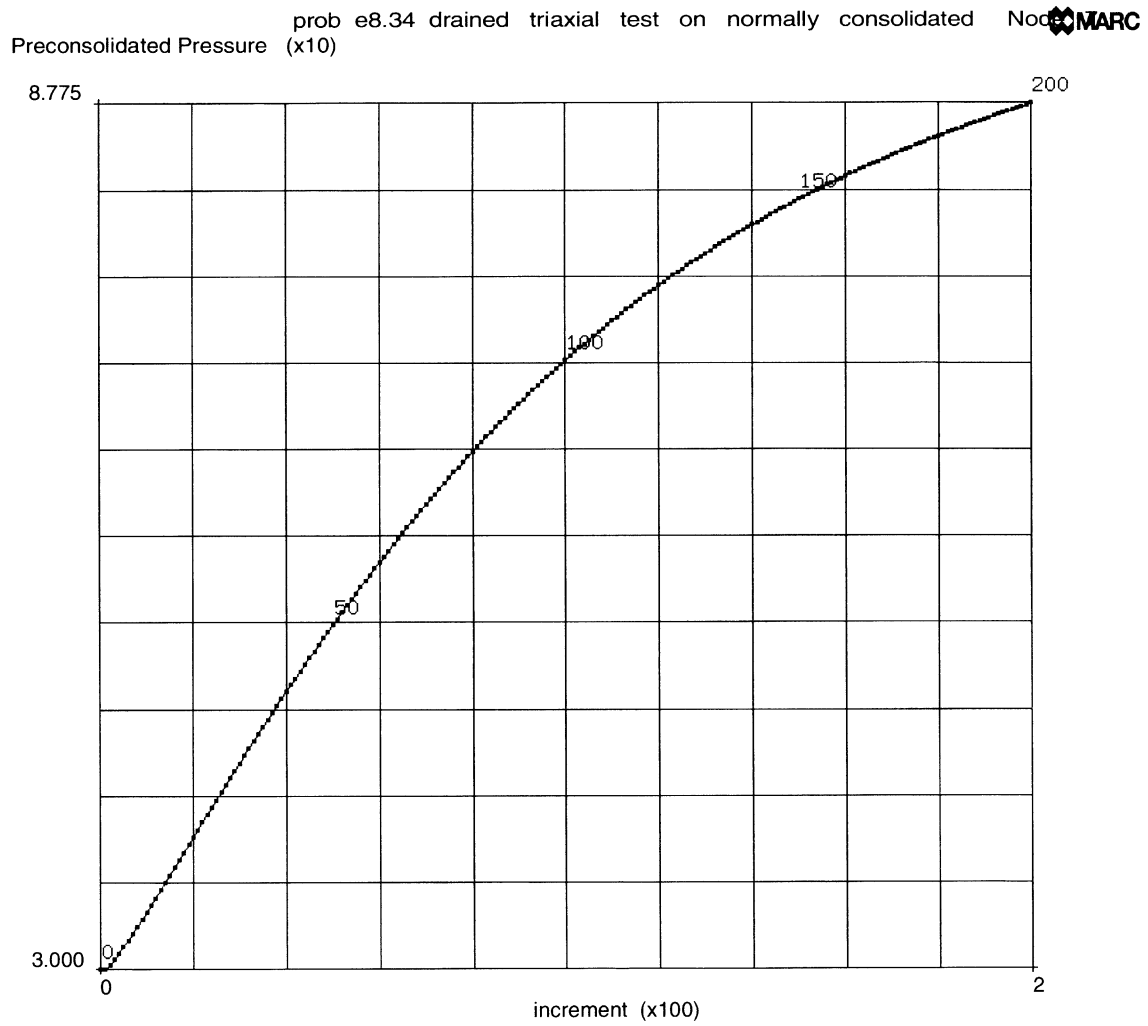


Figure 8.34-4 Time History of Preconsolidation Pressure



8.35 Soil Analysis of an Embankment

This problem demonstrates the use of MARC for a coupled pore pressure soil analysis. The I-95 embankment across the tidal marshes of Saugus, just north of Boston, is modeled under the conditions of plane strain. The original description was given by Wroth.

Parameters

The PORE, 2, 1 parameter indicates that a fully coupled pore pressure calculation is to be performed. The ISTRESS parameter indicates that an initial stress is applied in increment 0.

Model

Element type 32 is used in this analysis. This element is a Herrmann element which is normally used for incompressible material. When used in a pore pressure calculation, the fourth degree of freedom at the corner nodes is no longer the Lagrange multiplier, but instead the fluid pore pressure. The model consists of 126 elements and 427 nodes. The model consists of eight groups of elements that are used to define the different preconsolidation pressures. Three groups are used to define the material properties. These groups are shown in Figure 8.35-1.

Material Properties

The material properties are grouped into the fill, silt, and all of the rest (bbc). The properties are as follows:

	bbc	Silt	Fill
E (psi)	2.5×10^6	2.5×10^6	2.5×10^6
ν	0.4	0.4	0.4
ρ	0.000054	10.0	10.0
σ_y	0	0	0
K_{Fluid}	100	100	100
Dynamic viscosity of fluid – ν	0.1	0.1	0.1
Permeability	1	1	1
Virgin compression ratio – λ	0.147	0.147	0.147
Recompression ratio – κ	0.060	0.060	0.060
Slope of critical state line – M	1.05	1.05	1.05

This data is entered through the SOIL option.



When using the Cam-Clay model, Young's modulus, Poisson's ratio, and yield stress are ignored. The initial preconsolidation is dependent on the depth. The values entered through the INITIAL PC option are as follows:

Region	Initial Preconsolidation (psi)
Fill	10
Silt	10,000
Layer 1	95
Layer 2	80
Layer 3	71
Layer 4	70
Layer 5	57
Layer 6	50

A small hydrostatic initial stress is entered for all elements as 1 psi. It is entered as a negative value to indicate compression. The Cam-Clay model does not behave well when the hydrostatic stress is zero or positive (tensile).

The initial void ratio is 0.74 for all elements. This is entered through the INITIAL VOID option.

Boundary Conditions

The boundary conditions consist of no motion in the x direction on the right and left side. No motion in the y direction along the bottom surface. And the pore pressure is zero along the top surface. This is shown in Figure 8.35-2.

In increment 0, only the initial stress is on the structure.

In increment 1, a pressure of 1 psi is placed along the complete top surface (fill). A very small time step of 1×10^{-20} seconds is chosen.

A uniform body force/area is then applied of magnitude 0.6 psi/in² per increment for 15 increments or a total of 9 psi/in². Each time step is 10000 seconds \cong 2.78 hours.

This is followed by a distributed load of 0.5 psi/increment on the embankment and a load of 0.25 psi/increment on element 72. In the AUTO LOAD section, 290 increments are requested with each of a time step of 0.4138 seconds. Because the CONTROL option indicates 200 increments, this load sequence is not be completed.



Results

A contour plot of the vertical displacements on the superimposed deformed mesh is shown in Figure 8.35-3. The stress in the y-direction is given in Figure 8.35-4. The hydrostatic pressure is shown in Figure 8.35-5. The void ratio is shown in Figure 8.35-6. The preconsolidation stress is shown in Figure 8.35-7. The pore pressure is shown in Figure 8.35-8.

Parameters, Options, and Subroutines Summary

Example e8x34.dat:

Parameters	Model Definition Options	History Definition Options
ELEMENT	CONNECTIVITY	AUTO LOAD
END	CONTROL	CONTINUE
ISTRESS	COORDINATES	CONTROL
PORE	DEFINE	DIST LOAD
SIZING	DIST LOADS	TIME STEP
TITLE	FIXED DISP	
	INIT STRESS	
	INITIAL PC	
	INITIAL VOID	
	OPTIMIZE	
	POST	
	PRINT ELEM	
	PRINT NODE	
	RESTART	
	SOIL	
	SOLVER	

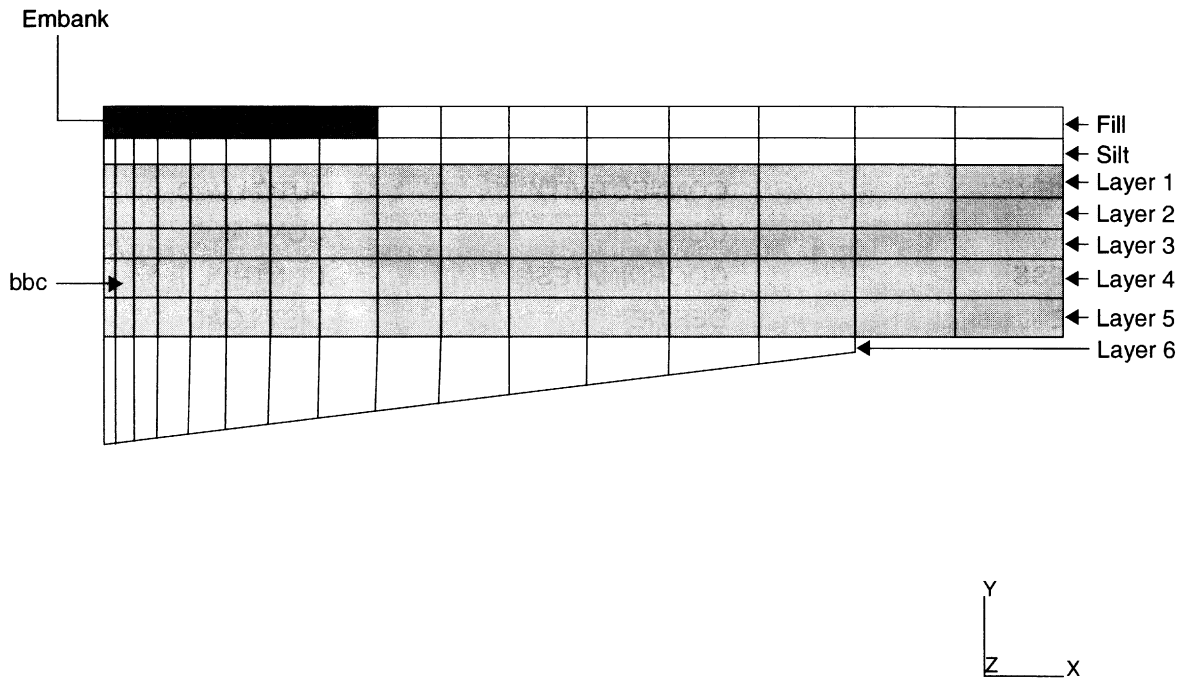


Figure 8.35-1 Mesh of Embankment with Sets used for Material Definition and Initial Preconsolidation

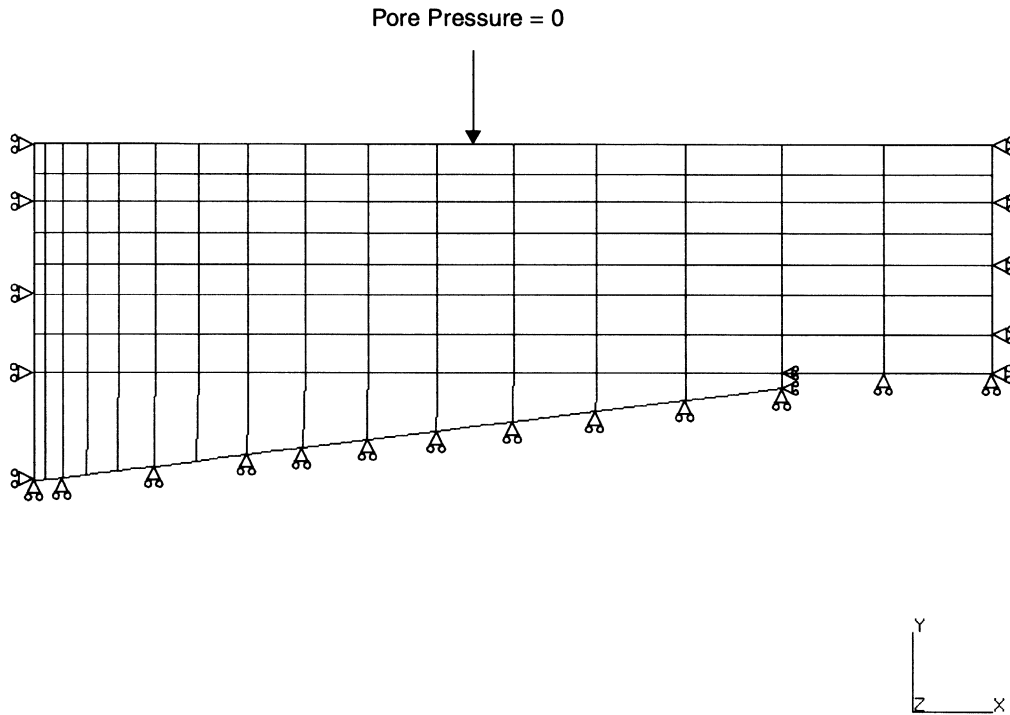
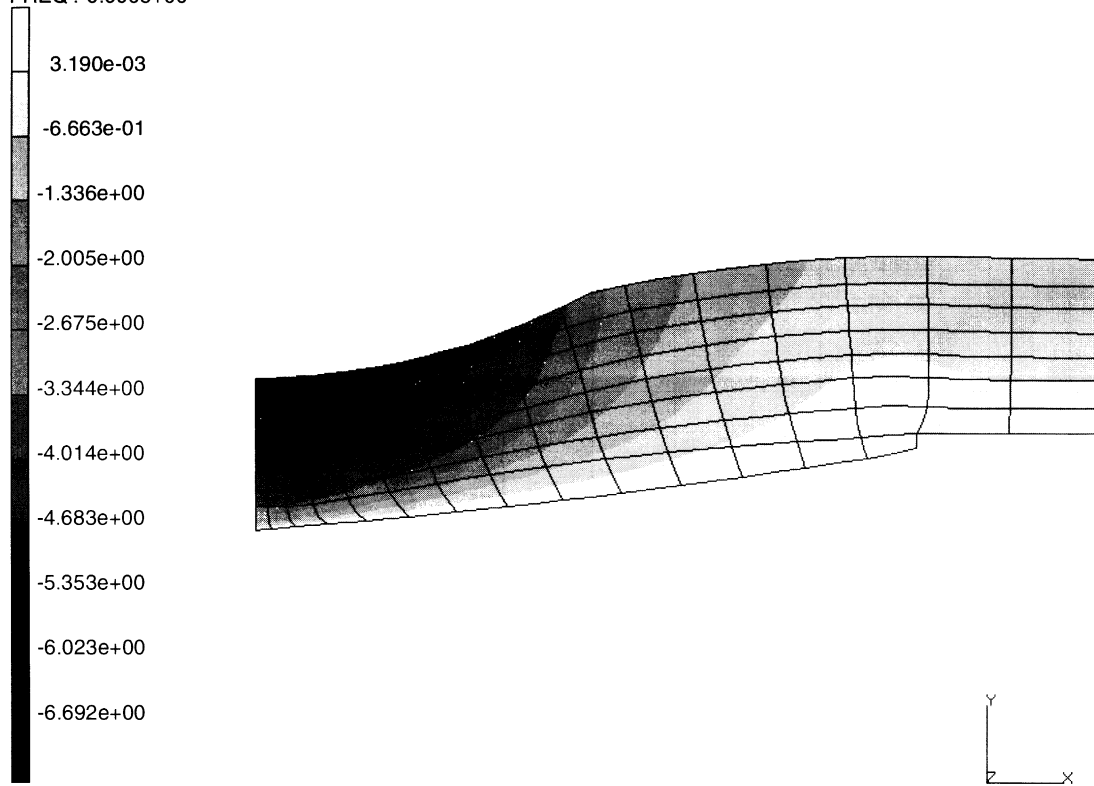


Figure 8.35-2 Boundary Conditions



INC : 199
SUB : 0
TIME : 1.501e+05
FREQ : 0.000e+00

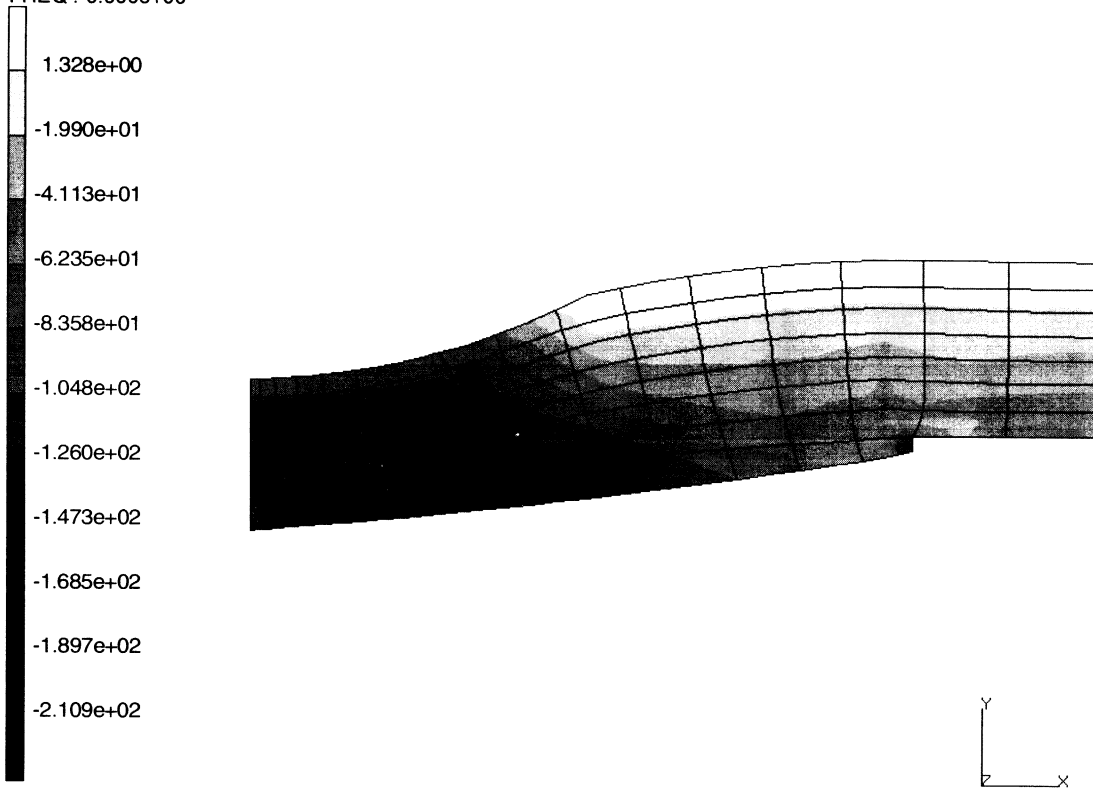


prob e8.35 i-95 embankment plane strain settlement boston blue
Displacements y

Figure 8.35-3 Contour of Settlement



INC : 199
SUB : 0
TIME : 1.501e+05
FREQ : 0.000e+00

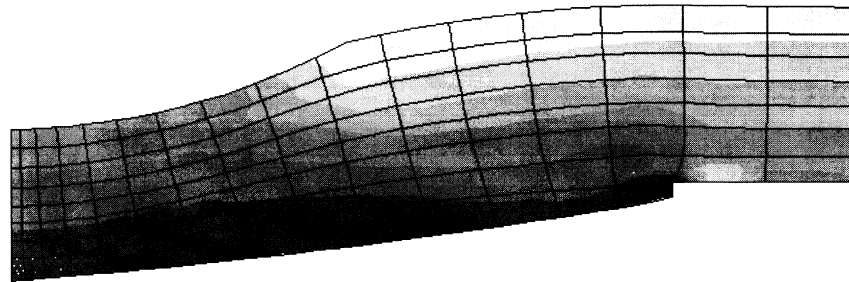
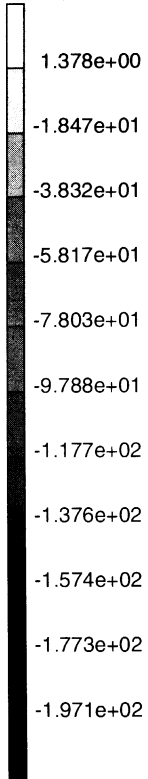


prob e8.35 i-95 embankment plane strain settlement boston blue
sigma-yy,

Figure 8.35-4 Vertical Stresses



INC : 199
SUB : 0
TIME : 1.501e+05
FREQ : 0.000e+00

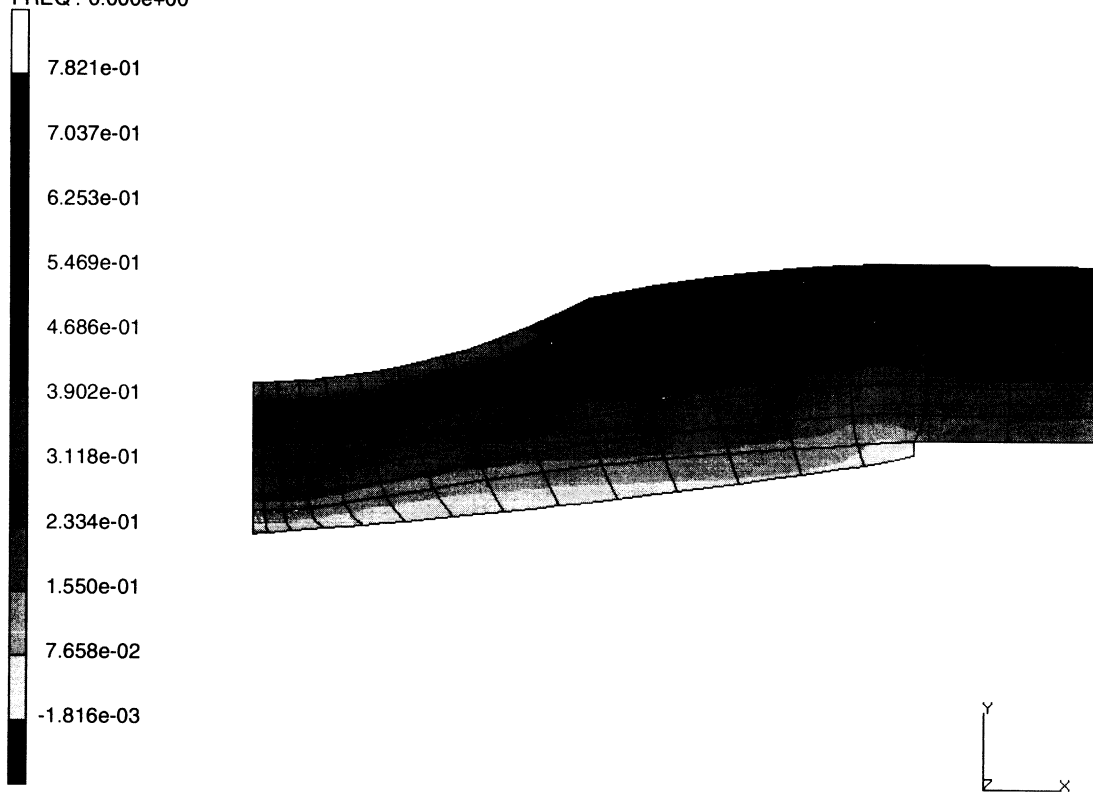


prob e8.35 i-95 embankment plane strain settlement boston blue pressure,

Figure 8.35-5 Mean Pressure in Soil



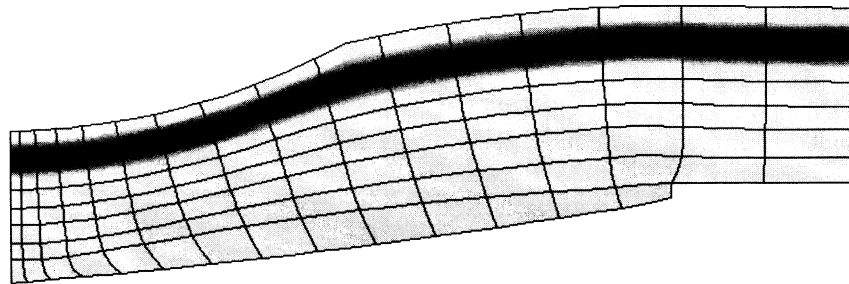
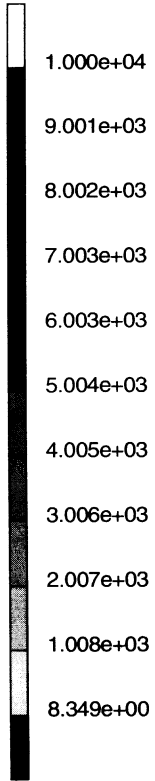
INC : 199
SUB : 0
TIME : 1.501e+05
FREQ : 0.000e+00



prob e8.35 i-95 embankment plane strain settlement boston blue
Void ratio,

Figure 8.35-6 Void Ratio

INC : 199
SUB : 0
TIME : 1.501e+05
FREQ : 0.000e+00

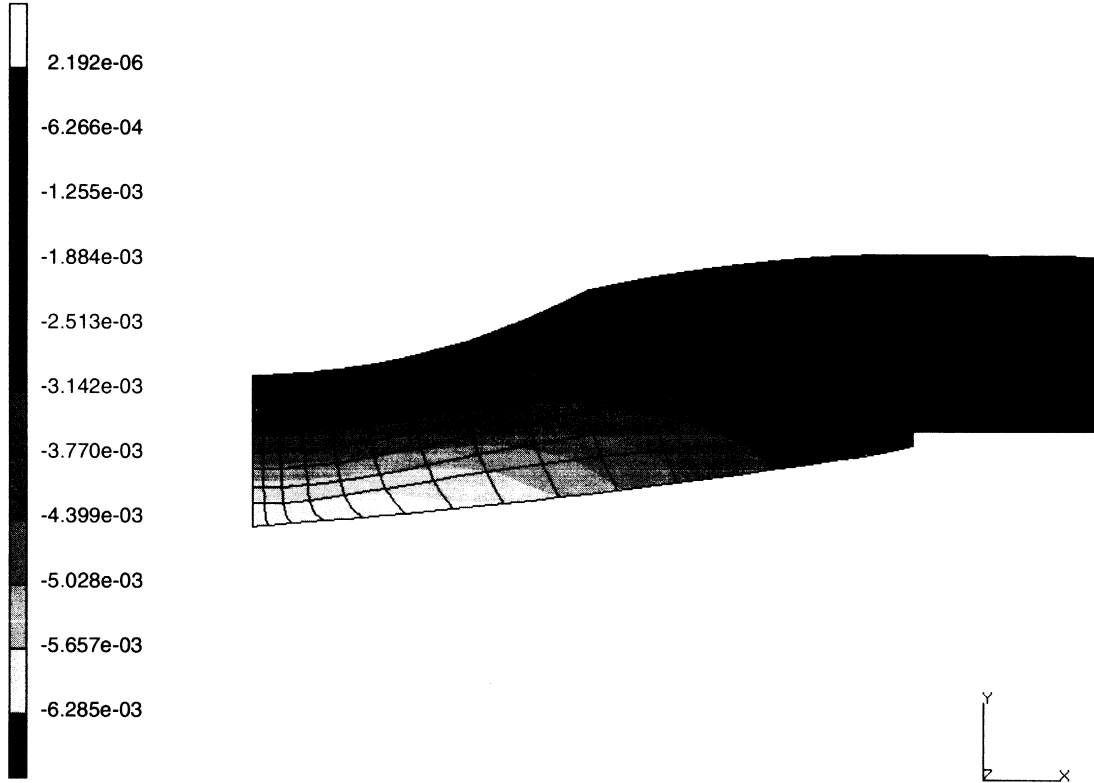


prob e8.35 i-95 embankment plane strain settlement boston blue
preconsolidation pressure,

Figure 8.35-7 Preconsolidation Pressure



INC : 199
SUB : 0
TIME : 1.501e+05
FREQ : 0.000e+00



prob e8.35 i-95 embankment plane strain settlement boston blue
pore pressure,

Figure 8.35-8 Fluid Pore Pressure



8.36 Interference Fit of Two Cylinders

This example demonstrates the interference fit capabilities and the use of symmetry planes in MARC. Two rings have an initial overclosure, and the resultant stress distribution is determined.

Element

Element type 116, a four node axisymmetric element with reduced integration and hourglass control, is used in this analysis. The mesh was originally defined using element type 10. The ALIAS option was used to switch it to type 116.

Loading

The line $z = 0$ is considered to be a symmetry boundary condition. A rigid surface (body 3) is defined and is given the characteristic of a symmetry plane. This means that the displacement of nodes initially in contact with this plane will be zero, and that the nodes cannot separate from this plane. No other loading or boundary condition is necessary.

The CONTACT option is used to specify that three bodies exist: inner cylinder, outer cylinder and the symmetry plane. There is no friction on any of the surfaces. A closure distance of 0.0001 is initially specified. This will be reset in the CONTACT TABLE option to be 0.0002.

The CONTACT TABLE option then specifies that body 1 and 2 have an interference distance of 0.001. It also specifies that body 1 and 2 are potentially in contact and that 1 and 2 are potentially in contact with 3. Note because of the geometries involved, this is more than a mere potential, but reality. The CONTACT TABLE option is a very powerful way to control the interaction between bodies. In this example, it was positioned in the LOAD INCREMENTATION block. This implies that this data can be changed during the incremental analysis.

Material Properties

The material is a high strength steel with Young's modulus = 30×10^6 psi, Poisson's ratio = 0.3, and the yield stress of 50,000 psi.

Control

The CONTROL option specifies that displacement control is being used with a tolerance of 10%. The convergence messages are written to the log file. A restart file and a post file is written for each increment. A single load step is performed with a time step of 0.03. The time step in this problem is totally arbitrary. A PRINT,5 option is included which generates additional messages in the output regarding contact.

**Results**

By examining the contact forces, you can calculate a total contact force of 44,177 pounds. This is available on the post file as the “EXTERNAL FORCES” and is given in the output.

Figure 8.36-2 shows the radial stress and the hoop stress as a function of the radius. Note that nodes 5 and 26 are the corresponding contact nodes between the inner and outer cylinder. You can easily observe that the inner cylinder has gone into compression (hoop stress) while the external cylinder has gone into tension. Also, observe the antisymmetries of the stress. Note that the radial stress should have gone to zero at nodes 1 and 30. The error is due to the extrapolation procedure employed.

Parameters, Options, and Subroutines Summary

Example e8x36.dat:

Parameters	Model Definition Options	History Definition Options
ALIAS	CONNECTIVITY	AUTO LOAD
ELEMENT	CONTACT	CONTACT TABLE
END	CONTROL	CONTINUE
PRINT	DEFINE	TIME STEP
SIZING	END OPTION	
TITLE	ISOTROPIC	
	POST	
	RESTART	

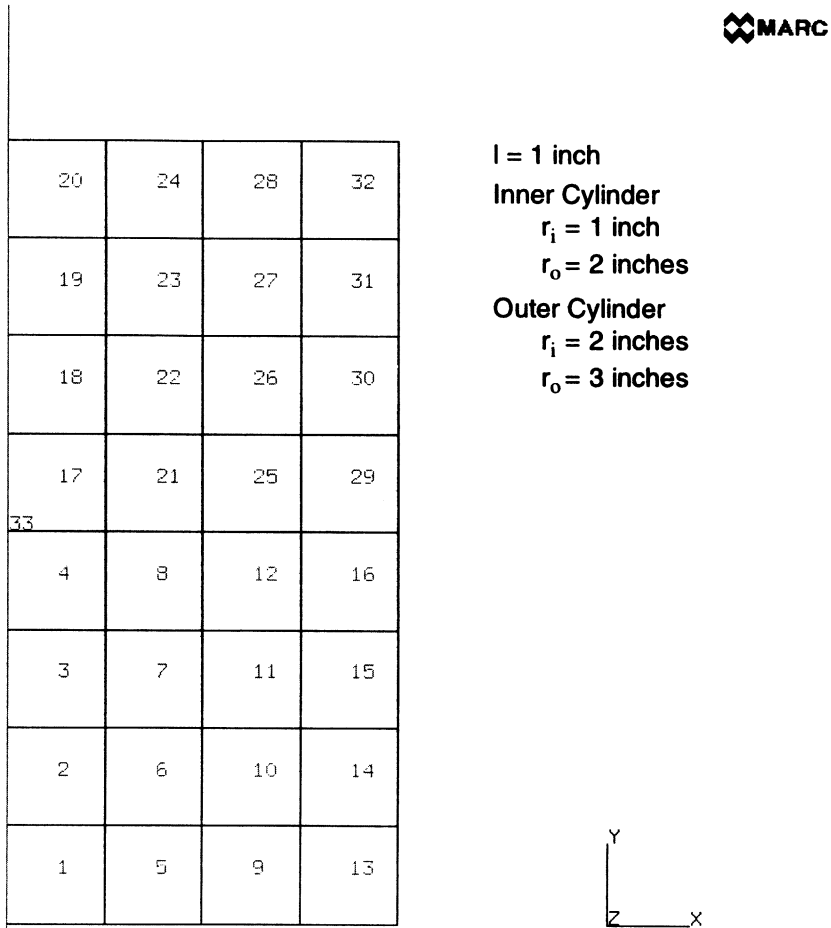



Figure 8.36-1 Two Cylinders

INC : 1 prob e8.36 interference fit analysis – axisymmetric: symmetric 
 SUB : 0
 TIME : 3.000e-02
 FREQ : 0.000e+00

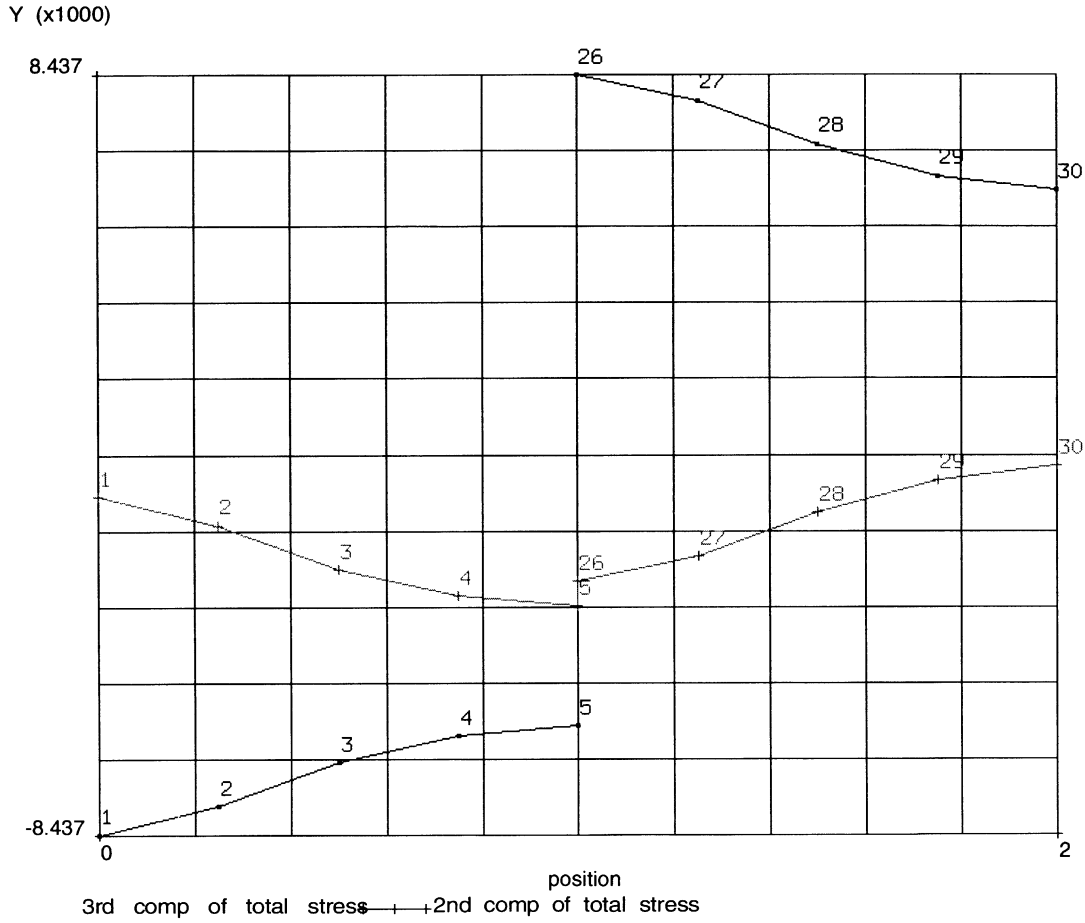


Figure 8.36-2 Radial and Hoop Stresses through Radius



8.37 Interference Fit Analysis

This example demonstrates the interference fit capabilities in MARC and the use of symmetry planes.

Element

Element type 11, a four node plane strain element, is used in this analysis. The model, as shown in Figure 8.37-1, consists of a 90° segment of two rings rotated by 45°. Ten elements (9° each) are used in the circumferential direction. The inner cylinder, with $r_i = 1$ inch and $r_o = 2$ inches, has five elements through the radius. The outer cylinder, with $r_i = 2$ inches and $r_o = 3$ inches, has six elements. Two symmetry surfaces at 45° and 135° are used. To prevent any rigid body motion, a spring was placed between the two bodies. While this was not necessary in this problem, it is often a good idea.

Loading

The kinematic boundaries are specified using the symmetry surfaces. This problem is driven by the overclosure fit of 0.01 inch specified through the CONTACT TABLE option.

Material Properties

The material is a high strength steel with a Young's modulus of 30×10^6 psi, a Poisson's ratio of 0.3 and a yield stress of 50,000 psi. The material remains elastic in this analysis.

Contact

There are four bodies defined: the inner cylinder, outer cylinder, symmetry surface at $\theta = 135^\circ$, and symmetry surface at $\theta = 45^\circ$.

No friction exists on any surface. Note the flag set on the fourth data block to indicate that surface 3 and 4 are symmetry surfaces. The CONTACT TABLE option is used to indicate which bodies can potentially contact others and to specify the closure distance and the overclosure amount. The overclosure was set to 0.01 inch.

Control

Displacement control was used with a convergence tolerance of 10%. A post file was created using POST and the output was suppressed using NO PRINT. A single increment with a time step of 0.03 second was performed. In this rate independent problem, the time step is arbitrary. The OPTIMIZE option is used to reduce the bandwidth. This is very important in deformable-deformable contact problems.



The PRINT,8 option was used to obtain additional information regarding the contact conditions, such as when a node comes into contact and the displacements relative to rigid surfaces.

Results

The reaction and contact forces are shown in Figure 8.37-2. You can observe a nice uniform pattern along the contact surfaces. The stresses σ_{xx} and σ_{yy} are shown through the radius at $\theta = 90^\circ$. These would be similar to the σ_{qq} and σ_{rr} components, respectively. Note that the stresses are an order of magnitude greater than in problem 8.36; but, on closer observation, the overclosure distance is also an order of magnitude larger. Note that accuracy could have been improved if the outer elements would have been offset relative to the inner elements by 4.5° . This would have resulted in a more accurate surface normal calculations.

Parameters, Options, and Subroutines Summary

Example e8x37.dat:

Parameters	Model Definition Options	History Definition Options
ELEMENT	CONNECTIVITY	AUTO LOAD
END	CONTACT	CONTACT TABLE
PRINT	CONTROL	CONTINUE
SIZING	COORDINATES	TIME STEP
TITLE	DEFINE	
	END OPTION	
	ISOTROPIC	
	NO PRINT	
	OPTIMIZE	
	POST	

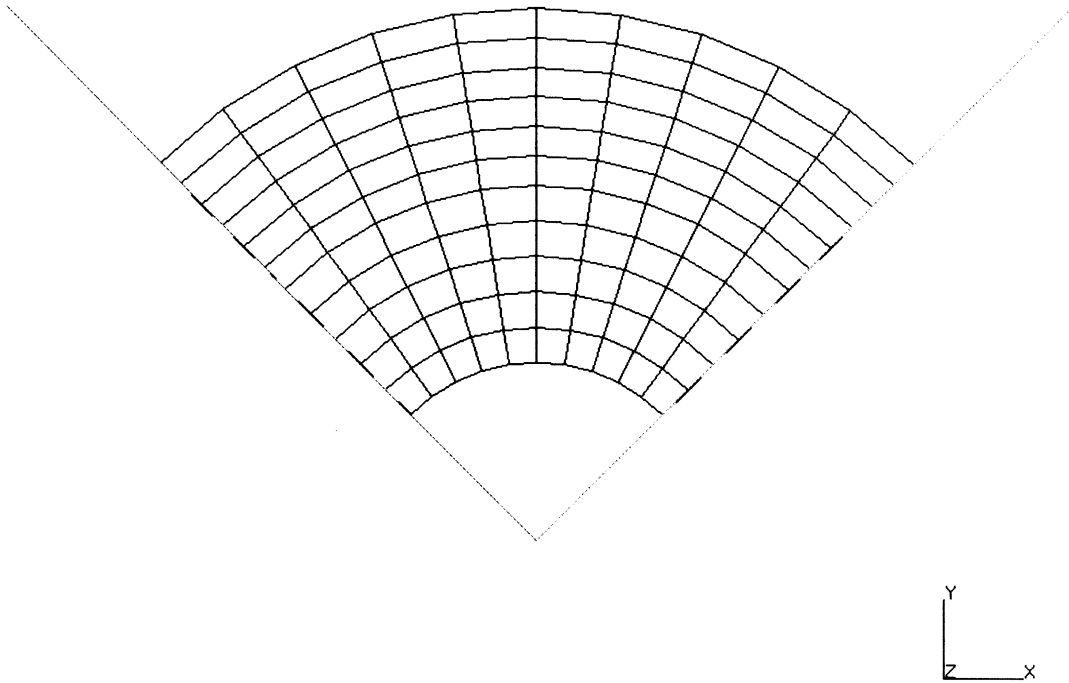
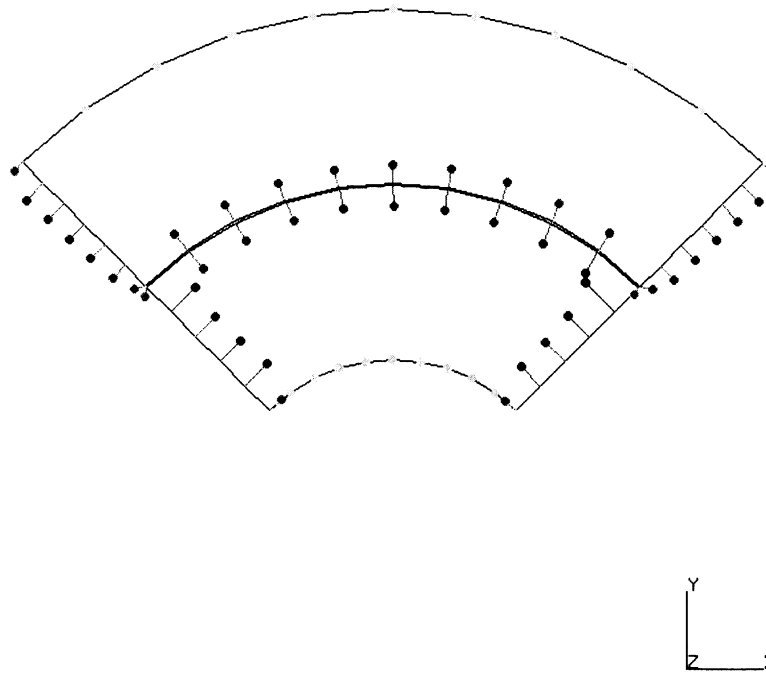
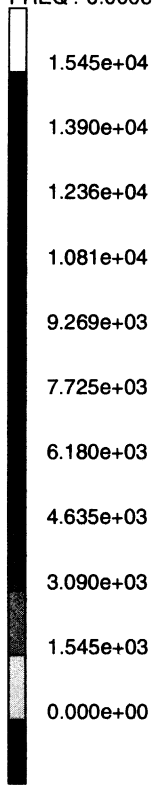


Figure 8.37-1 Finite Element Mesh with Symmetry Surfaces



INC : 1
SUB : 0
TIME : 3.000e-02
FREQ : 0.000e+00



prob e8.37 interference fit analysis – plane strain: dis
External Forces x

Figure 8.37-2 Reaction and Contact (Interference) Forces

8.38 Deep Drawing of a Box using NURB Surfaces

This example demonstrates the deep drawing of a box modeled with shell elements. The punch and holder are modeled with nurbs using the CONTACT option. The improvement in computational performance is demonstrated by the use of the sparse direct solver.

This problem is modeled using the four techniques summarized below.

Data Set	Element Type(s)	Number of Elements	Number of Nodes	Differentiating Features
e8x38a	75 or 139			
e8x38b				
e8x38c				
e8x38d				

Geometry

The sheet is made up of 636 element type 75 or element type 139 with dimensions of 225 cm by 220 cm. Element type 75 is a thick shell element which can also be used to simulate thin shells. Element type 139 is a thin shell element. The shell thickness (1.2 cm) is specified through the GEOMETRY option in the first field (EGEOM1).

Loading

The punch is given a constant velocity of 3 cm/second. The AUTO LOAD option with 112 step sizes is specified with each step size (0.25 seconds) specified through the TIME STEP option. The total motion is 84 cm.

Material Properties

The material is treated as elastic-plastic with a Young's modulus of $2.1e5 \text{ N/cm}^2$, a Poisson's ratio of 0.3, and an initial yield stress of 188.66 N/cm^2 . The yield stress is given through the WORK HARD DATA model definition option.

Boundary Conditions

One-quarter of the geometry is used due to symmetry. The appropriate nodal constraints are applied in the global x,y directions to impose symmetry. The box is deep-drawn by a punch having a constant velocity of 3 cm/sec.



Contact

This option had three bodies. The first body is a rectangle of 626 shell elements. The second body is a rigid die which is made up of 7 different NURBS. The third body is the rigid holder which has two major parts – a flat holder and a curved shoulder with 12 NURBS to describe the complete shoulder. The workpiece is firmly held by the rigid dies with 0.02 contact tolerance and high separation force entered to simulate the condition. To avoid unnecessary self contact check, the contact table is used.

Control

Displacement control was used with a convergence tolerance of 10%. No more than 20 recycles per increment is specified.

Results

Three bodies are declared in e8x38a.dat with nonanalytical form for NURBS used for the analysis. All surface defined as NURBS are discretized into 4-node patches.

The difference in e8x38b.dat is that the rigid dies are using the analytical form of NURBS to implement contact conditions. Computational performance is improved 10% by use of the analytical NURBS when comparing CPU time for e8x38a.dat and e8x38b.dat. Because an exact representation of the surface is made, the results are better.

Four bodies are declared in e8x38c.dat with the shoulder in the third rigid die in e8x38b.dat becoming the fourth body.

Figure 8.38-1 shows the geometry configuration for the deep-drawing analysis. Figure 8.38-4 shows the 7 NURBS rigid punch. Figure 8.38-5 shows the 12 NURBS rigid holder. The deformation of the sheet is shown at increments 20, 50, 80, and 110 in Figure 8.38-4 through Figure 8.38-7. The equivalent stress is shown in Figure 8.38-8. The equivalent plastic strain is shown in Figure 8.38-9. You can observe that the maximum plastic strain is 70%.



Parameters, Options, and Subroutines Summary

Example e8x38a.dat, e8x38b.dat, e8x38c.dat, e8x38d.dat:

Parameters	Model Definition Options	History Definition Options
ELEMENTS	CONNECTIVITY	AUTO LOAD
END	CONTACT	CONTINUE
FINITE	CONTROL	TIME STEP
CONTACT TABLE	COORDINATES	
LARGE DISP	END OPTION	
PRINT	FIXED DISP	
SHELL SECT	GEOMETRY	
SIZING	ISOTROPIC	
TITLE	NO PRINT	
UPDATE	OPTIMIZE	
	POST	

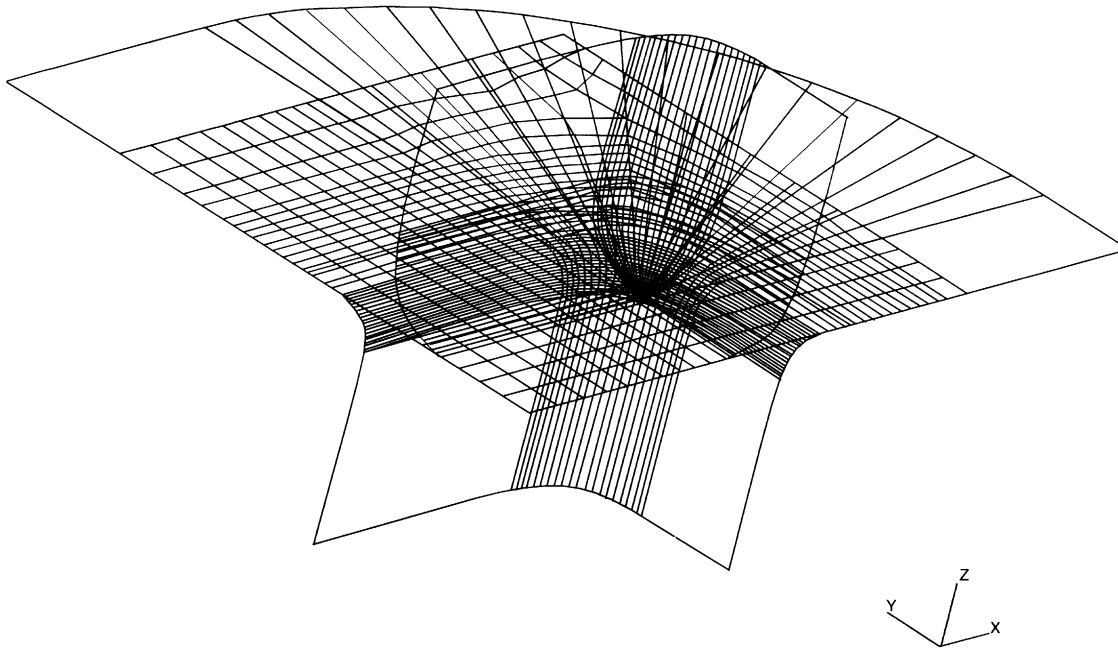


Figure 8.38-1 Plate with Rigid Surfaces

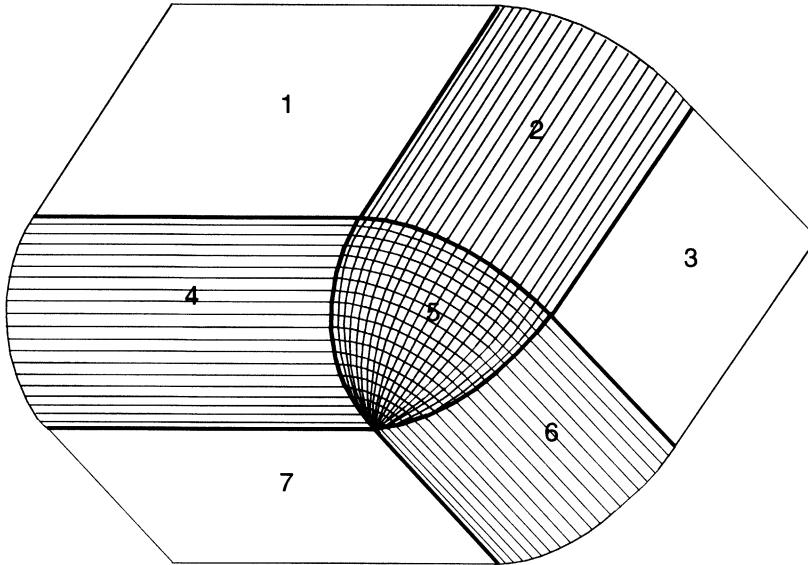


Figure 8.38-2 Male Punch Consisting of Seven NURBS

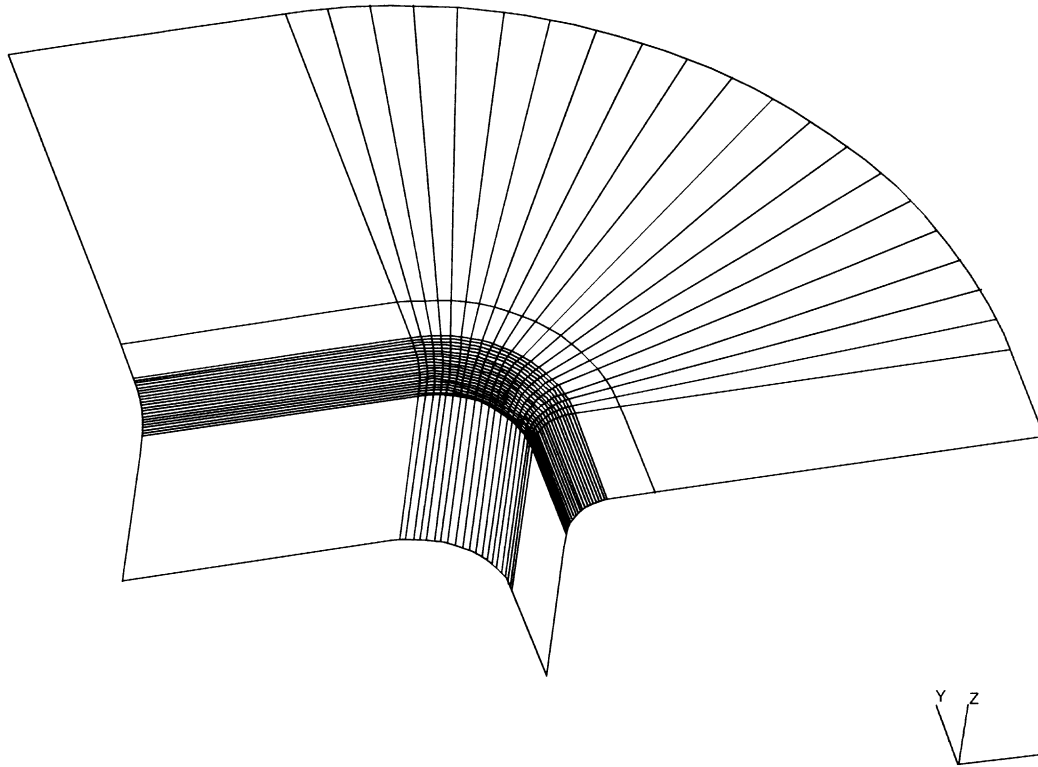
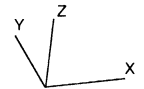
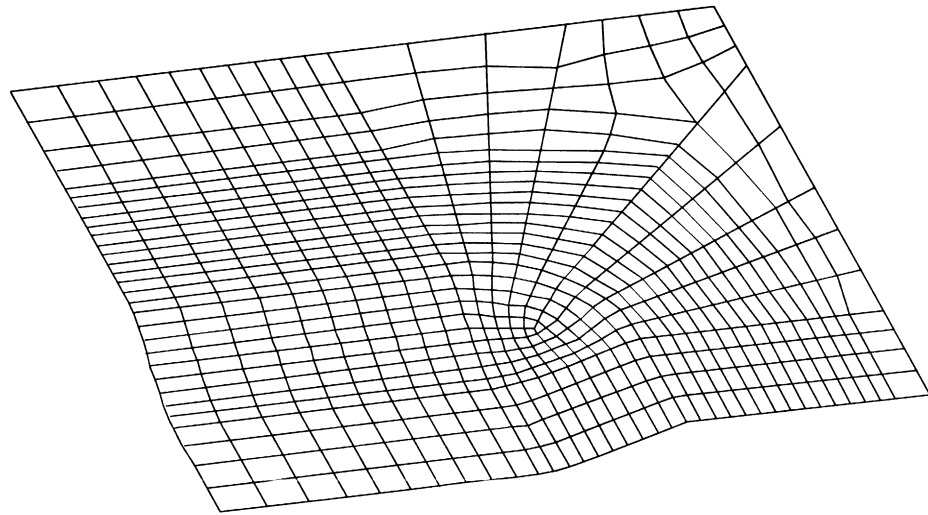


Figure 8.38-3 Blank Holder



INC : 20
SUB : 0
TIME : 5.000e+00
FREQ : 0.000e+00

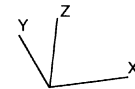
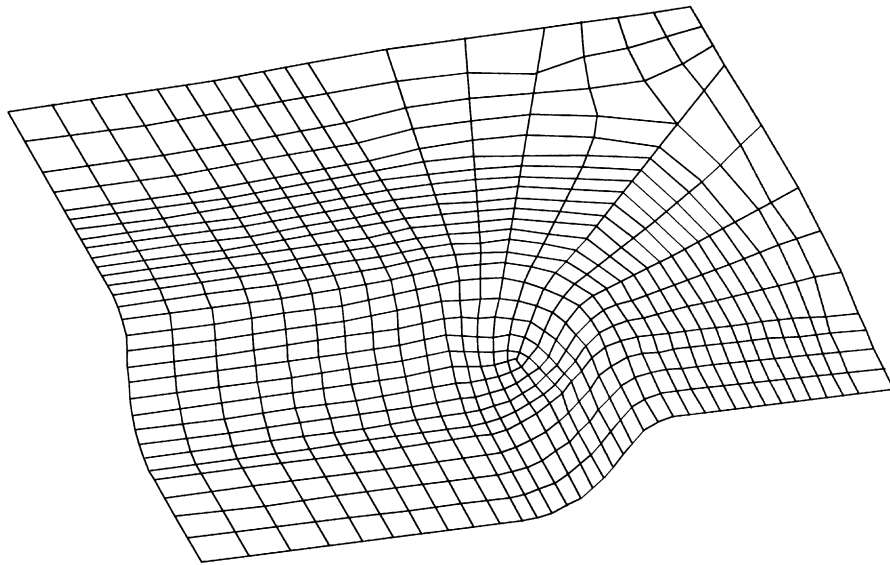


analytical solution of nurbs, two rigid bodies

Figure 8.38-4 Deformed Plate at Increment 20



INC : 50
SUB : 0
TIME : 1.250e+01
FREQ : 0.000e+00

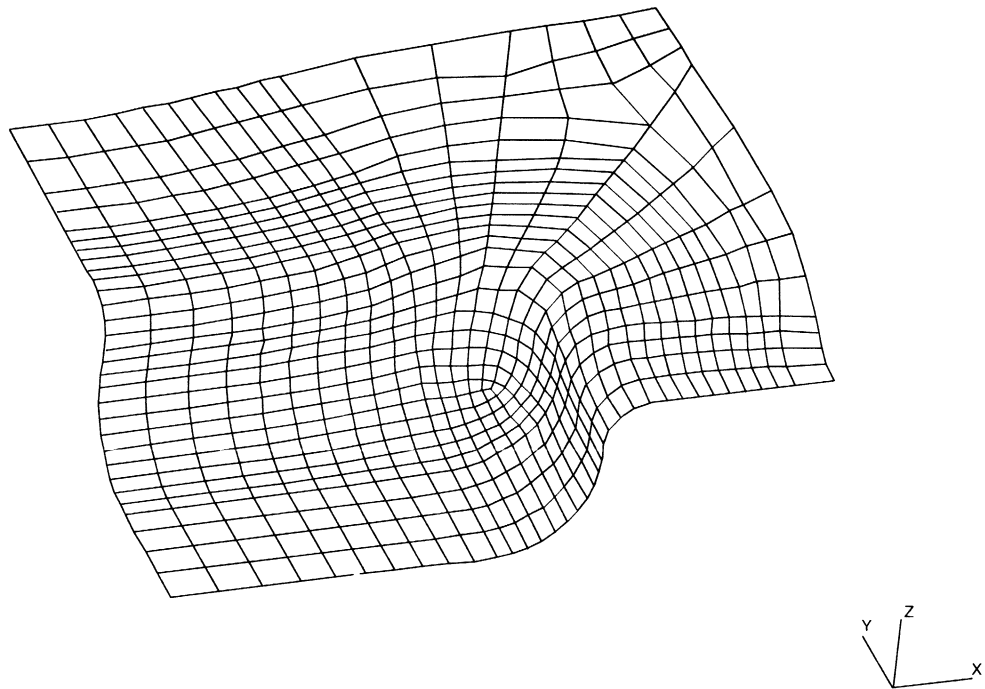


analytical solution of nurbs, two rigid bodies

Figure 8.38-5 Deformed Plate at Increment 50



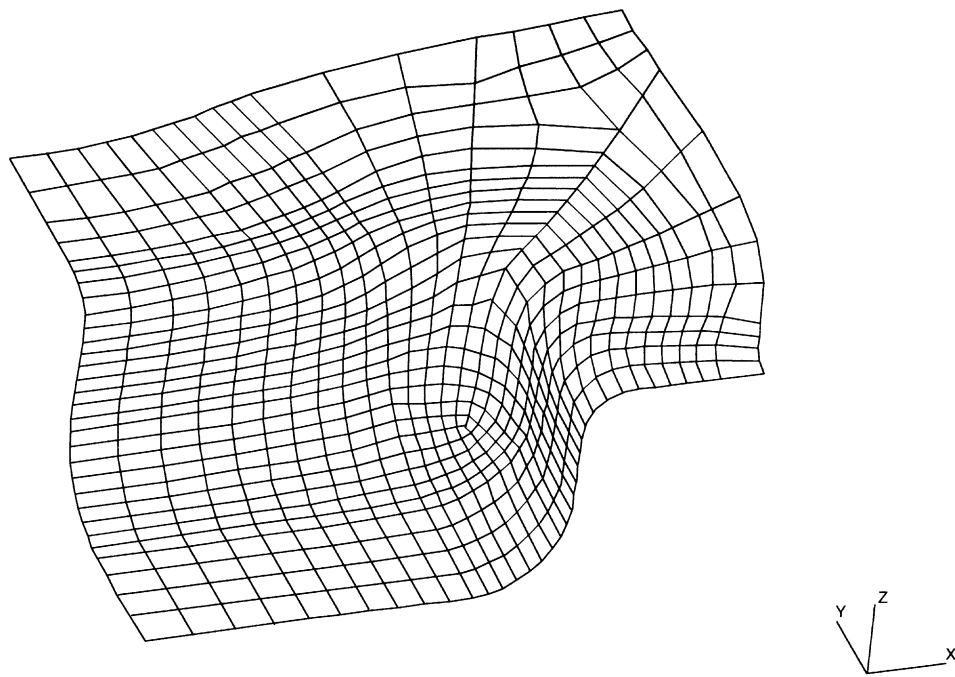
INC : 80
SUB : 0
TIME : 2.000e+01
FREQ : 0.000e+00



analytical solution of nurbs, two rigid bodies

Figure 8.38-6 Deformed Plate at Increment 80

INC : 110
SUB : 0
TIME : 2.750e+01
FREQ : 0.000e+00

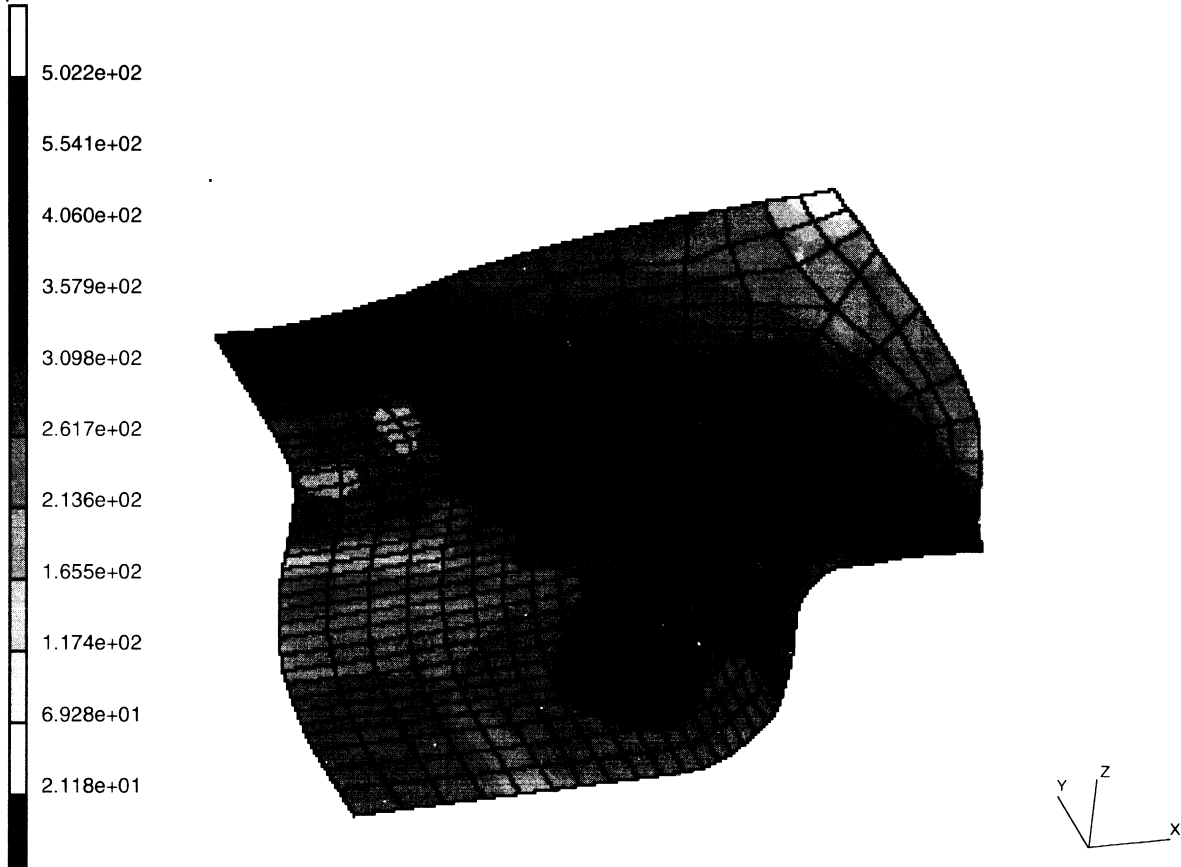


analytical solution of nurbs, two rigid bodies

Figure 8.38-7 Deformed Plate at Increment 110



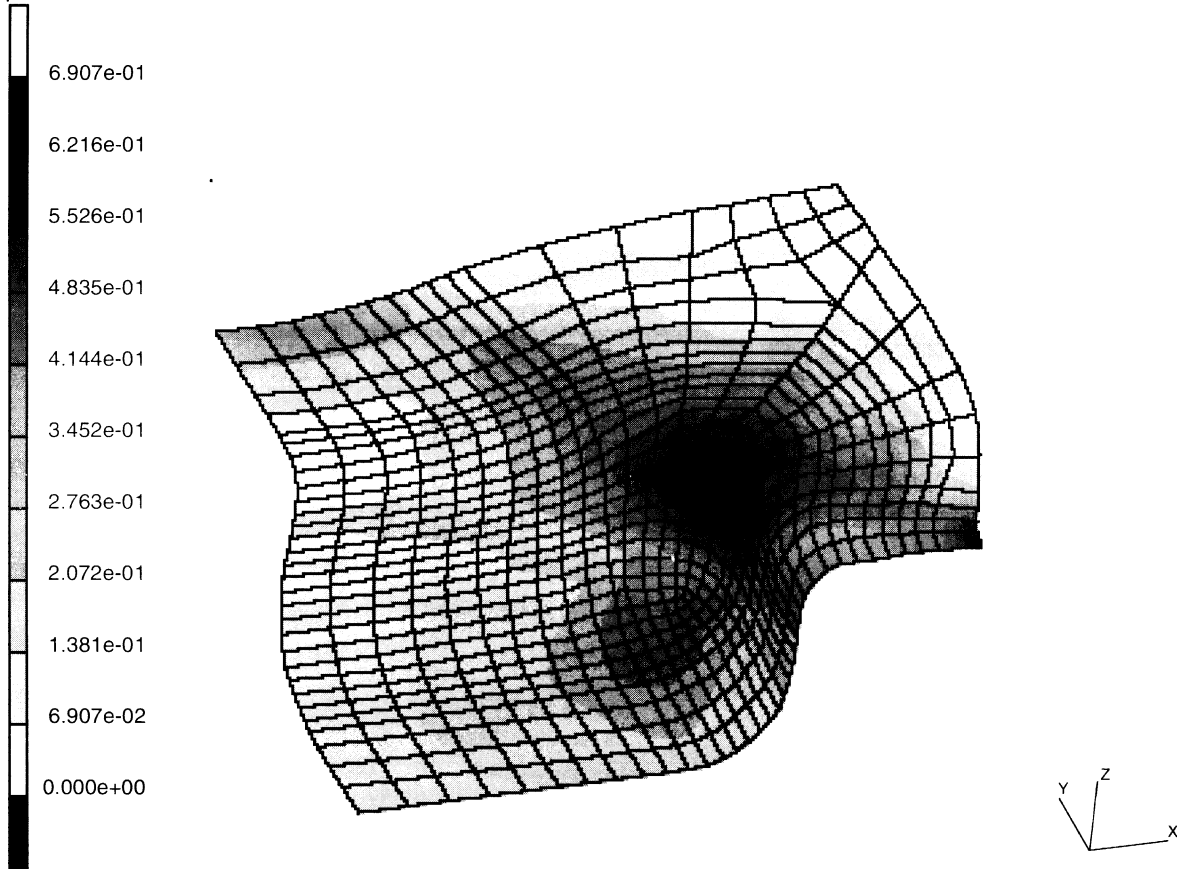
INC : 110
SUB : 0
TIME : 2.750e+01
FREQ : 0.000e+00



analytical solution of nurbs, two rigid bodies
Equivalent Von Mises Stress Layer 4

Figure 8.38-8 Equivalent Stress at Midsurface at Increment 110

INC : 110
SUB : 0
TIME : 2.750e+01
FREQ : 0.000e+00



analytical solution of nurbs, two rigid bodies
Total Equivalent Plastic Strain Layer 4

Figure 8.38-9 Equivalent Plastic Strain at Midsurface at Increment 110



8.39 Contact of Two Beams using AUTO INCREMENT

This problem demonstrates bringing two beams into contact as an example of large deflection which exhibits inelastic response. The AUTO INCREMENT option is used to control the magnitude of the load increment. A beam acted on by a point load eventually comes into contact with a second beam (Figure 8.39-1). The geometrically nonlinear problem is solved adaptively by the arc-length method. The procedure stops at the step before the upper beam slips from the lower beam (Figure 8.39-5).

Element

Element type 5 is 2-node rectangular-section beam-column with three global degrees of freedom per node.

Geometry

The beams are 80 inches in length with a distance of 20 inches separating the beams. The height of 2.5 is input in the first data field of GEOMETRY option. The cross-sectional area of 1 is input in the second data field (EGEOM2).

Material Properties

Linear elastic properties are specified in the ISOTROPIC option – Young’s modulus = 1,000,000 psi and Poisson’s ratio is 0.3333.

Boundary Conditions

Fully clamped conditions are applied to one end of each beam.

Geometric Nonlinearity

The LARGE DISP parameter indicates that geometric nonlinear analysis is to be performed.

Control

Residual-force control is used with a relative error of 10%. No more than 20 recycles per increment is specified.

Loading

The POINT LOAD option is used to enter the total applied load of 585 pounds at node 29 along the global Y-direction. The initial load is 1% of the total load in the first increment and subsequent loading is adjusted adaptively based on arc-length method.

**Contact**

This option declares that there are two flexible bodies. Each is made of 20 beam elements. Contact tolerance distance is 0.01.

Results

The deformed beams are shown in Figure 8.39-2 through Figure 8.39-5. The load deflection curve is shown in Figure 8.39-6. When the beams contact, the distance between the contacting node and the warm segment is equal to half the thickness of the beam. After the beams contact, the upper beam comes into contact with the lower beam at point A. The effect of stiffening due to the additional stiffness of the lower beam is observed until point B, as the contact node, slips onto the lower beam. At that moment, the pure bending dominates the response and corresponds to another type of instability until point C, at which time the upper beam will slip away the lower beam.

Parameters, Options, and Subroutines Summary

Example e8x39.dat:

Parameters	Model Definition Options	History Definition Options
ELEMENTS	CONNECTIVITY	AUTO INCREMENT
END	CONTACT	CONTINUE
LARGE DISP	CONTROL	POINT LOAD
PRINT	COORDINATE	
SIZING	END OPTION	
TITLE	FIXED DISP	
	GEOMETRY	
	ISOTROPIC	
	POINT LOAD	
	POST	
	PRINT ELEMENT	
	PRINT NODE	

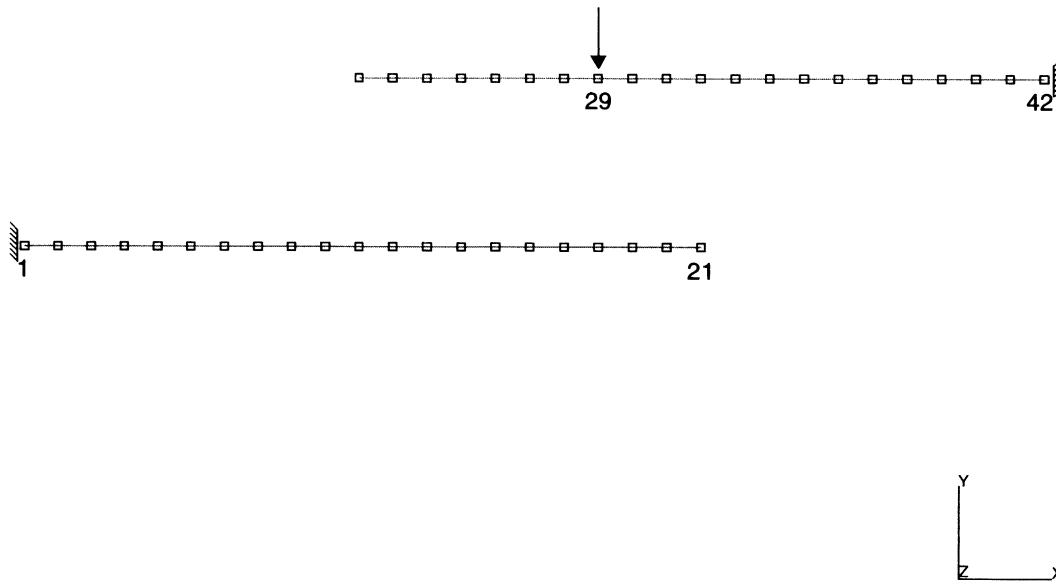
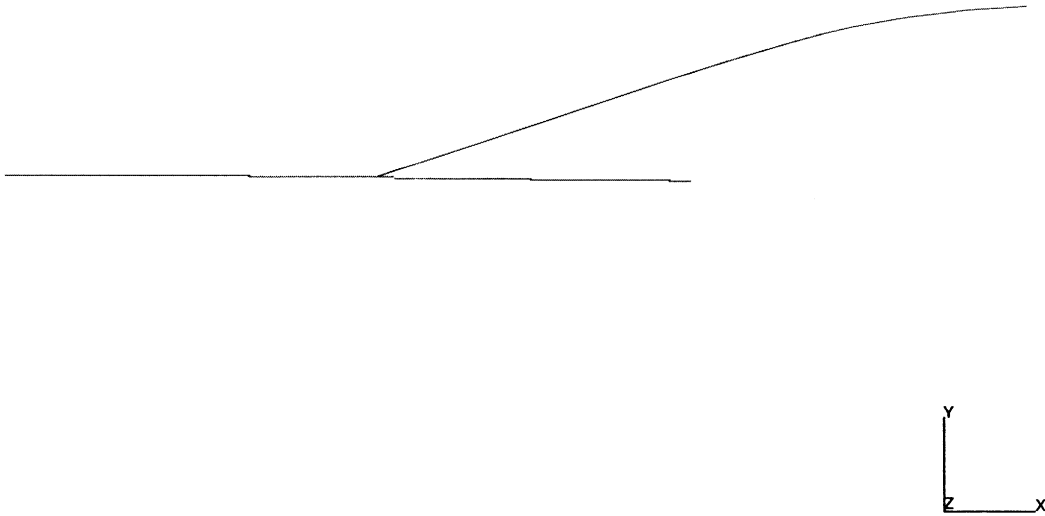


Figure 8.39-1 Mesh of Two Beams



INC : 11
SUB : 0
TIME : 2.581e-01
FREQ : 0.000e+00

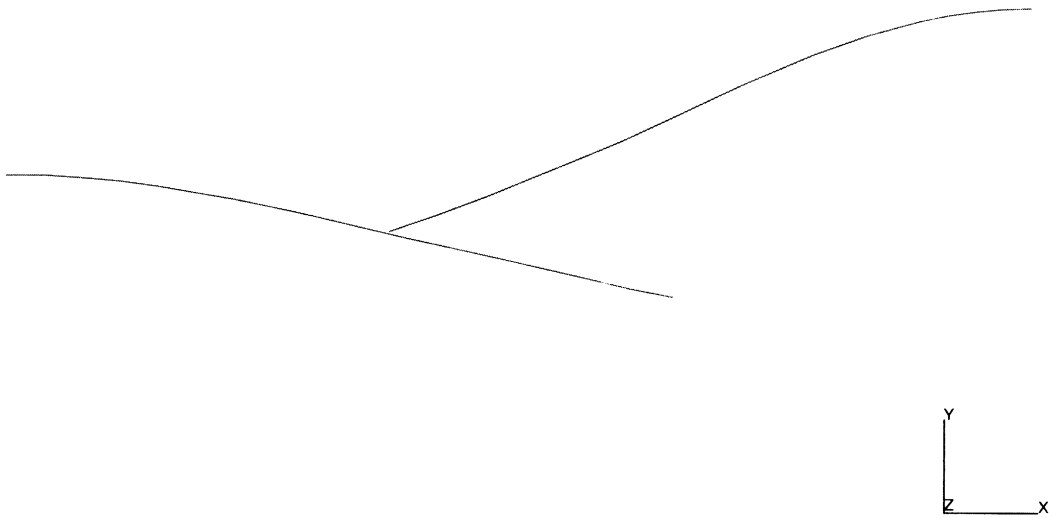


prob e8.39 : two-beam contact (auto inc + point load + c

Figure 8.39-2 Initial Contact of Beams



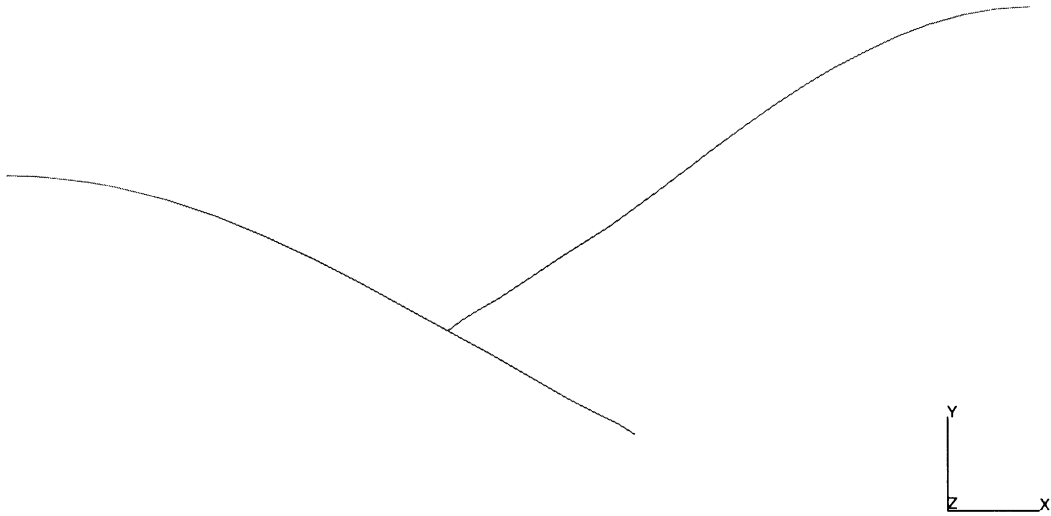
INC : 20
SUB : 0
TIME : 7.075e-01
FREQ : 0.000e+00



prob e8.39 : two-beam contact (auto inc + point load + c

Figure 8.39-3 Deformed Mesh at Increment 20

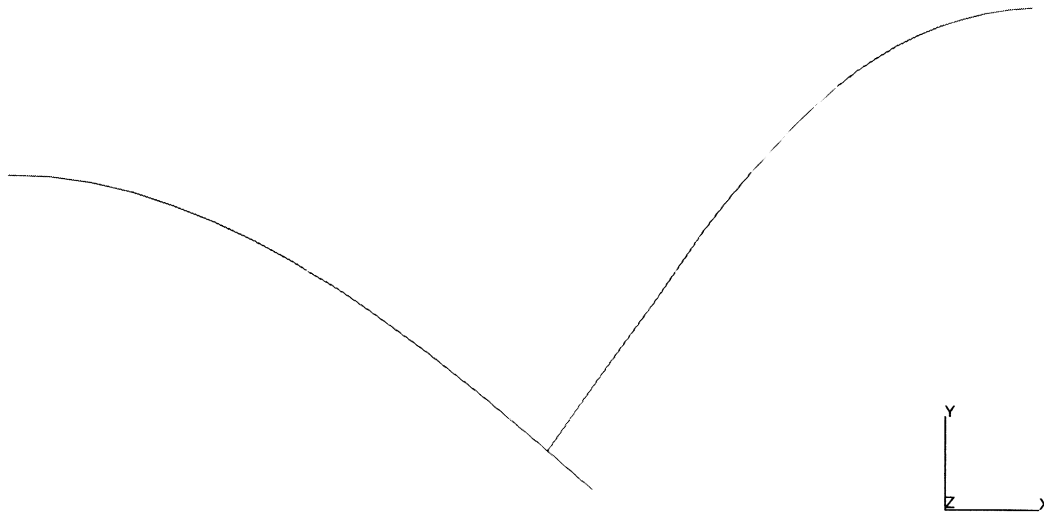
INC : 30
SUB : 0
TIME : 9.713e-01
FREQ : 0.000e+00



prob e8.39 : two-beam contact (auto inc + point load + c

Figure 8.39-4 Deformed Mesh at Increment 30

INC : 39
SUB : 0
TIME : 9.728e-01
FREQ : 0.000e+00



prob e8.39 : two-beam contact (auto inc + point load + c

Figure 8.39-5 Deformed Mesh at Increment 39

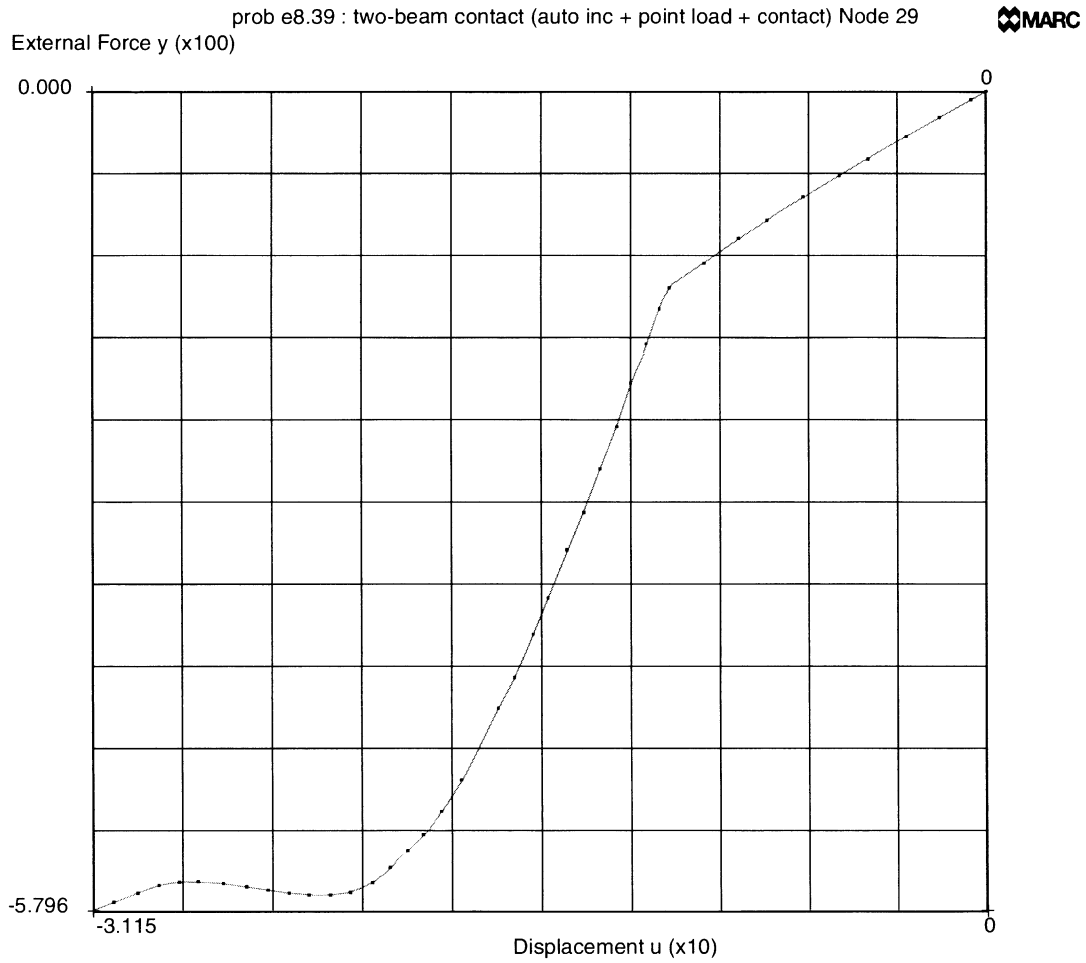


Figure 8.39-6 Load Deflection Curve



8.40 Circular Disk under Point Loads Using Adaptive Meshing

This problem illustrates the use of adaptive meshing for a simple geometry. A circular disk is crudely modeled, and MARC improves the finite element model.

Element

Element type 11, a 4-node linear isoparametric plane-strain element is used in the model.

Model

The original coarse mesh containing only four elements is shown in Figure 8.40-1. The disk has a radius of 1 mm and a unit thickness. The SURFACE option is used to define a circular curve which has this geometry. The ATTACH NODES option is used to specify that the boundary nodes are located on the curve. When new boundary nodes are created, they are automatically placed on the curve.

Geometry

No geometry is necessary as the default is used.

Material Properties

Young's modulus is 2.1×10^5 N/mm², and Poisson's ratio is 0.3. As new elements are created, they are given these material properties.

Boundary Conditions

The bottom point, node 9, is constrained in both directions. The top point, node 1, is constrained in the x-direction to insure no rigid body motion. Additionally, it is given a point load of 0.1 N vertically.

Adaptive Meshing

The ADAPTIVE parameter is used to indicate the maximum number of elements and nodes allowed. The ELASTIC parameter is used to indicate that the analysis is to be repeated until the adaptive criteria is satisfied. Only the loads applied in increment 0 are considered. The ADAPTIVE model definition option is used to indicate that an element should be refined if the stress is greater than 75% of the maximum stress. A limit of 4 levels of subdivisions is allowed. In theory, the maximum number of elements would be $4 \times 4^4 = 1024$; this is less than given on the parameter.

**Results**

The progression of meshes is shown in Figure 8.40-2 through Figure 8.40-5. You can observe the concentration of elements in the vicinity of the point loads. Furthermore, the nodes on the boundary take on the shape of the circle. As the mesh is improved, the solution converges to the correct results. Looking at the maximum y displacement, you can observe that the original solution is substantially incorrect.

Level	Maximum Displacement *10 ⁻⁶
0	.9070
1	.9054
2	1.067
3	1.331
4	1.548
5	1.549

Parameters, Options, and Subroutines Summary

Example e8x40.dat:

Parameters

ADAPTIVE
ELASTIC
ELEMENTS
END
PRINT
SIZING
TITLE

Model Definition Options

ADAPTIVE
ATTACH NODE
CONNECTIVITY
COORDINATE
END OPTION
FIXED DISP
ISOTROPIC
NO PRINT
POINT LOAD
POST
SOLVER
SURFACE



INC : 0
SUB : 0
TIME : 0.000e+00
FREQ : 0.000e+00

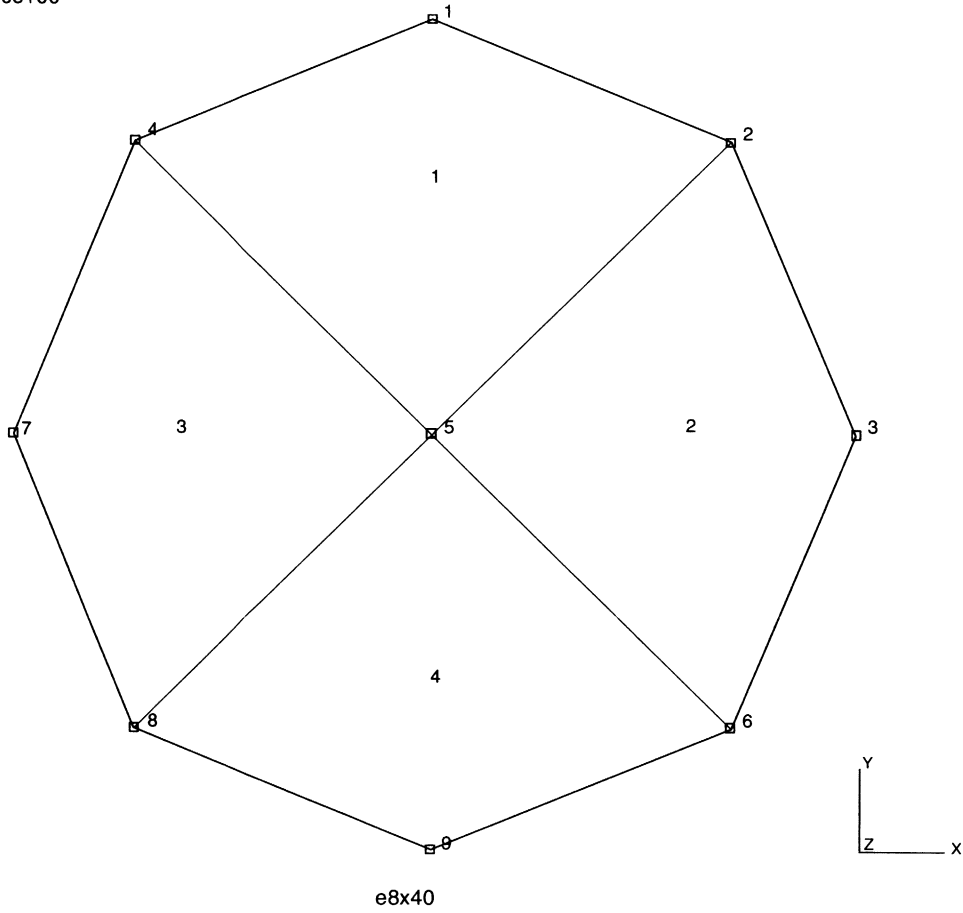


Figure 8.40-1 Original Mesh

INC : 0
SUB : 1
TIME : 0.000e+00
FREQ : 0.000e+00

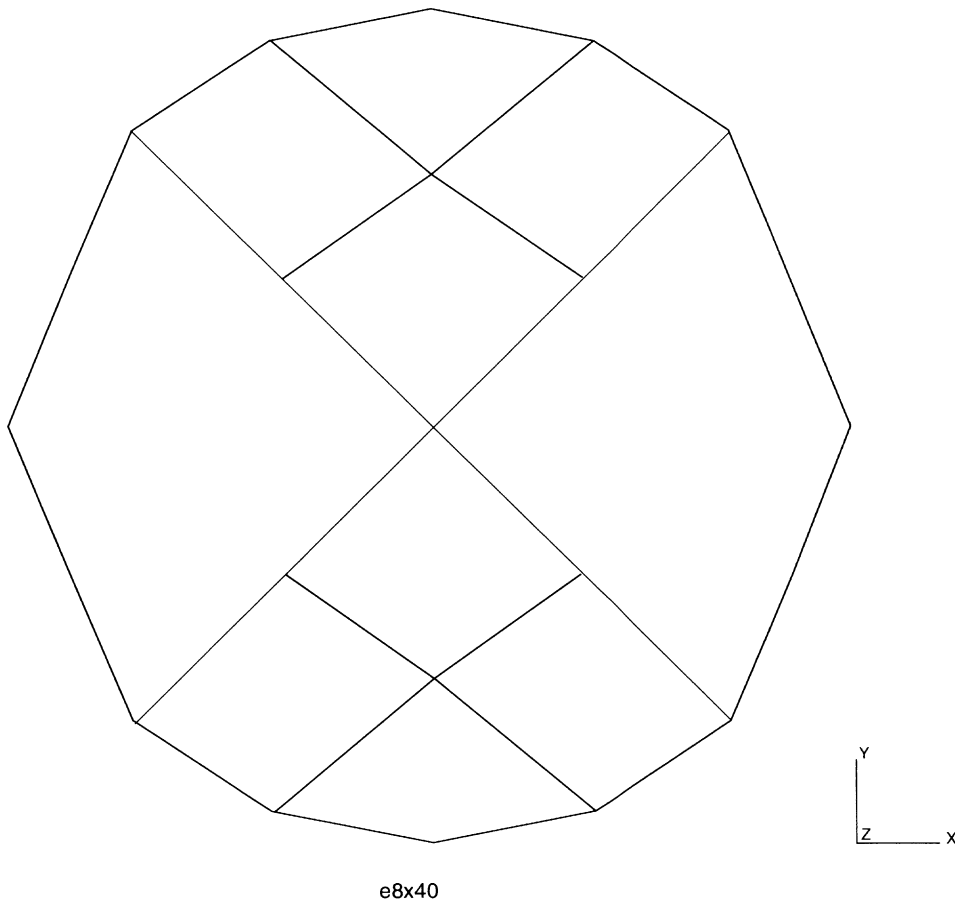


Figure 8.40-2 First Adaptive Mesh



INC : 0
SUB : 2
TIME : 0.000e+00
FREQ: 0.000e+00

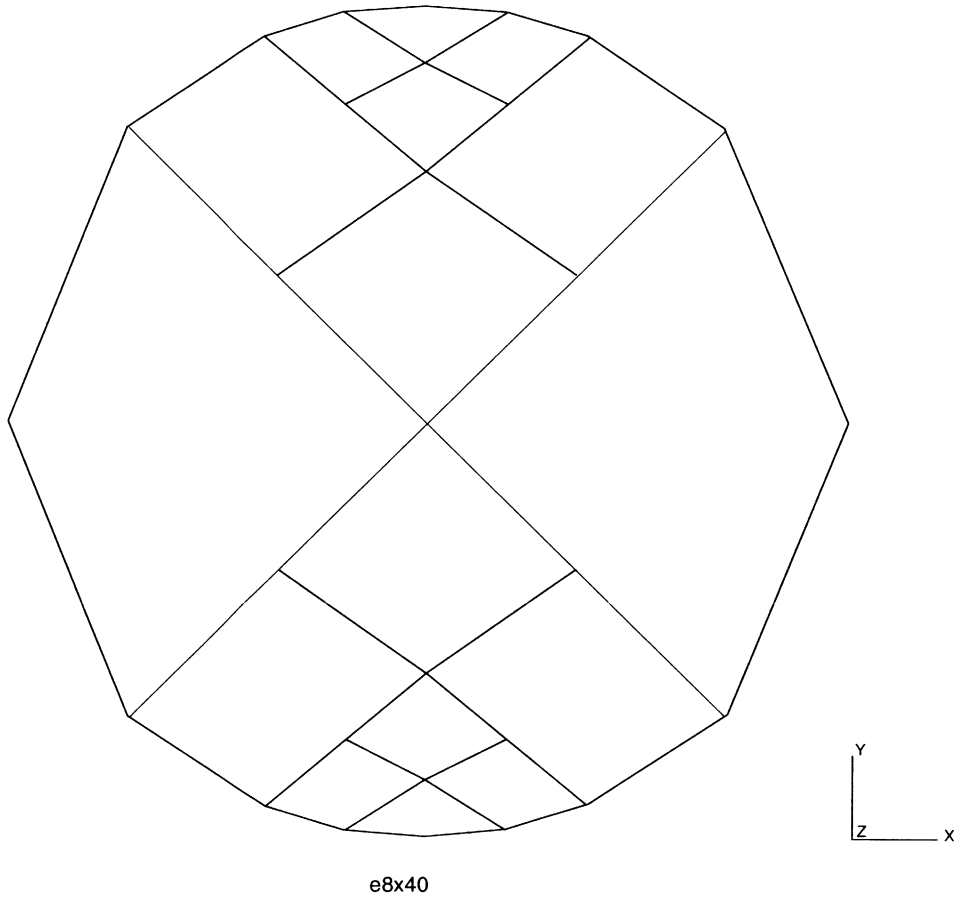


Figure 8.40-3 Second Adaptive Mesh

INC : 0
SUB : 3
TIME : 0.000e+00
FREQ : 0.000e+00

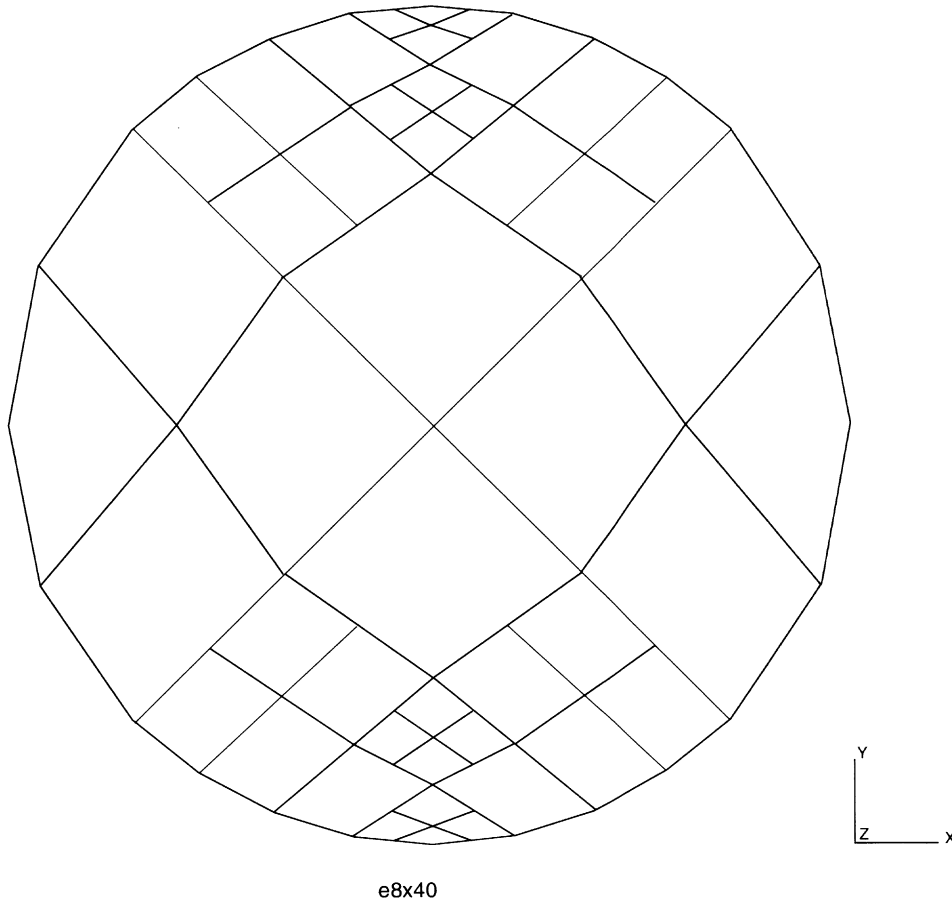


Figure 8.40-4 Third Adaptive Mesh



INC : 0
SUB : 4
TIME : 0.000e+00
FREQ : 0.000e+00

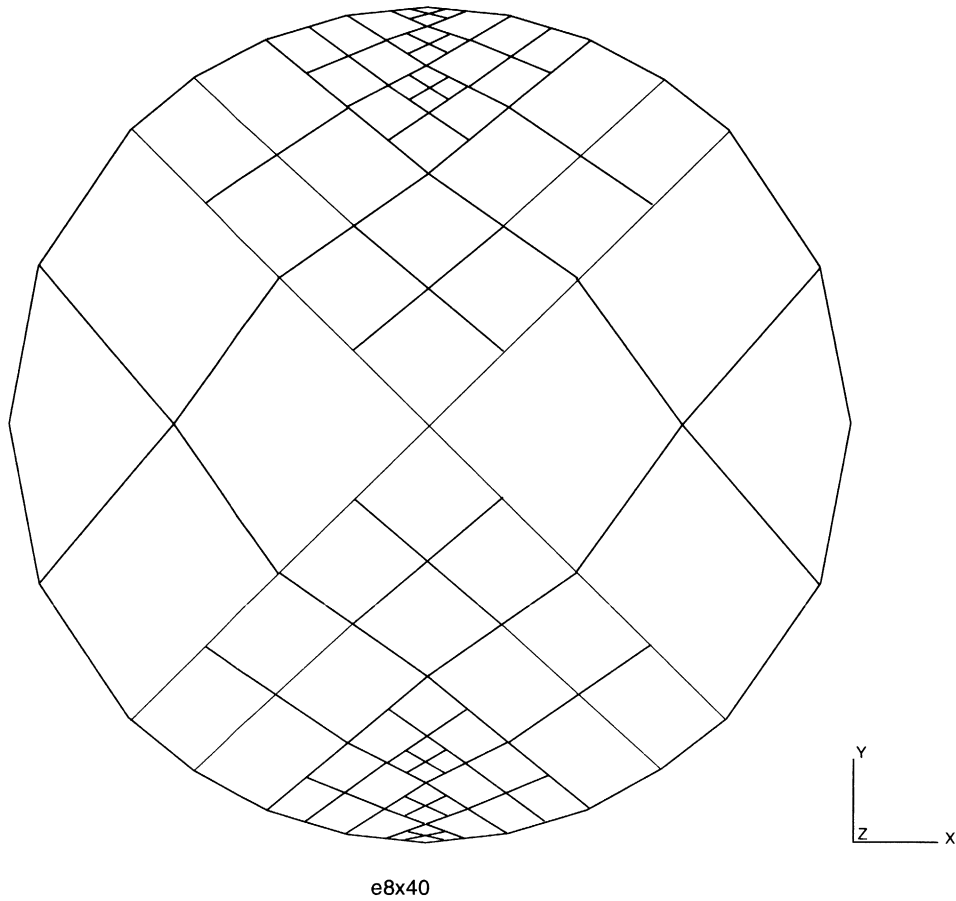


Figure 8.40-5 Fourth Adaptive Mesh





8.41 Stress Singularity Analysis using Adaptive Meshing

This problem demonstrates the use of adaptive meshing for the analysis of a stress singularity. The adaptive meshing increases the number of elements in the region of high stresses and/or high stress gradients.

Element

Element type 3, a 4-node plane-stress element, is used in this analysis.

Model

The plate is a square of dimensions of 100 inches with one-quarter cutout. The initial model, consisting of three elements and eight nodes is shown in Figure 8.41-1. A singular stress develops at node 5 because of the sharp corner.

Geometry

The plates are given a unit thickness.

Material Properties

The material is elastic with a Young's modulus of 30×10^6 psi and a Poisson's ratio of 0.3.

Boundary Conditions

Nodes 7 and 8 have constraints on y-motion while nodes 3 and 6 have constraints on x-motion. Nodes 1, 4, and 7 have a prescribed displacement in the negative x-direction of 0.01 inch. As new elements are created, displacement constraints are automatically generated as required.

Adaptive Meshing

The Zienkiewicz-Zhu error criteria is used with a very tight tolerance of 0.001. A limit of four levels of subdivisions is requested. In theory, the maximum number of elements that could exist at the end is $3 * 4^4 = 768$. The ELASTIC parameter is used to indicate that the analysis is to be repeated until the results satisfy the adaptive meshing error criteria. Additionally, the ERROR ESTIMATES option is used to evaluate the quality of the mesh.

**Results**

Figure 8.41-2 through Figure 8.41-6 show a progression of the created meshes. The stress at the corner node is shown below:

Iteration	$\sigma_{xx} \times 10^2$ psi	$\sigma_{xy} \times 10^2$ psi
0	2.33	3.469
1	2.376	4.825
2	2.892	6.535
3	3.229	9.615
4	4.271	13.56
5	4.498	14.80
6	4.583	14.56
7	4.577	14.53
8	4.583	14.53
9	4.583	14.54
10	4.583	14.54

Note that at higher iterations, the mesh refinement is propagating through the region. Because the number of levels is restricted to 4, the mesh is no longer being enriched at the corner. By iteration 7, the results do not substantially change. If the number of levels is allowed to increase, the solution will continue to change. The ERROR ESTIMATES option informs you that the aspect ratios and warpage is 1.0 and that the largest stress jump occurs at node 5.



Parameters, Options, and Subroutines Summary

Example e8x41.dat:

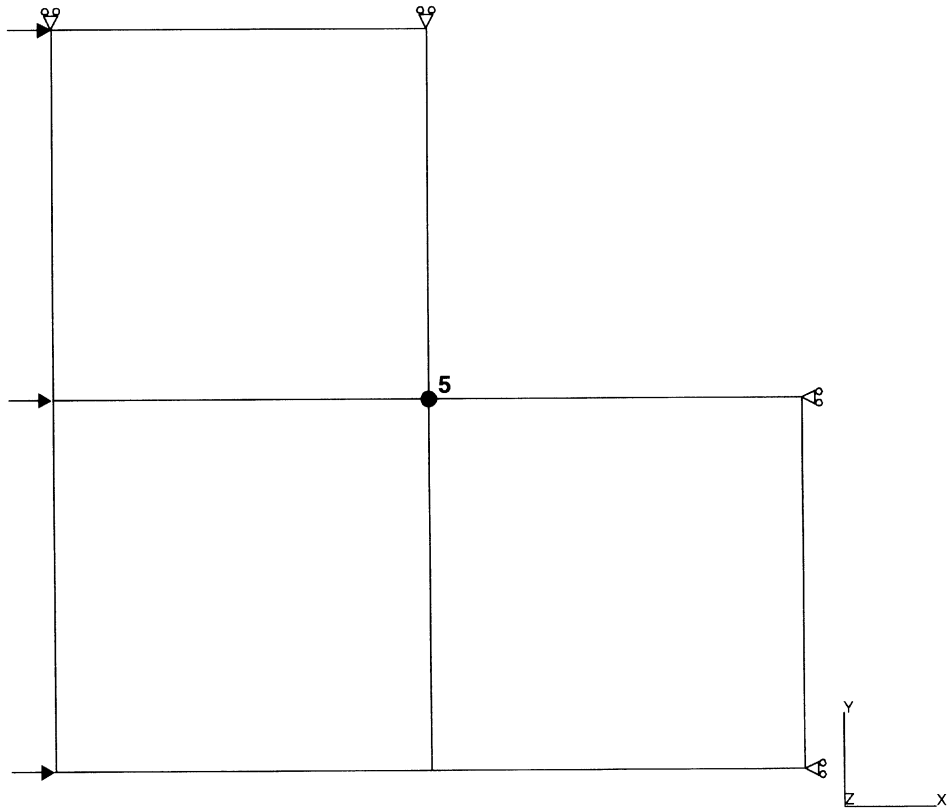
Parameters

ADAPTIVE
ALL POINTS
ELASTIC
ELEMENTS
END
PRINT
SIZING
TITLE

Model Definition Options

ADAPTIVE
CONNECTIVITY
CONTROL
COORDINATE
END OPTION
ERROR ESTIMATE
FIXED DISP
GEOMETRY
ISOTROPIC
POST

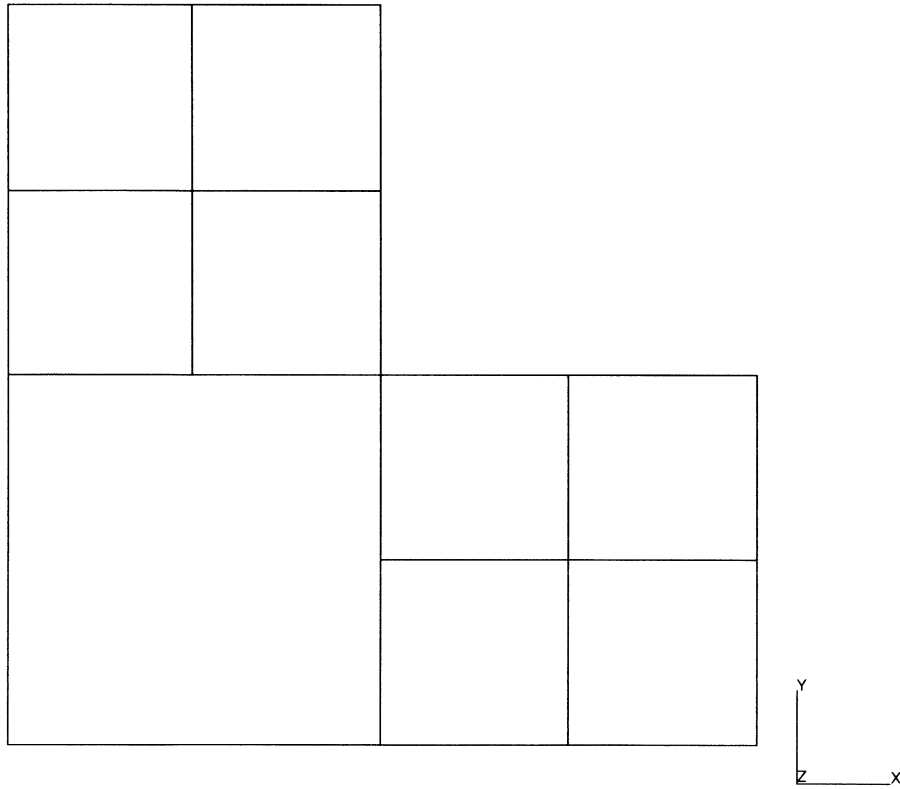
INC : 0
SUB : 0
TIME : 0.000e+00
FREQ : 0.000e+00



problem e8x41

Figure 8.41-1 Original Finite Element Mesh

INC : 0
SUB : 1
TIME : 0.000e+00
FREQ: 0.000e+00

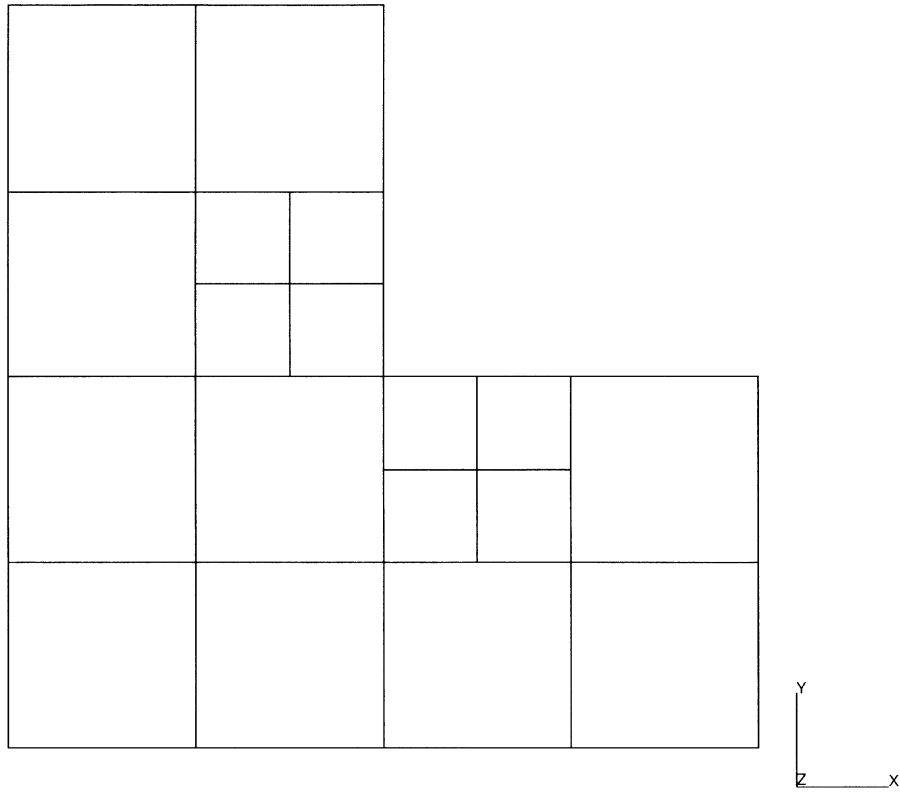


problem e8x41

Figure 8.41-2 First Adaptive Mesh



INC : 0
SUB : 2
TIME : 0.000e+00
FREQ : 0.000e+00

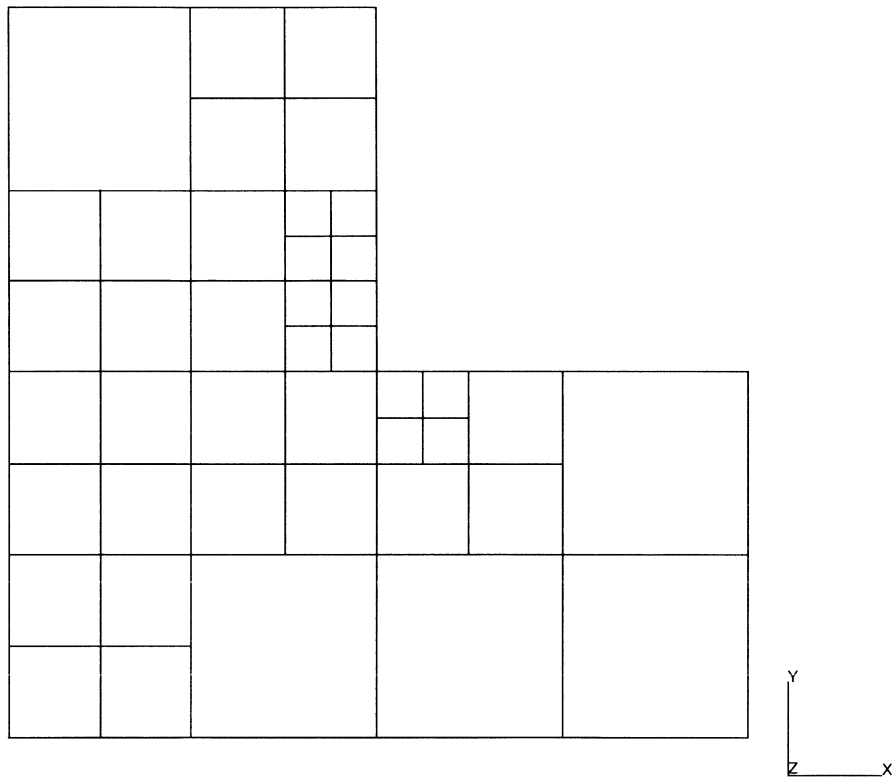


problem e8x41

Figure 8.41-3 Second Adaptive Mesh



INC : 0
SUB : 3
TIME : 0.000e+00
FREQ : 0.000e+00

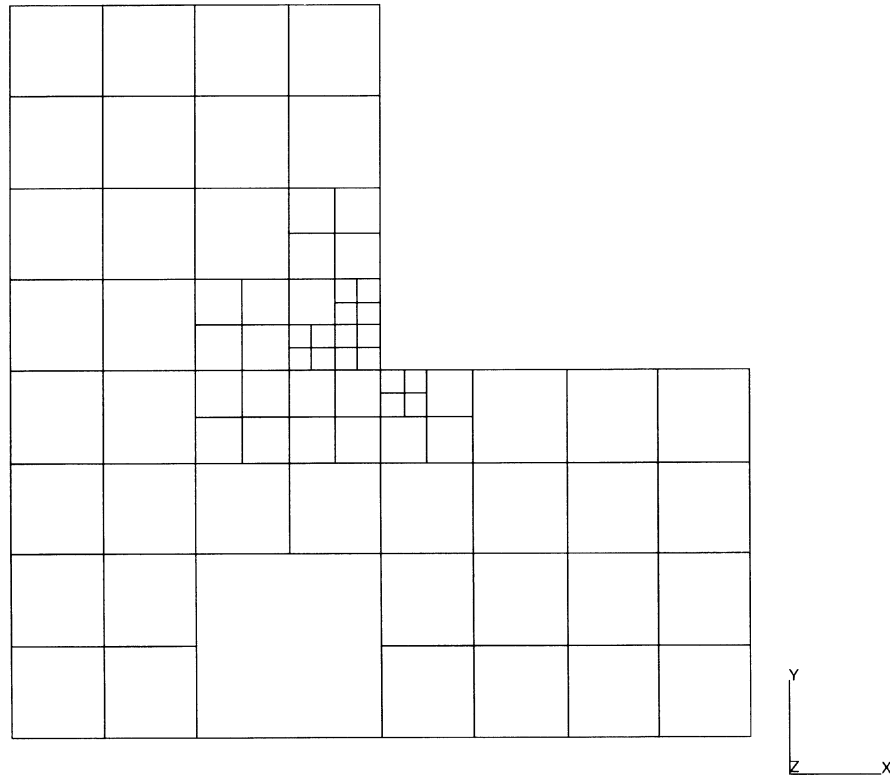


problem e8x41

Figure 8.41-4 Third Adaptive Meshing



INC : 0
SUB : 4
TIME : 0.000e+00
FREQ : 0.000e+00

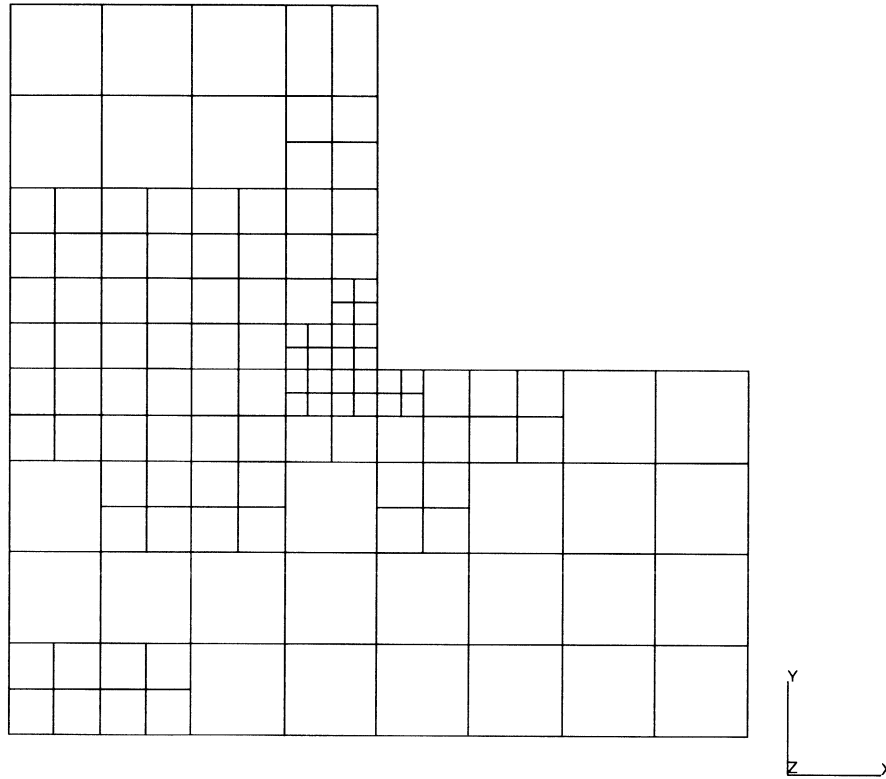


problem e8x41

Figure 8.41-5 Fourth Adaptive Mesh



INC : 0
SUB : 5
TIME : 0.000e+00
FREQ : 0.000e+00



problem e8x41

Figure 8.41-6 Fifth Adaptive Mesh





8.42 Contact Analysis with Adaptive Meshing

This problem demonstrates the capability of adaptive meshing analysis during a contact process. A rod is bent about a deformable roll by a rigid punch (Figure 8.42-1).

Geometry

The rod has a length of 0.28 m and a thickness of 0.02 m. The rigid roll has a radius of 0.31.

Material Properties

The material for all elements is treated as an elastic material with a Young's modulus of $1.5e7$ N/m² and a Poisson's ratio 0.3.

Boundary Conditions

The upper end of the rod is firmly fixed. To avoid the rigid body mode, the center of the roller is fixed.

Control

Residual-force control is used with a relative error of 10%. A maximum of 15 iterations is used per load step.

Contact

This option declares three flexible bodies. The first is a one-layer rod and the second is a roller. The third body is a rigid punch moving with .005 cm/second along the global x-direction. Contact tolerance distance is $1.e-4$ m. The ATTACH NODE option, in conjunction with the SURFACE option in an adaptive mesh analysis, allows new created nodes to attach to the surface. The surface the nodes are attached to is a circle with the center located at .037,2.6795 with a radius of .031. A list of nodes attached to this surface is the boundary nodes along the deformable roll.

Results

Initially, one element is placed through the thickness of the rod. As contact occurs between the punch and the rod, you can observe the mesh refinement. Similarly, where the rod contacts the deformable roll, both bodies show local mesh refinement. As the nonlinear process continues, adaptivity occurs when new regions come into contact. Finally, you can observe that the rod has been bent around and that the refinement has occurred on the rod through the thickness in the direction where contact has occurred. Two levels of refinement are allowed in this analysis. The deformed shape is shown in Figure 8.42-2 through Figure 8.42-5.



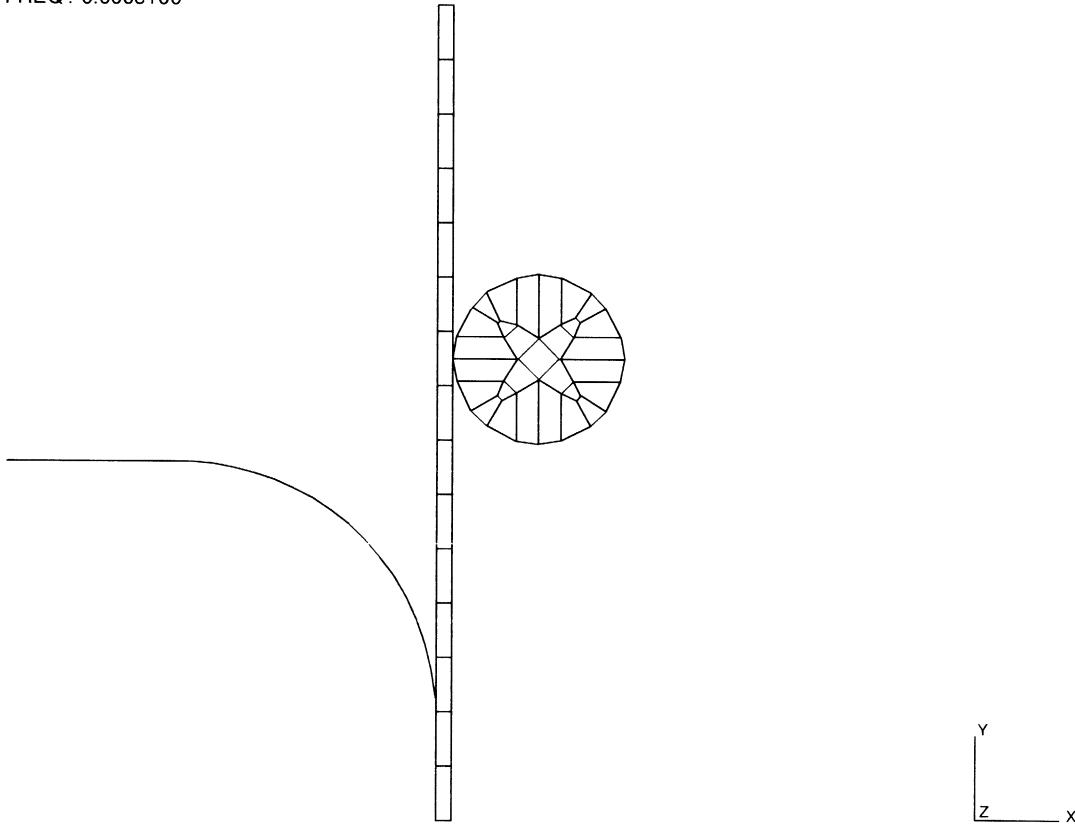
Parameters, Options, and Subroutines Summary

Example e8x42.dat:

Parameters	Model Definition Options	History Definition Options
ADAPTIVE	ADAPTIVE	AUTO LOAD
DIST LOADS	ATTACH NODE	CONTINUE
ELEMENTS	CONNECTIVITY	DIST LOADS
END	CONTACT	MOTION CHANGE
FOLLOW FOR	CONTROL	TIME STEP
LARGE DISP	COORDINATE	
PRINT	DEFINE	
SETNAME	DIST LOADS	
SIZING	END OPTION	
TITLE	FIXED DISP	
	GEOMETRY	
	ISOTROPIC	
	NO PRINT	
	OPTIMIZE	
	POINT LOAD	
	POST	
	RESTART	
	SOLVER	
	SURFACE	



INC : 0
SUB : 0
TIME : 0.000e+00
FREQ : 0.000e+00



problem e8x42

Figure 8.42-1 Original Mesh

INC : 30
SUB : 0
TIME : 3.000e+00
FREQ : 0.000e+00

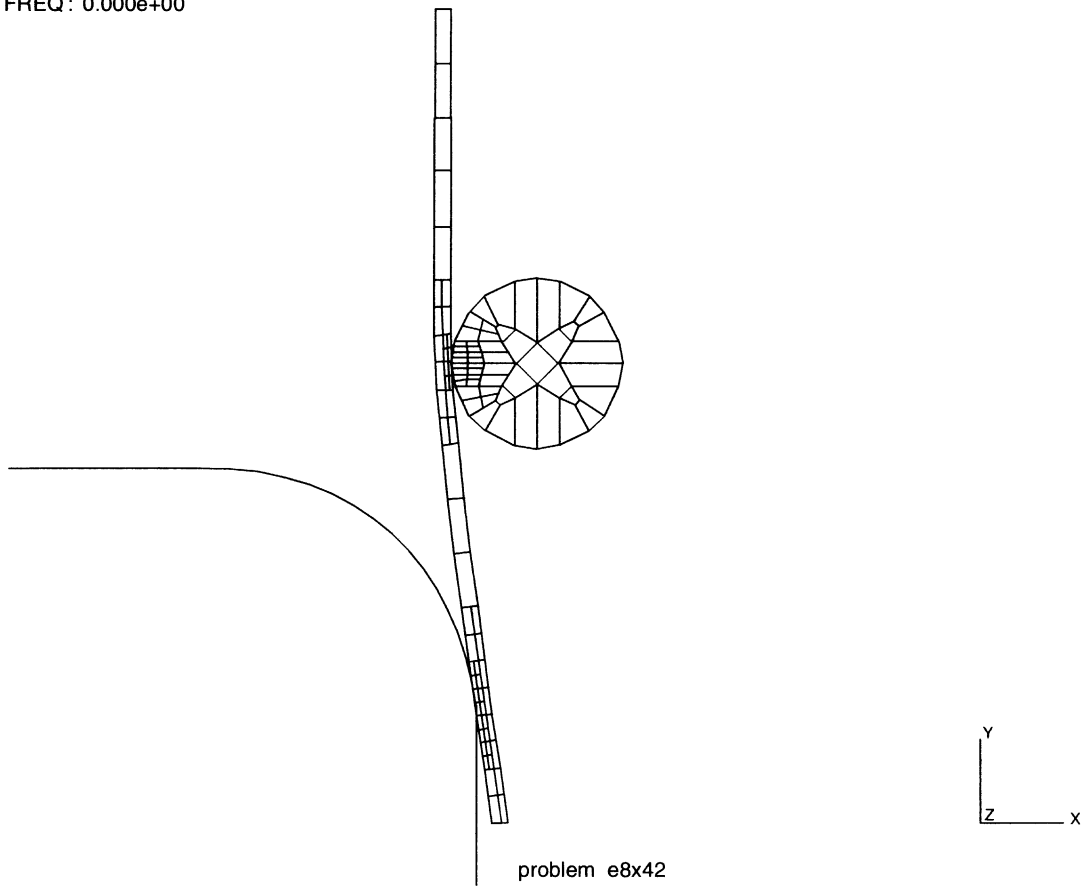


Figure 8.42-2 Deformed New Mesh at Increment 30



INC : 60
SUB : 0
TIME : 6.000e+00
FREQ : 0.000e+00

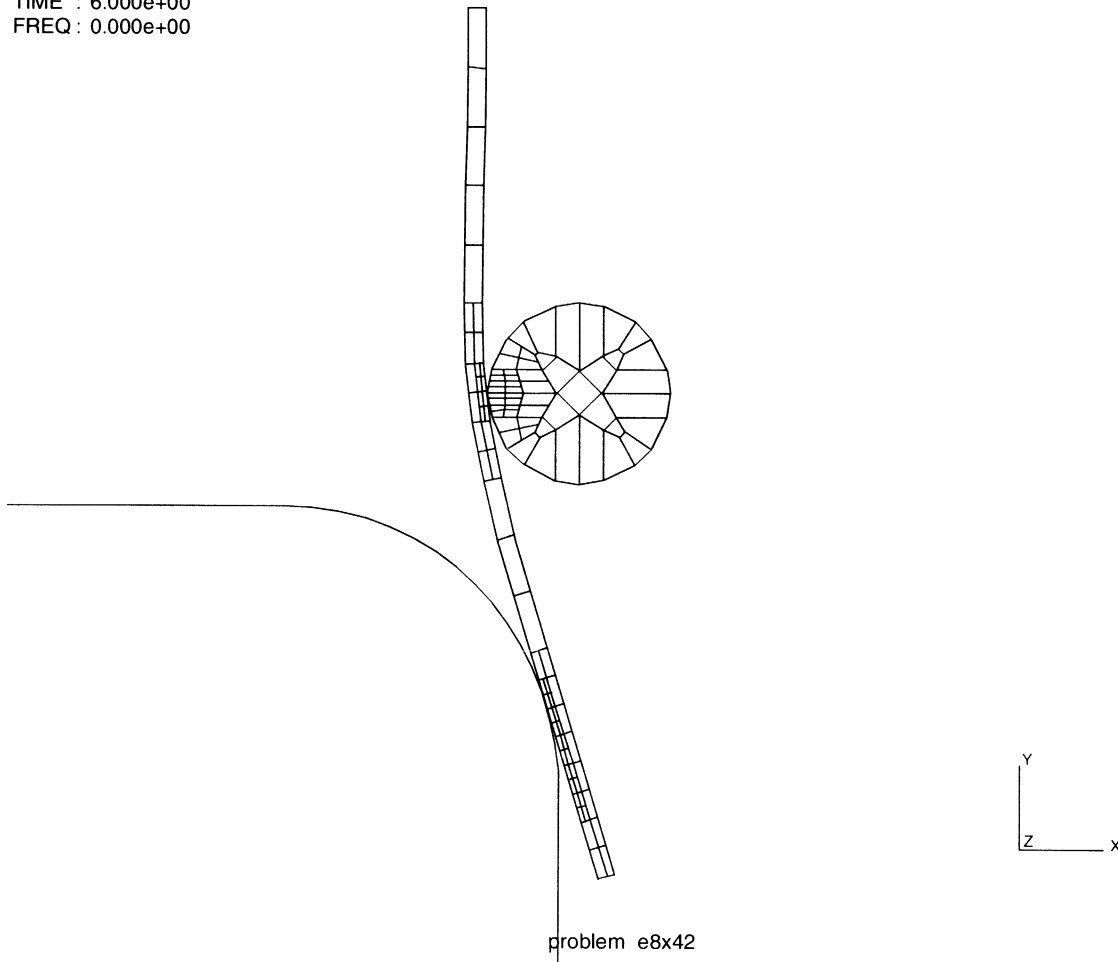


Figure 8.42-3 Deformed New Mesh at Increment 60

INC : 120
SUB : 0
TIME : 1.200e+01
FREQ: 0.000e+00

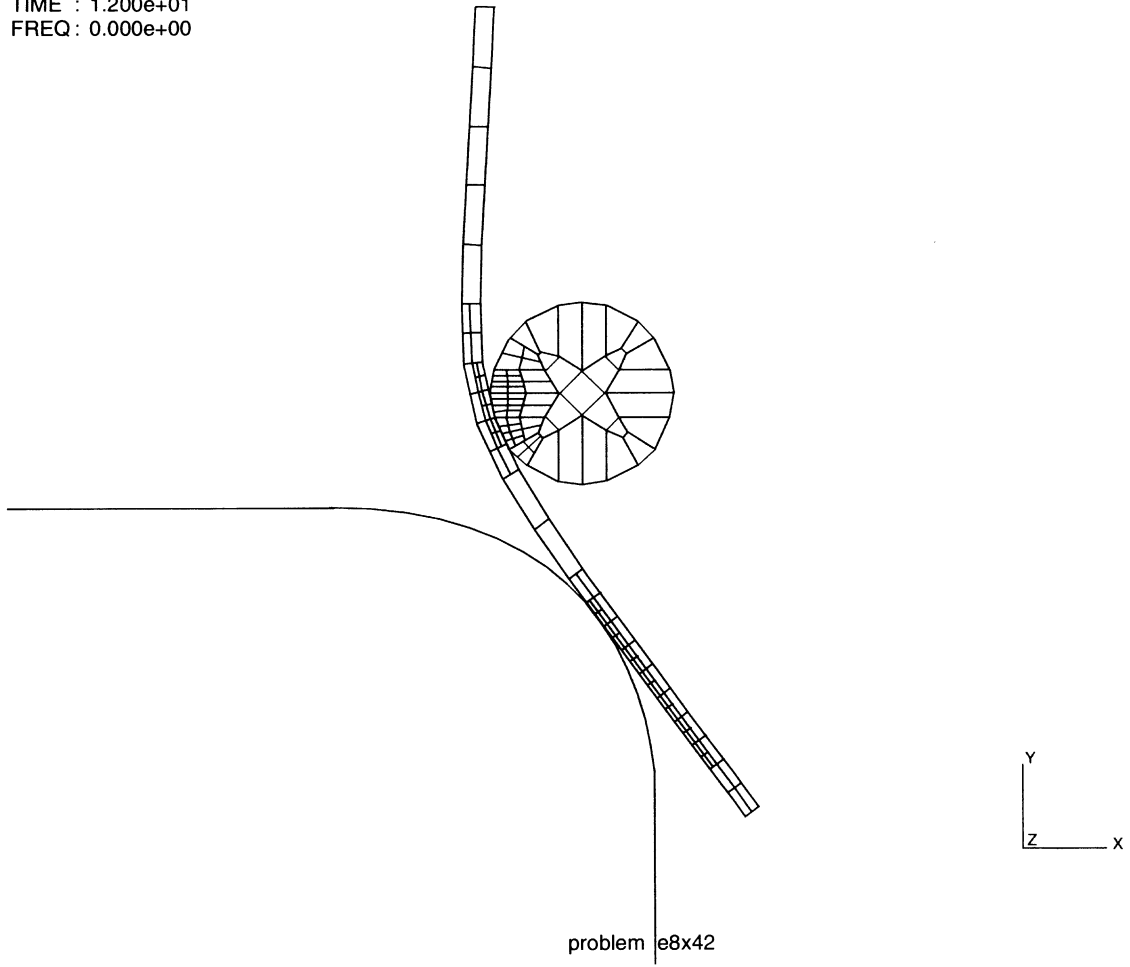


Figure 8.42-4 Deformed New Mesh at Increment 120



INC : 180
SUB : 0
TIME : 1.800e+01
FREQ : 0.000e+00

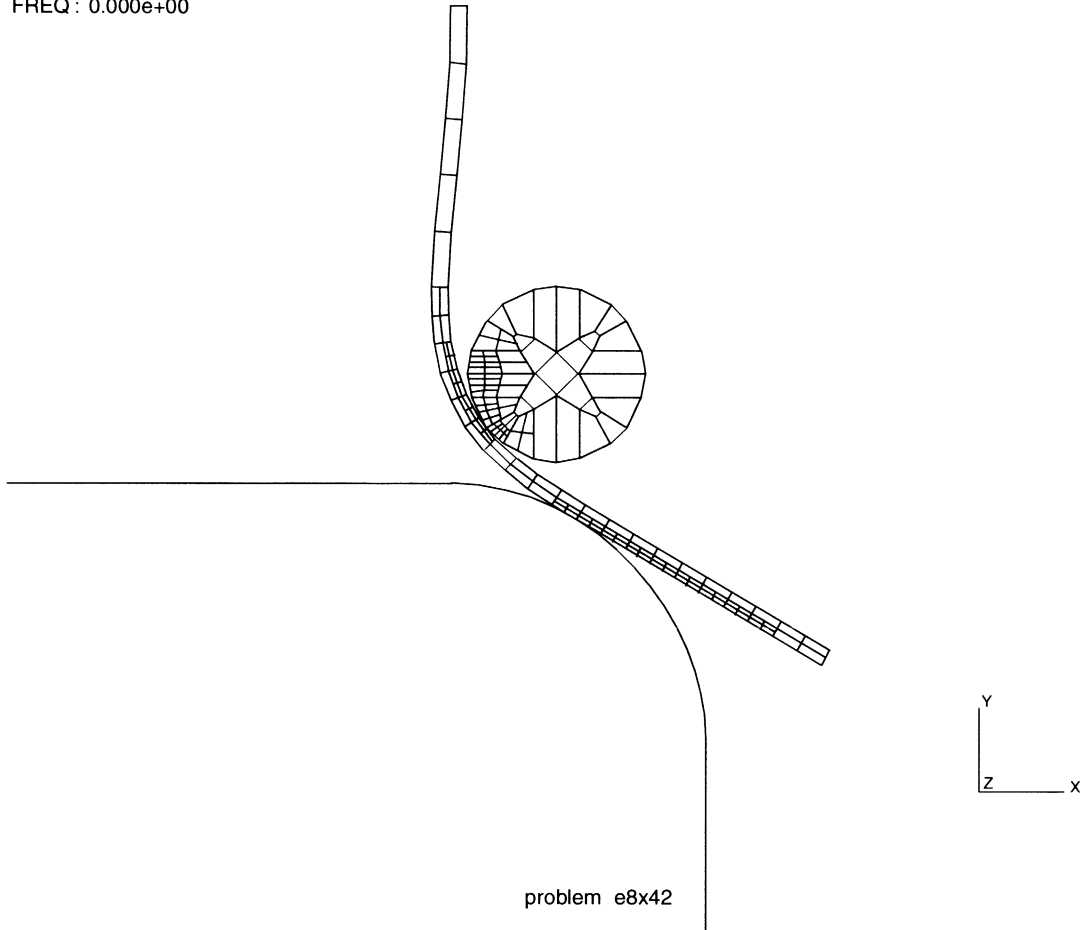


Figure 8.42-5 Deformed New Mesh at Increment 180





8.43 Rubber Seal Analysis using Adaptive Meshing

This problem demonstrates the use adaptive meshing in a nonlinear rubber analysis of a seal. In a nonlinear analysis, the mesh quality is checked at the end of each converged increment. If the mesh needs to be refined, this is performed before the beginning of the next increment. This model uses the Mooney material model. In the first analysis, the total Lagrange procedure is used. In the second and third analyses, the updated Lagrange procedure is used.

Hence, this problem is modeled using the three techniques summarized below.

Data Set	Element Type(s)	Number of Elements	Number of Nodes	Differentiating Features
e8x43	119	560	644	Total Lagrangian, reduced integration hourglass elements
e8x43b	10	560	644	Updated Lagrangian, full integration hourglass elements
e8x43c	116	560	644	Updated Lagrangian, reduced integration hourglass elements

Element

As the first analysis uses the total Lagrange approach, Herrmann elements are required. This example uses element type 119, a lower-order isoparametric axisymmetric element, using the modified Herrmann formulation. This element uses reduced integration with hourglass control. The four corner nodes have conventional displacement degrees of freedom with an additional degree of freedom representing the hydrostatic pressure. The original mesh was created using element type 82. The ALIAS option is used to convert element type 82 to element type 119.

In the second and third analyses, the updated Lagrange procedure is used and conventional displacement elements are used. Element type 10, a 4-node axisymmetric element, and element type 116, a 4-node axisymmetric reduced integration element, are used.

Model

The original model is shown in Figure 8.43-1 and consists of 560 elements and 644 nodes.

Material Properties

A two-term Mooney-Rivlin model is used with $C_{10} = 0.3 \text{ N/cm}^2$; $C_{01} = 0.04 \text{ N/cm}^2$.

**Boundary Conditions**

The region indicated in Figure 8.43-2 has prescribed displacement boundary conditions. In the first 8 increments, the tip of the seal is deflected 2 cm. In the next 12 increments, the tip is deflected an additional 3.0 cm. Additionally, a pressure load is placed on the region indicated which has a total magnitude of 0.25 N/cm^2 . The AUTO LOAD option is used to specify that fixed increment sizes are to be used. The time step used by the contact procedure is 1 second.

Control

The PRINT, 5, 8 parameter is used to obtain additional information regarding the progress of contact. The Cuthill-McKee optimizer is used. The bandwidth is re-optimized when new elements are created due to the adaptive procedure or when self contact occurs in the seal. The CONTROL option specifies the maximum number of elements is 100 and the number of iterations is 10. Displacement convergence checking is used with a 10% tolerance. The initial stress stiffness terms are subjected to compressive behavior and neglecting these terms may prevent a nonpositive definite matrix from occurring.

Adaptive

Two adaptive criteria are used. The first indicates that elements should be refined when they come into contact. In this problem, the seal comes into self contact and elements on both surfaces are refined. The second criteria is based on the stress levels in the element. It implies subdivision of those elements whose stress is greater than 75% of maximum stress. This results in the subdivision of elements in the bend region.

Contact

There is one deformable body that can go into self contact. If contact occurs, the surfaces use a Coulomb friction with a coefficient of 0.3. To improve convergence, the body is not allowed to separate unless the force is greater than 100 N. Based on the size of the element, MARC chooses its own contact tolerance.

Results

Figure 8.43-3 shows the deformation after ten increments. The initial mesh refinement is due to the stress level. Figure 8.43-4 shows the deformation just as contact is to occur. The results at increment 19, Figure 8.43-5 for the total Lagrangian case and Figure 8.43-6 for the updated Lagrangian case, show that mesh refinement has occurred due to contact. Moreover, the deformations, as expected, are identical in the two cases. At the end of the analysis, the number of elements is 560 and the number of nodes is 716.



Parameters, Options, and Subroutines Summary

Example e8x43.dat:

Parameters	Model Definition Options	History Definition Options
ADAPTIVE	ADAPTIVE	AUTO LOAD
ALIAS	CONNECTIVITY	CONTINUE
DIST LOADS	CONTACT	CONTROL
ELEMENTS	COORDINATE	DISP CHANGE
END	DIST LOADS	DIST LOADS
FOLLOW FOR	END OPTION	TIME STEP
LARGE DISP	FIXED DISP	
PRINT	MOONEY	
SIZING	NO PRINT	
TITLE	OPTIMIZE	
	POINT LOAD	
	POST	

Example e8x43b.dat:

Parameters	Model Definition Options	History Definition Options
ADAPTIVE	ADAPTIVE	AUTO LOAD
ALIAS	CONNECTIVITY	CONTINUE
DIST LOADS	CONTACT	CONTROL
ELASTICITY	COORDINATE	DISP CHANGE
ELEMENTS	DIST LOADS	DIST LOADS
END	END OPTION	TIME STEP
FOLLOW FOR	FIXED DISP	
LARGE DISP	MOONEY	
PRINT	NO PRINT	
SIZING	OPTIMIZE	
TITLE	POINT LOAD	
	POST	



Example e8x43c.dat:

Parameters

ADAPTIVE
ALIAS
DIST LOADS
ELEMENTS
END
FOLLOW FOR
LARGE DISP
PRINT
SIZING
TITLE
ELASTICITY

Model Definition Options

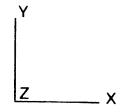
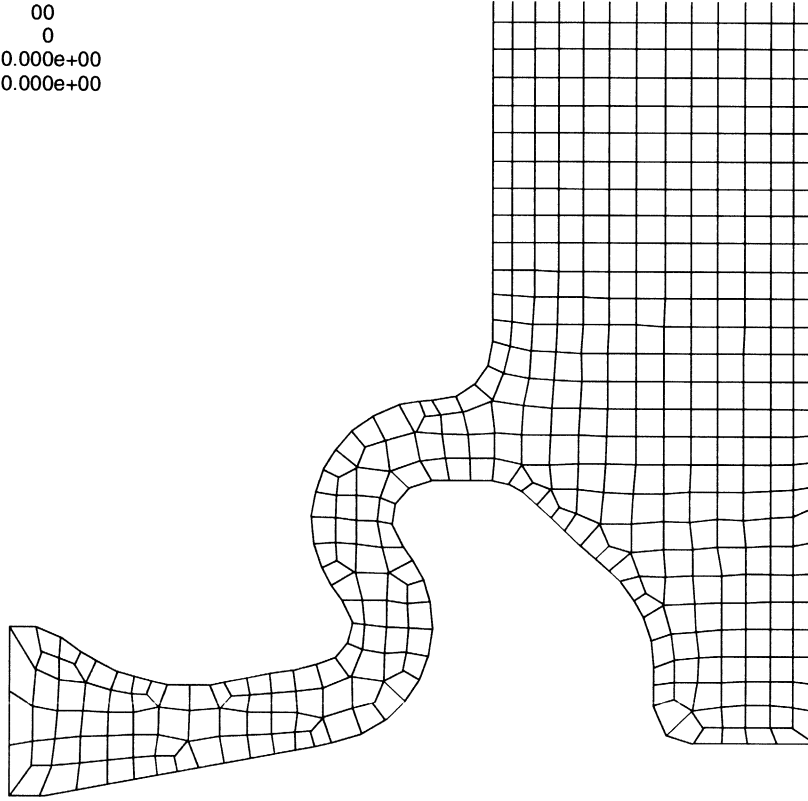
ADAPTIVE
CONNECTIVITY
CONTACT
COORDINATE
DIST LOADS
END OPTION
FIXED DISP
MOONEY
NO PRINT
OPTIMIZE
POINT LOAD
POST

History Definition Options

AUTO LOAD
CONTINUE
CONTROL
DISP CHANGE
DIST LOADS
TIME STEP



INC : 00
SUB : 0
TIME : 0.000e+00
FREQ : 0.000e+00



problem e8x43

Figure 8.43-1 Close-up of Original Finite Element Mesh

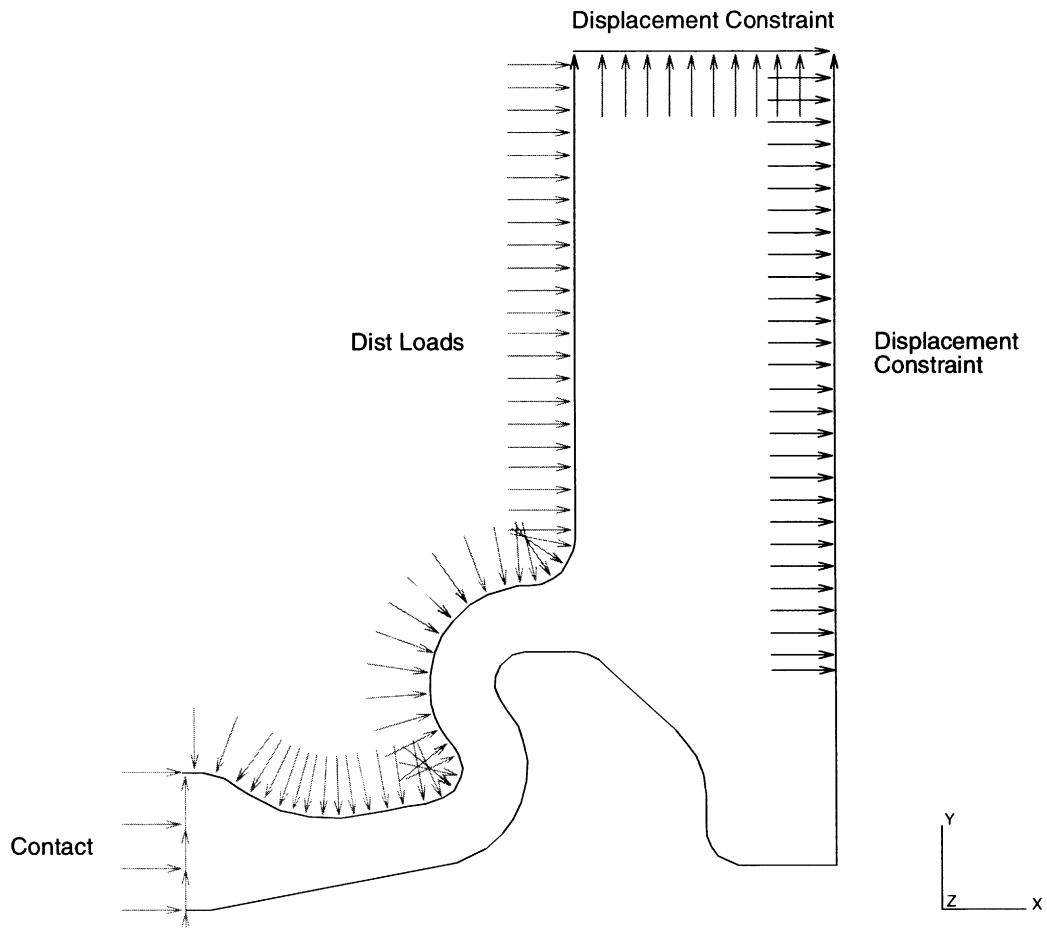
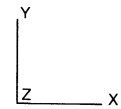
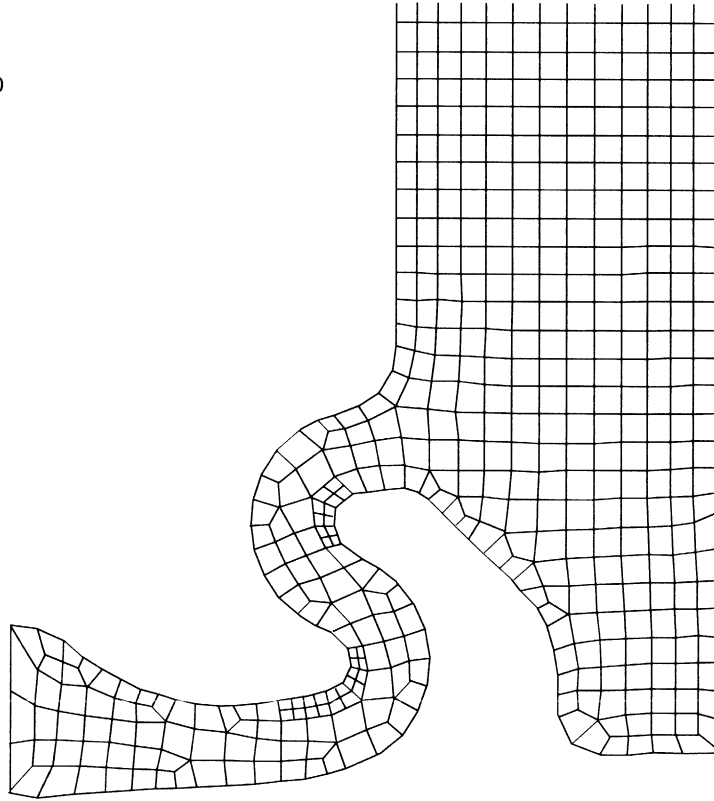


Figure 8.43-2 Seal with Prescribed Boundary Conditions

INC : 10
SUB : 0
TIME : 1.000e+01
FREQ : 0.000e+00

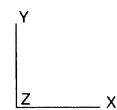
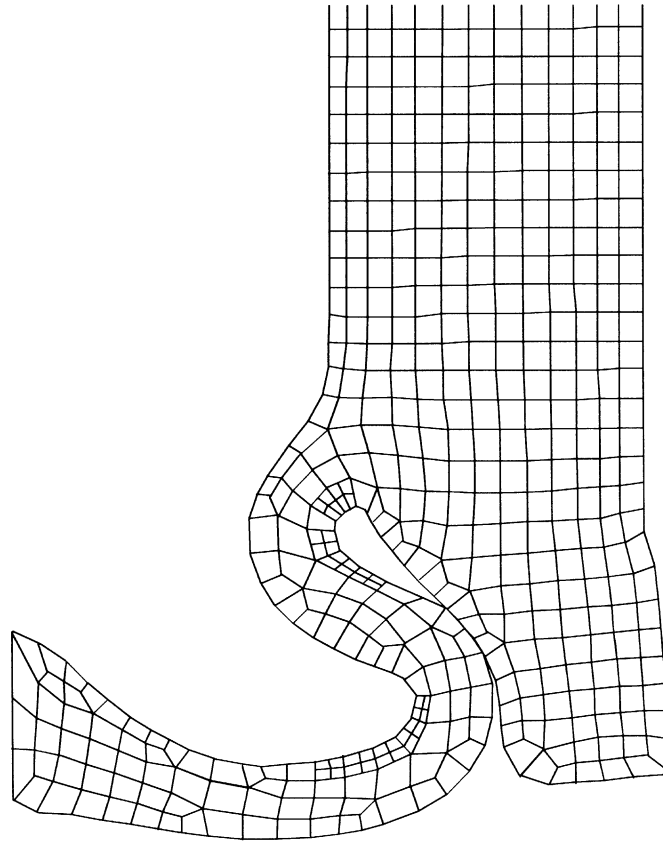


problem e8x43

Figure 8.43-3 Deformed Mesh showing New Elements



INC : 17
SUB : 0
TIME : 1.700e+01
FREQ : 0.000e+00

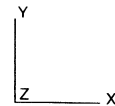
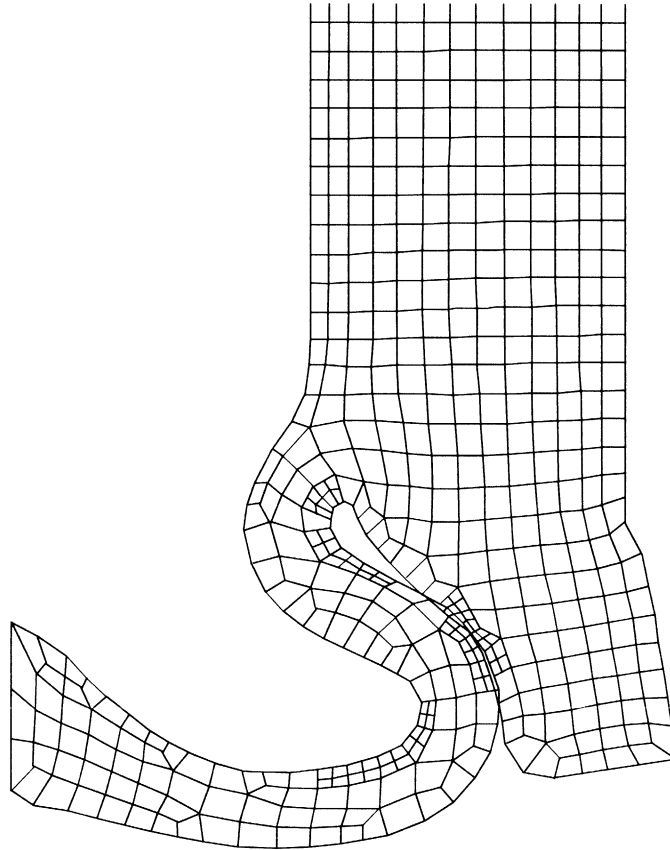


problem e8x43

Figure 8.43-4 Deformed Mesh at Initial Contact



INC : 19
SUB : 0
TIME : 1.900e+01
FREQ: 0.000e+00

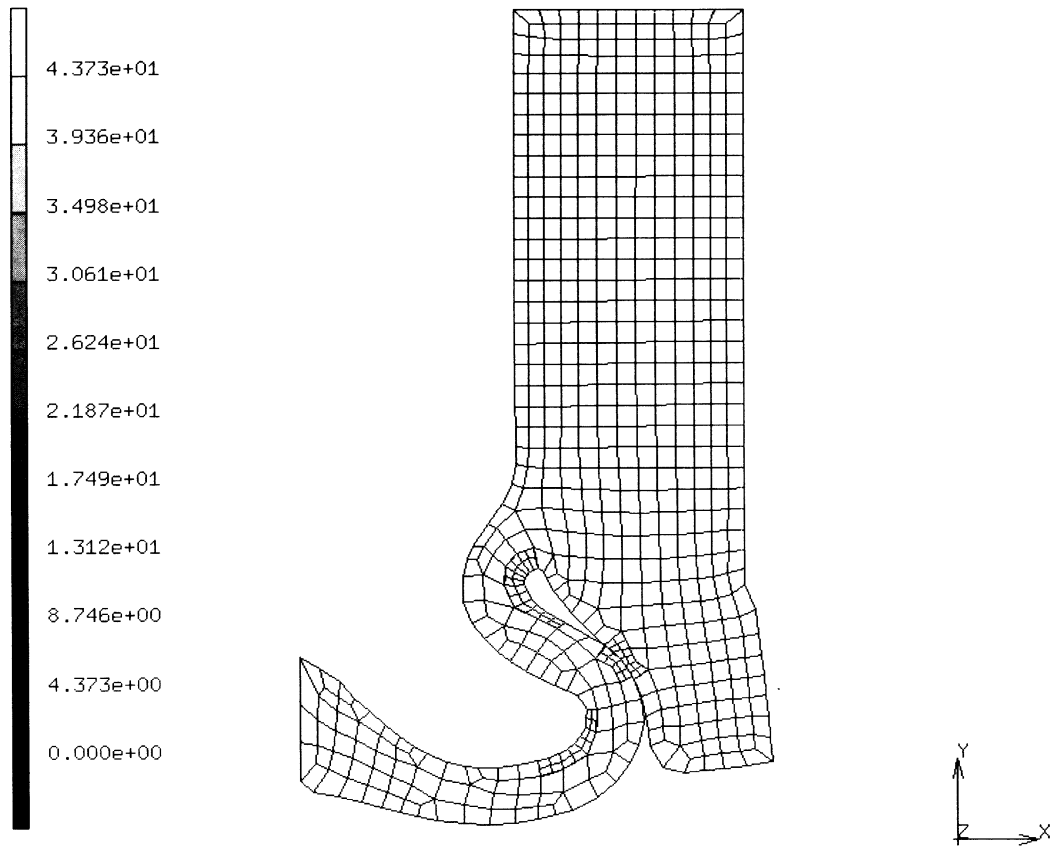


problem e8x43

Figure 8.43-5 Adaptivity Due to Contact



Inc : 19
Time : 1.900e+01



Rubber seal using Adaptive meshing
Final Deformed Geometry

Figure 8.43-6 Adaptivity Due to Contact (Updated Lagrange Formulation)

8.44 Simplified Rolling Example with Adaptive Meshing

This problem demonstrates the use of adaptive meshing by simulating the rolling of sheet. The adaptive meshing capability in MARC allows you to selectively refine the mesh using various criteria. This example uses three different data sets (problems e8x44, e8x44b, and e8x44c). Each data set uses a different criterion for adaptive meshing. However, the maximum number of levels an element is adapted(subdivided) is set to 2 for all three data sets.

Data Set	Adaptive Meshing Criterion Used
e8x44	Subdivide an element if at least one of the nodes falls within the imaginary box: $-3 < x < 3$; $-100 < y < 100$; $-100 < z < 100$
e8x44b	Subdivide an element if at least one of its nodes is in contact, or if it belongs to a segment that is contacted
e8x44c	Same as e8x44. In addition, if all nodes of an element leave the imaginary box, the already subdivided elements are merged together (unrefinement).

The initial model is the same for all three data sets.

Element

All three data sets use element 11, a 4-noded isoparametric plane strain element, to model the workpiece.

Model

The initial model for all three data sets is shown in Figure 8.44-1. The workpiece is 28 cm long and 1.025 cm thick. The roll radius is 64 cm and rotates at 1 radian/second. All three data sets employ 20 elements and 42 nodes to model the undeformed workpiece geometry. The number of nodes and elements change as the simulation proceeds due to the adaptive meshing processes of subdivision and merging.

Material Properties

The workpiece sheet is assumed to be made of high strength steel. The Young's modulus is 2.1×10^5 N/cm² and the Poisson's ratio is 0.30. The initial yield stress is 200 N/cm². The workhardening behavior is input using the WORK HARD DATA model definition option.

Geometry

The sheet is assumed to have a thickness of 1 unit. To model the incompressibility of the workpiece material, the constant dilatation option is chosen in the GEOMETRY model definition option.

**Boundary Conditions**

The model is assumed to be symmetric about the plane $y = 0$. Thus, all y displacements are set to zero on the surface $y = 0$.

Contact

There are three contact bodies in this model, the deformable workpiece (Body 1), the roller (Body 2), and the ram (Body 3) which pushes the workpiece into the roll gap. To enable efficient contact computations, the CONTACT TABLE option is used. This option details that Body 1 is allowed to contact only Body 2 and Body 3. This is because this problem will not realistically result in self contact of the deformable workpiece with itself.

Body 2 has its center of rotation at $[-5.9, 64.775]$. It is modeled a circular arc with 60 divisions. A friction coefficient of 0.10 is chosen for this body. Friction forces are based on the nodal contact forces.

Body 3 is modeled as a single straight line segment.

History Definition

The motion of the workpiece through the roll gap is modeled by defining a velocity for the contact bodies using the MOTION CHANGE history definition option. The roll is subjected to a constant angular velocity while the ram pushes the workpiece into the roll gap.

In the first 15 increments, the roll is subjected to an angular velocity of 1 radian/second (approximately 57.3 degrees/second). To avoid any slipping between the workpiece and the roll at entry, the ram is given a linear velocity identical to the linear velocity at the tip of the roll ($v = r \omega$) of -64 cm/second.

At the end of 15 increments, the ram is removed from the system using the RELEASE option for Body 3. For all subsequent increments, the ram is given a positive velocity of 20 cm/second in the x direction and moves continuously opposite the direction of motion of the workpiece motion.

The CONTACT TABLE option is also redefined to exclude Body 3 from any further contact checking calculations. For the remainder of the simulation, the roll continues to rotate and the friction between the roll and workpiece draws the workpiece further into the roll gap.

For data sets e8x44 and e8x44c, 140 further increments are taken. For data set e8x44b, 80 further increments are employed.

Control

This analysis uses displacement control with a tolerance of 10%. A maximum of 25 iterations are chosen for each increment to converge.

**Adaptive Meshing**

The adaptive meshing procedure is used to create more elements in areas of high deformation. The three data sets employ different criteria. The imaginary box used for data sets e8x44 and e8x44c is indicated in Figure 8.44-2. This box encloses the roll gap region, which can be expected to be the area where the workpiece undergoes maximum deformation.

Results

For the data set e8x44, the deformed mesh at increments 48, 75 and 100 are shown in Figure 8.44-3 through Figure 8.44-5. Comparing Figure 8.44-1 and Figure 8.44-3, it can be seen that the adaptive process has created more elements by subdividing elements that entered the imaginary box specified. However, the subdivided elements have not been merged together after exiting the roll gap. This merging option is shown by the results of e8x44c.

Figure 8.44-6 through Figure 8.44-8 shows the results for data set e8x44b. The adaptive process is shown to create elements upon contact. Figure 8.44-6 shows the deformed and adapted mesh at increment 3. New elements have been created at both the ram and roll contact elements. Figure 8.44-7 shows the deformed mesh at increment 50. The elements subdivided at contact bodies are shown to be not merged together after exiting the contact bodies. Figure 8.44-8 shows the adapted mesh at increment 80 for data set e8x44b.

Figure 8.44-9 through Figure 8.44-12 shows the adaptive process with the option for elements to be merged (data set e8x44c). Figure 8.44-9 shows the adaptive process doing both the subdivision of elements inside the imaginary box and the merging of elements that have exited the imaginary box at increment 48. Figure 8.44-10 shows the deformed mesh at increment 75. Figure 8.44-11 shows the deformed mesh at increment 100. Finally, Figure 8.44-12 shows the final mesh at increment 155. Figure 8.44-9 may be contrasted against Figure 8.44-3. Figure 8.44-10 may be contrasted against Figure 8.44-4. Figure 8.44-11 may be contrasted against Figure 8.44-5.



Parameters, Options, and Subroutines Summary

Example e8x44.dat, e8x44b.dat, and e8x44c.dat:

Parameters

ADAPTIVE
ELEMENTS
END
FINITE
LARGE DISP
PRINT
SIZING
TITLE
UPDATA

Model Definition Options

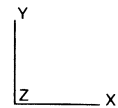
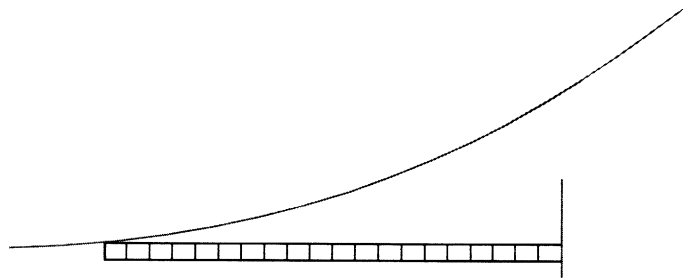
ADAPTIVE
CONNECTIVITY
CONTACT
CONTACT TABLE
CONTROL
COORDINATE
END OPTION
FIXED DISP
GEOMETRY
ISOTROPIC
NO PRINT
POST
RESTART
WORK HARD

History Definition Options

AUTO LOAD
CONTACT TABLE
CONTINUE
CONTROL
MOTION CHANGE
RELEASE
TIME STEP



INC : 0
SUB : 0
TIME : 0.000e+00
FREQ : 0.000e+00



problem e8x44

Figure 8.44-1 Original Finite Element Mesh for all 3 Data Sets

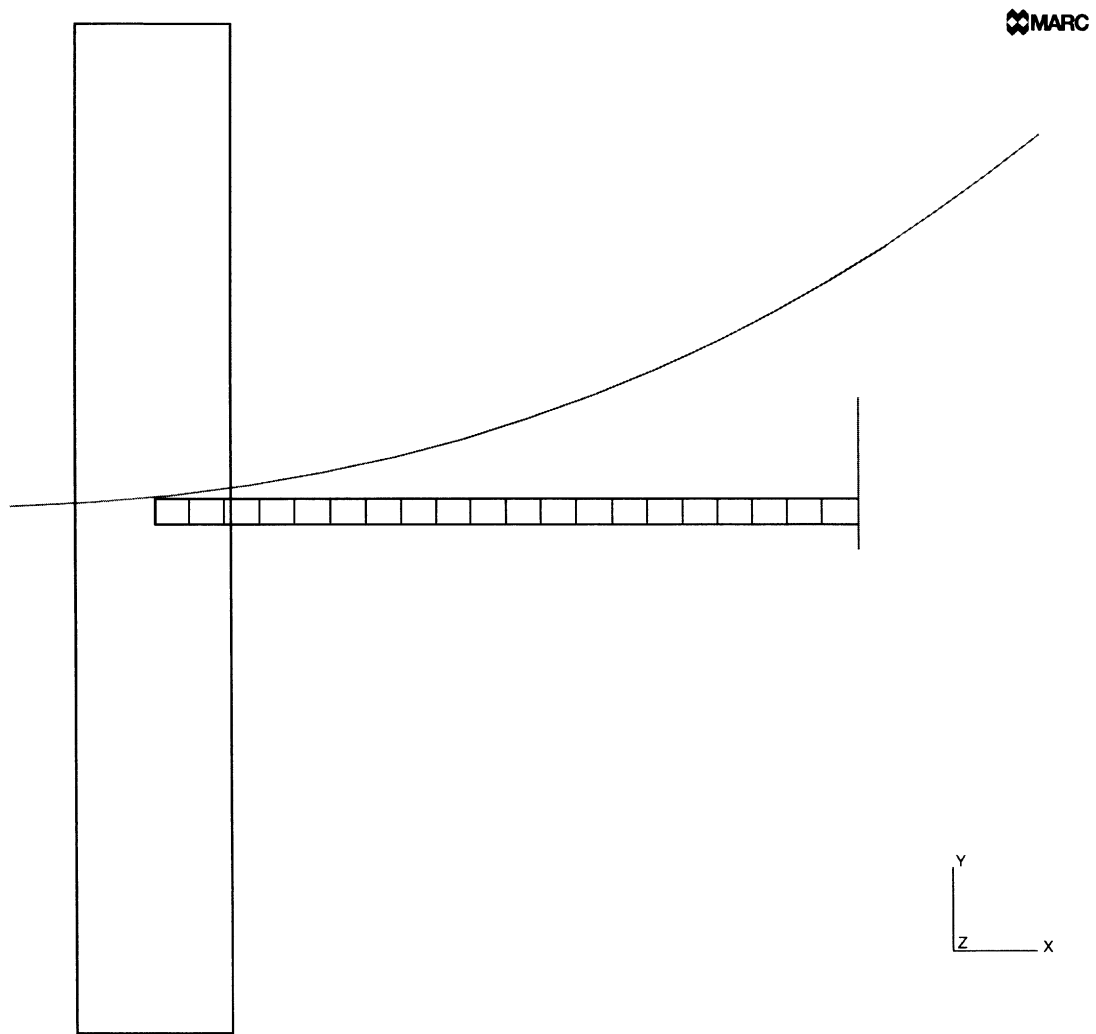
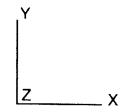
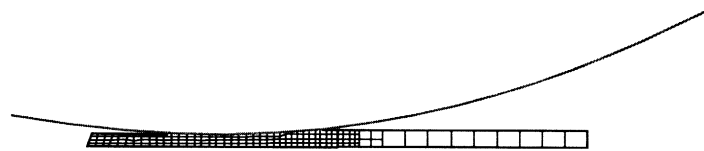


Figure 8.44-2 Adaptive Criteria Box for Data Set e8x44 and e8x44c



INC : 48
SUB : 0
TIME : 1.900e-01
FREQ : 0.000e+00

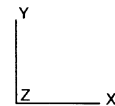


problem e8x44

Figure 8.44-3 Deformed Mesh at Increment 48 for Data Set e8x44



INC : 75
SUB : 0
TIME : 2.980e-01
FREQ: 0.000e+00

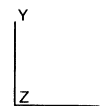


problem e8x44

Figure 8.44-4 Deformed Mesh at Increment 75 for Data Set e8x44



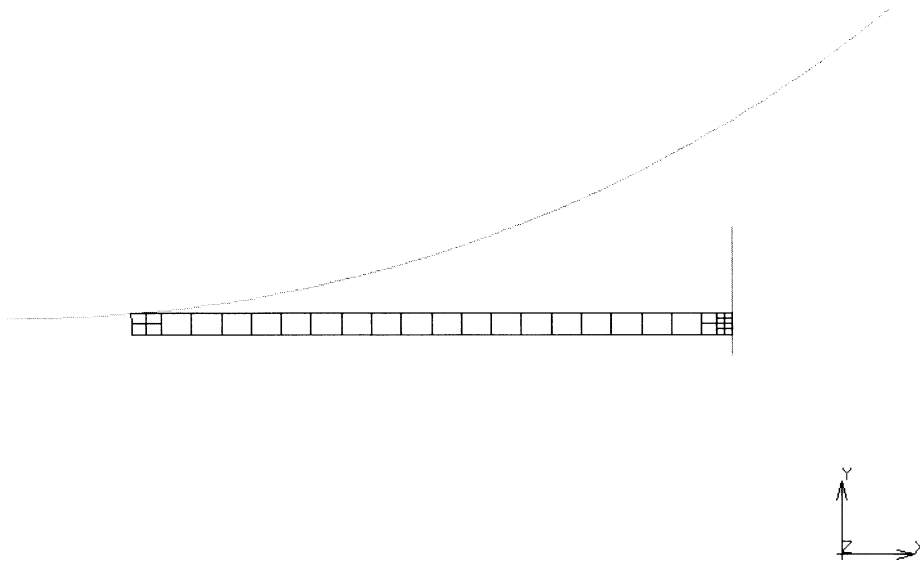
INC : 100
SUB : 0
TIME : 3.980e-01
FREQ : 0.000e+00



problem e8x44

Figure 8.44-5 Deformed Mesh at Increment 100 for Data Set e8x44

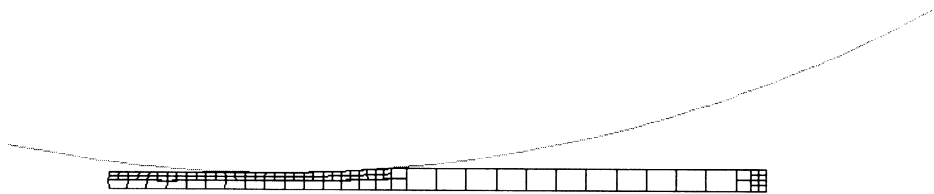
Inc : 3
Time : 1.200e-02



problem e8x44b

Figure 8.44-6 Deformed Mesh at Increment 3 for Data Set e8x44b

Inc : 50
Time : 2.000e-01



problem e8x44b

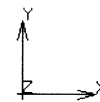
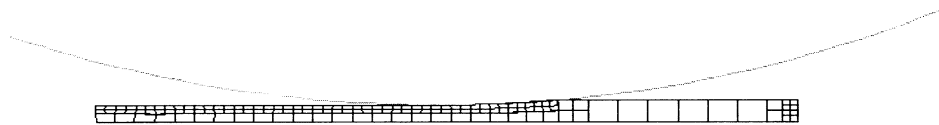


Figure 8.44-7 Deformed Mesh at Increment 50 for Data Set e8x44b



Inc : 80
Time : 3.200e-01

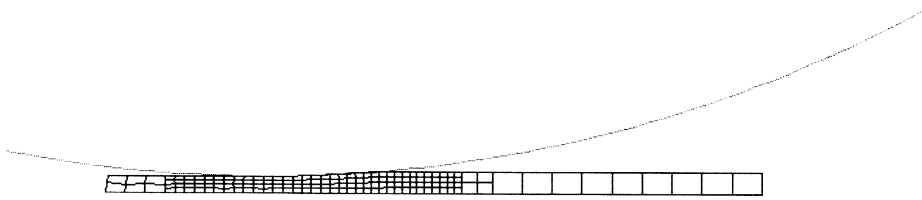


problem e8x44b

Figure 8.44-8 Deformed Mesh at Increment 80 for Data Set e8x44b



Inc : 48
Time : 1.900e-01



problem e8x44

Figure 8.44-9 Deformed Mesh at Increment 48 for Data Set e8x44c



Inc : 75
Time : 2.980e-01

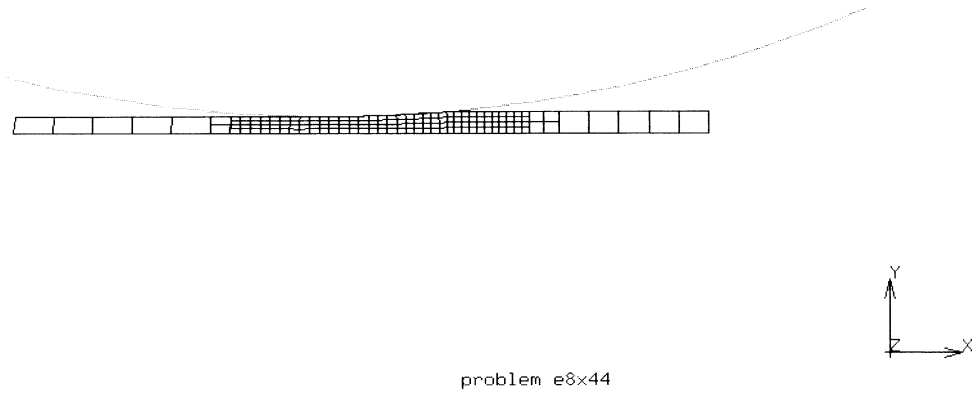
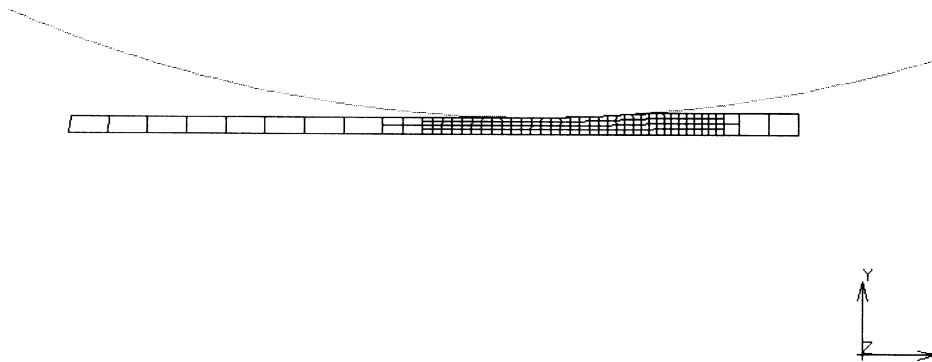


Figure 8.44-10 Deformed Mesh at Increment 75 for Data Set e8x44c



Inc : 100
Time : 3.980e-01

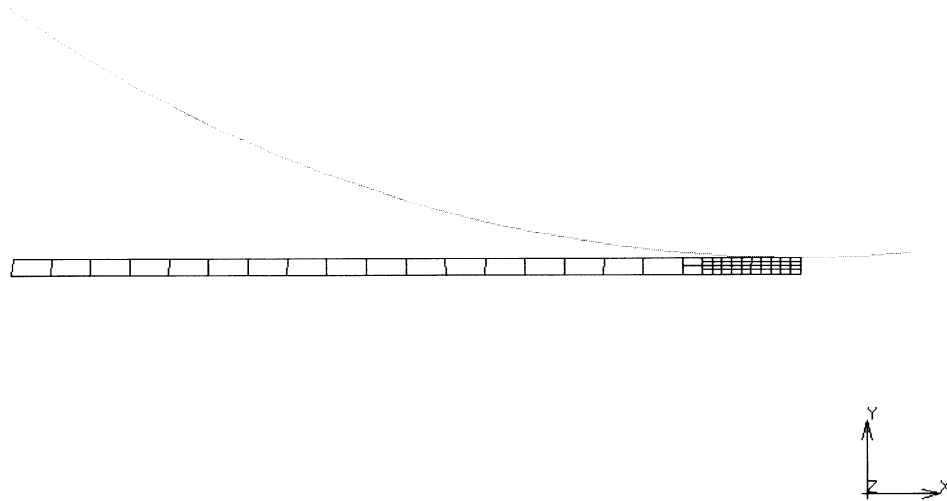


problem e8x44

Figure 8.44-11 Deformed Mesh at Increment 100 for Data Set e8x44c



Inc : 155
Time : 6.180e-01



problem e8x44

Figure 8.44-12 Deformed Mesh at Increment 155 for Data Set e8x44c



8.45 Use of the SPLINE Option for Deformable-Deformable Contact

This problem demonstrates the use of the SPLINE option in the simulation of problems involving deformable-to-deformable contact of bodies. In many cases, the accuracy of results in problems involving deformable-to-deformable contact depends on smoothness of the contact bodies can be defined, e.g. circular shafts. The SPLINE option can be used for 2D and 3D problems. This example illustrates a 2D plane strain case.

The geometry of the problem is shown in Figure 8.45-1. The model consists of two annular rings, each at a different temperature. The outer ring is hotter than the inner ring and gradually cools down to reach the temperature of the inner ring in five increments. The outer and inner rings are modeled as deformable bodies. The SPLINE option is applied to these two deformable bodies.

Element

Due to symmetry only a quarter of the rings are modeled using the isoparametric 4-noded element number 11. Elements 1 to 80 comprise the inner ring while elements 81 to 160 make up the outer ring. There are a total of 160 elements and 210 nodes in this model. The model is shown in Figure 8.45-2.

Material Properties

The deformable bodies have the same material properties. The Young's modulus is 2.1×10^6 GPa, and the Poisson's ratio is 0.33. The initial density is 1 Kg/m^3 . The coefficient of thermal expansion is $10^{-4}/^\circ \text{C}$.

Boundary Conditions

Symmetry is enforced by the definition of rigid symmetry bodies along the $x = 0$ and $y = 0$ plane.

Initial State

The initial temperatures of the two bodies are defined using the INITIAL STATE option. The outer ring has an initial temperature of 200°C , while the inner ring has an initial temperature of 20°C .

Contact

There are four contact bodies defined in this problem. Contact body 1 is the outer ring. Contact body 2 is the inner ring. Both these contact bodies are deformable and the SPLINE option is used to represent their outer surfaces. Contact body 3 is the rigid symmetry surface defining $x = 0$.



Contact body 4 is the rigid symmetry surface defining $y = 0$. An analytical form of these rigid surfaces are used by the appropriate choice of the CONTACT option. There is no friction assumed in the model.

Spline

The SPLINE option is used for the deformable contact bodies 1 and 2. The SPLINE option enables an exact definition of the normal. But for some nodes, a unique normal does not exist. The outer ring (Contact body 1) has four nodes: 106, 126, 210, and 190 at which the normal is not defined. Similarly, the inner ring (Contact body 2) has four nodes: 1, 21, 105, and 85 at which the normal to the curve is not defined. Such nodes must be excluded from the definition of the SPLINE option. This is done using the appropriate choice in the SPLINE option.

Post

The post file has output written for the equivalent or von Mises stress.

History Definition

The initial temperature of the outer ring is 200° C. The initial temperature of the inner ring is 20° C. The outer ring is cooled to equal the temperature of the inner ring in five increments. Thus, each increment cools the outer ring by 36° C. The inner ring is maintained at a constant temperature during the simulation. As the outer ring cools, it contracts and presses inward radially on the inner ring. This is the mode of deformation for the problem. The CHANGE STATE option prescribes the temperature change for the outer ring.

Control

The residual tolerance is set to 0.01. Ten iterations are made for each increment.

Results

The use of the SPLINE option results in a good solution for the problem. Figure 8.45-3 shows contours of the equivalent von Mises stress. These contours are seen to be axisymmetric. Even if the nodes on the outside surface of the inner ring do not lie coincident with the nodes of the inside surfaces of the outer ring, the SPLINE option will ensure correct results at the contact surface. Not employing the SPLINE option in such cases, may result in inexact results in contact regions.



Parameters, Options, and Subroutines Summary

Example e8x45.dat:

Parameters

ALL POINTS
ELEMENTS
END
EXTENDED
LARGE DISP
SETNAME
SIZING
TITLE

Model Definition Options

CHANGE STATE
CONNECTIVITY
CONTACT
CONTROL
COORDINATES
INITIAL STATE
OPTIMIZE
POST
SOLVER
SPLINE

History Definition Options

AUTO LOAD
CHANGE STATE
CONTINUE
MOTION CHANGE
TIME STEP

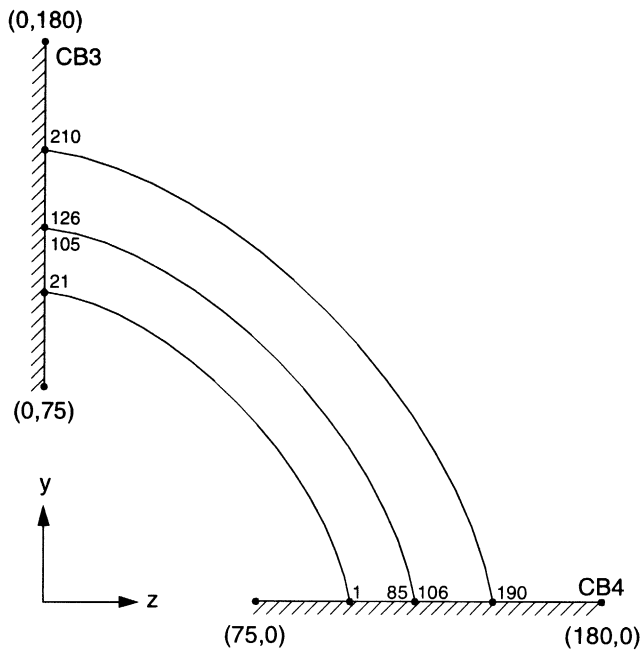


Figure 8.45-1 Geometry for Problem 8.45 to show the SPLINE Option

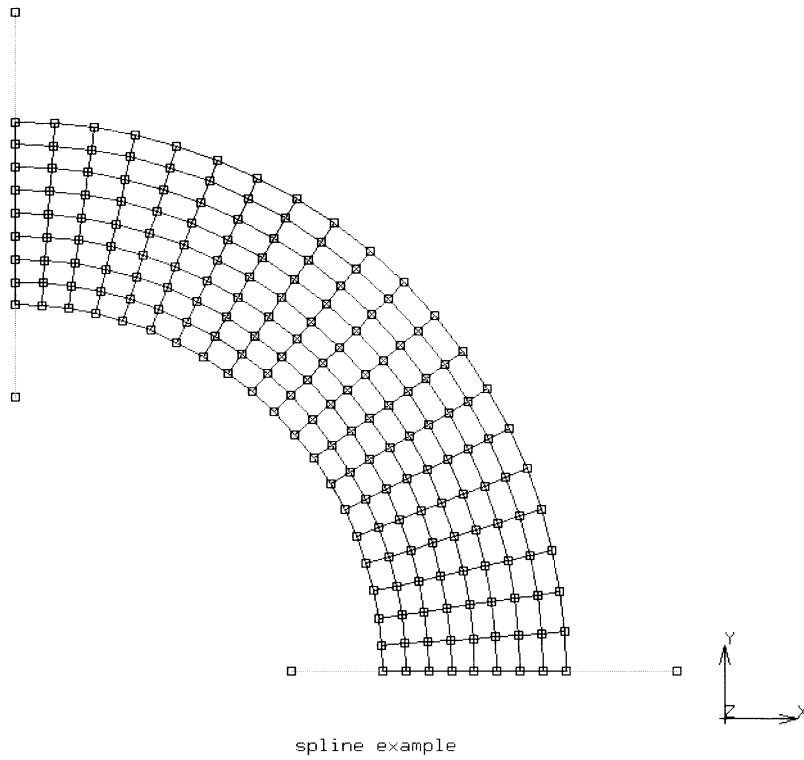


Figure 8.45-2 Initial Model for this Example



Inc : 5
Time : 1.000e+02

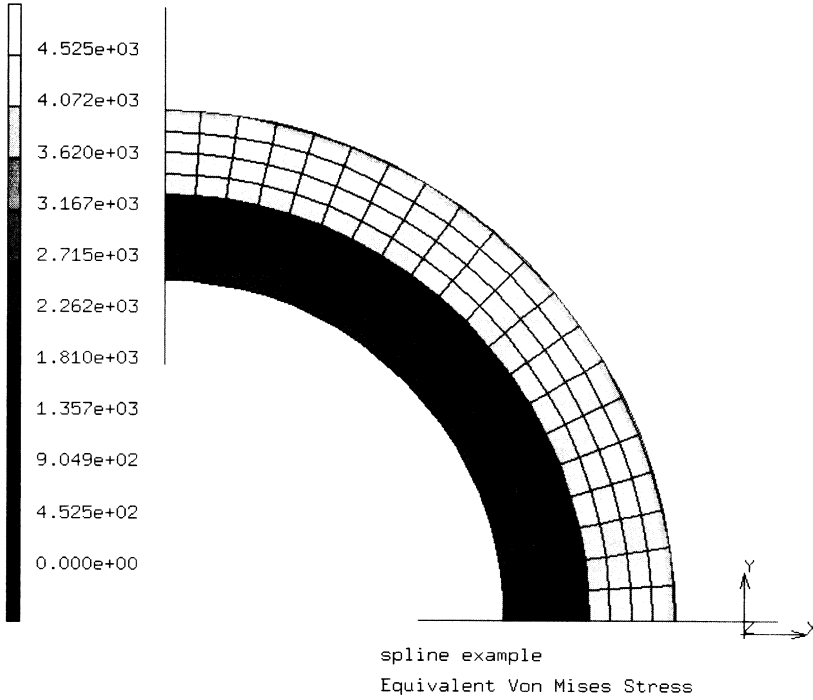


Figure 8.45-3 Contours of Effective von Mises Stress





8.46 Use of the EXCLUDE Option for Contact Analysis

This example shows the use of the EXCLUDE option for contact analysis. The EXCLUDE option is used in contact problems when you can, a priori, specify nodes which define certain segments that can be excluded from the contact calculations. This feature is especially helpful when there are sharp corners in a contact body or you want to restrict the motion of the body.

This example consists of three contact bodies. The initial model is shown in Figure 8.46-1. There are 12 elements and 27 nodes in the model. The elements associated with each contact body are given below.

Contact Body Number	Elements
1	1, 2, 3, 4
2	5, 6, 7, 8
3	9, 10, 11, 12

It can be seen that there are three segments here that can be excluded by you from the contact analysis. Each segment is defined by two nodes. Node 27 of Contact body 1 may slide along the segment defined by nodes 6 and 18 or along the segment defined by 6 and 19. However, it is physically unreasonable to expect that the node 27 may actually slide along the segment defined by nodes 6 and 19. Hence, you can EXCLUDE the segment defined by nodes 6 and 19 of Contact body 2. Similarly, once Contact body 1 slides down further, it would be better to exclude the segment defined by nodes 3 and 15 of Contact body 2, and the segment defined by nodes 25 and 26 of Contact body 3. Of course, if contact bodies 2 and 3 would be a single contact body, excluding the segments (3 & 5 or 25 & 26) would not be necessary.

Element

The 4-noded isoparametric plane stress quadrilateral element number 3 is used. There are 12 elements and 27 nodes in this model as shown by Figure 8.46-1.

Material Properties

All three contact bodies have identical isotropic material properties. The Young's modulus is $1 \times 10^5 \text{ N/m}^2$. The Poisson's ratio is 0.30.



Boundary Conditions

To restrain the rigid body modes, nodes 1, 21, 24, 2, 16, and 5 are prescribed to have zero x and y displacements.

Contact

There is no friction used in this example. The CONTACT TABLE model definition option is used to expedite the CONTACT calculations.

Control

Ten iterations are chosen as a maximum for each increment. The residual tolerance is set to 0.10.

Loading

The loading consists of a distributed load on elements 3 and 4 pointing in the negative y direction. Displacements of 5.5×10^{-2} units are applied in each increment along the negative x direction on nodes 8 and 13 using the DISP CHANGE history definition option. A total of ten increments are applied using the AUTO LOAD history definition option.

Results

The final deformed shape configuration at the end of 10 increments is shown in Figure 8.46-2.

Parameters, Options, and Subroutines Summary

Example e8x46.dat:

Parameters	Model Definition Options	History Definition Options
ALL POINTS	CONNECTIVITY	AUTO LOAD
DIST LOADS	CONTACT	DISP CHANGE
ELEMENTS	CONTACT TABLE	DIST LOADS
EXTENDED	COORDINATES	TIME STEP
LARGE DISP	EXCLUDE	
PRINT	FIXED DISP	
SIZING	ISOTROPIC	
TITLE	OPTIMIZE	

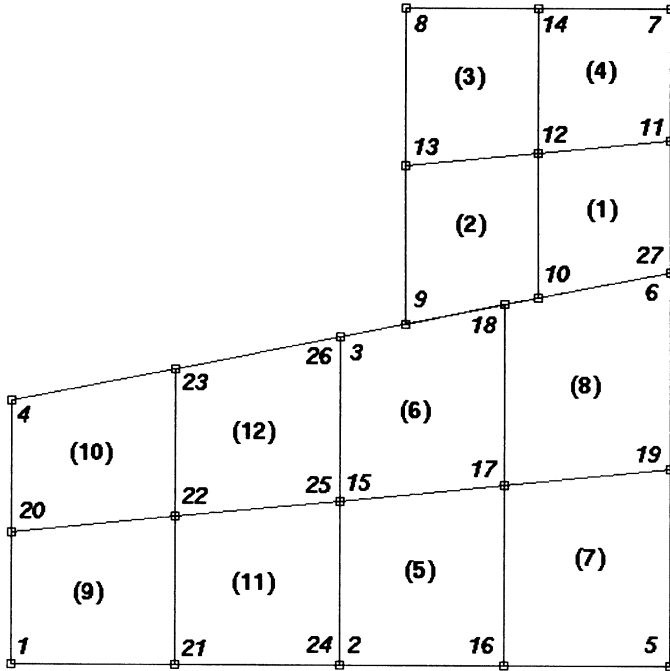
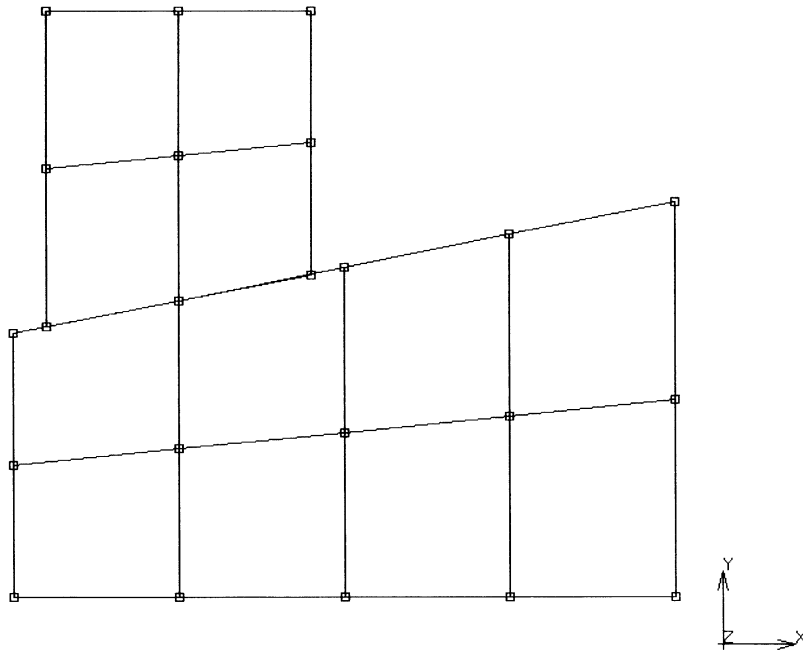


Figure 8.46-1 Initial Model



Inc : 10
Time : 1.000e+00



exclude example

Figure 8.46-2 Final Deformed Shape after 10 Increments



8.47 Simulation of Contact with Stick-Slip Friction

This example illustrates the use of the stick-slip friction model. The model consists of a deformable body on a rigid surface. The deformable body is subjected to a normal distributed load that holds it down onto the rigid surface. A distributed shear load is applied in order to cause slip on the rigid surface. A spring restrains the deformable body and stores energy when slip occurs.

Model

The initial model is shown in Figure 8.47-1. There are 20 elements and 31 nodes in the model. The four noded plane stress isoparametric element number 3 is used to model the deformable workpiece. A spring connects node 1 on the deformable body with the detached node 31. The spring is linear with a unit stiffness.

Material Properties

The workpiece is assumed to be isotropic. The Young's modulus is $2.1 \times 10^9 \text{ N/m}^2$, and the Poisson's ratio is 0.30. The spring is assumed to have a spring stiffness of 1.0 N/m.

Boundary Conditions

The detached node number 31 is restrained to have zero x and y displacements. Distributed loads are applied to the elements on the top surface of the deformable body (elements numbered 1, 5, 9, 13, 17) as shown in Figure 8.47-2. Both normal (P) and shear (τ) distributed loads are applied on these elements.

Contact

The stick-slip model is chosen in this problem. The slip to stick transition is assumed to be at a relative velocity of $1 \times 10^{-6} \text{ m/s}$. A contact bias factor of 0.99 is used. The default values of 1.05 for the friction multiplier and 0.05 for the relative friction force tolerance are assumed. There are two contact bodies in the problem. A friction coefficient of 0.05 is assigned to the rigid contact body.

Control

The maximum allowed relative error in residual forces is chosen to be 0.10. A maximum of ten recycles are allowed for each increment.

**History Definition**

The distributed loads are given in Figure 8.47-3. The shear distributed load is gradually increased in the negative sense and then reversed in sense to become positive. The normal distributed load increases to 1.0 units in increment 1. It is held at that value until increment 50. It is reduced to 0.80 units in increment 51. The loading proceeds for a total of sixty increments.

Results

The shear load is not high enough to cause slipping until increment 20. However, it is increased to -0.30 units in the 21st increment. This causes the deformable body to slip along the positive x direction for the first time in increment 21. The deformed and initial positions of the deformable body are shown in Figure 8.47-4. There is no load incrementation until increment 31 when the distributed shear load is reset to zero. The restoring force in the spring is however insufficient to cause the deformable body to slip again. Hence, it continues to stick until increment 40. In increment 41, the shear load is ramped up to +1.1 units. This now causes the body to slip along the negative x direction as shown in Figure 8.47-5. In increment 51, the normal distributed load is decreased in magnitude to 0.80 units. This causes the deformable body to slip further, along the positive x direction as shown in Figure 8.47-6. The x displacement of node 1 is shown in Figure 8.47-7 for the entire loading history.

Parameters, Options, and Subroutines Summary

Example e8x47.dat:

Parameters	Model Definition Options	History Definition Options
ALL POINTS	CONNECTIVITY	AUTO LOAD
DIST LOADS	CONTACT	CONTINUE
ELEMENTS	CONTROL	DIST LOADS
END	COORDINATES	TIME STEP
SETNAME	DIST LOADS	
SIZING	FIXED DISP	
TITLE	ISOTROPIC	
	OPTIMIZE	
	POST	
	SOLVER	
	SPRINGS	

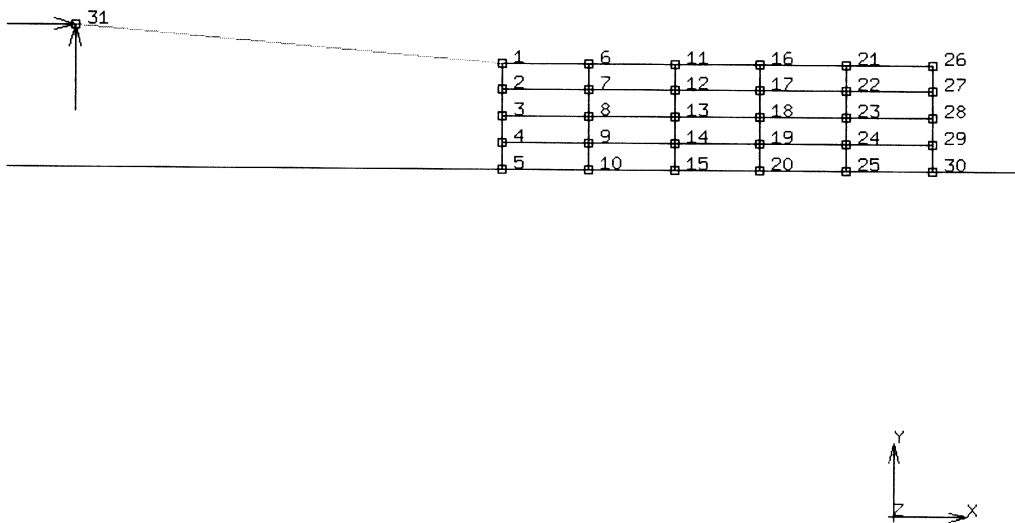


Figure 8.47-1 Initial Model for Stick-Slip Problem

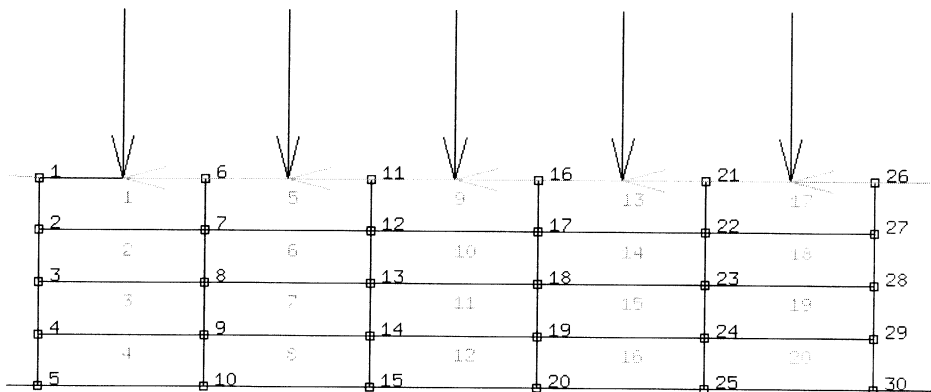


Figure 8.47-2 Distributed Load Boundary Conditions

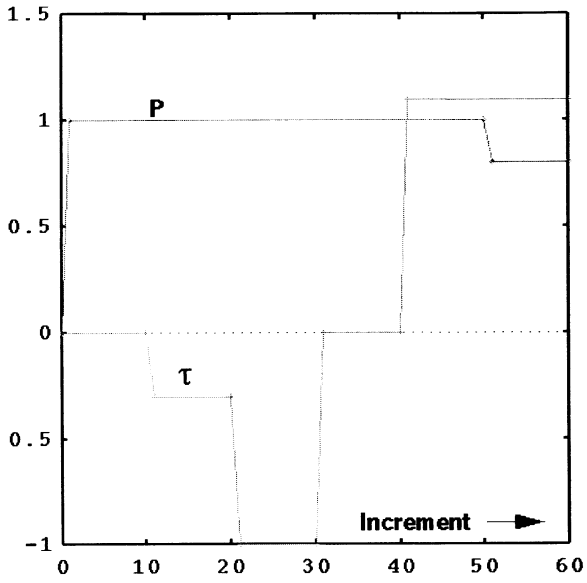
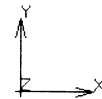
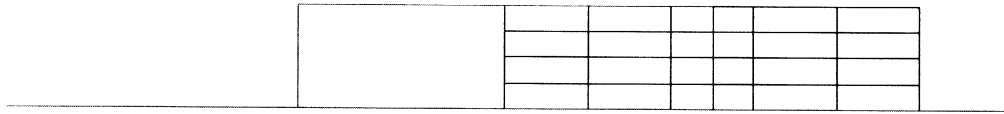


Figure 8.47-3 Loading History for the Distributed Loads



Inc : 21
Time : 2.100e-01

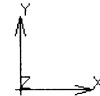
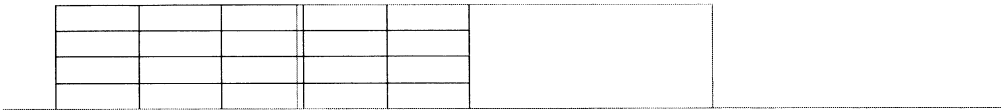


problem e8x47 - simple test of stick-slip model

Figure 8.47-4 First Slipping Motion (Increment 21)



Inc : 41
Time : 4.100e-01

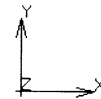
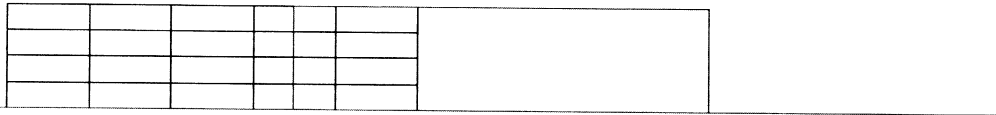


problem e8x47 - simple test of stick-slip model

Figure 8.47-5 First Slipping Motion (Increment 21)



Inc : 51
Time : 5.100e-01



problem e8x47 - simple test of stick-slip model

Figure 8.47-6 Final Slip occurring in Increment 51

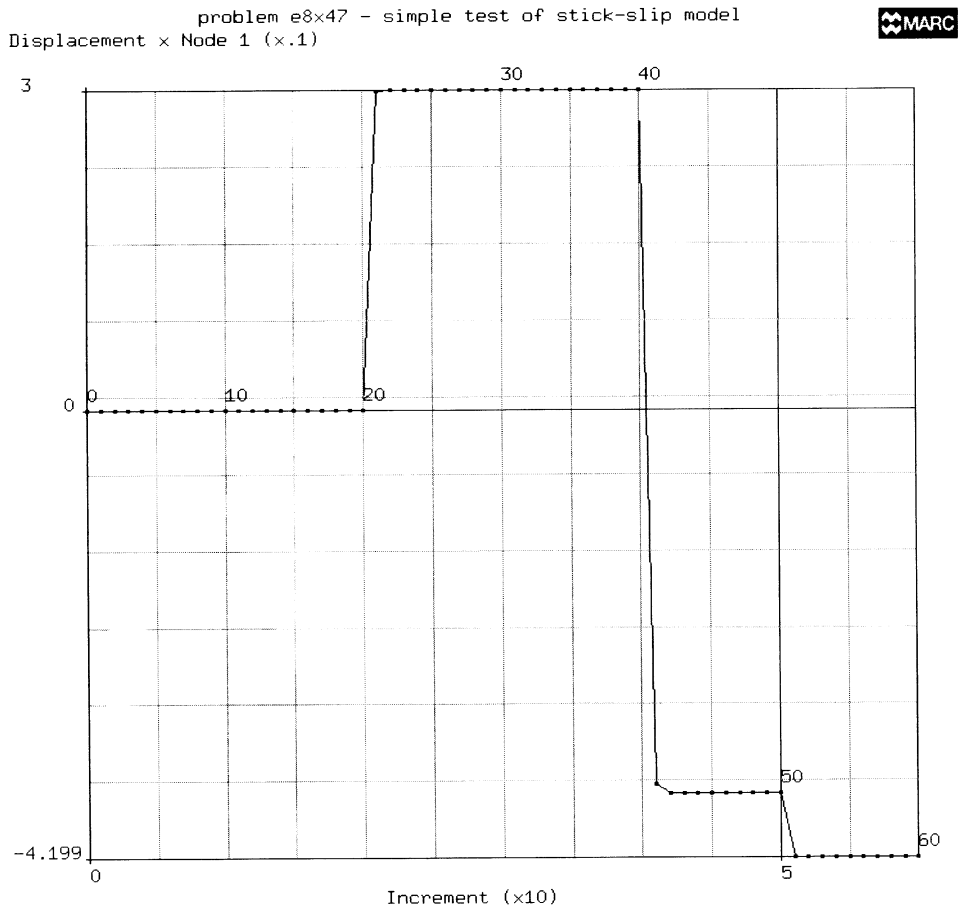


Figure 8.47-7 X Displacement History for Node 1



8.48 Simulation of Deformable-Deformable Contact with Stick-Slip Friction

This example illustrates the use of the stick-slip friction model in the simulation of the contact of two deformable bodies.

Model

The initial model is shown in Figure 8.48-1. There are 36 elements and 57 nodes in the model. The four noded plane stress isoparametric element number 3 is used to model the deformable workpiece. The body on top is contact body 1. The two nodes on the left most face of contact body 1 (nodes 51 and 46) are connected to detached nodes 57 and 56 by means of springs.

Material Properties

The two contact bodies are isotropic but have differing properties. The material properties are summarized below.

Contact Body	Comprised of Elements	E (N/m ²)	ν
1	33 to 36	3×10^9	0.30
2	1 to 32	2×10^{11}	0.30

Boundary Conditions

The detached nodes (nodes 56 and 57) are restrained to have zero x and y displacements. In addition, contact body 2 has its bottom surface fixed to have zero displacements. Thus, the x and y displacements are set to zero for nodes 1 to 9.

Contact

The stick-slip model is chosen in this problem. The slip to stick transition is assumed to be at a relative velocity of 1×10^{-5} units. A contact bias factor of 0.0 is used. The default values of 1.05 for the friction multiplier and 0.05 for the relative friction force tolerance are assumed. A friction co-efficient of 0.05 is used for contact body one and a friction co-efficient of 0.10 is used for the lower contact body.

Control

The maximum allowed relative change in displacement increments is chosen to be 0.05. A maximum of thirty recycles are allowed for each increment.

**History Definition**

There are a total of 20 increments in this problem. The loading consists of two distributed normal loads P_x and P_y , applied to contact body one as shown in Figure 8.47-1. The load P_y holds the upper contact body down on the lower contact body. P_y is ramped up to a value of $7.5 \times 10^6 \text{ N/m}^2$ in 10 increments and is then maintained constant until the 20th increment. P_x is maintained at a value of zero until the 10th increment. Then it is ramped to a value of $-15.0 \times 10^6 \text{ N/m}^2$ in the 20th increment. The distributed load history is shown in Figure 8.48-2.

Results

P_x remains at a value of zero until increment 10. Hence, there is no slip possible. From increment 11, P_x is ramped up. The first slip occurs in increment 13. The deformed shape is shown in Figure 8.48-3. As P_x is ramped up further, contact body 1 continues to slip until the last increment (increment 20). The final deformed shape is shown in Figure 8.48-4. Figure 8.48-5 shows the history plot of variation of x displacement at node 51 with increment number.

Parameters, Options, and Subroutines Summary

Example e8x48.dat:

Parameters	Model Definition Options	History Definition Options
ALL POINTS	CONNECTIVITY	AUTO LOAD
DIST LOADS	CONTACT	CONTINUE
ELEMENTS	CONTROL	DISP CHANGE
END	COORDINATES	DIST LOADS
LARGE DISP	FIXED DISP	TIME STEP
SIZING	GEOMETRY	
TITLE	ISOTROPIC	
	POST	
	SOLVER	
	SPRINGS	

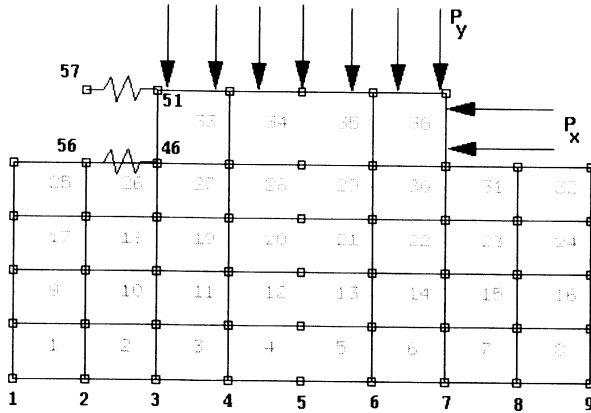


Figure 8.48-1 Initial Model for Stick-Slip Problem

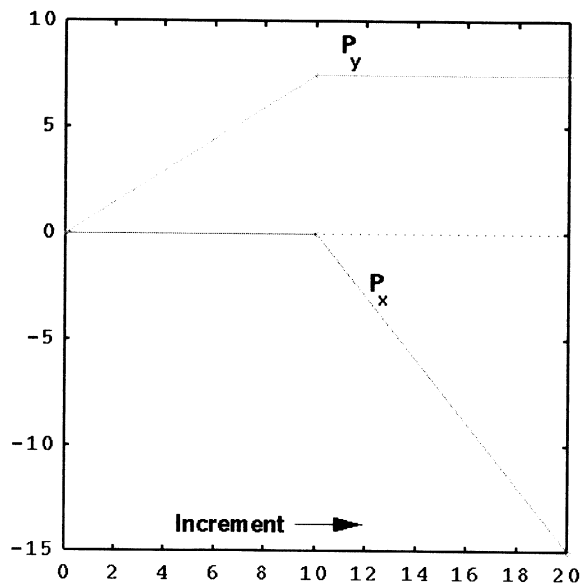
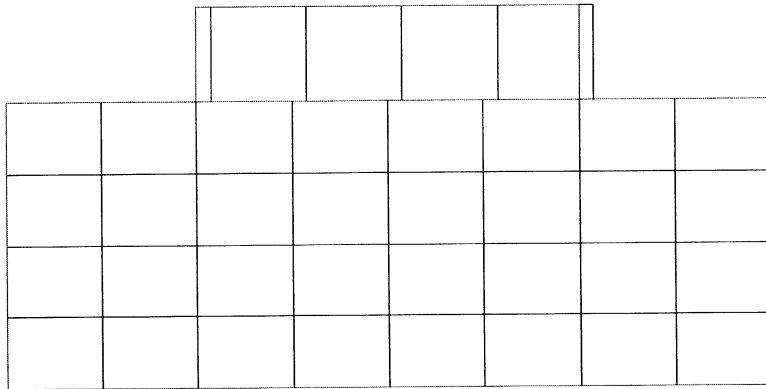


Figure 8.48-2 Loading History - Y Axis is Load Per Unit Area divided by 10^6



Inc : 13
Time : 1.300e+01

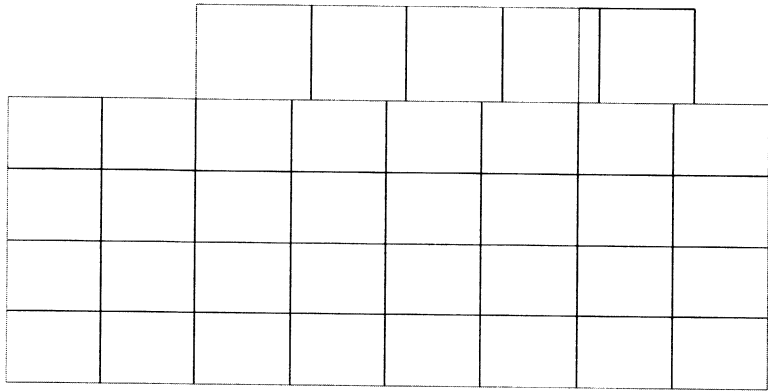


problem e8x48 - test stick-slip fricti

Figure 8.48-3 First Slip occurs in Increment 13



Inc : 20
Time : 2.000e+01



problem e8x48 - test stick-slip fricti

Figure 8.48-4 Final Deformed Shape in Increment 20

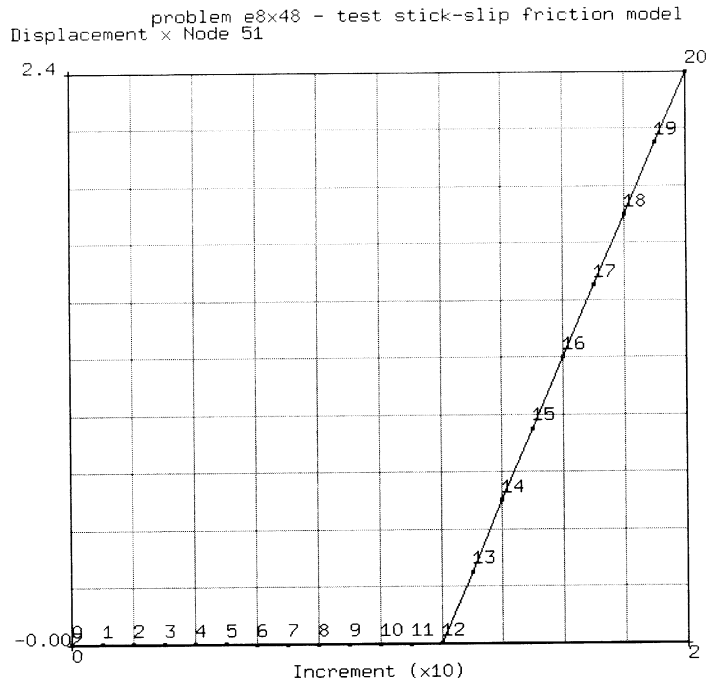


Figure 8.48-5 History Plot of x Displacement for Node 51



8.49 Rolling of a Compressed Rubber Bushing with Stick-Slip Friction

This example simulates the rolling of a rubber bushing with an off center compressed between two rigid surfaces. The rubber bushing material properties are assumed to approximate Mooney-Rivlin rubber material. The example shows large deformation behavior of rubber material along with contact simulated using the stick-slip algorithm.

Model

The initial model is shown in Figure 8.49-1. The bushing is modeled using element 80, which is a 4 noded isoparametric plane strain Herrmann element. The deformable bushing is modeled using 178 elements and 217 nodes. There are two rigid bodies in the model. The rigid body on top is contact body number 2. The bottom rigid body is contact body number 3. It is held fixed.

Material Properties

The deformable body is assumed to be made of Mooney-Rivlin material with constants given by $C_{10} = 8$ MPa and $C_{01} = 2$ MPa.

Boundary Conditions

Nodes 175 and 176 lie diametrically opposite on the equator of the off center hole in the bushing. Node 175 is constrained to have zero x displacement. Node 176 is constrained to have zero y displacement.

Contact

Contact is modeled with stick-slip friction. The default values of the stick-slip friction parameters are used. A value of 0.50 is used as a coefficient of friction for all contact bodies. The separation force is chosen to be 1 N.

Control

The maximum allowed relative error in residual forces is 0.01. A maximum of 10 recycles are chosen for each increment.



History Definition

The loading is imposed on contact body 2 using the MOTION CHANGE history definition option. Contact body 2 moves down and compresses the deformable bushing for 25 increments. Increments 26 and 27 involve a motion along the negative x direction in addition to compression of the cylinder. Subsequently, increments 28 to 51 involve the motion of contact body 2 along the negative x direction without any further displacement in the y direction.

Results

The deformed shape of the bushing in increment 25 is shown in Figure 8.49-2. It can be seen that more nodes have come into contact with the upper and lower contact bodies. The next two increments involve both x and y motion of the upper contact body. The friction between the contact bodies and the bushing enables the bushing to roll in response to the horizontal motion of contact body 2. The deformed shape of the bushing at the end of increment 27 is shown in Figure 8.49-3. Increments 28 through 51 involve further rotation of the bushing due to the translation of contact body 2 along the x direction. New nodes can be seen to come into contact with contact body two at the trailing edge of the bushing, while existing nodes at the periphery on the leading edge lose contact with contact body 2 as the rolling proceeds further. The deformed shapes of the bushing at the end of increments 40 and 51 are shown in Figure 8.49-4 and Figure 8.49-5 respectively.

Parameters, Options, and Subroutines Summary

Example e8x49.dat:

Parameters	Model Definition Options	History Definition Options
ALL POINTS	CONNECTIVITY	AUTO LOAD
DIST LOADS	CONTACT	CONTINUE
ELEMENTS	COORDINATES	MOTION CHANGE
END	FIXED DISP	TIME STEP
LARGE DISP	GEOMETRY	
SETNAME	MOONEY	
SIZING	OPTIMIZE	
TITLE	SOLVER	



Inc : 0
Time : 0.000e+00

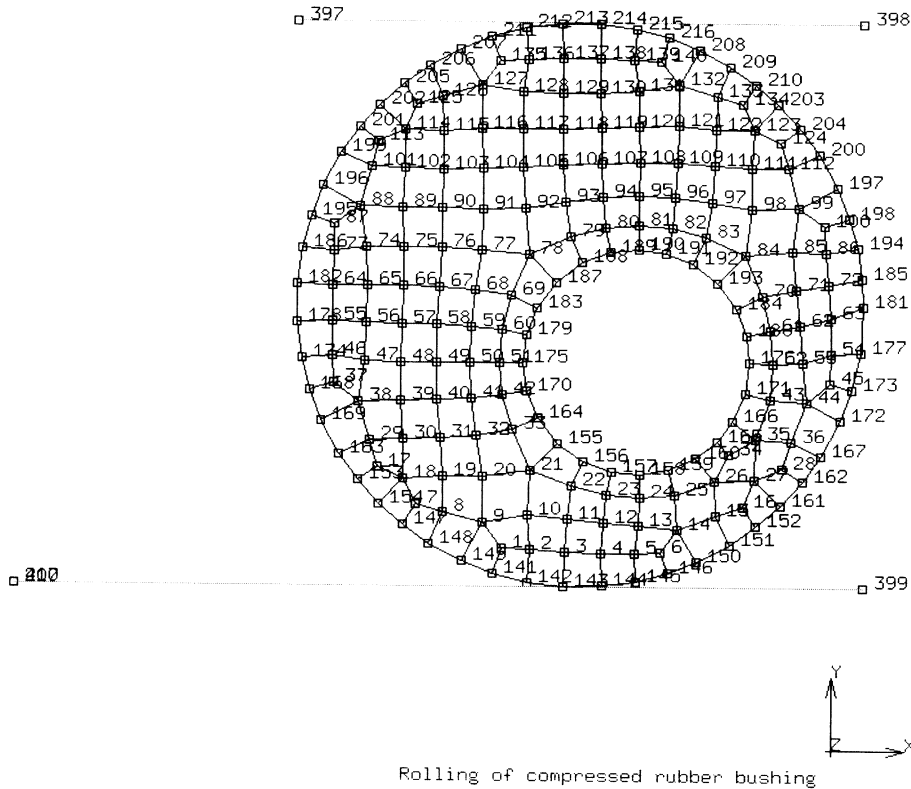
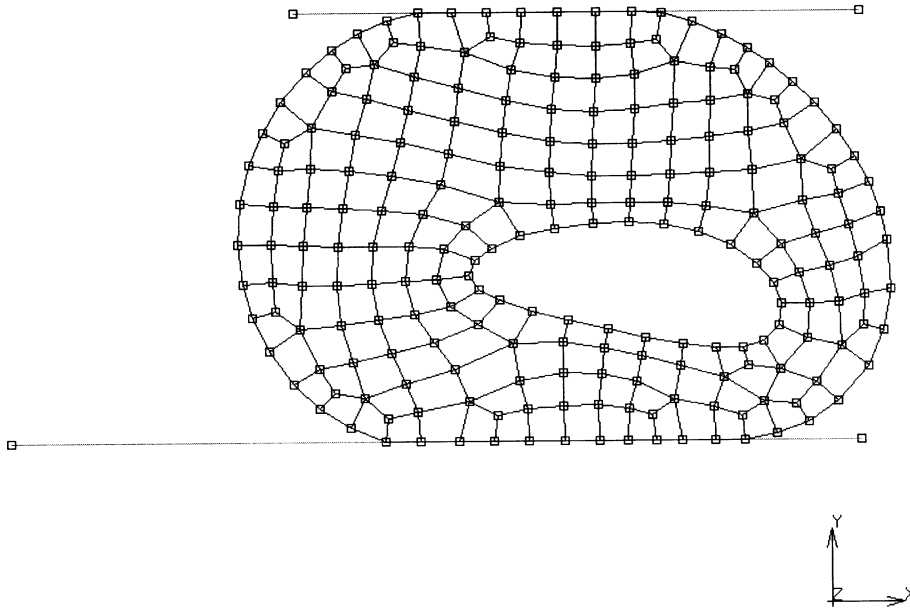


Figure 8.49-1 Initial Model



Inc : 25
Time : 9.652e-01



Rolling of compressed rubber bushing

Figure 8.49-2 Deformed Shape of Bushing at the End of Increment 25



Inc : 27
Time : 1.045e+00

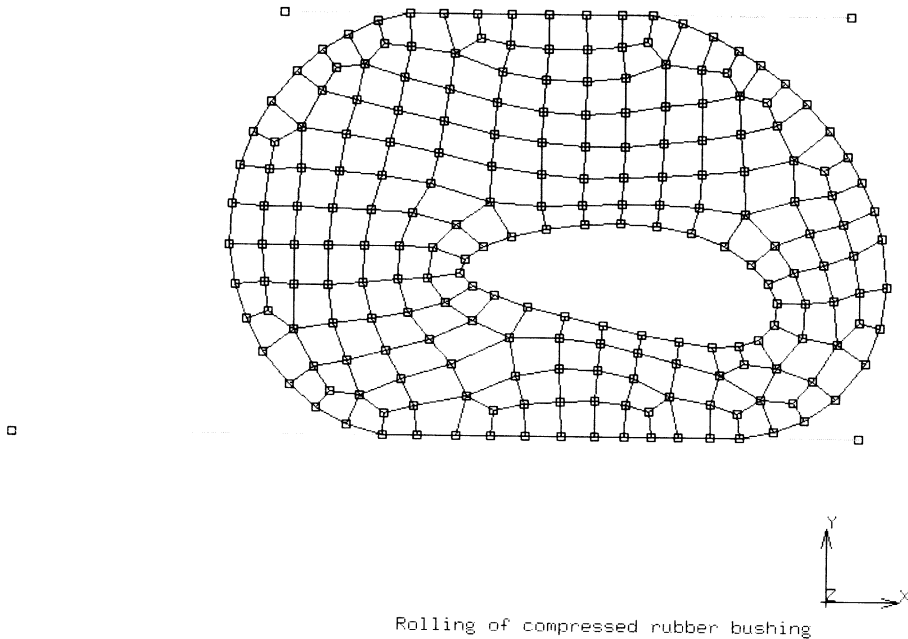
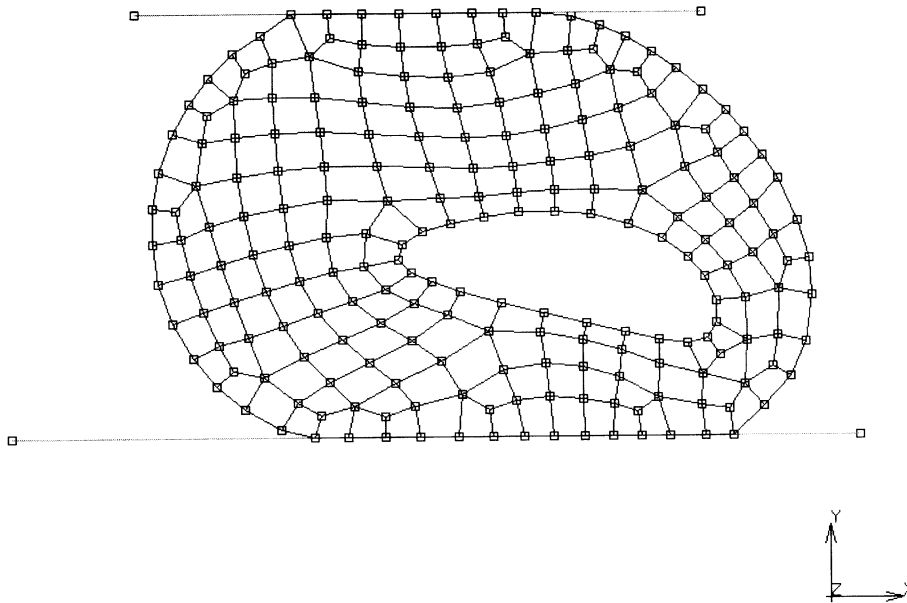


Figure 8.49-3 Deformed Shape of Bushing at the End of Increment 27



Inc : 40
Time : 1.562e+00



Rolling of compressed rubber bushing

Figure 8.49-4 Deformed Shape of Bushing at the End of Increment 40



Inc : 51
Time : 2.000e+00

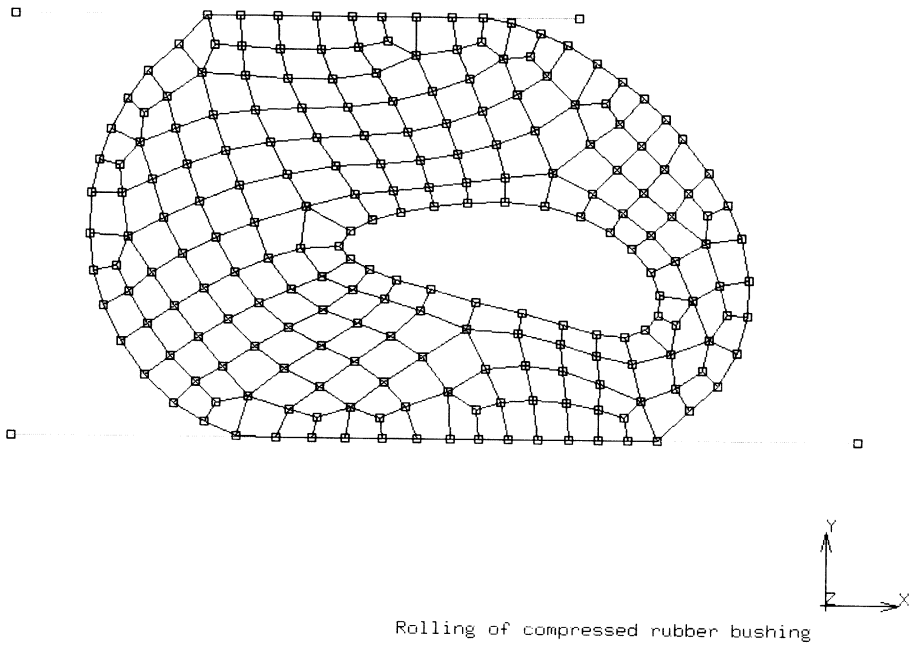


Figure 8.49-5 Deformed Shape of Bushing at the End of Increment 51



8 Advanced Topics

Rolling of a Compressed Rubber Bushing with Stick-Slip Friction



8.50 Compression Test of Cylinder with Stick-Slip Friction

This problem simulates the compression of an initially circular cylinder between rigid platens with stick-slip friction.

Model

The initial model is shown in Figure 8.50-1. The cylindrical billet is modeled using element number 10. Element 10 is an axisymmetric 4 noded isoparametric quadrilateral element. To model the billet, 160 elements and 187 nodes are used. The radial direction is along y while the axial direction is along x.

Material Properties

The billet is assumed to be made of an isotropic elastic plastic material. The Young's modulus is 5×10^3 Pa and the Poisson's ratio is assumed to be 0.30. The initial yield stress is taken to be 100 Pa. The workhardening data is input using the WORK HARD model definition block and is given below.

Plastic Strain	Flow Stress(Pa)
0.0	100.0
1.0	120.0
5.0	125.0

Contact

There are four contact bodies in the problem. The deformable billet is contact body 1. Contact body 2 is the fixed rigid platen and is the left most contact body in Figure 8.50-1. The moving rigid platen is contact body number 3 and is the right most contact body. Contact body 3 moves axially (along the negative x direction) at constant speed. Contact body 4 is the symmetry body represented by the line $y = 0$ in Figure 8.50-1. Stick-slip friction is used to model this problem, The slip to stick transition velocity is chosen as 10^{-6} m/s. A contact bias factor of 0.80 is used. A friction coefficient of 0.10 is assigned to contact bodies 2 and 3.

Control

The increments are controlled by a maximum allowed relative change in displacement increment of 0.01. A maximum of 10 cycles are allowed for each increment.



History Definition

The loading is accomplished by the motion of contact body 3 at a constant velocity. This is prescribed using the MOTION CHANGE option. A total of 50 increments are chosen.

Results

The deformed shape of the billet at the end of increment 25 is shown in Figure 8.50-2. The deformed shape of the billet at the end of increment 50 is shown in Figure 8.50-3. Figure 8.50-4 shows the load versus stroke profile for this example. The maximum load is seen to be 6.715×10^5 N.

Parameters, Options, and Subroutines Summary

Example e8x50.dat:

Parameters	Model Definition Options	History Definition Options
ELEMENTS	CONNECTIVITY	AUTO LOAD
END	COORDINATES	CONTINUE
FINITE	GEOMETRY	MOTION CHANGE
LARGE DISP	ISOTROPIC	TIME STEP
SIZING	OPTIMIZE	
TITLE	POST	
UPDATE	SOLVER	
	WORK HARD	



Inc : 0
Time : 0.000e+00

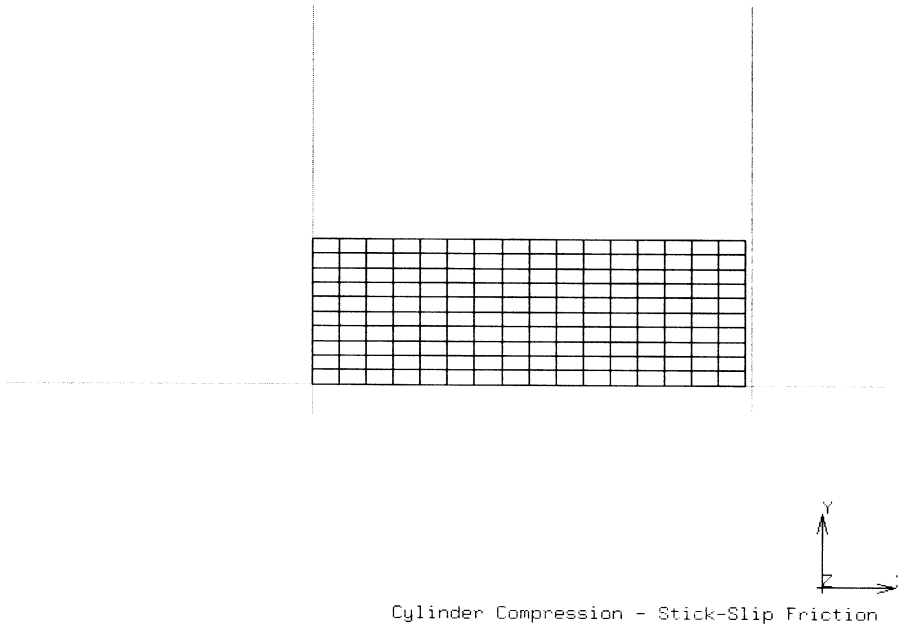
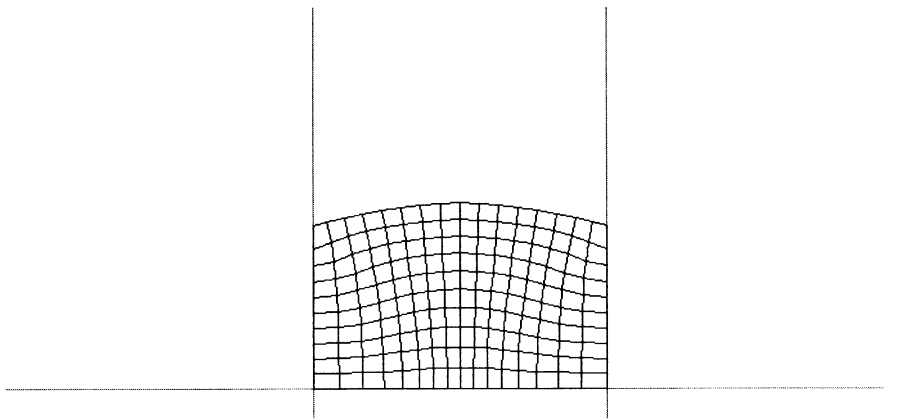


Figure 8.50-1 Initial Model

Inc : 25
Time : 4.800e-02



Cylinder Compression - Stick-Slip Friction

Figure 8.50-2 Deformed Shape at End of 25 Increments



Inc : 50
Time : 9.600e-02

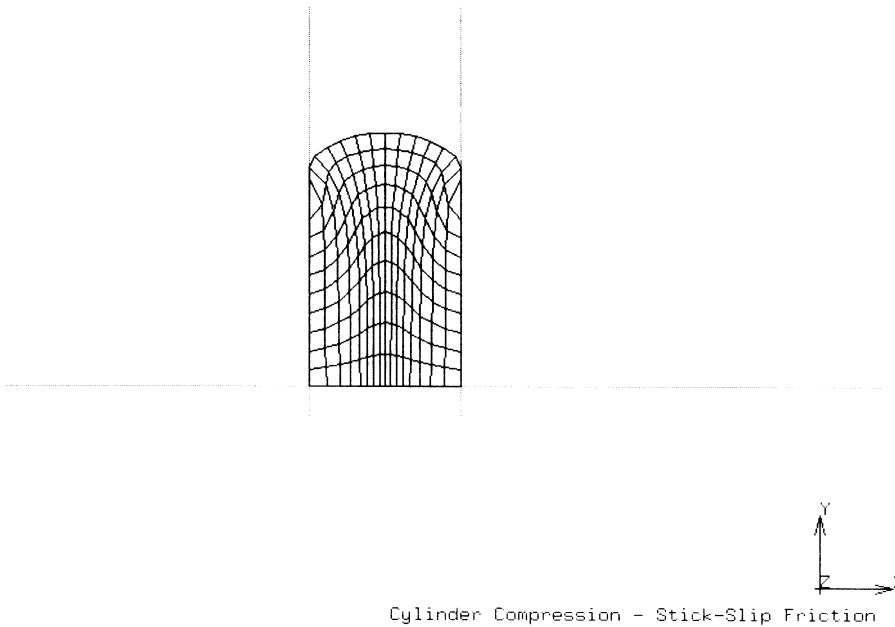


Figure 8.50-3 Deformed Shape at End of 50 Increments

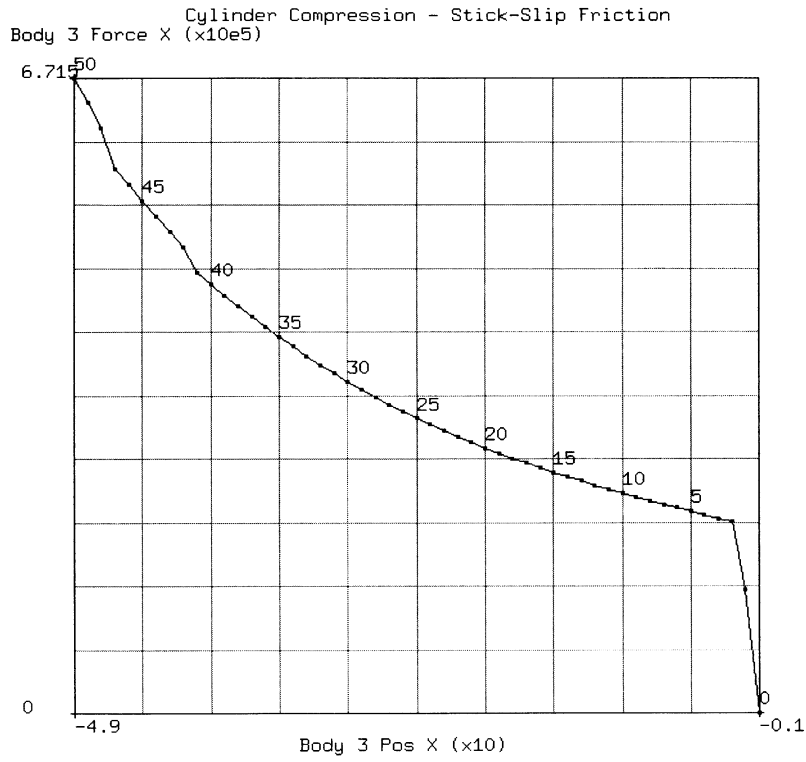


Figure 8.50-4 Load Stroke Curve for the Deformation



8.51 Modeling of a Spring

This example shows the shell contact capabilities MARC. A structure is a spring, made of shell elements is compressed between two rigid surfaces moving toward each other. Two cases are considered:

Data Set	Element Used
e8x51a	139
e8x51b	75

Model

The initial model is shown in Figure 8.51-1. The initial model is identical for both data sets with the exception of the element type used. There are 2790 4-node shell elements and 3354 nodes (Figure 8.51-2).

Element

Data set e8x51a uses element type 139. Element 139 is a 4-node bilinear thin shell element based on the discrete Kirchhoff theory. Element 75 is a 4-node bilinear thick shell element.

Material Properties

For both data sets, the shell elements are assumed to be modeled by a combined isotropic-kinematic workhardening behavior. The Young's modulus is 2.8×10^7 Pa and the Poisson's ratio is 0.30. The initial yield stress is 130×10^3 Pa. The workhardening data is input using the WORK HARD DATA option.

Boundary Conditions

The boundary conditions along the x-direction are imposed by the motion of the two contact bodies along the x-direction. The shell structure is restrained to have zero y and z displacements along the nodes 1, 2, 3, 4, 5, and 6 (edge AB in Figure 8.51-2) and along nodes 3349, 3350, 3351, 3352, 3353, and 3354 (edge CD in Figure 8.51-2).

Contact

The CONTACT option for the both data sets is identical except that in data set e8x51b (thick shell element 75) increment splitting is disallowed.



There are three contact bodies in this problem. There is no friction in the model. The distance below which a node is considered to touch a contact surface is assumed to be 10^{-3} m. The contact tolerance bias factor is assumed to be 0.90. Contact body 1 is a deformable body comprising all the elements in the model. Contact bodies 2 and 3 are rigid and each is made up of one four noded patch for contact definition. Contact body 2 is the planar surface defined by $x = -1$, while Contact body 3 is the planar surface defined by $x = +1$. The two rigid contact bodies compress the shell elements comprising the structure.

The CONTACT TABLE option is included to expedite the contact calculations. Contact body 1 is allowed to touch all the three contact bodies. Thus, self contact of the shell structure with itself is allowed. The two rigid bodies do not detect contact with each other.

History Definition

The MOTION CHANGE option specifies the motion of the rigid velocity controlled contact bodies. In increment zero, both contact bodies approach each other at constant velocity in order to just make contact with the shell structure. After increment zero, Contact body 2 is held stationary while Contact body 3 moves at constant speed in the -x-direction. There are a total of 25 increments of loading in this problem.

Results

For data set e8x51a, the deformed plots of the shell structure at increments 5, 10, 20, and 25 are shown in Figure 8.51-3 through Figure 8.51-6, respectively. For data set e8x51b, the deformed plots of the shell structure at increments 5, 10, 20, and 25 are shown in Figure 8.51-7 through Figure 8.51-10, respectively. On these deformed plots, the contours of the effective stress in layer 1 have been superimposed. It can be seen that both shell elements produce almost identical results. The comparison of x displacement for node 3351 is given below for the two data sets.

Increment Number	X Displacement at Node 3351	
	e8x51a	e8x51b
10	-0.3350	-0.3339
20	-0.3550	-0.3550



Parameters, Options, and Subroutines Summary

Example e8x51a.dat and e8x51b.dat:

Parameters	Model Definition Options	History Definition Options
ELEMENTS	CONNECTIVITY	AUTO LOAD
END	CONTACT	CONTINUE
FINITE	CONTACT TABLE	MOTION CHANGE
LARGE DISP	COORDINATES	TIME STEP
PRINT	FIXED DISP	
SETNAME	GEOMETRY	
SHELL SET	ISOTROPIC	
SIZING	SOLVER	
TITLE	WORK HARD	
UPDATE		

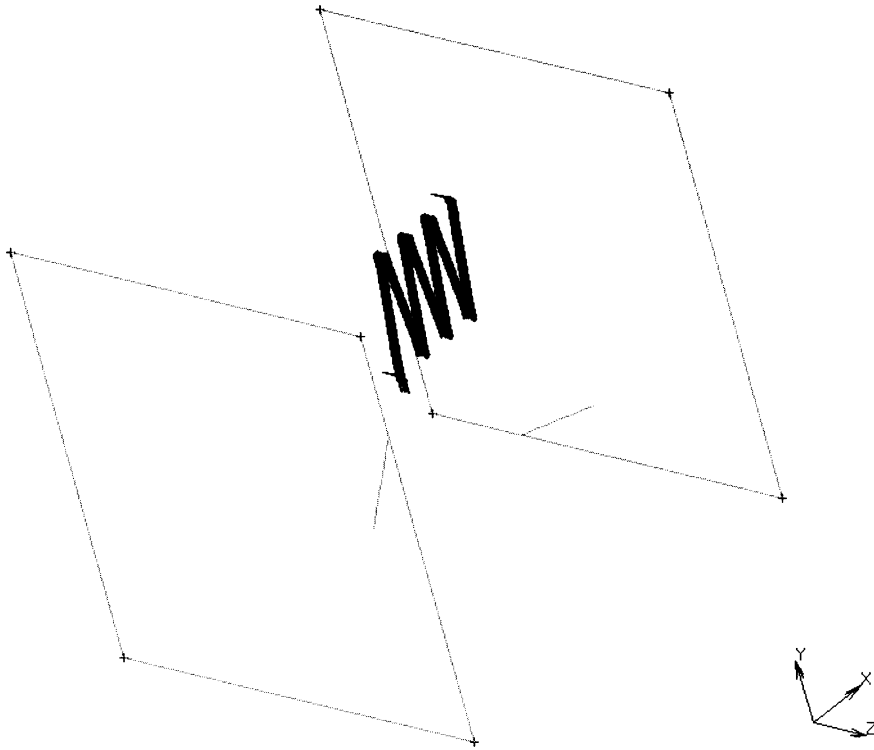


Figure 8.51-1 Initial Model for Both Data Sets

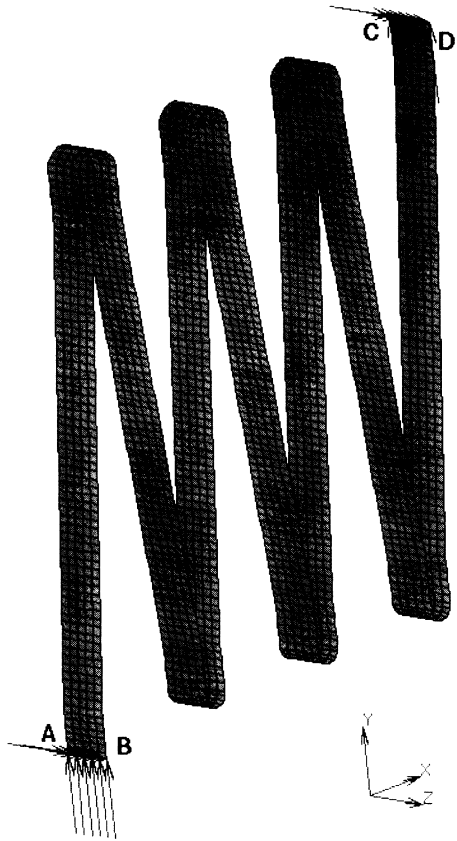


Figure 8.51-2 Boundary Condition Definition for Both Data Sets

Inc : 5
Time : 1.850e-01

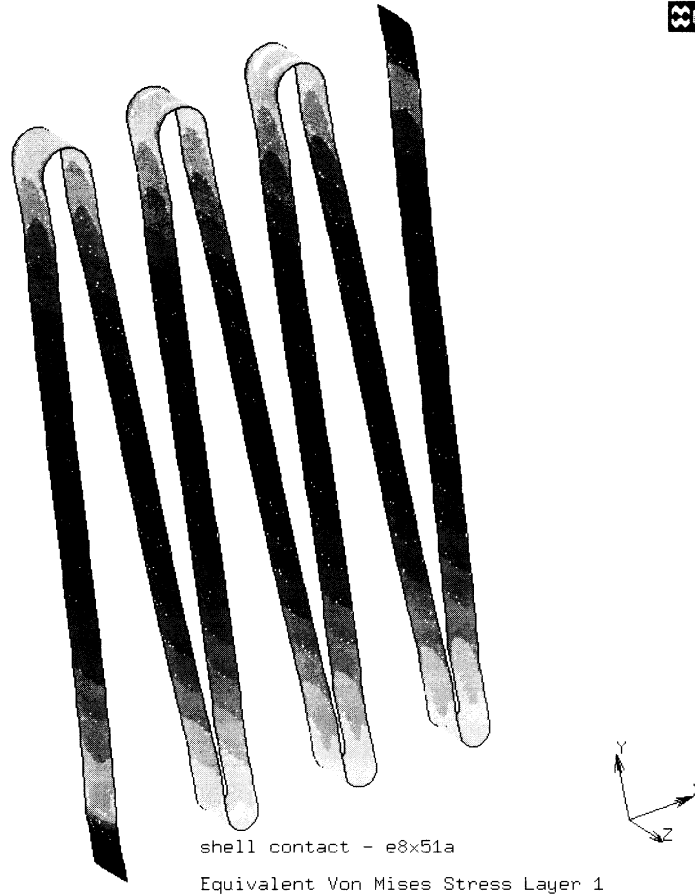
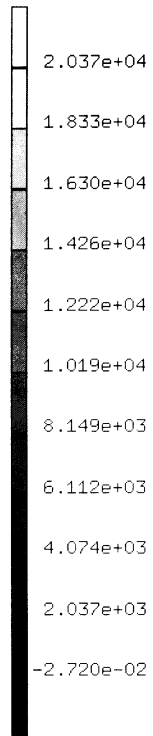


Figure 8.51-3 Deformed Shell Structure at Increment 5 for Data Set e8x51a



Inc : 10
Time : 3.350e-01

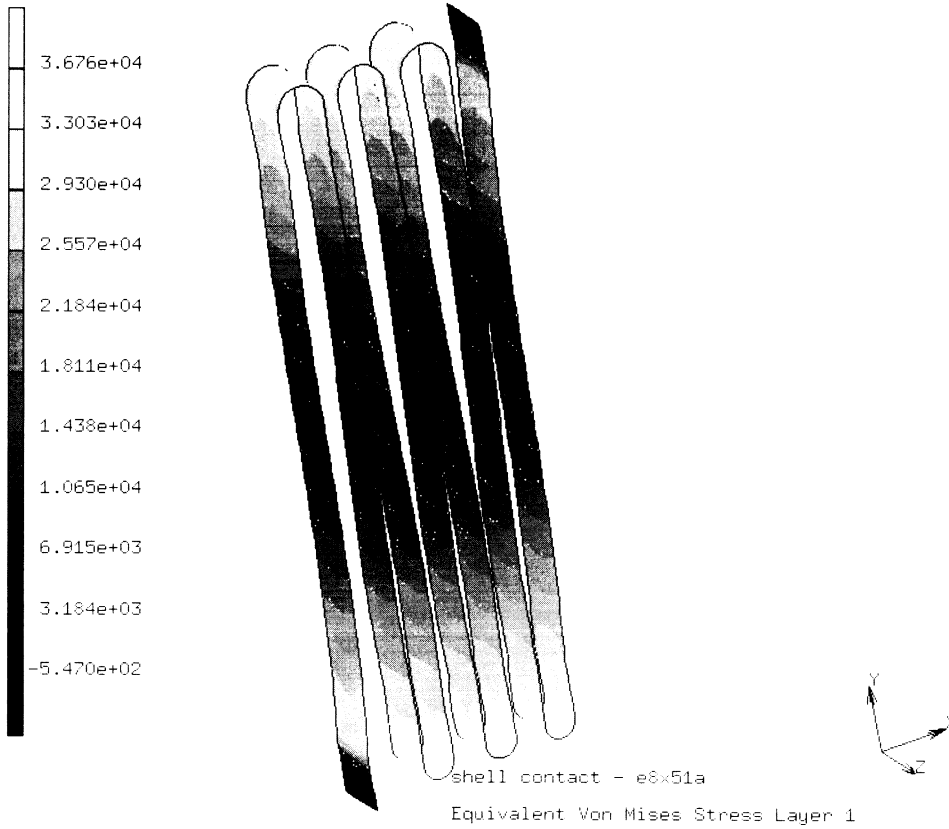


Figure 8.51-4 Deformed Shell Structure at Increment 10 for Data Set e8x51a



Inc : 20
Time : 3.550e-01

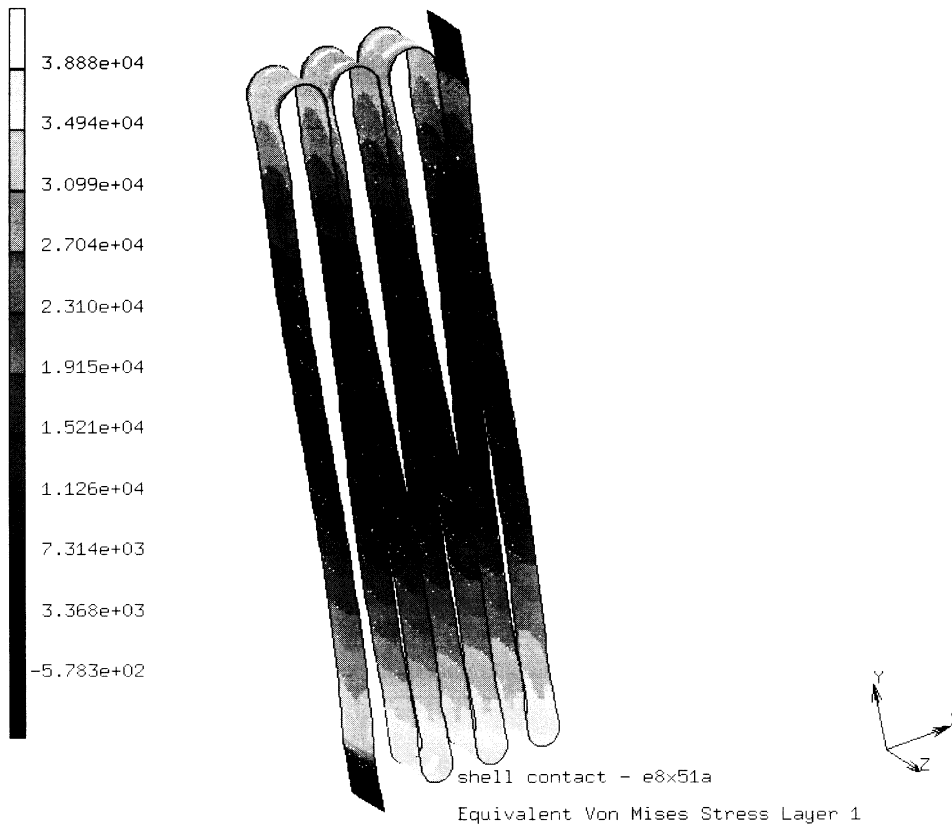


Figure 8.51-5 Deformed Shell Structure at Increment 20 for Data Set e8x51a



Inc : 25
Time : 3.650e-01

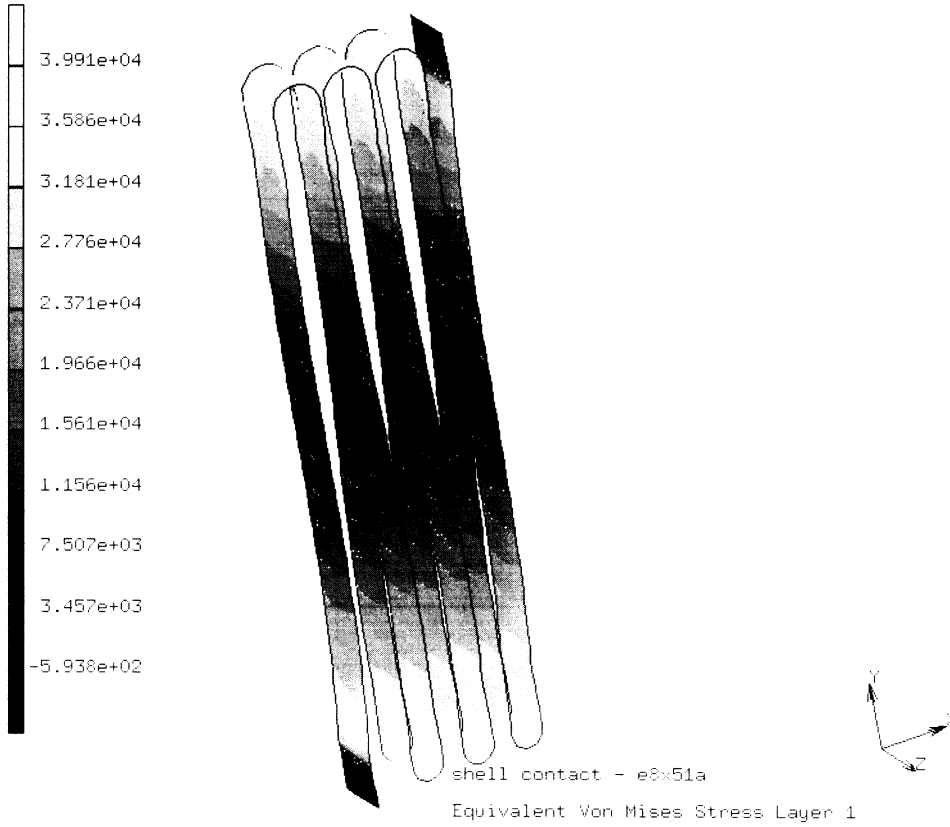


Figure 8.51-6 Deformed Shell Structure at Increment 25 for Data Set e8x51a



Inc : 5
Time : 1.850e-01

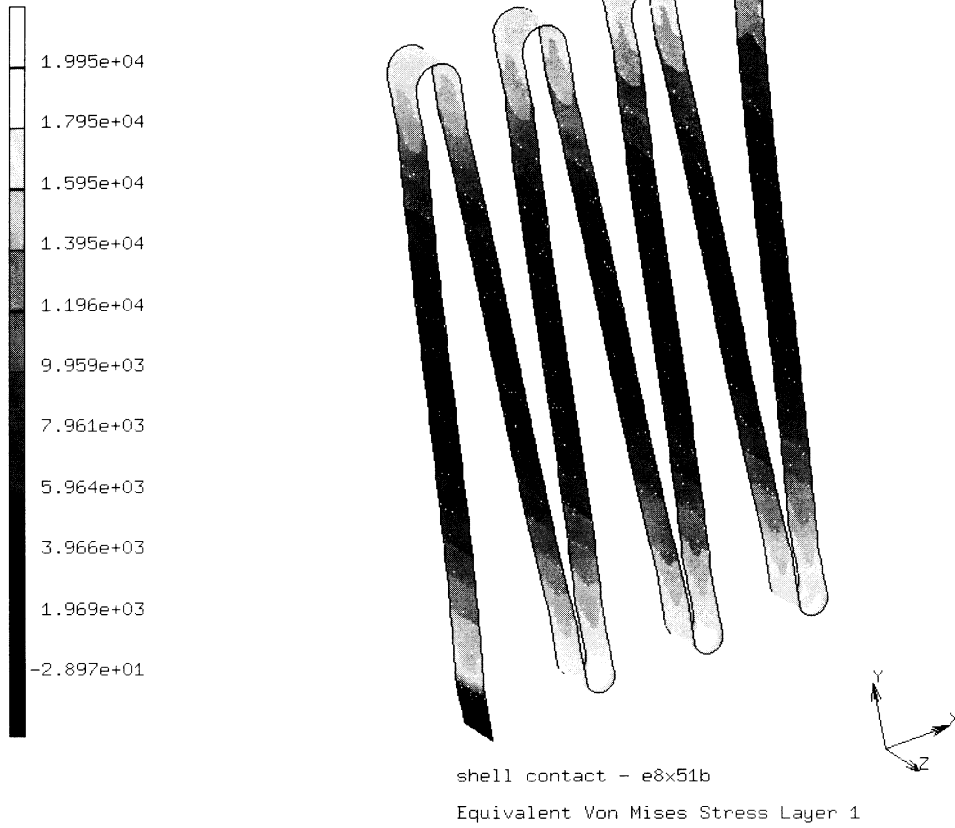


Figure 8.51-7 Deformed Shell Structure at Increment 5 for Data Set e8x51b

Inc : 10
Time : 3.350e-01

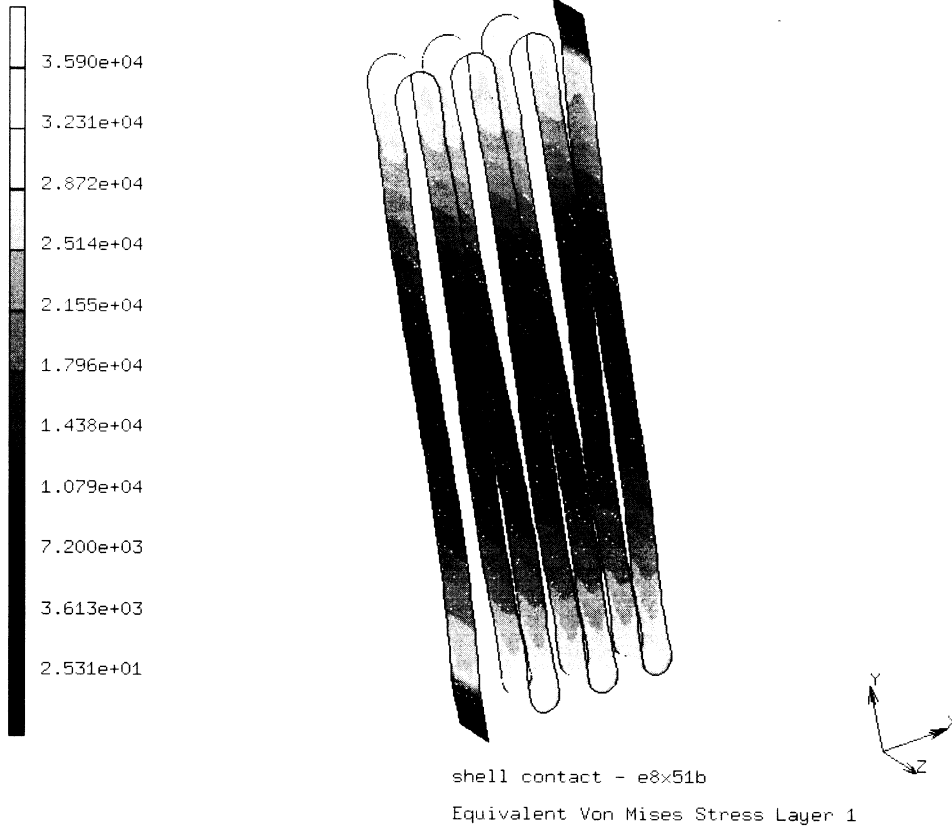


Figure 8.51-8 Deformed Shell Structure at Increment 10 for Data Set e8x51b

Inc : 20
Time : 3.550e-01

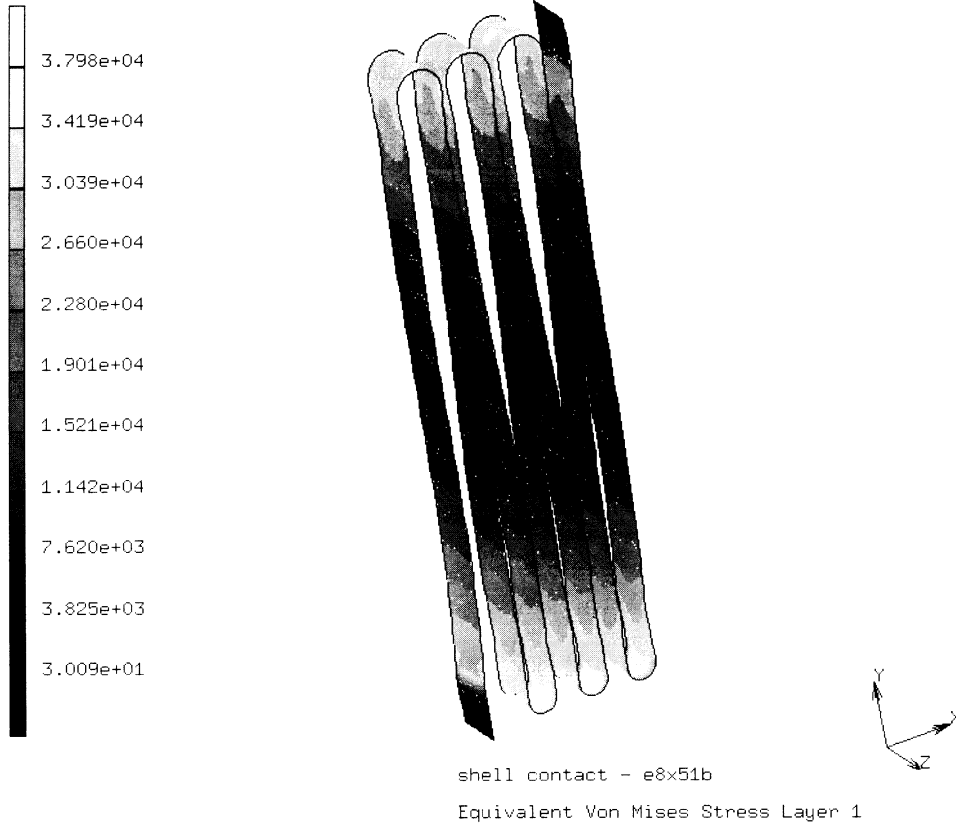


Figure 8.51-9 Deformed Shell Structure at Increment 20 for Data Set e8x51b



Inc : 25
Time : 3.650e-01

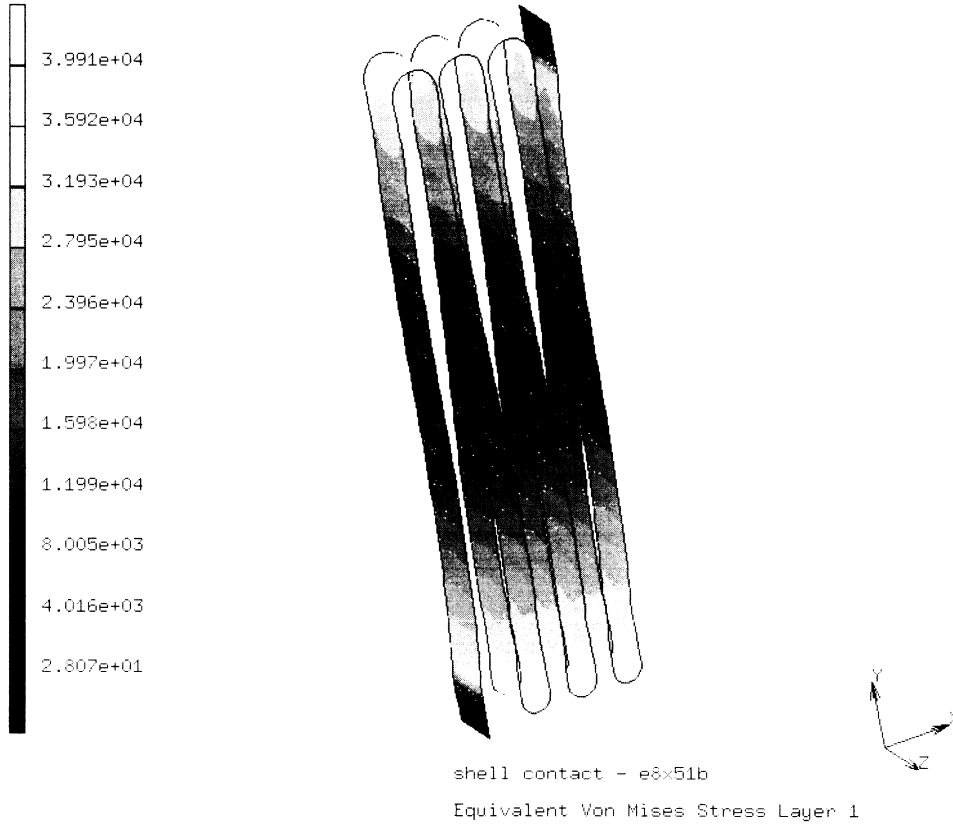


Figure 8.51-10 Deformed Shell Structure at Increment 25 for Data Set e8x51b





8.52 Deep Drawing of Sheet

This example shows the shell-shell contact capabilities. The example simulates the deep drawing of a sheet by a punch. The sheet is modeled using shell elements. The punch is also modeled using shell elements with stiffer material properties. Thus, the example shows a case of the contact of deformable-deformable shell-shell contact.

Model

The initial geometry for this problem is shown in Figure 8.52-1. Due to symmetry, only one quarter of this geometry is modeled. There are 792 elements and 848 nodes in the quarter model. Elements 1 to 360 comprise the sheet, while elements 361 to 792 constitute the punch. The deformable punch composed of stiffer shell elements stretches the sheet to form a cup.

Element

Both the sheet and punch are modeled using thick shell element number 75. Element 75 is a 4-node element.

Material Properties

Both the punch and the sheet are assumed to be modeled by an isotropic material. The material properties are:

Material	Young's Modulus (Pa)	Poisson's Ratio (Pa)	Initial Yield Stress
Sheet	6.90×10^{10}	0.30	1.59×10^8
Punch	1.38×10^{12}	0.30	1.00×10^{21}

The punch has a higher Young's modulus and an extremely high initial yield stress. Thus, the punch is stiffer than the sheet material. The workhardening behavior of the sheet material is input using the WORK HARD model definition option.

**Boundary Conditions**

The boundary conditions imposed are consistent with the four fold symmetry of the quarter model, about the z axis. Hence, the boundary conditions imposed are:

Sheet

On curve $x = 0$, $u_x = \theta_y = \theta_z = 0$.

On curve $y = 0$, $u_y = \theta_z = \theta_x = 0$.

On sheet circumference, $u_x = u_y = u_z = 0$

On sheet circumference, $\theta_x = \theta_y = \theta_z = 0$

Punch

On curve $x = 0$, $u_x = \theta_y = \theta_z = 0$.

On curve $y = 0$, $u_y = \theta_z = \theta_x = 0$.

Contact

There are two contact bodies in this simulation. Both contact bodies are deformable. Contact body 1 is the sheet and Contact body 2 is the punch. Coulomb friction is assumed with a coefficient of friction of 0.30. To prevent chattering, a node that contacts a contact body during an increment is prevented from separating during that increment. A contact bias factor of 0.99 is employed.

Control

The maximum allowed relative change in displacement increment is set to 0.05 and 20 recycles are chosen to the maximum for each increment.

History Definition

The deformable punch is moved downward by specifying a displacement increment along the negative z-direction on the nodes on the top circumference of the punch. The DISP CHANGE option is used. A total of 30 such increments are prescribed using the AUTO LOAD option.

Results

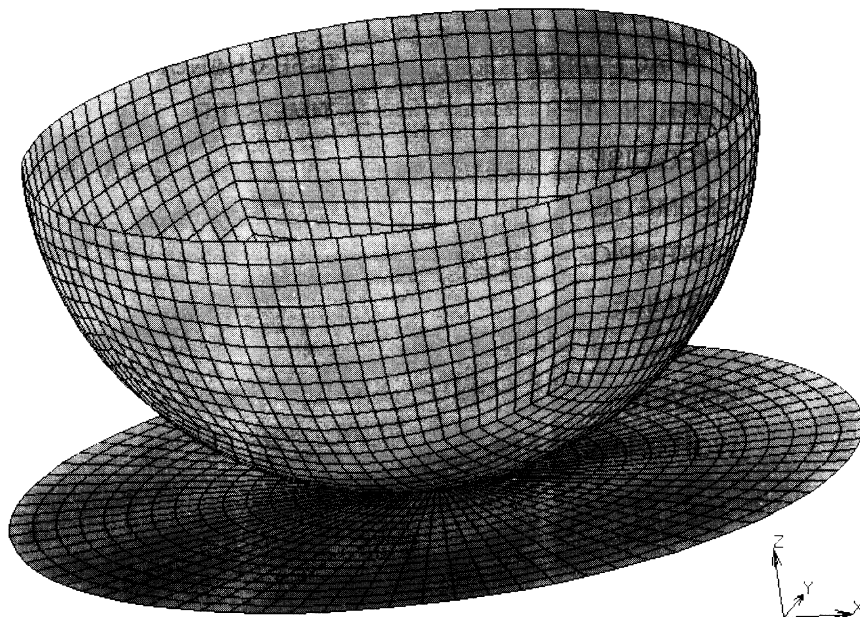
The deformed configuration for increments 10, 20, and 30 are shown in Figure 8.52-2, Figure 8.52-3, and Figure 8.52-4, respectively. The contours of effective plastic strain in the outer layer are plotted on the entire deformed geometry of the sheet in Figure 8.52-5.



Parameters, Options, and Subroutines Summary

Example e8x52.dat:

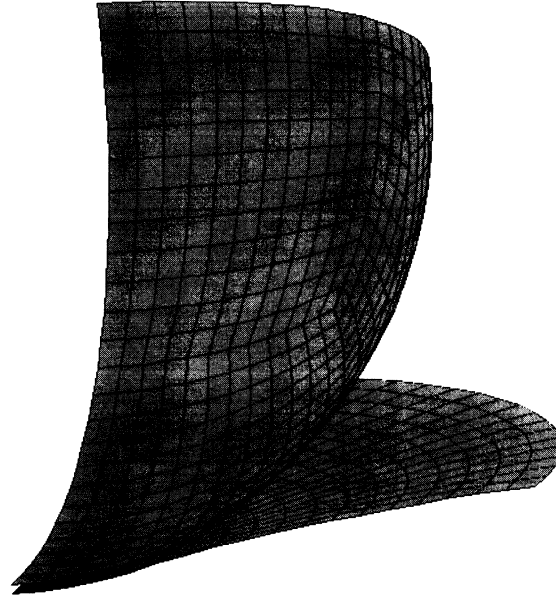
Parameters	Model Definition Options	History Definition Options
ELEMENTS	CONNECTIVITY	AUTO LOAD
END	CONTACT	CONTINUE
FINITE	CONTACT TABLE	DISP CHANGE
LARGE DISP	COORDINATES	TIME STEP
PRINT	FIXED DISP	
SETNAME	GEOMETRY	
SHELL SECTS	ISOTROPIC	
SIZING	OPTIMIZE	
TITLE	POST	
UPDATE	SOLVER	
	WORK HARD	



Deep Drawing Shell-Shell Contact

Figure 8.52-1 Initial Geometry - Only One Quarter is Modeled due to Symmetry

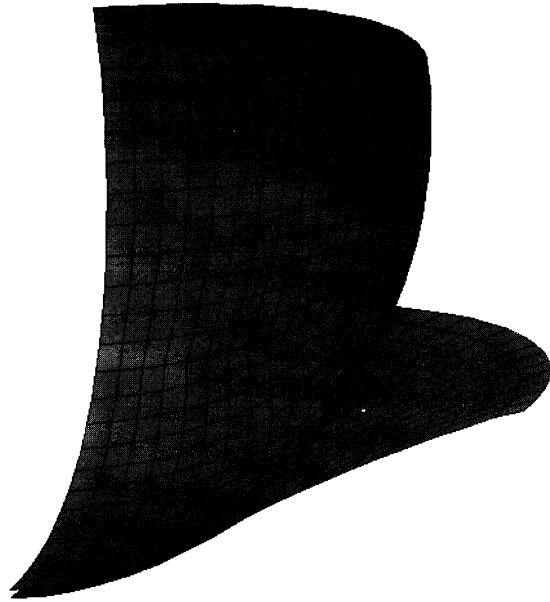
Inc : 10
Time : 8.333e-04



Deep Drawing Shell-Shell Contact

Figure 8.52-2 Deformed Geometry at the End of 10 Increments

Inc : 20
Time : 1.667e-03

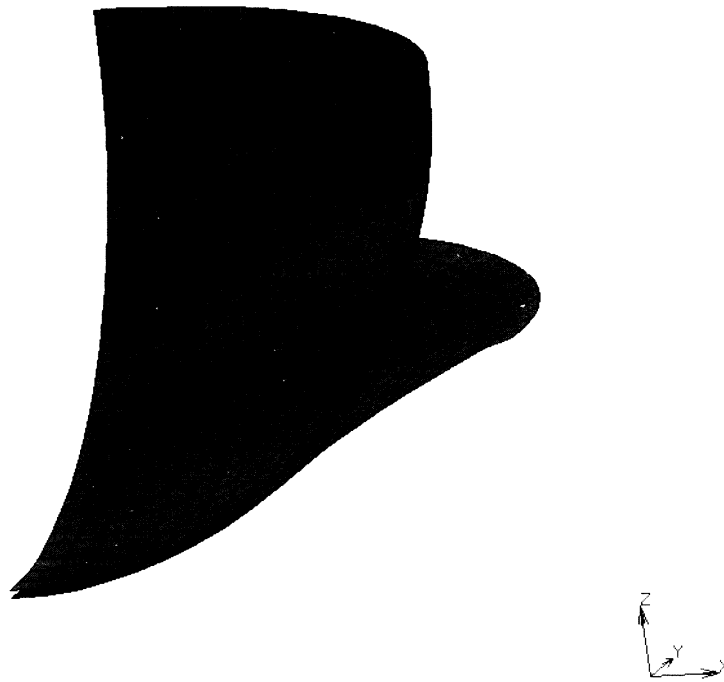


Deep Drawing Shell-Shell Contact

Figure 8.52-3 Deformed Geometry at the End of 20 Increments



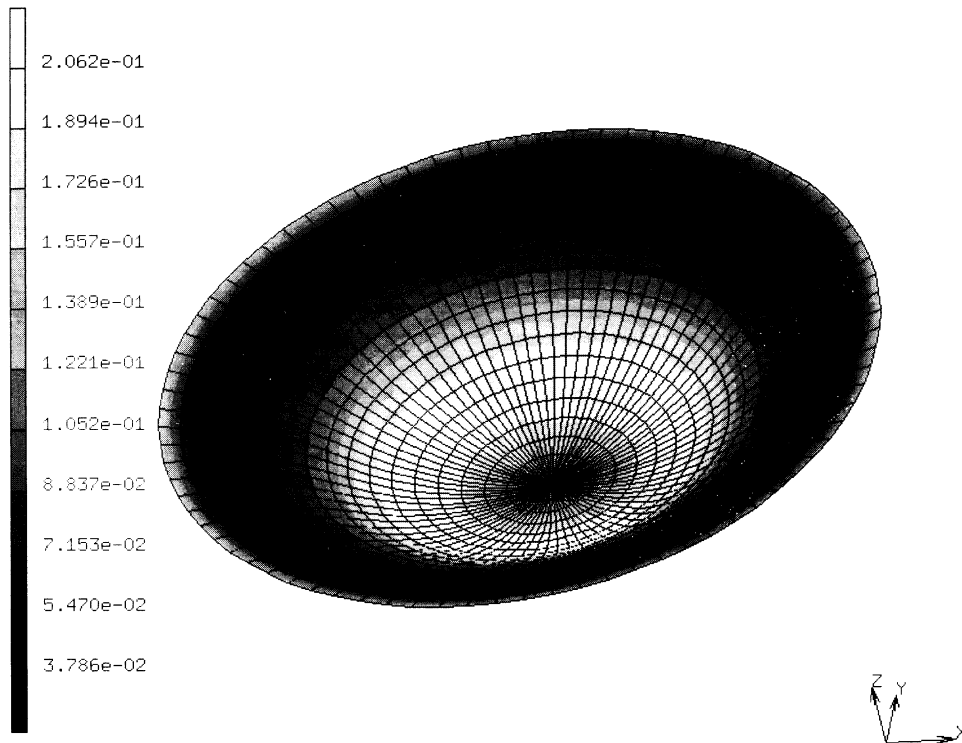
Inc : 30
Time : 2.500e-03



Deep Drawing Shell-Shell Contact

Figure 8.52-4 Deformed Geometry at the End of 30 Increments

Inc : 30
Time : 2.500e-03



Deep Drawing Shell-Shell Contact
eq plastic strain outer

Figure 8.52-5 Effective Plastic Strain Distribution at the End of 30 Increments



8.53 Shell-Shell Contact and Separation

This example shows the simulation of shell-shell contact and separation. Two data sets are shown in this example.

Data Set	Element Used
e8x53a	75
e8x53b	49

Model

The initial model is shown in Figure 8.53-1. Data set e8x53a uses element type 75 which is a 4-node thick shell element. Data set e8x53b uses element type 49 which is a 6-node finite rotation thin shell element. Data set e8x53a uses 400 elements and 505 nodes. Data set e8x53b uses 800 elements and 1809 nodes

Material Properties

For both data sets, all materials are treated as isotropic elastic. The Young's modulus is 2.1×10^5 Pa and the Poisson's ratio is taken to be zero.

Boundary Conditions

The boundary conditions applied in the two cases are summarized below:

Data Set	Line AB	Curve AC	Line CD	Curve BD
e8x53a	$u_x = u_z = 0, \theta_z = 0$		$u_x = u_y = u_z = 0,$ $\theta_x = \theta_y = \theta_z = 0$	
e8x53b	$u_x = u_z = 0, \phi = 0$	$\phi = 0$	$u_x = u_y = u_z = 0,$ $\phi = 0$	$\phi = 0$

Geometry

The shell elements in the bottom flat portion of the shell structure have a thickness of 0.05 m while the remaining shell elements have a thickness of 0.03 m. This holds for both data sets.

Contact

There is just one contact body in this problem. No friction is assumed. The distance below which an element is considered touching a contact surface is set to 0.002 m.



Control

Ten recycles are set as a maximum for each increment. The maximum allowed relative error in residual forces is set to 0.01.

History Definition

The loading history is the same for both data sets. The loading is carried out by defining distributed pressure loads acting on the top face of the shell structure as shown in Figure 8.53-1. The pressure load is ramped up from 0.0 Pa to 0.25 Pa in 20 increments in a linear fashion. Following this, the pressure load is reduced to 0.0 Pa in a further 20 increments. There are a total of 40 increments in this problem.

Results

The top surface of the shell structure contacts the bottom surface of the shell structure at the end of 14 increments for both data sets. The end view of the deformed and initial geometry for data set e8x53a after 14 increments is shown in Figure 8.53-2. The initial and deformed geometry at the end of 20 increments is shown in Figure 8.53-3 for data set e8x53a. Figure 8.53-6 shows the variation of the y reaction force of node 405 (point D in Figure 8.53-1) with increment for data set e8x53a. The end view of the deformed and initial geometry for data set e8x53b after 14 increments is shown in Figure 8.53-4. The initial and deformed geometry at the end of 20 increments is shown in Figure 8.53-5 for data set e8x53b. Figure 8.53-7 shows the variation of the y reaction force of node 405 (point D in Figure 8.53-1) with increment for data set e8x53b. As expected, the triangular shell element 49 shows a stiffer behavior compared to the 4-node element 75. For both cases, the shell is found to completely springback to the original configuration after 40 increments when the applied distributed load returns to zero.



Parameters, Options, and Subroutines Summary

Example e8x53.dat:

Parameters	Model Definition Options	History Definition Options
ALL POINTS	CONNECTIVITY	AUTO LOAD
DIST LOADS	CONTACT	CONTINUE
ELEMENTS	COORDINATES	DISP CHANGE (for e8x53b only)
LARGE DISP	DIST LOADS	DIST LOADS
SETNAME	END OPTION	TIME STEP
SHELL SECT	FIXED DISP	
SIZING	GEOMETRY	
TITLE	ISOTROPIC	
	OPTIMIZE	
	SOLVER	

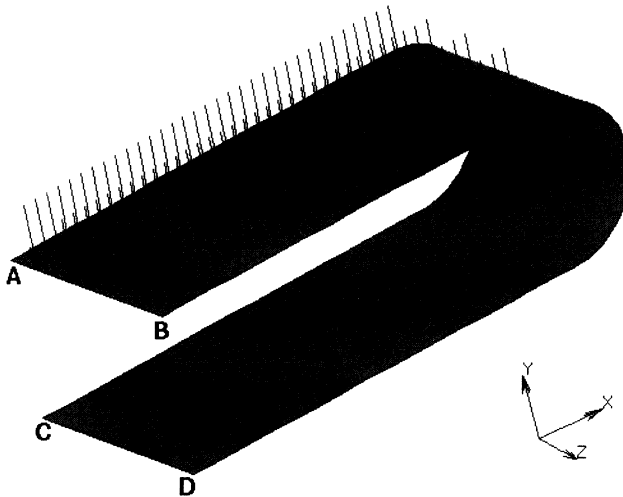
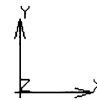
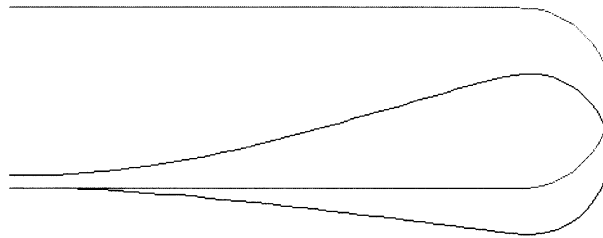


Figure 8.53-1 Initial Geometry for both Data Sets



Inc : 14
Time : 3.500e-01

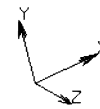
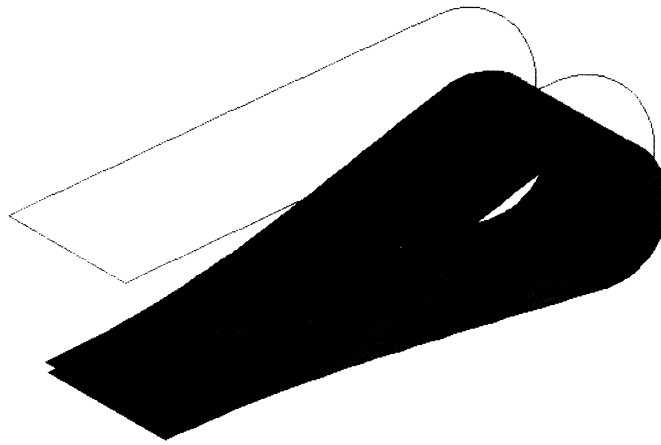


Shell self contact - e8x53a

Figure 8.53-2 End View of Original and Deformed Geometry after 14 Increments for Data Set e8x53a



Inc : 20
Time : 5.000e-01

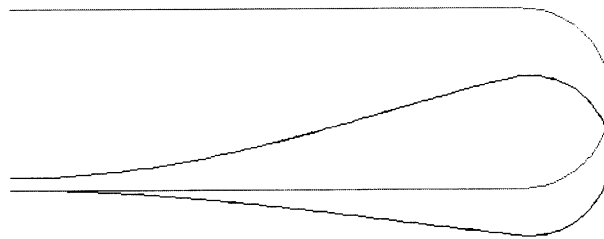


Shell self contact - e8x53a

Figure 8.53-3 Original and Deformed Geometry after 20 Increments for Data Set e8x53a



Inc : 14
Time : 3.500e-01

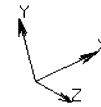
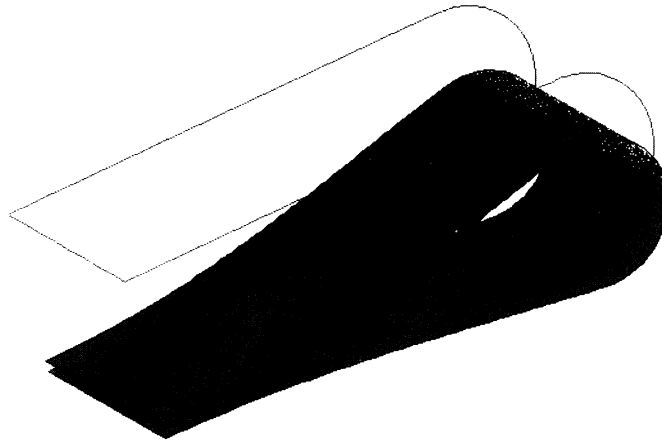


Shell self contact - e8x53b

Figure 8.53-4 Original and Deformed Geometry after 14 Increments for Data Set e8x53b - End View



Inc : 20
Time : 5.000e-01



Shell self contact - e8x53b

Figure 8.53-5 Original and Deformed Geometry after 20 Increments for Data Set e8x53b

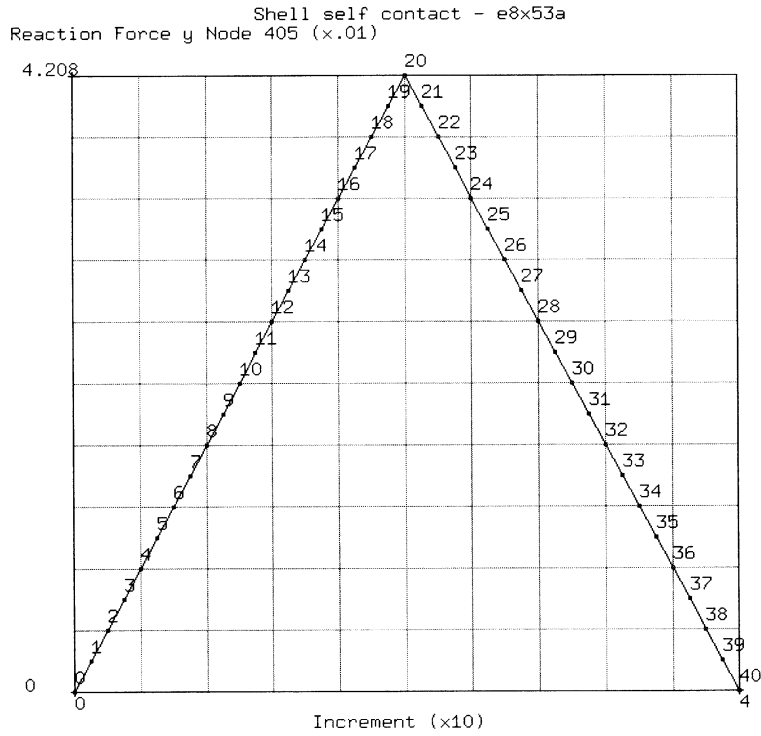


Figure 8.53-6 History Plot of the Variation of the y Reaction Force at Node 405 for Data Set e8x53a

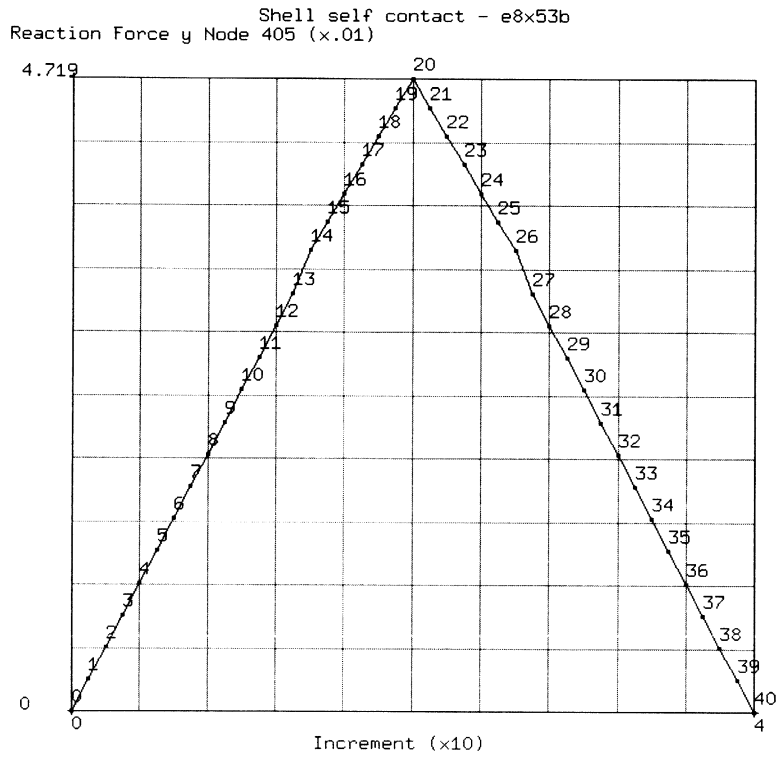


Figure 8.53-7 History Plot of the Variation of the y Reaction Force at Node 405 for Data Set e8x53b



8.54 Self Contact of a Shell Structure

This example shows the self contact of a shell structure. Even though there is little straining in this example, large displacements and finite rotations are involved which poses a numerical challenge to the computational algorithms in the code.

Model

The initial geometry of the model is shown in Figure 8.54-1 as a side view. The model is shown in Figure 8.54-2. There are 12 elements and 26 nodes in the problem. The 4-node thick shell element number 75 is used in the analysis.

Material Properties

The shell elements are assumed to be isotropic and elastic. The Young's modulus is 1.2×10^3 Pa and the Poisson's ratio is 0.295.

Boundary Conditions

The boundary conditions imposed on this problem are:

Nodes	Imposed Boundary Conditions
1, 2	$u_x = u_y = 0$
1 to 26	$u_z = \theta_x = 0$
25, 26	$u_y = 0$

Contact

There is just one contact body here and self contact is allowed. No friction is assumed. The distance below which a node is assumed to be in contact is 0.02 m.

Geometry

The thickness of all elements is assumed to be 0.20 m.

Control

The maximum allowed error in residual forces is assumed to be 0.10. A maximum of 10 cycles is allowed per increment.

**History Definition**

The loading is imposed by x displacements at nodes 25 and 26. An incremental x displacement of 0.2m is imposed on nodes 25 and 26 in each increment. A total of 10 increments are applied.

Results

The deformed shape of the structure is shown in side view in Figure 8.54-3 for increment 5. The deformed shape of the structure is shown in side view in Figure 8.54-4 for increment 10. In both figures, the initial configuration is also plotted. The deformed and initial configurations show the large rotation involved in this shell-shell contact example. Figure 8.54-5 shows the variation of reaction force x versus x displacement for node 26.

Parameters, Options, and Subroutines Summary

Example e8x54.dat:

Parameters	Model Definition Options	History Definition Options
ELEMENTS	CONNECTIVITY	AUTO LOAD
END	CONTACT	CONTINUE
LARGE DISP	COORDINATES	DISP CHANGE
PRINT	END OPTION	TIME STEP
SETNAME	FIXED DISP	
SHELL SECT	GEOMETRY	
SIZING	ISOTROPIC	
TITLE	OPTIMIZE	
UPDATE	SOLVER	



Inc : 0
Time : 0.000e+00

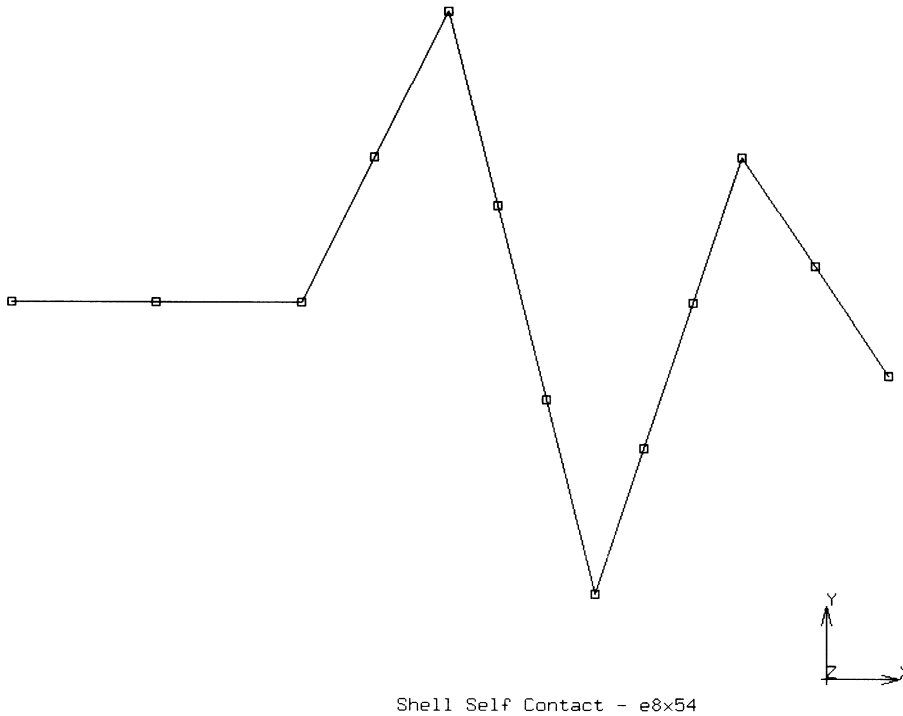
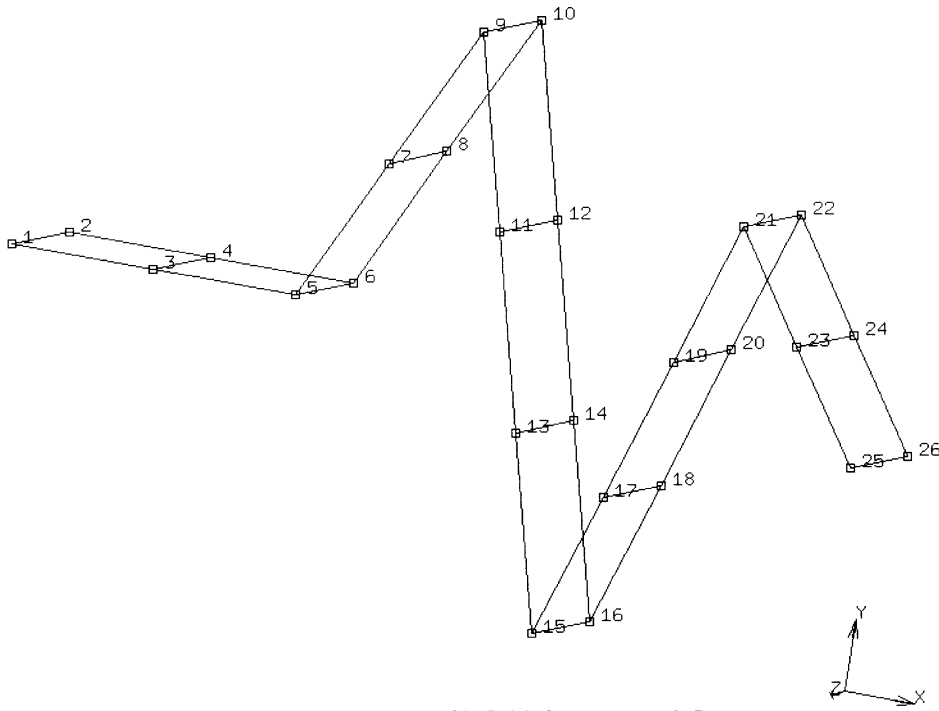


Figure 8.54-1 Side View of Initial Geometry



Inc : 0
Time : 0.000e+00



Shell Self Contact - e8x54

Figure 8.54-2 Initial Model of Structure



Inc : 5
Time : 5.000e+00

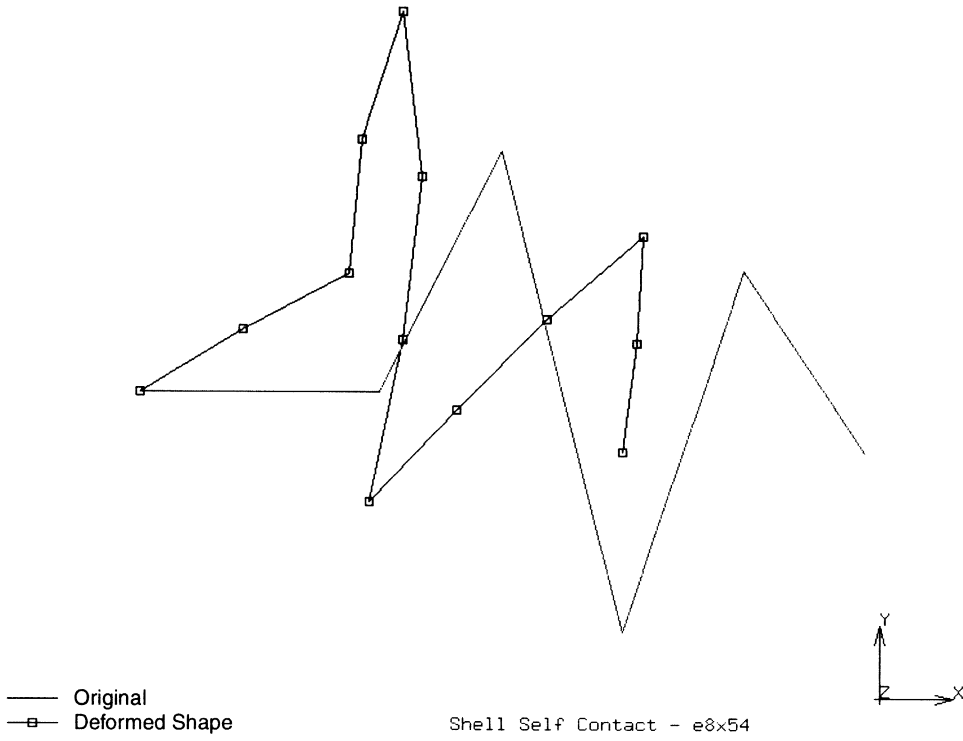


Figure 8.54-3 Deformed Shape of the Structure at Increment 5

Inc : 10
Time : 1.000e+01

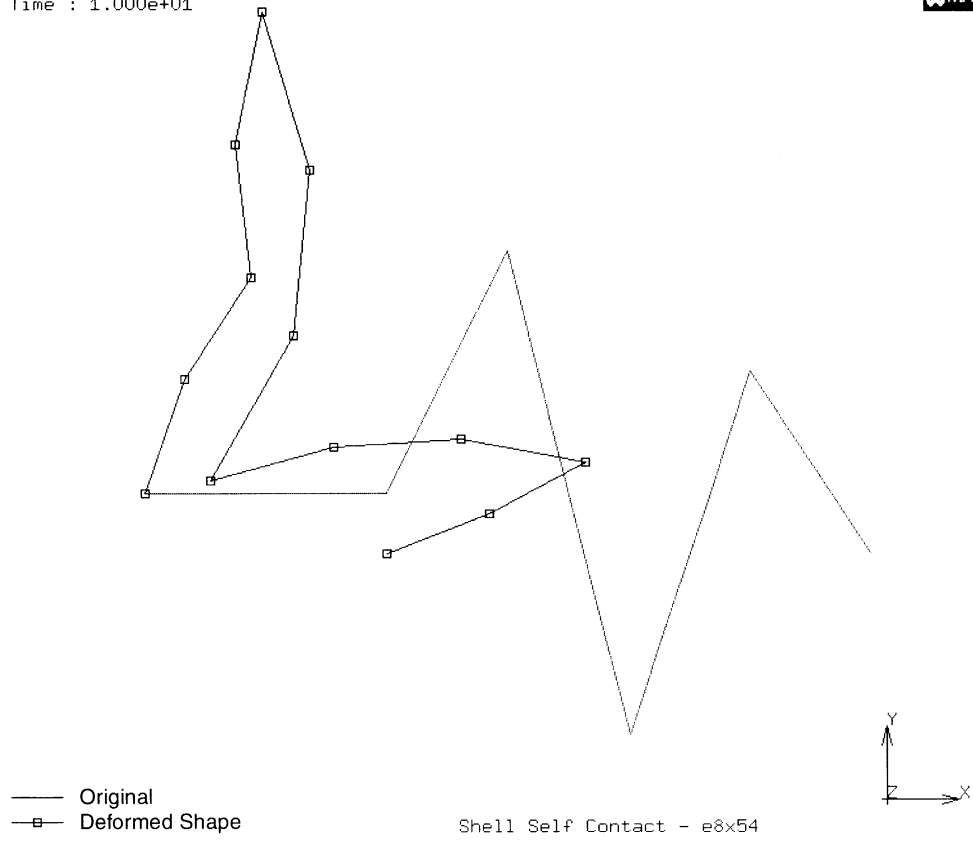


Figure 8.54-4 Deformed Shape of the Structure at Increment 10

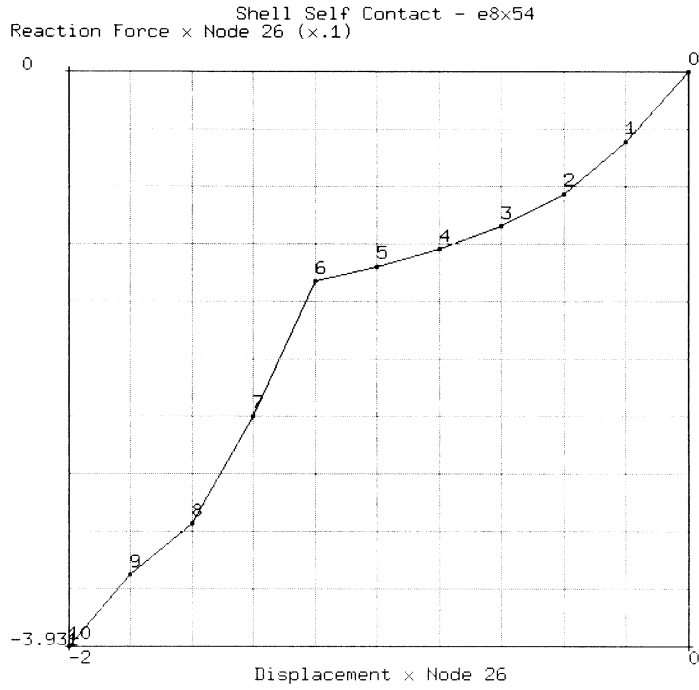


Figure 8.54-5 Displacement x versus Reaction Force X for Node 26



8 *Advanced Topics*

Self Contact of a Shell Structure



8.55 Deep Drawing of Copper Sheet

This example shows the deep drawing of a copper sheet. Shell elements are used to model the sheet. There are two data sets in this example. Data set e8x55a uses a velocity controlled punch. Data set e8x55b uses a load controlled punch. The effect of clamp down pressure is modeled using point loads.

Model

The initial model is shown in Figure 8.55-1. A 15° sector of the punch is used. The model consists of 79 elements and 121 nodes to model the sheet. There are four rigid bodies in the model, a punch, a lower die, and two symmetry bodies. In the case of data set e8x55b, an extra detached node (number 122) is associated with the rigid punch and a point load is applied to this node.

Element

The 4 noded thick shell element number 75 is used in this example to model the copper sheet.

Material Properties

The sheet is assumed to be isotropic with an elastic modulus of 17×10^6 psi and a Poisson's ratio of 0.33. The initial yield stress is assumed to be 1.08×10^4 psi. The workhardening characteristics of the sheet are given by the WORK HARD model definition option.

Boundary Conditions

The boundary conditions for this problem are imposed using the CONTACT option. Point loads are applied along the x direction on the nodes of elements 1 to 6 (Figure 8.55-2) to model the effect of the clamp down pressure to prevent wrinkling.

Contact

There are 5 contact bodies in this problem. Contact body 1 is the deformable body representing the sheet. Body 2 is a rigid body representing the punch. In the case of data set e8x55a, the punch is a velocity controlled body moving at a speed of 3.2 in/s along the +x direction. For data set e8x55b, the punch is load controlled. Contact body 3 represents the lower die. Contact bodies 4 and 5 represent the symmetry surfaces in the problem. Coulomb friction is used with a friction coefficient of 0.04. The distance below which a node is considered to be sticking to a contact surface is 8.75×10^{-4} in. A contact bias factor of 0.90 is used.

**Control**

The convergence control is displacement based. The maximum allowed relative change in displacement increment is 0.05.

History Definition

The effect of clamp down pressure is simulated by applying point loads to elements 1 to 6. In increment 1, the clamp down pressure is applied for both data sets. The clampdown pressure is unchanged for the entire simulation for both data sets. The clampdown pressure is detailed in the table below and is the same for both data sets.

Nodes	P_x (lb)
1, 3, 4, 6, 7, 9, 10, 12	2.6
2, 5, 8, 11	5.2

For data set e8x55a, the punch is moved along the +x direction at a speed of 3.2 in/s for a further 99 increments. For data set e8x55b, a load of 3.08 lbs per increment is applied along the x direction for 79 increments.

Results

The final deformed geometry is shown in Figure 8.55-3 for data set e8x55a. The contours of total effective plastic strain are superimposed. The final deformed geometry is shown in Figure 8.55-4 for data set e8x55b. The contours of total effective plastic strain are superimposed.



Parameters, Options, and Subroutines Summary

Example e8x55a.dat and e8x55b.dat:

Parameters	Model Definition Options	History Definition Options
ALL POINTS	CONNECTIVITY	AUTO LOAD
ELEMENTS	CONTACT	CONTINUE
END	CONTROL	POINT LOAD
FINITE	COORDINATES	TIME STEP
LARGE DISP	ISOTROPIC	
SHELL SECT	OPTIMIZE	
SIZING	POINT LOAD	
TITLE	WORK HARD	
UPDATE		

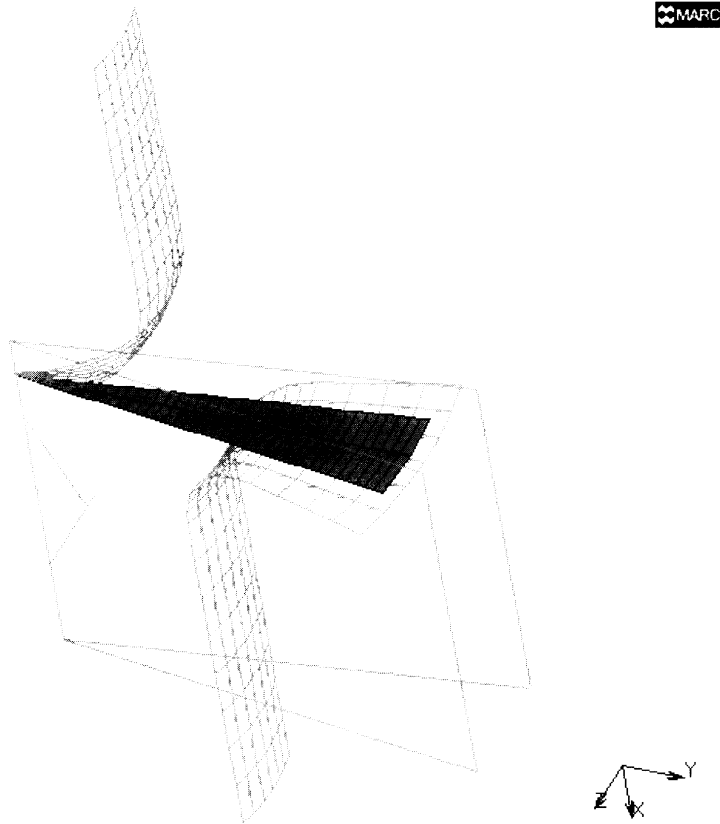


Figure 8.55-1 Initial Model

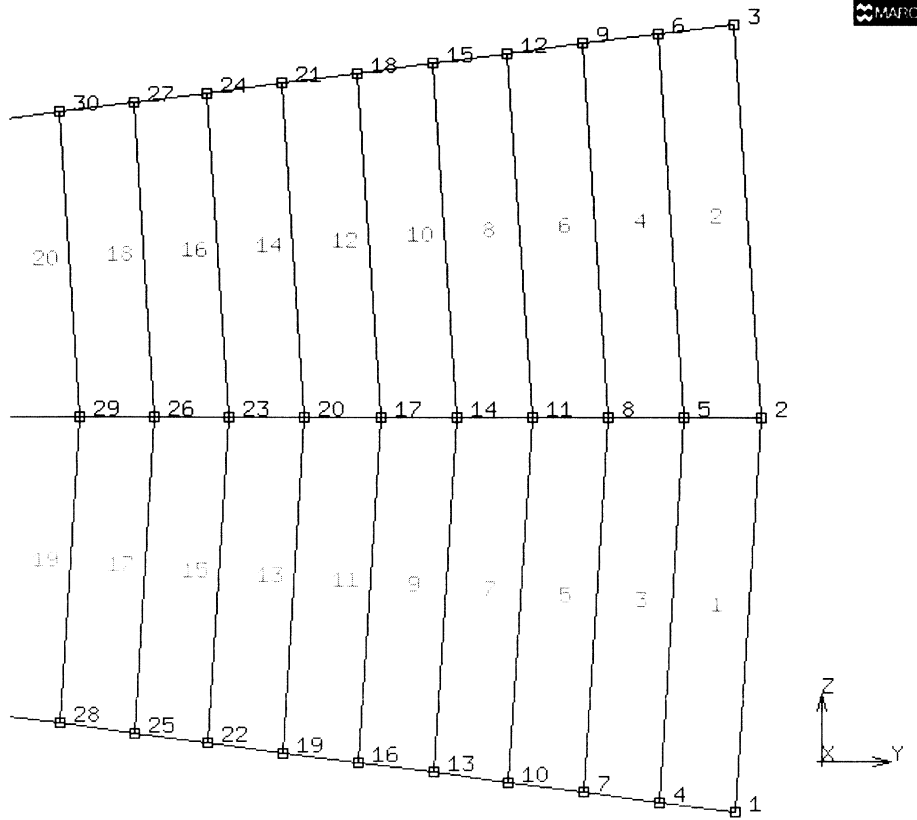


Figure 8.55-2 Elements to which Clamp Down Pressure is Applied



Inc : 100
Time : 5.000e-01

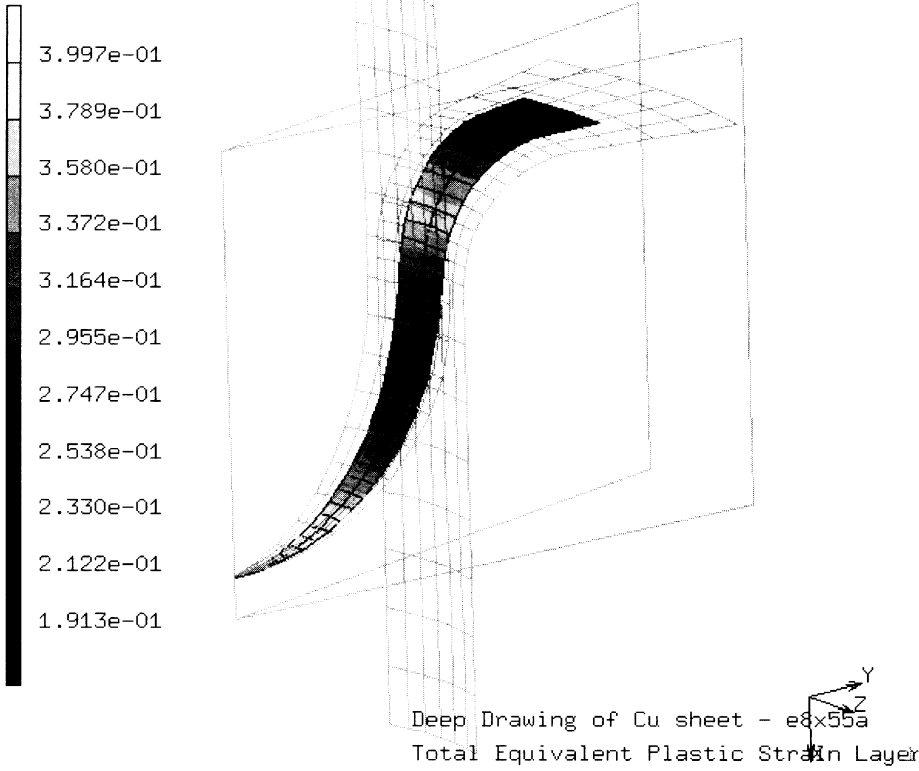


Figure 8.55-3 The Final Deformed Geometry for Data Set e8x55a



Inc : 80
Time : 4.000e-01

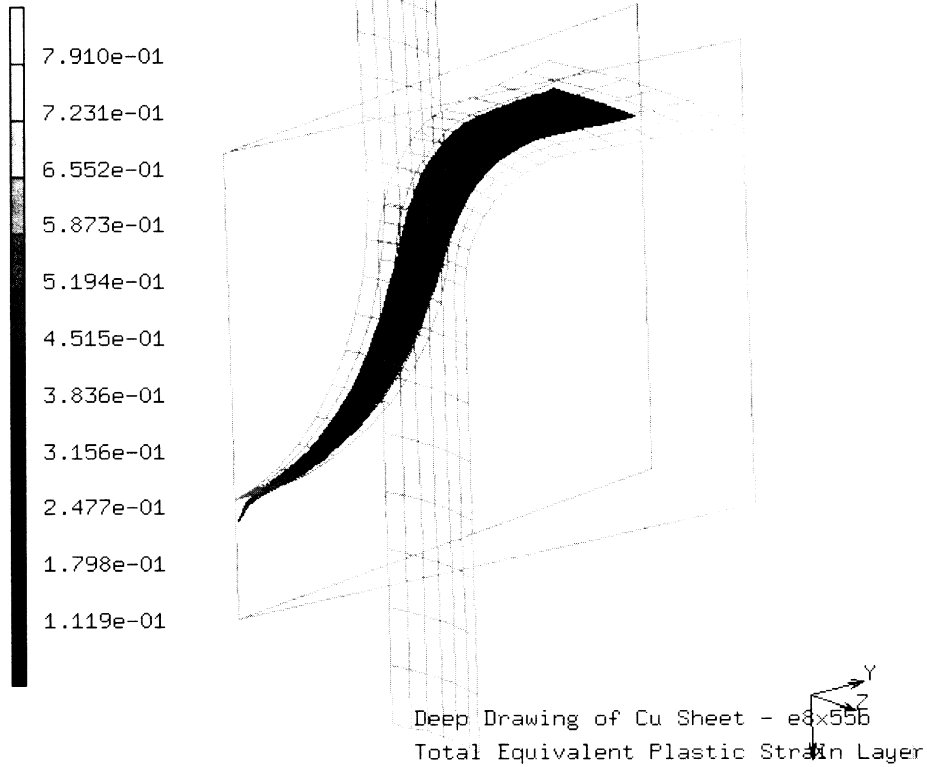


Figure 8.55-4 The Final Deformed Geometry for Data Set e8x55b





8.56 2D Contact Problem - Load Control and Velocity Control

This example shows the case of 2D contact. Two data sets are shown, one with load controlled contact bodies (e8x56a) and the other with velocity controlled contact bodies (e8x56b).

Model

The initial model is identical for both data sets and is shown in Figure 8.56-1. There are 320 elements and 405 nodes. An extra detached node (number 406) is added for data set e8x56b. This node is used to apply a point load to model the load controlled contact body in data set e8x56b.

Element

The axisymmetric 4-noded isoparametric element number 10 is used. The constant dilatation option is chosen.

Material Properties

The material properties are identical for both data sets. The Young's modulus is 3×10^7 psi and the Poisson's ratio is 0.70. The initial yield stress is 4×10^4 psi. The workhardening behavior is given using the WORK HARD model definition option.

Boundary Conditions

The nodes 1 to 5 are held to have zero x displacement. The boundary conditions along y are enforced by contact.

Contact

There are three contact bodies in this problem. Contact body 1 is the deformable body. Contact body 2 is the upper die and contact body 3 is the lower die. Contact body 2 is held stationary. Contact body 3 is velocity controlled for data set e8x56a. For data set e8x56b, contact body 3 is load controlled. A point load is applied along the +y direction to node 406 which is attached to contact body 3. Increment splitting is prevented for both data sets. The distance below which a node is considered to be sticking to a contact body is 0.001 in. The contact separation force is assumed to be 1×10^7 lb.

Control

Convergence control is displacement based. The maximum allowed relative change in displacement increment is set to 0.10.



History Definition

The loading is done using the CONTACT options. In data set e8x56a, the lower contact body (contact body 3) is velocity controlled. It is moved at a speed of 1 in/s along the +y direction. The first 18 increments are chosen with a time step of 0.1. Following this, 8 more increments are chosen with a time increment of 0.05.

For data set e8x56b, a point load of 1×10^5 lb is applied in every increment for the first 18 increments along the +y direction on node 406. Following this, load increments of 1×10^6 lb are applied for 24 more increments on node 406.

Results

The final deformed shape is shown in Figure 8.56-2 for data set e8x56a. The final deformed shape is shown in Figure 8.56-3 for data set e8x56b.

Parameters, Options, and Subroutines Summary

Example e8x56a.dat and e8x56b.dat:

Parameters	Model Definition Options	History Definition Options
ALL POINTS	CONNECTIVITY	AUTO LOAD
ELEMENTS	CONTACT	CONTINUE
END	CONTROL	DISP CHANGE
FINITE	COORDINATES	TIME STEP
LARGE DISP	FIXED DISP	
SIZING	ISOTROPIC	
TITLE	OPTIMIZE	
UPDATE	SOLVER	
	WORK HARD	

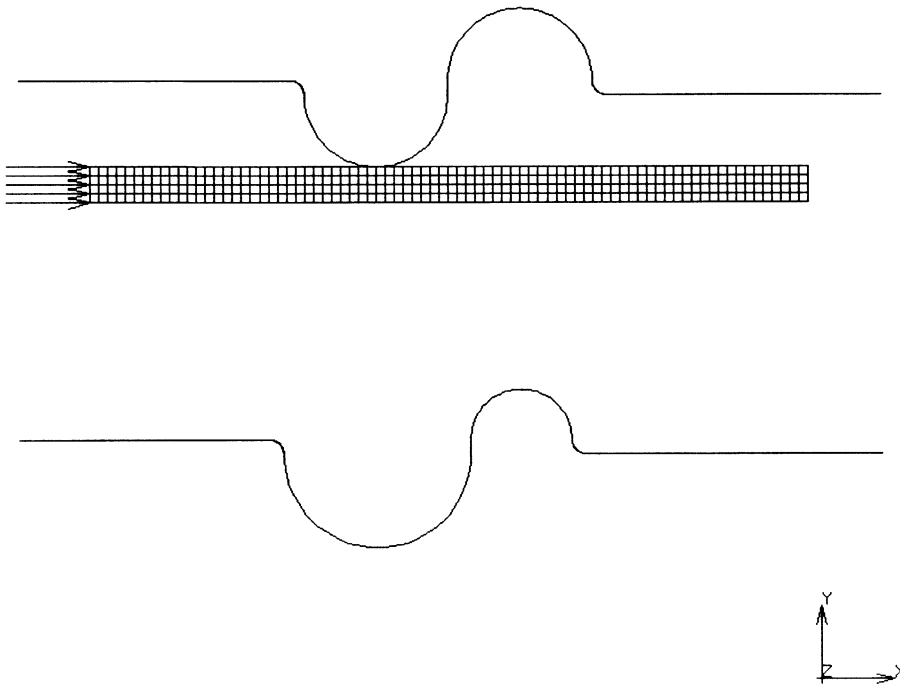
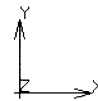
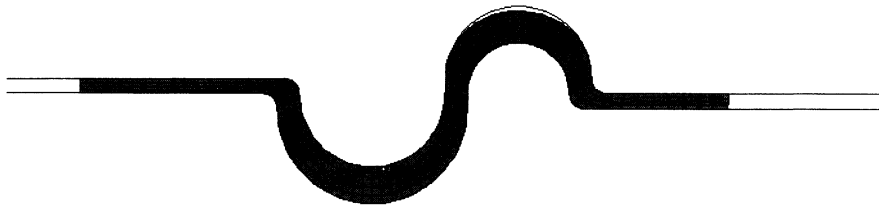


Figure 8.56-1 Initial Model for both Data Sets

Inc : 26
Time : 2.200e-01

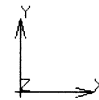


e8x56a - Velocity control

Figure 8.56-2 The Final Deformed Shape for Data Set e8x56a



Inc : 42
Time : 3.000e-01



e8x56b - Load control

Figure 8.56-3 The Final Deformed Shape for Data Set e8x56b



8.57 The ADAPTIVE Capability with Shell Elements

This example shows the ADAPTIVE capability in conjunction with shell elements. The example consists of four data sets, as given below.

Data Set	Element Used
e8x57a	4-node thick shell element number 75
e8x57b	3-node thin shell element number 138
e8x57c	4-node thin shell element number 139
e8x57d	4-node reduced integration thick shell element number 140

In each of these data sets, the problem involves the deformation of the structure under a point load. The ADAPTIVE model definition choice uses the Zienkiewicz-Zhu stress error as the criterion.

Model

The model consists of one 4-node element for data sets e8x57a, e8x57c, and e8x57d. Data set e8x57b consists of two 3-node triangular elements. All four data sets comprise of 4 nodes. The 4 nodes form a square of side 0.5 units in the x-y plane.

Material Properties

All four data sets have identical material properties. The Young's modulus is assumed to be 1.092×10^7 psi and the Poisson's ratio is assumed to be 0.30.

Boundary Conditions

The boundary conditions are identical for all four data sets and are given below.

Boundary Condition	Nodes
$u_x = u_y = \theta_z = 0$	1, 2, 3, 4
$u_z = 0$	2, 3, 4
$\theta_y = 0$	1, 4
$\theta_x = 0$	1, 2
$P_z = 1$	1

**Adaptive**

The ADAPTIVE model definition card is used to indicate that element refinement must be performed. A maximum of eight level of refinement are chosen. The Zienkiewicz-Zhu stress error criterion is used to flag the ADAPTIVE capability.

History Definition

The loading is imposed by the help of the model definition card POINT LOAD. The problem is elastic and a single increment is sufficient to solve the problem. However, the ADAPTIVE criterion requires successive subincrements for the single increment. No history definition cards are necessary in this single increment problem.

Results

The initial and deformed shapes with the adapted elements are shown at the end of the final subincrement of increment zero for data set e8x57a in Figure 8.57-2. The deformed shape is similar for all four data sets. Data sets e8x57a and e8x57d use six adaptive subincrements while e8x57b and e8x57c need seven subincrements. Figure 8.57-3 and Figure 8.57-4 show contours of the equivalent von Mises stress for data sets e8x57a and e8x57c respectively. As expected, the maximum value of the von Mises equivalent stress is higher for the discrete Kirchhoff quadrilateral element 139 (e8x57c) than the thick shell element 75 (e8x57a).

Parameters, Options, and Subroutines Summary

Example e8x57.dat:

Parameters	Model Definition Options
ADAPTIVE	ADAPTIVE
ELASTIC	CONNECTIVITY
ELEMENTS	COORDINATES
END	END OPTION
SHELL SECT	FIXED DISP
SIZING	GEOMETRY
	ISOTROPIC
	OPTIMIZE
	POINT LOAD
	SOLVER

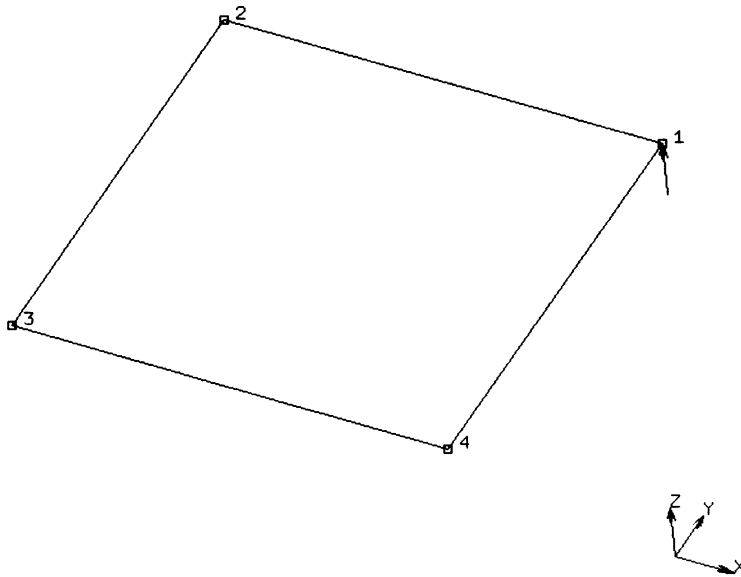


Figure 8.57-1 Initial Model with Point Load applied on Node 1



Inc : 0
Sub : 6
Time : 0.000e+00
Freq : 0.000e+00

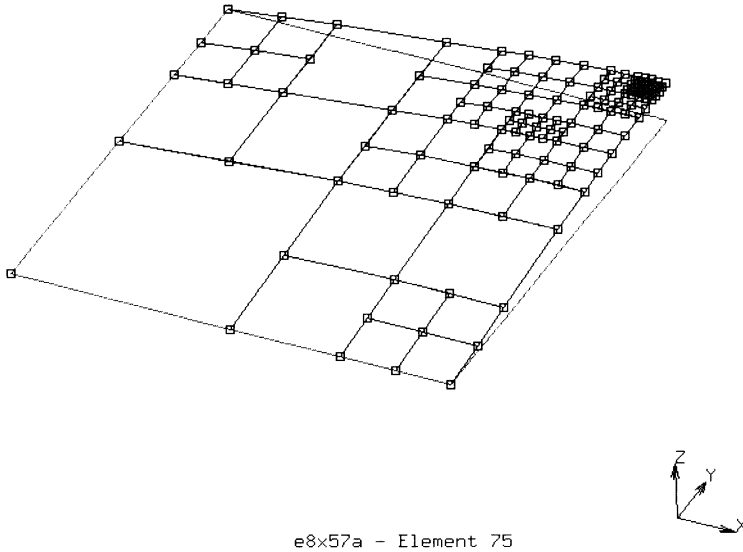


Figure 8.57-2 Initial and Deformed Shape for Data Set e8x57a

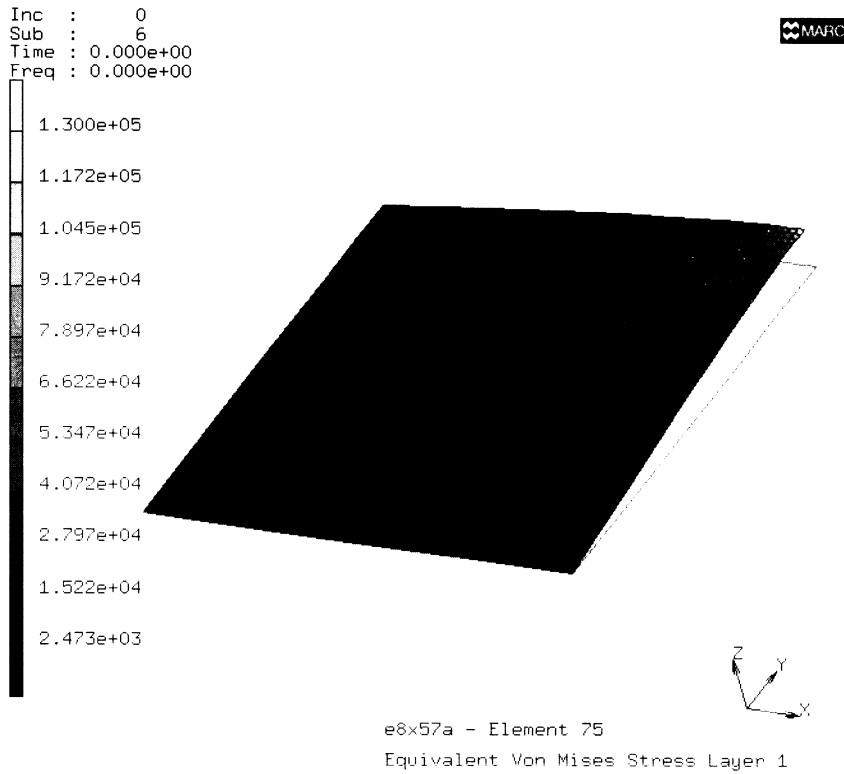


Figure 8.57-3 Equivalent von Mises Stress for Data Set e8x57a

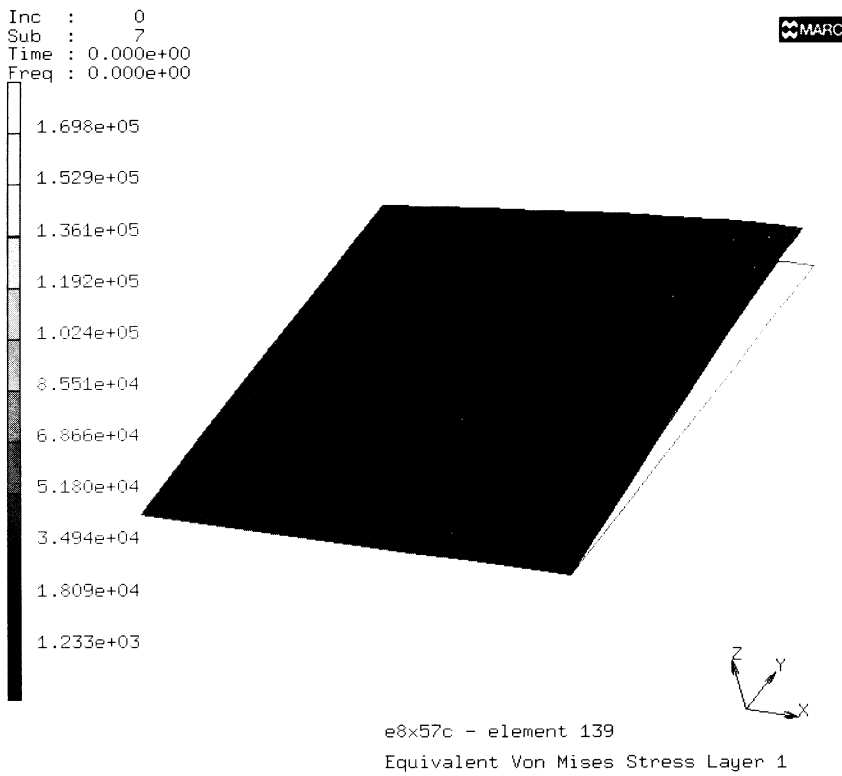


Figure 8.57-4 Equivalent von Mises Stress for Data Set e8x5c



8.58 Adaptive Meshing in Multiply Connected Shell Structures

This example shows the use of the ADAPTIVE criterion used at intersecting thin-walled structures.

Model

The model consists of three elements and 8-nodes. Element 75 which is a 4-node thick shell element is used. The initial model is shown in Figure 8.58-1.

Material Properties

All the three elements are linear elastic and have identical material properties with Young's modulus of 1.92×10^7 and a Poisson's ratio of 0.30.

Boundary Conditions

The nodal boundary conditions are summarized as follows.

Boundary Condition	Node Number
$u_x = u_y = u_z = 0$	1, 4, 5, 8
$\theta_x = \theta_y = \theta_z = 0$	1, 4, 5, 8

The loading is done by means of a face load (pressure) of $P_z = 0.01$ psi applied on elements 2 and 3.

Adaptive

The Zienkiewicz-Zhu stress error criterion is chosen with a maximum of eight levels of adaptation.

History Definition

The loading is accomplished in a single increment (increment zero) with the definition of the face loads on elements 2 and 3. No history definition cards are needed.

Results

A total of 9 subincrements are done in this example. The deformed geometry is shown in Figure 8.58-2. It can be seen that the subdivision takes place correctly at the areas of stress concentration, i.e. the intersection of the shell walls.



Inc : 0
Time : 0.000e+00

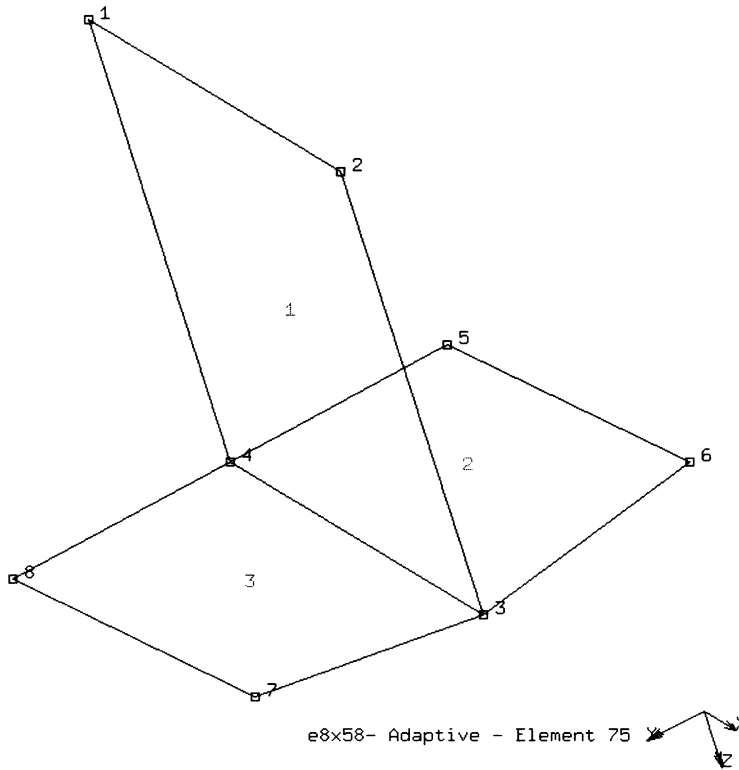


Figure 8.58-1 Initial Model



Inc : 0
Sub : 9
Time : 0.000e+00
Freq : 0.000e+00

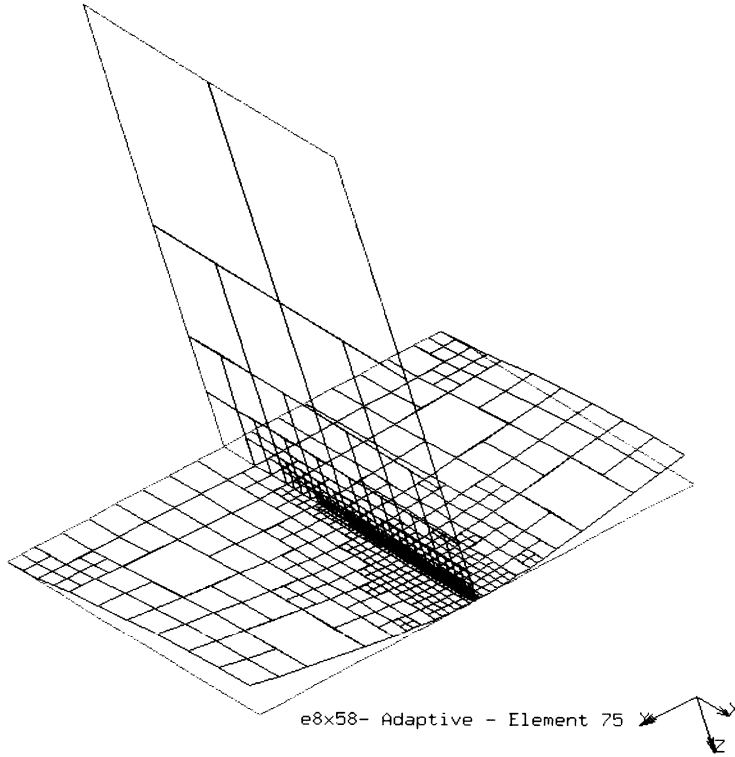


Figure 8.58-2 Deformed Geometry with the Adapted Mesh





8.59 Not Available



8 *Advanced Topics*

Not Available



8.60 Simulation of Sheet Bending

This example shows a simulation of the sheet bending process. A sheet is bent by deforming it with a punch into a die. In the sheet forming terminology, it is also called air bending or v-bending. This example demonstrates the forming and springback of the sheet.

Model

The sheet is modeled with 300 elements and 366 nodes. The punch and die are modeled as rigid bodies. The initial model is shown in Figure 8.60-1.

Element

The 4-node isoparametric quadrilateral plane strain element number 11 is used with the constant dilatation option.

Material Properties

The sheet is assumed to be isotropic. The Young's modulus is 3×10^7 psi and the Poisson's ratio is 0.30. The initial yield stress is 5×10^4 psi. The workhardening behavior is input using the WORK HARD model definition option.

Boundary Conditions

The boundary conditions along the x direction are enforced by setting a zero x displacement boundary condition on all nodes at the center line of the sheet. The boundary conditions along the y direction are enforced through the contact option.

Contact

There are a total of three contact bodies in the problem. Contact body 1 is the deformable sheet. Body 2 is a velocity controlled rigid surface and models the punch. Body 3 is also a rigid surface and represents the lower die. Shear friction is assumed with a coefficient of 0.10. The relative velocity below which a node is assumed to be sticking to a contact surface is set to be 1×10^{-3} in/s. The nodal reaction force required to separate a contacting node from its contacted surface is assumed to be 1×10^{-2} lb.

Control

The convergence control is governed by a relative displacement increment norm. The maximum allowed relative change in displacement increment is set to 0.10.



History Definition

The loading is done by moving the punch (contact body 2) along the negative y direction with a speed of -5×10^{-3} in/s for 120 increments. At the end of 120 increments, the direction of motion of the punch is reversed by prescribing a speed of 5×10^{-3} in/s along the positive y direction for a further 10 increments.

Results

The deformed shape is shown for increment 25 in Figure 8.60-2. The deformed shape is shown for increment 50 in Figure 8.60-3. The deformed shape is shown for increment 100 in Figure 8.60-4. At increment 118, the sheet contacts the flat portion of the lower die. For the next 2 increments, the sheet is driven into the lower die by the downward motion of the punch. The deformed shape is shown for increment 120 in Figure 8.60-5. For the next 10 increments, the punch moves upward and the sheet springs back. The final deformed configuration after springback is shown in Figure 8.60-6. A magnified view of contours of total effective plastic strain for increment 130 is shown in Figure 8.60-7.

Parameters, Options, and Subroutines Summary

Example e8x60.dat:

Parameters	Model Definition Options	History Definition Options
ALL POINTS	CONNECTIVITY	AUTO LOAD
ELEMENTS	CONTACT	CONTINUE
END	CONTROL	MOTION CHANGE
PLASTICITY	COORDINATES	TIME STEP
SETNAME	END OPTION	
SIZING	FIXED DISP	
TITLE	ISOTROPIC	
	SOLVER	
	WORK HARD	

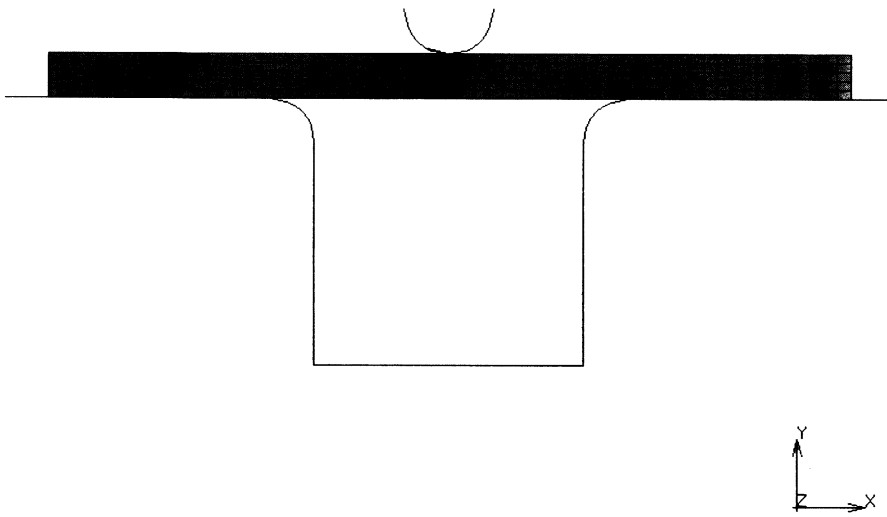
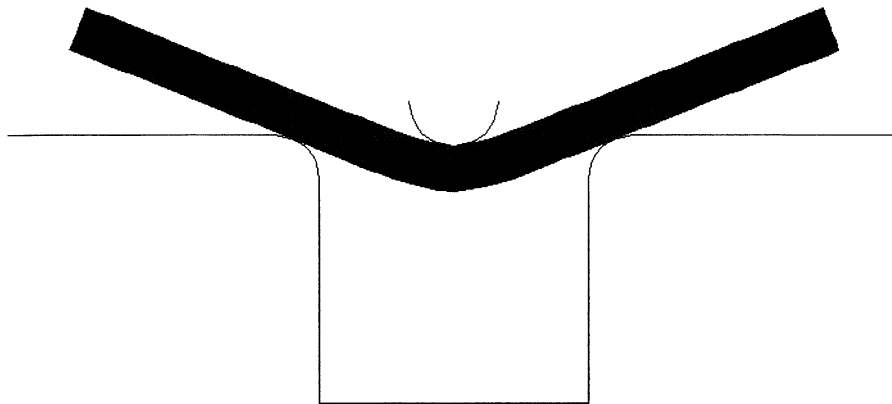


Figure 8.60-1 Initial Model



Inc : 25
Time : 2.500e+01



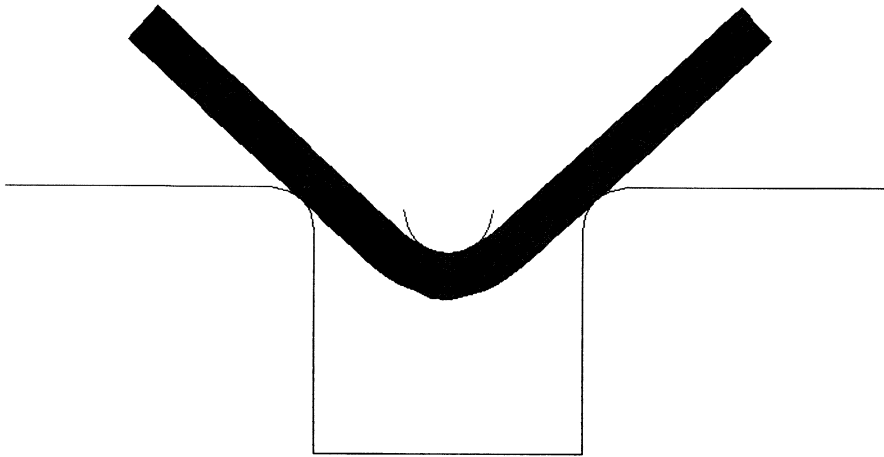
e8x60 - sheet bending



Figure 8.60-2 Deformed Geometry for Increment 25



Inc : 50
Time : 5.000e+01

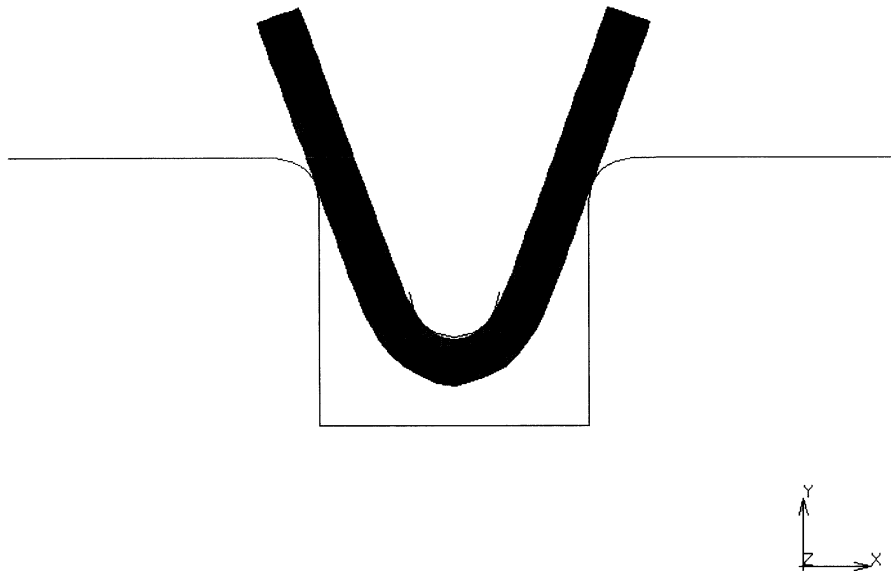


e8x60 - sheet bending

Figure 8.60-3 Deformed Geometry for Increment 50



Inc : 100
Time : 1.000e+02



e8x60 - sheet bending

Figure 8.60-4 Deformed Geometry for Increment 100



Inc : 120
Time : 1.200e+02

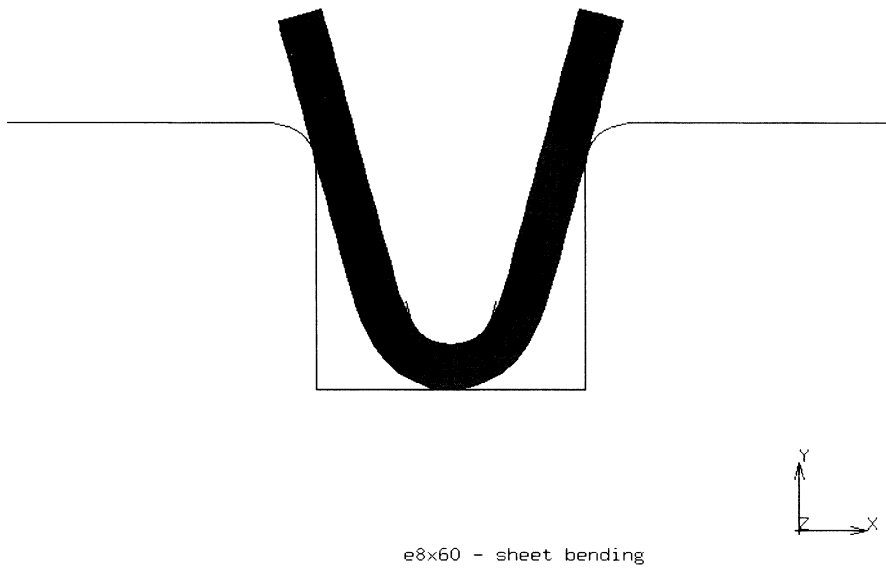
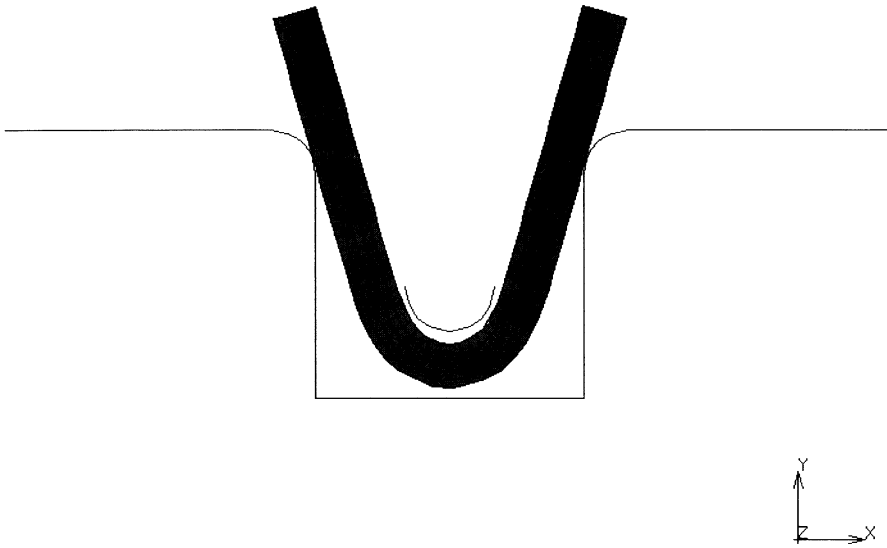


Figure 8.60-5 Deformed Geometry for Increment 120



Inc : 130
Time : 1.300e+02



e8x60 - sheet bending

Figure 8.60-6 Deformed Geometry for Increment 130

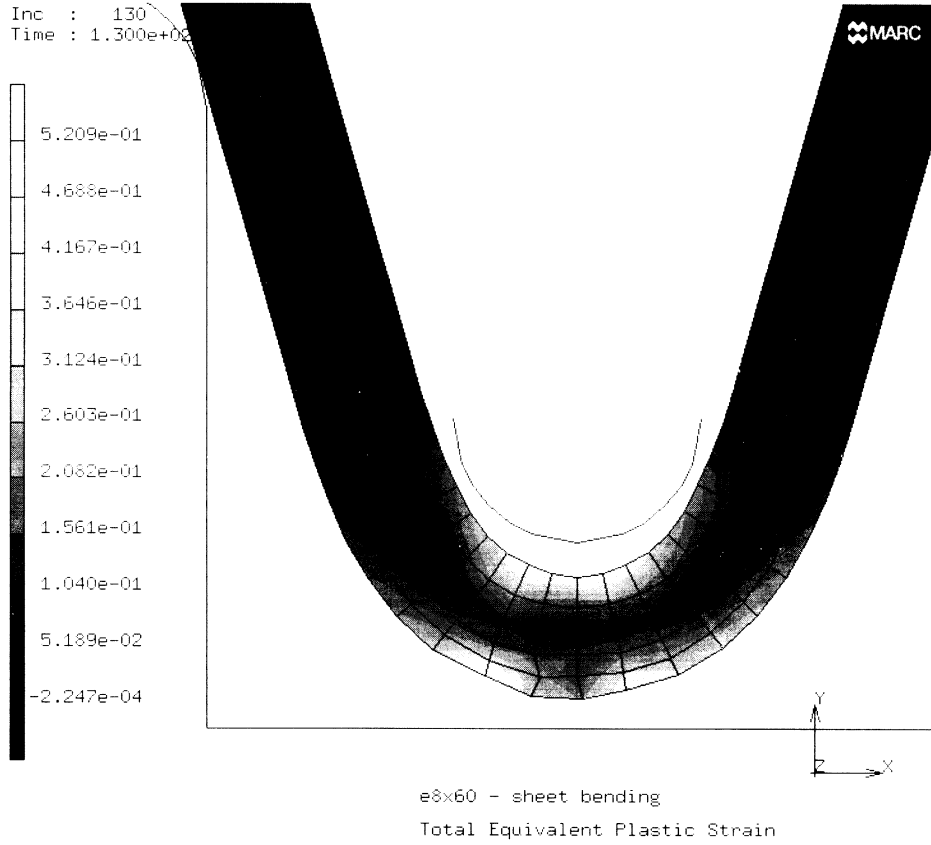


Figure 8.60-7 Magnified View of Contours of Total Effective Plastic Strain for Increment 130

